

The Palaeolithic Occupation of the Thar Desert

James Alexander Blinkhorn

Thesis submitted to the University of Oxford in partial fulfilment of the conditions in application for the Degree of Doctor of Philosophy

Michaelmas 2012

St. Hugh's College

University of Oxford

Research Laboratory for Archaeology and the History of Art

School of Archaeology

University of Oxford

The Palaeolithic Occupation of the Thar Desert

James Alexander Blinkhorn

St. Hugh's College

Submitted in partial fulfilment for the Degree of Doctor of Philosophy, Michaelmas 2012

Abstract

This thesis presents a comprehensive characterisation of the Palaeolithic occupation of the Thar Desert, which is located in western India and south-western Pakistan. This is achieved through a combination of extensive syntheses of existing palaeoenvironmental and archaeological evidence and the development of new, interdisciplinary evidence for Upper Pleistocene hominin occupation in the Thar Desert through surface survey and excavation. Patterns of environmental variability in the Thar Desert are described to identify when and where the Thar Desert may have been habitable to hominin populations. Evidence for over 900 Palaeolithic sites is synthesised to identify existing spatial, typological and chronological patterns in the Thar Desert. Typo-technological descriptions of new Palaeolithic assemblages are described, and placed within chronological and environmental contexts based upon associations with previously studied sediment formations. The results of chronological, environmental and archaeological analyses from a new excavated site, Katoati, are described, which presents a significant new benchmark for Palaeolithic studies, both for the Thar Desert and southern Asia. The excavated assemblages from Katoati indicate a Middle Palaeolithic occupation of the Thar Desert during episodes of enhanced humidity >91ka, and a further Middle Palaeolithic occupation 65-55ka. These Middle Palaeolithic assemblages indicate considerable cultural continuity and offer a chronometric framework for the results of the surface survey. The identification of a number of technologically and typologically distinct artefacts in both excavated and surface contexts indicate significant similarities with Middle Stone Age assemblages from Arabia and the Sahara and Middle Palaeolithic sites in South Asia. As a result, the Thar Desert can be identified as a pivotal location for investigating major changes in Upper Pleistocene hominin demography between Africa and across southern Asia.

Acknowledgements

The completion of this thesis has only been possible with the academic and personal support offered by a wide range of people and institutions, and this is gratefully acknowledged. Firstly, my thanks go to my academic supervisors, Mike Petraglia and Nicky Boivin, for their continuing encouragement, guidance and enthusiasm for my research in India. Hema Achyuthan has played a pivotal role in my D.Phil. research in India, as is thanked particularly for the enjoyable field season at Katoati, and the enlightening discussions over grape juice and idly.

My research has benefitted considerably from the intellectual environment at the School of Archaeology (University of Oxford), the Quaternary Geology and Palaeoclimate Lab (Anna University, Chennai), and in the field with my comrades in South Asian Archaeology - my thanks are extended to all involved. In particular, I thank the PalQuat-ers, Team Soup Thursday, and the Harcourt Open Arms Mic regulars and irregulars for making Oxford an enjoyable social environment. Special thanks are extended to Huw 'It's Sev-on' Groucutt and Ali Crowther for weekend ice creams and chomps. I am eternally grateful that my family support and encourage my adventures in the Palaeolicious. Finally, I thank my Cat, for her love and companionship, as well as her understanding for my dalliances with Mistress Archaeology.

Financial support from a number of sources is acknowledged. I have only been able to undertake D.Phil. research with support from the St. Hugh's College Graduate Scholarship. My fieldwork in the Thar Desert has primarily been funded by an Emslie Horniman Graduate Scholarship, awarded by the Royal Anthropological Institute in 2010. Further support for fieldwork activities has been provided a Meyerstein Research Fund Grant and a Rajiv Gandhi Travelling Scholarship. Radiocarbon dating of seven samples has been funded through a NERC Radiocarbon Facility award, awarded to Petraglia & Blinkhorn. The Archaeological Survey of India is thanked for permission to undertake research in Rajasthan.

Table of Contents

Abstract	i
Acknowledgements	ii
Table of Contents	iii
List of Figures	vi
List of Tables	xiv
Chapter 1 – Introduction	1
Research Methodology	6
Thesis Outline	6
Chapter 2 – Approaches to Palaeolithic Research in the Thar Desert	9
Development of South Asian Palaeolithic Systematics	10
Overview of Palaeolithic Archaeology in South Asia	21
History of Palaeolithic Research in the Thar Desert	29
Summary	39
Chapter 3 – Research Questions and Methodology	41
Research Questions	41
What spatial and chronological variation occurs in Pleistocene environments in the Thar Desert?	42
What variability occurs in the existing Palaeolithic record for the Thar Desert?	44
How does the organisation of lithic technology in the Thar Desert vary through time, space and across environments?	50
Summary	68
Chapter 4 – Geology, Ecology and Palaeoenvironments of the Thar Desert	69
Geology of the Thar Desert	70

Modern Ecology of the Thar Desert	74
Palaeoenvironments of the Thar Desert	78
Summary	113
Chapter 5 – Palaeolithic Archaeology of the Thar Desert	115
Defining the data set	116
Palaeolithic sites in the Thar Desert	117
Palaeolithic Industries in the Thar Desert	119
Palaeolithic lithic typology in the Thar Desert	122
Palaeolithic raw material use in the Thar Desert	133
Palaeolithic artefact sizes in the Thar Desert	141
Palaeolithic assemblage composition in the Thar Desert	159
Palaeolithic excavations and dated sites in the Thar Desert	155
Discussion	181
Chapter 6 – Survey in the Thar Desert	185
Survey sites with existing chronologies	186
Survey of lacustrine sites	205
Survey of Pushkar Valley	223
Discussion	235
Chapter 7 – Excavations at Katoati	239
Previous Research	240
Preliminary Research at Katoati	243
Excavations at Katoati	253
Site Formation Processes at Katoati	286
Pleistocene Landscapes at Katoati	291
Chapter 8 – Lithic Assemblages at Katoati	295
The Lithic Assemblages	295
Cores	297

Flakes	315
Flaked Pieces	330
Retouched Artefacts	332
Heavy Tools	339
Discussion	342
Chapter 9 – Discussion	345
The Katoati assemblages in their landscape context	345
Palaeolithic technology in the Thar Desert	352
Palaeoenvironments and Palaeolithic occupation in the Thar Desert	358
The Palaeolithic Occupation of the Thar Desert in its broader context	361
References Cited	371
Appendix A – Gazetteer of Palaeolithic Archaeology in the Thar Desert	391
Appendix B – Surface Survey Sites	459
Appendix C – Statistical results from Katoati	479

List of Figures

	Page Number
Figure 1.1: Location of Thar Desert in relation to major biogeographic provinces.	1
Figure 1.2: Maps indicating modelled annual rainfall: a) during the Last Glacial Maximum (LGM) with the Thar Desert (circled) experiencing hyper-aridity (<150mm rainfall/year) (above; following Braconnot et al. 2007); and b) during peak humidity of the last interglacial (Marine Isotope Stage 5e) (below; following Otto-Bliesner et al. 2006), with the Thar Desert (circled) typically experiencing sub-arid to sub-humid conditions (150-500+mm/ rainfall/yr).	2
Figure 1.3: Map indicating the location of Rajasthan, Gujarat, and Upper and Lower Sindh.	5
Figure 2.1: Bar chart of number of sites reported in Gujarat, Rajasthan and Sindh in five year periods.	37
Figure 2.2: Bar chart of sites reported using different terminology throughout the Thar Desert in five year periods.	38
Figure 4.1: Geological map of Rajasthan and Gujarat (Bakliwal & Wadhawan 2003; Figure 1).	71
Figure 4.2: Isohyet map of average annual rainfall (1950-2000) in the Thar Desert indicating eastward extent of sand dune formations.	74
Figure 4.3: A nilgai and cow by a canal that dissects the otherwise dry, sand dune-dominated plains at Chamu.	78
Figure 4.4: SPECMAP stacked $\delta^{18}O$ record for the past 600ka (following Imbrie et al. 1984).	80
Figure 4.5: The Indian Monsoon Index compared with the African Monsoon Index (grey scale on the right) and the Specmap oxygen isotope record for the last 140ka (Leuschner & Sirocko 2003; Fig. 4).	81
Figure 4.6: Indian Summer Moonson (ISM), temperatures, and ice. Reconstructed trends in (A) Northern Hemisphere ice volume, (B) ISM intensity, (C) Antarctic temperatures, and (D) Antarctic ice volumes over the last 900ka. Comparing the curves shows that the ISM started to strengthen before ice volumes reached their maxima. (A), (B) and (D) cover seven glacial-interglacial cycles; (C) covers five cycles. Thin gray lines illustrate each event; thick coloured lines represent the mean. The magnitude of each event is normalized. Time is also normalized: It is reset with the seven ISM minima lined up at 41 thousand years ago; each cycle is then rescaled so that the time between the ISM minimum and maximum becomes the average time of all seven events. The cycle between 700 and 780 thousand years ago was not included because it has a prominent interstadial during the glacial period (following Liu 2011).	83

Figure 4.7: Map of palaeodrainage network in the Thar Desert (Gupta et al. 2011).	84
Figure 4.8: Physical stratigraphy and OSL chronology of Quaternary alluvial successions in the mid-Luni Valley (Jain et al. 2005; Figure 7).	87
Figure 4.9: Stratigraphy and chronology of fluvial and aeolian sediments in the Sabarmati Valley (Srivastava et al 2001; Fig. 3).	88
Figure 4.10: Stratigraphic details and BGSL ages of the upper fluvial and aeolian succession resting on the marker red soil in the lower Mahi basin (Juyal et al. 2005; Figure 5).	89
Figure 4.11: Stratigraphic details and BGSL ages of Late Quaternary sediment succession in the Orsang Valley (Juyal et al. 2005; Figure 6).	90
Figure 4.12: Spatial variability of sediments to the south of the Katrol Range, Kachchh, and sediment profiles for sequences from which pedogenic carbonates have been dated (Maurya et al. 2008; Figure 4).	92
Figure 4.13: Excavated sediment profile and TL ages at 16R Dune (Singhvi et al. 2010; Figure 3).	95
Figure 4.14: Composite sediment stratigraphy and IRSL ages from Chamu (Dhir et al. 2010; Figure 2).	96
Figure 4.15: Sediment sequence, TL and IRSL ages, and stable isotope results from Shergarh Tri-Junction (Andrews et al. 1998; Figure 5).	97
Figure 4.16: Sediment sequences with radiocarbon and TL ages at Nachha, Bikampur and Awai (Chawla et al. 1992; Figure 2).	97
Figure 4.17: Stratigraphy and BGSL chronology of the aeolian sand overlying the fluvial sequences in the Mahi and Orsang basin (Juyal et al. 2005; Figure 7).	99
Figure 4.18: Composite results of stable isotope analyses on pedogenic carbonates at 16R Dune (Achyuthan et al. 2007), Chamu (Dhir et al. 2010); and Shergarh Tri-Junction (Achyuthan et al. 2007; Andrews et al. 1998).	101
Figure 4.19: Stable isotopic composition of pedogenic carbonates from 16R Dune, Chamu & Shergarh Tri-Junction plotted against date of parent matrix, or averaged date of age determinations bracketing samples.	102
Figure 4.20; Distribution of miliolite (Quaternary bioclastic carbonate) deposits in Saurashtra and Kachchh (Bhatt 2003; Figure 1).	104
Figure 4.21: Distribution of lakes in Rajasthan (Achyuthan et al. 2007; Figure 1).	106
Figure 4.22: Sedimentary section, radiocarbon dates and pollen diagrams from Bap Malar Lake (Deotare et al. 2004; modified from Figure 4).	107

Figure 4.23: Sedimentary section and radiocarbon dates from Borehole 1 at Sambhar Lake (Sinha et al. 2005; Figure 2).	109
Figure 4.24: Composite bar chart of all chronometrically dated aeolian deposits in the Thar Desert.	112
Figure 5.1: Map of all Palaeolithic sites in the Thar Desert.	118
Figure 5.2: Map displaying sub-regions of Thar Desert as used in this thesis.	119
Figure 5.3: Distribution of sites with a single Palaeolithic industry present.	121
Figure 5.4: Bar chart of occurrence (%) of different lithic artefact types in Palaeolithic sites in the Thar Desert separated by industry.	125
Figure 5.5: Distribution of sites with a typological inventory: a) Single industry sites (above); b) Multiple industry sites (below).	129
Figure 5.6: Distribution of raw material use in Palaeolithic sites in the Thar Desert: a) Igneous (previous page, top); b) Silicious (previous page, bottom); c) sedimentary and metamorphic (above).	135
Figure 5.7: Bar chart of raw material use in single industry Palaeolithic sites in the Thar Desert.	138
Figure 5.8: Scatter plot of individual Palaeolithic artefact size separated by raw material type.	142
Figure 5.9: Scatter plot of mean Palaeolithic artefact sizes separated by raw material type.	142
Figure 5.10: Scatterplot of individual and mean Palaeolithic artefact sizes separated by Palaeolithic industry.	144
Figure 5.11: Scatter plot of individual and mean flakes and blades separated by Palaeolithic industry.	144
Figure 5.12: Scatter plot of individual and mean retouched tools and microliths separated by Palaeolithic industry.	145
Figure 5.13: Scatter plot of individual and mean core sizes separated by Palaeolithic industry.	145
Figure 5.14: Scatterplot of individual and mean heavy tool sizes separated by Palaeolithic industry.	148
Figure 5.15: Distribution of sites with reported typological composition of Palaeolithic assemblage with more than 50 artefacts.	149

Figure 5.16: Mean proportional composition of lithic assemblage typological inventories separated by Palaeolithic industry (see text for exact proportion of flakes/debitage).	151
Figure 5.17: Distribution of sites with excavation or chronometric dating of Palaeolithic assemblages in the Thar Desert.	157
Figure 5.18: Plan of excavation at ZPS1 (Biagi et al. 1996; Figure 3).	158
Figure 5.19: Size of analysed complete un-retouched artefacts from ZPS1: a) E4 (left); b) (E6-7) (right)(Biagi et al. 1996; Figure 4a & 4b).	159
Figure 5.20: Unfinished Lower Palaeolithic Handaxes from ZPS1-E4 (Biagi et al. 1996; Figure 6).	160
Figure 5.21: Late Palaeolithic endscrapers (1 & 2) and cores (3-6) from ZPS1-E6-7 (Biagi et al. 1996; Figure 10).	160
Figure 5.22: Size of analysed complete un-retouched artefacts from ZPS2 (Biagi et al. 1998-2000; Figure 5b).	161
Figure 5.23: Cores from ZPS2 (Biagi et al. 1998-2000; Figure 10).	162
Figure 5.24: Artefacts from 797bis – refitting flakes with bidirectional detachments (1); flake with bidirectional detachments (2); fragments of cores with a debitage surface parallel to a cortical one (3 & 4) (scale 1:2) (Negrino & Kazi 1996; Figure 14).	163
Figure 5.25: Excavated profile at 16R Dune, identifying the location of archaeological horizons and chronometric dating sample locations and results (adapted from Singhvi et al. 2010).	165
Figure 5.26: Small tools from 16R-Sup (Gaillard 1993; Figure 89).	166
Figure 5.27: Heavy tools from 16R-Sup (Gaillard 1993; Figure 96).	167
Figure 5.28: Artefacts from 16R-Inf (Gaillard 1993; Figure 97).	169
Figure 5.29: Small tools from Singi Talav (Gaillard 1993; Figure 51).	174
Figure 5.30: Medium sized tools from Singi Talav (Gaillard 1993; Figure 58).	175
Figure 5.31: Handaxes (1-5) and a Cleaver (6) from Singi Talav (Gaillard et al. 2010; Figure 5).	176
Figure 5.32: Lower Palaeolithic handaxes from Umrethi (Baskaran et al. 1986; Figure 3).	178
Figure 5.33: Middle Palaeolithic artefacts from the Hiran Valley, Saurashtra (Baskaran et al. 1986; Figure 4).	179
Figure 6.1: Map of survey sites.	186

Figure 6.2: Stratigraphy of alluvial and aeolian deposits and associated luminescence dates at Karna (modified from Jain et al. 2005; Figure 4).	187
Figure 6.3: Lithic artefacts (circled) stratified in cemented multi-storied gravels at Karna in sediments dated to 79.8ka.	188
Figure 6.4: Map of locations of lithic assemblages recorded and sampled at Karna.	189
Figure 6.5: Rhyolite boulder core at KAR2.	190
Figure 6.6: Lithic scatter from which KAR3 assemblage was sampled.	190
Figure 6.7: Map of locations of lithic assemblages recorded and sampled at Chamu.	192
Figure 6.8: Quarry section observed at Shergarh Tri-Junction quarry, illustrating alternating colluvial and aeolian deposits overlain by a Holocene dune deposit.	193
Figure 6.9: Map of locations of lithic assemblages recorded and sampled at Shergarh Tri-Junction.	194
Figure 6.10: Lithic scatter from which TRI2 assemblage was sampled.	194
Figure 6.11: Lithic scatter from which SHR1 assemblage was sampled.	196
Figure 6.12: Cores from Shergarh Tri-Junctions. Top-left: Bidirectional Levallois core from TRI1 ; Top-right: bidirectional blade core from TRI1; Bottom-Left: Preferential Levallois core from TRI2.	199
Figure 6.13: Artefacts from SHR1. Top-left: Preferential Levallois Core; Top-right: Preferential point core similar to Nubian Type 2 cores; Bottom-left: Notched Flake; Bottom-right: Tongued Flake.	200
Figure 6.14: Artefacts from Chamu. Top-left: Shouldered flake from CHA1; Bottom-left: Levallois point from CHA1; Right: Bifacial stemmed point.	204
Figure 6.15: Map of locations of lithic assemblages recorded and sampled at Sambhar Lake.	207
Figure 6.16: Gneiss boulder core at SMB1.	207
Figure 6.17: Lithic scatter from which SMB6 assemblage was sampled.	208
Figure 6.18: Map of locations of lithic assemblages recorded and sampled at the Jaisalmer Raans	209
Figure 6.19: Lithic scatter from which KHA1 assemblage was sampled.	211
Figure 6.20: Lithic scatter from which KHA2 assemblage was sampled.	211
Figure 6.21: Tanged point from KHA1.	220

Figure 6.22: Delineated artefacts from SAM1. Top-left and Bottom-left: Nosed pieces; Right: Shouldered point.	221
Figure 6.23: Delineated gneiss artefacts from Sambhar Lake. Top-left: Tanged point; Top-middle: Tongued piece from SMB3; Right: Tanged point ; Bottom-left: Tanged point from SAM1.	222
Figure 6.24: Composite stratigraphy from Pushkar (Allchin & Goudie 1974; Figure 22).	224
Figure 6.25: Map of Pushkar Valley sites.	225
Figure 6.26: Lithic scatter from which the BPG1 assemblage was sampled.	226
Figure 6.27: Recently exposed red soil horizon at Hokra.	226
Figure 6.28: Blades cores from HOKF.	230
Figure 7.1: Location map of Katoati.	239
Figure 7.2: Location of Palaeolithic sites in Jayal area (Agrawal et al. 1980; Figure 3).	241
Figure 7.3: Scheme of quaternary deposition around Didwana (Misra 1995; Figure 3)	242
Figure 7.4: Site locations in Katoati landscape.	244
Figure 7.5: Detailed locations of JFL and KAT sites.	244
Figure 7.6: Ferricretised boulder conglomerate overlying sandstone basement at Ambali.	245
Figure 7.7: View over Katoati landscape from Ambali.	245
Figure 7.8: Uppermost horizon of calcretised horizon overlain by thin aeolian deposit.	246
Figure 7.9: Quarrying of calcrete horizon, with fluvio-aeolian deposits in background.	246
Figure 7.10: Schematic section drawing of sediment section at JFL1, showing location of OSL samples (modified from illustration by Dr. P. Ditchfield).	248
Figure 7.11: Schematic section drawing of sediment section at JFL2, showing location of OSL samples (modified from illustration by Dr. P. Ditchfield).	250
Figure 7.12: Prospection of fluvio-aeolian sediments in 2011, with Prof. H. Achyuthan.	252
Figure 7.13: Exposed clusters of ostrich eggshell at KAT2.	252
Figure 7.14: KAT1 prior to excavation.	254
Figure 7.15: KAT1 excavated section.	255

Figure 7.16: Schematic section diagram of excavation at KAT1 identifying individual strata (S1-S8) and showing the location of sedimentological (highlighted) and OSL sampling (black circles), and the excavation horizon yielding dated ostrich eggshell (Level 23).	256
Figure 7.17: Mean grain size, sorting, skewness and kurtosis (ϕ) by depth in excavated profile. A value of 1ϕ was subtracted from kurtosis values so positive values correspond to leptokurtic distributions and negative values correspond to platykurtic distributions.	265
Figure 7.18: Grain size (ϕ) distributions of sediment samples (listed by arbitrary depth in profile) from KAT1, separated into 1m groups: a) (top) 0-1m; b) 1-2m; c) 2-3m; d) 3-4m; e) (bottom) 4-4.5m.	266
Figure 7.19: Coarse sediment inclusions from excavated strata 4, 6 and 8, and granule-pebble horizon in situ in Stratum 3.	269
Figure 7.20: Proportional composition of aluminium, calcium, potassium and silicon within sedimentary samples from KAT1 based upon XRF analysis.	270
Figure 7.21: Percentage of calcite present in sediment samples plotted by depth.	272
Figure 7.22: Stable oxygen and carbon isotope results from pedogenic carbonates from KAT1.	273
Figure 7.23: Stable oxygen and carbon isotope results of pedogenic carbonates from KAT1 plotted by depth.	275
Figure 7.24: Stable oxygen and carbon isotope results of un-abraded ostrich eggshell samples from KAT1-KAT5.	278
Figure 7.25: Cumulative composition of lithic artefacts within each assemblage grouped by 10mm size classes.	280
Figure 7.26: Cumulative composition of lithic artefacts within each assemblage grouped by 10mm size classes and degree of rounding.	282
Figure 7.27: Boxplot of artefact surface area (mm^2) separated by weathering classes and lithic assemblage.	285
Figure 7.28: Schematic depiction of landscape development at Katoati: Top Left – existence of pre-Quaternary powerful fluvial system forming major boulder-cobble horizon overlying sandstone basement; Top Right – Tectonic uplift of sandstone basement alters depositional environment promoting deposition of overbank fine sediments; Middle Left – Weathering promotes ferricretisation of boulder horizon, while groundwater carbonate formation cements floodplain facies, making them resistant to erosion; Middle Right - Braided fluvial channels promote sedimentation, forming gravel and sand bars; Bottom Left – Aeolian deposition on top of fluvial horizons, with formation of pedogenic carbonates; Bottom Right – deflation of aeolian deposits and gullying of fluvio-aeolian horizons.	292

Figure 8.1: Levallois Cores: a) S8 - unidirectional (top left); b) S8 - convergent proximal and distal (top right); c) S5 proximal and divergent distal (middle left); d) S5 - proximal and convergent distal (middle right); e) S4 - proximal and divergent distal (Nubian Type 1-like) (bottom left); f) S6 -convergent proximal and distal (bottom right).	300
Figure 8.2: Levallois cores: a) S6 - distal and lateral (left); b) S4 - proximal and lateral convergent (Nubian Type 2-like) (right).	301
Figure 8.3: Levallois cores: a) S4 - distal divergent and lateral (Nubian Type 1/2-like) (left); b) S8 - distal divergent and lateral (right).	302
Figure 8.4: Radially flaked Levallois core from S6.	303
Figure 8.5: Levallois Cores: a) S8 - radial (left); b) S6 - recurrent centripetal (right).	303
Figure 8.6: Boxplots of core attributes separated by core type; a) number of scars (top-left); b) cortex (%) (top-right); c) maximum length (bottom-left); d) size corrected platform size (bottom-right).	307
Figure 8.7: Boxplots of core attributes separated by platform type: a) cortex (%) (top-left); b) maximum length (top-right); c) platform surface area mm ² (bottom left); d) platform shape (bottom right).	309
Figure 8.8: Levallois points: a) S6 (left); b & c) S4 (middle; right).	316
Figure 8.9: Boxplots of flake attributes separated by dorsal scar pattern: a) cortex (%) (top-left); b) maximum length (mm) (top-right); c) distal shape (bottom-left); d) size corrected platform area (bottom-right).	320
Figure 8.10: Box plot of complete flake maximum length separated by dorsal scar patterns and presence of retouch.	326
Figure 8.11: Bifacial point from S4; Ventral left, dorsal right; Platform at top.	333
Figure 8.12: Notched artefacts: a) S4 – notch (top-left); b) S5 – tanged point (top-right); c) S6 – shouldered point (middle-left); d) S6 – broken tanged artefact (middle-right); e) S8 – notch/shoulder (bottom-left).	336
Figure 8.13: Delineated artefacts: a) S4 – nosed flake (top-left); b) S4 – delineated flake (top-centre); c) S6 - bifacially delineated tongued flake (top-right); d) S6 – tongued flaked (middle-left); e) S6 – shouldered flake (middle-right); f) S6 - delineated flake (bottom).	337
Figure 8.14: Heavy tools: a) Ovate biface (left); b) bifacial heavy tool (right).	341
Figure 9.1: Biface observed in basal gravels in nalla at KAT1.	351
Figure 9.2: Large tanged point on silicious limestone from KHA1 (left) compared with small tanged point on gneiss from Sambhar Lake (right).	354

Figure 9.3: Synthesis of environmental and archaeological evidence from South Asia and Katoati, including genetic age estimates relating to human dispersals and suggested arrival of modern humans in South Asia by two models. Environmental evidence includes SPECMAP Oxygen Isotope curve and associated Marine Isotope Stages (MIS) (following Imbrie et al. 1984), Indian Monsoon Index based upon variability in insolation at 30°N due to orbital tilt, precession and eccentricity (Leuschner & Sirocko 2003), and estimated monsoonal minimum based upon time averaged patterns of monsoonal intensity across 9 Lower and Middle glacial-interglacial cycles (Liu 2012). Archaeological evidence presented from South Asia is discussed in Chapter 2 and 5 (see also Petraglia 2012a; Haslam et al. 2011). Genetic results indicate age estimates for: A) Genomic estimate of split of Eurasian from African populations 112-88ka (C.I. 150-63ka) (Xing et al. 2009); B) mtDNA estimate of appearance of Hg L3 at 72ka. (C.I. 87-56ka) (Soares et al. 2009); and C) genomic estimate of split of East Eurasians from proto-Eurasian group (Rasmussen et al. 2011). MIS 4/3 model for the arrival of *Homo sapiens* in South Asia derived from Mellars (2006), MIS 5 model for the arrival of *Homo sapiens* in South Asia derived from Petraglia et al. (2010; 2012b). 363

Figure 9.4: Above – Tanged point from Jwalapuram 22 ca. 74ka (Haslam et al. 2012); Below – Tanged point from Katoati S5 ca. 91ka. 364

Figure 9.5: Nubian Type 1 reduction strategy. Top-left: Schematic depiction of Nubian Type 1 reduction strategy (from Figure 2 [Rose et al. 2011]); Bottom-left: Example of Arabian Nubian Type 1 core from Aybut Al Auwal (from Figure 9 [Rose et al. 2011]); Top-right: schematic depiction of Nubian Type 1-like core from KAT 1-S4; Bottom-right: photo of Nubian Type 1-like core from KAT 1-S4. 366

Figure 9.6: Nubian Type 2 reduction strategy. Top-left: Schematic depiction of Nubian Type 2 reduction strategy (from Figure 2 [Rose et al. 2011]); Bottom-left: Example of Arabian Nubian Type 2 core from Aybut Al Auwal (from Figure 9 [Rose et al. 2011]); Top-right: schematic depiction of Nubian Type 2-like core from SHR1; Bottom-right: photo of Nubian Type 2-like core from SHR1. 367

List of Tables

	Page Number
Table 2.1: Summary of recognised Palaeolithic cultural phases throughout South Asian research history.	20
Table 2.2: Summary of broad cultural periodization in South Asian Palaeolithic.	28
Table 3.1: Cultural Group terminology reported in the literature and its relationship with terminology used in this thesis. aOnly aceramic sites are included in this group. b'Neolithic' sites have only been included from Foote (1916).	47
Table 3.2: Artefact types grouped by gross technological characteristics, based upon common categories reported in the Thar Desert.	49
Table 3.3: Assemblage scale attributes analysed and potential interpretation of results.	62
Table 3.4: Attributes recorded on cores indicating how they are recorded and potential interpretation of results.	64
Table 3.5: Attributes recorded on flakes indicating how they are recorded and potential interpretation of results.	65
Table 3.6: Attributes recorded on flaked pieces indicating how they are recorded and potential interpretation of results.	65
Table 3.7: Additional attributes recorded on retouched flakes or flaked pieces indicating how they are recorded and potential interpretation of results.	66
Table 3.8: Attributes recorded on heavy tools indicating how they are recorded and potential interpretation of results.	66
Table 4.1: Summary of fluvial activity in the Thar Desert.	93
Table 4.2: Synthesis of U/Th dates on miliolite deposits from Saurashtra and Kachch.	105
Table 5.1: Number of sites in the Thar Desert within each industrial group.	120
Table 5.2: Occurrence of different lithic artefact types in Palaeolithic sites in the Thar Desert.	123
Table 5.3: Number of sites with typological data with different industrial associations.	124
Table 5.4: Spatial patterns of variability in lithic artefact types in Palaeolithic sites in the Thar Desert.	131
Table 5.5: Number and percentage of sites containing different lithic raw materials.	134

Table 5.6: Presence of different raw material types in different regions of the Thar Desert.	137
Table 5.7: Mean number of raw materials in sites of each industry.	138
Table 5.8: Summarised description of Palaeolithic excavations undertaken in the Thar Desert.	156
Table 5.9: Summary of assemblage composition from 16R Dune following Gaillard 1993 (Tables 62, 63 and 69).	168
Table 5.10: Synthesis of U/Th, 14C and luminescence dates from 16R Dune.	170
Table 5.11: Summary of assemblage composition from Singi Talav following Gaillard (1993).	172
Table 6.1: Typological breakdown of artefact assemblages from Chamu, Karna and Shergarh Tri-Junction with chronology of associated sedimentary contexts.	196
Table 6.2: Raw material use at Chamu, Karna and Shergarh Tri-Junction.	197
Table 6.3: Number of artefacts with different levels of cortical coverage at Chamu, Karna and Shergarh Tri-Junction.	198
Table 6.4: Typological breakdown of artefact assemblages from Sambhar Lake and Jaisalmer Raans.	213
Table 6.5: Raw material use at Sambhar Lake and the Jaisalmer Raans.	214
Table 6.6: Number of artefacts with different levels of cortical coverage at Sambhar Lake and the Jaisalmer Raans.	214
Table 6.7: Typological breakdown of artefact assemblages from Pushkar Valley.	227
Table 6.8: Raw material use in Pushkar Valley sites.	228
Table 6.9: Number of artefacts with different levels of cortical coverage at Pushkar Valley sites.	229
Table 7.1: Preliminary OSL dates from JFL1 (pers. Comm. Prof. R. Roberts, 12/2011).	249
Table 7.2: Preliminary OSL dates from JFL2 (pers. Comm. Dr. R. Roberts, 12/2011).	250
Table 7.3: Results of AMS radiocarbon dating of OES fragments from KAT2, KAT3 and KAT4; the dates are presented in uncalibrated radiocarbon years (Half-life=5,568 years).	251
Table 7.4: Results of OSL dating of samples bracketing the OES assemblage at KAT2.	251
Table 7.5: Basal depths of excavated horizons.	257
Table 7.6: Description of sediment strata in excavated sequence at KAT1.	258

Table 7.7: OSL age estimates of samples from KAT1.	258
Table 7.8: Details of excavated lithic assemblages from KAT1, grouped by excavation horizon and assemblage, relating to sedimentary strata.	259
Table 7.9: Results of AMS radiocarbon dating of OES fragments from KAT1; the dates are presented in uncalibrated radiocarbon years (Half-life=5,568 years).	259
Table 7.10: Description of sediment samples characteristics following Folk and Ward (1957) method.	264
Table 7.11: Results of stable isotope analysis of pedogenic carbonates.	275
Table 7.12: Results of stable isotope analysis of ostrich eggshell. a $\delta^{13}\text{C}$ results from radiocarbon analyses.	277
Table 7.13: Total number of artefacts displaying different levels of rounding and weathering.	280
Table 7.14: Number of artefacts showing different degrees of rounding separated by excavation level and assemblage.	281
Table 7.15: Number of artefacts showing different degrees of weathering separated by excavation level and assemblage.	286
Table 8.1: Basic typology of artefacts from each stratum at KAT1. Counts in brackets indicate the number of blades present.	297
Table 8.2: Core types by stratum.	312
Table 8.3: Core platform types by stratum.	313
Table 8.4: Core platform preparation by stratum.	313
Table 8.5: Core last scar termination type by stratum	313
Table 8.6: Number of flakes with different scar patterns separated by stratum.	327
Table 8.7: Number of flakes with different scar patterns separated by stratum.	327
Table 8.8: Number of flakes with different platform type separated by stratum.	328
Table 8.9: Number of retouched and un-retouched flakes separated by stratum.	331
Table 8.10: Metric attributes of heavy tools from KAT1.	341
Table 9.1: Summary of hominin occupation at Katoati.	348

Chapter 1

Introduction

The Thar Desert occupies a major transitional zone between the arid, Palearctic landscapes of South-West Asia and the Sahara, and the monsoonal, Oriental biomes of South and East Asia (Figure 1.1), making it a critical location to investigate Palaeolithic hominin demography across southern Asia. This region presents a key topographic bottleneck between the mountainous Karakoram and Himalaya, and the Arabian Sea, which are likely to have significantly constricted potential routes of movement for hominin populations. Climatic fluctuation throughout the Pleistocene has resulted in significant oscillations between arid and humid environmental conditions (Figure 1.2) in the Thar Desert that may have either prevented or permitted hominin occupations. Characterising the Palaeolithic occupation of the Thar Desert is significant for understanding how hominin populations have adapted to environmental change in marginal habitats. Furthermore, understanding patterns in hominin occupations of the Thar Desert may offer insight into the nature and timing of major changes in hominin demography across southern Asia.

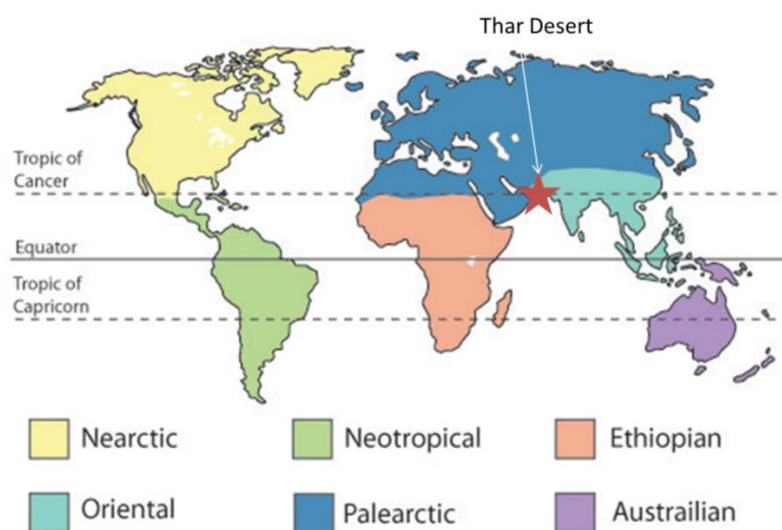


Figure 1.1: Location of Thar Desert in relation to major biogeographic provinces.

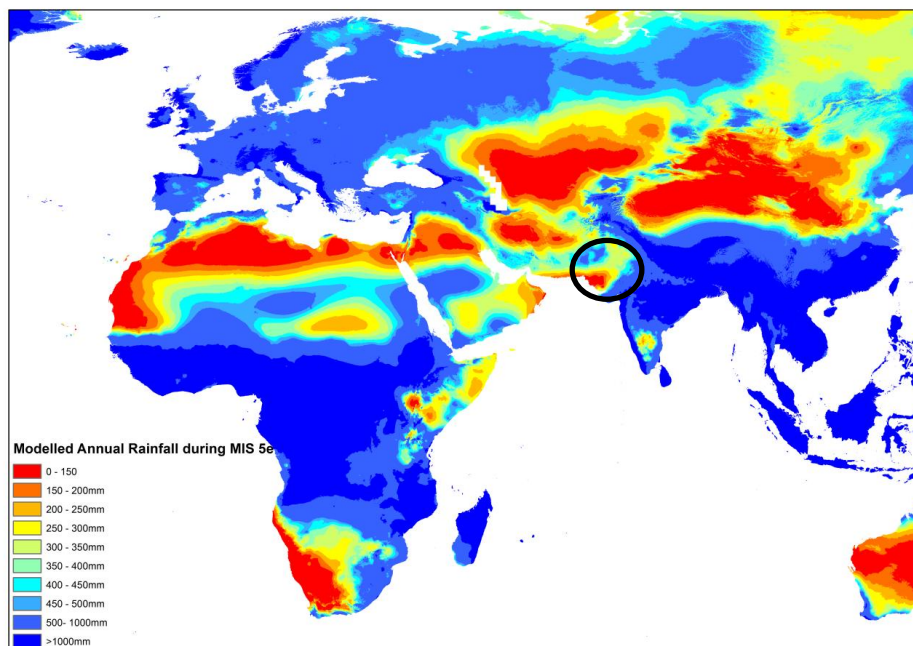
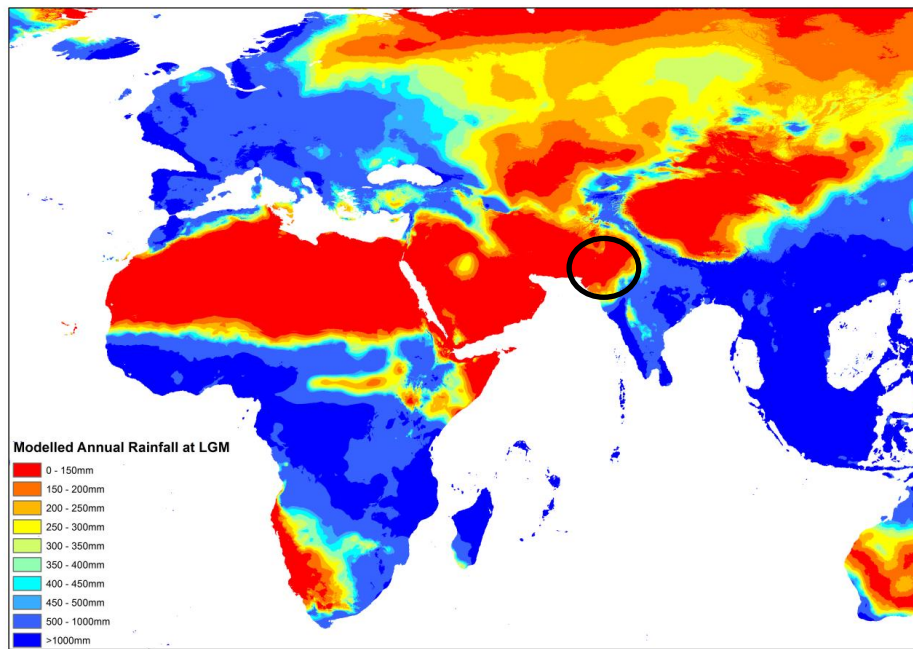


Figure 1.2: Maps indicating modelled annual rainfall: a) during the Last Glacial Maximum (LGM) with the Thar Desert (circled) experiencing hyper-aridity (<150mm rainfall/year) (above; following Braconnot et al. 2007); and b) during peak humidity of the last interglacial (Marine Isotope Stage 5e) (below; following Otto-Bliesner et al. 2006), with the Thar Desert (circled) typically experiencing sub-arid to sub-humid conditions (150-500+mm/ rainfall/yr).

Major changes in hominin demography have occurred in southern Asia during the Pleistocene, and much debate regarding these changes is framed by the over-arching concept of dispersals 'Out of Africa'. As African and Eurasian share only a narrow land-bridge, the Sinai Peninsula, comparing and contrasting archaeological, fossil and genetic evidence for hominin populations in these two landmasses has been a key feature of palaeoanthropological research. However, the binary opposition of Africa and Eurasia poorly reflects the environmental diversity of both regions as well as the similarities that occur between them. Dennell and Roebroeks (2005) propose 'Savannahstan' as a useful spatial unit for discussing Lower Pleistocene hominin demography and dispersals, focusing upon environmental similarities in grassland habitats that stretch from West Africa to North China, which includes the Thar Desert. As a major biogeographic transition occurs at the Thar Desert, research in this region may be critical to understand early expansions of hominins within these grassland habitats, and their capacity to colonise the monsoonal landscape of the east.

The Thar Desert is also a key location to investigate the dispersal of *Homo sapiens* from Africa into South Asia, which is currently a hotly debated topic due to recent research undertaken in South Asia (see Appenzeller 2012) with two distinct models that can currently be identified. One model for the modern human dispersal into South Asia suggests that a single dispersal of modern humans from Africa occurred ca. 60ka following a southern coastal route, and these populations produced lithic artefacts analogous to the Howieson's Poort industries of southern and eastern Africa (referred to as Late Palaeolithic in South Asia)(e.g. Mellars 2006a). An alternative model suggests multiple dispersals of *Homo sapiens* from Africa may have occurred, with modern humans arriving in South Asia between 130-70ka, potentially using continental routes, and these populations produced lithic industries analogous to Middle Stone Age assemblages (referred to as Middle Palaeolithic in South Asia) (e.g. Petraglia et al. 2010). The Thar Desert offers both coastal and continental routes for dispersal and preserves a

rich suite of sedimentary contexts spanning the Upper Pleistocene. As a result, archaeological research in this region is crucial to compare and contrast these alternate hypotheses.

Significantly, the Thar Desert is the eastern extent of the mid-latitude arid belt, stretching to the Atlantic Sahara in the west, which is a current focus for research into the dispersals of modern humans. Environmental approaches are illustrating periods of enhanced humidity in these arid landscapes as potential periods for human occupation of, and dispersals through, the arid belt (e.g. Drake et al. 2011; Fleitmann et al. 2011). Archaeological appraisals of the Aterian industries of the Sahara are indicating notable technological variability in lithic assemblages that share specific characteristic artefact types, tanged points (Scerri 2012).

Recent research in Arabia is illustrating the antiquity of hominin occupations (e.g. Armitage et al. 2011) and lithic industries with similarities African Middle Stone Age assemblages, most evident in the Nubian Complex of Dhofar (Rose et al. 2011). New archaeological research in the Thar Desert will help to develop this growing body of evidence for hominin occupations of the mid-latitude arid belt, and offers the potential for comparisons throughout this region.

The present extent of the Thar Desert is ca. 300,000km², occurring predominately in the Indian states of Rajasthan and Gujarat, and the Pakistani states of Upper and Lower Sindh (Figure 1.3). The east and western margins of the Thar Desert are marked by major topographic boundaries, with the Iranian Plateau in the West and the Arravallis to the East. For the purpose of this thesis, the southern boundary of the Thar Desert in mainland Gujarat is the northern watershed of the Narmada Valley, which lacks evidence of sand dune activity. The northern boundary is defined by the state boundary of Rajasthan, extended into Upper Sindh at a similar



Figure 1.3: Map indicating the location of Rajasthan, Gujarat, and Upper and Lower Sindh.

latitude. Substantial Quaternary sedimentation has preserved evidence of palaeoenvironmental conditions in the Thar Desert, making it one of the best documented regions for the impact of Upper Pleistocene climatic change across southern Asia. These same sedimentary contexts also contain a rich and diverse record for the production of lithic artefacts by Palaeolithic hominin populations, with an archaeological research history stretching back to the 19th century. Despite a number of intensive episodes of archaeological survey the character of Palaeolithic occupations of the Thar Desert is poorly understood and integrating this region into wider discussion of southern Asian hominin demography is problematic. The objective of this thesis is to characterise the nature of Palaeolithic lithic industries within the Thar Desert, and situate them within a chronological and environmental framework.

Research Methodology

In order to characterise the Palaeolithic occupation of the Thar Desert, existing palaeoenvironmental and archaeological records are synthesised with the results of interdisciplinary fieldwork undertaken in Rajasthan. Comprehensive literature reviews are used to develop new insights into palaeoenvironmental change and patterns within the distribution of Palaeolithic archaeological sites and their associated lithic assemblages. Surface surveys have been conducted at numerous sites in Rajasthan targeting sedimentary formations that have documented palaeoenvironmental and geochronological contexts, but have not been subject to archaeological inspection. Excavations undertaken at Katoati (Nagaur District, Rajasthan) and resulting geoarchaeological analyses present significant new findings for the characterisation of Upper Pleistocene hominin occupations of the Thar Desert. A range of sedimentological, geochemical and chronological studies are undertaken on sediment samples from the excavation. Assemblages of lithic artefacts from both the excavated horizons at Katoati and survey sites from Rajasthan have been subject to detailed attribute analyses. This permits a descriptive and comparative approach to characterising variability within lithic assemblages from the Thar Desert that that can address temporal and spatial change. Ultimately, by combining archaeological evidence with palaeoenvironmental and chronological studies it is possible to characterise the Palaeolithic occupation of the Thar Desert. This thesis presents a key step in integrating this critical region into global debates in Palaeoanthropology.

Organisation of the Thesis

Chapter 2 sets out the background to the research problem. The development of Palaeolithic systematics in South Asia is discussed, as this sets out the rationale for research in the Thar Desert. A key difference in the theoretical objective of between the majority of studies in

South Asia during the 20th century and more recent research is identified. Specifically, the underlying objective of South Asia's Palaeolithic research history has typically been to define broad cultural entities, whereas recent research explicitly aims to explain variability within and between these entities. The key features of Palaeolithic industries in South Asia are then described. The history of Palaeolithic research in the Thar Desert is presented and discussed within the context of the development of South Asian Palaeolithic systematics.

Chapter 3 presents three research questions that will structure the characterisation of the Palaeolithic occupation of the Thar Desert and the methodologies that will be used to address them. The first question relates to the palaeoenvironmental setting of hominin occupations and is addressed in Chapter 4 through a synthesis of the pertinent literature. The second question is focused upon developing an understanding of lithic artefact typological variability in published data sets, which is addressed in Chapter 5. The third question targets the integration of archaeological and environmental evidence to address patterns of variability in newly recorded lithic assemblages, and is dealt with in Chapters 6, 7 and 8.

In Chapter 4, a concise synthesis of literature regarding the geology, modern ecology and palaeoenvironments of the Thar Desert is presented. The distribution of geological resources indicates significant variability in the availability and quality of raw materials for the production of lithic artefacts. The synthesis of a wide range of proxies, included dated sediment formations and geochemical studies, is undertaken to develop a framework of palaeoenvironmental change, principally focused upon the Upper Pleistocene. The reports of over 900 Palaeolithic sites in the Thar Desert have been compiled to investigate patterns in typological, temporal and spatial variability, which are presented in Chapter 5. This indicates a number of repeated differences between Lower, Middle and Late Palaeolithic sites in the Thar Desert. More detailed description of a small number of dated and excavated sites provides

some means to integrate these trends into a more secure chronological and environmental context.

The analysis of lithic assemblages sampled from surface sites in six targeted locations in Rajasthan are described in Chapter 6. This survey focused upon a range of dated sediment formations and ecologically important locations. The results of this study indicate a number of distinctive patterns in the organisation of lithic technology and have revealed the presence of numerous typologically distinctive lithic artefacts.

The results of geoarchaeological and lithic attribute analyses from the excavated site of Katoati are reported in Chapters 7 and 8 respectively. Chapter 7 sets out the background to the excavations undertaken at Katoati, and identifies the natural formation processes at the site. The results of sedimentological, geochemical and chronological studies are then situated within their landscape context. Chapter 8 presents typological and technological descriptions and bivariate analyses of artefact assemblages from Katoati. These indicate that the assemblages can broadly be characterised as Middle Palaeolithic, although the oldest assemblage could indicate a Late Acheulean occupation.

The results of the preceding five chapters are discussed in Chapter 9. The artefact assemblages from Katoati are situated within their landscape context and compared with other dated excavated assemblages from Didwana, ca. 50km away, and the survey sites from Rajasthan. These technologically orientated studies are used to contextualise the synthesised results from previous, typological studies and integrated within their palaeoenvironmental context to characterise the Palaeolithic occupation of the Thar Desert.

Chapter 2

Approaches to Palaeolithic Research in the Thar Desert

Our knowledge of the Palaeolithic archaeology of the Thar Desert is inherently structured by the history of research, the theoretical assumptions of previous scholars, the problems they have chosen to address and the evidence that they have gathered to do so. The influence of these factors is best understood when situated within the broader regional and intellectual context of Palaeolithic research in South Asia. This, in turn, should also be viewed in the context of global developments in archaeological method and theory. Significantly, the questions that have become an important focus for Palaeolithic archaeological research in South Asia in the 21st century entail theoretical assumptions that are significantly different from those under which most of the evidence has been developed.

This is particularly evident in two areas of Palaeolithic research. Firstly, much of the scholarship undertaken in South Asia has been influenced from early on by the typological approach most prominently associated with Bordes (e.g. 1961). As a result, *fossil directeurs* have played an important role in assigning assemblages to different cultural phases. More recent approaches to investigating lithic variability focus upon understanding how patterns of raw material availability and variability, reduction intensity and forager mobility patterns may structure the archaeological record. The assessment of assemblage variability across space and time may vary significantly with the application of these new approaches. This has ramifications for both how we designate a particular assemblage to a broader cultural phase and how we identify transitions between such phases.

The second major difference is that for much of the post-Independence history of Palaeolithic research, the concept of 'migrations' have been considered out-dated for explaining cultural variability (e.g. Misra 1962; 1989; 2001). Indeed, prior to the 1990's, the regional differentiation of Middle Pleistocene hominin groups into modern populations of *Homo sapiens* offered an acceptable explanation for cultural continuity. The connections between biological taxa and how they mobilise their capacity for cultural behaviours is a complicated problem. Clear evidence for the dispersal of hominins into South Asia has begun to lead researchers to investigate what, if any, changes in the archaeological record of the subcontinent may herald the arrival of our species. As a result, understanding the nature of transitions between different cultural periods has taken on a new level of significance.

In order to engage with the existing Palaeolithic evidence of the Thar Desert, it is necessary to understand the broad theoretical framework in which the data was gathered, both at a regional and local scale. The aim of this chapter is to illuminate the history and structure of Palaeolithic evidence in South Asia and how broader developments within the subcontinent have influenced Palaeolithic research in the Thar Desert. Firstly, the development of Palaeolithic systematics in South Asia is examined. Secondly, a brief synthesis of the state of Palaeolithic evidence from South Asia is presented. Thirdly, the history of Palaeolithic research in the Thar Desert is reviewed and a historical description of the available evidence for Palaeolithic archaeology of the Thar Desert is outlined.

Development of South Asian Palaeolithic Systematics

The much-reported discovery of an Acheulean handaxe at Pallavarum, near Chennai (Madras) in 1864, by Foote (1866), is the first time the presence of Palaeolithic artefacts in the

subcontinent was clearly acknowledged. This offered the earliest indication of the antiquity of hominin occupation of South Asia, a concern that has since dominated Palaeolithic research in the subcontinent (Chauhan 2009; Dennell 2009; Gaillard et al. 2010; Pappu et al. 2011). During the earliest phase of research, a simple dichotomy of Palaeolithic and Microlithic was regularly employed to differentiate between the distinctive range of artefacts occurring in starkly different geological contexts (e.g. Sankalia 1946). However, numerous discoveries of more varied lithic industries with clear stratigraphic relationships to one another have since led to the repeated revision of Palaeolithic terminology (Subbarao 1958; Misra 1962; Sankalia 1964; Agrawal & Ghosh 1973; Sankalia 1974; Rendell et al. 1989; James and Petraglia 2005). The history of these changes is intimately related to the development of Palaeolithic research in South Asia, illuminating the questions that archaeologists have considered significant, and the evidence they sought to answer them.

Pre-Independence Era

Prior to the independence and partition of India and Pakistan, a number of regional terminologies were developed to describe cultural variability that were more detailed than the simple split of Palaeolithic-Mesolithic. The first, proposed by Cammiade and Burkitt (1930), split lithic assemblages discovered in the Eastern Ghats into four series based upon typology and stratigraphy. These included an industry of handaxes made on quartzite (Series 1), flake tools and more neatly crafted handaxes (Series 2), slender blades and implements with blunted backs alongside other flake tools based on flinty material (Series 3), and industries in which microlithic pieces significantly outnumber other elements (Series 4).

Numerous similarities can be noticed with the industrial sequence reported by Todd (1939), who was working on the western coast near Mumbai. The stratified sequence reported from the site of Khandivli, from the bottom upwards, includes: (i) rough tools and flakes recalling

Clactonian industries; (ii) similar tools and fine Acheulean handaxes; (iii) cores, blades, scrapers, and small handaxes on flakes; (iv) a blade-burin industry; (v) a developed blade-burin industry; and (vi) a microlithic industry, seen on the modern land surface. Although the terminology employed by Todd (1939) was more descriptive of the specimens he encountered, the similarities between this system and Cammiade and Burkitt's (1930) is apparent.

In a starkly different geological context, the work of de Terra and Patterson (1939) in the Siwaliks of the Soan Valley, northern Pakistan, produced some significant differences to the broad scheme for cultural succession in the Indian peninsula. They labelled the Palaeolithic artefacts they encountered pre-, early and late Soan industries, situated within a scheme of geological evolution. Significantly, these industries lacked an Acheulean component, which had previously been an integral character of the earliest industries in South Asia (see Dennell & Rendell 1991). This led Movius (1949) to place these Punjabi assemblages with the eastern Asian industries that were considered technologically isolated from the Acheulean tradition, which was widely evident throughout much of western Eurasia and Africa.

In the pre-Independence period, comparing the sedimentary and archaeological sequences of South Asian Pleistocene deposits and their parallels with better known sequences in Europe was a key endeavour. Critically, in this nascent phase of research, deriving evidence for cultural variability from stratified contexts (such as at Khandivli) offered a powerful means to integrate these results into a relative palaeoenvironmental and chronological framework.

The Nevasian and African Systems (1950's & 1960's)

Further support for this diverse cultural sequence was not clearly identified until excavations were undertaken by Sankalia (1956) at Nevasa. These provided a distinct and stratified flake tool assemblage that he labelled Series II. This industry was younger than the Acheulean

assemblages (Series I) and older than Microlithic (Series III) industries at the site. Following this discovery, Sankalia encouraged his students to undertake regional studies to identify intermediate industries, both typologically and stratigraphically, between those dominated by bifaces and microliths (e.g. Banerjee 1957; Issac 1960). This work offered a clear intermediary step between Acheulean and Microlithic industries, showing broad parallels with other regions of the Old World more clearly.

Subbarao (1958) argued that a distinct blade, scraper and burin industry based upon prepared core techniques and making use of new raw materials had become apparent, and labelled it the Middle Stone Age. This terminology was already employed in Africa, although Subbarao (1958) makes clear that the similarities in terminology were not intended to draw direct parallels:

“Just at present, Indian sequences does [sic] not fit into any mould, European or African. Let us discover our own pattern by intensive stratigraphic studies of more localities, and rely less on typology” (Subbaro 1958: 39).

The adoption of the African-style terminology was formalised at the ‘*International Conference on Asian Archaeology*’ held in New Delhi in 1961. As a result biface-dominated industries were identified as Early Stone Age, those based around flake tools were named Middle Stone Age, and microlith-dominated industries were called the Late Stone Age.

A number of researchers were critical of this terminology. Most prominent is the criticism offered by Misra (1962) and later supported by Sankalia (Agrawal & Ghosh 1973). Misra’s argument against the usage of the Nevasian or African-style terminology was principally semantic. The argument put forward for the adoption of the European nomenclature was that it captured all the broad technological stages known for Palaeolithic cultural evolution (i.e.

Lower, Middle and Upper Palaeolithic and Mesolithic) (Misra 1962). Although the Indian cultural sequence was not considered a direct parallel with the European sequence, Misra (1962) identified similarities in these culture history trajectories. Both sequences illustrated the technological development from core-tool cultures to flake tool cultures through the refinement of flaking techniques (Misra 1962). Further refinement of flaking techniques led to the development in Europe, West Asia and North Africa of blade-based cultures followed by microlithic industries (Misra 1962). This suggested to Misra (1962) that an (as yet) unknown blade-focused Upper Palaeolithic was necessary to explain the development of widely evidenced microlithic industries of South Asia. However, until such evidence was to be found, the majority of researchers, including Misra (e.g. 1967), retained the African-style terminology.

The European System (1970's to early 2000's)

During the *International Symposium on Radiocarbon and Indian Archaeology*, held in 1972 at the Tata Institute of Fundamental Research (Bombay), further discussion on the basis and terminology of periodization was held. Numerous objections to the adoption of European terminology were made. The lack of blade and burin industries throughout the subcontinent that were typologically and stratigraphically distinct from the MSA, widely reported to contain blades and burins (e.g. Sankalia 1964) was considered problematic (Agrawal & Ghosh 1973). Parallels with the European Upper Palaeolithic were seen as inappropriate as the term related not only to blade-focused lithic production, but also to a wide range of other typologically distinct artefacts, the use of organic materials and the production of art and ornamentation (Agrawal & Ghosh 1973). However, the usefulness of the European terminology for understanding Palaeolithic *development* was strongly put forward by Sankalia:

"These are now generalised terms denoting particular stages in the changing process of human civilisation" (Agrawal & Ghosh 1973:505).

Similarly, Misra argued that the development of Bordesian schemes of typological lithic variability would be a productive means to describe Palaeolithic assemblages in South Asia and ultimately illuminate the presence of Upper Palaeolithic industries (Agrawal & Ghosh 1973).

Unlike the 1961 meeting in Delhi, no consensus was reached over use of terminology. However the adoption of the European nomenclature in the second edition of Sankalia's *Prehistory and Protohistory of India and Pakistan* (1974), was highly influential. Throughout the 1970's numerous studies were undertaken that identified Upper Palaeolithic assemblages, notably the excavations undertaken by Murty (1974) in Kurnool District and by Wakankar (1973) and Misra (1978) at Bhimbetka. Significantly, at the latter site the Upper Palaeolithic horizons were part of a cultural sequence including Late Acheulean, Middle Palaeolithic and Mesolithic industries. Palaeolithic research in Pakistan was also undertaken for the first time since the pioneering research by de Terra and Patterson, and finds reported by both Khan (1979) and Allchin et al. (1978) adopted the European terminology readily.

Continued support for using the European terminology was found in the 1980's with excavations at sites such as Inamgoan (Badam 1977), Patne (Sali 1989) and 16R Dune (Misra & Rajaguru 1986). However, renewed research undertaken in northern Pakistan rejected both the local scheme developed by de Terra and Patterson (1939) and the European terminology, describing a suite of new discoveries as Early and Late Palaeolithic (Rendell et al. 1989).

The identification of South Asian Palaeolithic hominins

Prior to 1986, a century of research in South Asia had been undertaken without identifying which hominins were responsible for creating the Palaeolithic material culture that had been the focus of archaeological research. Indeed, the prevailing theory for modern human origins

had been one of the regional development of hominins into the contemporary populations of *Homo sapiens*, supported by the apparent gradual development of cultural assemblages (e.g. Clark 1977). This changed with the discovery of the only *pre-Homo sapiens* fossil known from South Asia, a calvarium discovered in gravels at the site of Hathnora in the Narmada Valley, associated with Late Acheulean artefacts (Sonakia 1985). This occurred at a time when the multiregional evolution of humans was coming under sustained scrutiny by researchers proposing a recent African origin for all modern humans (Mellars & Stringer 1989). The taxonomic identify of the Hathnora specimen has been a matter of some debate, and it is currently described simply as mid-Pleistocene *Homo* (Artheya 2007). This offers a glimpse of the earlier occupants of South Asia and the probable author of Late Acheulean industries (Haslam et al. 2011).

Burials of *Homo sapiens* in association with microlithic industries securely dated to the Upper Pleistocene in Sri Lanka retain a central place in modern discussions of the period. The discoveries at Fa Hien cave and Batadomba Lena (Deriyanagala 1992), dating to 31ka and 28ka respectively, remain the earliest evidence for the appearance of modern humans within South Asia. Until this point, there had been an implicit assumption that modern humans were responsible for the production of Upper Palaeolithic industries, and the development of microlithic technologies were a response to the environmental changes of the terminal Pleistocene and early Holocene (e.g. Misra 1989). Indeed, within India there was little new forthcoming evidence throughout the 1990's to change this status quo (e.g. Misra 2001).

The African origins of modern South Asians, albeit with some evidence for interbreeding with Eurasian hominins (Green et al. 2010; Reich et al. 2011), is currently overwhelmingly supported by genetic evidence (e.g. Kivisild et al. 1999; 2003; Macaulay et al. 2005), and to a lesser extent by fossil specimens. The ramifications of this are that, at some point, the hominin population

represented by the Hathnora specimen have disappeared, and modern humans dispersed into the subcontinent from Africa. Identifying such a change presents one of the largest challenges to interpreting the Palaeolithic record of South Asia. Beyond the theoretical and methodological issues associated with identifying the arrival of a new hominin by its cultural repertoire alone, this is problematic as it involves identifying a break in the cultural record of the subcontinent where previously continuity had been stressed. As a result, in the last decade there has been a radical shift in some of the fundamental assumptions that have underlain the study of Palaeolithic assemblages in South Asia.

21st Century Approaches

Due to the recent focus upon modern human dispersals, the use of the term 'Upper Palaeolithic' has once more come under scrutiny. The South Asian Upper Palaeolithic shares little in common with its European counterpart, which may itself be a highly regionalised phenomenon, rather than the cultural or technological universal that Misra (1962) argued for. Recently the appearance of microlithic technologies within numerous 'Upper Palaeolithic' industries (James & Petraglia 2005; James 2011) has been emphasised. This indicates that no simple separation between 'Upper Palaeolithic' and Mesolithic industries can be made on purely typological grounds. As Misra (1962) argued that chronological terms were unsuitable for referring to cultural assemblages, it would appear that the term Upper Palaeolithic may have run its course.

The rejection of the term Upper Palaeolithic is further supported by recent excavations in the Jurreru Valley, southern India, where, for the first time, a microlithic industry of comparable age to the Sri Lankan sites of Fa Hien and Batadomba Lena has been excavated. At the site of Jwalapuram 9, a deep and continuous microlithic sequence has been excavated, dating the emergence of microlithic technologies to 35ka (Clarkson et al. 2009). Significantly, the regional

development of microlithic industries from preceding Middle Palaeolithic assemblages have been established in the Jurreu Valley where Middle Palaeolithic assemblages are dated between 78-38ka (Clarkson et al. 2012). This is supported by a recent reappraisal of the lithic industry at Patne, where the gradual development of Middle Palaeolithic industries in those dominated by the production of geometric microliths by 25ka, originally labelled Upper Palaeolithic (Sali 1989; James 2011). In neither case is there a distinct, intermediate lithic industry between the Middle Palaeolithic and Microlithic, although further work in a range of geographic settings is required to validate this trend.

The term Late Palaeolithic has been proposed to encompass the diverse range of industries that are seen within South Asia after ca. 35-30ka (Rendell et al. 1987; James & Petraglia 2005) and apparently derive from preceding Middle Palaeolithic assemblages (James & Petraglia 2005). The basis of the division between Late Palaeolithic and Mesolithic is mostly chronological, rather than purely cultural, something that Misra (1962) had argued against. Unfortunately, we currently lack sufficient well dated and analysed assemblages to identify whether clear patterns of variation exist between microlith-dominated assemblages between the Terminal Pleistocene and Early Holocene, to truly warrant the use of the term. However, microlithic industries from excavated Early Holocene contexts are typically considered more highly standardised than their Pleistocene counterparts.

Discussion

A summary of changing terminology for the South Asian Palaeolithic is presented in Table 2.1. The major changes to Palaeolithic systematics in South Asia during the 20th Century have involved the insertion of new terms to describe what have been considered typologically intermediary industries within a culture history framework. The adoption of the Middle Stone Age acknowledged a distinct step between Acheulean and microlithic industries. The use of the

term Upper Palaeolithic was deployed to describe the blade focused technologies deemed necessary for progression from the flake based industries of the Middle Palaeolithic to the microlithic industries of the Mesolithic period.

A significant challenge presented by this is that our understanding of what each cultural phase consists has been based upon a few excavated and stratified assemblages. These have subsequently been supported by surface discoveries that may well be palimpsests, and have often focused upon certain key artefacts types at the expense of understanding the full range of assemblage variability. As a result, the broad periodisations of the South Asian Palaeolithic are largely self-affirming entities, monolithic in character and impervious to change. Assessing what constitutes these broad cultural groups, whether they do reflect clear and distinct technological strategies, and how they vary have remained open questions.

Broad critiques of previous approaches are apparent in the shifting priorities of South Asian Palaeolithic research in the 21st Century. The typological basis of the major cultural units of analysis is questionable, and may not stand up to sustained scrutiny (e.g. James & Petraglia 2005; 2009). Underlying this is a global shift in the theoretical basis and objectives of lithic analysis, moving away from the style-function debates rooted in ideas of finished artefact forms that dominated the mid-20th century toward various explanations of the continuum of variability in lithic artefact form (see Bradbury & Carr 2011; Sorressi & Geneste 2011).

Furthermore, implicit in the culture history framework of analysis is a sense of gradual progressivism - that behavioural change and the refinement of lithic production techniques were an inevitable consequence of the period over which these cultures developed.

Period	Terminological System	Cultural Phases	Description	References
19 th Century- mid 20 th Century	'Foote's system'	Palaeolithic	'Madrasian' handaxes	Sankalia 1946; Foote 1866
		Microlithic	Microliths	
1930's-1940's	'Burkit's system'	Series I	Handaxes	Cammiade & Burkit 1930
		Series II	Flake tools and refined handaxes	
		Series III	Long slender blades & backed implements	
		Series IV	Microlithic	
1950's	Nevasian	Series I	Handaxes	Sankalia 1956
		Series II	Prepared cores, scrapers, points	
		Series III	Microliths	
1960's	African	Early Stone Age	Bifaces and crude cores	Subbarao 1958; Sankalia 1962
		Middle Stone Age	Prepared core technologies; scrapers, burins, points and blades	
		Late Stone Age	Microliths	
1970's-early 2000's	European	Lower Palaeolithic	Bifaces with prepared core and flake tool component	Misra 1962; Sankalia 1974;
		Middle Palaeolithic	Prepared cores, scrapers, blades, points & diminutive handaxes	
		Upper Palaeolithic	Blade focused industries	
		Mesolithic	Microlithic technologies	
Mid 2000's to present	South Asian	Lower Palaeolithic	Bifaces with prepared core and flake tool component	James & Petraglia 2005
		Middle Palaeolithic	Prepared cores, scrapers, points, blades and diminutive handaxes	
		Late Palaeolithic	Mosaic of Late Pleistocene flake, blade and microlith focused industries	
		Mesolithic	Holocene blade and microlith focused industries	

Table 2.1: Summary of recognised Palaeolithic cultural phases throughout South Asian research history.

The orientation of Palaeolithic research in South Asia has seen some significant changes, particularly in the last decade. Where once the goal for many archaeologists was to establish the presence of typologically distinct intermediate cultural entities between existing

categories, there is a growing focus upon explaining the changes between them. The current concern with hominin dispersals has focused attention on the transitions between the major culture history phases as potentially relating to substantial biological changes. Although the dispersal of *Homo sapiens* from Africa into South Asia is broadly attested, many simpler explanations for change within lithic assemblages must be explored before we can attribute them to such high order explanations as the arrival of a new species. Both inter- and intra-assemblage variability need to be explored with respect to more prosaic explanations than either gross cultural stability or biological overhaul. Such assessments can be facilitated by a suite of recent approaches to understanding the factors that drive both innovation and diversity in lithic assemblages (see Chapter 3). However, to integrate the more detailed evidence of Palaeolithic variability from the Thar Desert into its regional context, it is necessary to provide an overview of the archaeological evidence of the major cultural phases of the Palaeolithic in South Asia, however problematic these designations may be.

Overview of Palaeolithic South Asia

The choice of terminology with which to describe the Palaeolithic industries in South Asia is problematic. This is due to the history of use, the underlying assumptions and patterns of continuity between the terms that leave no clear means to divide them. Nevertheless, broad patterns in cultural variability are regularly reported in the South Asian archaeological record, relating to the prominence of bifacial tools, prepared core technologies, and the reliance on blades or microliths. Here, I will employ the terms Lower, Middle and Late Palaeolithic to structure these three groups of assemblages. Although a critical analysis may show that the validity of these terms does not hold, it should also highlight new areas of research that may lead to more productive means of describing Palaeolithic variability.

The Lower Palaeolithic

The Lower Palaeolithic in South Asia is characterised by the presence of heavy tools, particularly Acheulean handaxes, with the exception of northern Pakistan. Until recently, evidence for hominin occupation of South Asia >1ma has been equivocal (e.g. Chauhan 2010; Gaillard et al. 2010a; 2010b). Given the occupation of Southwest and South-East Asia at this time, the lack of evidence for a hominin occupation has appeared anomalous (Dennell 2009). Recent evidence from the site of Attirampakam, southern India, has demonstrated Acheulean artefacts in primary context securely dating to between 1.07-1.9ma, based on palaeomagnetic dating (Pappu et al. 2011). This lends significant support to proponents of a long chronology for the occupation of South Asia (e.g. Dennell 2009), and requires a critical review of numerous elements of industrial change. For example, an examination of whether typological refinement increases in younger sites (Petraglia et al. 1998), and whether the development of prepared core technologies was a local development or relates to a possible hominin dispersal (Foley & Lahr 1997; James & Petraglia 2009).

Although the upper age limit for the Lower Palaeolithic of South Asia has tended to see considerably more debate, the lower age limit has also been poorly defined. This is due both to difficulties in attributing assemblages to either Late Acheulean or early Middle Palaeolithic industries, and the paucity of directly dated assemblages. Recently, two Late Acheulean sites in the Son Valley, Bamburi and Patpara, have yielded an industry that is technologically distinct from the succeeding Middle Palaeolithic, despite some typological continuity, which is robustly dated to the MIS 6-5 boundary (Haslam et al. 2011).

The dominant material used for Lower Palaeolithic industries is quartzite. Other raw materials that occur in suitably large exposures have also been used, included various volcanic materials, such as dolerites, basalts and granites, and sedimentary materials, principally sandstones.

Beyond the production of large cutting tools and simple flakes, the use of prepared core technologies is evident, e.g. Isampur (Petraglia & Paddaya 2005), but variable in Lower Palaeolithic contexts. It is typically reported as a more important assemblage component and executed with more control within Late Acheulean industries (Chauhan 2009). Similarly, blade production also occurs within the Lower Palaeolithic, e.g. Bhimbetka (Misra 1982), although incidence rates are comparatively low and there is no evidence to suggest this was a formalised pursuit.

Lower Palaeolithic sites occur principally in the major river basins of central and peninsular India and the foothills of the Himalaya, and are notably lacking in the Ganges valley and north-west India. This may in part be explained by site visibility, but factors such as ecological and raw material constraints cannot be ruled out. The number of Late Acheulean sites, found principally in later Middle Pleistocene contexts, appear more numerous than their Early Acheulean counterparts. Korisettar (2007) has suggested that a number of 'purana' basins offered a core area for Lower Palaeolithic populations. The nature of the geological and geographical position of these basins is likely to have offered suitable raw material resources and stable resource structures, even in the face of palaeoclimatic changes.

The Middle Palaeolithic

Middle Palaeolithic industries in South Asia are focused upon the production of flakes from prepared cores, although separating them from Late Acheulean assemblages on either technological or chronological grounds remains problematic. Middle Palaeolithic assemblages can be securely dated from 78-38ka (Petraglia et al. 2009). The most securely dated Middle Palaeolithic assemblages occur in the Jurreru Valley, where they are found in both primary and secondary contexts underlying the 74ka Toba tephra horizon, and in sediments overlying this ash horizon dating to ca. 50ka and 38ka (Petraglia et al. 2007; 2009; Clarkson et al. 2011). The

Middle Palaeolithic horizons from 16R Dune may indicate the chronology of these industries extends into the early periods of MIS 5 ca. 120ka, although the sample size is small (Raghaven et al. 1989; Singhvi et al. 2010).

With regards to lithic technology, the reduction in size in both flake cores and resulting flakes from the preceding period is broadly evident (James & Petraglia 2005). This may be partly due to a wider change in lithic reduction behaviour, i.e. a focus on finer raw materials. Although use of materials like quartzite continues, the proportion of artefacts made on finer silicious materials, such as chalcedony, quartz, jasper and chert increases dramatically amongst Middle Palaeolithic assemblages (James & Petraglia 2005).

A concomitant factor of the use of finer raw materials is the diversification of their source. Many finer raw materials are available as smaller clasts, such as cobbles and pebbles in river gravels, which are apparent in a broader range of landscape settings than major rock outcrops. Therefore, the capacity to exploit a broader range of smaller, finer raw material types appears to have facilitated the more widespread occupation of the subcontinent by Middle Palaeolithic populations. This is evident in the Middle Palaeolithic occupation of regions such as the central Thar Desert and the Ganges Valley. This may suggest that Middle Palaeolithic populations were able to adapt to more diverse ecological settings with different resource structures than in the Lower Palaeolithic, which could also facilitate more intensive occupation of the subcontinent.

A recent study (James 2011), comparing the proportion of artefacts from 153 surface and excavated contexts from across South Asia provides the clearest and most up to date synthesis of variability amongst lithic assemblages reported as Middle Palaeolithic. Amongst this sample of assemblages, core technology can be characterised as: 63% have unclassified core types, 60% have unprepared cores, 32% have discoidal cores, 24% have Levallois cores, 24% have

blade cores, 17% have prepared cores and 8% have flake-blade cores (James 2011). No strongly regional patterns in core reduction technologies are apparent, although variation in the level of detail provided by different researchers has been highlighted as a potential cause. Core tools are reported as a fairly regular occurrence in Middle Palaeolithic assemblages, including core scrapers (26%), chopping tools (22%), choppers (19%) and cleavers (16%) (James 2011).

Establishing patterns of variability in flake blanks also presents problems due to variable reporting of un-retouched flakes. However, two categories of flake blank that do appear to be well reported are blades, which occur in 51% of the sites, and Levallois flakes, occurring in 34% of the sites (James 2011). These values are notably higher, particularly for blades, than the proportion of either core type reported, which further highlights the inconsistency in reporting both cores and flakes. Blades are a dominant component of many assemblages in the regions considered, with the exception of the far south of the peninsula (James 2011). Microliths are reported in two Middle Palaeolithic sites (1.3%).

Retouched flakes are generally well reported amongst most of these assemblages, and also exhibit some notable regional variations. Scrapers are ubiquitous, occurring in 96% of all assemblages, and often in relatively high proportions (10-20%) (James 2011). Borers follow as next most common (45%), with points (38%), handaxes (35%) and burins (27%) also fairly regular occurrences, although these four artefact types occur in relatively low numbers in the assemblages in which they occur (~5%) (James 2011). Backed artefacts are apparent in 11% of the sites, once more in low frequency when present (James 2011). In terms of regional variability, burins were reported in highest frequency from the Thar Desert and Pakistan, but are poorly represented elsewhere. Points dominate the Krishna and Penner River regions, and south of the Narmada a package of scrapers, points and borers is commonly reported. The greatest variety amongst retouched tool types is apparent in the far south of the peninsula.

The Late Palaeolithic

The earliest sites that fall within the Late Palaeolithic are the microlithic sites of Sri Lanka, now dating to 38ka (Perera 2011), and Jwalapuram 9, dating to 35ka (Clarkson et al. 2009). A potentially earlier site that straddles the definitions offered here is Site 55 (Riwat) in Pakistan, an assemblage with a blade component, but described by the excavators as either late Early Palaeolithic or early Late Palaeolithic (Rendell et al. 1989; Dennell et al. 1992). Dating change within this period is somewhat problematic, as many dates available for Late Palaeolithic assemblages were produced over 20 years ago, using traditional radiocarbon methods, bulk samples, and outdated calibration curves. This is equally pertinent to many dated Mesolithic sites that may fall within the Terminal Pleistocene if re-dated using AMS techniques and advanced pre-treatment chemistries.

A number of trends seen within the Middle Palaeolithic become accentuated in the Late Palaeolithic. Raw material usage is dominated by silicious materials, artefacts show evidence of more intensive reduction sequences and overall artefact sizes decrease. True 'Upper Palaeolithic' industries have been considered rare and geographically restricted due to the severe aridity of the LGM (e.g. Misra 1989; 2001). However, when combined with evidence for aceramic microlithic sites there is a dramatic change in the number of sites and their spread across the subcontinent, becoming virtually ubiquitous. Even though this assessment is likely to include some Early Holocene material, the shorter timespan in which these industries have occurred compared to the preceding Middle Palaeolithic emphasises the increased intensity of occupation of the subcontinent after 35ka (Petraglia et al 2009b).

Blade production within these industries is both ubiquitous and dominant. James' (2011) analysis of 563 assemblages indicates that blades are found throughout the subcontinent in 90% of assemblages and contributing substantially to assemblage proportions, up to 20% at

some sites. However, within the data set used by James (2011) there seems to be a strong bias to record the presence and proportion of blades more than to investigate the other reduction strategies employed, leading to only 7% of sites reporting unprepared flakes, despite 56% yielding unprepared cores. Levallois core technologies are virtually absent, occurring in 1% of the sites, although Levallois flakes are more common, occurring in 4% of sites, sometimes comprising >20% of the assemblage. Scrapers remain the dominant form of retouched flakes, occurring within 87% of the assemblages, a slight drop from the Middle Palaeolithic. Other widespread retouched types include microliths (63%), points (53%), burins (44%) and borers (35%). Backed artefacts occur within 19% of the assemblages, though frequently in low numbers.

With regards to spatial variability, Sri Lanka is notable as despite the dominance of blades and microliths, unprepared and discoidal cores are the major core component (James 2011). This highlights the fact that a heavy reliance on blades may not necessitate the production of typical, prismatic blade cores. The presence of assemblages with high numbers of blades, burins and Levallois flakes and cores in Pakistan sets them apart from the rest of mainland South Asia, where microliths and scrapers dominate (James 2011).

A number of other forms of material culture enter the archaeological record during the Late Palaeolithic, including ornaments, human burials, structures and the use of ochres (James & Petraglia 2005; Blinkhorn 2008). These occur in limited numbers, and appear widely distributed in both time and space, lacking any coherent burst of symbolic activity that is suggested to represent modern human behaviour (e.g. Klein 1995; 2000) and the incursion of *Homo sapiens* into South Asia (Mellars 2006).

Summary

This broad scheme for cultural changes throughout South Asia (Table 2.2) provides the backdrop into which a more detailed assessment of variability within the Thar Desert will be set in Chapter 9. Interestingly, within each major period the Thar Desert appears to occupy a significant typological boundary. The relative dearth of Lower Palaeolithic sites in the central Thar presents a major geographic gap between the Soanian traditions of north-western Pakistan and the Acheulean/Madrasian traditions of peninsular India.

	Lower Palaeolithic	Middle Palaeolithic	Late Palaeolithic
Chronology	>1.07ma-ca.130ka	78-38ka	38ka onwards
Settlement Pattern	Major river valleys of central and peninsular India and Siwaliks	More numerous sites throughout subcontinent including Thar Desert, Ganges Valley and Konkan Coast	Ubiquitous and in denser concentration than Middle Palaeolithic
Raw Materials	Predominately quartzites and volcanic materials where available in large package sizes	Continued exploitation of quartzites and volcanic materials, exploitation of small package size silicious materials (e.g. chert, chalcedony, jasper, quartz)	Predominately silicious materials (e.g. chert, chalcedony, jasper, quartz), continued exploitation of quartzites and volcanic materials
Technology	Acheulean industries dominated by LCT production with decrease in LCT size and increased presence of prepared core technologies in Late Acheulean; flake tools include scrapers and flake blanks include blades in very low numbers; Soanian industries comprise core tool and flake industry but lack Acheulean bifaces	Prepared core technologies predominate, including Levallois, discoidal, multi- and uni-directional cores; scrapers are ubiquitous with points, burins and borers common; blades occur in numerous assemblages in moderate numbers; small bifaces and choppers a regular occurrence	Blade and microlithic cores dominant, although Levallois, discoidal and flake cores persist; blades and microliths dominate assemblages, with scrapers and points common retouched forms.
Regional Variation	Major split between Soanian (northern Pakistan) and Acheulean/Madrasian (India)	Variation in retouched tool assemblages particularly between NW India and Pakistan, central India and southern India	Variation observed primarily between Sri Lanka and India in proportion of retouched pieces, and India and Pakistan in presence of burins and scrapers in latter.

Table 2.2: Summary of broad cultural periodization in South Asian Palaeolithic.

During the Middle Palaeolithic, James (2011) identified the (eastern) Thar region showing similarities with Pakistan and subtle differences with the rest of South Asia, whereas during the Late Palaeolithic the (eastern) Thar region showed greater affinities with peninsular India in contrast to Pakistan. Clearly, a more detailed understanding of the Late Pleistocene archaeology of the Thar Desert, as set out in this thesis, offers the means to investigate the validity of these differences and a more nuanced attempt to explain them.

History of Palaeolithic research in Thar Desert

The history of Palaeolithic research in the Thar Desert shares a number of parallels with the scheme outlined above for the subcontinent as a whole. Indeed, a number of discoveries in the Thar region have played a significant role for the development of research throughout the subcontinent. The following section will outline the history of Palaeolithic research in the Thar Desert; a comprehensive synthesis of the Palaeolithic archaeological evidence from the region is presented in Chapter 5. The concerns of the earliest Western explorers in the Thar Desert were principally geographical and geological. These were particularly focused upon understanding the configuration of drainage networks and nature of the 'sandhills' (Allchin et al. 1978). Explorations by various members of the Geological Survey of India (GSI) during the second half of the 19th century were more organised than previous efforts. These identified sand dunes that frequently bore the scars of erosion through the action of water (Blanford 1877), suggesting more humid environmental conditions at some point in the past. Further comments upon environmental change were made by Heron and La Touche, who suggested that the rarity of 'Stone Age' implements in the region was due to aridity (La Touche 1910).

Pre-Independence

The earliest collections of Palaeolithic artefacts in the Thar were made near Sukkur, Sindh, first by Dickinson in 1867, then by Burgess in 1886 (Biagi 1997). In Rajasthan, a few quartzite blades were reported by A.C. Carlleyle, working for the Archaeological Survey of India (ASI) (Allchin et al. 1978). Acheulean implements were reported by Hackett, working for the GSI, both in the region of Jaipur during the 1870's (Allchin et al. 1978). During his appointment as State Geologist in the service of the Maharaja of Baroda, R. Bruce Foote was the first to collect Palaeolithic artefacts from the Thar region and to record their stratigraphic position (1898). Foote's work in the Sabarmati and Orsang valleys of Gujarat were to be the only Palaeolithic discoveries reported for 40 years. During the early 20th Century, the ASI began their investigations of the Indus Civilisation sites, such as Mohenjo Daro and Harappa, which dominated research interests amongst archaeologists in this region.

In their seminal work on the Pleistocene and Palaeolithic deposits of the Siwaliks, de Terra and Patterson (1939) also reported evidence from the Rohri Hills, Sindh. They noted archaeological artefacts matching the Early and Late assemblages known from the Soan Valley (see Rendell et al. 1989 for further discussion). Significant steps forward in the sphere of Palaeolithic exploration in the Thar were made following Independence, beginning with the publication of Sankalia's *Investigations into the Prehistoric Archaeology of Gujarat* (1946), revisiting the archaeological sites identified by Foote. This work was rapidly followed by Zeuner's volume *Stone Age and Pleistocene Chronology in Gujarat* (1950) in which he integrated a chrono-stratigraphic sequence for the appearance of Palaeolithic, microlithic and Iron Age artefacts with palaeoclimatic interpretations.

The Nevasian and African Style Systems (1950's & 1960's)

Investigations into Stone Age sites were continued by Subbarao (1958), although with a focus on the younger, microlithic sites occurring upon sand-dunes. Throughout the 1960's a steady stream of Palaeolithic discoveries in Gujarat were reported principally using the African-style terminology by teams from the Western Circle of the ASI, Maharaja Sayajirao University, Baroda and the Deccan College, Pune. These studies were partly focused upon identifying Harappan sites, an important endeavour in post-partition India as the major urban centres of the Indus Civilisation were now located west of the border with Pakistan. As a result, the majority of sites that were located in this period were microlithic, occurring in similar geomorphological contexts to Harppan sites.

The Palaeolithic archaeology of Rajasthan was virtually unknown prior to the pioneering work of V.N. Misra, who undertook a series of surveys both in the Thar Desert (Misra 1961; 1963; 1968) and the river valleys to the east of the Aravallis (Misra 1967). Instigated by his Ph.D. supervisor, H.D. Sankalia, his aim was to identify Palaeolithic occurrences in hitherto unexplored regions. Misra's explorations in the Luni Valley led to the discovery of numerous sites which were first labelled Series II, and subsequently MSA (although not without protest). The sites occurred within significantly different geological contexts to those known in peninsular India or the Siwaliks. This region lacked both the general river terrace sequences that had proved vital to establishing relative Pleistocene chronologies elsewhere, or the presence of Lower Palaeolithic artefacts. Misra (1963) suggested a mid-late Pleistocene chronology for this industry, but called for more detailed geological work to establish the sequence of Pleistocene deposition.

The discovery of the site of Baridhani, reported by Mohpatra et al. (1963), was significant for its location within the modern arid zone of western Rajasthan. At a similar time, the

geomorphology and alluvial stratigraphy of southeast Baluchistan and southern Sindh and their related lithic industries were under investigation by Prof. A. R. Khan, University of Karachi, as reported in the popular press, although this work was not published until 1979.

The European System (1970's-1990's)

A series of six seasons of fieldwork undertaken by B. Allchin, an archaeologist, A. Goudie, a physical geographer, and K. Hedge, a geochemist, in the early 1970's remains the only research to have investigated Palaeolithic contexts in Rajasthan, Gujarat and Sindh. Their volume *Prehistory and Palaeogeography of the Great Indian Desert* (Allchin et al. 1978) is the only attempt to synthesise archaeological and palaeoenvironmental evidence from across the Thar Desert. A significant contribution made by this research team was the identification of Upper Palaeolithic assemblages in the Pushkar Valley in Rajasthan, Visadi in Gujarat, and the Rohri Hills in Sindh, supporting these assertions with a metric approach to typological variability in comparison to Middle Palaeolithic and microlithic assemblages. Following the work of Zeuner (1950) in Gujarat, Allchin et al. (1978) highlighted the repeated association between Middle and Upper Palaeolithic assemblages and weather resistant, pedogenised, ancient sand dunes within Gujarat and at numerous locations in Rajasthan. Due to the comprehensive nature of their study, they were able to argue for broad patterns of cultural continuity through time, punctuated with some regional discontinuities and variation resulting from different patterns of raw material acquisition and use. Ultimately, they associated the geographically restricted Lower Palaeolithic with the penultimate arid phase, attribute the Middle Palaeolithic to the last humid phase, permitting occupation within the arid core of the desert, and argued the development of Upper Palaeolithic industries offered a more versatile and mobile technological system to adapt to increasing aridity. Numerous methodological advances were made rapidly after the completion of this work, such as the application of chronometric dating

techniques and the excavation of archaeological assemblages, which remain poorly synthesized with other forms of evidence from surface sites from across the region.

Within the alluvial plains of Gujarat, a wealth of LSA/microlithic/Mesolithic sites continued to be identified throughout the 1970's, accompanied by relatively fewer, earlier sites. A couple of shallow excavations were conducted at the Mesolithic sites of Udrel (IAR 1970-71) and Maheswari Hill (IAR 1974-75), recovering microlithic implements stratified underneath later Prehistoric and Historic period material. However, within Saurashtra, more numerous Lower and Middle Palaeolithic sites were being identified in this period, particularly in the Bhadar Valley (Lele 1972) and Hiran Valley (Marathe 1981). Both studies focused upon understanding the Late Quaternary geology of the region, incorporating stratified archaeological discoveries within this framework. As a key feature of the Late Quaternary geology of the region, identifying the origin and timescale for the miliolite formations in Saurashtra has been an important focus of palaeoenvironmental research. The application of U-Th techniques to dating the miliolite deposits have help to situate Palaeolithic assemblages within a chronological context (Baskaran et al. 1986).

In 1978 V.N. Misra started an interdisciplinary project, entitled "Early man and his environment in north-west India with special reference to the Luni basin in Rajasthan", with a range of other scholars focusing upon archaeological, palaeoenvironmental, ethnobotanical, ethnoarchaeological and geomorphological studies in central and western Rajasthan. Widespread archaeological survey and palaeoenvironmental research was undertaken that resulted in new discoveries in previously unexplored regions of Rajasthan. Excavations undertaken within the vicinity of Didwana Lake, Nagaur District, as part of this study have had a significant impact on Palaeolithic archaeology throughout the subcontinent. In the late 1970's, excavations were undertaken at Jayal, Singi Talav and Indola-ki-Dhani that identified Lower Palaeolithic occurrences further into the Thar Desert than previous surface discoveries

(IAR 1979-80; 1980-1981; 1981-82). These assemblages were found principally within a massive clayey loam (Amarapura Formation) overlying a large boulder conglomerate (Jayal Formation) (Misra 1995). It was apparent that the Lower Palaeolithic occupation around Didwana occurred during an exceptionally humid phase thought to have occurred in the mid-Pleistocene. This was preceded by the presence of a huge and powerful river system in the early Pleistocene, whose drainage had been disrupted either by headwater capture or tectonic disturbance (Misra 1995). In order to relate the evidence from the excavations to the wider evidence from the region typically associated with more arid landforms, an excavation through a large sand dune, known as 16R Dune, was undertaken (Misra & Rajaguru 1986). This excavation remains one of very few sites in the subcontinent where excavators have reported a cultural sequence including Lower, Middle and Upper Palaeolithic and microlithic horizons, and the production of a series of Thermoluminescence, Uranium-Thorium series and radiocarbon dates offered the means to integrate the archaeological and palaeoenvironmental evidence from the site within a clear, chronometric framework (Misra & Rajaguru 1986; Raghavan et al. 1989).

During the late 1980's and early 1990's research undertaken by archaeologists at MSU Baroda, particularly Sonawane and Ajithprasad, resulted in a new phase of archaeological reconnaissance in the Orsang and Sukhi valleys, which included the identification of a range of Mesolithic, Middle and Lower Palaeolithic sites, some of which occurred in primary context and provided an index of the chronology of cultural deposits and the environment of their deposition. These researchers began excavations at a number of Mesolithic sites, namely Loteshwar, Jaidak II, Shaktari, Santhli, Ambakut and Datrana (IAR). Ajithprasad's work in the Sukhi Valley included a component of excavation, including 3 trenches at Jogpura, yielding Late Acheulean and transitional Middle Palaeolithic assemblages (IAR 1986-7). In the Orsang Valley, Ajithprasad has also reported Late Acheulean and transitional Middle Palaeolithic industries

from stratified contexts, which can now be associated with luminescence dates from more recent palaeoenvironmental study of the valley sediments (Ajithprasad 2005b; Juyal 2005).

More recent research on the Palaeolithic period in Gujarat has been limited.

Recent Approaches

Following another substantial lull in activity, research on the Palaeolithic period in Sindh has flourished following the instigation of the 'Joint Rohri Hills Project' in 1993, a collaboration between Pakistani and Italian researchers. This project has dominantly been survey work, focusing upon re-investigation of the Rohri Hills, studied previously by Allchin et al. (1978) and de Terra and Paterson (1939) before them. Due to the continued use of the Rohri Hills as a raw material source from the Lower Palaeolithic period to the present separating lithic industries and assemblages has not been facile. Such separation is based primarily upon typological concerns, facilitated to some extent by the shallow excavation of a Late Acheulean and two Late Palaeolithic sites (Biagi et al. 1996; Negrino & Kazi 1996, Biagi et al. 1998-2000). Further recent investigations have expanded beyond the Rohri Hills. Shaikh et al. (2002-2003) have undertaken extensive survey work in the Veesar Valley. Situated within the alluvial plains of the Indus, these sites are the first sites reported from the region that occur within a modern, desert context. Biagi's work in Lower Sindh has also involved re-evaluating the assemblages from Ongar, reported by Khan (1979) and Allchin et al. (1978), and undertaking new survey work in the area (Biagi 2007). Most recently, Biagi (2011) has undertaken survey at a series of Late (Upper) Palaeolithic site called Jhampir, Lower Sindh, including some shallow and undated excavation.

In Rajasthan, there has been minimal Palaeolithic research since the mid-1980's. A few discoveries have been reported in the western districts of Jaisalmer and Barmer, notably including Lower Palaeolithic occurrences (IAR 1999-2000). Palaeolithic artefacts were observed

by a team of palaeoenvironmental scientists within the vicinity of Sambhar Lake (Sinha et al. 2006), whereas two small assemblages of stratified and dated artefacts were recovered by a team investigating the mid-Luni valley (Mishra et al. 1999).

Discussion

A number of trends are apparent in this review of the history of Palaeolithic research in the Thar Desert. Firstly, Rajasthan, Gujarat and Sindh have been subject to very diverse research trajectories, illustrated by the number of Palaeolithic sites identified through time (Figure 2.1). Importantly, the Palaeolithic of the Thar Desert has only been brought together as a single analytical unit only for the comprehensive review offered by Allchin et al. (1978).

Archaeological research in Gujarat has led to a fairly constant stream of Palaeolithic discoveries through survey since the 1950's by a wide range of scholars with a diverse range of motives. The inclusion of stratigraphic studies in the 1970's and excavations, albeit sporadically, from the 1980's illustrate a more problem-oriented and interdisciplinary outlook to research. In contrast, Palaeolithic research in Rajasthan has been more punctuated, with clear spikes in activity in the late 1950's, the early 1970's and the late 1970's-early 1980's, but with clearer research objectives focused upon Palaeolithic questions. Until the 1990's, Palaeolithic research in Sindh can be described, at best, as sporadic, and as a result, much of the recent activity involves filling out blank areas through survey, an activity that has occurred much earlier elsewhere.

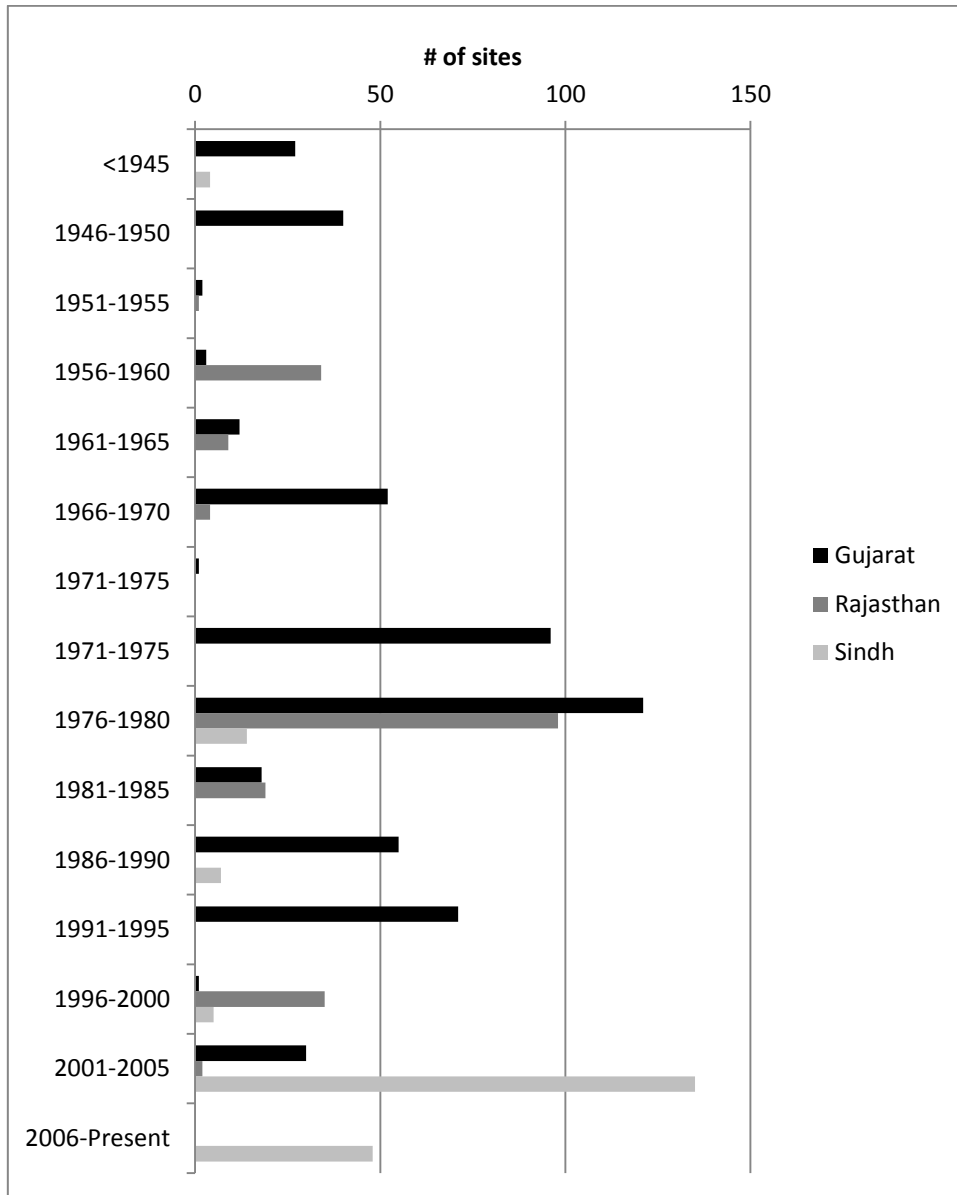


Figure 2.1: Bar chart of number of sites reported in Gujarat, Rajasthan and Sindh in five year periods.

Secondly, a broad range of terminology has been used to describe the Palaeolithic assemblages of the Thar Desert throughout its research history (see Figure 2.2). The changes in usage of terminology, broadly matching the pattern outlined for South Asia, present considerable issues for synthesising existing evidence and contributing new data to the Palaeolithic record of the Thar Desert. The use of terms of the African-style system, or those such as Series II, can largely be regarded an artefact of the development of Palaeolithic study

in South Asia. The contrast between the use of European terminology in India compared to the use of the pared down nomenclature in Pakistan proposed by Rendell et al. (1989) is more problematic.

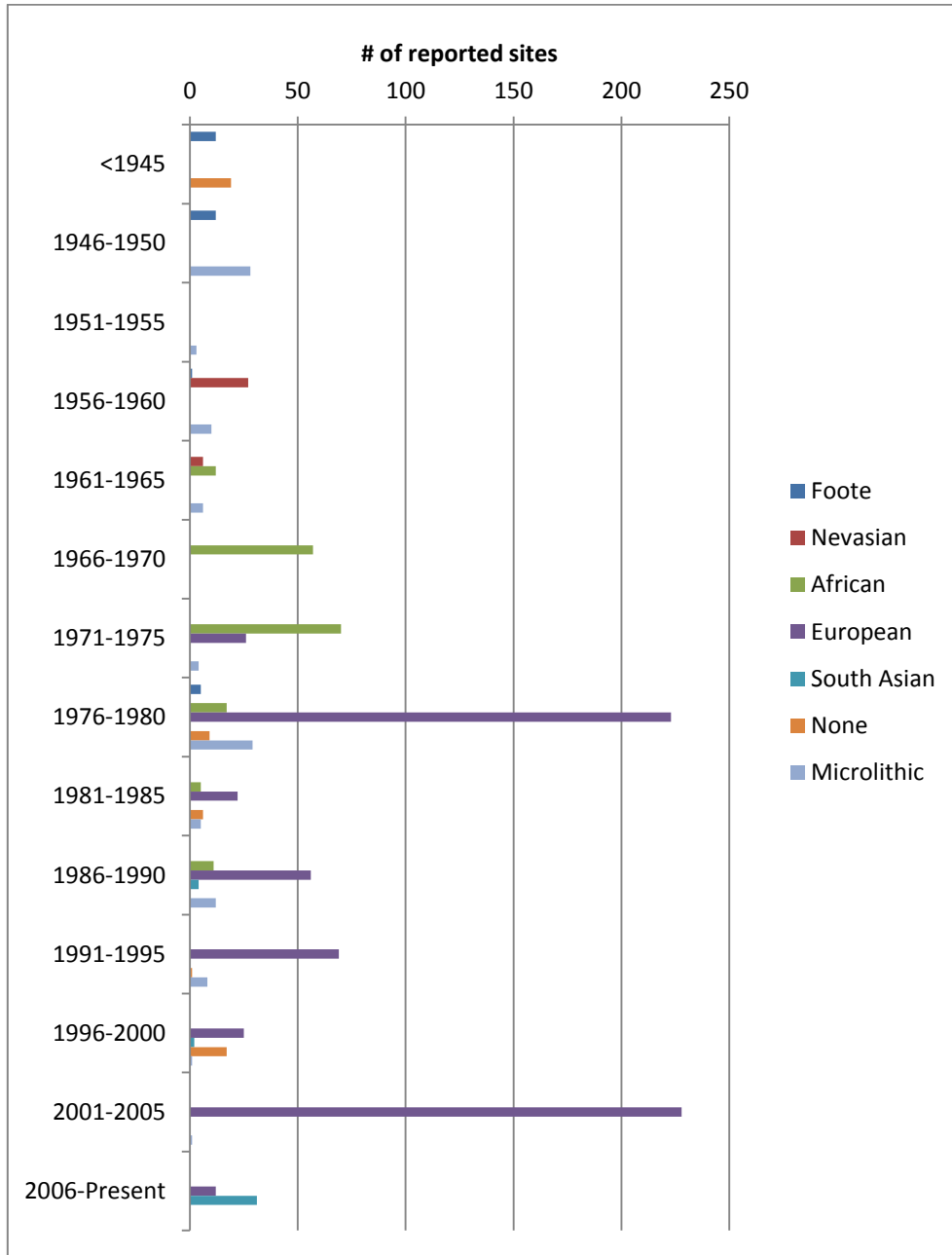


Figure 2.2: Bar chart of sites reported using different terminology throughout the Thar Desert in five year periods.

Finally, the type and quality of data recorded throughout the history of Palaeolithic research in the Thar Desert also varies between the 'dot-on-a-map' approaches of many surface surveys,

lists of typologically and technologically characteristic pieces identified through more detailed surveys (e.g. Misra 1963; Allchin et al. 1978), to the typo-technological analysis of excavated assemblages that are associated with palaeoenvironmental evidence within a geochronological framework, as at 16R Dune (Gaillard 1993; Misra & Rajaguru 1986). Any analysis of this data must take into account the different scales of analysis that are possible with the different sorts of evidence these offer.

Summary

The foregoing review of the history of research in South Asia, and particularly Rajasthan, Gujarat and Sindh, has highlighted numerous pertinent factors to be considered when approaching the Palaeolithic record of the Thar Desert. Most prominent is that, as the body of archaeological evidence has grown and theoretical approaches to understanding lithic assemblages have developed, the main questions being approached by Palaeolithic archaeologists in South Asia have changed from defining the sequence of Palaeolithic cultures to explanations of change between them.

Typological assessments of lithic assemblages, which have been the mainstay of Palaeolithic research in South Asia, were well suited to self-affirming definitions of broad cultural phases. Engaging with this data is essential to provide the context into which new research can be integrated, but this must be undertaken cautiously and critically, with explicit recognition of where contradictions lie between modern concerns in lithic analysis and the theoretical assumptions made when the data were reported.

Broad assessments of Palaeolithic assemblages within South Asia have highlighted significant differences on either side of the Thar Desert. Palaeolithic assemblages from the Thar Desert appear to share similarities with India during the Lower Palaeolithic, Pakistan during the

Middle Palaeolithic and India again during the Late Palaeolithic. A more detailed understanding of the Palaeolithic assemblages of the Thar Desert may, therefore, offer significant new insights into patterns of cultural variability and diachronic change in South Asia. In particular, the role of palaeoenvironmental variability for understanding hominin demographics and ecology deserves further examination to understand when, why and how the cultural (typological) affiliation of lithic industries from this region switched from west to east.

Chapter 3

Research Questions and Methodology

In reviewing the development of Palaeolithic research in South Asia and the Thar Desert, it is evident that major research questions are currently undergoing a significant re-orientation, stimulated by contemporary global debates in palaeoanthropology. As a result, different rationales and methodologies are required to approach the varied types of evidence necessary to undertake a comprehensive evaluation of the Palaeolithic archaeology of the Thar Desert. This is particularly pertinent for understanding how the occupation of this region may inform broader debates regarding hominin dispersal. This chapter will set out the specific research questions that the thesis will address in order to characterise the Palaeolithic occupation of the Thar Desert. This chapter also addresses the various methodologies that will be employed to assess both existing data and new lines of evidence developed in the thesis.

Research Questions

Three types of evidence, archaeological, environmental and chronological, can be marshalled to assess the Palaeolithic occupation of the Thar Desert, given the absence of fossil hominin remains. Whereas distinct questions and methodologies are applicable to archaeological and environmental evidence, both are reliant upon chronological information in order to structure patterns of change. As a result, issues relating to chronology are addressed in research questions focused upon both environmental and archaeological change.

In order to characterise the Palaeolithic occupation of the Thar Desert, three research questions need to be addressed:

1. What spatial and chronological variability occurs in Pleistocene environments in the Thar Desert?
2. What variability occurs in the existing Palaeolithic record for the Thar Desert?
3. How does the organisation of lithic technology in the Thar Desert vary through time, space and across environments?

Below, the significance of each question for the overarching goal of the thesis will be detailed.

A methodology to address each question will be set out and the chapters in which each question will be addressed is identified.

What spatial and chronological variability occurs in Pleistocene environments in Thar Desert?

Pleistocene environmental conditions in the Thar Desert present the fundamental backdrop to understanding patterns of hominin occupation of the region. Major global climatic changes have occurred throughout the Pleistocene, and as part of the mid-latitude desert belt, the Thar Desert is prone to extreme changes in environmental conditions, driven primarily by the availability of water. In order to assess the Palaeolithic occupation of the Thar Desert, it is necessary to understand where and when it may have been habitable to hominin populations. More broadly, the geological and geographic composition of the region play a significant role in structuring both aquatic and geological resources whose exploitation in antiquity have provided the only evidence for the Pleistocene hominin occupation of the Thar Desert.

A novel and comprehensive synthesis of published literature will be undertaken to identify and characterise patterns of spatial and chronological variability in environments within the Thar

Desert, which will be presented in Chapter 4. This synthesis will encompass current ecological conditions in the Thar Desert, the contemporary geographic and geological make-up of the region, and the influence of global patterns of Pleistocene climate change. Although partial syntheses covering these topics are currently available in the literature (e.g. Juyal et al. 2005; Sivaperuman et al. 2009b), these are typically geographically restricted. In addition, these studies are not orientated toward palaeoanthropological research questions. As a result, undertaking a new interdisciplinary literature review is a significant endeavour for integrating the Thar Desert into broader debate surrounding Pleistocene hominin demography and potential routes of dispersal.

The geological and geographic structure of the region has a significant bearing for understanding patterns of hominin resource exploitation. Comparing patterns of raw material use with known distributions of geological resources offers a key means to identify patterns of primary lithic reduction and subsequent mobility throughout the landscape. Similarly, spatial patterns in availability of different raw material types may have had a significant impact on lithic reduction sequences that could ultimately lead to variation in exploitation and occupation of the Thar Desert. Synthesis of the existing geological literature is therefore necessary to address questions relating to variability in the archaeological record.

Palaeoenvironmental reconstructions are somewhat reliant on analogies with modern ecological conditions, and so a brief description of current conditions in the Thar Desert will be presented. Understanding patterns of palaeoenvironmental change are important to evaluate how hominin populations have responded to varying conditions. The growing interest in modern ecological degradation in the Thar Desert offers a unique opportunity to understand not only the modern ecology of the region, but also how floral and faunal communities are changing in relation to both climatic and anthropogenic impacts upon the environment. Developing modern analogies for the processes of palaeoenvironmental change is important

to provide explicative frameworks for understanding change in the archaeological record, particularly at a finer scale of resolution than currently possible from palaeoenvironmental studies alone.

While detailing global patterns of climate change is important to provide a broader context for palaeoenvironmental change in the Thar Desert, regional proxies offer more detailed information regarding how large scale climate processes were manifest in the region. In contrast to much of South Asia, a range of recent and well dated palaeoenvironmental studies have been undertaken in the Thar Desert. The synthesis in Chapter 4 will present an up to date review of all chronometrically dated terrestrial palaeoenvironmental contexts, providing new insights into patterns of palaeoenvironmental variability in the Pleistocene. In the concluding chapter (Chapter 9), the results of this synthesis will be returned to in order to explore how spatial and chronological patterns of Pleistocene palaeoenvironmental conditions relate to the archaeological record.

What variability occurs in the existing Palaeolithic record for the Thar Desert?

As indicated in the preceding chapter, a considerable amount of Palaeolithic research has been undertaken in the Thar Desert. Yet, the only synthesis of the archaeology of this region (Allchin et al. 1978) was undertaken before any excavations or absolute dating had been conducted, and before substantial research was performed in Sindh. Furthermore, the majority of this research undertaken in the Thar Desert was designed to address different questions from the contemporary research problems that provide the context for this thesis. However, the extensive archaeological record for the region cannot be overlooked, and offers a key means to characterise the Palaeolithic occupation of the Thar Desert. In addition, by undertaking a comprehensive synthesis of the existing data, new patterns may become illuminated in the

archaeological record. The synthesis and analysis of the existing Palaeolithic archaeological record of the Thar Desert will be presented in Chapter 5.

The major issues with the current Palaeolithic record of the Thar Desert are the nature of field sampling. Unfortunately, samples typically comprise unsystematic surface collections and have only rarely included excavation or application of chronometric techniques. Moreover, the methods of reporting the lithic assemblages frequently include reporting of unspecified artefacts from an industrial group (e.g. Lower Palaeolithic) or poorly defined artefact types. These present significant methodological hurdles for the synthesis of existing evidence and for making robust inferences from the patterns that they present.

The majority of sites are reported by the closest village, a typical means for recording archaeological site locations in South Asia. Often, precise information regarding collection location and the sedimentary context are typically lacking. Generally, it is not possible to determine whether surface assemblages may have undergone substantial post-depositional disturbance or whether they may have undergone vertical disturbance (i.e. deflation), or that are relatively undisturbed. Equally, there is generally insufficient detail to appraise the nature of palimpsests from which collected assemblages derive, which could range from a single spatially segregated knapping episode to heavily re-used and time averaged sites. As a result, it must be assumed that the aggregated results of Palaeolithic research in the Thar Desert comprise a range of site types that have undergone varied levels of post-depositional modification. In a similar vein, where details regarding sampling techniques have not been explicitly stated, it is safest to assume that no systematic methodology has been employed and thus collections may be biased towards grab samples of culturally 'diagnostic' artefacts. Similarly, where small samples sizes are reported, 'diagnostic' artefacts may be more prominent.

As a result, emphasis will be placed upon the results presented by researchers that clearly delineate collection strategies and assemblage contexts, although this is a somewhat limited group. The bulk of researchers do not report these methodological and contextual data, and wholesale rejection of this data may overlook a significant source of information regarding lithic variability that may be useful to identify topics for more detailed analysis. A broader appraisal of the entire data set will be presented first, before more detailed consideration of evidence from systematically sampled sites. Evaluation of results from the entire data set must remain cautious, although consistent and repeated patterns may indicate trends in archaeological data beyond that which may be explained by different research strategies. More extensive scrutiny of results from excavated and dated contexts provides the opportunity to corroborate the results of analyses from the broader data set.

A more formal strategy is required to synthesise the diverse quality and quantity of data presented regarding the lithic assemblages themselves. Indeed, a number of sites provide no data about the lithic assemblages, and serve only to identify locations in which Palaeolithic artefacts have been recorded. With these exceptions aside, all reported Palaeolithic sites make use of either or both a cultural phase (e.g. LSA) and artefact typologies (e.g. point, Levallois core, cleaver). The review of the development of Palaeolithic cultural groupings in South Asia presented in Chapter 2 indicates a tripartite split of nomenclature has prevailed throughout most of the history of research in the Thar Desert, and maintaining this division is likely to capture the diversity reported by the majority of researchers.

A standardised set of terms is used to discuss the broadest cultural groupings evident in the Thar Desert (Table 3.1). The category of 'Lower Palaeolithic' includes sites reported as Series I, Madrasian, Early Stone Age, Lower Palaeolithic and Acheulean. Similarly, the 'Middle Palaeolithic' category will include Series II, Middle Palaeolithic and Middle Stone Age sites. Finally, Upper Palaeolithic, Microlithic, Mesolithic and Later Stone Age sites are reported here

as ‘Late Palaeolithic’. Sites that indicate the presence of either ceramics or metalwork have been rejected (which appear in the Thar Desert after 6ka [Possehl 2002], as are sites dated to <10ka. In addition, a small number of sites reported by Foote (1916) as ‘Neolithic’ can be included in this category, as the majority have subsequently been reclassified as Mesolithic by Sankalia (1948). This last category is perhaps most problematic as these sites may well include Holocene assemblages, although as the antiquity of Late Palaeolithic assemblages extends to 38ka elsewhere in South Asia (Petraglia et al. 2009; Perera et al. 2011), it is reasonable to suggest many of these sites may derive from the Pleistocene.

Cultural Group reported in literature	Cultural Group used in this thesis
Madrasian	Lower Palaeolithic
Series I	
Early Stone Age	
Acheulean	
Lower Palaeolithic	
Series II	Middle Palaeolithic
Nevasian	
Middle Stone Age	
Middle Palaeolithic	Late Palaeolithic ^a
Upper Palaeolithic	
Microlithic	
Later Stone Age	
Mesolithic	
‘Neolithic’ ^b	

Table 3.1: Cultural Group terminology reported in the literature and its relationship with terminology used in this thesis. ^aOnly aceramic sites are included in this group. ^b‘Neolithic’ sites have only been included from Foote (1916).

A much broader range of terms have been deployed to describe individual Palaeolithic artefact types. Broadly adopted from geological and palaeontological traditions, artefact typologies have been as much of a significant feature in the research history of South Asia (Kennedy 2000) as they have globally. However, South Asia has lacked clear delineation and cataloguing of these artefact types, as occurred in Europe (e.g. Bordes 1961), which prevent easy comparisons. In the Thar Desert, Allchin et al. (1978) are notable for providing descriptions of

artefact types that they report, although this has not been adopted as a standardised catalogue by other researchers. Modern approaches to lithic variability reject the suggestion that artefact types reflect deliberate finalised forms, whether functional or cultural, focusing instead upon the impact of artefact life-history and patterns of reduction intensity have upon artefacts that enter the archaeological record (e.g. Rolland and Dibble 1990; Clarkson 2007; Andrefsky 2009; Bleed 2011).

Despite problems inherent in the simplistic use of artefact typologies, they do provide the main source of evidence regarding artefact variability in the existing Palaeolithic record from the Thar Desert. Indeed, in her typological analysis of Middle and Late Palaeolithic assemblages from across South Asia, James (2011) identified evidence of a significant change within the Thar Desert between these two periods. James' (2011) analysis indicates greater similarities between Thar Desert and Pakistani assemblages in the earlier period, shifting to a more Indian affiliation in the later period. The analysis presented in Chapter 5 has been undertaken in full acknowledgement that these categorisations are entirely the construct of archaeologists, and may mask artefact life histories, but these may offer meaningful insight into existing bodies of evidence that can help direct future research.

In order to compare artefact typologies across the Thar Desert, a single composite list of commonly used categories has been derived from the literature (Table 3.2). This list is intended for use as a heuristic device to explore variability in the existing reports of Palaeolithic sites from the Thar Desert, and does not present a catalogue of clearly delineated artefact types for this region or any other. 'Heavy Tools' is used to group a range of artefact types which may be produced on both cores and large flakes through the application of either unifacial or bifacial reduction. Artefacts reported simply as 'large flake tool', 'core tools' or 'bifaces' are classed together in the category 'Heavy Tool'.

Artefact Group	Artefact Type
Debitage	Flake/Debitage
Debitage - Blades	Blade
	Parallel Blade
	Flake Blade
	Backed Blade
	Crested Blade
Debitage - Retouched	Retouched/Tools
	Point
	Borer
	Burin
	Awl
	Denticulate
	Notch
	Scraper
	Knife
Debitage - Microliths	Microlith
	Geometric Microlith
	Non-geometric Microlith
	Lunate/Crescent
	Triangle
	Trapeze
	Micro-blade
	Backed bladelet
Core	Core
	Fluted Core
	Blade Core
	Prepared/Levallois Core
	Discoid/Discoidal Core
	Microlithic Core
	Polyhedron/Polyhedral Core
Heavy Tools	Heavy Tools
	Handaxe
	Chopper
	Chopping Tools
	Cleaver
	Pick
	Ovate

Table 3.2: Artefact types grouped by gross technological characteristics, based upon common categories reported in the Thar Desert.

Analysis of the complete data set in Chapter 5 will firstly cover the spatial distribution of all Palaeolithic sites. Following this, analysis will be organised around the broadest cultural groups (Table 3.1) reported, including distribution patterns, raw material use, presence/absence of artefact types with assemblages, proportional typological composition of assemblages and artefact size. A detailed synthesis of excavated sites and chronometrically dated assemblages will follow, with more varied evidence presented, dependent upon original report. In the conclusion of Chapter 5, a concise summary of the patterns evident from these analyses will be presented to offer a clear characterisation of variability in the Palaeolithic archaeology of the Thar Desert. This summary will be revisited in Chapter 9 and integrated with the results of new evidence presented in this thesis.

How does the organisation of lithic technology in the Thar Desert vary through time, space and across environments?

Contemporary approaches to lithic analysis are substantially different, both in terms of theoretical underpinnings and methodological practices, from those under which the majority of existing evidence from the Thar Desert has been developed. In particular, modern practices of lithic analysis focus upon Organisation of Technology or *Chaîne Opératoire* approaches, both of which incorporate an explicit concern for reduction sequences and artefact life-histories (see Carr & Bradbury 2011; Soressi & Geneste 2011). New lithic analyses presented in this thesis have been undertaken in following Organisation of Technology approaches, which permit better integration with palaeoenvironmental data to investigate how Pleistocene hominin lithic technologies have been variably deployed in the Thar Desert in the face of climatic change. Common methodologies have been applied to two seasons of fieldwork, which consist of a program of targeted surface surveys at a number of sites in Rajasthan,

reported in Chapter 6, and excavations undertaken at the site of Katoati, Rajasthan, reported in Chapters 7 and 8.

Archaeological Sampling Strategy

The methods employed by archaeologists in the recovery of Palaeolithic assemblages can have a significant bearing upon the patterns of variability that are identified. The majority of Palaeolithic fieldwork requires a sampling strategy, as exhaustive collection methods are generally not practical. By explicitly stating the sampling strategy employed in the field, an assessment can be made of potential restrictions of variability that result from archaeological practice, rather than site formation processes or the patterns of hominin behaviour under investigation. The ability to evaluate the impact of natural site formation processes upon cultural assemblages is heavily dependent upon the use of sampling strategies that aim to address these issues. For example, it may not be possible to address post-depositional size sorting of artefacts if archaeological sampling has been unsystematic or is biased toward larger, 'diagnostic' artefacts.

Two different sampling strategies have been employed while undertaking new fieldwork in the Thar Desert. Firstly, a targeted surface survey of a number of sites in the Rajasthan has been undertaken, the results of which are reported in Chapter 6. Due to restrictions on time available to undertake this fieldwork, and the need to perform lithic analyses in the field, unsystematic collection strategies have been employed. This places some restrictions upon the kinds of conclusions that can be drawn from the recorded evidence, but the sampling strategy employed allowed an assessment of lithic assemblages from more varied spatial, palaeoenvironmental and geochronological contexts than would otherwise have been possible. This spatially diverse surface survey is complementary to the excavation undertaken at the site of Katoati, the results of which are reported in Chapters 7 and 8. Excavation

practices facilitated a more clearly defined sampling strategy, based upon recovery of artefacts from arbitrary horizons following sediment sieving (see Chapter 7 for further details), permitting more nuanced analysis of the resultant lithic assemblages (presented in Chapter 8).

The methodology for assessing the organisation of lithic technology for both sampling strategies can be split into two distinct components. Evaluation of site location, palaeoenvironmental context and site formation processes depends upon a range of evidence including the landscape context, site sedimentology, geochronology and allied palaeoenvironmental proxies, described below as Contextual Attributes. The remaining aspects of technological organisation depend upon an attribute analysis of lithic assemblages, described below as Lithic Attributes.

Contextual Attributes

A number of contextual factors can affect the diversity of lithic assemblages analysed by archaeologists, many of which cannot be inferred from the artefacts alone. These stem both from the nature of hominin behaviour, in the short, medium and long term, and depositional context. A range of researchers have highlighted the importance of considering mobility, risk reduction and time stress to understand the technological decisions and practices undertaken by hunter-gather populations (see Clarkson 2007). Underlying these approaches is the concept that technological behaviour has both energetic costs and benefits which need to be balanced for successful subsistence strategies and ultimately permit a population's reproductive viability. A range of idealised strategies have been proposed relating to optimal technological decisions in a variety of circumstances (see Clarkson 2007), however sufficient resolution to assess these factors thoroughly is extremely rare, and certainly not yet present in the Thar Desert.

Nevertheless, a number of insights from this area of research may help to provide a broad framework for interpreting lithic assemblages. Different strategic and energetic constraints

may influence the organisation of technology and lithic reduction sequences in places with variable access to both raw material and subsistence resources. As a result, lithic assemblages recovered in different locations within the landscape may differ in response to the availability of different resources, and strategies for their procurement. Assessing the location of an archaeological site within a landscape with regards to the availability of different raw materials, water resources and palaeoenvironmental conditions therefore offers critical information for interpreting the results of attribute analysis.

Cultural processes of site formation can also have a significant impact upon the variability of lithic assemblages recovered by archaeologists. All archaeological sites can be considered as forms of palimpsest deposit (Bailey 2007). In the majority of cases, material culture from multiple, temporal separated behavioural episodes may form a single horizon, which are not distinct in the archaeological record. Furthermore, the level of spatial and temporal resolution available to archaeologists typically prevents direct associations between sampled sites. As a result, lithic assemblages sampled by archaeologists typically represent an aggregate record of reduction activities, which may compress varied behavioural responses to short term variability in resource availability. As a result, the Palaeolithic assemblages analysed from the Thar Desert may provide more robust indications of change in reduction behaviours beyond the scale of individual or even contemporary group activities.

Comparisons between discrete archaeological horizons, whether stratified at a single site or occurring in varied locations across a landscape offer the means to address change in lithic reduction behaviour at a scale beyond the experience of Pleistocene hominins. A range of demographic factors may influence long term change in lithic reduction practices, with changing population sizes influencing the frequency of adaptive innovation and cultural drift (Shennan 2001; Powell et al. 2009). Hominin population sizes may have varied dramatically in response to fluctuating palaeoenvironmental conditions in the Thar Desert. In extreme cases,

population extinction may have occurred in the Thar Desert, which would cause a complete break in regional cultural transmission, and subsequent re-colonisation could introduce novel reduction practices. Similarly, the dispersal of new populations into the Thar Desert could introduce new lithic reduction behaviours, either in whole or in part. Developing an integrated chronological framework for climatic and archaeological change is key to assessing the impact of these demographic processes, which may operate over hundreds or thousands of years.

Natural processes of site formation can fundamentally transform variability in material culture, and the potential to differentiate between behavioural episodes at various different temporal scales (Schiffer 1987; Bailey 2007; Schiffer 2010). The extent and means by which artefacts are transported by natural agency prior to deposition in the sedimentary contexts from which they are recovered determine the degree to which an excavated assemblage accurately reflects the cultural processes that lead to its formation. The rate of sedimentary burial of lithic assemblages coupled with the level of resolution permitted by chronometric dating techniques to differentiate depositional episodes provide the key means to address issues of long-term change in hominin behaviour.

In the Thar Desert, two natural processes may lead to the displacement of some or all of a lithic assemblage with different consequences. Deflation of sediment deposits by aeolian activity can lead to the vertical transport of artefact assemblages, as wind power is rarely capable of horizontal mobilisation of any clast >2mm. As a result, conflation of discrete reduction episodes can occur upon a sediment horizon that is more resistant to erosion. Essentially, this results in the formation of a palimpsest record of hominin behaviour rather than the mobilisation of artefacts away from the site of reduction activity.

The flow of water, whether as sheet-wash over a gently sloped surface or as channelized activity in rills, gullies, streams or rivers, has the potential to transport some or all lithic

artefacts from an assemblage away from the site at which they were created or discarded. Experimental studies have indicated that increasingly energetic depositional environments typically result in a greater degree of displacement of larger sized artefacts (Schick 1984). However, the degree of artefact transport has been observed to correlate with the length of assemblage exposure rather than simply relating to sedimentary or geomorphic context (Petraglia & Potts 1994). Significantly, smaller artefacts, particularly <20mm, are particularly susceptible to disturbance by the flow of water (Schick 1984), whereas larger artefacts are notably less prone to transport (Petraglia & Potts 1994). Experimental studies of the influence of flowing water suggests that the gross composition of an assemblage may not be substantially altered amongst larger size classes (>10g) (Schick 1984; Petraglia & Potts 1994). As a result, lithic assemblages that only include restricted size classes of artefacts present the clearest means to identify contexts in which significant winnowing has occurred or downstream lag deposits have formed.

The degree to which edge rounding and artefact weathering have occurred may provide further information regarding patterns of exposure and transportation. Microscopic analyses of lithic edges offer a robust means to quantify the extent of rounding present upon an artefact (e.g. Shackley 1974), although this may require bespoke experimental data to compensate for raw material variability, which are not broadly available. Macroscopic analyses of both artefact rounding and weathering depend upon qualitative assessments of appearance of edges and surfaces presented by lithic artefacts. Artefact rounding and weathering may occur as a result of either mechanical or chemical activity. Transportation of artefacts in water may cause both rounding and weathering, although exposure to flowing water with suspended sediments or smaller clasts may have a similar impact for exposed surfaces of non-mobile artefacts (Petraglia & Potts 1994). Exposure to sediments mobilised by aeolian activity presents a further means of mechanical rounding and weathering of artefacts that are only

likely to impact exposed surfaces. Finally, chemical weathering occurring once artefacts have been buried may mimic the impact of rounding and weathering caused by mechanical weathering. The potential extent of chemical effects upon lithic artefacts may vary due to the nature of the raw material and the context in which they are buried. An integrated assessment of artefact transport, weathering and rounding is therefore required to understand potential post-depositional distortion of lithic assemblages.

Methods

Evaluation of the contextual attributes of sampled sites for both the surface survey and excavation include a desk-based assessment of existing sources of evidence and corroboration of these data in the field during sampling. In addition, sedimentological and geochronological sampling at the site of Katoati has permitted further laboratory analyses to be conducted to refine the understanding of context of lithic assemblages.

Desk-based assessment for the surface survey focused upon the identification of suitable contexts for recovery of lithic assemblages for which palaeoenvironmental and geochronological studies have previously been conducted and reported within the literature. In particular, this has focused upon sites with chronometrically dated Upper Pleistocene geomorphological units or where palaeoenvironmental evidence provides an indication of the influence of humid climatic regimes. Luminescence dating techniques provide the most secure means for understanding geomorphological development and palaeoenvironmental change through time in the Thar Desert (e.g. Dhir et al. 2010). In some instances, traditional radiocarbon dates are also available, but are treated with greater caution as they typically fall beyond the range of reliable calibration curves and are liable to be superseded by application of either AMS ^{14}C or luminescence dating techniques. In cases where existing geochronological

information is available, the relationship between the sample location and published data will be examined to establish the extent to which any lithic assemblages can be integrated into an existing chronological framework.

A variety of sedimentological and palaeoenvironmental evidence is available in the literature that has helped to shape the surface survey program. At the coarsest level, these published data offer some insight into relative humidity/aridity at the sample locations. This dichotomy can be illustrated by the presence of coarser or finer fluvial sediments, alternation of aeolian and lacustrine sediments or colluvial sediments, and accretion, deflation or pedogenesis of sand dunes. These offer a baseline for interpreting potential site formation factors that have influenced sampled archaeological assemblages. In addition, the presence and development of pedogenic carbonates offer a widespread means to assess pedogenic development in sedimentary units, which in some cases have undergone isotopic analyses to derive further proxy evidence for the influence of humid climatic regimes and local composition of vegetation. Finally, a number of geomorphological observations made in the field while conducting the survey help to support and extend commentaries made by earlier researchers, and further contribute to understanding the site location, palaeoenvironmental setting and site formation processes that relate to sampled archaeological assemblages.

Limited published evidence is available for sites near Katoati. Whereas some research has been undertaken in the region, geomorphological units that have undergone either geochronological or sedimentological analyses are too remote (ca. 50km away) to draw direct analogies. However, this research does offer a number of useful insights into the long term geomorphological processes and associations with archaeological occurrences within the Katoati landscape, which supported by additional observations from the field. A preliminary study at Katoati has yielded both sedimentological and geochronological information, which have helped guide the choice of excavation site at Katoati. Two sedimentological logs have

been recorded, detailing a succession of aeolian and fluvial sediments within close vicinity of the excavation site. A single AMS ^{14}C date and a number of preliminary OSL age estimates provide the means to set out a provisional scheme of sedimentological development at Katoati.

Detailed information regarding the palaeoenvironmental context and site formation processes at Katoati are derived from laboratory analyses of sedimentary samples and an assessment of size sorting, weathering and rounding of lithic artefacts. Here, a basic description of which analytical approaches have been conducted will be provided, with a more detailed description of sampling methodology and analytical procedure reported in Chapter 7.

Sediment grain size analysis of fine sediments (<2mm) and an informal appraisal of coarse sediments provide the basic means to establish the depositional context in which lithic assemblages have been preserved, supported by field logs of the excavated sedimentary section. Palaeoenvironmental proxy evidence is developed through the use of X-Ray Fluorescence, %CaCO₃ and stable isotope analyses, which are used to identify patterns in pedogenesis and variations in both soil humidity and local vegetation composition.

Geochronological studies include the analysis of a number of sediment samples using OSL methods, and the application of AMS ^{14}C dating to establish age estimates for a small number of ostrich eggshell samples derived both from the excavated site and a nearby location. These provide a chronological framework for the interpretation of both sedimentological studies, and the analysis of lithic assemblages. Finally, an analysis of artefact size sorting, weathering and rounding is undertaken to establish the extent to whether the archaeological deposits have undergone any substantial natural disturbance or either physical or chemical weathering prior to burial, and to what extent these factors vary between excavated horizons.

Lithic Attributes

A number of inferences regarding past hominin reduction behaviours can only be made following attribute analysis of each artefact within sampled assemblages, although some factors, such as site use and reduction intensity, are best assessed in relation to their broader context. Site use and reduction intensity are intrinsically linked to site location in relation to contemporary resource structure and subsistence strategies. However, the influence of these factors is recorded in patterns of variability within lithic assemblages. As the production of lithic artefacts is a reductive process, increasing exploitation of raw material clasts can be identified by the reduction in artefact sizes and increase in evidence for previous removals present on an artefact (Andrefsky 2005; Clarkson 2007; Andrefsky 2009). Patterns of site use may be indicated by the presence or absence of different parts of reduction sequences, which in part relates to analysis of reduction intensity. For example, the lack of cortical artefacts at a site may indicate that primary reduction/decortification has taken place elsewhere and that partially reduced raw materials had been imported from elsewhere (Andrefsky 2005). However, as conflation of different reduction sequences both at an individual scale (e.g. discard of artefacts broken through extended use and production of a replacement) and over more extended periods of time are likely to occur, identification of site use is likely to capture the variety of activity at a site. The level of reduction intensity and the elements of reduction sequences present at a site play a significant role in structuring further evidence for organisation of technology.

Raw material variability also has significant influence upon reduction strategies (Rolland & Dibble 1990; Andrefsky 2005; 2009). While clast size and availability may have an impact upon strategies for resource procurement, variability in raw material fracture mechanics can affect its suitability for different levels and techniques of reduction and functional demands, leading to variability in lithic assemblages (Rolland & Dibble 1990; Andrefsky 2005; 2009). Raw

materials with finer crystalline structures are typically easier to control during more extensive reduction sequences, but may be more prone to breakage when used for heavy-duty tasks. In contrast, coarse grained raw materials are typically more resilient when used for heavy-duty tasks, but are difficult to control in the manufacture of smaller tools. As a result, differences in reduction intensity and reduction sequences structured around raw material variability may relate to different fracture mechanics or functional demands, as well as patterns of availability and clast size.

While mitigated by potential impacts of site use, reduction intensity and raw material variability, differences in individual proficiency and culturally transmitted reduction techniques can also affect the size and shape of artefacts produced (Whittaker 1994). Indeed, these factors may also play a significant role in determining the extent to which clasts of different materials and sizes can be reduced. Differences in reduction technique may become manifest in a number of ways (Andrefsky 2005). Variability in size, shape and type of platform surfaces with respect to the clast size and existing flake scar pattern may indicate attempts to control reduction sequences through preferred reduction techniques. Similarly, flake size and shape may result from technical choices made by hominins during the reduction process. The production of blades or blade-proportioned flakes is a good example of this, as to produce a flake at least twice as long as it is wide requires of control of both platform and flaking surfaces (e.g. Whittaker 1994). The application of specific core reduction strategies, such as the Levallois technique (see Van Peer 1992), provides another example of how reduction techniques can influence flake size and shape. Equally, the ability to proficiently remove flakes while leaving a core suitable for further reduction may be indicative of a certain degree of technical expertise. Evidence for aberrant terminations, such as hinges and steps, on cores or flakes may indicate where flaking technique has not matched material constraints (Andrefsky 2005).

Beyond material constraints and technical ability, patterns in artefact size and shape may indicate functional or cultural preferences. Comparisons between the size and shape attributes of flakes, last flake scars on cores and retouched flakes provide some means to identify such preferences. The absence of flakes matching the size and shape of the last flake scars from cores may indicate the removal of these artefacts from the site. Similarly, differences in size and shape of retouched and un-retouched artefacts may indicate preferences in choice of flakes for further reduction. Finally, functional or cultural preferences may be manifest in artefact typologies, although separating such preferences from material constraints and technical ability is problematic, particularly when artefact life histories are taken into account (Rolland and Dibble 1990).

Methods

A common methodology for lithic analysis has been applied to both surface and excavated assemblages, although it has been possible to record a more extensive range of lithic attributes for the latter. Analysis of the archaeological assemblages requires a split into gross artefact types, comprising cores, debitage and heavy tools, with debitage further split into both flakes and flaked pieces and retouched and un-retouched pieces. Comparisons of the differing proportions of these basic artefact types and patterns of raw material exploitation can be analysed at the assemblage-wide scale (Table 3.3).

Assemblage Attribute	Interpretation
Core:Debitage ratio	Increased proportion ofdebitage present may indicate increased reduction intensity, raw material fracture mechanics or different patterns of site use.
Flake:Flaked Pieces ratio	Increased presence of flaked pieces may reflect less precise control over reduction technique, or relate to raw material fracture mechanics.
Retouched:Unretouched ratio	Increased presence of retouched artefacts may indicate increased reduction intensity or different patterns of site use.
Raw Material Use	Use of different raw materials may inform upon availability, procurement strategies and associated energetic costs; clast size and fracture mechanics may impose restrictions upon reduction strategies..

Table 3.3: Assemblage scale attributes analysed and potential interpretation of results.

Typological descriptions of artefacts have been undertaken using nomenclature set out by Inizian et al. (1993). A range of nominal, ordinal and scalar technological attributes have been recorded for each artefact that can be used to assess one or more aspects of the organisation of technology. The attributes recorded and the aspects of technological organisation that can be inferred from them are presented in Tables 3.4-3.8. It is important to note that variation in artefact attributes may be interpreted in a number of ways, which may not be mutually exclusive.

Attribute	Description	Interpretation
Max Length	Largest length in any direction (mm)	Decreased size attributes may reflect raw material clast size, increased reduction intensity; variability in size may reflect the degree of control of flaking technique, or either functional or cultural preferences.
Max Width	Largest measurement perpendicular to Max Length (mm)	
Medial Thickness	Thickness at mid-point of core (mm)	
Axial Length	Length along axis of last percussion from striking platform (mm)	
Axial Proximal Width	Perpendicular to axial length at proximal end of core (mm)	
Axial Medial Width	Perpendicular to axial length at mid-point of core (mm)	
Axial Distal Width	Perpendicular to axial length at distal end of core (mm)	
Maximum Surface area	Maximum Length x Maximum Width (mm ²)	
Distal Thickness	Perpendicular to Distal Width (mm)	

Attribute	Description	Interpretation
Proximal Shape	Axial Proximal Width/Axial Medial Width (1=parallel edges; >1=contracting edges; 1>=expanding edges)	Variability in core shape may be indicative of different reduction techniques, or functional of cultural preferences.
Distal Shape	Axial Medial Width/Axial Distal Width (1=parallel edges; >1=contracting edges; 1>=expanding edges)	
Axial Elongation	Axial Length/Axial Medial Width	
Flatness	Axial Medial Width/Medial Thickness	
Platform Width	Width of platform orientated by flaking axis (mm)	Decreased platform size may reflect raw material clast size, increased reduction intensity; variability in size may reflect the degree of control of flaking technique, or either functional or cultural preferences.
Platform Thickness	Perpendicular to platform width at point of percussion (mm)	
Platform Area	Platform Width x Platform Depth (mm ²)	
Platform Type	Cortical, Plain (no clear negative scar morphology), Single Conchoidal (single flake scar), Dihedral (sharp angled intersection between two flake scars), Multiple Conchoidal (multiple flake scars), Punctiform (very thin surface), Crushed (fractured surface).	Increased number of flake removals present on platform may indicate increased reduction intensity or preferences for reduction technique.
Platform Preparation	Overhang removal (small flake scars at proximal end of dorsal face removed from platform), Faceting (small flake scars on platform removed from proximal dorsal face)	Presence of platform preparation may indicate need to strengthen platform due to increased reduction intensity or preferred reduction technique.
Platform Shape	Platform Width/Platform Depth	Variability in platform shape may be indicative of different reduction techniques, or functional of cultural preferences.
Size corrected Platform Area	Platform Area/Maximum Surface Area	Variability in platform size relative to core size may reflect the degree of control of flaking technique, or either functional or cultural preferences.
Last Termination Type	Feather (tapered), Hinge (curved over), Step (broken), Outrepassé (terminating on surface opposite to flaking surface), Axial (split along axis)	Aberrant terminations may indicate either increased reduction intensity or reduced control of reduction technique.
Last Scar Length	Axial length of last scar removal >1/3 core length (mm)	Decreased size attributes may reflect raw material clast size, increased reduction intensity; variability in size may reflect the degree of control of flaking technique, or either functional or cultural preferences.
Last Scar Face Length	Maximum length of flaking face on flaking axis (mm)	
Last Scar Medial Width	Perpendicular to Last Scar length at mid-point of scar (mm)	
Last Scar Elongation	Last Scar Length/Last Scar Width	Increased elongation indicates greater control over flaking technique, and may relate to functional or cultural preferences.
# Core rotations	Number of times flaking direction has changed	Increased number of core rotations, exploited platform quadrants and number of scars indicates increased reduction intensity, and may indicate different discard thresholds for different reduction practices.
# Platform Quadrants	Split the platform into four quadrants and record the number with flaking present, with the first quadrant starting on the left of the last scar and working anticlockwise (Clarkson 2004; Jones 2007)	
# Scars	Count of scars greater than 1/3 of core length	
Cortex %	Estimated in 10% increments	Decreasing cortical coverage indicates increased reduction intensity.

Attribute	Description	Interpretation
Flaking Pattern	Single Platform (unidirectional reduction from a single platform), Bidirectional (bidirectional reduction from opposed platforms), Multi Platform (reduction from more than one platform in different directions), Prepared (presence of distinct preparatory and flaking surfaces)	Reduction from a greater number of platforms in a greater number of directions indicates greater reduction intensity; variability in flaking pattern may reflect different control of reduction, or functional or cultural preferences.

Table 3.4: Attributes recorded on cores indicating how they are recorded and potential interpretation of results.

Attribute	Description	Interpretation
Max Length	Largest length in any direction (mm)	Decreased size attributes may reflect raw material clast size, increased reduction intensity; variability in size may reflect the degree of control of flaking technique, or either functional or cultural preferences.
Max Width	largest measurement perpendicular to Max Length (mm)	
Medial Thickness	Thickness at mid-point of flake (mm)	
Axial Length	Length along axis of percussions from striking platform (mm)	
Axial Proximal Width	Perpendicular to axial length at proximal end of flake (mm)	
Axial Medial Width	Perpendicular to axial length at mid-point of flake (mm)	
Axial Distal Width	Perpendicular to axial length at distal end of flake (mm)	
Maximum Surface area	Maximum Length x Maximum Width (mm ²)	
Proximal Shape	Axial Proximal Width/Axial Medial Width (1=parallel edges; >1=contracting edges; 1>=expanding edges)	Variability in flake shape may be indicative of different reduction techniques, or functional of cultural preferences.
Distal Shape	Axial Medial Width/Axial Distal Width (1=parallel edges; >1=contracting edges; 1>=expanding edges)	
Axial Elongation	Axial Length/Axial Medial Width	
Flatness	Axial Medial Width/Medial Thickness	
Platform Width	Width of platform orientated by flaking axis (mm)	Decreased platform size may reflect raw material clast size, increased reduction intensity; variability in size may reflect the degree of control of flaking technique, or either functional or cultural preferences.
Platform Thickness	Perpendicular to platform width at point of percussion (mm)	
Platform Area	Platform Width x Platform Depth (mm ²)	
Platform Type	Cortical, Plain (no clear negative flake scar morphology), Single Conchoidal (single flake scar), Dihedral (sharp angled intersection between two flake scars), Multiple Conchoidal (multiple flake scars), Punctiform (very thin surface), Crushed (fractured surface).	Increased number of flake removals present on platform may indicate increased reduction intensity or preferences for reduction technique.
Platform Preparation	Overhang removal (small flake scars at proximal end of dorsal face removed from platform), Faceting (small flake scars on platform removed from proximal dorsal face)	Presence of platform preparation may indicate need to strengthen platform due to increased reduction intensity or preferred reduction technique.

Attribute	Description	Interpretation
Size corrected Platform Area	Platform Area/Maximum Surface Area	Variability in platform size relative to flake size may reflect the degree of control of flaking technique, or either functional or cultural preferences.
Termination Type	Feather (tapered), Hinge (curved over), Step (broken), Outrepassé (terminating on surface opposite to flaking surface), Axial (split along axis)	Aberrant terminations may indicate either increased reduction intensity or reduced control of reduction technique.
Flake Scar Pattern	Cortical (min 50% cortex cover and no clear flaking direction for removals on dorsal surface) Proximal (all scars originate from proximal), Distal (all scars originate from distal) Bidirectional (scars originate from proximal and distal), Opposed (scars originate from left and right), Perpendicular (scars originate from either a) proximal or distal and b) right and left), Weakly Radial (scars originate from three directions), Radial (scars originate from at least three directions and lack cortex)	Increased number of dorsal scar directions may indicate increased reduction intensity; variability in dorsal scar pattern may reflect differences in reduction technique, or functional or cultural preferences.
Cortex %	Estimated in 10% increments on dorsal and platform surface	Decreasing cortical coverage indicates increased reduction intensity.

Table 3.5: Attributes recorded on flakes indicating how they are recorded and potential interpretation of results.

Attribute	Description	Interpretation
Max Length	Largest length in any direction (mm)	Decreased size attributes may reflect raw material clast size, increased reduction intensity; variability in size may reflect the degree of control of flaking technique, or either functional or cultural preferences.
Max Width	largest measurement perpendicular to Max Length (mm)	
Medial Thickness	Thickness at intersection of max length and width (mm)	
Maximum Surface area	Maximum Length x Maximum Width (mm ²)	
Cortex %	Estimated in 10% increments on dorsal and platform surface	Decreasing cortical coverage indicates increased reduction intensity.

Table 3.6: Attributes recorded on flaked pieces indicating how they are recorded and potential interpretation of results.

Attribute	Description	Interpretation
Index of Invasiveness	Each segment on single flake surface with retouch present (combinations of Proximal End, Proximal Left, Proximal Right, Meidal Left, Medial Right, Distal Left, Distal Right, Distal End on both flake margins and flake interior on both dorsal and ventral surfaces) scores 0.5. Sum of scores divided by total assessed segments provides Index of Invasiveness (see Clarkson 2002)	Increased score indicates increased retouch intensity.
Retouch location	Single End, Single Side, Single End & Single Side, Single End Double Side, Double End, Double Side, Double End Double Side	More numerous retouched margins indicates increased retouch intensity.
Retouch width	Straight length between start and end points of longest retouched margin (mm)	Increased size indicates increased retouch intensity.
Retouch depth	Largest perpendicular measurement between Retouch width axis and retouched margin (mm)	Increased size indicates increased retouch intensity.

Table 3.7: Additional attributes recorded on retouched flakes or flaked pieces indicating how they are recorded and potential interpretation of results.

Attribute	Description	Interpretation
Axial Length	Distance from proximal to distal end	Decreased size attributes may reflect raw material clast size, increased reduction intensity; variability in size may reflect the degree of control of flaking technique, or either functional or cultural preferences.
Max Width	Largest measurement perpendicular to Axial Length (mm)	
Surface Area	Maximum Length x Maximum Width (mm ²)	
1/4 width	Width, perpendicular to axial length, measured at 1/4 of axial length	
1/2 width	Width, perpendicular to axial length, measured at 1/2 of axial length	
3/4 width	Width, perpendicular to axial length, measured at 3/4 of axial length	
1/4 thickness	Thickness, perpendicular to 1/4 width, measured at 1/4 of axial length	
1/2 thickness	Thickness, perpendicular to 1/2 width, measured at 1/2 of axial length	
3/4 thickness	Thickness, perpendicular to 3/4 width, measured at 3/4 of axial length	
Max thickness	Maximum thickness perpendicular to axis	
Cleaver Edge Length	Distal width of cleaver	
Biface Butt Length	Distance from proximal end of artefact to maximum width	
Cortex %	Estimated in 10% increments	

Table 3.8: Attributes recorded on heavy tools indicating how they are recorded and potential interpretation of results.

The results of the technological attribute analysis from surface sites discussed in Chapter 6 will be presented as a discussion of basic descriptive statistics, as neither the sampling strategy nor sample sizes analysed are suitable for comparative statistical approaches. Only limited potential to assess a range of site formation processes is presented by this attribute analysis. However, due to the association with known palaeoenvironmental and dated geomorphic contexts, this analysis can provide insights into the organisation of lithic technology in the Thar Desert beyond that which is present through the analysis of existing research alone.

The discussion of lithic assemblages from Katoati, set out in Chapter 8, includes a typological description of artefacts and univariate description of artefact variability encompassing the entire assemblage. Comparative analyses focus upon the three largest assemblages recovered from excavations. The remaining assemblages are excluded due to small sample size and different levels of post-depositional disturbance that make them inappropriate for inclusion in statistical analyses. Bivariate analyses are structured around nominal lithic attributes as well as artefact assemblages separated by strata.

Preliminary testing has identified that the metric lithic attribute data are not normally distributed, and as a result non-parametric tests have been used. Comparisons between more than two categories of scalar and ordinal data have been conducted using Kruskal-Wallis tests. Pair-wise comparisons of scalar and ordinal data, including post-hoc analysis following Kruskal-Wallis tests, have been conducted using Mann-Whitney U-tests. Nominal data sets have been analysed using Fisher's Exact test with Monte Carlo resampling of 10,000 tables to provide a 99% model of p values; these have been employed as test data did not meet the criteria for chi-squared tests. A Benjamini-Hochberg procedure (Benjamini & Hochberg 1995) has been employed where a number of tests within the same family have been conducted to control for Type 1 errors. As a result a critical level of significance of $p \leq 0.05$ is maintained for all results reported as significant.

The result will be the most comprehensive analysis of the organisation of lithic technology undertaken in the Thar Desert to date that will offer a new benchmark for the region. In Chapter 9, the results of contextual and attribute analyses from both the survey and excavation will be synthesised with evidence from elsewhere in the Thar Desert to present a new characterisation of the Palaeolithic occupation of the Thar Desert.

Summary

This chapter has set out the major research questions for assessing the Palaeolithic occupation of the Thar Desert. This chapter has also identified the methodological approaches that will be employed to address the research questions. As indicated above, the first two research questions will be addressed primarily by a comprehensive synthesis of existing evidence, presented in Chapters 4 and 5 respectively. The third research question is primarily addressed with new evidence resulting from two seasons of fieldwork undertaken in Rajasthan, which will be presented in Chapters 6, 7 and 8. Chapter 9 will combine the results of analyses presented in Chapters 4-8 to offer a concise appraisal of the research undertaken in order to characterise the Palaeolithic occupation of the Thar Desert. This comprehensive synthesis will provide the opportunity to make comparisons with adjacent regions and assess what role the Thar Desert may have played in broader dynamics in Pleistocene hominin demography.

Chapter 4

Geology, Ecology and Palaeoenvironments of the Thar Desert

The evidence under review in this chapter has a significant impact upon both the availability of archaeological evidence and explanations for variability within lithic assemblages dependent upon the nature of raw materials and environmental factors. Firstly, the geological structure of the region is described, which is critical to understand the distribution and nature of lithic raw material sources that have been available for exploitation by Pleistocene hominins. Details of the modern ecology of the Thar Desert will then be set out, and how evidence of modern climate change may be informative for past processes is set out. Turning toward the palaeoenvironmental context, the nature of orbital-scale and monsoon-driven climate change will be set out, which are the two major forces driving palaeoenvironmental variability for the Thar Desert. A synthesis of chronometrically dated terrestrial proxy evidence for palaeoenvironmental change from the Thar Desert will be presented, including fluvial, aeolian, lacustrine and eustatic proxies and focusing predominately upon MIS 6-2. This will expand on existing syntheses, which focus either on single forms of proxy data (e.g. Jain & Tandon 2003; Singhvi & Kar 2004) or are geographically restricted (e.g. Juyal et al. 2005) to offer a clear and concise review of existing and chronometrically dated palaeoenvironmental proxies. In summary, I will discuss how palaeoenvironmental variability may have influenced the nature of hominin occupations of the Thar Desert in the Late Pleistocene and to what extent this may have determined access to different raw material resources.

Geology of the Thar Desert

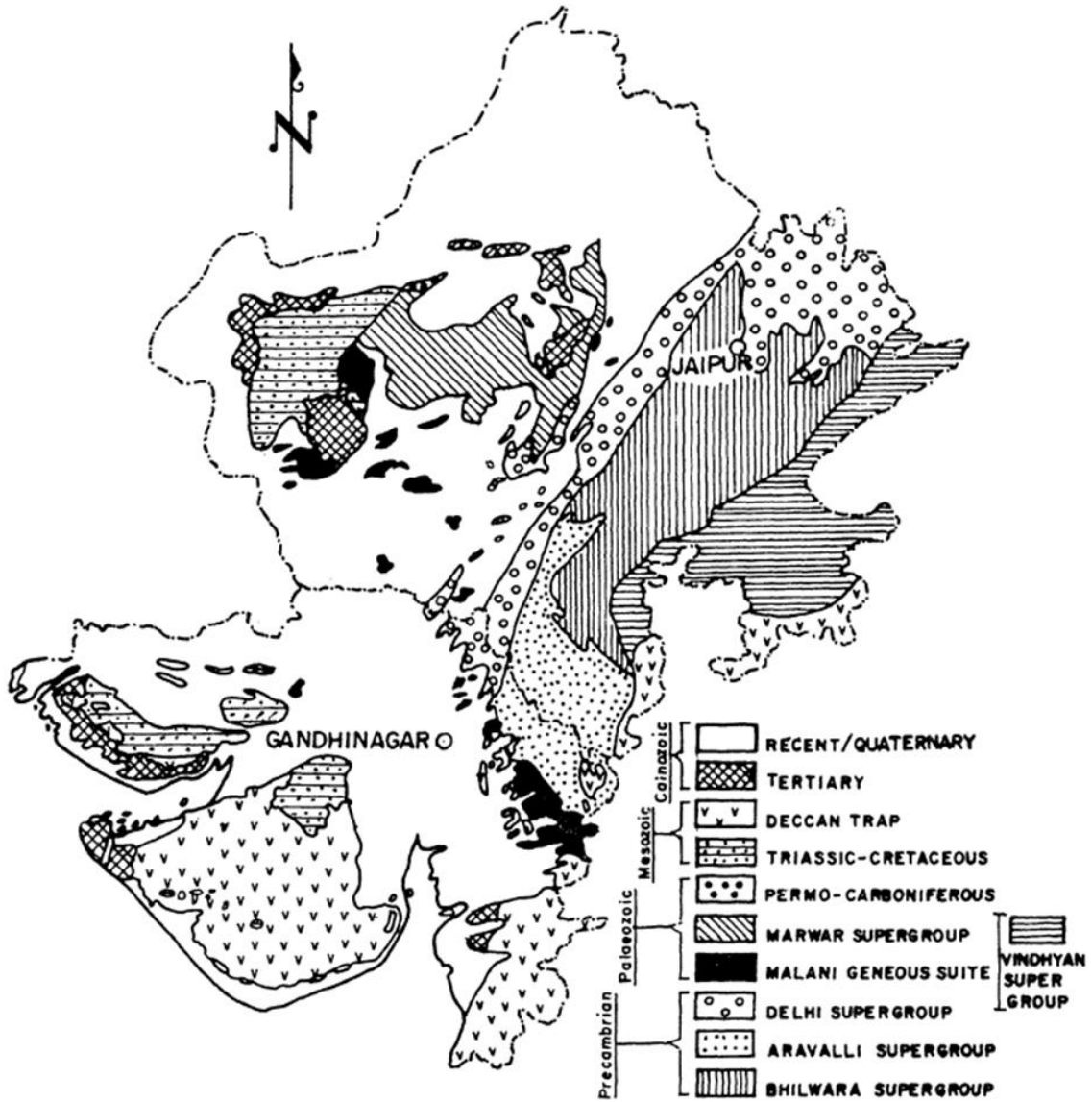
The geological evolution of the Thar Desert, involving both tectonic (crustal accretion, rifting, faulting, basin development, magmatic rock emplacement, ore deposit formation and crustal deformation) and eustatic controls, is complex (Biswas 1987; Roy & Jakher 2001; Laghari 2004). The basic framework is due to the fragmentation of the western Indian Shield, relating to the collision of the Indian and Eurasian plates. To the west, the Iranian Plateau provides evidence of a distinct geological evolution, and the boundary with the Thar Desert, and the Indian tectonic plate, is evident in the sharp drop in relief, associated with the alluvial plains of the Indus.

Broadly SW-NE trending foldbelts led to the formation of the Aravalli and Delhi Supergroups, that form the Aravalli Range (Figure 4.1). The present Aravallis are merely a stub of the most ancient hill ranges in South Asia, and their northward extension, the subsurface Delhi-Haridwar ridge, appears to be the watershed between the Himalayan rivers flowing to the Arabian Sea and the Bay of Bengal (Roy & Jakher 2001). The Aravalli and Delhi Supergroups are comprised of quartzites, limestones, granites, gneisses and schist, and in some areas, the underlying Archean banded gneiss complex is present, although mostly to the east of the Aravallis and beyond the scope of this study.

To the west, in the area surrounding Pali, Sojat and the east of Jodhpur, extrusive granites, rhyolites and gneiss's have formed in the late Proterozoic, referred to as the Malani Igneous suite (Laghari 2004). Malani volcanics are also widely observed in District Barmer, at a number of locations within the Luni Valley, as well as at Nagar Parker in Pakistan (GSI 1999; Laghari 2004). However, this extrusive formation is heavily buried by both geological and sedimentation.

GEOLOGICAL SURVEY OF INDIA
LITHOSTRATIGRAPHIC MAP OF RAJASTHAN AND GUJARAT
 SCALE

km 100 0 100 200 300 km



(Map source: Rec.Geol.Surv. Ind., 1989, V-122, Pt.7, Ext. Abs. F. S. 1987-88)

Figure 4.1: Geological map of Rajasthan and Gujarat (Bakliwal & Wadhawan 2003; Figure 1).

Central Rajasthan is dominated by the Marwar supergroup, which includes a suite of Palaeozoic geological formations that overlie the Malani igneous formations, forming the dominant source of relief in the Bikaner/Nagaur/Pokaran Basin (Pandey & Bahadur 2009). The Marwar Supergroup comprises of the Nagaur Group, formed of sandstone, siltstone and claystone, the Bilara Group, formed of cherty dolomitic limestones and inter-bedded dolomites and limestones, and the Jodhpur Group, formed of gritty sandstones (Kumar & Pandey 2010). These are dominantly sedimentary formations laid down within marine conditions (Pandey & Bahadur 2009). Again, although the Marwar supergroup is known to have a wide spatial extent, its appearance above the swathes of quaternary sediments is much more limited.

Further west, a range of Mesozoic formations are apparent within the Jaisalmer Basin, presenting further evidence for marine sedimentation in the form of sandstones, limestones and claystones (GSI 1999). These are topographically more prominent than either the Marwar or Malani groups, and hence have not been buried so heavily by alluvium or dune sands. The Rohri Hills (Sindh) are the deeply dissected remnant of a limestone plateau that may share a common origin with the sedimentary formations of the Jaisalmer basin. However, their appearance in the modern landscape appears to relate to neotectonic uplift of these bedded limestones above the surrounding alluvial plains of the Indus, which otherwise lack substantial geological outcrops (Biagi & Cremaschi 1988). To the south, sedimentary Mesozoic formations provide some relief in mainland Kachchh, presenting a similar range of geological materials. However, Saurashtra is dominated by Deccan Trap, forming flat topped ridges with extensive wall-like dykes protruding from the surface (Chamyal et al. 2003). Although limestones also occur here, the geology is dominated by Deccan volcanic formations (Chamyal et al. 2003), i.e. basalts and dolerites.

Two large exposures of largely quartzitic boulders are present in the Thar Desert, seen at Bap and Jayal. These present upstanding fluvial features and are most likely to have been deposited by a powerful and coherent river draining the Himalaya and Karakorum ranges. They are both currently upstanding features of the landscape, raised above surrounding recent sediments, due to both cementation of these deposits and the lack of a suitable agency to mobilise these clasts, which measure upto 30cm (Misra 1995). The Bap boulder bed is suggested to have been laid down prior to the development of the Jaisalmer basin Mesozoic formations during the Permo-Carboniferous period (GSI map). The Jayal Gravel ridge is argued to have been the product of a tectonically disrupted fluvial regime from the early Pleistocene (Misra 1995) potentially an ancient course of the Ghaggar.

Quartz and various crypto-crystalline raw materials, such as chalcedony and jasper, are also present in the Thar Desert, occurring as outcrops within other geological formations and as fluvially transported gravels. Outcrops of these materials within other rock types offer increased diversity of raw materials available for exploitation although crypto-crystalline lithic sources tend to be more limited in size and availability than the typically coarser parent geology. Fluvial transported gravels offer more limited prospects for use as a raw material resource due to size limitations, although they may have been significant within a landscape blanketed in quaternary sediments.

The geology of the Thar Desert will have structured the raw materials available and employed by Pleistocene hominins. Large areas of the Thar lack access to substantial lithic raw material sources as they are covered in quaternary sediments, suggesting that their occupation, or at least the intensity of occupation, may be limited by potential to import raw materials or to exploit smaller lithic packages. Most notably, it is the lower alluvial plains of the major rivers that present the least diverse and available raw material sources, although these may have offered other desirable resources, including water, flora and fauna.

Modern Ecology of the Thar Desert

Under modern conditions, true arid desert, defined by annual rainfall of <150mm, is confined to the west of the Thar region (see Figure 4.2). The current zone of sand dune mobility is too heavily impacted by pastoral and agricultural activity to offer clear information with regards to how similar activity should be inferred in the past. However, the presence of sand dunes far beyond the modern arid zone indicate that sufficient wind speeds (>6m/s) and sediment supply were, at some remote period, available across the Thar Region.

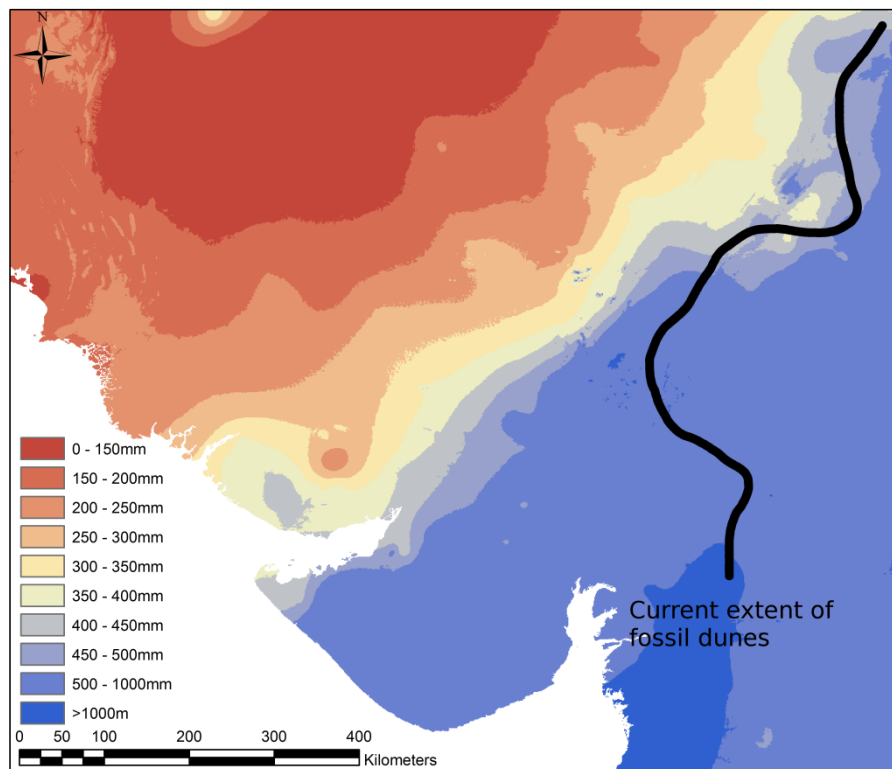


Figure 4.2: Isohyet map of average annual rainfall (1950-2000) in the Thar Desert indicating eastward extent of sand dune formations.

Similarly, it is difficult to disentangle endemic ecological patterns from the various and increasingly intense anthropic influences on the Thar Desert. Irrigation-fed agriculture, groundwater pumping, hunting, introduction of assorted livestock and fossil-fuel explorations are all disrupting the ecology of the Thar Desert, and on the whole this impact is greatest upon

arid-adapted species (Idris et al. 2009; Sharma & Mehra 2009). The Orsang, Mahi, Sabarmati and Indus rivers remain perennial fluvial features in the Thar region, whereas both the Gharggar-Hakra and Luni Rivers are only active during the monsoon season, receding into fragmented, saline pools during the dry season. Despite their present salinity, the lakes of Rajasthan present reserves of biotic diversity in the Thar Desert, although after the monsoon numerous localised pools form in disrupted drainage channels, which evaporate leaving a saline crust.

Flora

The floral communities of the Thar Desert are dominated by xerophytic varieties that are capable of tolerating extreme fluctuations in moisture availability and temperature, and myriad edaphic settings. Arid and semi-arid regions, covering most of the Thar Desert, are grasslands dominated by associations of *Dicanthium-Lasiurus-Cenchrus*, with patchy xeromorphic woodland including stunted, thorny or prickly shrubs and perennial herbs which are resistant to drought (Sharma & Mehra 2009). Stabilised sand dunes are colonised by a range of psammophytic grasses, such as *Aristida adescensionis*, and shrubs such as *Calotropis procera*, *Acacia senegal*, and *Prosopis cineraria* (Shetty 1994). The upland areas, principally within the Aravallis and Saurashtra, but also dotted across the Thar, are covered with mixed xeromorphic thorn forest and with dry, deciduous species present. Aquatic habitats include the salt lakes and Raans of Kachchh, which are often seasonally inundated, and their margins dominated by a range of grasses and sedges, such as *Eleusine compressa*, *Eragrostis ciliaris* and *Dactyloctenium aegyptium* (Sharma & Mehra 2009).

Fauna

The Thar Desert exhibits a high biodiversity amongst its native fauna, due in part to the location at the juxtaposition between different biogeographical zones, and heavily influenced

by the Thar Desert lakes that offer suitable habitats for migratory avifauna from northern Asia (Sharma & Mehra 2009). Over 250 bird species are known from Rajasthan alone, including vultures and the endangered Indian Bustard, as well as migratory species that include the Imperial sand grouse, houbara and demoiselle crane (Sharma & Mehra 2009). Sixty-eight mammals are known to inhabit the Thar Desert, and although smaller creatures such as gerbils, hares, squirrel and porcupines are adapted to extract sufficient water from their food, the range of larger mammals is heavily restricted by water availability (Sharma & Mehra 2009). Both the Asiatic Lion and Asiatic cheetah were present in the Thar before the 20th century, and other prominent carnivores include the desert cat, caracal, desert fox and wolves (Sharma & Nehra 2009). Amongst the herbivores, chinkara (Indian desert gazelle), nilgai (blue bull) and blackbuck are notable, whilst the grasslands of Kachchh offer the final preserve for the Wild Ass (Sharma & Nehra 2009). Snakes and lizards are well represented in the region, particularly capitalising upon the temperature stable environments that exist within burrows in sand dunes, which also support insect communities, such as the dung beetle (Rao 2009). Beyond this, crocodiles and turtles are known from the Thar, as are twelve desert adapted amphibians. Halophytic invertebrate populations thrive in the salt lakes of the Thar Desert, feeding upon similarly salt-tolerant algae and bacteria, and providing a key nutritional resource for both migratory and non-migratory fauna (Kumar 2008).

Modern perspectives on environmental change

Unsurprisingly, access to water is a major determining factor in the distribution of modern flora and fauna, although soil salinity is also a major issue. Most grasses sprout following the onset of the monsoon and reach maturity by the end of the monsoon, although different grasses appear to prosper with different levels of soil humidity (Rao 2009). Shrubs and trees currently provide vital fodder for herbivores during periods of drought, as they are capable of

drawing upon deeper water resources. For considering past faunal resources within the Thar Desert, it is important to realise that different fauna have specific dietary requirements, and species such as chinkara particularly focus upon grasses with high nutrient and water contents.

Two modern examples of the impact of fluctuating water availability are, perhaps, illustrative as to what types of impacts palaeoclimatic change may have had. The significance of soil condition for the overall health of an ecosystem, measured in both number of herbaceous species and overall vegetal biomass, has been illustrated from a case study in Gujarat. Here, significant changes to floral composition occur with increasing sand content in soils, relating to decreased capacity to hold water (Pandey et al. 1999). Increasing concentrations of calcium, magnesium, potassium and sodium, and decreasing concentrations of carbon, nitrogen and phosphorus, were a concomitant change in areas facing increasing aridification and soil moisture fluctuations, putting further pressure on non-halophytic flora (Pandey et al. 1999). Soil texture and mineral composition may be critical for a given area to respond rapidly to increasing humidity, with soils that already include higher proportions of silts and clays best suited to encourage ecosystem recovery.

A second case-study comes as a result of the Indira Gandhi Nahar Project, which has involved the construction of a massive canal delivering Himalayan water to central Rajasthan for irrigation purposes. In numerous locations, significant leaks in irrigation channels have formed inter-dunal accumulations of surface water as well as driving up local ground water levels, permitting the expansion of hydrophytic flora (Sivarperuman & Baqri 2009). This in turn has promoted an increase in insect and other invertebrate populations (Sivaperumen & Baqri 2009), offered both fodder and water for herbivores, such as nilgai (Figure 4.3), chikara and wild boar (Dookia et al. 2009; Sharma & Mehra 2009) and suitable feeding and breeding grounds for numerous avifauna (Idris et al. 2009; Sivaperuman et al. 2009). The extension of irrigation canals into the Thar Desert cannot provide a simple analogy for the return of humid

conditions in the Thar, but it does illustrate that both flora and fauna rapidly capitalise upon the availability of freshwater supplies.



Figure 4.3: A nilgai and cow by a canal that dissects the otherwise dry, sand dune-dominated plains at Chamu.

Palaeoenvironments of the Thar Desert

Broad scale climatic trends in the Thar Desert are influenced by two global factors: orbital-scale climate change and the South Asian monsoon system. These provide explanations of the overarching patterns of climatic change throughout the Late Pleistocene that are significant beyond the immediate region under consideration. The terrestrial palaeoenvironmental proxy record of the Thar Desert, on the other hand, presents evidence for how the impact of orbital-scale climate change and monsoonal variability were manifest in the Thar Desert.

Global Explanations of Late Pleistocene Climate Change

Orbital Climate Change

Orbital factors appear to have had the dominant effect upon global Pleistocene climates, driving the glacial-interglacial cycle. Put simply, variations to the Earth's orbit, namely precession, obliquity/tilt and eccentricity, vary the seasonal and latitudinal distribution of solar radiation, which promote the development or decay of continental ice sheets (Cronin 2010). The formation of continental ice masses results in the preferential uptake of the lighter ^{16}O isotope, leaving marine (and therefore meteoric) water reserves enriched in ^{18}O (Cronin 2010). The ratio of $^{18}\text{O}:^{16}\text{O}$, relative to a standard (SNOW) and expressed as $\delta^{18}\text{O}$ ‰, therefore indicates patterns of relative cool/arid vs. warm/humid, which, following the study of deep sea marine cores and various ice-cores, has led to the definition of Marine Isotope Stages (MIS) (Cronin 2010). The production of stacked oxygen isotope records averaged from numerous cores, most notably SPECMAP (Figure 4.4) (Imbrie et al. 1984), that have been tied in to a range of absolutely dated phenomena present a significant means to correlate other forms of palaeoenvironmental proxies (Cronin 2010).

Through the study of orbital-scale palaeoclimatic records, a number of cycles are evident. Berger & Loutre (1991) identified precession driven cycles occurring every 19ka and 23ka, a 41ka obliquity cycle, and eccentricity cycles occurring every 100ka and 400ka. Notably, within the Middle and Upper Pleistocene oxygen isotope records indicate interglacials occurring in phase with insolation maxima every 100ka, although the significance of greenhouse gas feedbacks may also play an important role (Cronin 2010). Numerous proxies now exist that detail broad patterns of palaeoclimatic change during the Pleistocene, recording concentrations of greenhouse gases, sea-surface temperatures, glacio-chemical patterns etc. (Cronin 2010). However, for the scale of analysis undertaken within this thesis, the glacial-

interglacial regime can broadly be inferred to indicate cooler, drier conditions during glacial phases, and warmer, humid conditions during interglacial phases.

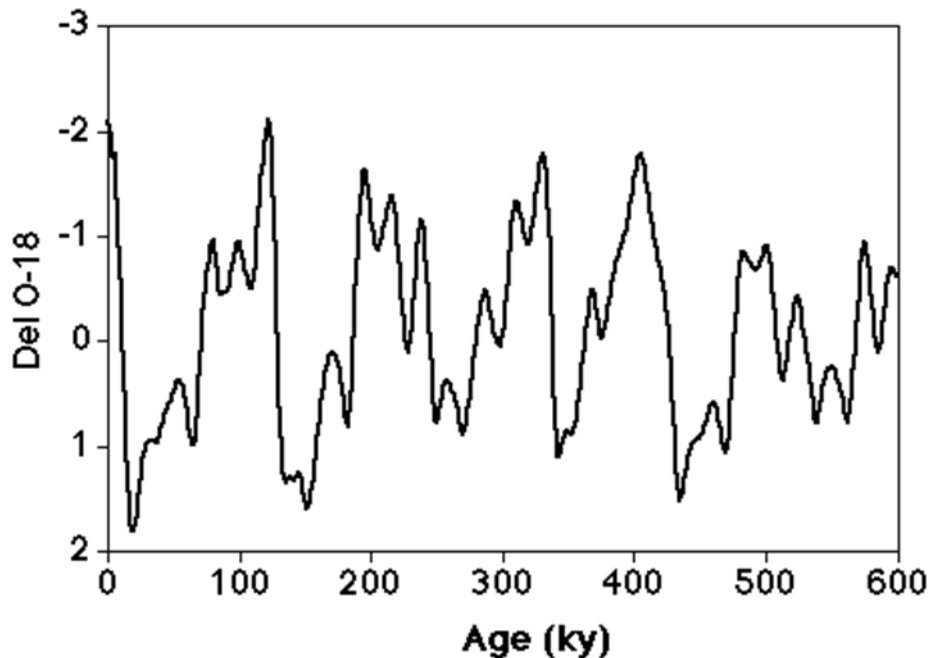


Figure 4.4: SPECMAP stacked $\delta^{18}\text{O}$ record for the past 600ka (following Imbrie et al. 1984).

The South Asian Monsoon System

The South Asian Monsoon System has the dominant effect on environmental conditions within the subcontinent today, and the presence of monsoon conditions across much of South-East and East Asia has resulted in much shared biota of the Oriental biogeographic zone. The monsoon system is driven by a cross-equatorial atmospheric pressure gradient, resulting from differential heating of the Asian landmass, principally the Tibetan Plateau, and the Mascarene high pressure zone in the southern Indian Ocean (Clemens et al 1991; Leuschner & Sirocko 2003). This leads to a unique cross-equatorial transfer of heat and momentum bringing strong southwesterly winds to South Asia, which also deliver the majority of the subcontinent's precipitation as a result of evaporation from the Arabian Sea (Clemens et al 1991; Leuschner &

Sirocko 2003). The relative cooling of the Tibetan Plateau over winter results in a weaker, north-easterly wind that delivers significantly less precipitation and this is more regionally restricted (Clemens et al 1991; Leuschner & Sirocko 2003).

The standard model for relating the South Asian Monsoon System to the orbitally induced glacial-interglacial scheme of palaeoclimate change suggests that the 100ka peaks of solar insolation relating to interglacial periods should also correlate with maximum monsoonal intensity, and minimal monsoonal intensity occurs during troughs in solar insolation relating to glacial maxima (Liu 2011). Moving beyond this simple correlation, a monsoonal index has been developed by Leuschner and Sirocko (2003) that acknowledges the influence orbital factors of precession, tilt and eccentricity would have at 30° N, which may be significant for understanding SST's and rates of evaporation, relevant both to the strength of monsoonal winds and precipitation (Figure 4.5).

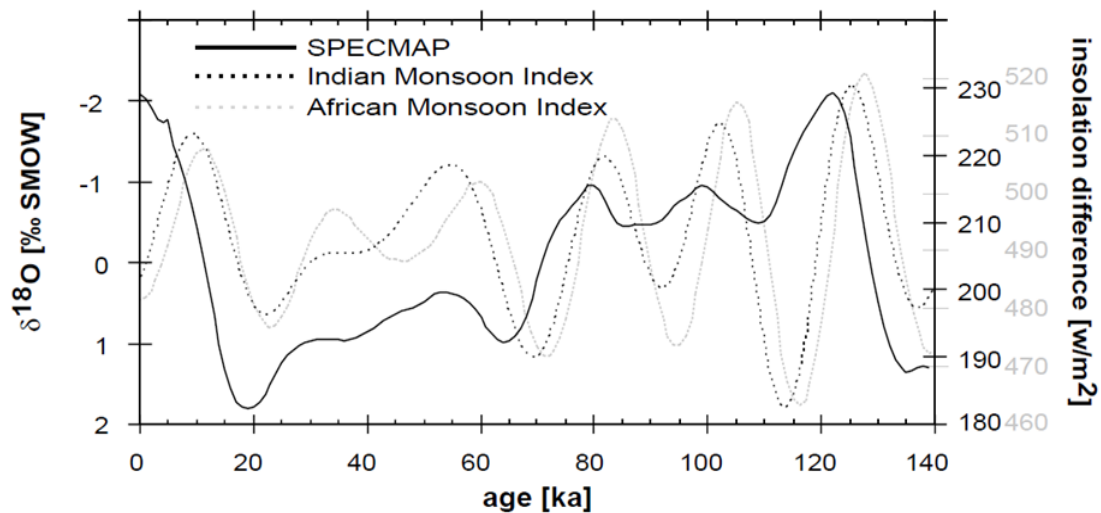


Figure 4.5: The Indian Monsoon Index compared with the African Monsoon Index (grey scale on the right) and the Specmap oxygen isotope record for the last 140ka (Leuschner & Sirocko 2003; Fig. 4).

However, recent research by An et al. (2011) has indicated further complexity within the monsoon system due to its interaction with both southern and northern hemisphere climatic patterns. This suggests that although maximum monsoonal intensity occurs in phase with the

interglacial maximum every ca. 90ka, the minimum monsoonal intensity occurs ca. 20ka prior to the glacial maximum, by which point monsoonal intensity has already begun to intensify (Figure 4.6)(An et al. 2011; Liu 2011). Interestingly, this implies that although (relatively) higher SST's and rates of evaporation were locally present in the Arabian Sea during MIS 3, weaker winds related to the monsoonal minimum may have been less able to deliver precipitation inland. Conversely, strengthening monsoon winds would have been present over the LGM, although reduced SST's and rates of evaporation may have limited potential precipitation.

Terrestrial Proxies for Palaeoenvironmental conditions in the Thar Desert

A range of chronometrically dated palaeoenvironmental terrestrial proxies are available to illuminate the impact that orbital-scale climate change and the waxing and waning of monsoonal intensity within the Thar Desert. The most widespread and deepest records are presented by fluvial and aeolian sequences. More chronologically and geographically restricted records of climate change are presented by the lacustrine record and proxies for eustatic changes. I will present a synthesis of the terrestrial palaeoenvironmental evidence from the Thar Desert focusing predominately upon evidence from MIS 6-2.

Fluvial Records

Beyond providing evidence for the response of riverine systems to climate change, fluvial records are also significant for understanding the availability of water resources for flora, fauna and hominins. Two exogenous rivers have flowed through the Thar Desert. The Indus and Ghaggar-Hakra rivers drain the Tibetan Plateau and Himalaya before debouching in the Arabian Sea, drawing minimal additional waters in their lower reaches as it flows through the

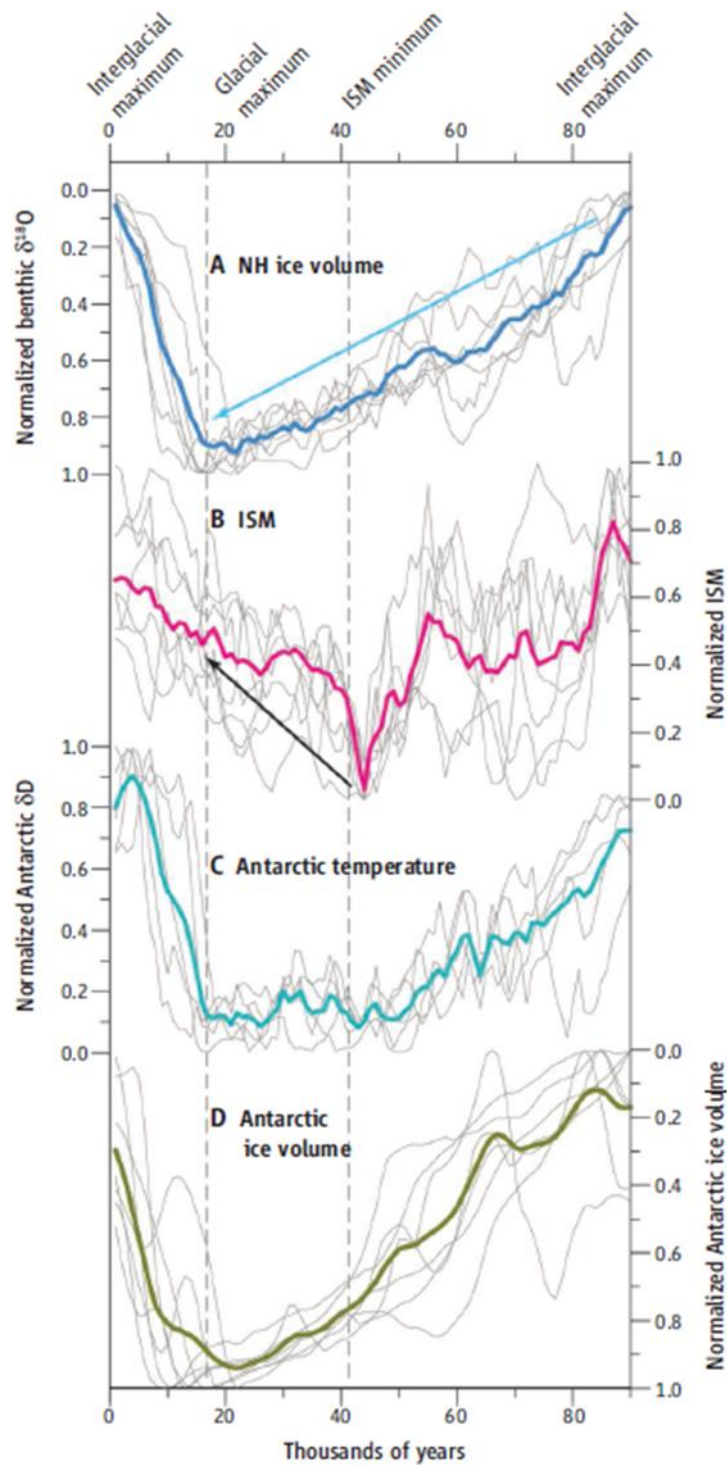


Figure 4.6: Indian Summer Moonson (ISM), temperatures, and ice. Reconstructed trends in (A) Northern Hemisphere ice volume, (B) ISM intensity, (C) Antarctic temperatures, and (D) Antarctic ice volumes over the last 90ka. Comparing the curves shows that the ISM started to strengthen before ice volumes reached their maxima. (A), (B) and (D) cover seven glacial-interglacial cycles; (C) covers five cycles. Thin gray lines illustrate each event; thick coloured lines represent the mean. The magnitude of each event is normalized. Time is also normalized:

It is reset with the seven ISM minima lined up at 41 thousand years ago; each cycle is then rescaled so that the time between the ISM minimum and maximum becomes the average time of all seven events. The cycle between 700 and 780 thousand years ago was not included because it has a prominent interstadial during the glacial period (following Liu 2011).

arid Thar landscape. A number of endogamous rivers are also present, and the largest and best studied rise from the Aravallis, including (from north to south) the Luni, Banas, Saraswati, Rupen, Sabarmati and Mahi rivers. Additionally, the Orsang, currently a tributary of the Narmada, will be considered as it may represent the captured headwaters of the Dhadar River. A number of smaller rivers rise in the uplands of Saurashtra and Kachchh and drain in a radial fashion, as both are surrounded by low-lying terrain. However, remote sensing studies have illustrated that fluvial networks in the Thar Desert have been much more extensive than at present (Rajawat et al. 2003; Gupta et al. 2011), which are likely to have developed under consistently humid regimes that promote more stable fluvial systems (Figure 4.7).

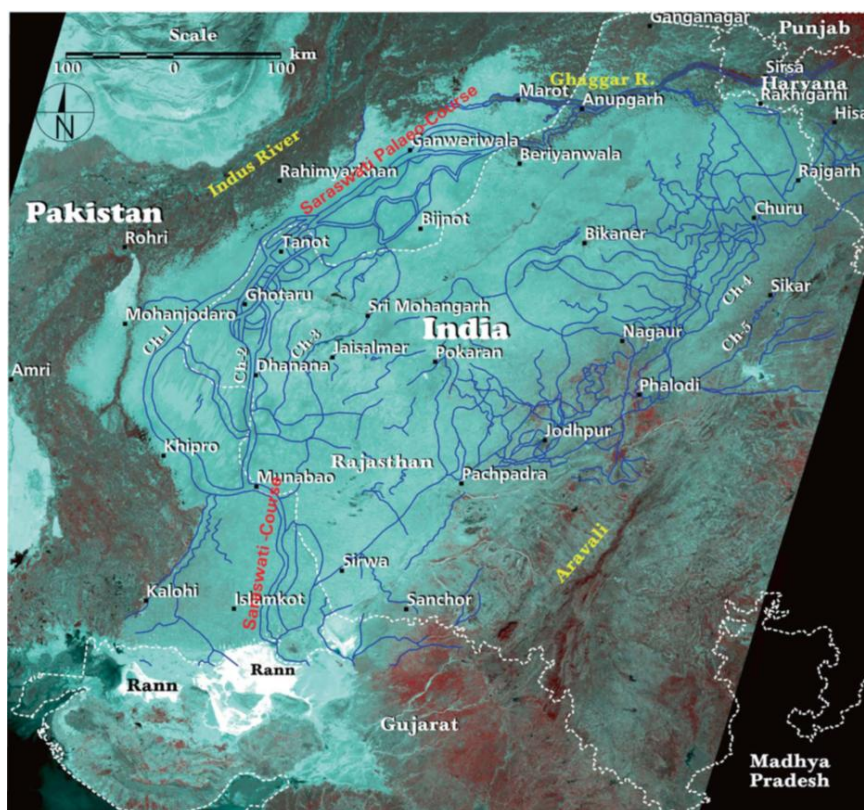


Figure 4.7: Map of palaeodrainage network in the Thar Desert (Gupta et al. 2011).

Exogenous Rivers

Unfortunately, there is little clear, well dated evidence for the behaviour of either the Indus or the Ghaggar-Hakra Rivers from the Thar Desert during MIS 6-2, partly due to the high rates of alluvial sedimentation that have occurred during the Holocene. The presence of inland delta formations in the Rann of Kachchh as well as patterns of terrigenous sediment supply and incision in the Indus marine fan indicate that eustatic changes have had some impact upon these fluvial regimes (Prins et al. 2000; Roy & Jakher 2001). The modern Indus discharge is heavily dependent upon melt waters, which contribute over half of downstream waters (Immerzeel et al. 2010), although the nature of balancing output with sediment discharge within and between the upper and lower stretches of the Indus remains understudied.

The westward migration of the Ghaggar-Hakra River is suggested by the sequence of palaeochannels evident in remote sensing surveys, perhaps indicating this river once flowed through central Rajasthan and connecting with the Luni (Rajawat et al. 2003; Gupta et al. 2011). The chronology of this migration is not constrained, although recent tectonic impacts on other rivers indicates this certainly should be considered as a potential cause. A more tangible aspect of the influence of these rivers palaeoenvironmental role in the Late Pleistocene is as presenting a source of material for aeolian mobilisation. Through a range of geochemical analyses, Tripathi et al. (2004) suggest that Ghaggar-Hakra alluvium is found as reworked aeolian deposits throughout the Thar Desert.

This is unfortunate as these two rivers may have been critical in preserving flora and fauna in the desert during periods of heightened aridity as, unlike the endogamous rivers, they deliver waters from a reliable source, i.e. Himalayan melt waters. As a result, these two rivers present potential source populations for the re-colonisation by biotic populations of deserted areas with the return of more humid conditions.

Endogamous Rivers

Luni River

Currently, the river is seasonal, flowing principally during and directly after the monsoon period, after which the surface waters fragment into isolated ponds, although a period of deep incision, apparently occurring in the Holocene wet phase presents large cliff sections in a number of areas in which the Late Pleistocene behaviour of the Luni can be discerned. In a study of six sections from the Mid-Luni Valley, Jain et al. (2005) have defined two distinct alluvial successions (Figure 4.8). The first (Type 1) consists of an extensive suite of vertically stacked, upward fining cycles deposited by gravelly braided streams that progress to form floodplain facies, but these were beyond the age range of the applied OSL techniques to >300ka (Jain et al. 2005). While the occurrence of cemented gravels at the base of the sequence from Chamu may not directly relate to the Luni drainage system, it occurs underlying a date of 155ka, offering broad support for fluvial activity during the Mid-Pleistocene (Dhir et al. 2010).

The second sequence (Type 2) illustrates depositional environments dating from MIS 5-1. Humid phases are evidenced during MIS 5 by the deposition of braided stream channel deposits, during MIS 5, dating to >86ka and 86ka at Khudala and >79ka and 79ka at Karna (Juyal et al. 2005). A period of pedogenesis is chronologically constrained to the period ca. 70-30ka, and ephemeral stream deposits are evident at the transition between MIS 3-2 (Jain et al. 2005). The appearance of aeolian horizons at 27ka indicates significant decline in fluvial activity, with incision ca. 22-14ka and the deposition of gravel braided, mixed load meandering and ephemeral sand bed channel deposits between ca. 14-8ka indicating the considerable fluvial flux with the transition from MIS 2-1 (Jain et al. 2005).

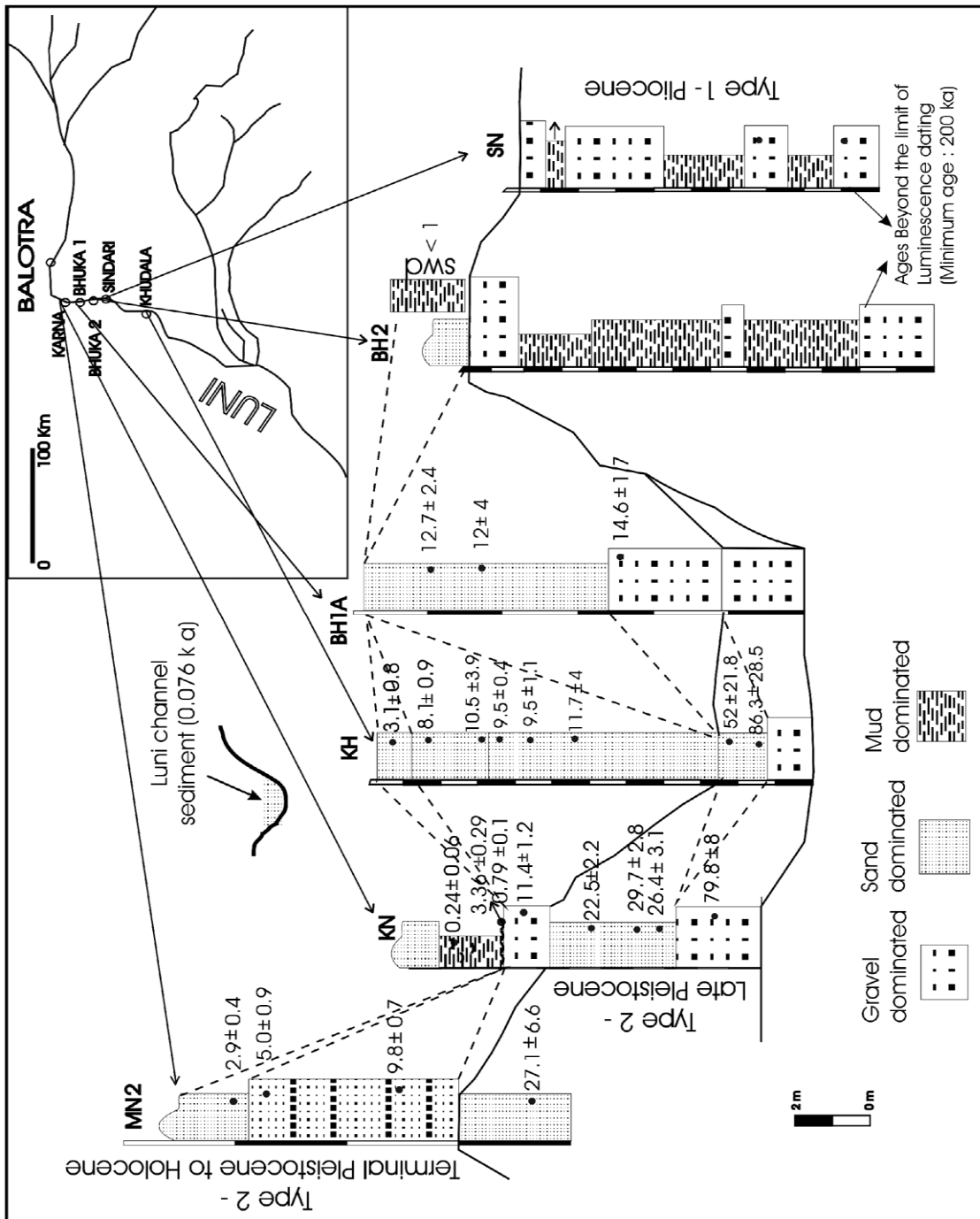


Figure 4.8: Physical stratigraphy and OSL chronology of Quaternary alluvial successions in the mid-Luni Valley (Jain et al. 2005; Figure 7).

Eastern Gujarati Rivers

The Sabarmati (Figure 4.9), Mahi (Figure 4.10) and Orsang (Figure 4.11) rivers display considerable similarities in their responses to Late Pleistocene climate change. Geographically, they all rise in the Aravallis and pass through buried pediments and alluvial plains before debouching in the tectonically structured Gulf of Cambay. The start of observable fluvial sequences in all three valleys extends beyond reliable chronological dating, including floodplain deposits and cross stratified gravels >98ka at Bahadurpur and Aritha (Orsang)(Juyal et al. 2005), a conglomerate horizon at Vijaypur (Sabarmati)(Tandon et al. 1997), and pedogenised marine clays, cross stratified gravels and pedogenised floodplain facies >74ka at Rayka (Mahi)(Juyal et al. 2000; 2005). These are all most likely to relate to interglacial conditions during MIS 5, with the marine clay at Rayka (Mahi) related to high sea levels in MIS 5e (Juyal et al. 2000).

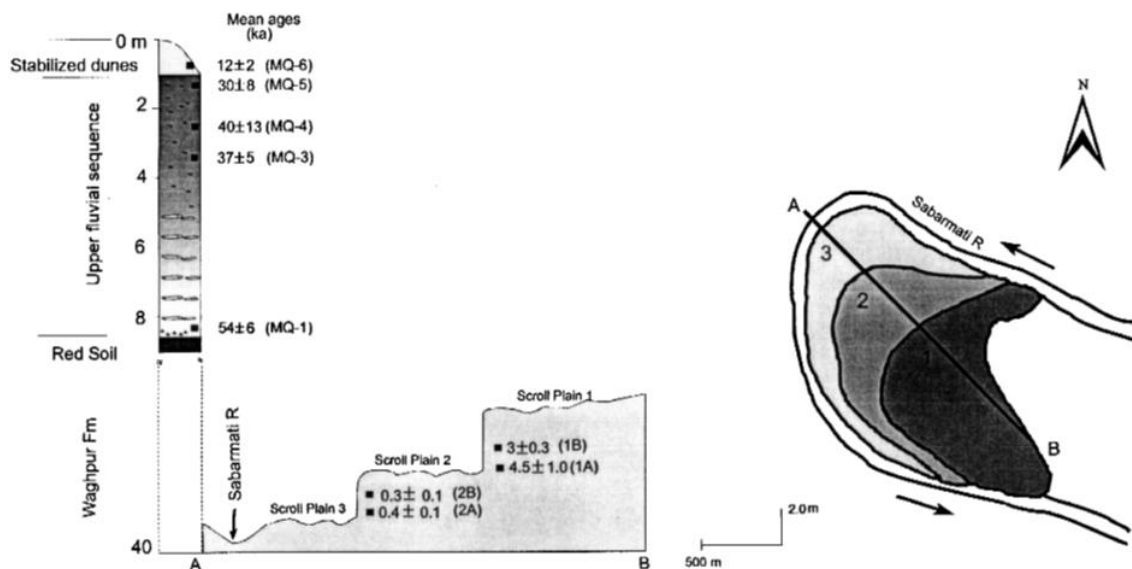


Figure 4.9: Stratigraphy and chronology of fluvial and aeolian sediments in the Sabarmati Valley (Srivastava et al 2001; Fig. 3).

Dated horizons from MIS 5 include evidence for low sinuosity channel deposits with bedded calcretes dating to 98ka from Aritha (Orsang), and a cross-stratified gravel, dating to 74±24ka

at Rayka (Mahi)(Juyal et al. 2005). The only dated deposits from MIS 4 come from the Orsang valley, where two sites present evidence for the development of a wide, shallow bedload river, dated to 69-60ka at Bahadurpur and 62ka at Aritha (Juyal et al. 2005).

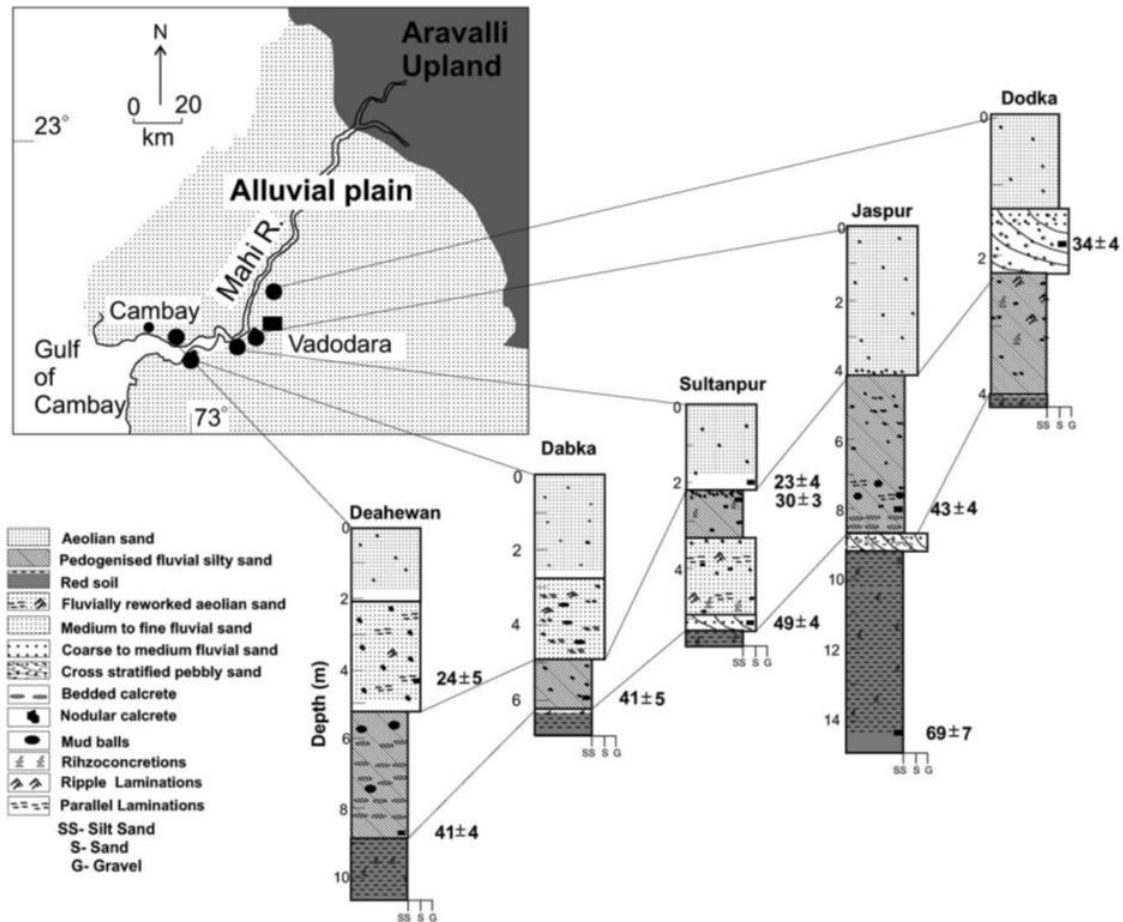


Figure 4.10: Stratigraphic details and BGSL ages of the upper fluvial and aeolian succession resting on the marker red soil in the lower Mahi basin (Juyal et al. 2005; Figure 5).

Palaeoenvironmental conditions during MIS 3 are much more richly attested to in all three valleys. In the Orsang Valley, pedogenised silty sand is interpreted to have been deposited in a flood plain setting, dating to 48ka at Bahadurpur, suggesting reduced fluvial discharge, and the lack of further deposition permitted pedogenesis and possible channel avulsion (Juyal et al. 2005). In the Mahi Valley, the appearance of cross-stratified gravels at Sultanpur dates to 49ka (Juyal et al. 2005). Thick weathered deposits are seen at all sites in this study, indicative of a persistent fluvial regime promoting floodplain development dating between 43-41ka at the

bottom of the deposit, and 30ka at the top (Juyal et al. 2003; 2005). Stable periods following deposition permitted the exposure of floodplain sediments to sub-aerial weathering (Juyal et al. 2005). A further cross-bedded gravel is present at Dodka at 34ka (Juyal et al. 2005). In the Sabarmati valley pale red sands are dated to 58ka, and reddening is suggested to occur prior to the deposition of an overlying fine silty sand with an erosional contact, dating to 39ka Pushpawati (Tandon et al. 1997). The sequence at Pushpawati is capped by undated floodplain and reworked aeolian sediments (Tandon et al. 1997). At the base of the sequence at Mahudi, this formation is dated to 54ka, and 40ka, 37ka, and 30ka toward the top at this site (Srivastava et al. 2000). Thick bedded calcretes are seen at the base of these deposits at Mahudi, suggesting a fluctuating water table, and moderate pedogenesis is evident toward the top (Srivastava et al. 2000).

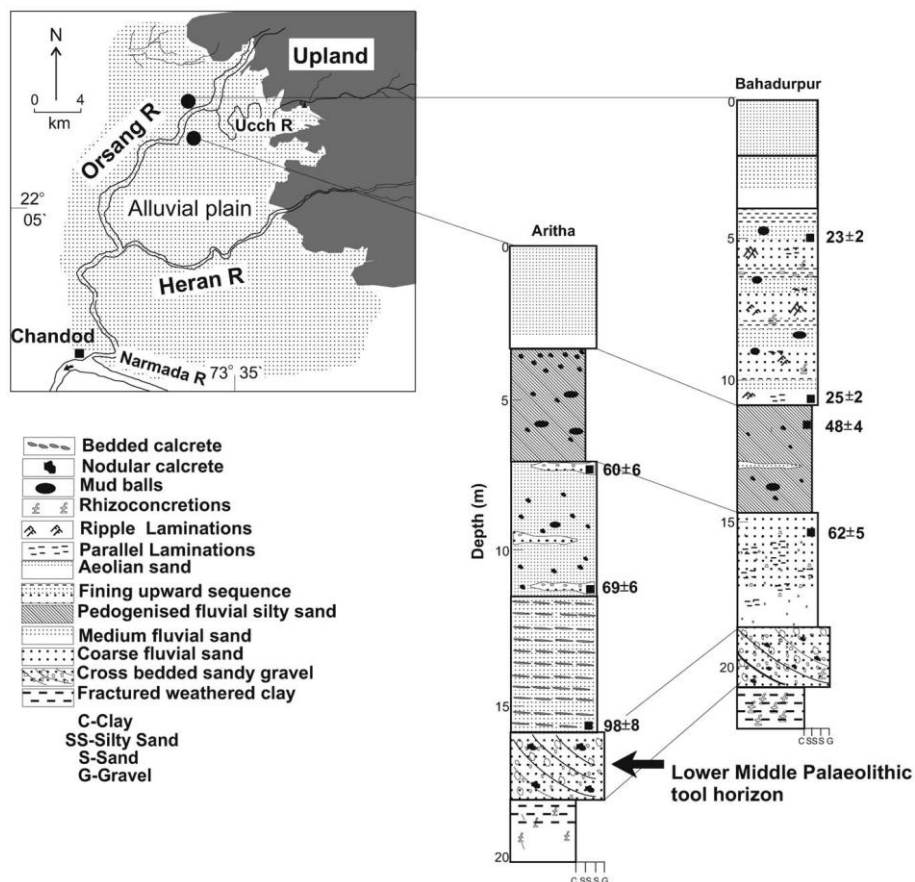


Figure 4.11: Stratigraphic details and BGSL ages of Late Quaternary sediment succession in the Orsang Valley (Juyal et al. 2005; Figure 6).

A sequence of 4 upward fining deposits occur at Bahadurpur (Orsang), dating to 25-23ka, that are suggested to have been deposited by streams, originally scouring the underlying deposit to reach the trunk channel, with fluvial sands deposited during flood conditions, gradually fining to silts and clays toward the end of flooding (Juyal et al. 2005). In the Mahi Valley, fluvial reworking of aeolian sands form distinctive units at Deahewan, at 24ka, and Sultanpur at 23ka (Juyal et al. 2005). In all three valleys, there has been a period of aeolian deposition that caps these fluvial sequences (discussed below), which appear to have been revealed as a result of post LGM incision.

Saurashtra and Kachchh Rivers

In contrast to the Eastern Gujarati rivers, the fluvial geomorphology of Saurashtra and Kachchh offers little well dated evidence for investigating palaeoenvironmental variability. In both areas, debates surrounding Quaternary deposition have been heavily dominated by the miliolite question (see below). As a result fluvial sequences in Saurashtra and Kachchh are known to occurring before, during and after the broad period of miliolite formation (Bhatt & Bonde 2006; Chowesky et al. 2011), but are otherwise poorly understood. An exception to this is the study of fluvial sequences on the southern margin of the Kachchh mainland. Following the study of numerous fluvial sequences to the south of the Katrol hills, Maurya et al. (2008), document cross stratified gravels covered by red/brown soils, with an overlying and erosive sandy gravel and weakly pedogenised sandy silt (Figure 4.12). Dated pedogenic carbonates from Geladia and Kothara indicate the pedogenesis of the red/brown soils occurred prior to 18-22ka (Maurya et al. 2008).

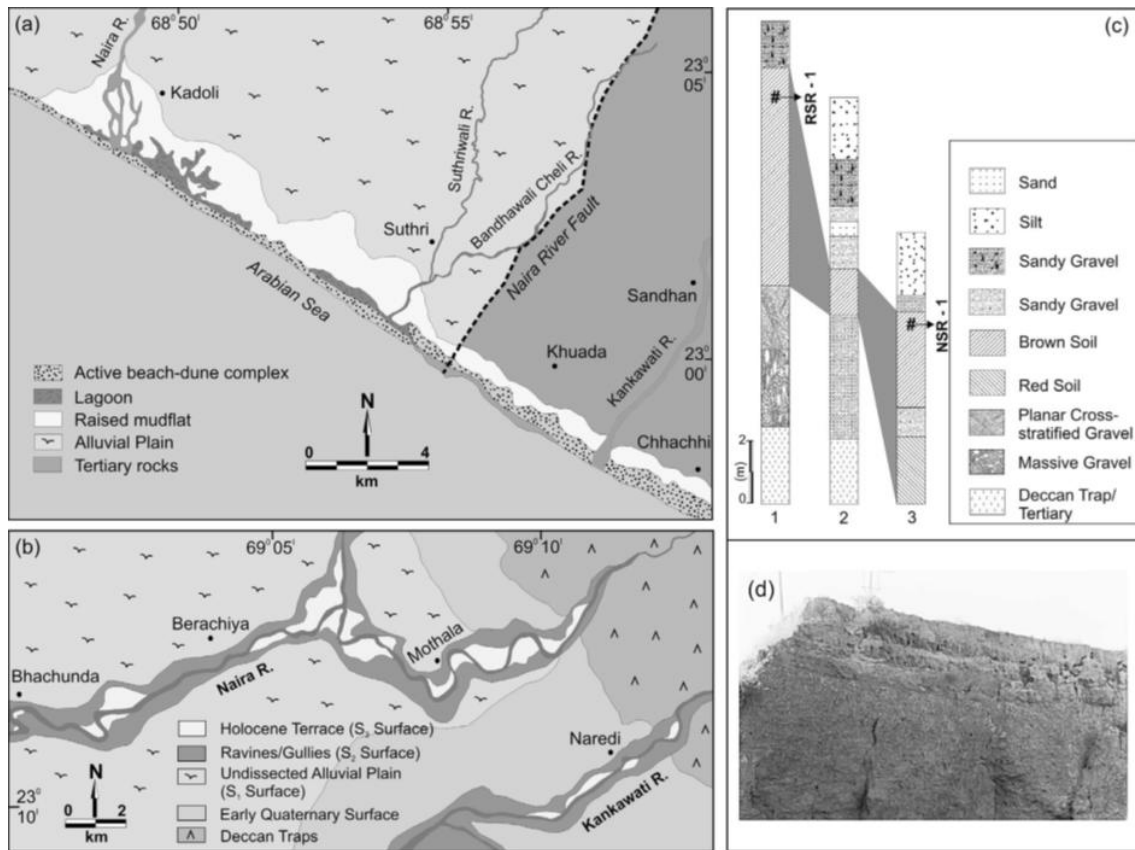


Figure 4.12: Spatial variability of sediments to the south of the Katrol Range, Kachchh, and sediment profiles for sequences from which pedogenic carbonates have been dated (Maurya et al. 2008; Figure 4).

Summary

Amongst the evidence from the endogenous rivers of the Thar Desert, some broad patterns are apparent (Table 4.1). Evidence from MIS 5 suggests that more coherent fluvial networks were present than are apparent today, with periods of stability suggesting limited flux in fluvial output facilitated by well vegetated catchments (Juyal et al. 2005). The only evidence dated to MIS 4 comes from the southernmost river, the Orsang, indicating low intensity fluvial activity, perhaps supporting minimal activity in the more northern rivers. Fluvial activity is widely apparent in MIS 3, although overall it indicates reduced intensity to MIS 5. The end of riverine activity in MIS 3 and at the start of MIS 2 are marked by presence of ephemeral stream channels and fluvially reworked aeolian sands, indicating decreasing discharge and blocked

drainages. The resumption of fluvial activity is first evident in a period of widespread incision that appears to begin after the LGM, although the diverse forms of fluvial activity evident in the Luni Valley, paralleled elsewhere, suggest considerable flux in response to changing climatic conditions at the transition between MIS 2-1.

Period	Inferred environmental processes
MIS 2	Incision and mixed fluvial and aeolian deposition occurring after 22ka; Aeolian deposition and ephemeral sand beds 30-20ka;
MIS 3	Initial increase in fluvial discharge marked by gravel deposits ca 60-50ka, followed rapidly by regional floodplain aggradation and subsequent pedogenesis up to 30ka
MIS 4	Ephemeral fluvial activity and pedogenesis
MIS 5	Braided channel deposition, followed by periods of floodplain aggradation and pedogenesis after 100ka; marine transgression, braided channel deposition, followed by periods of floodplain aggradation and pedogenesis before 100ka

Table 4.1: Summary of fluvial activity in the Thar Desert.

Aeolian Records

Aeolian processes are influenced by a range of factors, of which the supply of material, strength of winds, rainfall, vegetative cover and land surface conditions appear to have the dominant effects (Singhvi & Kar 2004). Although aeolian activity tends to be most dominant in areas of maximum aridity, which prevent high levels of vegetative growth and soil moisture that would otherwise limit sediment mobility, many of the aeolian records from the Thar Desert come from areas beyond the modern arid zone. This is because it is at the edge of the zone of potential aeolian activity that minor changes in climatic conditions are likely to have amplified effects upon sediment stabilisation and pedogenesis or reactivation, whereas at the core of the desert, continual aeolian reworking prevents the same level of preservation (Singhvi & Kar 2004).

Current aeolian activity is promoted primarily by the degradation of sand dunes through agropastoralism within the modern arid zone, providing unconsolidated sediments. The main

period of aeolian activity occurs between March and June, and wind speeds typically reach 20km/hr and above prior to the onset of monsoonal rains, that effectively prohibit further aeolian sediment mobilisation (Singhvi & Kar 2004). Long term weathering of sand dunes, leading to pedogenesis, builds a resistance to remobilisation by increasing sediment cohesion, with higher levels of silt and clay that also promotes vegetative growth, as well as the formation of pedogenic carbonates, as a result of mobilisation and precipitation of calcretes (Allchin et al. 1978; Singhvi & Kar 2004). These factors appear to have been significant in the preservation of widespread sand dunes of the 'old' system compared to the more limited distribution of sand dunes of the 'new system (Kar 1996; Singhvi & Kar 2004), which may simply be too young to have undergone significant weathering.

Dating sand dune formations offers information on both periods and extent of aeolian mobility, which can be directly dated. In addition intervening periods of stability and soil formation, evidenced by weathered profiles and the formation of pedogenic carbonates, can be identified within the brackets provided between episodes of deposition. Evidence of aeolian activity in the Thar Desert is principally available from sand dune sequences, with more regionalised evidence apparent in the formation of miliolites in the coastal areas of Saurashtra and Kachchh.

Sand dunes

The origins of aeolian activity and the Thar Desert itself have been debated, with some suggestions that recent, anthropogenic factors were responsible (see Allchin et al. 1978). However, the dating of aeolian sediments into the Mid-Pleistocene clearly proves the existence of fluctuating aridity within the region over a period of hundreds of thousands of years (Raghaven et al. 1989; Dhir et al. 2010; Singhvi et al 2010). Two sand dune sequences provide evidence for Mid-Pleistocene activity, dating to 187ka and 140ka at 16R Dune (Figure

4.13; Singhvi et al. 2010) and 155ka at Chamu (Figure 4.14: Dhir et al. 2010). These sites also provide the only dated evidence for aeolian activity during MIS 5, with aggradational events occurring both before (Unit III) and between (Unit IV) 81-105ka at Chamu (Dhir et al. 2010) and at 130-109ka and 80k at 16R Dune (Singhvi et al. 2010).

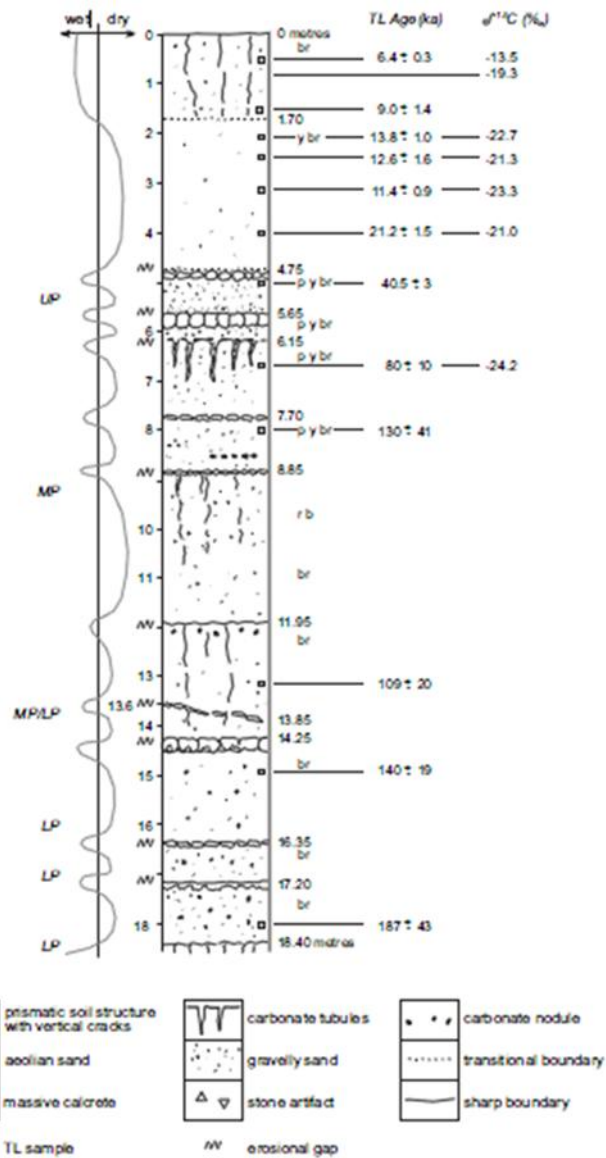


Figure 4.13: Excavated sediment profile and TL ages at 16R Dune (Singhvi et al. 2010; Figure 3).

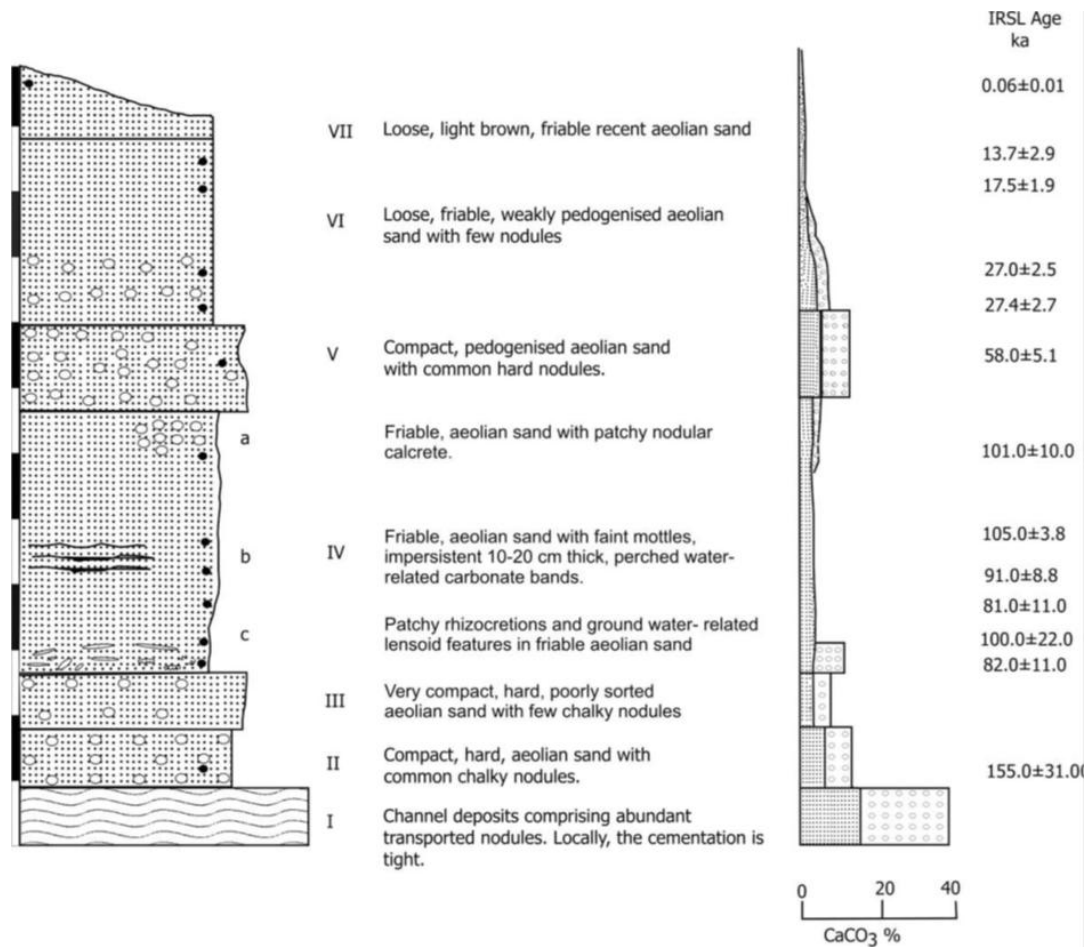


Figure 4.14: Composite sediment stratigraphy and IRSL ages from Chamu (Dhir et al. 2010; Figure 2).

There is little evidence dating aeolian activity to MIS 4, with the exception of aeolian horizons at Shergarh Tri-Junction dating to 60ka and 64ka (Figure 4.15; Andrews et al. 1998), although these dates do not occur in stratigraphic order and their error ranges overlap considerably with MIS 3. There is a significant body of evidence for intermittent aeolian activity during MIS 3. Aggradation events are seen dating to: 55±6ka and 43±5ka at Shergarh Tri-Junction (Andrews et al. 1998); 58ka at Chamu (Dhir et al. 2010); 40ka at 16R Dune; and 40-36ka at Awai (Figure 4.16; Chawla et al. 1992). All the aeolian deposits from MIS 6-3 show considerable pedogenesis and calcrete formations, as nodular calcretes and as laterally extensive bands.

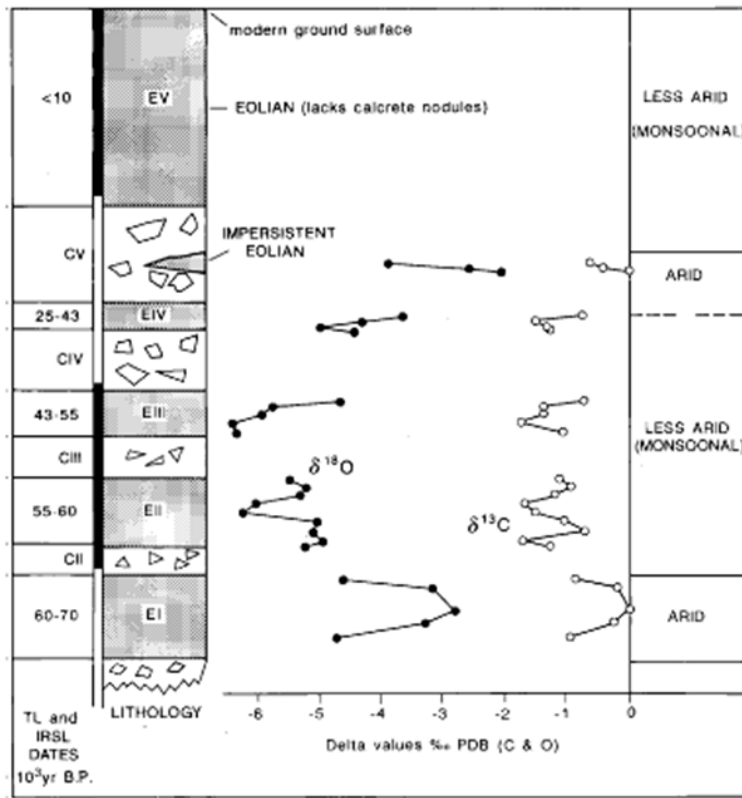


Figure 4.15: Sediment sequence, TL and IRSL ages, and stable isotope results from Shergarh Tri-Junction (Andrews et al. 1998; Figure 5).

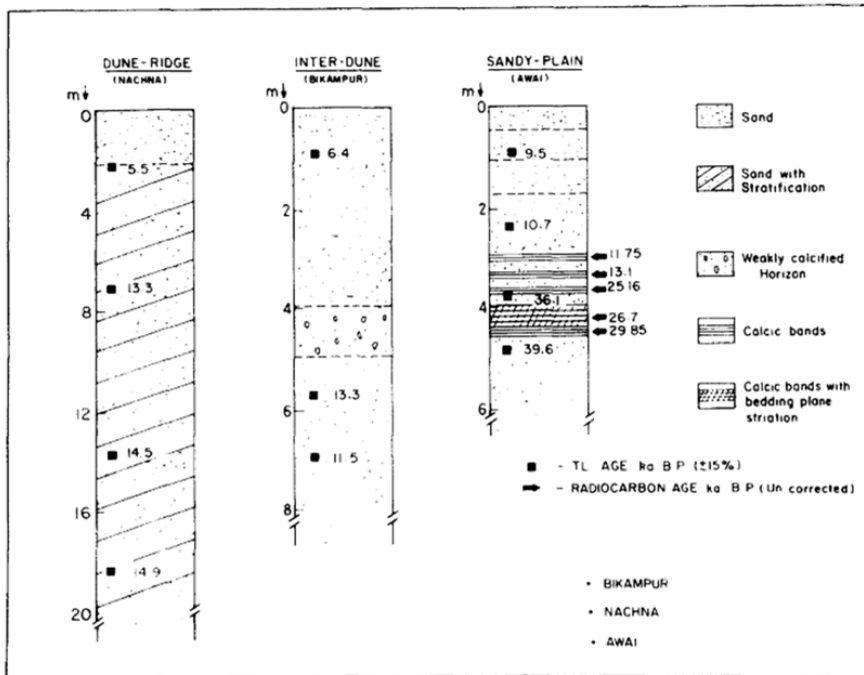


Figure 4.16: Sediment sequences with radiocarbon and TL ages at Nachna, Bikampur and Awai (Chawla et al. 1992; Figure 2).

Chronometrically dated evidence for aeolian activity during the transition of MIS 3-2 and the LGM is mostly evident from the alluvial plains of Gujarat, with only one recorded horizon dating to this period (27ka) from Chamu in central Rajasthan (Dhir et al. 2010). In Gujarat, this transition is recorded at Jaspur (Mahi) at 28ka, and at Dharoi-II (Sabarmati) at 25ka and Akhaj (Sabarmati) at 26ka (Juyal et al. 2003). However, more extensive evidence for aeolian activity is apparent over the LGM with aggradation events occurring at: 22ka at Sultanpur, 22ka at Dabka and 23ka, 22ka and 20ka at Tajpura-II (Mahi); 21-26ka at Dharoi-I and Dharoi-II (Sabarmati); and 22-21ka Orsang) (Figure 4.16). A horizon dated to 21ka at 16R Dune is the only preserved and dated evidence for aeolian activity in Rajasthan at the LGM. Post LGM aggradation occurs in the Mahi Valley at: 19ka at Dabka; 17ka at Tajpura-I; and 18ka at Tajpura-II (Juyal et al. 2003; 2005). These deposits typically display more limited evidence of pedogenesis, with less developed carbonate formations.

Preserved and dated evidence for aeolian activity becomes more geographically widespread for the post-glacial transition (MIS 2-1). Within Rajasthan aggradations occur at 17-13ka at Chamu (Dhir et al. 2010) between 15-13ka at Nachna (Chawla et al. 1992); 10-9ka at Awai (Chawla et al. 1992); at 13ka, 12ka, 11ka and 9ka at 16R Dune (Singhvi et al. 2010); 13.5-11.5ka at Bikampur (Chawla et al. 1992); 9ka at Shergarh Tri-Junction (Andrews et al. 1998). Within Gujarat, sand dune horizons from the MIS 2-1 boundary occur at: 14-12ka at Tajpura-1, 13ka at Jaspur and 11ka Deahewan (Mahi) (Juyal et al. 2003;2005); and 12-6ka at Dharoi-I, 11-7ka at Akhaj, and 12ka at Mahudi (Sabarmati)(Juyal et al. 2003; Srivastava et al. 2000).

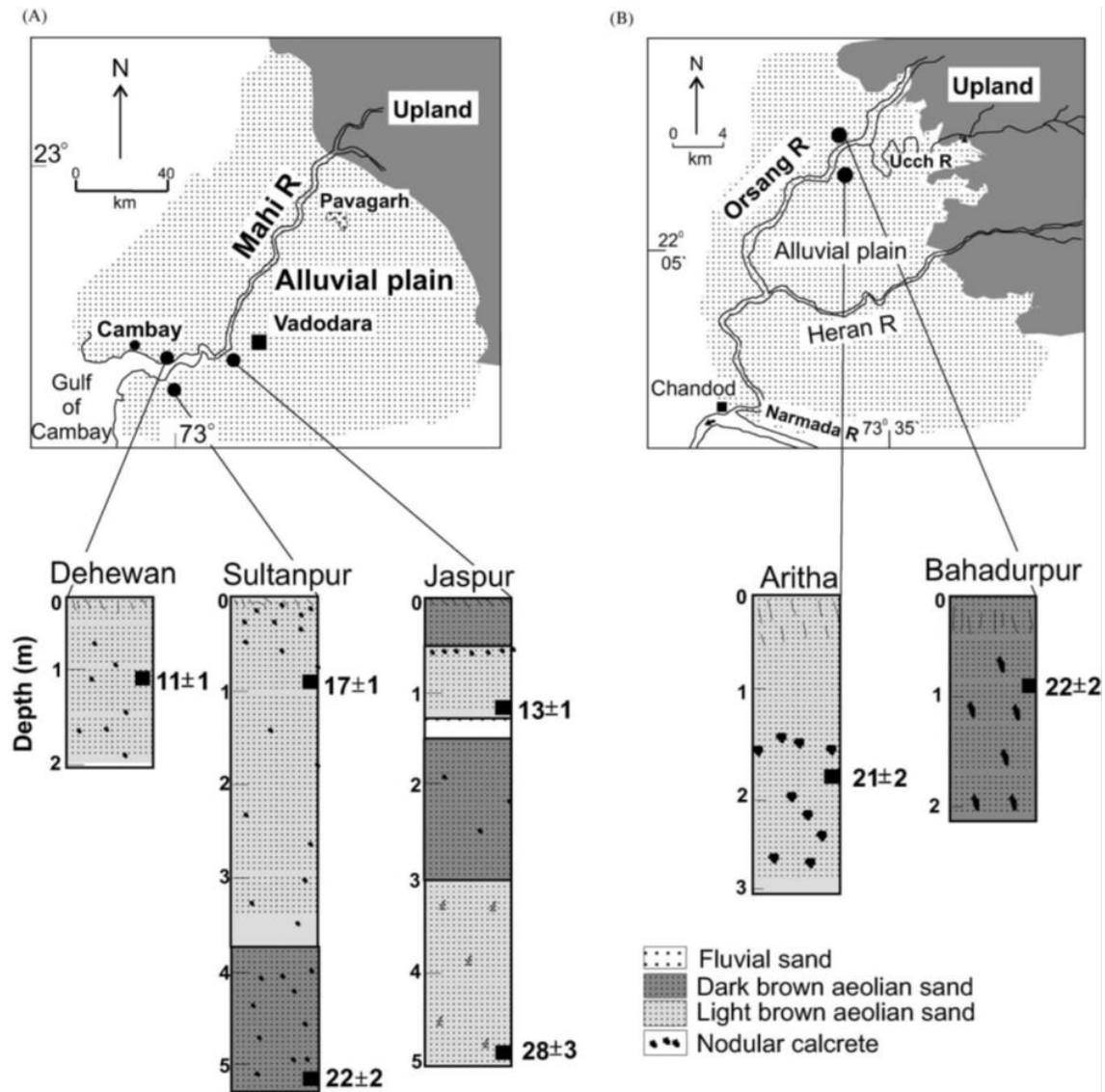


Figure 4.17: Stratigraphy and BGS chronology of the aeolian sand overlying the fluvial sequences in the Mahi and Orsang basin (Juyal et al. 2005; Figure 7).

Stable Isotope studies of sand-dune pedogenic carbonates

In both aeolian and fluvial sedimentary sequences within the Thar Desert evidence for pedogenesis occurs, indicating periods of stability in the depositional environment permitting post-depositional alteration to sediments, i.e. the formation of palaeosols. Due to the prevailing arid and semi-arid climatic regime, the Thar Desert preserves a rich record of climatic change through the formation of pedogenic carbonates. Pedogenic carbonates are

formed in the context of fluctuating groundwater levels, leading to the precipitation of calcite, initially as powder, then discrete nodules and finally as fused bands of nodules, which occurs during dry periods (Breeker et al. 2009). Pedogenic carbonates form in isotopic equilibrium with soil water for oxygen isotopes, and with soil CO₂ for carbon isotopes, predominately documenting patterns in meteoric waters and the ratio of C₃ to C₄ vegetation types (Breeker et al. 2009). Understanding the chronology of this isotopic record is complex, as pedogenic carbonate form as a series of over-printing laminae and partial dissolution of outer lamina and re-equilibration with soil carbon is possible, indicating that radiocarbon dating can be problematic (Trumbore 2000). Within the Thar Desert, at the sites of Awai (Chawla et al. 1992) and 16R Dune (Misra & Rajaguru 1986; Singhvi et al. 2010) highlight this issue, illustrating a 10ka time gap between ¹⁴C dated pedogenic carbonates and OSL dates for the depositional matrix in which they have formed. Stable isotope analyses on pedogenic carbonates may be best interpreted as time averaged signals of palaeoenvironmental conditions over a number of millennia for nodular carbonates, and perhaps a more extended chronology for hardpan calcretes.

A total of 128 pedogenic carbonate samples have undergone stable isotope analysis that can be reliably associated with chronometrically dated horizons (Figure 4.18 and 4.19). This includes 68 samples from 16R Dune (Achyuthan et al. 2007), 34 samples from Chamu (Dhir et al. 2010) and 26 from Shergarh Tri-Junction (Andrews et al. 1998). δ¹³C results from Chamu and Shergarh Tri-Junction fall within the range of -3.8 to 0.6‰ seen at 16R Dune, indicating that throughout the late Pleistocene the vegetation has almost exclusively been C₄ with some periods exhibiting a minor C₃ component. As two of these three sites are large sand dune formations, the dominance of grasses over trees and shrubs is perhaps not surprising, and further studies of pedogenic carbonates from alluvial settings may present a more varied picture of floral communities.

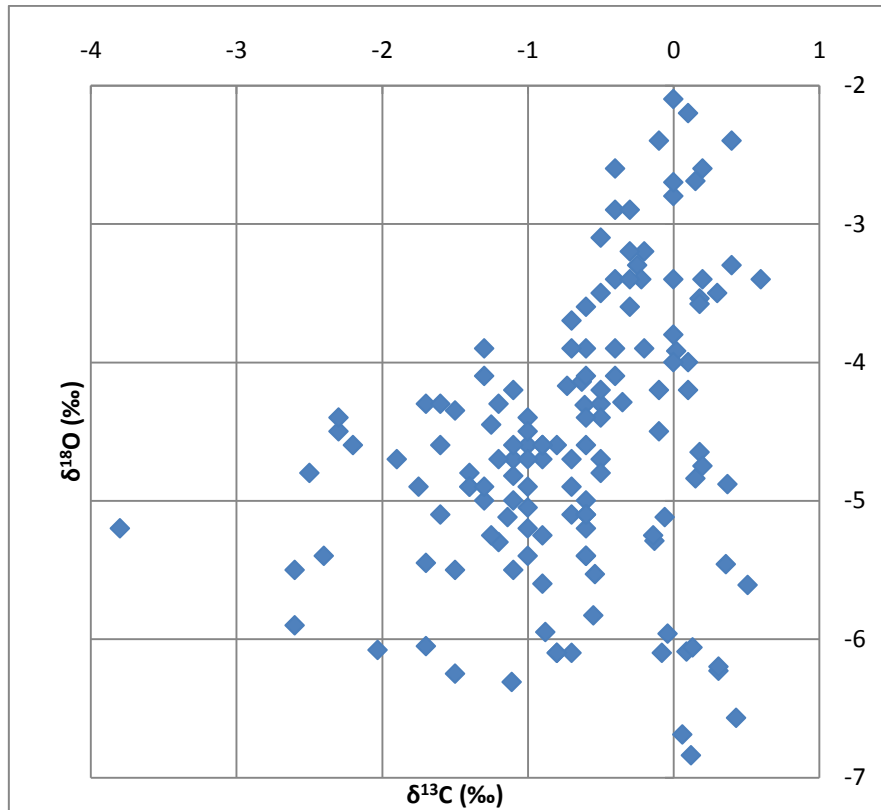


Figure 4.18: Composite results of stable isotope analyses on pedogenic carbonates at 16R Dune (Achyuthan et al. 2007), Chamu (Dhir et al. 2010); and Shergarh Tri-Junction (Achyuthan et al. 2007; Andrews et al. 1998).

The $\delta^{18}\text{O}$ signal is likely to represent two inter-related factors: the isotopic composition of meteoric water and the degree to which soils have been affected by evaporation. Evaporation of soil water is significant both for any surface accumulations as well as within the soil profile (Deutz et al. 2002; Brecker et al. 2009). All three sites show a very similar range of $\delta^{18}\text{O}$ values, ranging between -6.84 to -2.1‰, suggesting none has undergone significant more evaporation than the others. Direct matching of these terrestrial records to global oxygen isotope archives is problematic due to the time lag in formation of pedogenic carbonates, although broad changes are clearly recognisable, including increased aridity after MIS 5e, during MIS 4 and the LGM, and increased humidity during MIS 5c and MIS 3.

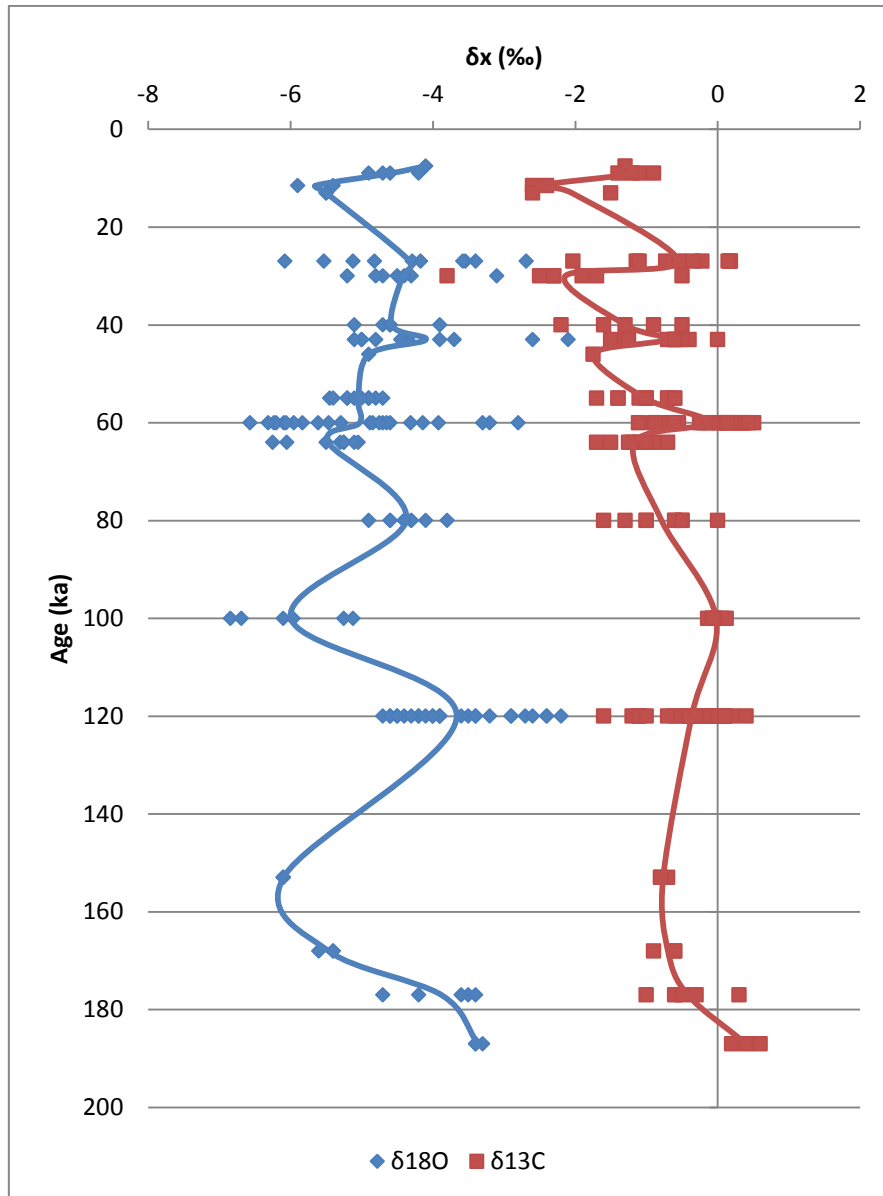


Figure 4.19: Stable isotopic composition of pedogenic carbonates from 16R Dune, Chamu & Shergarh Tri-Junction plotted against date of parent matrix, or averaged date of age determinations bracketing samples.

The relationship between these stable isotopic records indicates a marked threshold between periods when C_3 vegetation becomes a more significant component of floral communities.

When $\delta^{18}O$ values are greater than -4‰ dominantly C_4 vegetation is indicated by $\delta^{13}C$ values greater than -0.8‰ (Cerling 1999). A significant expansion of range in $\delta^{13}C$ values, up to -3‰ , occurs when $\delta^{18}O$ values are lower than -4‰ . This marks a considerable change to the

vegetation at these sites, suggesting that within the Thar Desert $\delta^{18}\text{O}$ records may be instructive regarding broader palaeoenvironmental changes.

Miliolite

Extensive Quaternary bioclastic carbonate formations, known as miliolite, are present both in the coastal regions and major river valleys of Saurashtra and mainland Kachchh (Figure 4.19). Despite earlier suggestions for their marine origin (e.g. Baskaran et al. 1986), the miliolites appear to have formed through the aeolian mobilisation and deposition of marine carbonate sands (Bhatt 2003). In the coastal regions of Saurashtra, large cliffs, stacks and coastal platforms of miliolite have formed whereas in inland locations, both in Saurashtra and Kachchh, the nature of miliolite occurrences is heavily dominated by pre-miliolite topography (Bhatt 2003). Within Saurashtra, Miliolite deposition has been suggested to be concentrated within three periods, dated using U-series to 50-70ka, 75-115ka and 140-200ka (Baskaran 1985; Baskaran et al. 1986; 1989). While this assessment largely stands, a number of dates now extend into MIS 2 (see Table 4.2). As marine derived aeolian deposits, these miliolites appear to preserve evidence of both an exposed continental shelf and periods of high winds capable of mobilising marine carbonate sands.

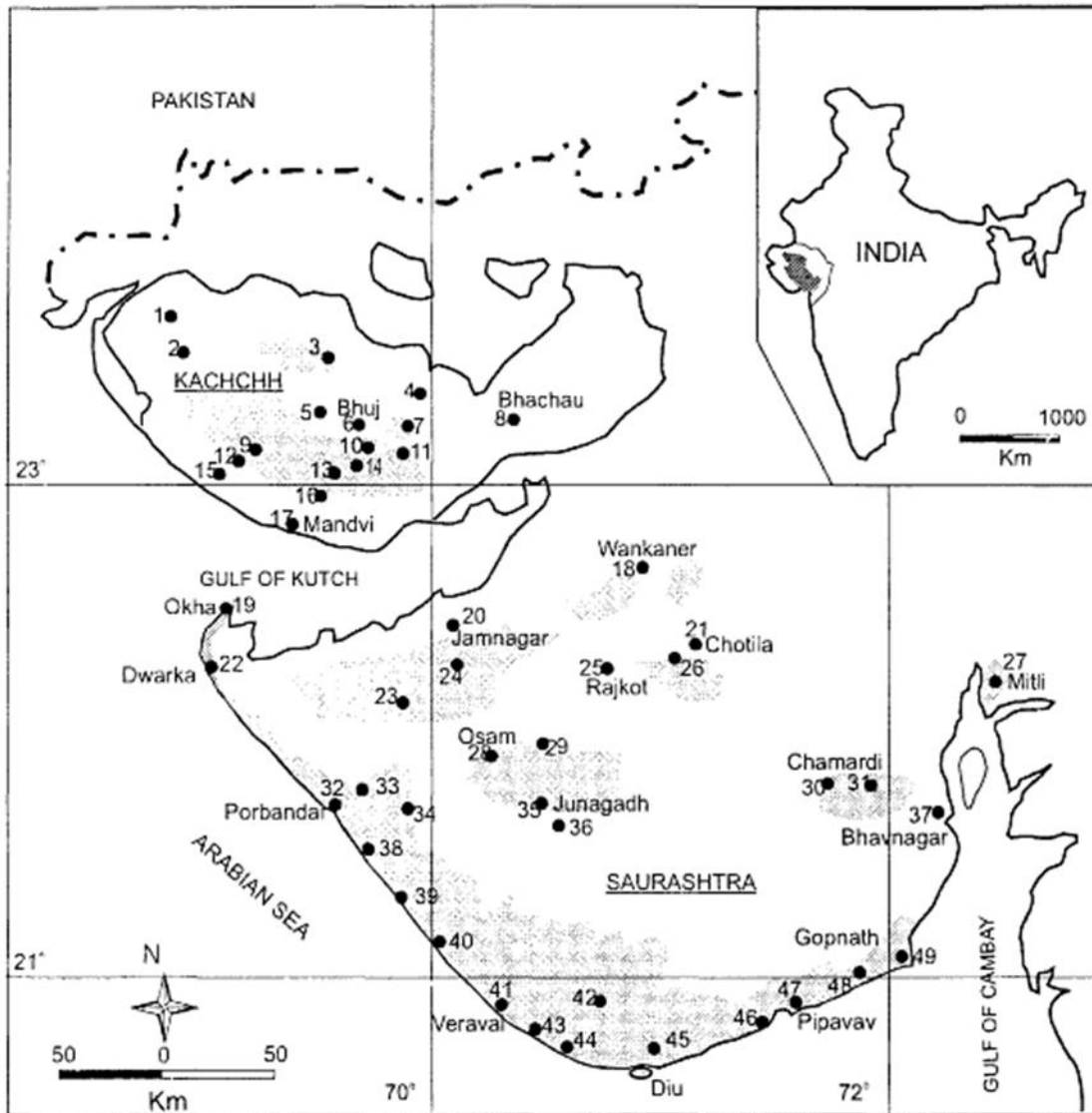


Figure 4.20; Distribution of miliolite (Quaternary bioclastic carbonate) deposits in Saurashtra and Kachchh (Bhatt 2003; Figure 1).

Region	Site	U/Th age estimate (ka)	Reference
Kachchh	Bhupadungar	22.8±2.6	Chakrabarti et al. 1993
Kachchh	Mukuda	36.9±1.5	Chakrabarti et al. 1993
Kachchh	Kothara	54.8±5.1	Chakrabarti et al. 1993
Kachchh	Roha	138.6±13.9	Chakrabarti et al. 1993
Saurashtra	67	29.5+1.3/-1.2	Baskaran et al. 1989
Saurashtra	38	33.4+4/-3.9	Baskaran et al. 1989
Saurashtra	Bad Pachosra	39.9±3	Chakrabarti et al. 1993
Saurashtra	Walmut	46.3±3.2	Chakrabarti et al. 1993
Saurashtra	31-Jan	48.9+3.1/-3	Baskaran et al. 1989
Saurashtra	Strand Lines Sample 29	52+3.2/-3.1	Baskaran et al. 1987
Saurashtra	46	52+3.2/-3.1	Baskaran et al. 1989

Region	Site	U/Th age estimate (ka)	Reference
Saurashtra	18-Jan	53.6+4.9/-4.7	Baskaran et al. 1989
Saurashtra	83	53.6±3.2	Baskaran et al. 1989
Saurashtra	Tanakia	54.8±6.8	Chakrabarti et al. 1993
Saurashtra	Strand Lines Sample 31-2	55.2+3.3/-3.2	Baskaran et al. 1987
Saurashtra	Walmut	56.4±3.4	Chakrabarti et al. 1993
Saurashtra	47-2	56.8+5.1/-4.8	Baskaran et al. 1986
Saurashtra	15-Jan	58.5+3.4/-3.3	Baskaran et al. 1989
Saurashtra	18-Feb	63.6+3.6/-3.4	Baskaran et al. 1989
Saurashtra	Wankaner	65.1±7.1	Chakrabarti et al. 1993
Saurashtra	57-2	65.4+3.6/-3.5	Baskaran et al. 1986
Saurashtra	Strand Lines Sample 31-1	65.4+5.5/-5.2	Baskaran et al. 1987
Saurashtra	Gop Hill	69.5±5.7	Chakrabarti et al. 1993
Saurashtra	49-1	69+3.8/-3.6	Baskaran et al. 1986
Saurashtra	49-5	69+3.8/-3.6	Baskaran et al. 1986
Saurashtra	62	69+5.7/-5.4	Baskaran et al. 1989
Saurashtra	Dhepar Village	76.1±6.1	Chakrabarti et al. 1993
Saurashtra	Bamanbore #115	76.2±4.1	Chakrabarti et al. 1993
Saurashtra	88	78.7+13.1/-11.5	Baskaran et al. 1989
Saurashtra	42	78.7+6.3/-5.9	Baskaran et al. 1989
Saurashtra	Ranji Sagar Dam	80.7±6.4	Chakrabarti et al. 1993
Saurashtra	61-1	80.8+6.4/-6.1	Baskaran et al. 1989
Saurashtra	Bamanbore #116 (overlies #115)	82.2±4.2	Chakrabarti et al. 1993
Saurashtra	10-Jan	87.2+6.9/-6.4	Baskaran et al. 1989
Saurashtra	68	91.8+12.2/-11	Baskaran et al. 1986
Saurashtra	45	94.1+7.4/-6.9	Baskaran et al. 1989
Saurashtra	36	96.5+7.5/-7	Baskaran et al. 1986
Saurashtra	Strand Lines Sample 24	99+16.1/-14	Baskaran et al. 1987
Saurashtra	64	107+8	Baskaran et al. 1989
Saurashtra	Chorbedi Hill	111.6±10.9	Chakrabarti et al. 1993
Saurashtra	Strand Lines Sample 20	112+9/-8	Baskaran et al. 1987
Saurashtra	10-Apr	121+10/-9	Baskaran et al. 1989
Saurashtra	63	142+16/-14	Baskaran et al. 1986
Saurashtra	Strand Lines Sample 22	142+26/-21	Baskaran et al. 1987
Saurashtra	60-1	158+32/-24	Baskaran et al. 1986
Saurashtra	Strand Lines Sample 30	168+22/-18	Baskaran et al. 1987
Saurashtra	Strand Lines Sample 34	177+19/-17	Baskaran et al. 1987
Saurashtra	52-2	178+26/-20	Baskaran et al. 1989
Saurashtra	37	178+41/-26	Baskaran et al. 1989
Saurashtra	57-1	190+29/-22	Baskaran et al. 1986
Saurashtra	Strand Lines Sample 27	204+35/-26	Baskaran et al. 1987
Saurashtra	Strand Lines Sample 32	235+36/-27	Baskaran et al. 1987

Table 4.2: Synthesis of U/Th dates on miliolite deposits from Saurashtra and Kachchh.

Lacustrine Records

Rajasthan contains numerous salt lakes (playas) (Figure 4.21) that provide another archive of palaeoenvironmental variability, although dated evidence is predominately restricted to the terminal Pleistocene and Holocene. These lakes typically occupy closed basins of riverine ancestry, and many display a NE-SW orientated long axis as a result (Roy 1999). A range of explanations for the cause of drainage disruption that promoted the development of the lakes have been suggest, including blockage by sand dunes, stream trapping and neotectonism (Roy 1999). As the majority of studied and dated sequences present evidence of lacustrine facies that post-date the LGM, and the associated aridity at this time resulted in both decreasing fluvial discharge and increased aeolian mobility, sand dune blockage and stream trapping appear the most parsimonious explanations for this.

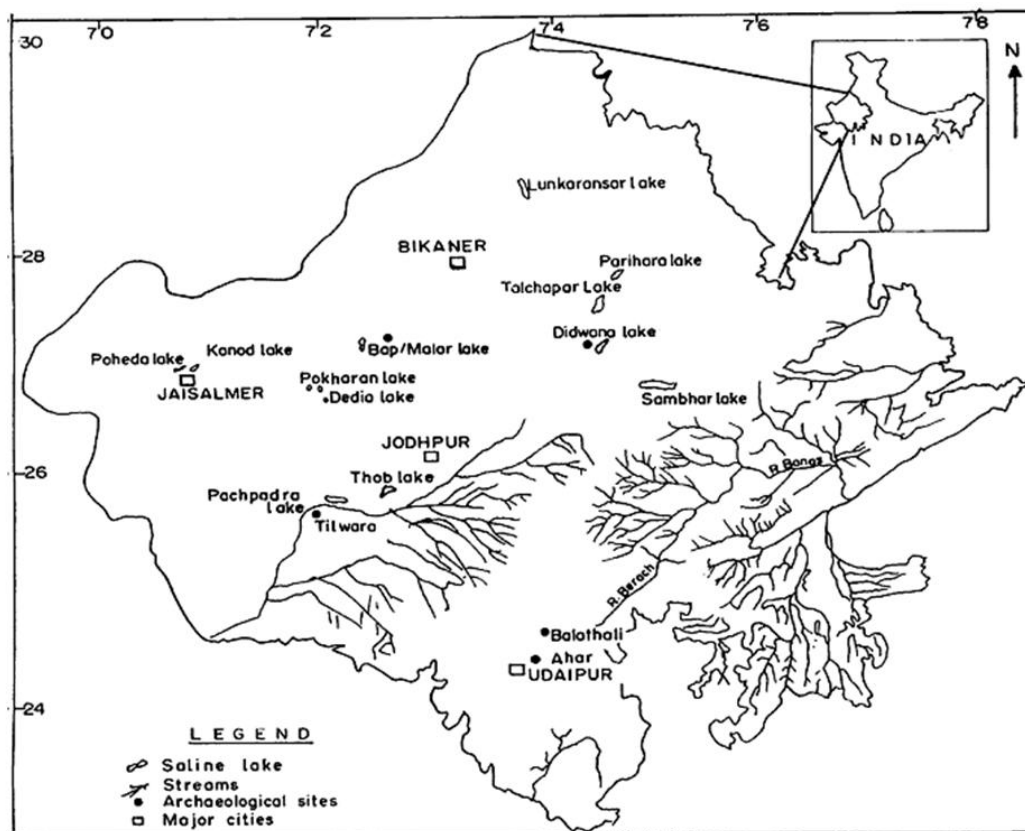


Figure 4.21: Distribution of lakes in Rajasthan (Achyuthan et al. 2007; Figure 1).

At Bap Malar a relatively shallow sedimentary succession is observed down to bedrock (Figure 4.22), and Deotare et al. (2004) suggest their 3m excavations at Kanod come close to the bedrock, identified by a previous study at 3-5m depth. At Tal Chappar, weathered bedrock and a thin palaeosol is observed underlying the lacustrine sequence, and the sharp erosive contact between the lacustrine and palaeosol deposits indicates the removal of earlier Pleistocene sediments (Achyuthan et al. 2003). Similar erosive events may have also occurred at Bap Malar and Kanod, prior to the onset of lacustrine deposition. Didwana provides the clearest evidence for the formation of the lake in a depression initially formed by a disrupted drainage channel, with evidence for pedogenised alluvial deposits underlying the lacustrine sequence (Wasson et al. 1984).

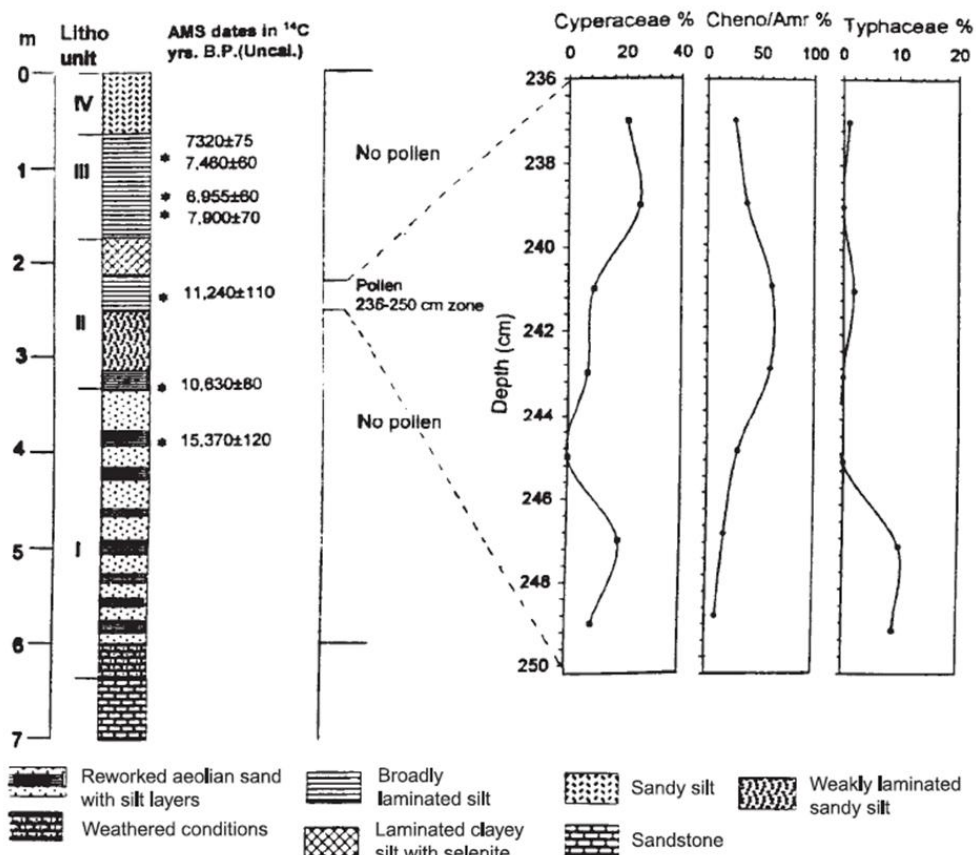


Figure 4.22: Sedimentary section, radiocarbon dates and pollen diagrams from Bap Malar Lake (Deotare et al. 2004; modified from Figure 4).

The earliest evidence for lacustrine formations includes reworked aeolian sands and gravels, suggesting the emergence of ephemeral lakes settings occurred from 15ka at Bap Malar (Deotare et al. 2004), >12ka at Didwana (Wasson et al. 1984) and >13ka at Tal Chappar (Achyuthan et al. 2003). These are followed by laminated deposits indicating high levels of salinity and occasional desiccation ca. 10ka at Bap Malar, Didwana, Kanod, Tal Chappar and Lukaransar. Rapid deposition of laminated lake sediments with low levels of salinity occurred ca. 7ka at all studied lakes, relating to peak humidity in the early-mid Holocene, with many lakes becoming increasing saline and ephemeral from ca. 4ka onwards (Wasson et al. 1984; Enzel et al. 1999; Achyuthan et al. 2003; Deotare et al. 2004).

Sambhar Lake, the largest playa within the Thar Desert, does not fit simply with this pattern. This closed basin has been formed as a graben within the Aravalli Range, although it is unclear whether this tectonic feature occurred through movements along strike-slip planes or fault bounded blocks (Roy 1999). Sinha et al. (2006) have provided dated evidence of the Late Pleistocene evolution of the lake sediments through the recovery of a 23m lake core (Figure 4.23). Three major litho-units have been described, including (Unit III) an upper organic rich mud ¹⁴C dated between 6.8ka to modern overlying a carbonate mud dating to 7.5-9.5ka, sand and silt dominated Unit II dating to 19-22ka, and Unit I, a carbonate mud capping a thick carbonate sand (Sinha et al. 2006). Although evidence for heightened aridity is evident during the LGM and between 7.5-6.8ka, this research suggests that Sambhar Lake has not been completely desiccated throughout this observed history (Sinha et al. 2006). Significantly, Sambhar is the only lake in the Thar Desert that clearly was present prior to the LGM.

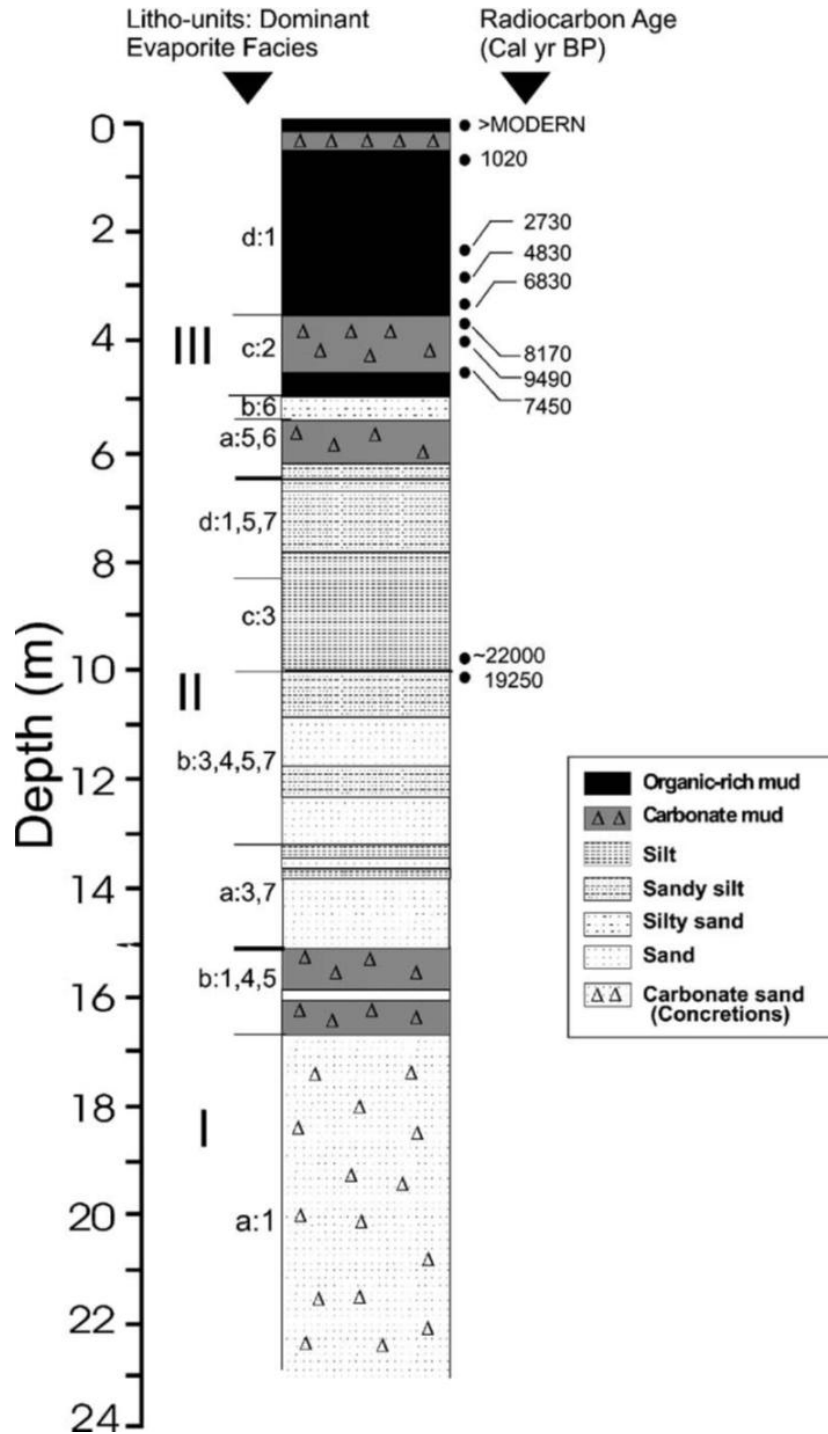


Figure 4.23: Sedimentary section and radiocarbon dates from Borehole 1 at Sambhar Lake (Sinha et al. 2005; Figure 2).

Eustatic Records

Eustatic controls on sea level, resulting from varying levels of water stored in continental ice sheets compared to the oceans, have also left their mark on the Pleistocene palaeoenvironmental history of the Thar Desert. Although most evident at the shoreline, changing sea levels also have significant impacts upon fluvial systems. While discussing fluvial sequences (above) two impacts of sea level change have been noted: marine transgression in MIS 5e evident in the deposition of marine clays at the base of the fluvial sequence in the Mahi Valley; the appearance of delta formations inland in the Raans of Kachchh indicate a period of marine transgression during MIS 1. A number of further proxies present evidence for both episodes.

Widespread evidence for coral formation above sea level in Kachchh appears to represent the period of marine transgression in MIS 5e, which have subsequently been exposed to destructive processes during LGM low sea stands at 18ka (Michael et al. 2009). Oyster and clam beds, sampled from 13 locations in Saurashtra by Juyal et al. (1995) provide an indicator of changing sea-levels in the past, which fall into three discrete periods based on U-series dating. These beds are argued to offer good indicator of past seas levels as they only form in intertidal marine conditions and require a firm rock substrate (Juyal et al. 1995). The first period appears to represent high sea levels in MIS 5e, with oyster and clam shells between 119-132ka occurring at 13-12m and 1-2m above modern sea-levels, argued to relate to a maximum 7m AMSL when tectonic uplift is accounted for (Juyal et al. 1995). The second period relates to MIS 5a, with oyster shell deposits currently 3-2m AMSL that date to 71-87ka, originally relating to sea-levels 13m below present levels (Juyal et al. 1995). The final period relates to the mid-Holocene high sea levels, with oyster beds dating to 8.6-6.4ka and 3.3-2.5ka between 3-4m AMSL, although the tectonic component is difficult to interpret here (Juyal et al. 1995).

Further evidence for Late Pleistocene sea level changes are evident in raised marine terraces and notches located on the southern coastline of Saurashtra. Pant and Juyal (1993) have suggested that raised marine terraces indicate MIS 5 sea levels were ca. 7m AMSL, having accounted for tectonic uplift. Notches are erosive features, recorded at three locations between Bararkot and Jafrabad and three sites surrounding Diu, are found on raised shore platforms and cliff sections and provide evidence for higher sea levels, although neotectonic uplift complicates their interpretation (Bhatt & Bonde 2006). Notches occurring at 12-15m AMSL are related to MIS 5 high sea levels, and are argued to have seen between 6-9m uplift to match global figures for high stands (Bhatt & Bonde 2006). Similarly, notches related to the mid-Holocene high-stands, globally suggested to have been ca. 2m above present levels, occur 4-5m AMSL, again suggesting some tectonic influence (Bhatt & Bonde 2006).

Summary

Combined, the fluvial and aeolian sequences of the Thar Desert offer the clearest picture of palaeoenvironmental change. Two cycles of fluvial deposition appear to have occurred during MIS 5 with a further, less powerful cycle occurring in MIS 3. Following an initial period of incision, upward-fining cycles of riverine deposition are apparent, starting with the deposition of gravels under strong fluvial regimes, sometimes preserving evidence for the erratic and flashy nature of these drainage systems, before the formation of more stable river courses and the development of floodplains. As fluvial activity wanes, these alluvial deposits undergo weathering and pedogenesis, and the onset of aridity is marked by ephemeral stream channels and the deposition, and occasional reworking, of aeolian deposits.

Aeolian activity appears to be a persistent feature of the Thar Desert, although episodes of deposition are likely to be rapid and may have been geographically restricted (Figure 4.23). Sand dunes only encroach upon the Gujarati alluvial plains during the LGM, whereas they have

been regularly deposited within central Rajasthan throughout the Late Pleistocene, though both the LGM and MIS 4-3 boundary are notable for peaks in aeolian accretion. Stable isotopic studies in the Thar Desert appear to identify a key threshold in relative humidity for the increased presence of C_3 plants, certainly in dune settings. The MIS 4-3 boundary is also the peak period of miliolite formation, although only the Holocene is notable for the lack of dated miliolite deposits.

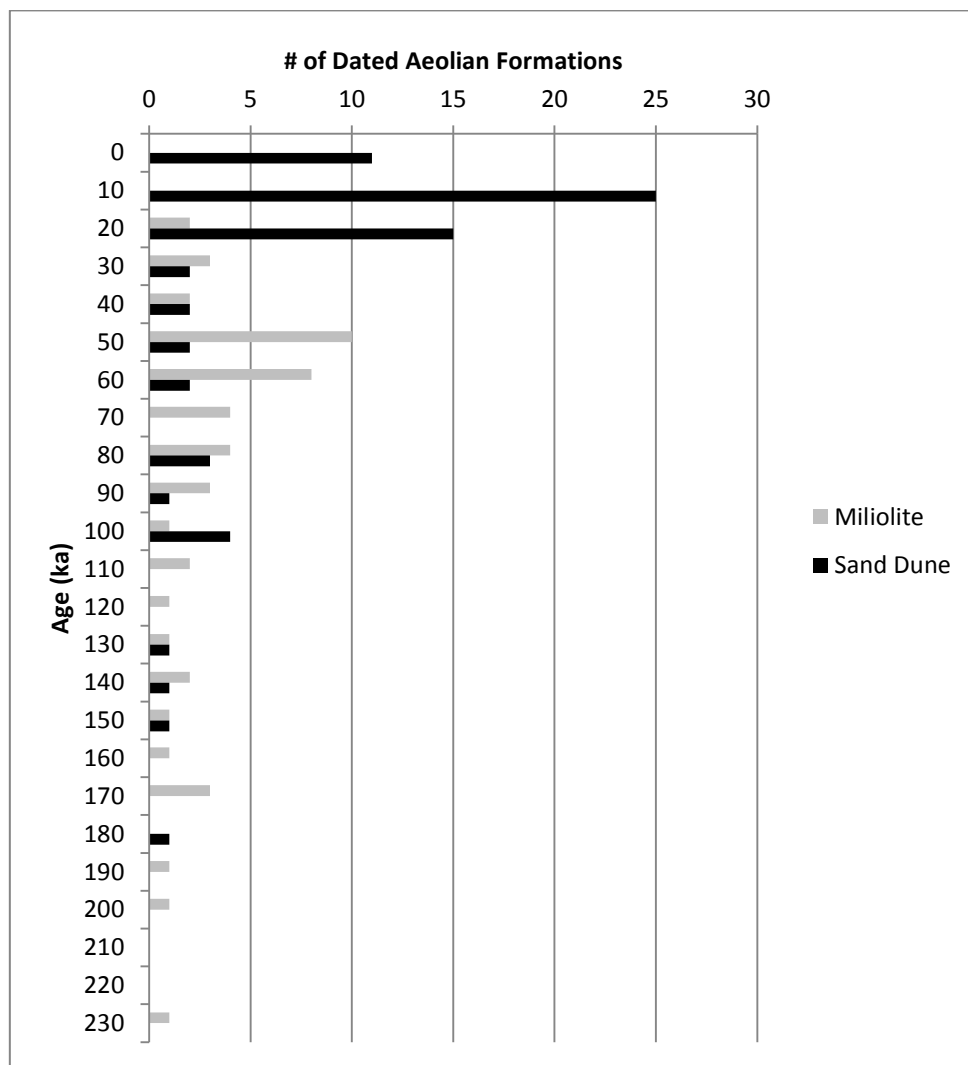


Figure 4.24: Composite bar chart of all chronometrically dated aeolian deposits in the Thar Desert.

The importance of the lacustrine record for understanding palaeoenvironmental change is limited, although significant for understanding the re-colonisation of the Thar Desert after the

LGM. It may, perhaps, offer a useful analogy for the colonisation of the desert after earlier peak arid events, in periods when increased humidity led to reactivation of palaeochannels temporarily blocked by aeolian deposits. However, Sambhar Lake may have played a significant role as a source location for expansions of various biota as palaeoenvironmental conditions improved following arid events.

Eustatic changes over the Late Pleistocene serve a clear reminder not only of the changing impact that sea levels may have had over the distribution of resources and and behaviour of fluvial systems, but also as the most tangible index of the impact that tectonic activity has had upon the Thar Desert. Unfortunately, the timing of these impacts and hence their own role upon the changing nature of the various drainage networks remain something of a 'known-unknown'. The same can be said of the two largest fluvial features of the Thar Desert, the Indus and Ghaggar-Hakra rivers, which are likely to have been highly significant refugia for numerous biota during arid periods, and seasonally dangerous flood-prone areas during periods of peak humidity, although they remain poorly understood for the period in question.

Summary

The evidence under review in this chapter has indicated a number of potential constraints upon Palaeolithic hominin populations that have occupied the Thar Desert. The potential for rapid colonisations of the Thar Desert by various biota has been illustrated by case studies of both modern flora and fauna, as with the IGNP canal. Indeed, investigating how soil moisture and CO² varies amongst modern floral communities may provide a useful guide to understand what kind of change in vegetation may correspond to the apparent threshold that has been identified in the isotopic record. It is worthwhile noting that although it is the hominin occupation of the Thar Desert under consideration here, a number of other large and medium

sized carnivores would also have been extending their ranges to track the response of herbivores to the opening up of new pastures, offering a significant line of resource competition.

The geology of the Thar Desert is spatially diverse, and this trend may be expected to be evident in the archaeological assemblages of the region. Both the quality and package size of lithic raw materials can be expected to be heterogeneous, which may have a significant bearing upon the ways in which Palaeolithic hominins have been able to occupy various areas of the Thar Desert. This is particularly pertinent in the central regions of the Thar, where low lying outcrops of higher quality materials may have been covered or uncovered by prevailing conditions of aeolian deposition.

Orbital scale climate change and variations in monsoonal intensity have set the tempo of regional palaeoenvironmental variability that have been outlined. The rhythm of sea level changes, fluvial cycles and aeolian mobility will have been a major factor in determining the habitability of the Thar Desert. It is inevitable that the archaeological record of the Thar Desert will be tied into the record of palaeoenvironmental change that has been set out. This is not only because this provides the context in which Palaeolithic hominins lived, but also because these are the depositional environments in which archaeological phenomena have been preserved. Indeed, those landforms that have been least exposed to taphonomic disturbance, whether through relative youth, such as with the wide visibility of post-LGM dune deposits, or resistance to erosion and deflation, such as pedogenised alluvial deposits of MIS 3, are likely to offer more numerous and higher resolution archives of hominin activity than sand dunes that have been repeatedly deflated, or even alluvial landscapes buried by more recent sedimentation. These factors must be kept in mind throughout the ensuing review of existing archaeological evidence from the Thar Desert in Chapter 5 and have played a significant role in structuring the fieldwork that will be reported in Chapters 6, 7 and 8.

Chapter 5

Palaeolithic Archaeology of the Thar Desert

Engaging with the work of earlier researchers on the Palaeolithic occupation of the Thar Desert is a critical endeavour to enable the identification of both lacunae and contradictions in existing evidence. As a result, this is a crucial task for targeting future research in the region that can address both gaps in the local data set and palaeoanthropological questions of global significance. Nevertheless, there are several problems inherent in synthesising the existing evidence for the Palaeolithic occupation of the Thar Desert. Although the overall sample size for Palaeolithic sites in the region is large, the number of sites decreases rapidly with increasing resolution of archaeological detail.

The objective of this chapter is to present a comprehensive synthesis of the existing archaeological evidence for the Palaeolithic occupation of the Thar Desert. The scope of this synthesis is considerably wider than that of the last comprehensive study of the region as a single analytical unit by Allchin et al. (1978), including approximately 8 times as many sites. The chapter is structured such that, having defined the source of the data set, the largest number of sites is dealt with first, at the coarsest level of archaeological resolution, and the number of sites under consideration will decrease as the resolution of archaeological evidence increases. Attention will then turn to a restricted number of sites that offer more robust evidence for the Palaeolithic archaeology of the Thar Desert, either through the application of clearly defined sampling strategies or chronometric dating techniques.

Defining the Data Set

Given the varying types of description offered by earlier researchers, as discussed in Chapters 2 and 3, it is necessary to offer a clear indication of the grounds upon which reports of sites have been included in this synthesis. The majority of sites have been reported as occurring within a Palaeolithic industry (e.g. Series II), and are unproblematic to include in the synthesis. A number of sites have been simply reported as Palaeolithic or as occurrences of 'stone artefacts', and where the latter group do not occur with clearly Holocene material culture they have been included, although offer limited analytical utility.

As discussed in Chapter 3, the inclusion of Mesolithic and Neolithic sites is more problematic. The Upper Pleistocene antiquity of some microlithic industries in South Asia (e.g. Patne [Sali 1989; James 2011]; Jwalapuram 9 [Clarkson et al. 2009]; Batadomba Lena & Fa Hien Cave [Perera et al. 2011]) is well established. It is therefore likely that some Mesolithic sites, including Neolithic sites reported by Foote (1916), typically associated with the presence of microliths, may also share similar antiquity in the Thar Desert. However, the continued use of such technologies into the Holocene is well illustrated by excavations in the region, such as at Langhnaj (Sankalia 1968). Mesolithic sites have been included where they show no association with ceramics or other material culture from Holocene contexts (e.g. metals), and sites with chronometric dates <10ka have been rejected. It is acknowledged that this is unlikely to accurately discriminate between Upper Pleistocene and Holocene microlithic industries, and thus presents an inherent problem with the available data (in the interests of brevity, this sample will be referred to throughout the rest of the thesis as Palaeolithic, but the potential inclusion of early Holocene material is recognised).

A sizeable literature has been reviewed for data collection. The majority of these sites are reported in *Indian Archaeology – A Review* (1955-56 to 1999-2000) and *Ancient Sindh* (v.1-7),

although numerous other sources (Foote 1916; de Terra & Patterson 1939; Sankalia 1946; Misra 1961; Allchin et al. 1978; Misra et al. 1980; Marathe 1981; Misra et al. 1982; Baskaran et al. 1986; Biagi & Cremaschi 1988; Biagi et al. 1996; Negrino & Kazi 1996; Biagi & Shaikh 1998-1999; Mishra et al. 1999; Deotare et al. 2004; Biagi 2003-2004; Ajithprasad 2005a; 2005b; Biagi 2005; 2008; 2011) have also been reviewed. While the synthesis of data has attempted to be as complete as possible, it is inherently determined by the availability of sources either within the University of Oxford or on the internet, and it is difficult to gauge what further detail may be added with the inclusion of difficult to access or unpublished work (e.g. Ajithprasad 1988). In total 971 reports of archaeological sites fitting the criteria set out above have been collected, of which 939 reports offer unique data (see Appendix A.1), whereas the 32 reports have been excluded from further study repeat data that has already been recorded.

Palaeolithic Sites in the Thar Desert

At the widest level, it is possible to discuss some basic features of the distribution of all 939 Palaeolithic sites in the Thar Desert (Figure 5.1). There is a broader distribution and greater density of sites in Gujarat than Rajasthan, whereas Palaeolithic occupation in Sindh is limited to a few concentrations. There is a dearth of Palaeolithic sites in eastern Sindh, and to a lesser extent in western Rajasthan, although the practicality of undertaking research close to the Indian-Pakistani border and limited archaeological visibility due to contemporary sand dune activity offer a likely explanation for this.

There also appears to be a discontinuation in the distribution of sites between Gujarat and Rajasthan. This may be partly explained by the different research histories in the two states. Institutions such as MSU Baroda and the Department of Archaeology (Government of Gujarat) have undertaken long term and widespread archaeological survey in Gujarat throughout the

state. In contrast, many of the sites in Rajasthan have been identified by research teams with specific objectives, with greater focus upon central regions (e.g. Allchin et al. 1978; Misra et al. 1980), rather than systematic state-wide programs of exploration.

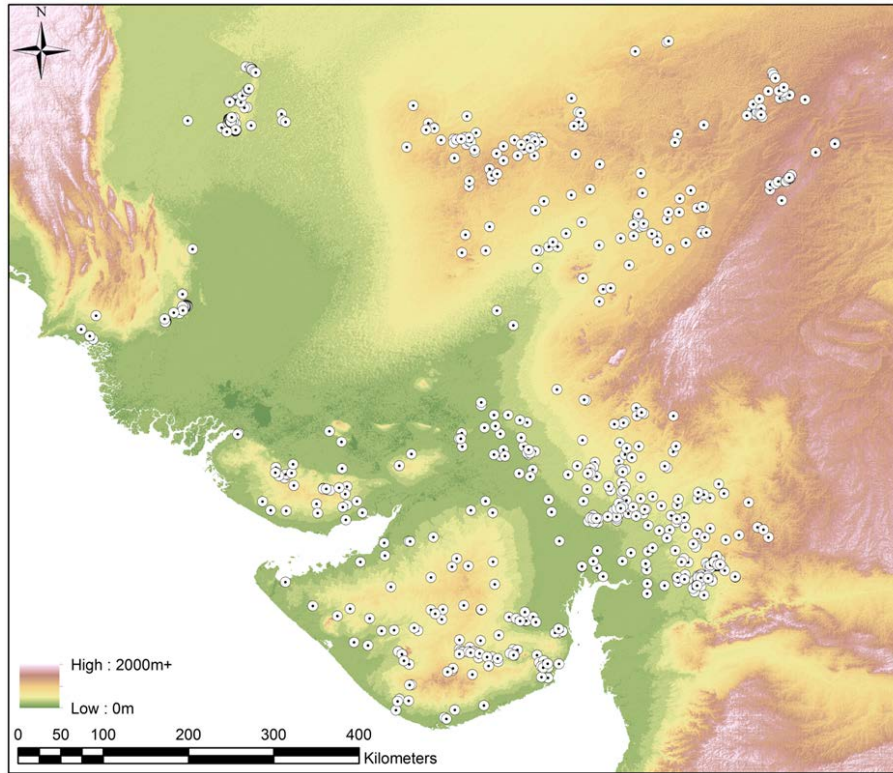


Figure 5.1: Map of all Palaeolithic sites in the Thar Desert.

Many of the Palaeolithic sites in the Thar Desert can be found associated with one of three geographic features: roads, rivers or hills. The location of numerous sites along modern transport routes most likely indicates that the increased access and visibility of such areas to archaeologists has increased the chances of any Palaeolithic occurrence being identified. Many archaeological surveys have specifically focused upon river courses (e.g. Misra 1963; Marathe 1981), and the association of numerous sites close to modern river courses is likely to reflect this to some extent. In addition, erosive fluvial activity in the Holocene has probably had a significant impact upon the visibility, and mobility, of Pleistocene sediments, which may have increased archaeological visibility of Palaeolithic sites. However, the focus upon both rivers

and hills probably also reflects both assumed and actual patterns of Palaeolithic resource exploitation and archaeologists researching this period are likely to focus upon sources of fresh water and raw materials as a result.

For the purposes of this thesis, spatial analysis within the Thar Desert will be undertaken in six sub-regions (Figure 5.2): a) The Rohri Hills region, including all sites in Upper Sindh; b) Lower Sindh; c) Western Rajasthan; d) Central Rajasthan; e) Mainland Gujarat; f) Saurashtra and Kachchh.

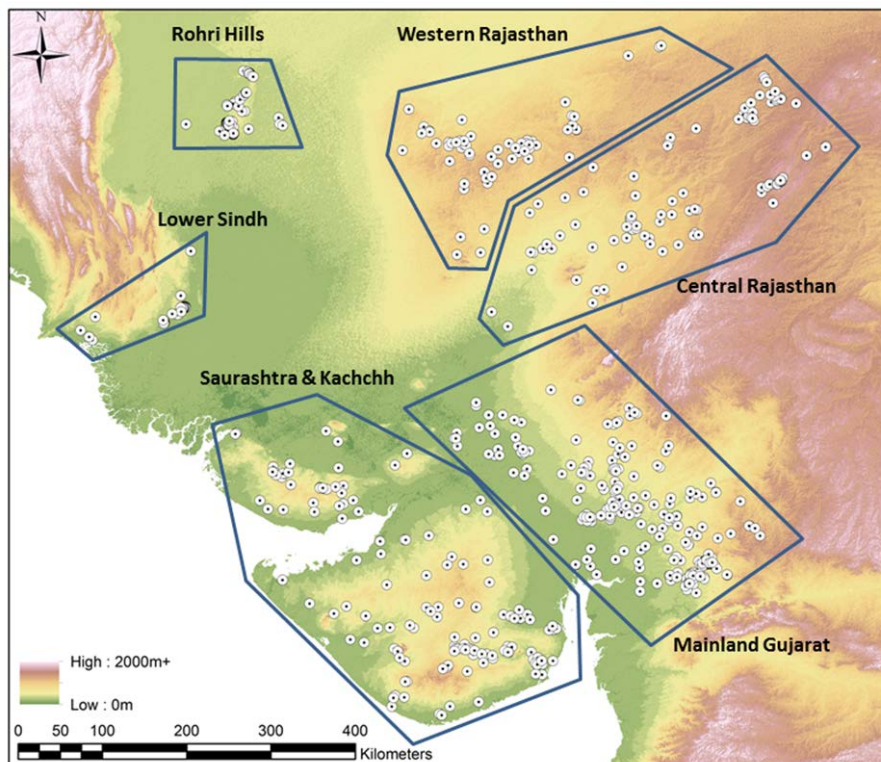


Figure 5.2: Map displaying sub-regions of Thar Desert as used in this thesis.

Palaeolithic Industries in the Thar Desert

The standardised terminology for Palaeolithic industries proposed in Chapter 3 (Lower, Middle and Late Palaeolithic) offers the broadest means by which the 939 sites can be partitioned

(Table 5.1). A total of 79 sites cannot easily be included in any of these three industrial groups.

This group includes sites where artefacts are in too low numbers to ascribe an industry securely (e.g. Karna [Mishra et al. 1999]) or only offer typological descriptions that occur in more than one category, such as hand axes.

Industry	# of sites
Lower Palaeolithic	143
Middle Palaeolithic	113
Late Palaeolithic	460
Lower and Middle Palaeolithic	43
Lower and Late Palaeolithic	5
Middle and Late Palaeolithic	81
Lower, Middle and Late Palaeolithic	15
Unid.	79

Table 5.1: Number of sites in the Thar Desert within each industrial group.

The majority of Lower Palaeolithic sites are located in Gujarat (Figure 5.3), with significant concentrations of sites occurring in the Orsang and Hiran Valleys, which can partly be explained by detailed survey of these regions by Ajithprasad (1988; 2005a; 2005b) and Marathe (1981) respectively. Another concentration of sites occurs in central Rajasthan near Didwana and in the Pushkar Valley, identified through the work of Misra et al (1980; 1982) and Allchin et al. (1978). Few sites are located in Western Rajasthan and relatively little data is available for these. Few Lower Palaeolithic sites also occur in the Rohri Hills and Lower Sindh.

Middle Palaeolithic sites are less numerous yet more widespread than Lower Palaeolithic. Fewer sites only reported as Middle Palaeolithic occur in mainland Gujarat, whereas they are widespread within Saurashtra and Kachchh. The prominence of the Luni Valley for this sample can be attributed to the work of Misra (1961), although a number of researchers have expanded upon this early and significant contribution. The surveys undertaken by Allchin et al. (1978) identified many of the sites in Western Rajasthan, indicating a more prominent Middle Palaeolithic presence. Both Lower Sindh and the Rohri Hills present Middle Palaeolithic sites.

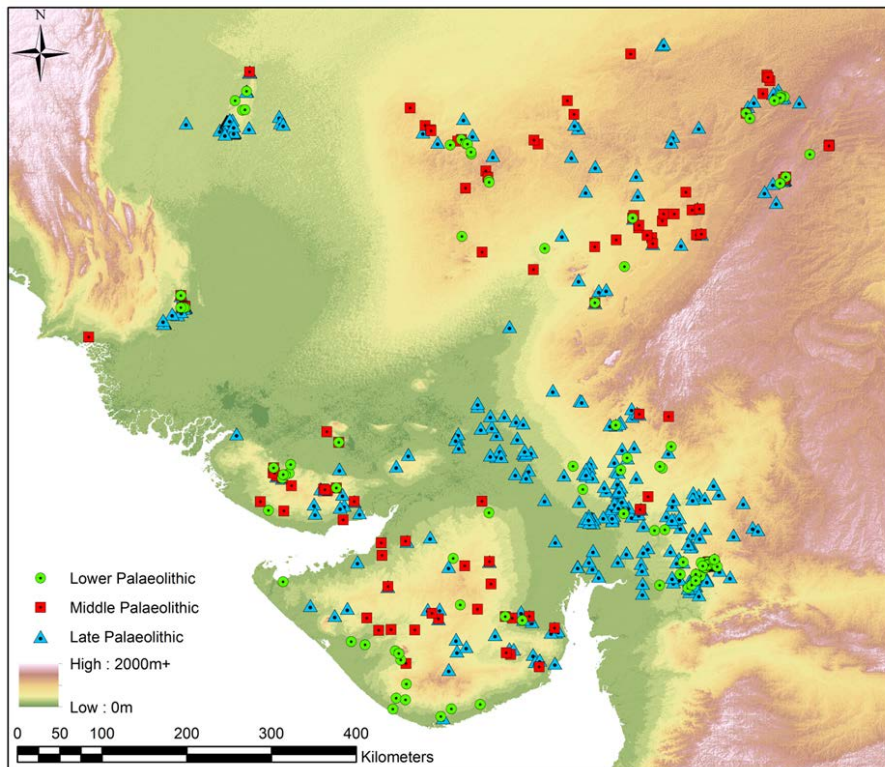


Figure 5.3: Distribution of sites with a single Palaeolithic industry present.

Late Palaeolithic sites are three times as numerous as either Lower or Middle Palaeolithic sites, with the majority of occurrences located in Mainland Gujarat, and particularly in alluvial settings that lack a significant Lower or Middle Palaeolithic presence. Late Palaeolithic sites are also found in large numbers throughout Saurashtra and Kachchh. The distribution of Late Palaeolithic sites in Rajasthan is similar to that of the Middle Palaeolithic, although slightly more numerous. In Sindh, a large number of sites are reported, including more dispersed concentrations within the Rohri Hills region, and at the Lower Sindh region of Jhimpir, predominately identified by Biagi et al. (1996) and Shaikh et al. (2002-3).

The large number of Late Palaeolithic sites reported in the Thar Desert and their regional variability may reflect a number of factors, such as increased archaeological visibility due to their occurrence in more recent and abundant sedimentary contexts. However, elsewhere in

South Asia rapid demographic growth is associated with the development of Late Palaeolithic technologies (Petraglia et al. 2009), and so more intensive occupation of the Thar cannot be discounted.

The distribution of sites reported as Lower and Middle Palaeolithic broadly matches the distribution of both individual industries, while indicating a greater presence of Middle Palaeolithic sites in mainland Gujarat. In contrast, sites with both Middle and Late Palaeolithic archaeology show a more discrete distribution occurring in east Saurashtra and central Rajasthan, as well as many of the well sampled areas of Sindh. The relatively large number of sites reported as Middle Palaeolithic and either Lower or Late Palaeolithic may indicate problems in the accurate attribution of transitional industries and explain the relatively low number of sites with only Middle Palaeolithic archaeology reported. The number of sites with Lower and Late Palaeolithic archaeology is low, and the distribution is broadly in keeping with the distribution of the individual industries. Sites with all three industries present are limited in number, and are widely dispersed. Finally, sites without industrial affiliation are most numerous in west Rajasthan, with prominent occurrences in mainland Gujarat, as well as appearing in Saurashtra and Sindh.

Palaeolithic Lithic Typology in the Thar Desert

A total of 521 Palaeolithic sites in the Thar Desert present information on the presence of certain artefact types (Table 5.2; Appendix A.2). When broken down into different Palaeolithic industries, the presence of certain artefact types shows considerable structuring in the 521 sites (Figure 5.4). The majority of sites have been attributed to a single Palaeolithic industry (Table 5.3), permitting discussion of the different typological characteristics of each industry.

After these typological trends are detailed, the evidence from sites with more than one industry present will be examined.

Artefact Group	Artefact Type	# of sites	% of sites
Debitage	Flake/Debitage	349	66.97
Debitage - Blade	Blade	104	19.96
	Parallel Blade	10	1.92
	Flake Blade	43	8.25
	Backed Blade	29	5.57
	Crested Blade	16	3.07
Debitage -Retouched	Retouched/Tools	84	16.12
	Point	188	36.08
	Borer	69	13.24
	Burin	79	15.16
	Awl	29	5.57
	Denticulate	13	2.49
	Notch	9	1.73
	Scraper	315	60.46
	Knife	64	12.28
Debitage - Microlithic	Microlith	35	6.72
	Geometric Microlith	7	1.34
	Non-geometric Microlith	11	2.11
	Lunate/crescent	48	9.21
	Triangle	42	8.06
	Trapeze	28	5.37
	Micro-blade	7	1.34
	Backed bladelet	3	0.58
Cores	Core	275	52.78
	Fluted Core	19	3.65
	Blade Core	65	12.48
	Prepared Core	12	2.3
	Discoid/Discoidal Core	46	8.83
	Microlithic Core	18	3.46
	Polyhedron/Polyhedral Core	69	13.24
Heavy tools	Heavy tools	16	3.07
	Handaxe	158	30.33
	Chopper	39	7.49
	Chopping Tools	97	18.62
	Cleaver	129	24.76
	Pick	4	0.77

Table 5.2: Occurrence of different lithic artefact types in Palaeolithic sites in the Thar Desert.

Industry	# of sites
Lower Palaeolithic	105
Middle Palaeolithic	81
Late Palaeolithic	194
Lower and Middle Palaeolithic	31
Lower and Late Palaeolithic	3
Middle and Late Palaeolithic	26
Lower, Middle and Late Palaeolithic	10
Unid.	71

Table 5.3: Number of sites with typological data with different industrial associations.

Lower Palaeolithic

A basic package of flakes, scrapers, cores and heavy tools are reported as comprising the majority of the 105 Lower Palaeolithic sites. Flakes are reported as present at 78.09% of sites. Retouched tools (40.95%) and scrapers (65.71%) are the most widely reported small tool types, with rarer occurrences of knives (18.09%), denticulates (4.76%), points (2.86%), notches (1.90%) and burins (0.95%). Cores are reported at half the Lower Palaeolithic sites (50.47%), and polyhedrons (36.19%) are also a regular occurrence, whereas discoids (7.62%) and blade cores (1.91%) are much rarer. Handaxes (80%) and cleavers (70.48%) are the most commonly reported heavy tools. Chopping tools (49.52%) and ovates (31.43%) are also a prominent feature, while choppers (14.28%), undifferentiated heavy tools (6.67%) and picks (2.86%) form a minor component.

Middle Palaeolithic

The 81 Middle Palaeolithic sites show a significant diversification of retouched tool and cores types compared to the Lower Palaeolithic, while including a less prominent heavy tool component. Flakes are again widely reported (61.73%), and both blades (16.05%) and blade flakes (13.58%) are a regular feature. Scrapers (80.25%) and points (61.72%) are the most

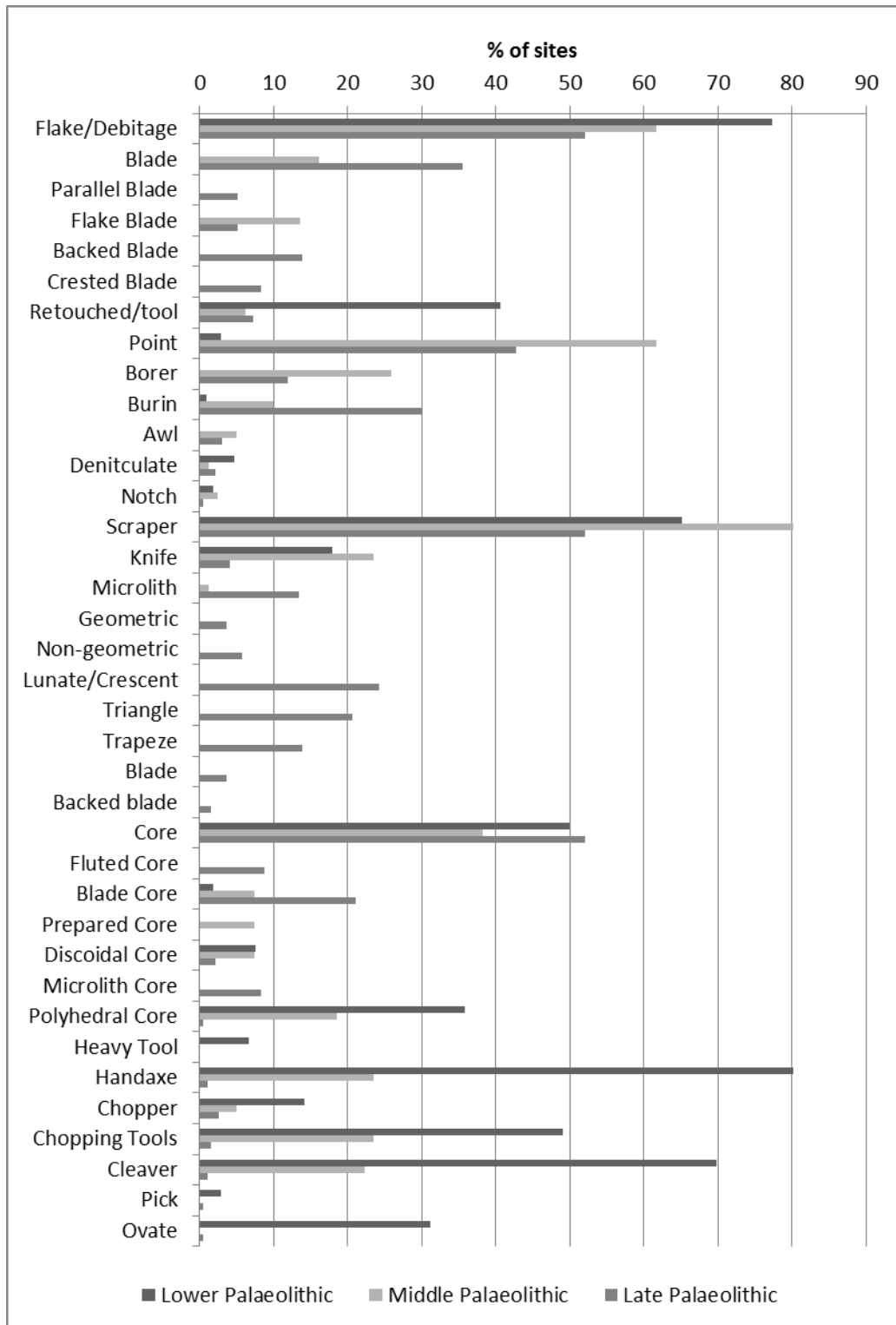


Figure 5.4: Bar chart of occurrence (%) of different lithic artefact types in Palaeolithic sites in the Thar Desert separated by industry.

widely reported retouched tool types. Borers (25.93%) and knives (23.46%) are also a common assemblage component, whereas a range of other tool types are reported at lesser frequencies (<10%). Cores (38.27%) are regularly reported in Middle Palaeolithic assemblages, although a range of specific core types, including polyhedral (18.52%), blades (7.41%), discoidal (7.41%) and Levallois cores (6.17%) form a notable, additional component. Heavy tools are regularly reported from Middle Palaeolithic sites, including handaxes and chopping tools (23.46% each), cleavers (22.22%) and choppers (4.94%).

Late Palaeolithic

Blade production and products appear to be the major component of the 192 Late Palaeolithic sites. Flakes are reported at 54.12% of sites, and blades are a common feature (37.63%).

Backed blades (13.91%) are also regularly reported, with more restricted presence of crested blades (8.24%), parallel blades (5.15%) and flake blades (5.15%). Scrapers (53.61%), points (43.81%) and burins (31.96%) are the most commonly represented retouched tool types, and with the exception of borers (11.86%) the remainder all occur at low frequencies (<5%).

Microlithic debitage are regularly reported in Late Palaeolithic sites, with lunates/crescents (24.23%), triangles (20.62%) and trapezes (13.92%) most common. Microliths (15.46%), geometric microliths (3.61%) and non-geometric microliths (5.67%), as well as bladelets (3.61%) and backed bladelets (1.55%), are reported in low frequencies. Besides non-specific cores (54.12%), blade cores (22.68%) are most common, with fluted cores (8.76%) and microlith cores (8.25%) a rarer inclusion, and few discoidal (2.06%) and polyhedral (0.52%) types are reported. Heavy tools are absent from the majority of sites, although a minor component of choppers (2.58%), chopping tools (1.55%), handaxes and cleavers (1.03% each) is notable.

Mixed Industries

The differences between individual Palaeolithic industries offer some insight into sites reported with more than a single Palaeolithic industry present. The 31 sites with both Lower and Middle Palaeolithic industries presenting the package of flakes, scrapers, cores and heavy tools that is common ground between the two, but with a significant addition of points, which are commonly associated with Middle Palaeolithic industries.

Only 3 sites with Lower and Late Palaeolithic assemblages occur, amongst a range of typically Late Palaeolithic types, included microliths and backed blades appear with heavy tools. Whilst choppers were the most common heavy tools amongst Late Palaeolithic assemblages, the appearance of handaxes and cleavers in these three sites may have influenced the decision to brand these sites Lower Palaeolithic.

Twenty-six sites are reported as both Middle and Late Palaeolithic. The broad typological similarities between Middle and Late Palaeolithic sites are evident in this sample, and the main means to distinguish the two groups, the presence of microlithic artefacts, is notably absent. Although these sites do present evidence for a focus upon blade production, this alone appears insufficient to distinguish the two industries.

Ten sites include components of all three industries, and unsurprisingly this sample presents a varied typological package including a diverse range of retouched tools and heavy tools whereas microliths are poorly represented. A very similar scenario is present amongst the 71 sites without any industrial affiliation, with a variety of retouched tools and heavy tools, few blades, and minimal reports of microliths.

Spatial Variation in Palaeolithic typology

The investigation of spatial patterning in Palaeolithic lithic typology of the Thar Desert offers a means to address environmental and, potentially, cultural influences upon variability. Figure 5.5 present the distribution of sites for which a typological inventory is available. As the Lower to Middle Palaeolithic, and Middle to Late Palaeolithic groups have been identified as illustrating considerable typological diversity and offer some level of control of industrial change, these will be included in the discussion, whereas the remaining groups offer little additional information by way of either typological or industrial variability, and are therefore excluded. The result of this analysis is presented in Table 5.4.

Variation in site typology varies considerably by region. Central Rajasthan is notable for illustrating the widest typological inventory, followed by Mainland Gujarat, and Saurashtra and Kachchh. Western Rajasthan shows the least diverse typological inventory, whereas the Rohri Hills show a greater degree of typological diversity than those in Lower Sindh. In assessing these patterns, it remains important to consider the history of research in these regions as a primary explanation for diversity, as Central Rajasthan has seen numerous important research projects, but this alone does not explain the evident diversity. The typological inventories of sites in Pakistan are somewhat less varied than those in the Indian regions, which may result from the more recent and technologically, rather than typologically, focused work.

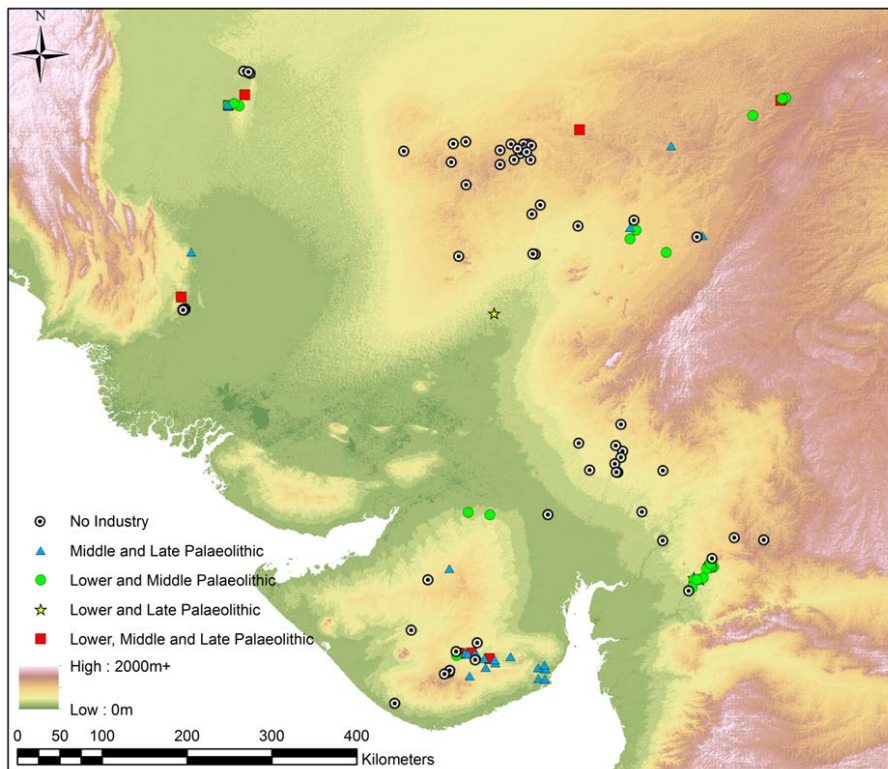
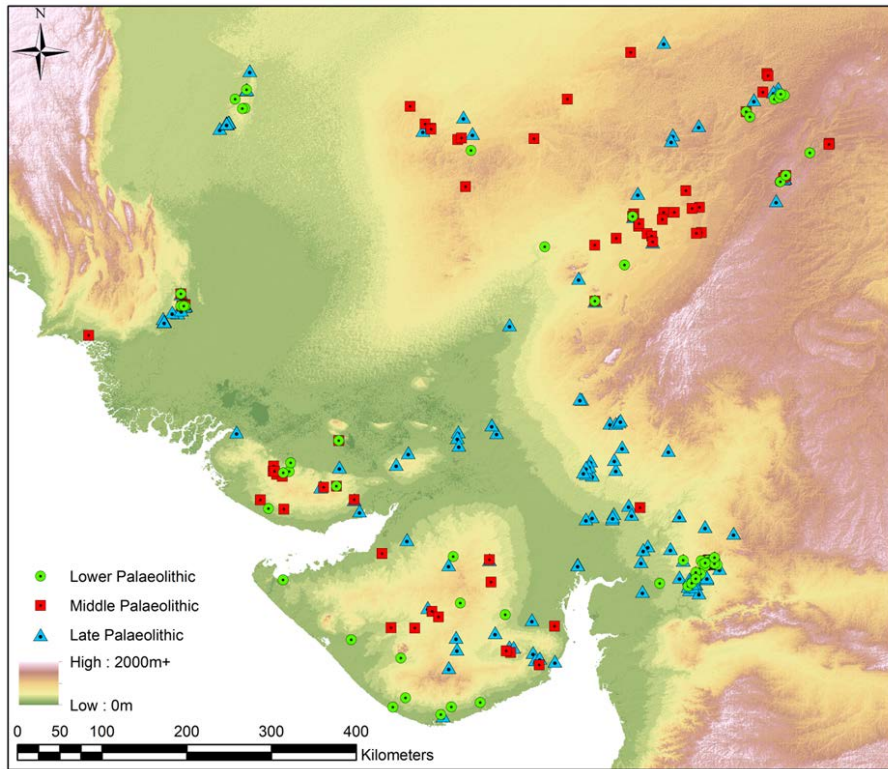


Figure 5.5: Distribution of sites with a typological inventory: a) Single industry sites (above); b) Multiple industry sites (below).

	Rohri Hills	Lower Sindh	Western Rajasthan	Central Rajasthan	Mainland Gujarat	Saurashtra and Kachchh
Lower Palaeolithic	Notch, Scraper	Scraper	Retouched Tools	Burin, Denticulate, Knife, Notch, Denticulate, Point, Scraper, Retouched Tools	Scrapers, Knives, Retouched Tools	Scrapers, points, borers
	Core, Blade Core	Core, Blade Core	Core	Core, Discoidal Core, Polyhedral Core	Cores, Polyhedral Cores	Cores
	Handaxe	Chopping Tools, Cleaver, Handaxe, Heavy Tool		Chopping Tools, Chopper, Cleaver, Handaxe	Chopping Tools, Cleaver, Handaxe, Heavy Tool, Pick	Chopper, Cleaver, Handaxe
Lower to Middle Palaeolithic				Blade, Flake Blade		Flake Blade
	Denticulate, Scraper			Borer, Denticulate, Knife, Point, Scraper	Knife, Point, Scraper, Retouched Tools, Ovate	
	Core			Blade Core, Core, Discoidal Core, Polyhedral Core, Prepared Core	Cores, Polyhedral Cores	Cores
				Chopping Tools, Chopper, Cleaver, Handaxe	Chopping Tools, Cleaver, Handaxe, Heavy Tool, Ovate	Chopper, Cleaver, Handaxe, Ovate
Middle Palaeolithic		Flake Blade	Blade	Blade, Flake Blade	Blade	Blade, Flake Blade
		Point, Scraper	Awl, Borer, Point, Retouched Tools, Scraper	Awl, Borer, Burin, Denticulate, Knife, Notch, Point, Scraper	Knife, Point, Scraper	Awl, Borer, Burin, Knife, Point, Scraper
		Prepared Core	Blade Core, Core, Prepared Core	Blade Core, Core, Discoidal Core, Prepared Core, Polyhedral Core	Polyhedral Cores	Cores, Discoidal Cores
			Chopping Tools, Chopper, Cleaver	Chopping Tools, Chopper, Cleaver, Handaxe	Chopping Tools, Cleaver, Handaxe	Chopping Tools, Chopper, Handaxe

(Continued Below)

	Rohri Hills	Lower Sindh	Western Rajasthan	Central Rajasthan	Mainland Gujarat	Saurashtra and Kachchh
Middle to Late Palaeolithic	Blade			Backed Blade		Flake Blade
	Burin, Point, Scrapers			Awl, Burin, Point, Scraper		Awl, Borer, Point, Scraper
	Blade Core, Core, Discoidal Core, Polyhedral Core, Prepared Core	Microlithic Core		Blade Core, Core, Discoidal Core		Cores, Discoidal Cores
	Cleaver, Handaxe			Chopping Tools, Cleaver, Handaxe		Chopping Tools
Late Palaeolithic	Blade, Backed Blade, Crested Blade, Flake Blade	Blade, Crested Blade, Flake Blade	Blade, Backed Blade	Blade	Blade, Backed Blade	Blade, Backed Blade, Crested Blade, Flake Blade
	Burin, Knife, Retouched Tools, Scraper	Burin, Notch, Retouched Tools, Scrapers	Awl, Burin, Scraper	Awl, Burin, Denticulate, Point, Scraper	Point, Awl, Borer, Burin, Denticulate, Knife, Scraper, Retouched Tools	Point, Borer, Denticulate, Knife, Scraper
	Blade Core, Core, Discoidal Core, Microlithic Core	Blade Core, Core, Microlithic Core	Blade Core, Core	Blade Core, Core, Fluted Core, Microlithic Core	Cores, Blade Cores, Fluted Cores, Microlith Cores, Discoidal Cores	Cores, Blade Cores, Fluted Cores, Microlith Cores, Discoidal Cores
	Pick	Chopper, Cleaver, Handaxe	Chopping Tools	Chopping Tools, Cleaver	Chopper, Handaxe	Ovate

Table 5.4: Spatial patterns of variability in lithic artefact types in Palaeolithic sites in the Thar Desert.

A number of spatial trends are also apparent between the different industrial groups. The appearance of Lower Palaeolithic blade cores in Sindh appears anomalous, and is not matched within the flake inventory, or followed by further blade production in the Middle Palaeolithic. In the Middle Palaeolithic, blade production is mostly restricted to the Luni Valley, whereas flake blade production is more widespread, including Saurashtra and Lower Sindh. Blade production expands considerably during the Late Palaeolithic, whereas crested blades are only seen in Sindh in this period, suggesting some diversity to blade technologies.

Amongst retouched tools, site inventories expand considerably in sites with a Middle Palaeolithic element, with scrapers and points are a common theme. In contrast, burins are not reported in Lower Sindh or Mainland Gujarat until the Late Palaeolithic, borers and awls are absent in the Pakistani sites, and knives are a repeated component of sites in the Central Rajasthan, Mainland Gujarat and Saurashtra and Kachchh.

Many sites are reported as containing cores, and although the limited detail of core reduction methods precludes in-depth discussion, some patterns are apparent in the basic typology. Discoidal reduction is seen in all industrial periods in Central Rajasthan except for the Late Palaeolithic, whereas in the Rohri Hills, and Saurashtra and Kachchh they appear in Middle and Late Palaeolithic contexts. Levallois cores are notably absent from Gujarati sites, appearing in the regions of Rajasthan and Sindh from the Middle Palaeolithic. Fluted cores are restricted to Central Rajasthan and the two Gujarati regions in the Late Palaeolithic. As previously noted, blade cores appear, albeit rarely, in Lower Palaeolithic contexts in both regions of Sindh, in Middle Palaeolithic contexts in Rajasthan, before becoming ubiquitous in the Late Palaeolithic.

Less diverse packages of heavy tools are apparent in the Pakistani sites than their Indian counterparts throughout all the industrial groupings. Central Rajasthan and Mainland Gujarat repeatedly have the most diverse range of heavy tools present, whereas handaxes are a notable absence from Western Rajasthan. Across all regions, heavy tool diversity is reduced in the Late Palaeolithic, with three regions presenting only a single type, although variation in heavy tool type between regions is evident.

Discussion

This analysis of the Palaeolithic archaeology of the Thar Desert indicates trends in lithic typological between different industries and different sub-regions. A common typological package is widespread in the Lower Palaeolithic of the Thar Desert, featuring heavy tools,

flakes, cores and scrapers. In the Middle Palaeolithic, the retouched tool inventory expands considerably, and this diversification appears spatially structured. Greater variety in lithic type inventories is present in the desert margins than in the desert core, and different packages of retouched types occur in the different sub-regions (see below for further discussion). Flake blades and blades occur in numerous Middle Palaeolithic sites across the Thar Desert, but evidence for more systematic blade production occurs in the Late Palaeolithic with the widespread appearance of blade cores. The presence of crested blades in Sindh suggests some technological diversity in methods of blade production, indicating that the possible independent development of blade technologies on different sides of the Thar Desert. In contrast, heavy tools become less commonplace and fewer types occur after the Lower Palaeolithic, but their continued presence in Late Palaeolithic assemblages is notable. Core types diversify in Middle Palaeolithic sites to include a range of forms, and this appears to be spatially structured.

Palaeolithic Raw Material Use in the Thar Desert

Information regarding raw material use are present at 449 sites from the Thar Desert of which 333 instances come from single industry sites, while 49 sites provide no detail on Palaeolithic industry. At the broadest level of resolution it is possible to discuss overall raw material use throughout the Thar Desert (Figure 5.6; Table 5.5; Appendix A.3). The most frequently used raw material is quartz, appearing in the inventory of 197 sites, followed by chert (n=168) and quartzite (n=167). Other raw material types that have seen repeated use include chalcedony (n=121), flint (n=82), agate (n=60), jasper (n=46) and rhyolite (n=36). A range of other raw materials have seen very limited use including sandstone, shale, basalt, dolerite, volcanic rock or lava, ochre (including iron ore, raw sienna and haematite), tachylite, SHR, trap, and various silicious rocks (including carnelian, lydium, moonstone, bloodstone, greenstone, sard and

silicified wood). The number of raw materials at a site varies from 1 to 7, with a mean of 2.11 across the Thar Desert.

Type	# of sites	% of sites
Silicious	19	4.23
Chalcedony	121	26.95
Agate	60	13.36
Jasper	46	10.25
Chert	168	37.42
Flint	82	18.26
Quartz	197	43.88
Quartzite	167	37.19
Sandstone	9	2
Shale	9	2
Granite	1	0.22
Dolerite	5	1.11
Basalt	7	1.56
Rhyolite	36	8.02
Tachylite	4	0.89
Trap	3	0.67
Volcanic	5	1.11
SHR	1	0.22
Ochre	5	1.11

Table 5.5: Number and percentage of sites containing different lithic raw materials.

Distribution of Raw Material Use

The distribution of geological resources has a significant influence over the appearance of different raw material types found in archaeological sites. Spatial variation in raw material use is presented in Table 5.6.

A number of striking spatial differences in raw material use are evident in the Palaeolithic record of the Thar Desert. Most obviously, the two Pakistani regions stand in stark contrast to the Indian regions as only flint and chert are reported in the former whereas all four Indian regions show the use of at least seven different raw material types. This reflects differences in the distribution of geological resources (see Chapter 4). As a result, chert appears to be the

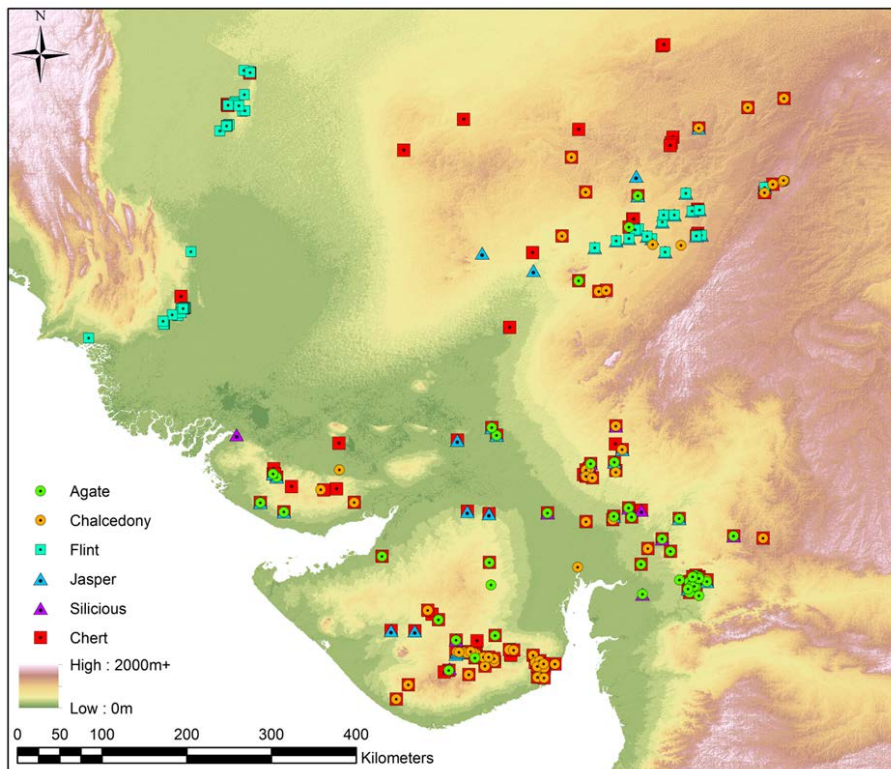
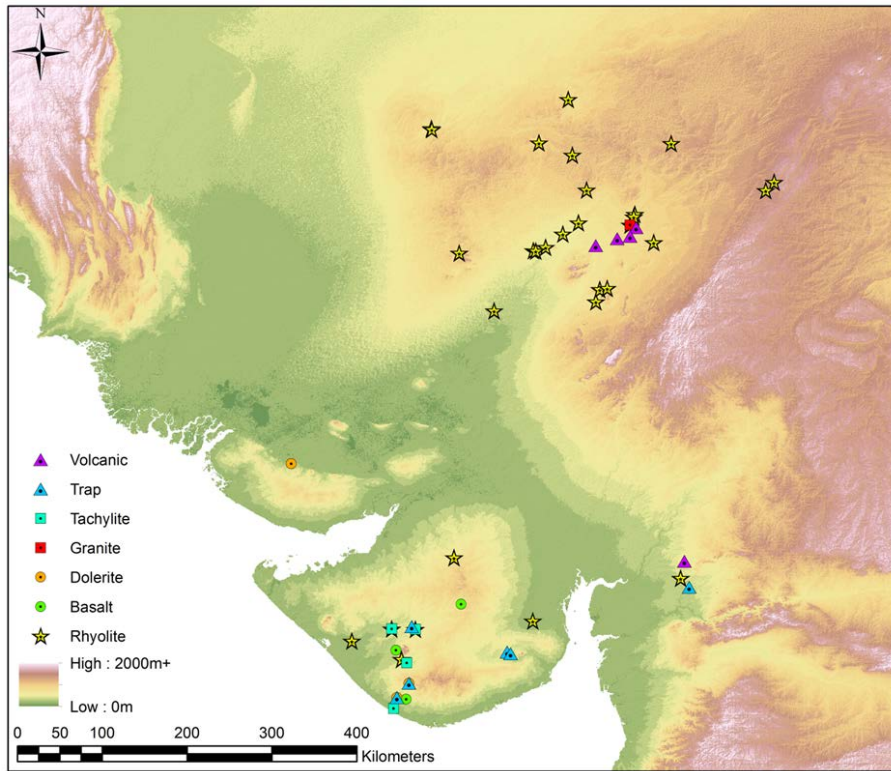


Figure 5.6: (Cont.)

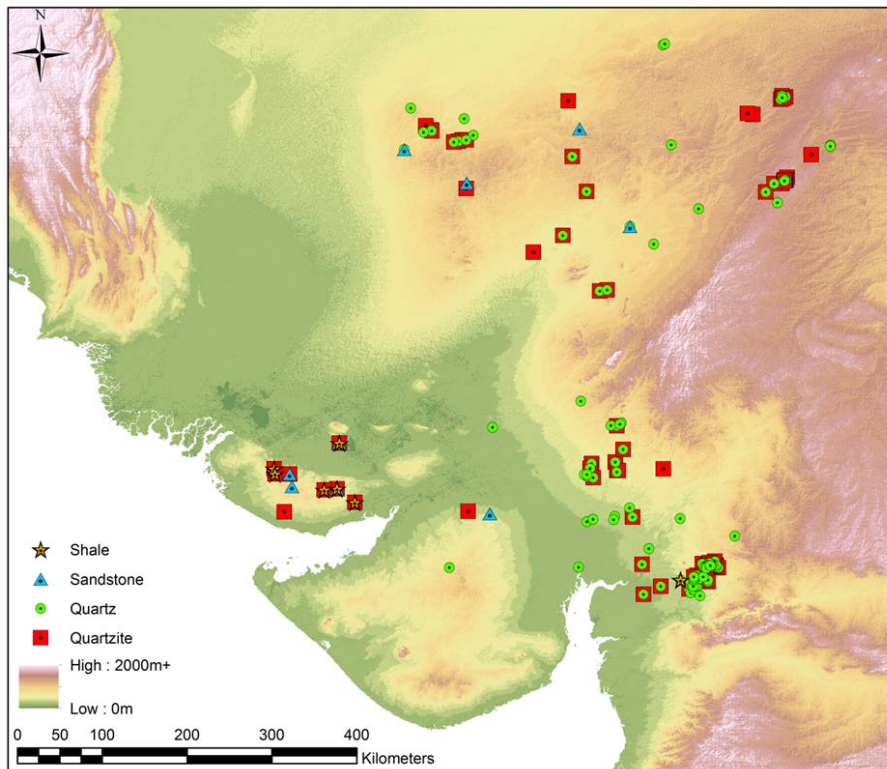


Figure 5.6: Distribution of raw material use in Palaeolithic sites in the Thar Desert: a) Igneous (previous page, top); b) Silicious (previous page, bottom); c) sedimentary and metamorphic (above).

most widespread raw material employed in the Palaeolithic period, appearing in all six regions. Jasper, quartz, quartzite and rhyolite are also widespread, and are present in all four Indian regions, although their distribution is not even. Rhyolite makes a single appearance in Mainland Gujarat. Quartzite is used in Kachchh but not Saurashtra, and quartz occurs only once in this region. Similarly, jasper is only seen at one site in Western Rajasthan. Saurashtra and Kachchh include the majority of sites that present use of igneous raw materials, including dolerite, basalt, tachylite and trap. Sandstone is limited to the two Rajasthani regions, whereas shale is restricted to the two Gujarati regions. Agate and chalcedony are found in three regions, although see their greatest concentration in Mainland Gujarat.

Type	Rohri Hills	Lower Sindh	Western Rajasthan	Central Rajasthan	Mainland Gujarat	Saurashtra & Kachchh
Silicious	-	-	-	X	X	X
Chalcedony	-	-	-	X	X	X
Agate	-	-	-	X	X	X
Jasper	-	-	X	X	X	X
Chert	X	X	X	X	X	X
Flint	X	X	-	X	-	-
Quartz	-	-	X	X	X	X
Quartzite	-	-	X	X	X	X
Sandstone	-	-	X	X	-	X
Shale	-	-	-	-	X	X
Granite	-	-	-	X	-	-
Dolerite	-	-	-	-	-	X
Basalt	-	-	-	-	-	X
Rhyolite	-	-	X	X	X	X
Tachylite	-	-	-	-	-	X
Trap	-	-	-	-	X	X
Volcanic	-	-	-	X	X	-
SHR	-	-	X	-	-	-
Ochre	-	-	-	-	X	X

Table 5.6: Presence of different raw material types in different regions of the Thar Desert.

Variability in Raw Material Use by Palaeolithic Industry

At a gross level, there are subtle differences in the mean number of different raw materials occurring at a site in each individual industry, with a trend to include a greater number of raw materials from Lower to Late Palaeolithic (Table 5.7). Clearer trends are apparent when individual raw material use is detailed by industry (Figure 5.7).

Industry	Mean # of raw materials
Lower Palaeolithic	1.67
Middle Palaeolithic	1.95
Late Palaeolithic	2.57
Lower and Middle Palaeolithic	2.24
Lower and Late Palaeolithic	3.67
Middle and Late Palaeolithic	1.84
Lower, Middle and Late Palaeolithic	1.9
None	1.45

Table 5.7: Mean number of raw materials in sites of each industry.

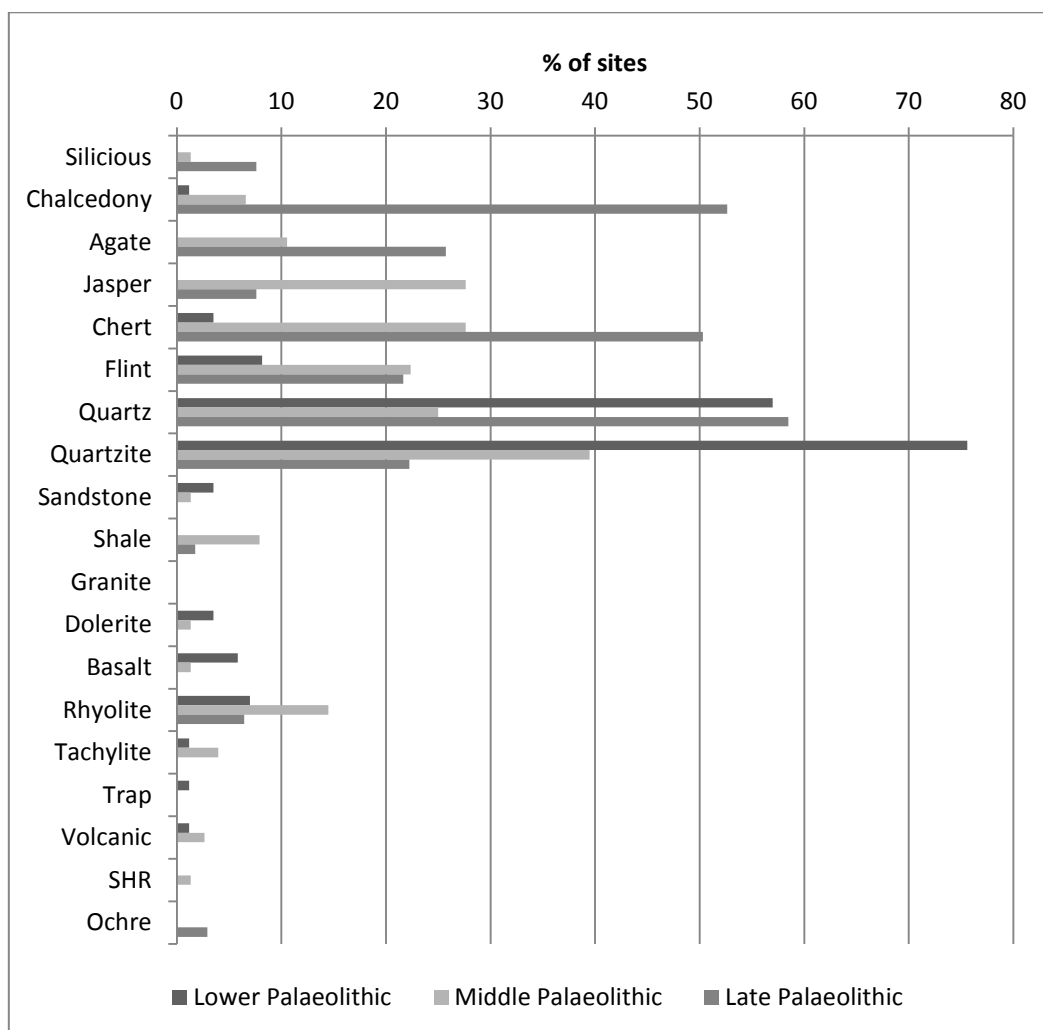


Figure 5.7: Bar chart of raw material use in single industry Palaeolithic sites in the Thar Desert.

Lower Palaeolithic

Of the 86 Lower Palaeolithic sites with raw material reported, three quarters include quartzite (75.58%) and just over half include quartz (56.98%). Besides these, flint (8.14%), rhyolite (6.98%) and basalt (5.81%) and most frequently reported, with few sites (<5%) reported with chalcedony, chert, sandstone, dolerite, tachylite or trap.

Middle Palaeolithic

A more diverse picture of raw material use is present in the 76 Middle Palaeolithic sites with available information. Quartzite (39.47%) remains the most frequently reported raw material type. Roughly equal use of chert and jasper (27.63% each), quartz (25%) and flint (22.37%) indicate a significant focus upon the use of silicious materials, also supported by the more limited use of agate (10.53%) and chalcedony (6.58%). Use of igneous raw materials is also evident, dominated by rhyolite (14.47%) and smaller proportions of tachylite (3.95%), trap (2.63%), dolerite (1.31%) and basalt (1.31%). Limited use of sedimentary rocks is also present with the occurrence of shale (7.89%) and sandstone (1.32%).

Late Palaeolithic

A clear focus upon silicious raw materials is evident from 171 Late Palaeolithic sites. While quartz (58.48%) is most common, both chalcedony (52.63%) and chert (50.29%) are found at over half of these sites. Agate (25.73%), quartzite (22.22%) and flint (21.64%) also show regular use, whereas jasper (7.6%) and other silicious types (9.37%) are more uncommon. Limited use of rhyolite is present (6.43%), and minor use of haematite (2.92%) and shale (1.75%) is evident.

Mixed Sites

Lower and Middle Palaeolithic sites show a similar pattern of raw material use as Middle Palaeolithic sites, with a diverse range of both silicious and igneous materials employed, but with a more dominant presence of both quartz and quartzite that is akin to the Lower Palaeolithic pattern. A similar situation is evident in the Lower and Late Palaeolithic sites, although sample size has already been noted as an issue here. The Middle and Late Palaeolithic sites are dominated by the use of chert (92%) and chalcedony (56%) with isolated occurrences of other raw materials. Flint is most common in sites with either all three industries present or no industrial affiliation, with a number of silicious materials used in low incidence.

Discussion

Raw material use appears to be strongly structured between the Palaeolithic industries and the different regions of the Thar Desert. Lower Palaeolithic raw material use is highly restricted to quartzite and quartz, except for sites in Sindh where flint and chert are the only available materials, resulting in some typologically more refined specimens. This is drastically different to the pattern evident amongst Middle Palaeolithic sites, suggesting a wide use of materials suitable for lithic reduction, most clearly apparent in the decreased emphasis on quartzite. In contrast to this, Late Palaeolithic sites see high concentrations of use of silicious materials, and much more limited use of other types. Many of the silicious materials that have been used permit much greater control over lithic reduction due to their crypto-crystalline structure, but typically occur in much smaller package sizes, such as pebbles and cobbles. The engagement with a greater number of more diverse materials that begins in the Middle Palaeolithic and intensifies in the Late Palaeolithic may relate to a range of factors, such as the capacity or requirement for finer control over lithic reduction or expansion into regions that lack larger

raw material packages. In contrast, the focus upon quartzite in the Lower Palaeolithic may reflect functional requirements for edge durability amongst heavy tools. The continuity seen in raw material choice in the Pakistani regions is likely to reflect the abundance and easy access of flint and chert, which may have a significant impact upon both typological and technological factors.

Palaeolithic Artefact Sizes in the Thar Desert

Length and width measurements of 225 individual artefacts as well as 201 mean length and width measurements are available from 87 sites in the Thar Desert, whereas 195 individual artefact widths and 125 mean widths are also available (Appendix A.4). As discussed below, a range of factors are likely to determine the size of lithic artefacts, including raw material variability, typology, lithic reduction techniques and intensity.

Artefact size by raw material type

Trap, rhyolite and quartzite have been used to make the widest variety of artefact sizes, with lengths ranging from >150mm and <40mm (Figure 5.8). Flint and chert, which are often poorly differentiated from one another, cover a similar size range, although it is notable that Lower Palaeolithic artefacts dominate the larger flint range. Quartz shows a rather restricted size range, with artefacts measuring typically <40mm, and are almost entirely Late Palaeolithic artefacts. Lava is only represented by Middle Palaeolithic artefacts occurring in a 70-120mm size range. The remaining raw material types (jasper, silicified wood, agate and chalcedony) only occur in low numbers, mostly <120mm. The mean artefact size population suggest some similar patterns (Figure 5.9). Quartz and chalcedony artefacts are almost entirely <40mm. In contrast, the majority of quartzite, rhyolite and chert artefacts fall between >40mm and

<140mm. Although some trends in artefact size can be identified through analysis of raw material type, this appears insufficient to explain the majority of variability that is evident.

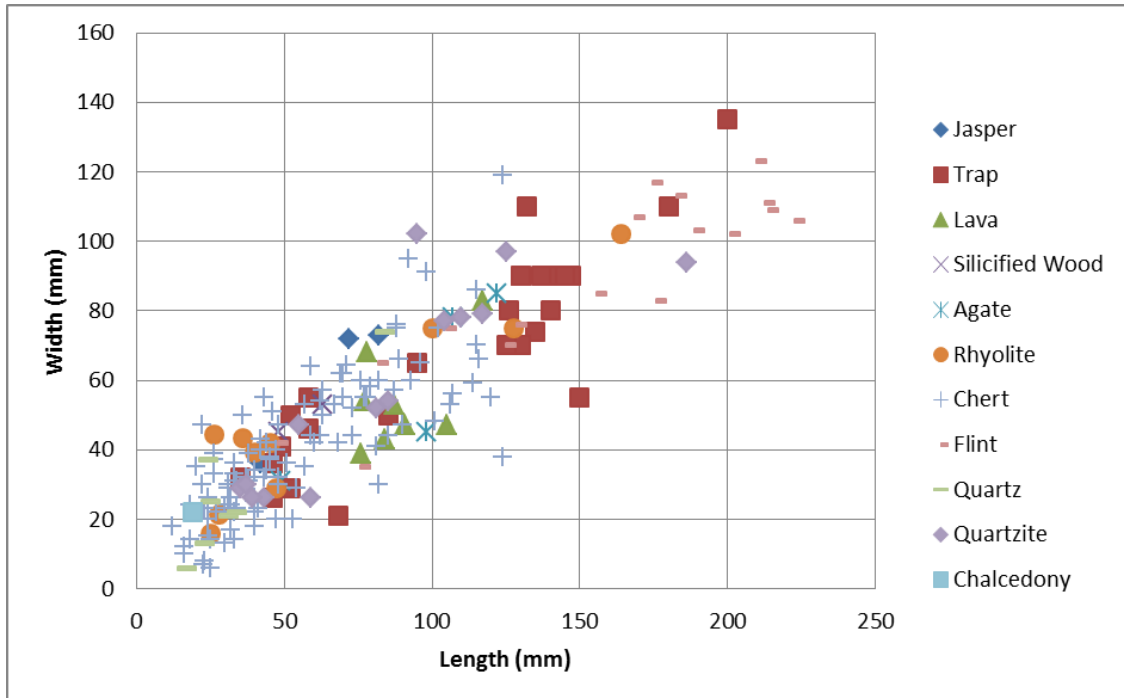


Figure 5.8: Scatter plot of individual Palaeolithic artefact size separated by raw material type.

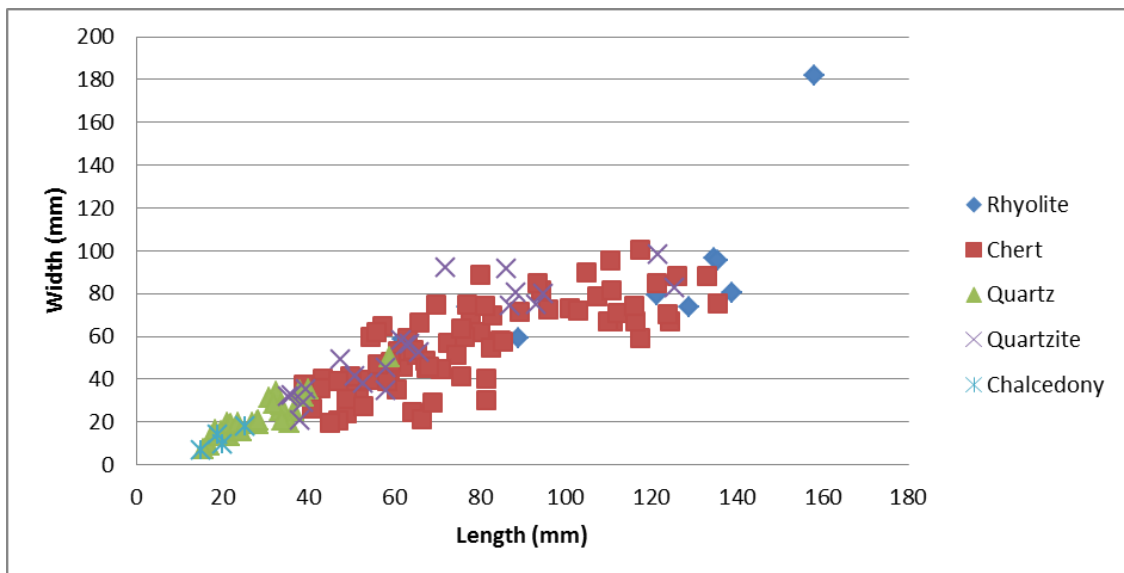


Figure 5.9: Scatter plot of mean Palaeolithic artefact sizes separated by raw material type.

Artefact size by Palaeolithic Industry

Within this sample, the three major Palaeolithic industries are fairly well discriminated by size (Figure 5.10), although the variety of artefact types that occur in each group is likely to be an important factor driving this. Amongst both individual and mean measurements, the majority of Lower Palaeolithic artefacts are >100mm in length, although the number of mean measurements may mask the smaller size ranges. Middle Palaeolithic artefacts almost entirely fall between 40-120mm length. Late Palaeolithic artefacts are mostly <50mm in length, although there is also a significant overlap with the Middle Palaeolithic range, with numerous artefacts ranging up to 120mm length.

Artefact size by artefact type

Flakes, blades and retouched tools

When broken down by artefact type, the trend of decreasing artefact size from Lower to Late Palaeolithic industries remains apparent (although sample size is an issue). Amongst flakes and blades, Lower Palaeolithic artefacts are largest (90-140mm length), Late Palaeolithic are the smallest (10-80mm length) and Middle Palaeolithic artefacts overlap with both ranges (30-120mm length)(Figure 5.11). The presence of only a single mean measurement prevents discussion of Lower Palaeolithic retouched tool types. Middle Palaeolithic retouched artefacts occur within the range of 30-120mm length, matching the range for flakes and blades in for this industry (Figure 5.12). The majority of Late Palaeolithic retouched artefacts range between 10-60mm, with few instances of larger pieces.

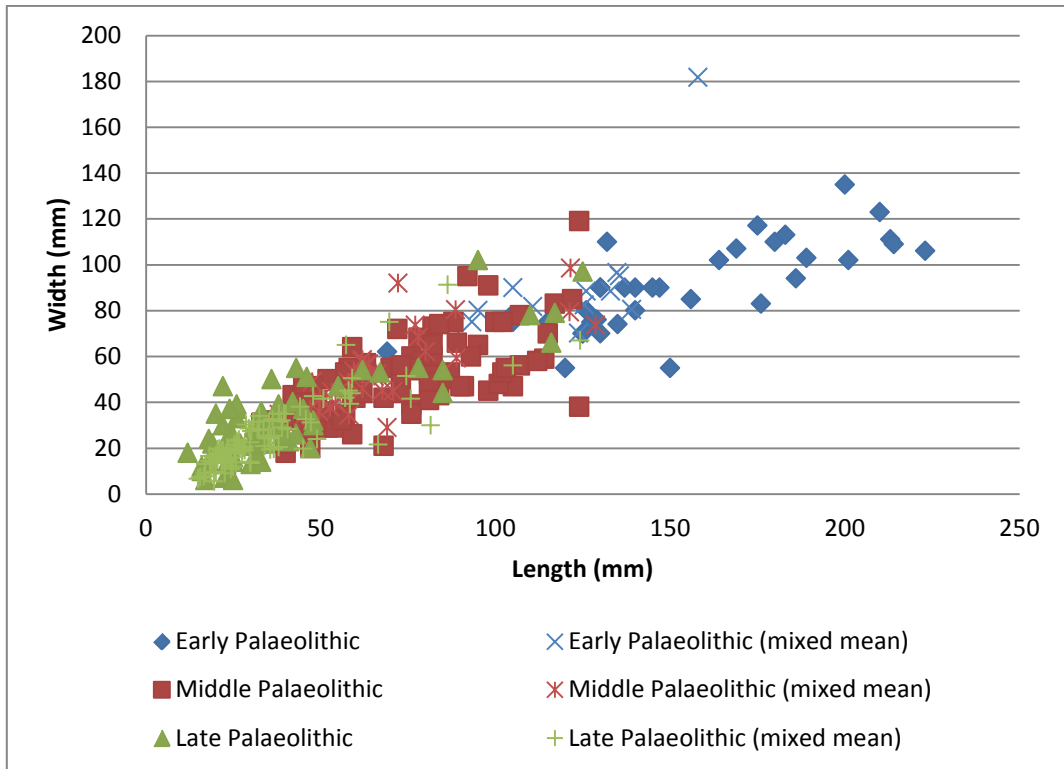


Figure 5.10: Scatterplot of individual and mean Palaeolithic artefact sizes separated by Palaeolithic industry.

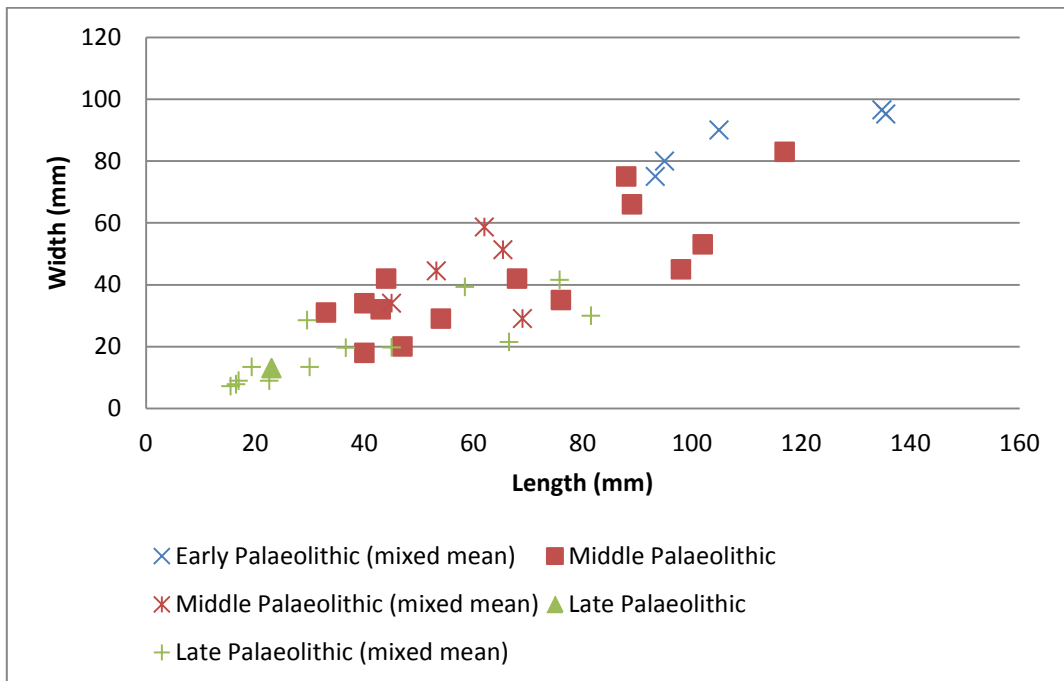


Figure 5.11: Scatter plot of individual and mean flakes and blades separated by Palaeolithic industry.

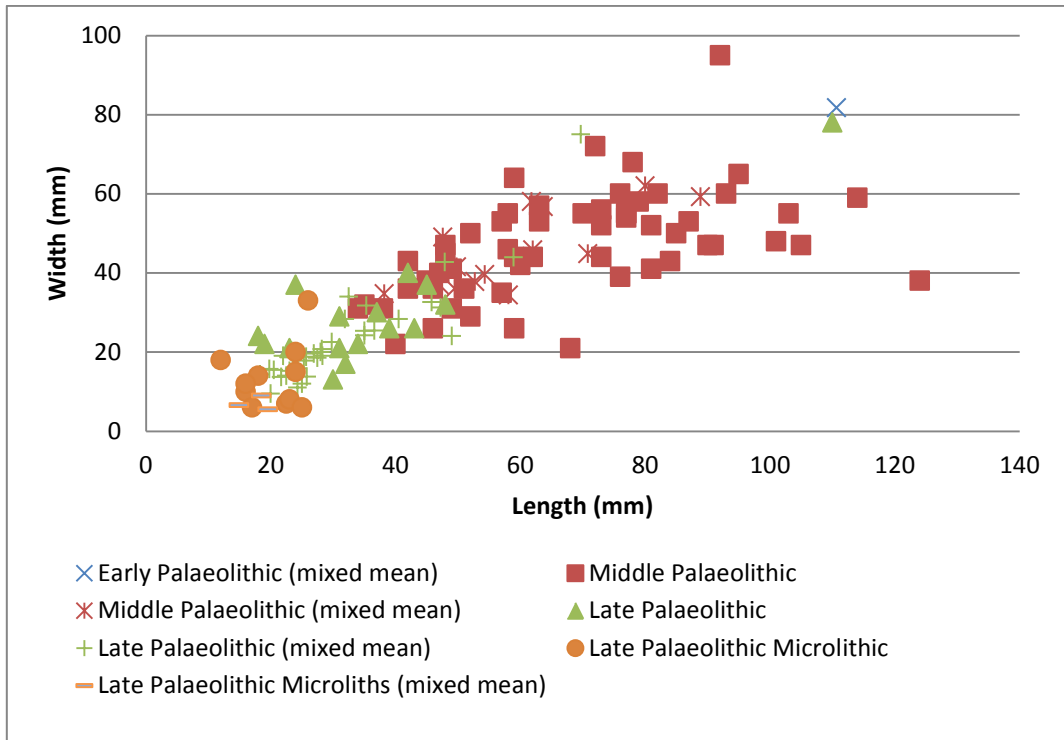


Figure 5.12: Scatter plot of individual and mean retouched tools and microliths separated by Palaeolithic industry.

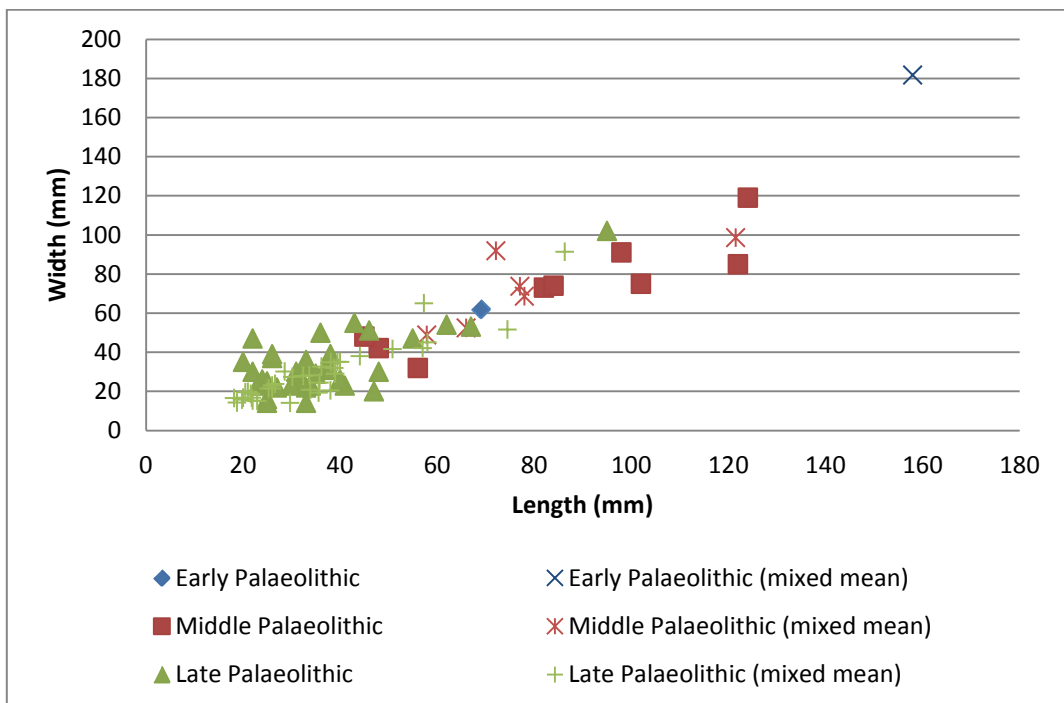


Figure 5.13: Scatter plot of individual and mean core sizes separated by Palaeolithic industry.

Middle Palaeolithic flakes are mostly thinner than 25mm and have an elongation index (Length/Width) ranging between 1-2.5, whereas the larger sample of retouched tools shows greater diversity, including a number of artefacts ranging up to 50mm thickness, and two artefacts with an elongation index above 2.5. The greater proportion of retouched pieces have an elongation index <1.5 , suggesting some variability in the requirement of elongate flake blanks for retouching.

Amongst the Late Palaeolithic sample, clear differences are apparent between retouched pieces and microlithic pieces. Microlithic pieces occur at a thickness $<10\text{mm}$ with a elongation index between 0.5-4.5, with the exception of a single artefact with a thickness of 40mm. Retouched Late Palaeolithic artefacts are predominately $<15\text{mm}$ thick, but a proportion range up to 3cm thick. The elongation index of Late Palaeolithic retouched artefacts is predominately <1.5 , with only a small proportion ranging up to 2.25. This suggests that different blank products appear to have been selected for the production of microliths to other Late Palaeolithic retouched artefacts. There is, however, a significant overlap between the Middle and Late Palaeolithic retouched artefacts, although the Middle Palaeolithic retouched artefact ranges are greater for both thickness and elongation index.

In contrast to the index of elongation, there is limited overlap between Middle and Late Palaeolithic flake and retouched artefact surface areas. Middle Palaeolithic pieces typically range between $1000\text{-}7000\text{mm}^2$, whereas Late Palaeolithic pieces are typically $<2000\text{mm}^2$. This suggests that while there are similarities in the shape of flakes produced in both of these industries, Middle Palaeolithic artefacts are notably larger.

Cores

One individual and one mean measurement of Lower Palaeolithic cores indicates a broad range of 70-160mm length, and thus extends beyond that suggested for flakes and retouched

artefacts (Figure 5.13). The length range for Middle Palaeolithic cores is 40-120mm, matching well with the flake and retouched tool size range. Late Palaeolithic cores mostly range from 20-70mm in length, with a small number extending to 100mm length, commensurate with the size of flakes and retouched tools.

The comparison of surface area and thickness offers a broad index of core volume. Core volume will impact the precision of both location and force of percussion for lithic reduction, and potentially the requirement for using different percussive techniques (e.g. bidirectional flaking, indirect percussion or pressure flaking). Variation in core volume amongst Palaeolithic artefacts may also relate to patterns of discard. Middle Palaeolithic core surface areas range between 20-150cm² and thicknesses range between 20-80mm, and these factors are broadly correlated. Late Palaeolithic cores show much tighter variation, with most core surface areas <4000mm², although rare examples extend to 10,000cm². Similarly, Late Palaeolithic core thicknesses are mostly <30mm, with fewer examples ranging up to 55mm. Overall, this indicates clear differences between Middle and Late Palaeolithic core volumes.

Heavy tools

Lower Palaeolithic Heavy tools range between 100-230mm length, There is little size differentiation between Middle and Late Palaeolithic artefacts (Figure 5.14), which mostly occurring between 50-120mm length, although a single Late Palaeolithic example is significantly smaller (mean length 30mm).

Amongst the Heavy tool sample, the Middle and Late Palaeolithic examples exhibit broad similarities and can be differentiated from the Lower Palaeolithic artefacts. This distinction is most apparent in thickness, with Lower Palaeolithic Heavy tools ranging between 25-95mm compared to 20-60mm for Late Palaeolithic and 20-50mm for Middle Palaeolithic. The

elongation index range for all three Palaeolithic industries overlap considerably, although the Lower Palaeolithic heavy tools tend toward a greater elongation.

Surface area also presents a greater degree of separation between Heavy tools than Index of Elongation for Palaeolithic industries. Whereas the majority of Lower Palaeolithic heavy tools have a surface area $>10,000\text{mm}^2$, the surface area of the majority of Middle and Late Palaeolithic heavy tools is $<10,000\text{mm}^2$.

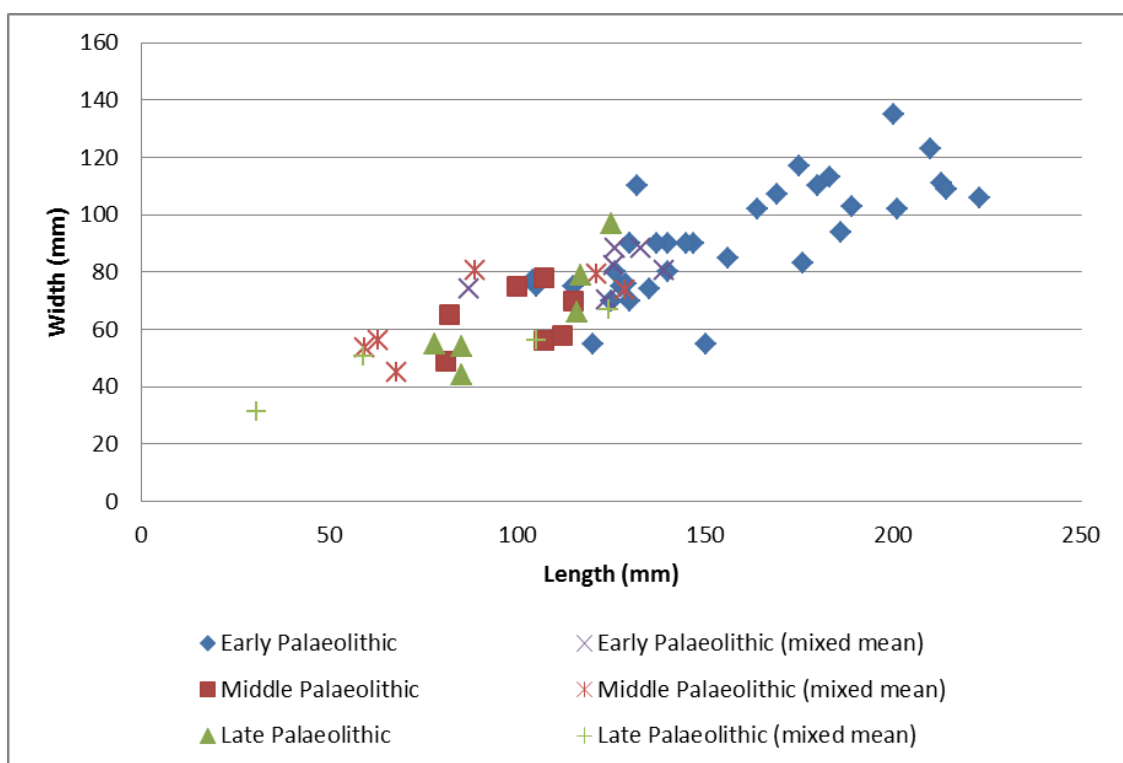


Figure 5.14: Scatterplot of individual and mean heavy tool sizes separated by Palaeolithic industry.

Discussion

Although both the sample of artefacts sizes and range of data available are limited, as well as being derived from a geographically diffuse group of sites, a number of trends are apparent in lithic artefact sizes. Some of variability in assemblages may be explained by the different raw materials used in the three Palaeolithic industries, although typology appears to be a more

dominant factor. Middle and Late Palaeolithic industries demonstrate considerable similarities in terms of artefact shape across the typological categories, but can be better differentiated upon the basis of artefact size. Differences in size and, to a lesser extent, shape of heavy tools indicate Lower Palaeolithic artefacts are different from Middle and Late Palaeolithic artefacts.

Palaeolithic Assemblage Composition in the Thar Desert

Determining patterns in proportional assemblage composition offers an approach to identifying patterns of hominin behaviour. A restricted number of sites present a detailed breakdown of the assemblage proportions, and many include relatively few artefacts. This analysis has therefore been restricted to those which number 50 artefacts or more (Figure 5.15; Appendix A.5). A total of 64 assemblages from 60 sites meet this criterion.

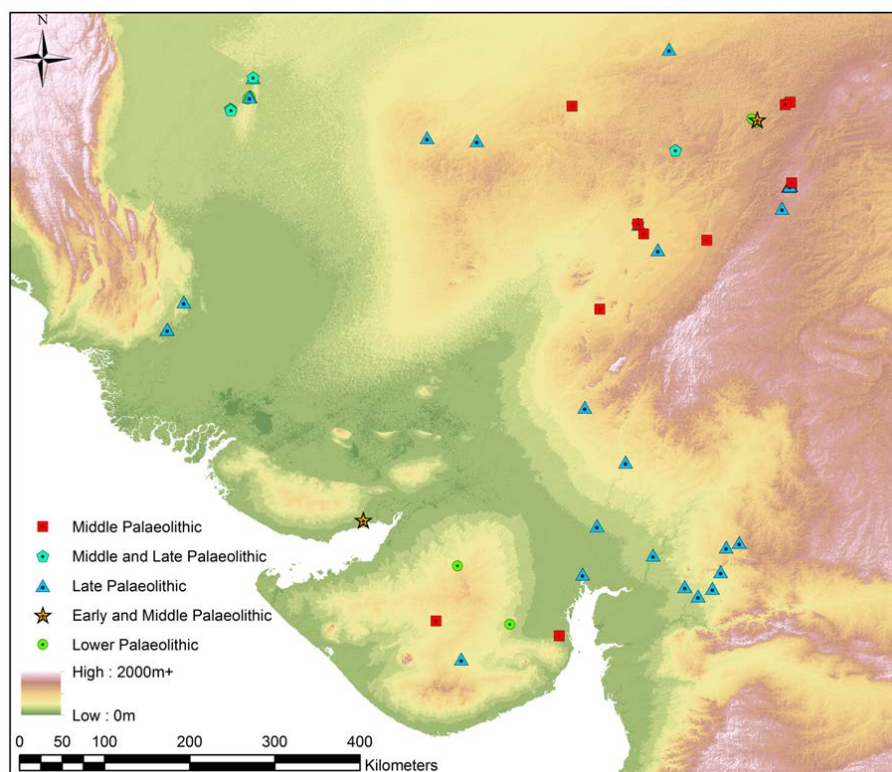


Figure 5.15: Distribution of sites that report the typological composition of Palaeolithic assemblages and include 50 or more artefacts.

Lower Palaeolithic

Twelve Lower Palaeolithic sites provide proportional details of assemblage composition, five of which have come from excavations and three have derived from controlled collections. As a result, the total number of artefacts in each assemblage is high, ranging from 891 to 63, with a mean of 419. Overall, the patterns of presence/absence of artefact types match well with broader typological sample discussed above, with all or most sites reporting flakes, scrapers, cores and various heavy tools (Figure 5.16). However, besides flakes (mean= 47.38%), these other artefact types all occur at very low levels (<10%) in most assemblages. Scrapers (mean=6.67%) occur in much higher frequencies than the other retouched tool types, with unspecified tools (mean = 2.12%) the only type with mean frequency >1%. Cores regularly occur in low frequency (mean=4.07%), with rare incidence of discoidal (mean=0.2%) or polyhedral (mean=0.33%) core types. Amongst heavy tools, handaxes are the most frequent occurrence (mean= 3.97%), followed by choppers (mean=2.11%), cleavers (mean=2.12%) and picks (mean=1.17%).

The spatial distribution of this sample is highly limited, principally deriving from sites close to Didwana, and including three excavated horizons from the site of Singi Talav. Sites from Gujarat and Sindh in the sample show no divergence with the trends identified amongst the sites near Didwana.

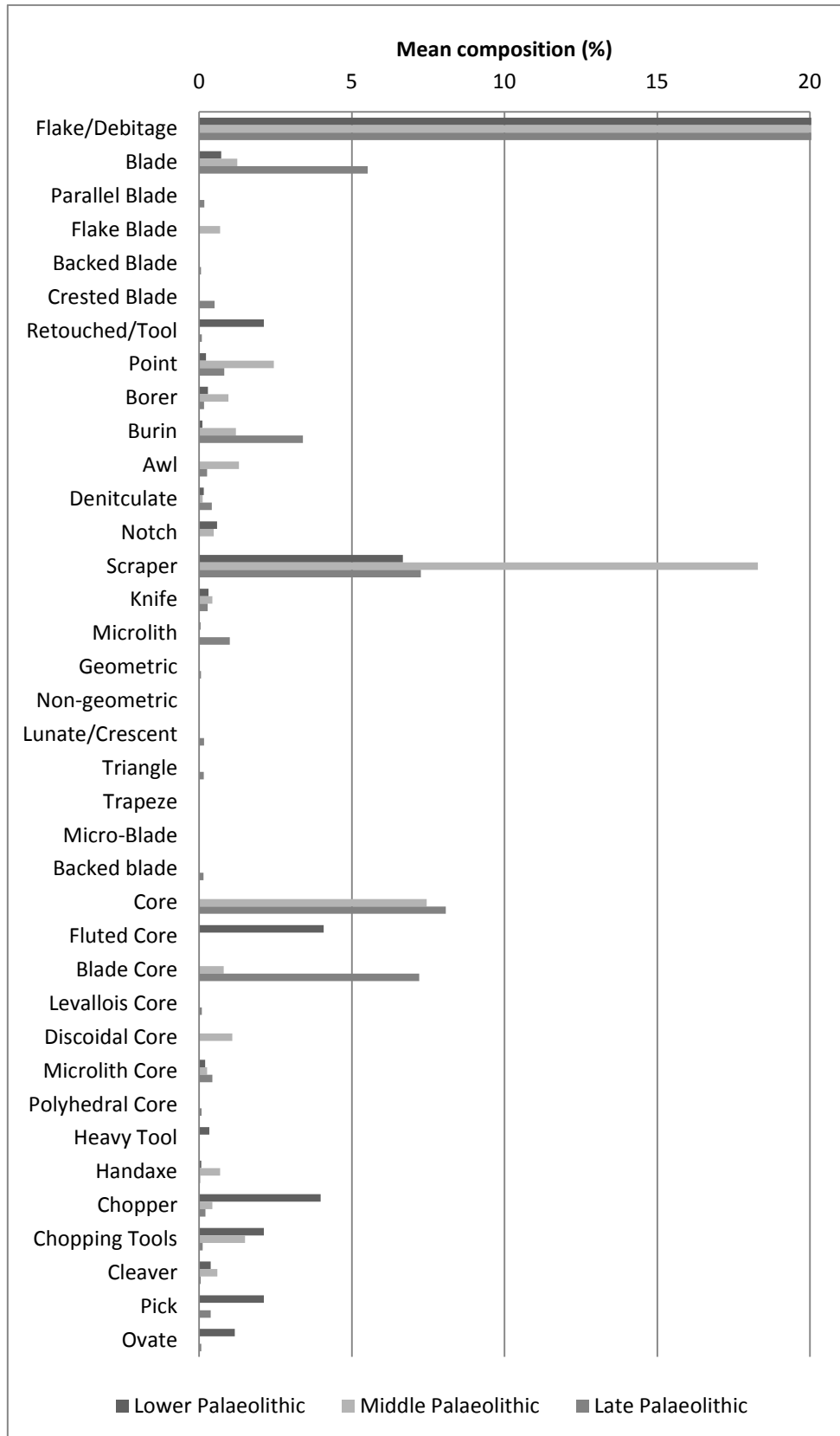


Figure 5.16: Mean proportional composition of lithic assemblage typological inventories separated by Palaeolithic industry (see text for exact proportion of flakes/debitage).

Middle Palaeolithic

Ten Middle Palaeolithic sites include proportional details of assemblage composition, two of which derive from excavations. The range of total number of artefacts is much lower than the Lower Palaeolithic group, ranging between 683 to 50, with a mean count of 186. This sample broadly reflects the patterns evident in the wider typological sample, but the average proportions of artefacts are generally low. Flakes generally account for half of the assemblages (mean=51.55%), whereas blades (mean=1.24%) and flake blades (mean=0.68%) are rare. Amongst retouched tool types, scrapers appear twice as common than in the preceding industry (mean= 18.29%), and points (mean=2.44%), awls (mean=1.3%) and burins (mean=1.2%) comprise retouched types >1%. Cores are more abundant in Middle Palaeolithic assemblages (mean=7.45%), including a discoidal core (mean=1.08%) and blade core (mean=0.81%) component, and rare microlithic cores (mean=0.26%). Chopping tools (mean=1.5%) are the most common heavy tool, with handaxes (mean=0.69%), cleavers (mean=0.59%) and choppers (mean=0.43%) a rare occurrence.

This Middle Palaeolithic sample derives from sites surrounding Didwana, the Pushkar Valley and Luni Valley, all of which fall within the Eastern Region. They therefore offer little prospect to investigate spatial changes in assemblage composition across the Thar.

Late Palaeolithic

The Late Palaeolithic sample is relatively large, comprising 45 sites, including evidence from ten controlled collections. The range of total number of artefacts is heavily skewed by two sites with very high numbers of artefacts (n=7505; n=4794), with the rest presenting between 426 to 50 artefacts, resulting in a high mean of 399. The number of flakes is slightly lower (mean=42.16%), and the number of blades (mean=5.42%) slightly higher in Late Palaeolithic

assemblages, with other blade variants occurring in low frequency (<0.5%). Scrapers are less common than either preceding industry (mean=6.87%), but burins form a more substantial part of assemblages (mean=3.68%). With the exception of points (mean=0.86%), all other retouched types occur <0.5%. Microliths (mean=1.27%) appear poorly accounted for, with specific microlith types all occurring <0.2%. Cores (mean=7.81%) and blade cores (mean=7.13%) are both common, whereas microlith cores (mean=0.4%) have a minimal presence. Heavy tools show a minimal contribution to artefact inventories, occurring at a mean frequency <0.2%.

When split into regional groups, a number of spatial trends can be identified, although the impact of sample size is evident. Saurasthra and Kachchh are represented by a single site, indicating a concentration of borers and denticulates not seen in other regions. Five sites appear in Lower Sindh, and due to the manner in which these assemblages have been reported, they offer little typological insight into their composition. The Rohri Hills region, with six sites, is notable for the highest percentage of blade cores, the appearance of picks, and an absence of retouched types except for scrapers, which may once more be a factor of differences in typological reporting. Both regions in Sindh present evidence for crested blades that are not seen elsewhere. Three sites appear in the Central Region, presenting a basic typological package, with the highest proportions of burins, second highest proportion of blade cores and the only instances of backed blades, triangles and chopping tools. The sixteen sites from the Eastern region present a generalised picture of assemblage composition, which may be a factor related to averaging a larger number of sites. As a result, it records low numbers (<1% unless specified) of most types seen across the Thar, including blades (3%), burins (5%), scrapers (4%), points (1%), awls, denticulates, microliths (2%), cores, blade cores, chopping tools and cleavers. Similarly, fourteen sites are present in Mainland Gujarat, offering a generalised Late Palaeolithic package including a high proportion of blades (10%) and

scrapers (12%), as well as points (2%), burins (3%), awls, denticulates, knives, microliths (2%), geometric microliths, lunates, cores (18%), blade cores (2%), Levallois cores, microlithic cores, polyhedral cores, choppers and ovates.

Mixed Industries

Seven sites presenting Middle and Late Palaeolithic artefacts present suitable numbers of artefacts for comparison, ranging between 350 to 70, with a mean count of 190. These sites share common features with the Late Palaeolithic sample, including relatively large numbers of blades (mean=4.89%), and blade cores (mean=8.3%), and a lower numbers of scrapers (mean=6.06%), but include a slightly higher heavy tool presence including handaxes (mean=0.63%), chopping tools (mean=0.62%) and cleavers (mean=0.64%). This matches the Middle Palaeolithic sample more closely.

Discussion

The analysis of assemblage composition highlights typological differences between the Lower, Middle and Late Palaeolithic industries in the Thar Desert. Quantitative as well as qualitative differences in the presence of different artefact types can be discerned. Heavy tools offer a prime example, as they occur in high numbers in many Lower Palaeolithic sites, and although they feature in both Middle and Late Palaeolithic inventories, they occur in low numbers. In contrast, although cores are a feature of Lower Palaeolithic sites, they occur in lower numbers than either Middle or Late Palaeolithic sites, which could suggest either that these later periods have a greater focus upon flake production, or differences in site use.

It is unfortunate that small sample size effectively prevents useful discussion of spatial variation in assemblage composition for the Lower and Middle Palaeolithic. However, spatial trends are apparent in the Late Palaeolithic samples. In particular, significant differences are

discernible between the Pakistani and Indian sites, and some more subtle differences occur between the larger samples of the Eastern Region and Mainland Gujarat.

Palaeolithic Excavations and Dated Sites in the Thar Desert

Nineteen excavations have been undertaken in the Thar Desert, concentrated in the area around Didwana, the Orsang and Sabarmati Valleys, Saurashtra and Sindh (see Figure 5.17).

The data from these excavations have been included in foregoing discussion, although there is rarely sufficient detail provided upon the chronological context or assemblage variability to warrant further discussion. Table 5.8 summarises details of these excavations

Site	Description
Chhajoli (Misra et al. 1980)	Limited evidence is available for the excavations undertaken at Chhajoli, suggesting simply that excavations were undertaken within the vicinity of the Jayal gravel ridge revealing similar results to the excavations at Jayal, i.e. a Lower Palaeolithic industry.
<i>Indola-ki-Dhani (Misra et al. 1982)</i>	Also occurring within the vicinity of the Bangur Canal, a 4x4m trench has been excavated opposite the village of Indola-ki-Dhani. Excavations were undertaken to a depth of 3.85m, and with a 2x2m area to a depth of 5.15m. Archaeological artefacts from the excavation were grouped into three horizons: Horizon 1 (1.35-1.85m) a Middle Palaeolithic assemblage numbering 266 artefacts; Horizon 2 (1.85-3.85m) a Late Acheulean (Lower Palaeolithic) assemblage concentrated mostly between 2.85-3.35m depth numbering 441 artefacts; and Horizon 3 (4.46-5.05m) a Middle Acheulean (Lower Palaeolithic) collection of 10 artefacts. The artefactual horizons occur beneath two layers of dune sands with loam and gravelly sand horizons with stronger evidence of carbonate precipitation between 1.35-2.72m.
Jayal (Misra et al. 1982)	Four 1x1m trenches have been excavated on the Jayal gravel ridge. The first (Jayal I) was excavated on top of a gravel ridge, whereas the other were excavated at the base (Jayal II), crest (Jayal III) and mid-slope (Jayal IV) of another gravel ridge. A composite stratigraphy from the site indicates that Lower Palaeolithic tools occur to a depth of 0.40m, although the excavations continued to 1m depth, illustrating that archaeological finds were restricted to the upper loam (0-0.2m) and the uppermost layer of a boulder gravel (0.2-1m). The majority of archaeological finds occur in Jayal IV (n=154; 45.3%), with a greater number occurring at the base of the ridge (Jayal II – n=117; 34.7%), than on the crest (Jayal III – n=68; 20%). Including the finds from Jayal I, a total of 456 artefacts have been recovered and are effectively reported as a single assemblage.
<i>Tarsang (IAR 1977-78)</i>	Excavations undertaken at Tarsang rock shelter in the late 1970's revealed an aceramic Mesolithic deposit overlain by Chalcolithic and Early Historic material culture, with an overall thickness of 0.8m. A total of 80,000 lithic artefacts were recovered with a rich typological inventory, with little further detail available about this assemblage, although presence of rock art at the site is a relatively rare feature for the region.
<i>Udrel (IAR 1970-71)</i>	Excavations at a surface sand dune site near the village of Udrel recovered a microlithic assemblage. The 1x1m trench was excavated to a depth of 0.5m, but archaeological artefacts including a range of microlithic material and partially fossilised bone fragments were only recovered from the top 0.1m.

Site	Description
<i>Samadhiala (IAR 1976-77)</i>	The site of Samadhiala is the only excavated site in Saurashtra, located 1km from the Kalubhar River. A 3x3m trench revealed an artefact bearing horizon, typified as a poorly sorted rubbly gravel, between 0.61-1.2m depth, although the gravel itself extended beyond 2.5m. The tools, characterised as Acheulean (Lower Palaeolithic) are reported as very fresh, with a large number of light tools and waster products, suggesting a semi-primary context. The gravel is seen stratified under alluvium, which is presumed to be an Upper Pleistocene deposit.
<i>Datrana IV & V (IAR 1994-95)</i>	A 5x5m excavation has been undertaken at Datrana IV, with particular interest in investigating blade production. An aceramic Mesolithic horizon 0.5-0.6m thick was identified stratified beneath a Chalcolithic deposit, with marked technological differences noted between the two, particularly the absence of long and crested blades. A small faunal sample was also encountered, indicating the presence of marine fish at the site. Datrana V is located ca. 300m away from Datrana IV, and revealed a similar sequence.
<i>Ambakut (IAR 1994-95)</i>	Ambakut is a rock shelter site in the Sukhi Valley, and 20m ² has undergone excavation. Two distinct archaeological deposits made up the 0.3-0.8m thick sequence, Mesolithic and Medieval, of which the former comprised ca. 0.6m at the deepest point. A broad range of typological evidence is available from the site, including the presence of worked red ochre.
<i>Santhli (IAR 1993-94)</i>	Four 5x5m trenches have been excavated at Santhli, revealing a cultural deposit of 0.4m thickness, dominated by aceramic Mesolithic deposits, which account for 0.25-0.3m. As well as a typical Late Palaeolithic lithic inventory, a rich faunal assemblage is present including numerous wild cattle skulls, although the reported presence of sheep/goat is a likely indicator that the site is from the Holocene.
<i>Jaidak II (IAR 1991-92)</i>	The site of Jaidak II occurs on a mound ca. 5m above the surrounding alluvial plain, with a Mesolithic deposit 0.8-0.9m thick occurring directly upon alluvium. The lithic inventory includes a range of geometric and non-geometric microliths, though predominately the latter. A substantial faunal assemblage is reported, although only the appearance of ostrich eggshell is reported.
<i>Jogpura (Ajithprasad 2005b)</i>	Three trenches have been excavated at Jogpura, located on top of a hilly ridge in the Sukhi Valley. The first measured 10x5m and ranged from a depth of 0.15m to 0.8m. The base of the sequence only includes abraded artefacts, overlain by an Acheulean horizon of 0.15-0.2m of both fresh and abraded artefacts. A 0.25m sterile layer separates this from a Middle Palaeolithic assemblage with similarly mixed states of preservation. A second trench, excavated to a depth of 0.5-0.6m, yielded a large quantity of Acheulean material, predominately debitage with some diagnostic pieces. A third trench, measuring 3x2m was excavated to a depth of 0.8m, with Middle Palaeolithic artefacts occurring in the uppermost 0.2m, with early Middle Palaeolithic and Late Acheulean artefacts found beneath this horizon, some of which are seen in association with a hearth.
<i>Shaktari Timbo (IAR 1992-93)</i>	During substantial excavations for drought relief work, a large Chalcolithic site was exposed at Shaktari, which has also yielded a thin (0.2m thick) aceramic Mesolithic horizon at the base of a 0.9m occupational deposit. A range of microlithic artefacts are reported as present, as well as a faunal assemblage encrusted in salts.
<i>ZPS4 (Biagi 2004)</i>	The site of ZPS 4 was selected for excavation because of the presence of bifacial picks. The excavation covered a total 16m ² , recovering 7505 Late Palaeolithic artefacts from thin, surficial aeolian sand deposits.

Table 5.8: Summarised description of Palaeolithic excavations undertaken in the Thar Desert.

A number of 'excavated' surface sites from the Rohri Hills present technological description of artefacts that are of use. Two sites, 16R Dune and Singi Talav, deserve individual discussion as they have been subject to more detailed analyses. In addition, chronometric dating of

stratified but unexcavated assemblages at a small number of sites provides further means to understand chronological patterns in the Palaeolithic archaeology of the Thar Desert.

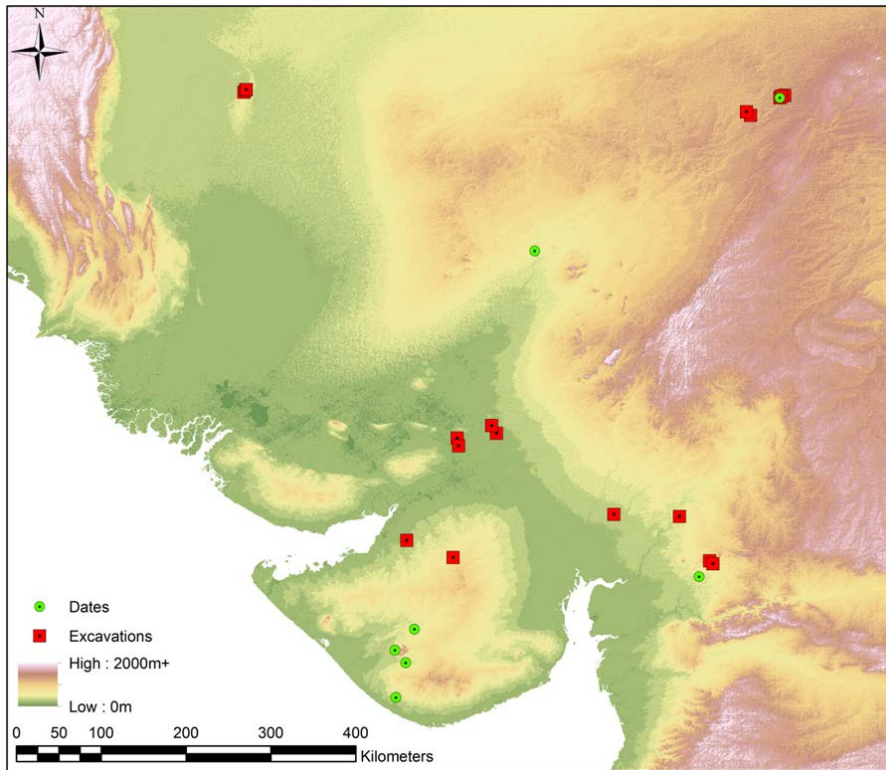


Figure 5.17: Distribution of sites with excavation or chronometric dating of Palaeolithic assemblages in the Thar Desert.

Rohri Hills

The 'excavations' at 797bis, ZPS1 and ZPS2 are notable as although the recovered assemblages are rarely found stratified in sediment, they appear to have undergone minimal post-depositional transportation and have been subject to technological analysis. These sites all occur associated with major limestone outcrops in the Rohri Hills, which have been exploited by Pleistocene populations, and more extensively in the Harappan period (Biagi 2004). Differing levels of patination accompanied with typological variability are used to separate these assemblages into Lower (Acheulean) Palaeolithic and Late (Upper) Palaeolithic (Biagi et al. 1996; Negrino & Kazi 1996; Biagi et al. 1998-2000).

ZPS1 (Biagi et al. 1996)

The excavation at ZPS1 recovered 29,047 artefacts from a 2x6m area, split into square metres. (see Figure 5.18) Three squares have been analysed in detail: E4 is reported to contain a pure Acheulean assemblage comprising 811 complete and 4,984 broken artefacts; E6 and E7 contain evidence of a Late (Upper) Palaeolithic workshop comprising 398 complete and 826 broken artefacts.

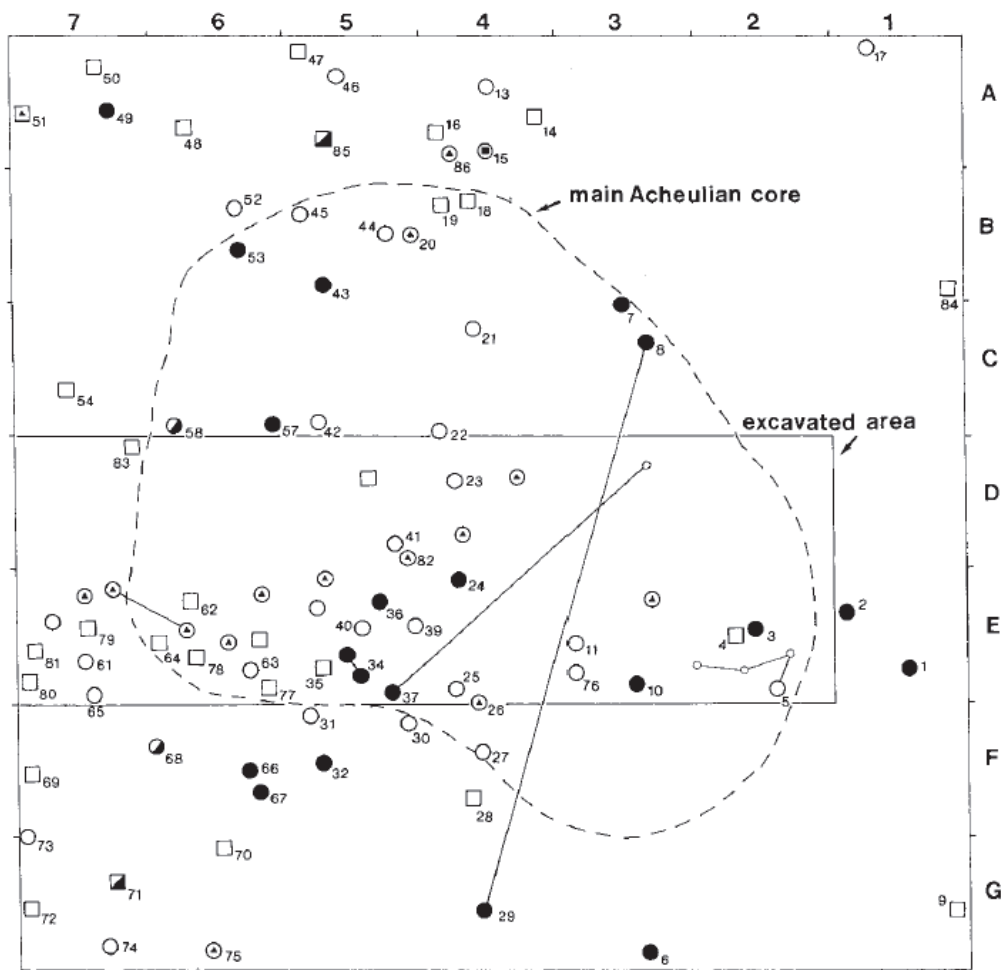


Fig. 3. Site ZPS1: distribution map of the tools.

- | | |
|---|---|
| 1. heavily patinated early Palaeolithic core, ● | 6. Late (Upper) Palaeolithic end-scrapers, ■ |
| 2. Acheulean hand-axes, ● | 7. Late (Upper) Palaeolithic cores, □ |
| 3. Acheulean side scrapers, ● | 8. Late (Upper) Palaeolithic hammerstone, ▣ |
| 4. Acheulean cores, ○ | 9. refitting Acheulean flakes, ○ |
| 5. Acheulean hammerstones, ● | 10. other refittings (drawn by F. Negrino), ○ |

Figure 5.18: Plan of excavation at ZPS1 (Biagi et al. 1996; Figure 3).

Amongst the complete and un-retouched Acheulean artefacts from E4 flake surfaces are predominately non-cortical (70%), with only 13% displaying more than 50% cortical coverage. Platforms are mostly flat (68%), linear (12%) or natural (11%), with a notable number of faceted pieces (6%). The majority of artefacts are larger than 60mm in either length or width, with 41% larger than 80mm in either dimension (see Figure 19a). Blade proportioned artefacts are rare (4%), with the majority of flakes presenting an elongation of 0.75-1.5 (62%). In addition, 18 bifacial handaxes in varied stages of reduction (see Figure 5.20), 2 side scrapers, 27 cores and 13 hammerstones were recovered.

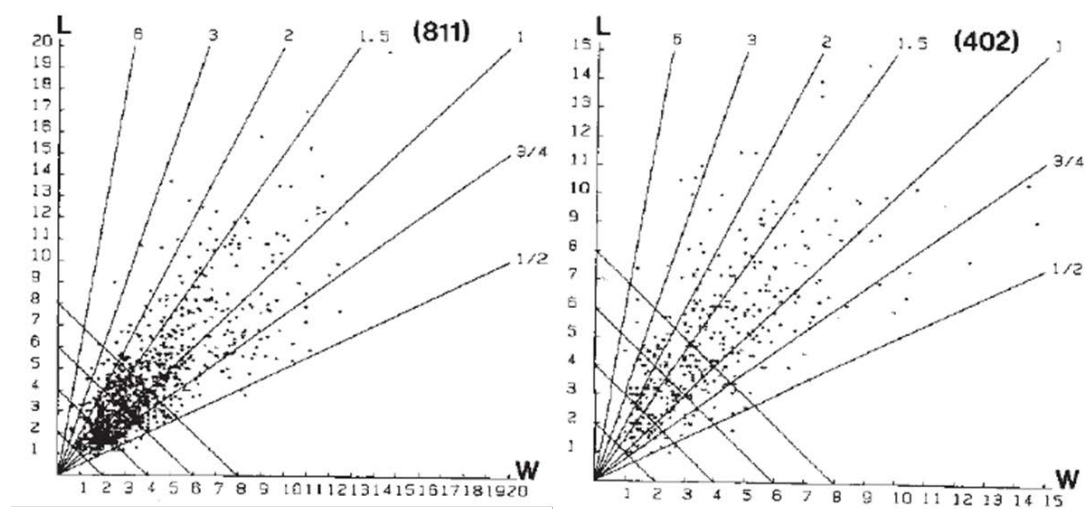


Figure 5.19: Size of analysed complete un-retouched artefacts from ZPS1: a) E4 (left); b) (E6-7) (right) (Biagi et al. 1996; Figure 4a & 4b).

For the Late (Upper) Palaeolithic assemblage, 51% of complete un-retouched pieces are non-cortical and a large component (16%) have >90% cortical coverage. Platform types are mostly flat (76%), with a lower proportion of natural and linear types (10% each), and rare faceted (2%) and dihedral (1%) types. Nearly half (48%) of artefacts are larger than 80mm (See Figure 19b), with 13% of flakes presenting an elongation greater than 2. Twenty-six subconical or prismatic blade cores were recovered, along with a hammer stone and two atypical carinated scrapers (Figure 5.21).

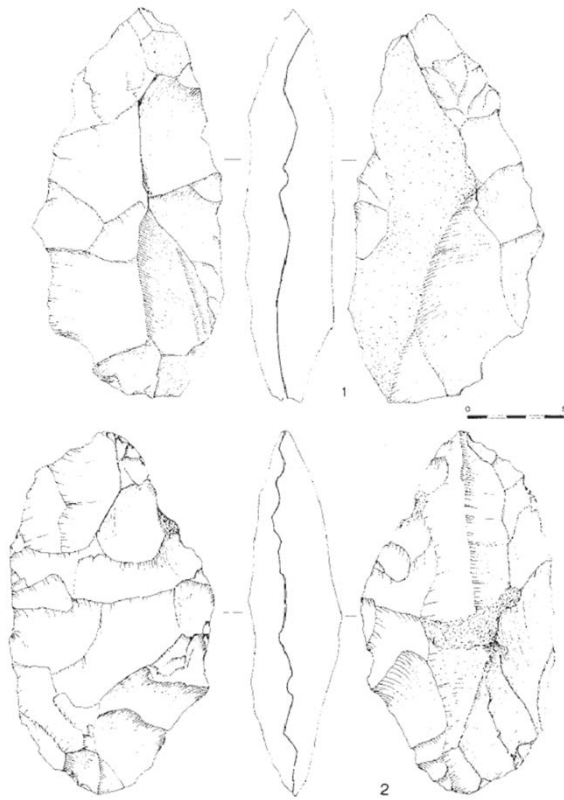


Figure 5.20: Unfinished Lower Palaeolithic Handaxes from ZPS1-E4 (Biagi et al. 1996; Figure 6).

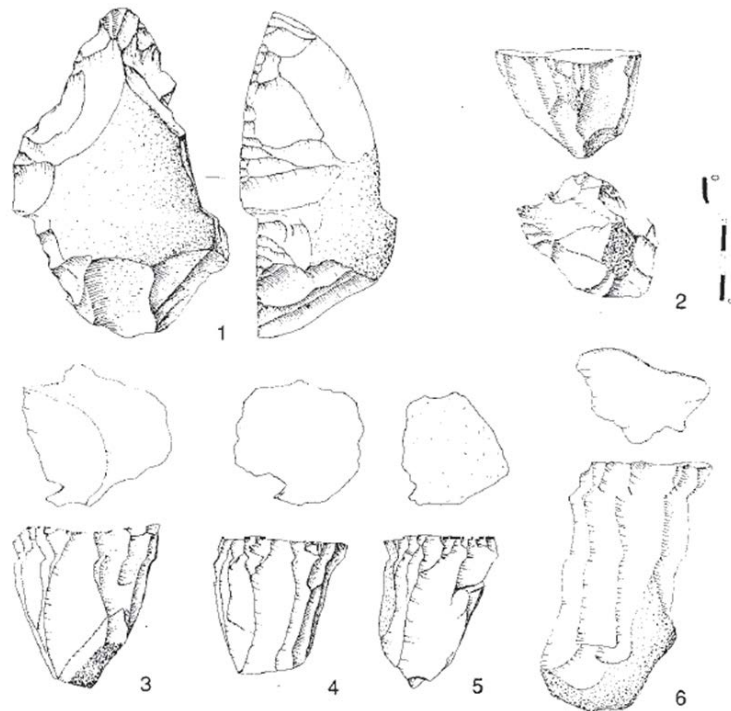


Figure 5.21: Late Palaeolithic endscrapers (1 & 2) and cores (3-6) from ZPS1-E6-7 (Biagi et al. 1996; Figure 10).

ZPS2 (Biagi et al. 1998-2000)

A 13m² excavation at ZPS2 yielded 4,794 artefacts following screening through 3mm mesh, which are characterised as a Late (Upper) Palaeolithic assemblage. 1,074 complete and un-retouched artefacts have been subject to more detailed analyses. Roughly one quarter of the artefacts measure 40-60mm (24%) and 60-80mm (26%) each in either length or width, with a larger proportion (39%) greater than 80mm in either dimension (see Figure 5.22). While the majority of artefacts present an elongation between 1-2 (61%), 14% display blade proportions (>2). A sub-sample of 99 artefacts indicated that flat (n=42) and natural (n=42) platform types were dominant, whereas pointed (n=11), dihedral (n=3) and faceted (n=1) types were rare. Fifty-seven cores and thirteen pre-cores were also recovered. Fifty-six of the cores are categorised as sub-conical with blade-like detachments and plain platforms and range from 31-94mm in length (see Figure 5.23).

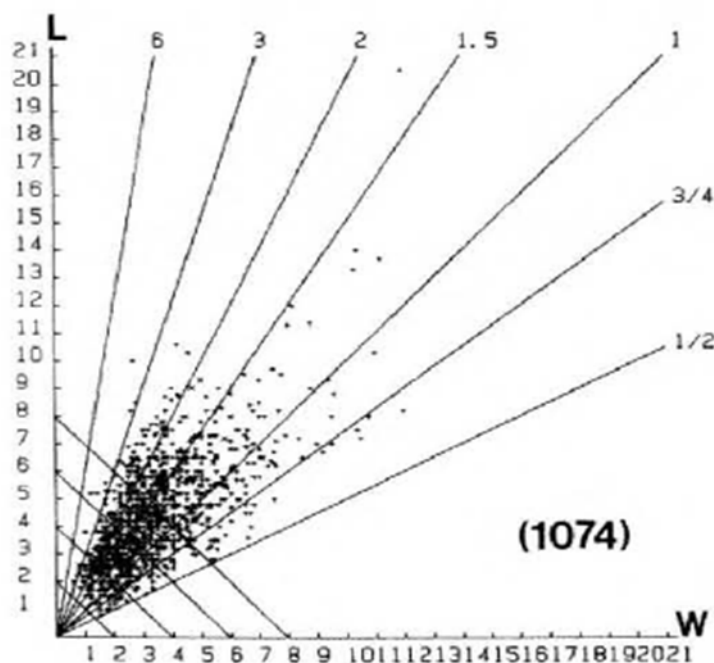


Figure 5.22: Size of analysed complete un-retouched artefacts from ZPS2 (Biagi et al. 1998-2000; Figure 5b).

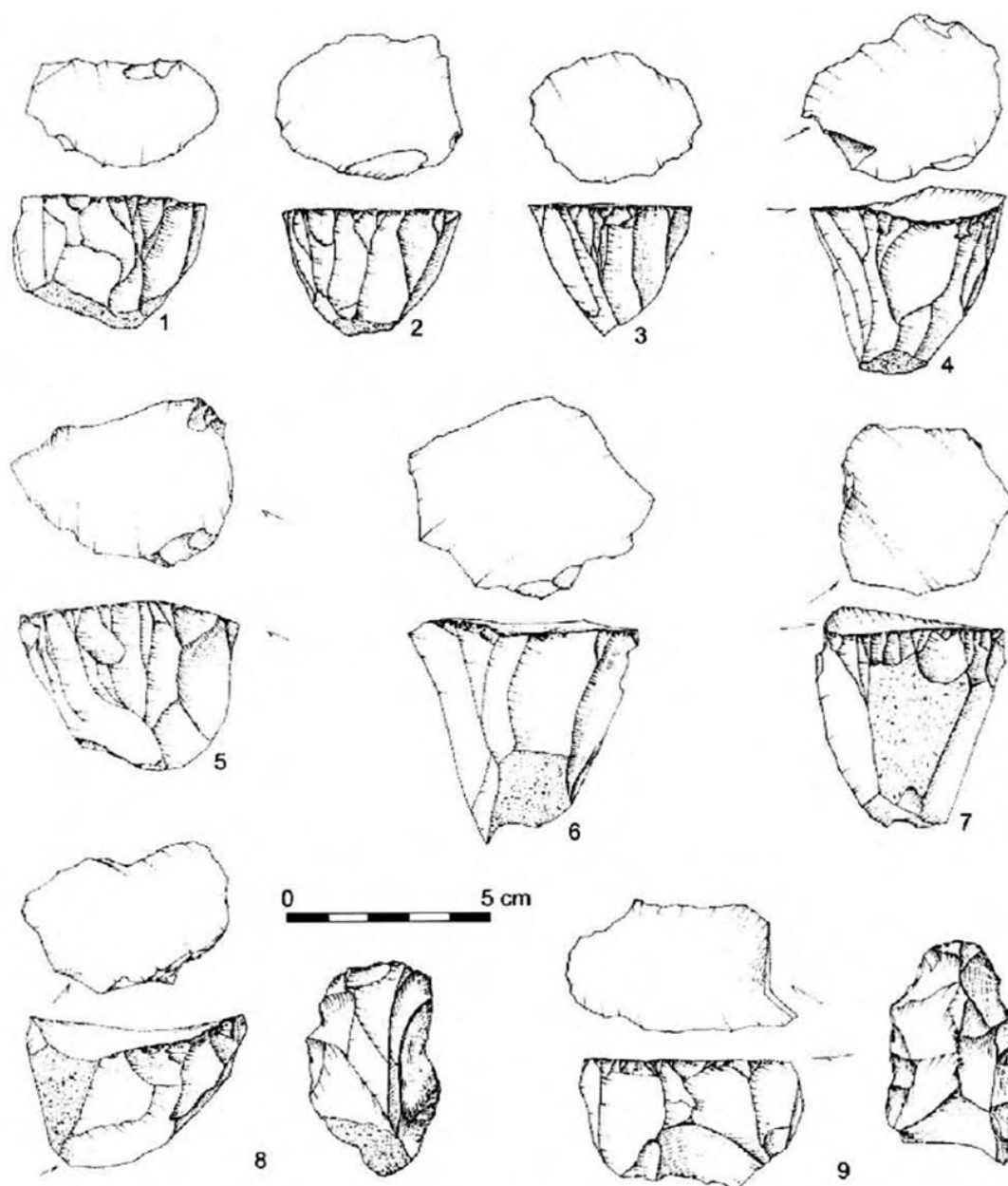


Figure 5.23: Cores from ZPS2 (Biagi et al. 1998-2000; Figure 10).

Site 797bis (Negrino & Kazi 1996)

Located to the south of the ZPS sites, a collection of 743 artefacts from an in situ assemblage across 80m² was made. A sub-sample of 638 artefacts showed similar levels of patinisation and were ascribed to Series 3 (Acheulean) and 315 complete pieces were subject to detailed

analysis (see Figure 5.24). The majority of flakes (55%) were between 80-100mm in either length or width, followed by artefacts with at least one dimension between 60-80mm (28%). Flakes rarely matched blade proportions ($n=7$), and the majority of artefacts present an elongation of 0.75-1.5. Platforms are almost exclusively flat (53%) and natural (44%). Dorsal surfaces are relatively unorganised, typically displaying between 1-3 scars (80%), matching the 80% of artefacts with less than 50% cortex on their surface. The direction of flaking is predominately unidirectional (84%), followed by bidirectional (16%). A number of refitting pieces are present, attesting to the relative integrity of the site.

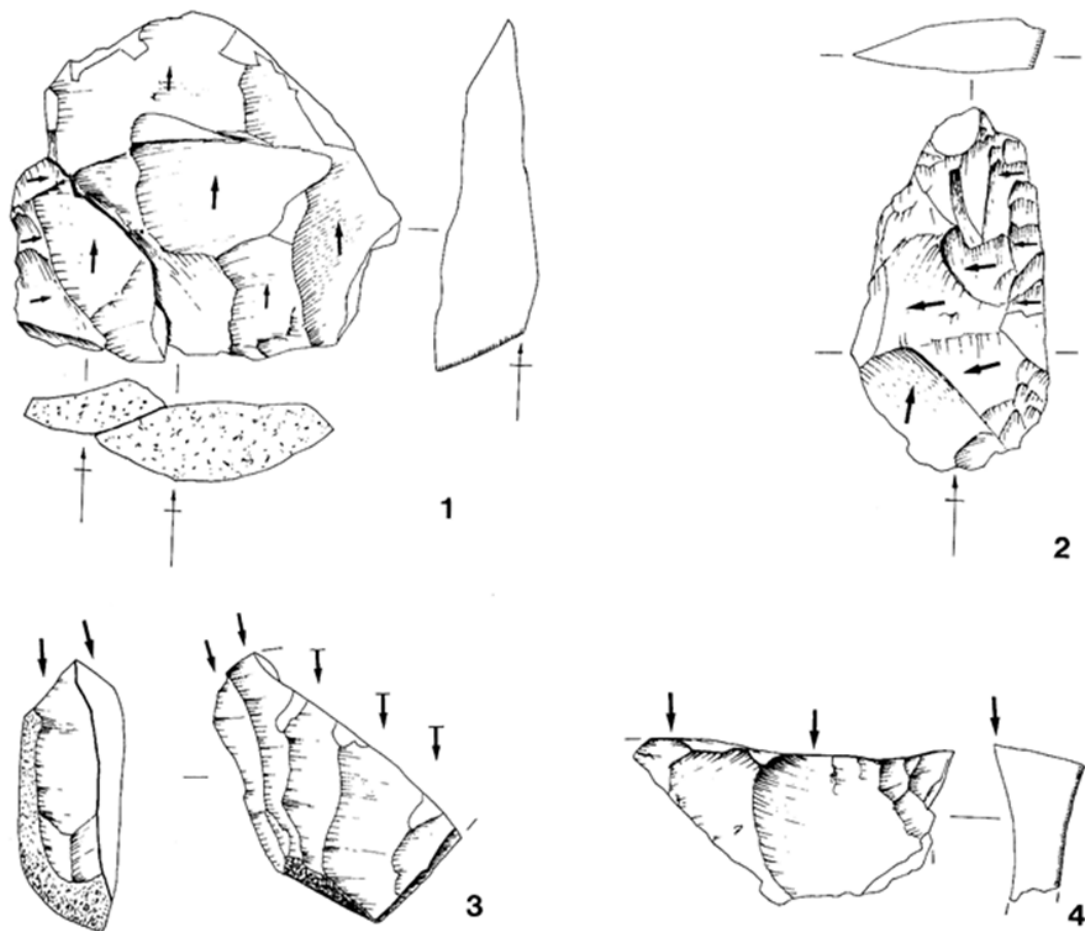


Figure 5.24: Artefacts from 797bis – refitting flakes with bidirectional detachments (1); flake with bidirectional detachments (2); fragments of cores with a debitage surface parallel to a cortical one (3 & 4) (scale 1:2) (Negrino & Kazi 1996; Figure 14).

Summary

The excavators of these assemblages identify two distinct reduction strategies, and evidence for different levels of patina formation supports the assertion of chronologically separated reduction activity. The Acheulean sites appear to have focused upon biface production whereas the Late (Upper) Palaeolithic sites clearly concentrate upon systematic blade production. Although no absolute chronological framework can be derived from this evidence, technological differentiation of these reduction strategies serve to highlight the more basic, typological differences previously noted with a greater level of detail.

16R Dune

The site of 16R Dune is situated in the defunct Bangur Canal, to the south-west of Didwana Lake. The excavations extended to a depth of 18.5m originally revealing five artefact bearing horizons, two of which were labelled Lower Palaeolithic and single assemblages recorded as Middle and Upper Palaeolithic and Mesolithic (Figure 5.25)(Misra & Rajaguru 1986). The recent reanalysis of the sediment profile by Singhvi et al. (2010) has been discussed in Chapter 4. The Upper Palaeolithic assemblage was recovered from excavations covering 30m², the Middle Palaeolithic horizon was recovered from 10m² of excavations, while the Lower Palaeolithic assemblages were recovered from a 6m² sondage. While Mesolithic artefacts were encountered during excavation, they were not collected and given the absence of any clearly Holocene material culture may be considered as Late Palaeolithic for the purpose of this thesis. A re-evaluation of the industrial affiliations of these assemblages suggests the Upper Palaeolithic horizon can be more suitably assigned to the Middle Palaeolithic, whereas the lower assemblages can be described as Middle or Lower Palaeolithic (Gaillard 1993; 2006).

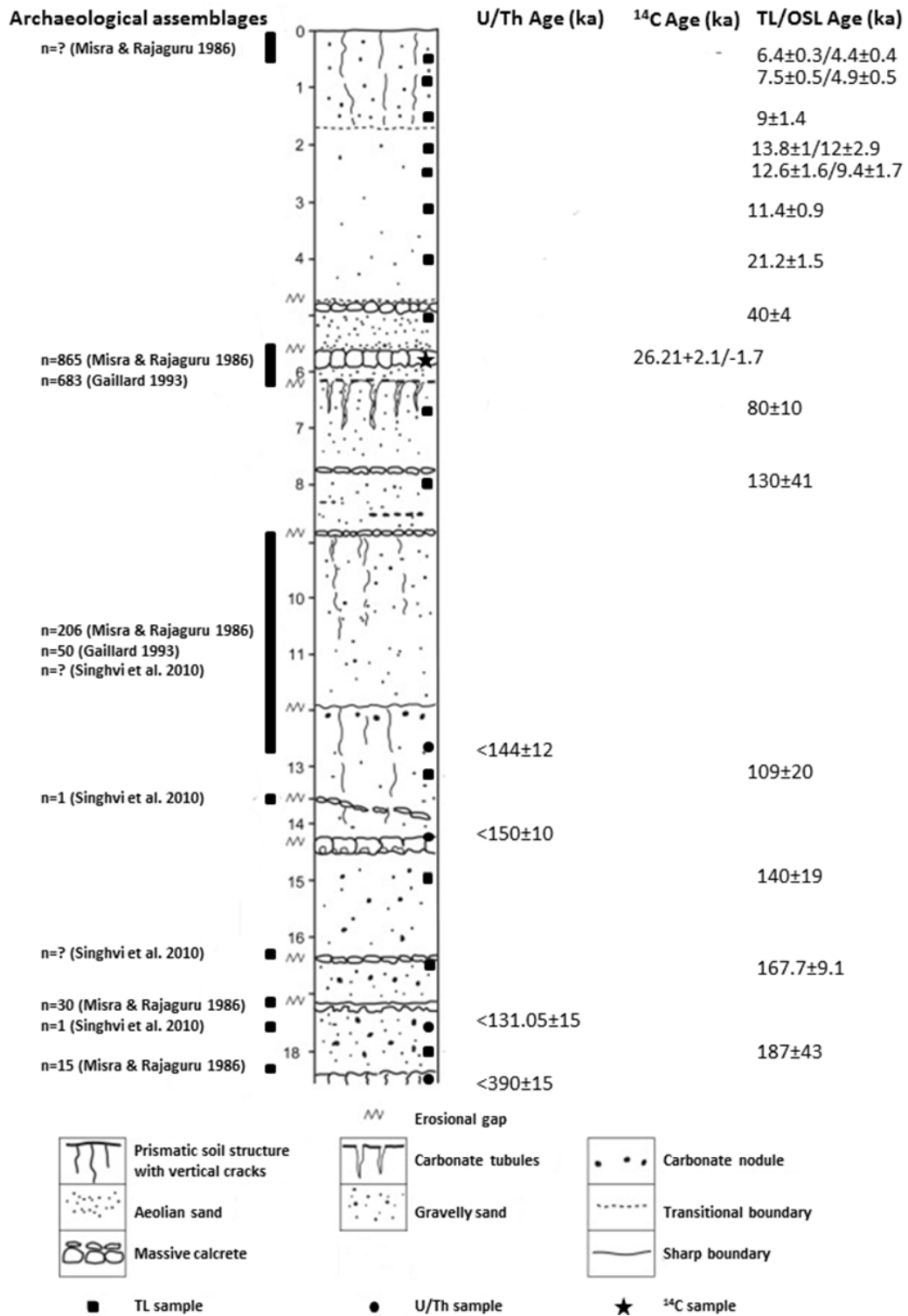


Figure 5.25: Excavated profile at 16R Dune, identifying the location of archaeological horizons and chronometric dating sample locations and results (adapted from Singhvi et al. 2010).

Gaillard (1993) presents the most detailed techno-typological description of the artefacts recovered from 16R Dune, separated into two assemblages: 16R-Sup. comprising 683 artefacts from 5.4-6.1m depth (see Figure 5.26 & 5.27); 16R-Inf. comprising 63 artefacts including 50 from 12m depth, with the remaining artefacts from the lowest deposits (Table 5.9; Figure 5.28). The dominant raw materials for both groups are grey quartzite, white quartzite and quartz, which are mostly available in from the hills close to the site. The majority of pieces are fresh, or show light weathering, although approximately 20%, dominantly debris, shows moderate to heavy weathering. Almost all pieces (95%) lacked any cortical surfaces. Striking platforms are dominantly plain (62%), with reduced, convex, and dihedral platforms occurring in equal proportions.

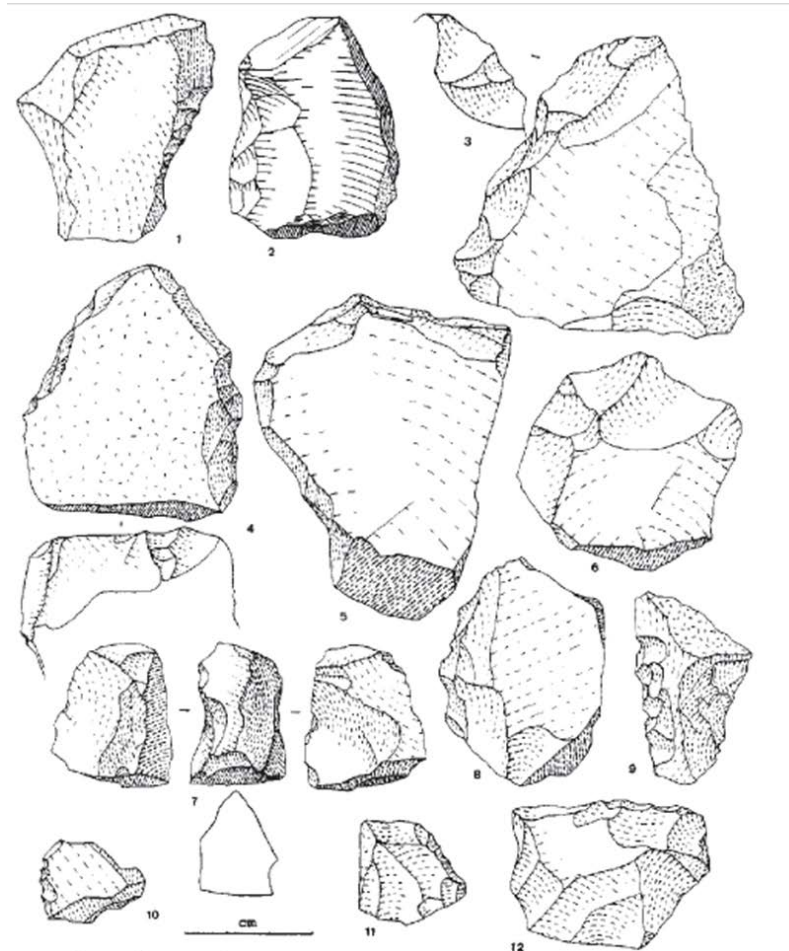


Figure 5.26: Small tools from 16R-Sup (Gaillard 1993; Figure 89).

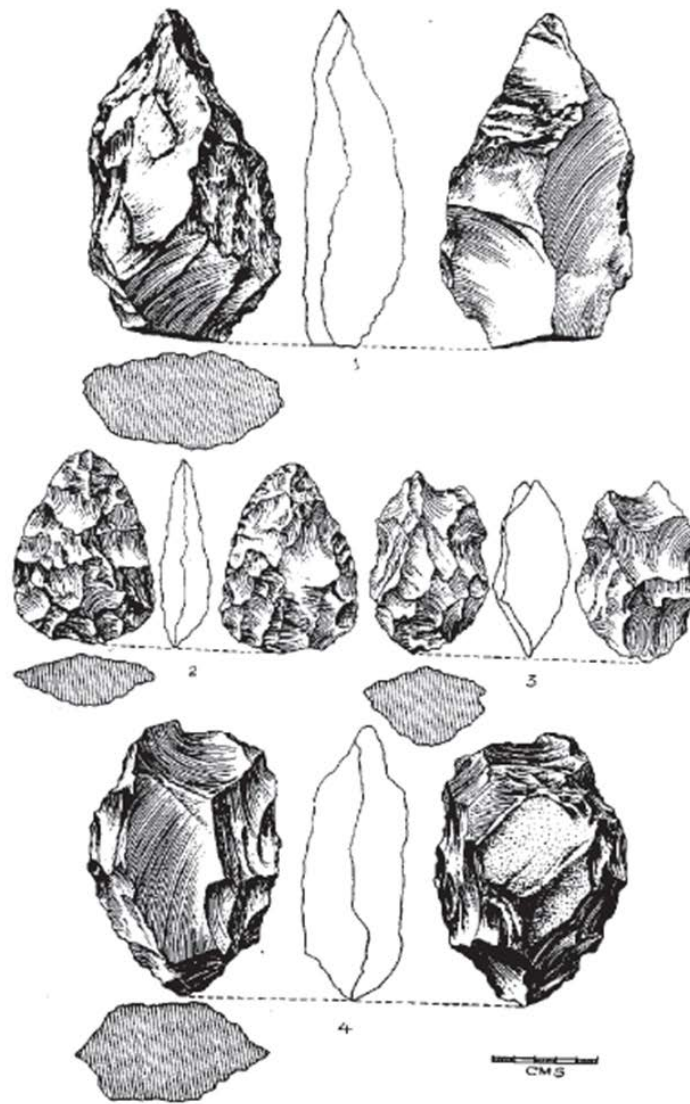


Figure 5.27: Heavy tools from 16R-Sup (Gaillard 1993; Figure 96).

The majority of both 16R Sup. and 16R Inf. comprises flakes, which are on average smaller in 16R Sup. than in 16R Inf. (mean LxWxT: 16R Sup. 26.3x24.3x9.7mm; 16R Inf. 40.2x34.7x14mm). This is due to the presence of numerous (n=73) small flakes (<20mm) in 16R Sup., which mostly occur on quartz. These are suggested to be industrial debris due to the fracture properties of the raw material on onsite reduction with minimal disturbance, rather than an intended product, supported by the lack of retouched small flakes. In 16R Sup., 85% of flakes have an elongation index (L/W) between 0.6-1.6, with an overall mean of 1.16. The elongation index for 16R Inf. shows two clusters at 0.7 and 1.4. Most flakes bear scars of 2-3 (16R Sup.) or 2-4

(16R Inf.) previous removals, although there is no clear Levallois component to either assemblage. Much of the debris is in the form of quartz chunks, generally ca. 30mm³ some of which have been selected to be retouched.

Type	16R Sup. (n)	16R Sup (%)	16R Inf. (n)	16R Inf. (%)
Flake (blade)	329 (10)	48.2 (1.5)	37 (5)	58.7 (7.9)
Debris	246	36	9	14.3
Scrapers	24	3.5	5	7.9
Denticulates	8	1.2	-	-
Borer	8	1.2	-	-
Notch	6	0.9	2	3.2
Burin	3	0.4	-	-
Point	1	0.1	-	-
Biface	7	1	2	3.2
Chopper	13	1.9	4	6.4
Chopping Tools	15	2.2	-	-
Cores	23	3.4	4	6.4
Total	683	99.9	63	100.1

Table 5.9: Summary of assemblage composition from 16R Dune following Gaillard 1993 (Tables 62, 63 and 69).

The remaining component of the assemblage has been analysed as small, medium and large tools, with cores included in the two latter categories. Small tools comprise 7% (n=49) of 16R Sup. and 8% (n=5) of 16R Inf. The average size of these artefacts combined (LxWxT=50x33x20mm) is larger than that for flakes in either assemblage. There is no clear discrimination between retouched flakes (54%) and retouched debris (46%), and quartz is the dominant raw material. Retouch is generally marginal, with rare cases of abrupt retouching.

A relatively high proportion (40%) of the medium and large tools exhibit medium/heavy weathering. The 16R Sup. assemblage includes the only medium tools at the site, comprising 5 micro-choppers and 4 cores. Large tools in 16R Sup. include a particularly finely worked diminutive handaxe, but are dominated by choppers/chopping tools. In addition, 19 cores are present, of which 6 exhibit only single removals. 16R Inf. contains 2 bifaces, more crudely

worked than in 16R Sup., and 11 cores, one of which exhibits a large blade removal and is derived from the lowest horizon (Figure 5.28).

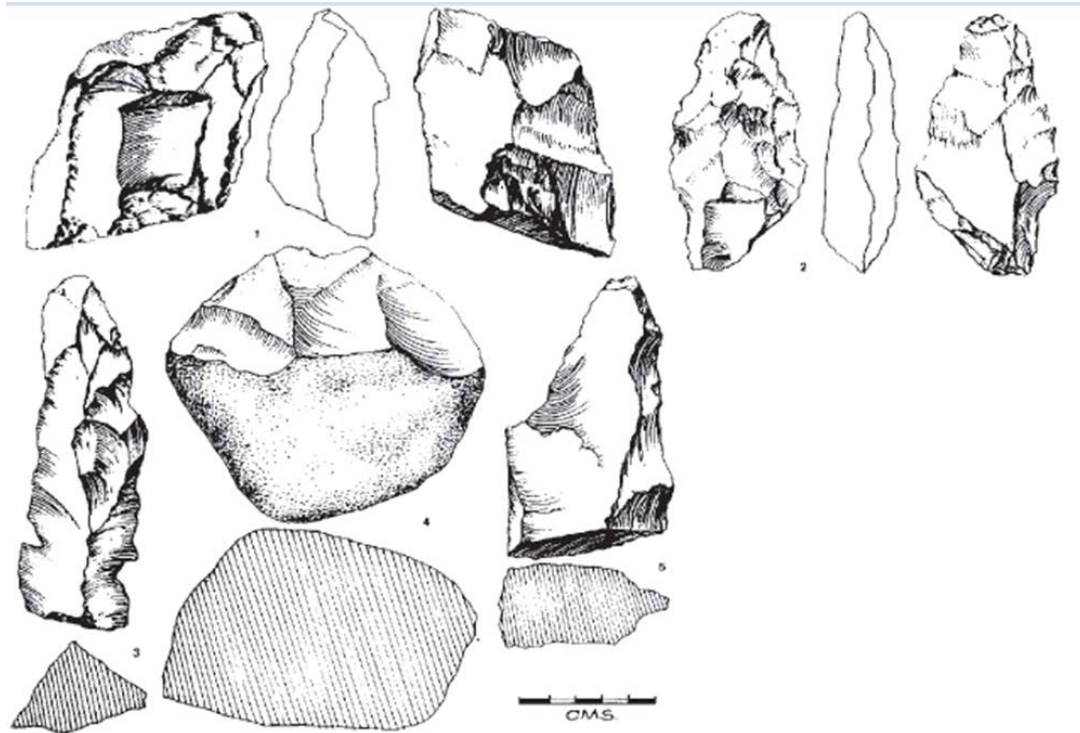


Figure 5.28: Artefacts from 16R-Inf (Gaillard 1993; Figure 97).

In addition, Singvi et al. (2010) report a small number of artefacts in the lower portion of the sequence. A significant implication of these archaeological discoveries is that numerous artefacts are found upon calcrete horizons (Singhvi et al. 2010), and may, therefore, represent deflated accumulations, rather than discrete behavioural episodes. Nevertheless, the appearance of artefacts on numerous calcrete layers in the lower part of the 16R sequence supports earlier suggestions that the site saw repeated, if somewhat brief, occupation during the formation of the site.

The application of chronometric dating (U/Th series and ^{14}C) at the site of 16R Dune (Raghaven et al. 1989) has had an enduring impact upon South Asian Palaeolithic archaeology. Recent re-dating of the sedimentary sequence using luminescence techniques at the site has provided a

more comprehensive chronology for the site (Table 5.10) (Achyuthan et al. 2007; Singhvi et al. 2010). This broadly matches the U/Th series dates, but substantially revises the date associated with the 16R-Sup. horizon. Pedogenic carbonates are problematic for dating as they are post-depositional features with the potential for repeated episodes of overprinting and equilibration with younger soil carbon sources (Amundson et al. 1994; Trumbore 2000). ¹⁴C dating of pedogenic carbonates are likely to underestimate the actual age of deposition, and analogies with other sites in the Thar Desert indicate that up to 10ka difference between radiocarbon and luminescence dating may occur (Chawla et al. 1992). Therefore, the new luminescence age bracket for the 16R-Sup. assemblage is considered more reliable and supersedes the earlier ¹⁴C chronology.

Sample Depth (m)	Age (ka) U/Th	Age (ka bp) ¹⁴ C	Age (ka) – Multiple Aliquot TL	Age (ka) – Single Aliquot OSL
0.52-0.64	-	-	6.4±0.3	4.4±0.4
0.82-0.91	-	-	7.5±0.5	4.9±0.5
1.5-1.6	-	-	9±1.4	-
2.14-2.22	-	-	13.8±1	12±2.9
2.5-2.6	-	-	12.6±1.6	9.4±1.7
3.34-3.48	-	-	11.4±0.9	-
4.16-4.28	-	-	21.2±1.5	-
5.2-5.38	-	-	40±3	-
5.4-6.1	-	26.21±2.1/-1.7	-	-
6.65-6.95	-	-	80±10	-
8.2-8.3	-	-	130±41	-
12.65	<144±12	-	-	-
13.2-13.3	-	-	109±20	-
14.25	<150±10	-	-	-
14.9-15.1	-	-	140±19	-
16.5-16.6	-	-	-	167.7±9.1
17.55	<131.05±15	-	-	-
18.2-18.3	-	-	187±43	-
18.66	<390±15	-	-	-

Table 5.10: Synthesis of U/Th, ¹⁴C and luminescence dates from 16R Dune.

The combination of Gaillard's (1993) analysis of 16R-Sup. and the new chronological framework for the site (Achyuthan et al. 2007; Singhvi et al. 2010) provide the most secure benchmark for understanding hominin lithic behaviour in the Upper Pleistocene. 16R-Sup appears to present evidence of a secondary reduction site, with decortified raw materials brought to the site from nearby raw material resources, bracketed by dates of 80-40ka. Relatively amorphous cores and limited evidence for blade production suggested reduction activity remained relatively simple, supported by only marginal application of retouch. In contrast, the presence of bifaces is more notable and indicate their continued production into the middle Upper Pleistocene. Overall, 16R-Sup presents evidence of the use of Middle Palaeolithic technologies in the Thar Desert between MIS 5a and early MIS 3. Due to the limited sample sizes analysed from the lower horizons, any conclusions drawn from these assemblages must be more limited. However, the presence of artefacts at various levels indicates repeated occupation of the site in MIS 6 and early MIS 5. The presence of both a blade and a core with a blade removal at the lowest excavated level as well as bifaces and choppers offers limited indication of technological continuity with the overlying layers.

Singi Talav

The Singi Talav depression is separated from Didwana Lake by a NE-SW sand dune, of which the site lies to the South. A total of 72m² has been excavated in the depression, extending to a maximum depth of 1.2m from surface, although in some areas excavation was limited to 0.8m as no artefacts had been identified below this level in the deeper parts of the trench. A deep sounding continued to a depth of ca. 4m, which identified minimal artefacts below 0.8m depth and sterile deposits below 2m. The excavations at Singi Talav revealed fine sediments associated with the Amarpura formation, a greenish grey, crudely laminated calcareous loam with prominent *kankar* (carbonate) horizons (Misra 1995). This low energy depositional

context appears to have preserved the evidence of reduction activity without any post-depositional disturbance (Misra 1995), supported by the presence of large numbers (21-26%) of small flakes (<20mm) in all three horizons (Gaillard 1993).

Artefacts have been identified in three horizons. The first occurs within the top 0.2m of excavation and comprises 401 artefacts (Couché 3). The second occurs between 0.2-0.6m and comprises 891 artefacts (Couché 4). The final assemblage was recovered at a depth of 0.65-1.1m yielding 173 artefacts (Couché 5). These top two assemblages were initially reported as Middle and Late Acheulean assemblages respectively, but following analysis by Gaillard (1993), both can be considered Late Acheulean (Lower Palaeolithic).

Type	Couché 3	%	Couché 4	%	Couché 5	%
Flake	167	41.6	357	40.1	61	35.3
Point	5	1.2	5	0.6	1	0.6
Borer	3	0.7	7	0.8		
Burin			5	0.6	1	0.6
Denitculate			3	0.3		
Notch	3	0.7	9	1.0	1	0.6
Scraper	14	3.5	32	3.6	2	1.2
Core	8	1.9	3	0.3		
Discoidal Core	1	0.2	3	0.3		
Polyhedral Core	6	1.4	5	0.6		
Handaxe	4	0.9	20	2.2		
Chopper	4	0.9	5	0.6		
Chopping Tool	6	1.4	6	0.7		
Cleaver			3	0.3		
Pick			1	0.1		
Debris	171	42.6	407	45.7	100	57.8
(unspecified)	9	2.2	20	2.2	7	4.0
Total	401		891		173	

Table 5.11: Summary of assemblage composition from Singi Talav following Gaillard (1993).

The majority of raw materials used at the site comprise assorted quartzites, which derive from the Balia Hills, 3km away near 16R Dune. A lower number of river cobbles from further afield, ca. 20km, are also evident. A particular grey schistous quartzite from the Balia Hills is more

frequently found in Couché 4 and 5 than in Couché 3 (Gaillard 1993), and it's repeatedly associated with reduction of handaxes from flat blocks or slabs (Gaillard 1996). In contrast, white quartzites are more common in Couché 3 (Gaillard 1993).

The high number of flakes lacking cortical surfaces (92%) suggests that primary reduction was undertaken elsewhere, and partially reduced clasts were imported to the site. Few differences in flake attributes occur between the three horizons (Gaillard 1993). The majority of flakes (54%) have simple platforms, with 20% presenting reduced platform types. Two or three scars are present on the majority of flake dorsal surfaces. Feather terminations are most common (72%), with step terminations also common (19%). No real differences occur between the three assemblages with regards to flake size, with 62% flakes between 10-30mm long, 67% between 10-30mm wide, and 73% between 5-15mm thick. Less than 10% longer or wider than 50mm. Blade proportioned flakes are rare (2.8%), with a mean elongation of 1.13. Overall, the majority of flakes are either fresh (55%) or lightly weathered (32%); heavily weathered artefacts are rare (1%). Flaking debris shows many similarities with the flake populations, in that they are typically small (50% weigh less than 10g) and mostly fresh (27%) or lightly weathered (33%). Grey schistose quartzite is particularly abundant (10%) amongst the flaking debris.

Tools from all levels at Singi Talav show similar size distributions, presenting an overall mean size (LxWxT) of 43.4x31.1x16.1mm for small tools and 46.3x38.5x29.8mm for medium tools. Scrapers and denticulates are the most common form of small tool (30%), typically made on flakes, whereas end scrapers (25%) are generally made on flaking debris (see Figure 5.29). Medium tools include micro-choppers, -discoids, -spheroids and -polyhedrons, and only three examples of micro-cores (see Figure 5.30). The presence of medium tools is considered a characteristic trait of the Singi Talav industry (Gaillard 1993). Bifaces, including handaxes, cleavers and picks, are more common in C4 (n=24) than in C3 (n=4) and present averaged sizes

of (LxWxT) 113.3x70.6x37.8mm (see Figure 5.31). Bifaces display a significantly larger number of flake scars than either medium tools or core tools, indicating they were produced through a distinct reduction strategy. The combined size of cores and core tools, principally choppers or chopping tools, is somewhat smaller at (LxWxT) 76.9x64.3x49.6mm, with simple cores more common in C3 compared to C4. Overall, Gaillard (1996) suggests considerably more energy has been expended in collecting and transporting the raw materials than on their reduction.

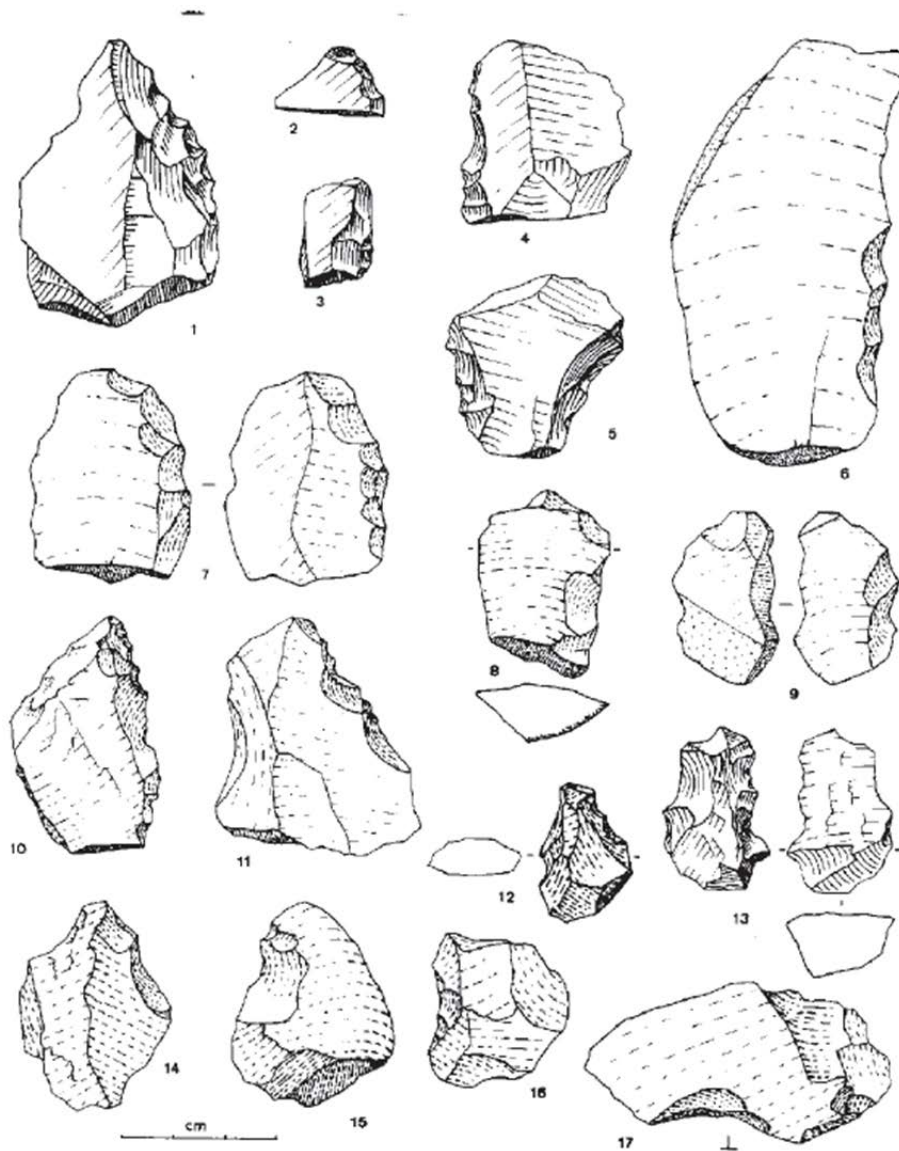


Figure 5.29: Small tools from Singi Talav (Gaillard 1993; Figure 51).

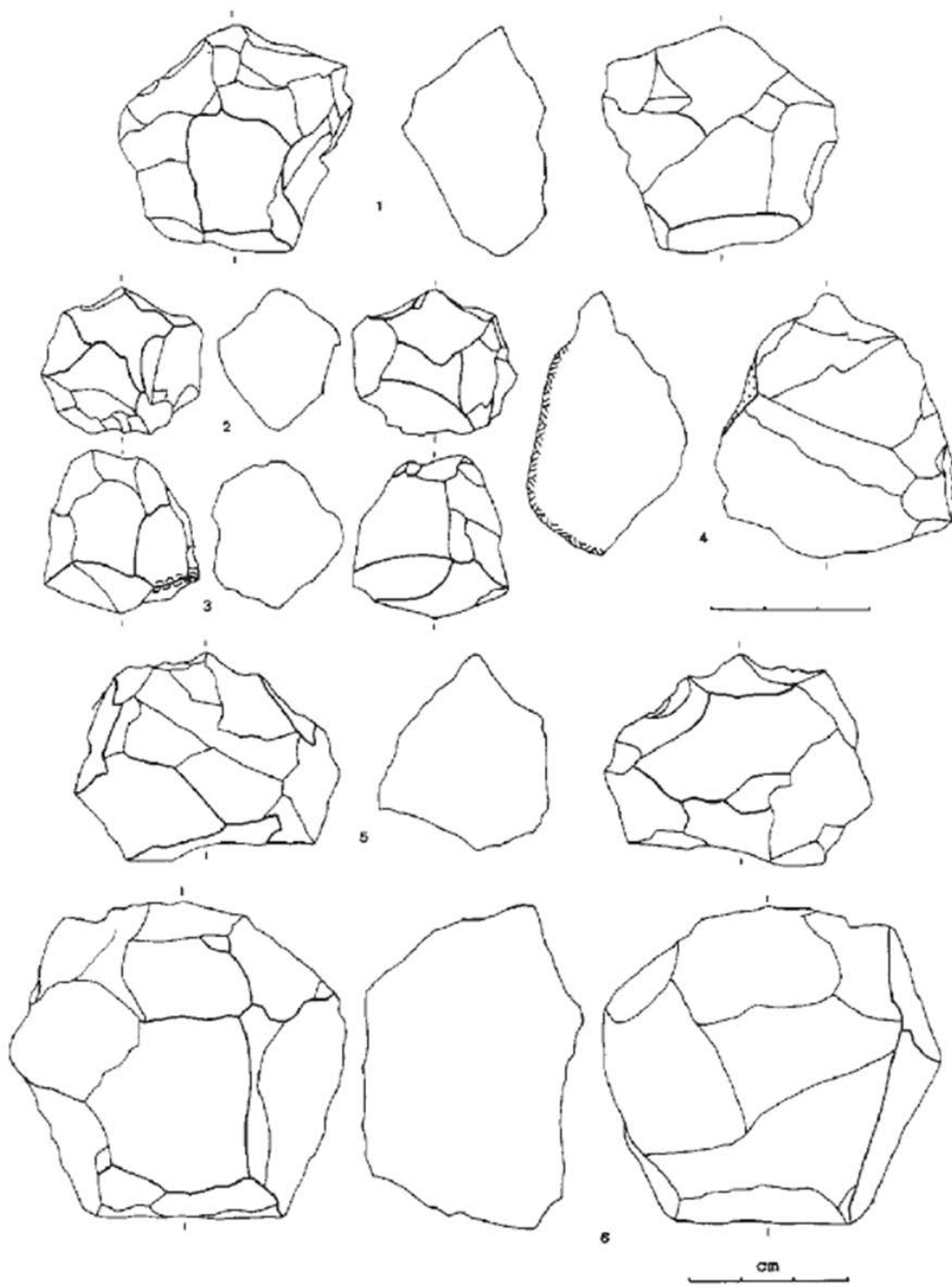


Figure 5.30: Medium sized tools from Singi Talav (Gaillard 1993; Figure 58).

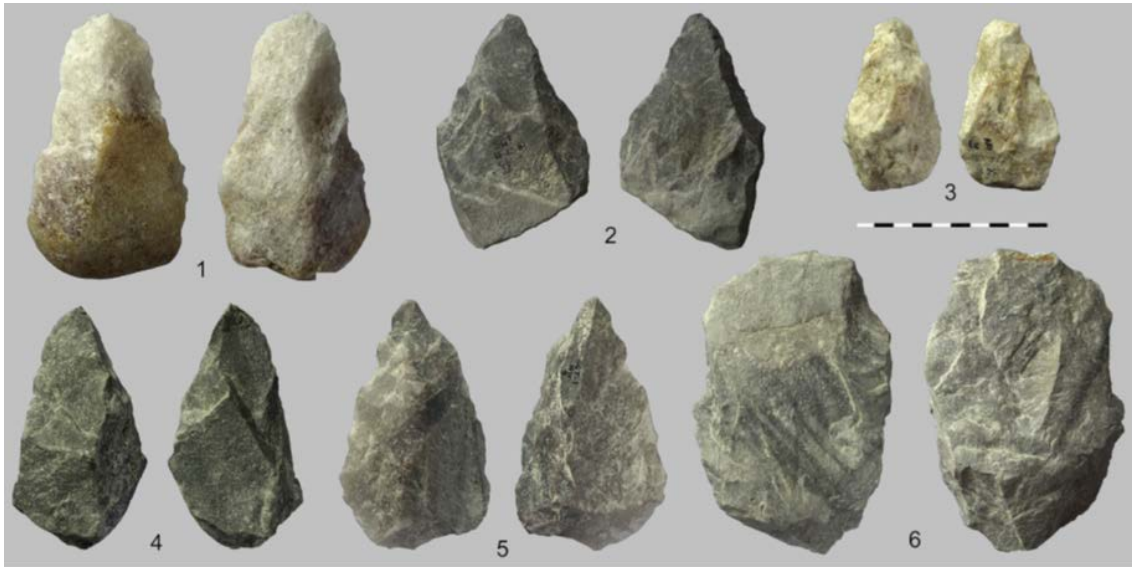


Figure 5.31: Handaxes (1-5) and a Cleaver (6) from Singi Talav (Gaillard et al. 2010; Figure 5).

The presence of 6 quartz crystals in C4 is somewhat enigmatic. Given their depositional context, they must have been transported to the site in a similar manner to all artefacts at Singi Talav. However, they show no clear evidence for any modification and are distinct from the other raw materials present at the site. No use for these artefacts is readily apparent, and as they are an isolated occurrence within South Asia, it is problematic to offer any clear interpretation for their presence.

No chronometric dating has been undertaken at the excavation site. The excavators have suggested that the sediment formation at the site should be older than those at the base of 16R Dune (Misra 1995). However, as some inter-stratification of these deposits was observed and the topographical contexts are clearly distinct, no straightforward chronological comparisons are possible. A single sample recovered from Amarpura Quarry yielded an Electron Spin Resonance age of >797ka (Kailath et al. 2000), which Gaillard (2006) and Gaillard et al. (2010) suggest this offers a useful age estimate for the assemblages from Singi Talav. However, as the stratigraphic and sedimentary provenance of the dated sample is unclear, and

the sampling location may be up to 3km away from Singi Talav, the suggested association between the excavated assemblages and the dated sample can be rejected (Chauhan 2010). As a result, the evidence from Singi Talav presents high resolution detail upon typological and technological aspects of Late Acheulean (Lower Palaeolithic) hominin behaviour in the Thar Desert, but may only be safely assigned to the Middle or early Upper Pleistocene.

Chronometrically Dated Sites

Two small undiagnostic assemblages have been identified at the site of Karna in the mid Luni Valley. Luminescence dating indicates that 6 flakes found cemented in a gravel horizon can be dated to 79.8 ± 8 ka, whereas 6 flakes and an ostrich eggshell fragment found on top of the gravel have been covered by a fluvial sand deposit dating to 26-29ka.

A number of sites from the Orsang Valley can be associated with different alluvial strata, for which luminescence dates are available, although they are not directly correlated with archaeological assemblages. A loose pebbly gravel in the Orsang Valley has been dated to 125-97ka (Juyal et al. 2004), which has been observed to contain both Lower and Upper Acheulean artefacts (Ajithprasad 2005). Similarly, early Middle Palaeolithic artefacts are seen occurring on a buried soil, dating to 49ka, and sandy silt, dating to 63ka, as well as within a thin, coarse gravel that overlies both of these dated deposits (Ajithprasad 2005).

Palaeolithic sites in the Hiran and Bhadar Valleys have been reported by a number of investigators, often occurring beneath or between miliolite deposits. At Umrethi in the Hiran Valley, a 22m section exposed a substantial miliolite horizon, dated by U/Th series to 190 ± 29 -22ka, overlying a pebbly sand, which yielded three fresh handaxes reported as Lower Palaeolithic (Figure 4.32). A similar scenario is presented at Junagadh, where a 30m miliolite deposit, dating to 69 ± 3.8 /-3.6ka, overlies a boulder gravel containing Lower Palaeolithic artefacts. At Jetpur, a thin miliolite layer is dated to 56.8 ± 5.4 /-4.8 that overlies a sandy, pebbly

gravel containing a large number of Middle Palaeolithic artefacts (Figure 5.33). Finally, at Badalpur, Middle Palaeolithic artefacts are seen in a sandy, pebbly gravel bracketed between an oyster bed, dated using ^{14}C to 25ka, and a miliolite layer, dated to 158+32/-24ka.

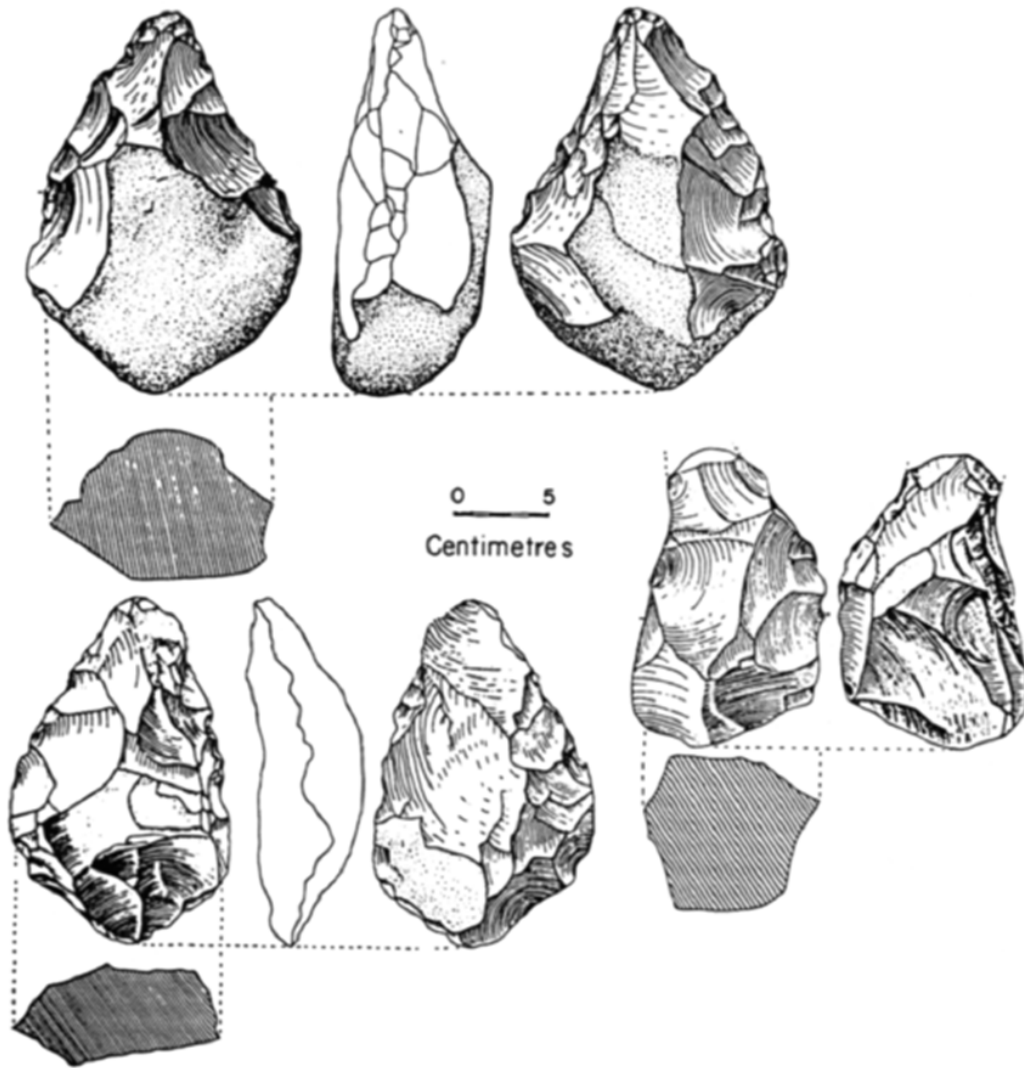


Figure 5.32: Lower Palaeolithic handaxes from Umrethi (Baskaran et al. 1986; Figure 3).

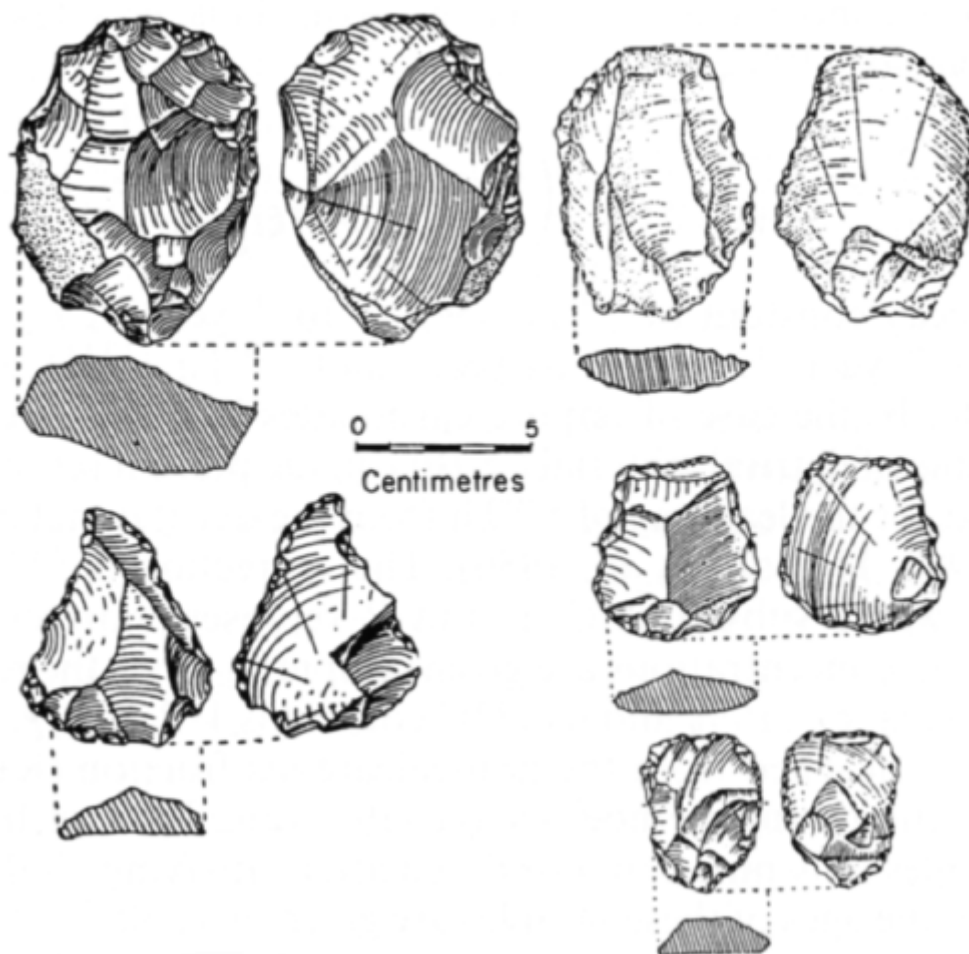


Figure 5.33: Middle Palaeolithic artefacts from the Hiran Valley, Saurashtra (Baskaran et al. 1986; Figure 4).

Summary

Chronometric dating and technological analyses of lithic assemblages offer a more secure basis from which to identify patterns in hominin behaviour in the Palaeolithic period, but the number of assemblages with such detail is highly limited. However, a number of trends are evident in the few sites where more detailed analyses have been conducted that are of use in corroborating trends identified in the appraisal of the broader corpus of evidence.

Where chronometric dates are available, the Lower Palaeolithic appears to occur in contexts >100ka, and given the potential secondary context of the younger sites this may present a minimum age. Middle Palaeolithic sites appear in contexts <100ka, and this is most securely attested at 16R Dune. The boundary between the Middle and Late Palaeolithic cannot be clearly identified, as no firm dates can be attributed to the latter. The Late Palaeolithic assemblage from 16R Dune is poorly reported, but the maximum age attributable to them is 21ka, and the suite of younger ages toward the top of the excavation may indicate they were recovered from a Holocene context.

With regards to technology, the Lower and Late Palaeolithic industries can be clearly differentiated in Sindh, focused upon biface and blade production respectively, although it is unclear whether this pattern would hold elsewhere in the Thar Desert where silicious limestones are not abundant. The continued production of bifacial tools, observed both in Sindh and at Didwana indicate that their presence alone does not offer a clear means to differentiate between the three cultural phases. The presence of bifacial picks in ZPS4 (Late Palaeolithic) and bifacial handaxes at ZPS1 (Lower Palaeolithic) may also relate to the nature of site use, exploiting the easily available limestone resources, and so may not be indicative of behaviour elsewhere in the Thar. Although rare, the presence of bifacial tools, including a finely crafted diminutive handaxe, in 16R-Sup indicates the continuity of biface production and use into the middle Upper Pleistocene. This complicates the separation of Lower and Middle Palaeolithic industries, suggesting their differences may relate to the proportional emphasis placed upon biface production, such as between 16R-Sup and Singi Talav Couché 4. As a result, the chronological boundary between these periods may be inherently diffuse.

Discussion

The foregoing synthesis has expanded considerably upon the last time such an exercise has been undertaken for the Palaeolithic archaeology of the Thar Desert. A much larger sample of sites have been evaluated, with a broader range of evidence available. However, a number of conclusions drawn by Allchin et al. (1978) regarding the distribution of sites of different industries, typological and basic technological changes between industries, and their relative chronology remain remarkably relevant. This, perhaps, indicates a widespread, if unstated, understanding of what the key features of each industry are, which is now more apparent as a result of this synthesis.

The comparatively low number of Lower Palaeolithic sites in Western Rajasthan commented upon by Allchin et al. (1978) remains evident today. Although the count of such sites has grown, the majority do not provide suitable levels of detail to investigate them further. Both Middle and Late Palaeolithic sites are more widespread within the central region of the Thar Desert. This may result from a number of factors, of which visibility is most prominent, but differences in resource exploitation patterns cannot yet be excluded.

Based upon patterns of typological presence/absence, the three Palaeolithic industries appear to have distinctive packages. Synthesis of this data has permitted an engagement with one of the widest available forms of archaeological data, despite the issues surrounding artefact typologies. Lower Palaeolithic artefact inventories are least diverse, particularly with regards to retouched artefacts, but heavy tools are a prominent feature. Retouched tools are particularly diverse amongst Middle Palaeolithic sites, with points appearing at a large number of sites, as well as borers, burins and knives to a lesser extent. Similarly, there is some evidence to suggest more varied core reduction strategies in Middle Palaeolithic sites. Blades and blade cores are more prominent in Late Palaeolithic assemblages, and burins are notably

more common in this period. Some overlap does occur, as with certain heavy tool types, which may indicate that artefact type alone has not been used to ascribe industrial affiliation to assemblages.

Both Middle and Late Palaeolithic industries appear more diverse at the edge of the desert in contrast to the central region. A wider range of raw materials and ecological resources are also available at the margin of the desert compared to the core. Greater diversity in typological packages could represent more varied functional demands of stone tools in response to either, or both, of these factors. As cultural diversity may be linked to population size (Shennan 2001; Powell et al. 2009), the more varied typological packages evident in the desert margins could indicate that larger populations were sustained in the more humid parts of the Thar Desert, or these groups featured in information exchange networks extending beyond the Thar region.

At a gross level, patterns of raw material use offers a useful means to discriminate between the Palaeolithic industries, though similarities between Middle Palaeolithic assemblages with both preceding and succeeding exist. A couple of general patterns are evident in these data. Firstly, raw material use is highly limited in the Lower Palaeolithic sites, and this may have played an important factor in limiting the potential for occupation of the central desert region, where quartzite, quartz, flint and chert are rare, and only occur as small clasts where present. Considerable diversification and experimentation appears to have occurred in the Middle Palaeolithic period, suggesting the lithic reduction techniques employed were adaptable to raw material variability, which may have in turn facilitated the formation of a broader distribution of sites and artefact types. In contrast, the Late Palaeolithic sites in the Thar Desert show a strong focus upon silicious materials with fine and very predictable fracture properties, which may indicate that these qualities were sought after, or required, for the techniques of lithic reduction that were employed.

Artefact size offers a more clear-cut means for differentiating the different industries, and may well have been used as a rapid index for a number of researchers for their identification.

Significantly, there are differences in size between the artefact types shared between Lower and Middle Palaeolithic sites, predominately heavy tools, and Middle and Late Palaeolithic sites, predominately retouched types and cores. A large number of Late Palaeolithic artefacts appear <40mm, which has been used by a number of researchers in South Asia, including researchers working in the Pakistani Thar (e.g. Biagi et al. 1996) and the thoroughly documented sites in the Jurreru Valley (Clarkson et al. 2012), as the size at which artefacts can be described as microlithic. Although it is important to understand localised variations in artefact size frequencies to identify where such metric definitions may be useful, the relatively low number of microliths reported in Late Palaeolithic assemblages may be explained by the lack of application of a clear definition.

A similar trend is apparent amongst the sample of sites that offer details of the proportional composition of assemblages, indicating that where there is overlap in site inventories between Middle Palaeolithic assemblages and both preceding and succeeding industries, the overlapping artefact occur in significantly different proportions. For example, although a range of heavy tools are reported in Middle Palaeolithic sites, they are half as numerous, where present, than Lower Palaeolithic sites. The diversity amongst retouched types remains evident in Middle Palaeolithic sites, although the different artefact types are only present in small numbers. The spatial patterns of variability highlighted amongst the presence/absence of artefact types remain evident in Late Palaeolithic sites with details of proportional assemblage composition.

The excavated evidence for Palaeolithic industries in the Thar matches some of the trends presented by the surface sites. Lower Palaeolithic sites appear to present reduction strategies focused upon heavy tool production, with limited further reduction of debitage. A greater

range of small, retouched tools is employed at the lone Middle Palaeolithic site, although the presence of heavy tools indicates that reduction strategies are not entirely focused upon debitage production. Late Palaeolithic reduction schemes from Pakistan include systematic blade production, a trend apparent in the surface sites beyond Pakistan. A tentative chronological division between Lower and Middle Palaeolithic sites appears to occur between 100-80ka, and no evidence for Late Palaeolithic sites is apparent prior to the Last Glacial Maximum.

Overall, it appears that previous research undertaken in the Thar Desert has broadly conformed to an implicit model of what constitutes the Lower, Middle and Late Palaeolithic, that can be supported by the limited sample of excavated and dated sites. As a result, a number of the trends identified throughout this synthesis present themselves as working hypotheses that require further research so that the differences between the Palaeolithic industries can be made explicit. For example, how do heavy tool reduction sequences vary through time? Are different core reduction strategies associated with the diversification of retouched tool types? Perhaps most critical to this goal is research that enables archaeological assemblages to be recovered from secure contexts and can be dated using chronometric methods, as it remains possible that the different industries are poorly chronologically structured and that differences between some Lower and Middle Palaeolithic sites, for example, relate to functional aspects of raw material use or availability.

Chapter 6

Survey in the Thar Desert

Surface surveys currently provide the most widespread form of evidence for the Palaeolithic occupation of the Thar Desert, as outlined in the preceding chapter. In light of evidence from sites which record the proportional composition of lithic assemblages, it is clear that surface surveys focused upon detailing only the presence of different retouched tool types are too reliant upon a relatively minor feature of lithic evidence to investigate variability in Palaeolithic technological activity. Technological analyses of un-retouched flakes and cores, as well as retouched pieces, from surface sites offer a new approach to investigating variability in the Palaeolithic record of the Thar Desert. In particular, such studies can assess the impact of reduction intensity and strategy, as well as raw material variability, upon our understanding of lithic artefact variability through time and in different ecological settings.

In order to undertake such analyses, a program of fieldwork has been undertaken in the Rajasthan Thar Desert, offering a broad transect from the eastern edge of the Thar Desert to the central core (Figure 6.1). Originally, the aim of this research was to undertake excavations in a range of landscape contexts, but limited funding and restricted excavation permits prevented this. Therefore, to offer a broad spatial perspective on Palaeolithic lithic technology, a targeted surface survey was devised to investigate chronological variability in lithic assemblages, the presence and nature of Palaeolithic occupation of lake sites at the core and periphery of the desert, and the evidence for technological evolution relating to the Middle-Late Palaeolithic transition. All recording was undertaken in the field, and time limitations prevented the systematic sampling of Palaeolithic sites. Instead, a range of cores, flakes and retouched pieces were selected to characterise each assemblage. As a result, the surface assemblages reported in this chapter and detailed in Appendix B typically include 20 to 50

artefacts. Simple technological statistics are provided to describe the sampled artefacts, but due to the size and nature of sub-sampling, these may not accurately characterise the whole assemblage.

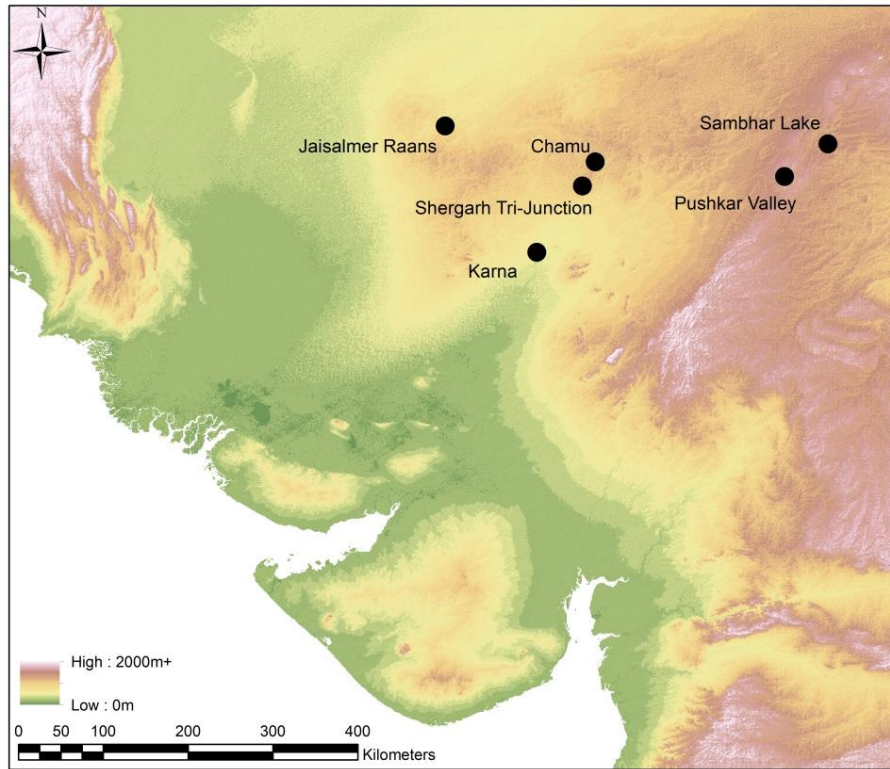


Figure 6.1: Map of survey sites.

Survey of Sites with Existing Chronologies

Three areas were chosen for survey where existing chronological evidence is present for sedimentary sequences. At two locations, Karna and Chamu, sediment deposits dating between MIS 1-5 and MIS 1-6 are present, whereas the third area chosen, Shergarh Tri-Junction, offers a more limited chronological range, from MIS 4-2. These three locations occur in significantly different geographic contexts, located in a river valley, sand dune and hill-side settings. As a result, different levels of access to raw material resources occur, which may influence the nature of lithic assemblages at these sites.

Karna

Karna is located on the Luni River, which preserves a rich record of Upper Pleistocene sedimentation (see Figure 4.8) and Palaeolithic occupation. The research undertaken by Misra (1963) in the Mid-Luni Valley to the north-east of Balotra is significant for our understanding of the archaeology of central Rajasthan, cementing the importance of this region for studying the Palaeolithic of the Thar Desert. Further recent research by Mishra et al. (1999) and Juyal et al. (2005) has presented a more detailed understanding of palaeoenvironmental and chronological patterns of alluvial sedimentation in the Mid-Luni Valley. Two small samples of lithic artefacts from the sites near Karna were identified within and upon a cemented gravel, dated to ca. 79ka (Figure 6.2; Chapter 5), indicating the potential for further archaeological discoveries.

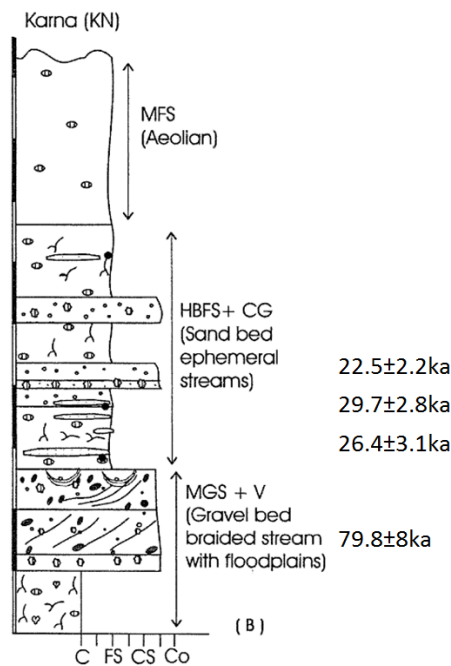


Figure 6.2: Stratigraphy of alluvial and aeolian deposits and associated luminescence dates at Karna (modified from Jain et al. 2005; Figure 4).

The basal sedimentary succession presented by Jain et al. (2005) for Karna consists of cemented multi-storied gravel sheets, dating to 79.8ka, associated with an overbank calcic

vertisol, is an easy landscape feature to identify. Although a number of lithic artefacts have been identified cemented in the gravel horizon by Jain et al. (2005), corroborated by the author (Figure 6.3), it has not been possible to recover and analyse them. As a result the presence of artefacts within the dated horizon can be confirmed but it has not been possible to provide further technological details.



Figure 6.3: Lithic artefacts (circled) stratified in cemented multi-storied gravels at Karna in sediments dated to 79.8ka. Largest artefact approx. 30mm.

During the survey at Karna reported here, two lithic scatters (KAR1 & KAR2) were encountered close to one another near the current course of the Luni River (Figure 6.4). A small sample of 10 artefacts was recovered at KAR1 at the eroding interface between a sandy gravel and an underlying pedogenised sand deposit, displaying well developed pedogenic carbonate nodules. At KAR2, a number of rhyolite boulders that display a number of large flake scars occur on top of a cemented gravel horizon (Figure 6.5), and a sample of 20 artefacts have been analysed from the immediate vicinity. A discrete lithic scatter (KAR3) was identified on top of the calcic

vertisol (Figure 6.6) and the presence of numerous very small lithic fragments (<10mm), the fresh appearance of the artefacts and their occurrence as a spatially discrete cluster suggest minimal natural disturbance; a sample of 20 artefacts were analysed. Given the stratigraphic position of all three assemblages, it is possible to suggest that they post-date the multi-storeyed gravel sheets in the area, which date to 79.8ka (Jain et al. 2005), however, it is not possible to offer an *ante quem* date for these samples.

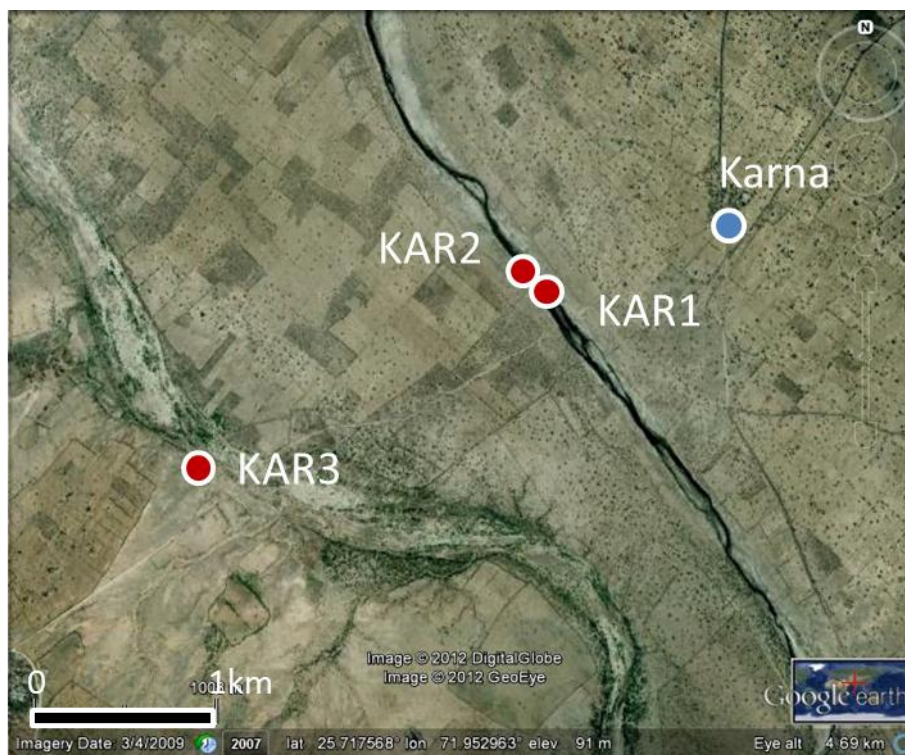


Figure 6.4: Map of locations of lithic assemblages recorded and sampled at Karna.



Figure 6.5: Rhyolite boulder core at KAR2 (150mm scale on boulder edge).



Figure 6.6: Lithic scatter from which KAR3 assemblage was sampled (150mm scale in lithic scatter).

Chamu

The construction of an irrigation canal near the village of Chamu (Figure 6.7 & 4.3) resulted in substantial excavations through a large dune deposit, revealing laterally extensive and deep sedimentary sections. Dhir et al. (2010) have produced a dated composite stratigraphy for the sedimentary sequence exposed near Chamu (Figure 4.14). Although no Palaeolithic artefacts have been reported from Chamu by Dhir et al. (2010), dune sites, such as 16R Dune, have proven to be profitable locations for research.

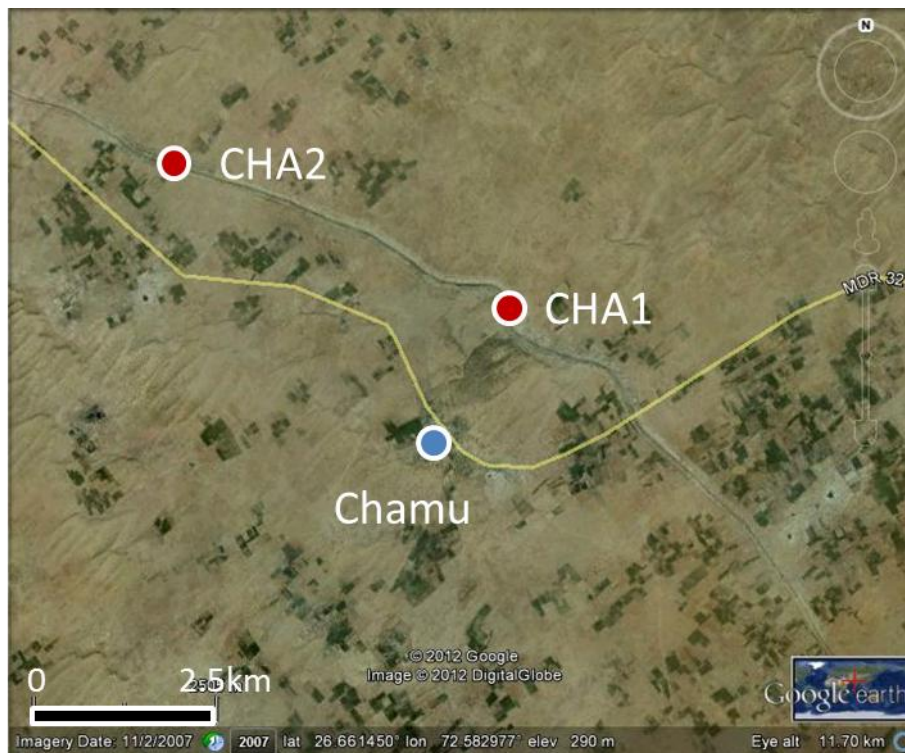


Figure 6.7: Map of locations of lithic assemblages recorded and sampled at Chamu.

New survey work at Chamu, undertaken by the author, resulted in two lithic assemblages being recorded, each comprising of 50 artefacts. The first (CHA1) was recovered from the surface of Horizon V, suggesting the assemblage should post-date the age of 58ka attributed to the horizon. It is likely that this assemblage pre-dates the formation of the friable, weakly

pedogenised deposits of Horizon VI ca. 27ka, although the relationship between these two horizons was not directly evident.

The context of the CHA 2 assemblage is more problematic, occurring as a dump of material on top of Horizon V. The surrounding area is comprised of Horizon V sediments, with minimal amounts of recent (Horizon VII) aeolian accumulation. The bank of the canal has been formed from the deposition of excavated material from the canal channel. As a result, it is suggested that the sandstone accumulations are dumps of material from the excavation of the canal channel. As Horizon V is the lowest observable deposit in this location, this is the youngest deposit from which this material may derive. It is also plausible that the material derives from the upper levels of Horizon IV. As a result, the CHA 2 assemblage can be constrained by the dates of these two horizons, providing an age bracket of 58ka to 81-105ka.

Shergarh Tri-Junction

Luminescence dating of a quarry section at Shergarh Tri-Junction by Andrews et al. (1998) provided an important early benchmark for palaeoenvironmental studies in the Thar Desert, particularly with its focus upon stable isotope geochemistry (Figure 4.15). The site occurs at the foot of a prominent rhyolite hill, where a quarry reveals alternating colluvial gravel and aeolian deposits (Figure 6.8). A report of rich surface Middle Palaeolithic and Mesolithic (Late Palaeolithic) sites has been made in the area (IAR 1978-79), indicating the importance of local raw material sources.

Following survey work undertaken for this thesis, two lithic assemblages have been recorded at the site (Figure 6.9). The first (TRI1) comprises 50 artefacts and was recovered from the quarry floor and predominately recovered from dumps of pedogenic carbonates that are found at the edge of the quarry. On the basis of the presence of large pedogenic carbonates nodules and the paucity of gravel content, it is suggested that this assemblage is likely to

derive from the dated aeolian horizons at the site, which have been deposited between 60-43ka.

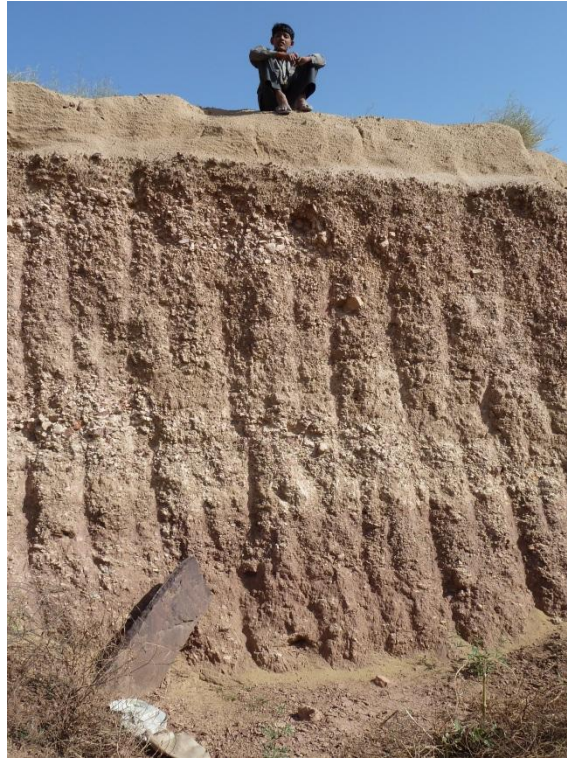


Figure 6.8: Quarry section observed at Shergarh Tri-Junction quarry, illustrating alternating colluvial and aeolian deposits overlain by a Holocene dune deposit.

The second assemblage (TRI2) is smaller, comprising of 20 artefacts. This assemblage was sampled from a spatially discrete surface scatter located on top of the upper-most colluvial unit (Figure 6.10). Occurring with a number of pedogenic carbonates and rhizo-concretions on an exposed surface, it is possible that this assemblage has been deflated. However, as the assemblage appears spatially confined and with similar levels of artefact weathering, there does not appear to have been substantial mixing. As a result, it is possible to suggest that the age of this assemblage is <43ka.

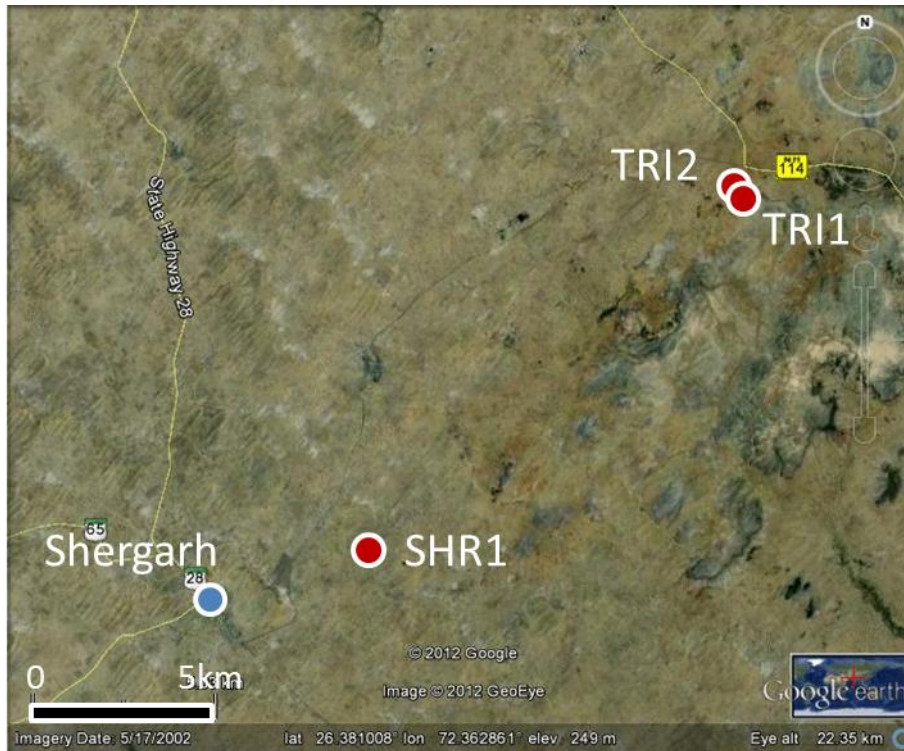


Figure 6.9: Map of locations of lithic assemblages recorded and sampled at Shergarh Tri-Junction.



Figure 6.10: Lithic scatter from which TRI2 assemblage was sampled.

Survey work undertaken closer to the village of Shergarh revealed further evidence of Palaeolithic occupation, although unrelated to any existing chronometrically dated landforms. A prominent rhyolite hill was inspected and numerous Palaeolithic artefacts were apparent on the slopes of the hill. A large Palaeolithic knapping floor was identified on the top of the hill (Figure 6.11). Although the site lacks a clear chronological context, the spatial integrity of the site is more certain, with little chance for material to be removed by natural agency. The nature and colour of the raw material used on the hill top, a striped, bright orange and purple rhyolite, was not immediately available, suggesting it was imported to the site. This may have occurred as this raw material was more silicious and presented fewer crystalline inclusions compared to the immediately available exposures of rhyolite. However, the bright and distinctive colour of the raw material may have also been an important factor in its selection, based on ethnographic and archaeological analogies (Gould 1968; Taçon 1991). A sample of 50 artefacts was recorded from the site (SHR1).

Analysis of lithic assemblages

A preliminary chronological framework for investigating change amongst these assemblages can be devised (Table 6.1). One assemblage, CHA2, can be attributed to MIS 5-4, and three further assemblages, KAR1, 2 and 3, may also date to a similar period. The remaining three assemblages with a dating bracket can be attributed to MIS 3-2. Significantly, the latter group overlaps the time period for the appearance of Late Palaeolithic industries illustrated elsewhere in South Asia, and may therefore offer some insight into similar technological changes in the Thar Desert.



Figure 6.11: Lithic scatter from which SHR1 assemblage was sampled.

Site	CHA1	CHA2	KAR1	KAR2	KAR3	SHR1	TRI1	TRI2
Associated Chronology (ka)	58 – 27	58 – (81- 105)	<79	<79	<79	N/A	60 – 43	43 – 9
Artefact Type								
Single Platform Core	0	1	0	4	0	0	6	1
Bidirectional Core	0	0	0	0	0	0	2	0
Multi Platform Core	0	1	1	1	1	3	8	8
Prepared Core	0	1	0	1	0	3	7	4
Flake	20	30	4	8	16	27	15	5
Broken Flake	18	9	1	3	1	8	4	1
Flake Piece	9	3	1	2	1	3	2	1
Broken Flaked Piece	0	0	0	0	0	1	0	0
Single End	1	0	0	0	0	0	1	0
Single Side	0	1	0	0	1	2	4	0
Single Side (FP)	1	0	0	0	0	0	0	0
Single End Single Side	1	3	2	0	0	3	0	0
Single End Double Side	0	1	1	1	0	0	0	0
Double Side	0	0	0	0	0	0	1	0
Total	50	50	10	20	20	50	50	20

Table 6.1: Typological breakdown of artefact assemblages from Chamu, Karna and Shergarh Tri-Junction with chronology of associated sedimentary contexts.

The use of local raw material resources is certainly evident in TRI1, TRI2 and SHR1, which exclusively make use of rhyolites available in the vicinity of the sampled sites (Table 6.2). The artefacts at Karna (KAR1, 2 & 3) are mostly comprised of rhyolite, which can be found both on site, as with the boulder cores at KAR2, and in a range of hills 3km away. The presence of both quartzite and chert amongst the KAR1 assemblage may indicate the use of gravel horizons as raw material sources, although they may also be exogenous. Both CHA1 and CHA2 are comprised entirely of sandstone, and no source of raw material is apparent in the modern landscape, although widespread and deep coverage by sand dunes may prevent the identification of raw material availability in the immediate vicinity.

Site	Rhyolite	Sandstone	Quartzite	Chert
CHA1	-	50	-	-
CHA2	-	50	-	-
KAR1	6	-	2	2
KAR2	20	-	-	-
KAR3	20	-	-	-
SHR1	50	-	-	-
TRI1	49	1	-	-
TRI2	20	-	-	-

Table 6.2: Raw material use at Chamu, Karna and Shergarh Tri-Junction.

No artefacts with cortical surfaces were recorded amongst the TRI1 and TRI2 assemblages, suggesting preliminary reduction was not taken place on site. In contrast, in the SHR1 assemblage show some presence of cortex on seven flakes and a retouched flake (Table 6.3). Two flakes in each assemblage at Chamu preserve cortical surfaces, whereas the presence of a number of artefacts with a high percentage of cortical coverage at KAR2 and KAR3 suggests some primary reduction activity has occurred at these sites.

Site	10%	20%	30%	40%	50%	60%	70%	80%	90%	100%
CHA1	-	-	-	-	-	-	-	1	-	1
CHA2	-	-	-	1	-	-	-	-	1	-
KAR1	-	-	-	-	-	-	1	-	-	-
KAR2	-	-	2	1	-	-	-	-	-	2
KAR3	-	-	1	2	-	-	-	1	-	3
SHR1	-	2	-	1	-	4	-	1	-	-

Table 6.3: Number of artefacts with different levels of cortical coverage at Chamu, Karna and Shergarh Tri-Junction.

Cores

Typological description

Cores at both Karna and Chamu appear informal and infrequently, whereas more formalised types appear at Shergarh Tri-Junction. A bidirectional core from TRI1 exhibits a number of parallel longitudinal arises and blade removals (Figure 6.12). Four Levallois cores are present at TRI1, two of which present preferential removals, whereas the other two exhibit unidirectional and bidirectional flaking patterns (Figure 6.12). Three further preferential Levallois cores are recorded at TRI2 (Figure 6.12), and a single preferential Levallois core is evident at SHR1 (Figure 6.13). A single core from SHR1 exhibits flake removals from the left, distal and right of the core with a single pointed preferential removal (Figure 6.13). This reduction pattern closely matches the description of Nubian Type 2 point cores (Rose et al. 2012).

Technological description

Single and Multiplatform reduction strategies are most widespread and common. A single prepared core is identified at KAR2, whereas prepared and multi-platform cores occur at the Shergarh Tri-Junction sites in equal proportions. Average core sizes from this sample is 72.3x53.2x25.54mm, with some variation by core type. The bidirectional cores are notably smaller (mean length=54.5mm) compared to other core types (group mean length=72.3mm). However, they are encompassed in the size range of other core types (37.2-145.8mm).

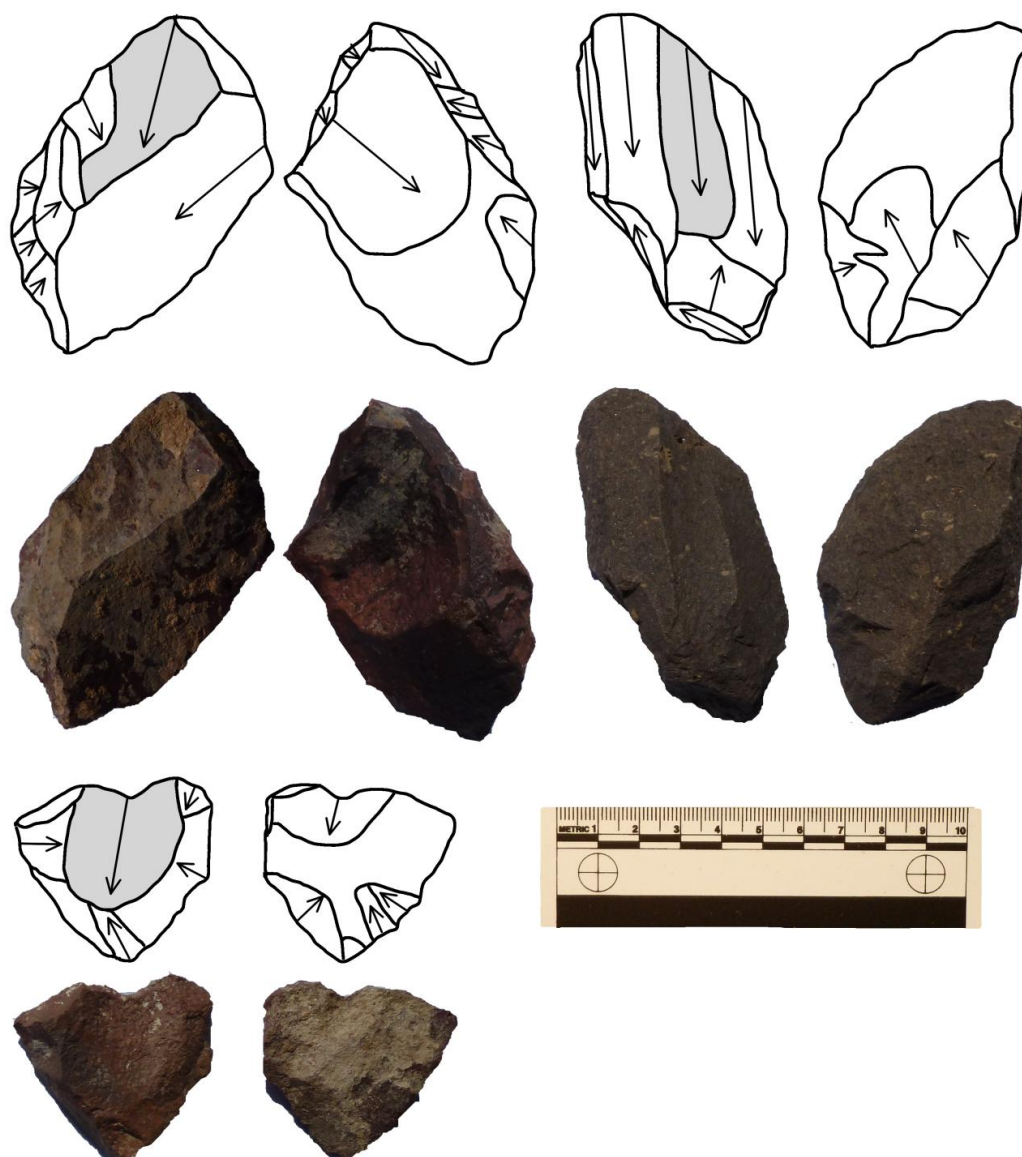


Figure 6.12: Cores from Shergarh Tri-Junctions. Top-left: Bidirectional Levallois core from TRI1 ; Top-right: bidirectional blade core from TRI1; Bottom-Left: Preferential Levallois core from TRI2.

Platform width varies with core type, with the average width of prepared cores (mean=37.5mm) largest, followed by Multi-Platform (mean=33mm), single platform (mean=27.9mm) and bidirectional cores (mean=21.1mm). A large proportion of the cores (n=16; 30.8%) exhibited faceted platforms, followed by dihedral (n=11; 21.2%) and plain (n=11; 21.2%). Single conchoidal (n=7; 13.4%) and multiple conchoidal (n=4; 7.7%) platforms were



Figure 6.13: Artifacts from SHR1. Top-left: Preferential Levallois Core; Top-right: Preferential point core similar to Nubian Type 2 cores; Bottom-left: Notched Flake; Bottom-right: Tongued Flake.

less common, and other platform types are isolated occurrences. The majority of final flake scars present feather terminations (n=35; 67.3%), with axial types the other most common type (n=12; 23%).

The two bidirectional core both exhibit blade proportioned scars, and examples of blade-proportioned removals are present on all core types (max range=2.09-4.25), although the overall average is below this threshold (mean=1.46). Except for flake scars on bidirectional cores, which are substantially narrower, little variability is observed by core type with regards to last scar size.

A number of differences are apparent between assemblages. The cores from TRI1, TRI2 and SHR1 are mostly smaller than those from CHA2, KAR2 and KAR3. The lower length range from the Shergarh Tri-Junction sites is 37.2-55.9mm, whereas from the remaining sites it is 72.8-145.8mm, which is similar to the upper range from TRI1, TRI2 and SHR1 (94.1-114mm). A similar pattern is apparent across the size variables. Despite a number of highly elongate last scars present in TRI1 and TRI2, on average there is no variation between assemblages with regards to elongation. Faceted, dihedral and plain platforms are most common at the Shergarh Tri-Junction sites, with few clear patterns evident elsewhere.

Flakes

Typological Description

Two complete flakes present dorsal scar morphologies matching descriptions for Levallois points, both of which derive from CHA1 (Figure 6.14). The remaining flakes do not fall into clear typological categories.

Technological Description

Complete flakes are the most numerous artefacts recorded amongst this group of sites, and were found at all eight sites. Considerable size differences in flake size have been observed, with maximum dimension ranging from 25-199mm, although half of the flakes recorded occur between 51-86mm. The average dimensions of flakes are 69.8x47.7x17.9mm, although

average axial measurements are 50.1x54.7mm, and average platform size is 45.3x14.3mm.

Average flake elongation is 0.99, with the most elongate flake indicated by a value of 2.21.

Proximal dorsal scar patterns are most common (34%), followed by weakly radial (17.4%) opposed/perpendicular (16.5%) and side (15.5%). Radial flakes account for 10% of the samples; distal (3.9%) and cortical (1.9%) types are rare. Plain platform types are most common (33.3%), followed by single conchoidal platforms (24.4%). Dihedral platforms account for 13.8% of platform types, with remaining types occurring <10%. Termination types are mostly feather (86.8%), with few axial (6.7%), hinge (4.1%) and step (2.5%) types.

The two cortical flakes present are have larger maximum dimensions than average, but overage there is little difference in flake size with regards to dorsal scar pattern. With regards to axial dimensions, the lower range of all types is broadly similar (ca. 25x24mm), but flakes with distal, opposed/perpendicular and radial scar patterns do not show as large an upper range, below <100mm in both dimensions. Perpendicular and proximal flakes exhibit the only blade-proportioned flakes.

The flakes from KAR2 (mean length= 104.7mm) are notably larger than the remaining sites (group mean length=69.8mm) across the size variables recorded. Flakes from KAR1 (mean=52.1mm), TRI1 (mean=61.9mm) and TRI2 (mean=59.8mm) are typically smallest, although considerable overlap occurs between the assemblages. TRI2 is the only site containing blade-proportioned flakes, although both TRI1 (max=1.95) and KAR3 (max=1.86) contain more elongate flakes than average. The proportion of dorsal scar pattern types in each assemblage is broadly comparable. A greater proportion of simple (plain and single conchoidal) platform types are present at CHA1 and CHA2, whereas more complex forms (dihedral, multiple conchoidal, faceted) types occur at TRI1, TRI2 and SHR1.

Retouched Pieces

Typological Description

A number of distinct retouched types are apparent amongst these assemblages. A number of these exhibit varying intensities of delineation. Individual tanged pieces are present at KAR1, KAR2 and CHA2. Tongued pieces are recorded at KAR3 and SHR1 (Figure 6.13). Shouldered pieces are present at CHA1 (Figure 6.14), KAR1 and SHR1. In these cases, the delineated margin appears at one end of the maximum axis of the artefact, with converging margins present at the opposite end. Two notched artefacts are present (Figure 6.13) one of which helps to delineate a stem on a bifacially flaked point (Figure 6.14). A single burin is recorded at SHR1.

Technological Description

The average dimensions of retouched artefacts are 72.6x46.1x17.7mm, with the typical extent of retouch measuring 42.5x12.8mm. Average maximum, axial and platform dimensions are typical of the broader flake population outlined above, and there is little indication for selection of elongate flakes.

Summary

Despite the greatest proximity to raw material resources, the artefacts from Shergarh Tri-Junction are typically smaller than those from the other two sites, suggesting that this size difference may relate to differences in reduction strategy, rather than limitations imposed by raw material package size. This is supported by the focus upon specialised core reduction strategies. Conversely, the Chamu sites often present the largest sized artefacts across all categories without a clearly identified raw material resource in the vicinity. Despite the relative dearth of cortical artefacts, the high number of broken flakes and flaked pieces may

indicate that the large size of these artefacts may relate to an earlier stage of reduction than those at Shergarh Tri-Junction, supported by the simpler suite of platform types and scar patterns. TRI1 and TRI2 are notable for the lack of retouched pieces with delineated tangs, tongues or shoulders from this group. As the potentially youngest sites, this may indicate a chronological shift in reduction focus, although overlap in chronometric dates and the large proportion of cores present at the site preclude a clear distinction. Nevertheless, these assemblages all match current descriptions of Middle Palaeolithic industries in the Thar Desert.

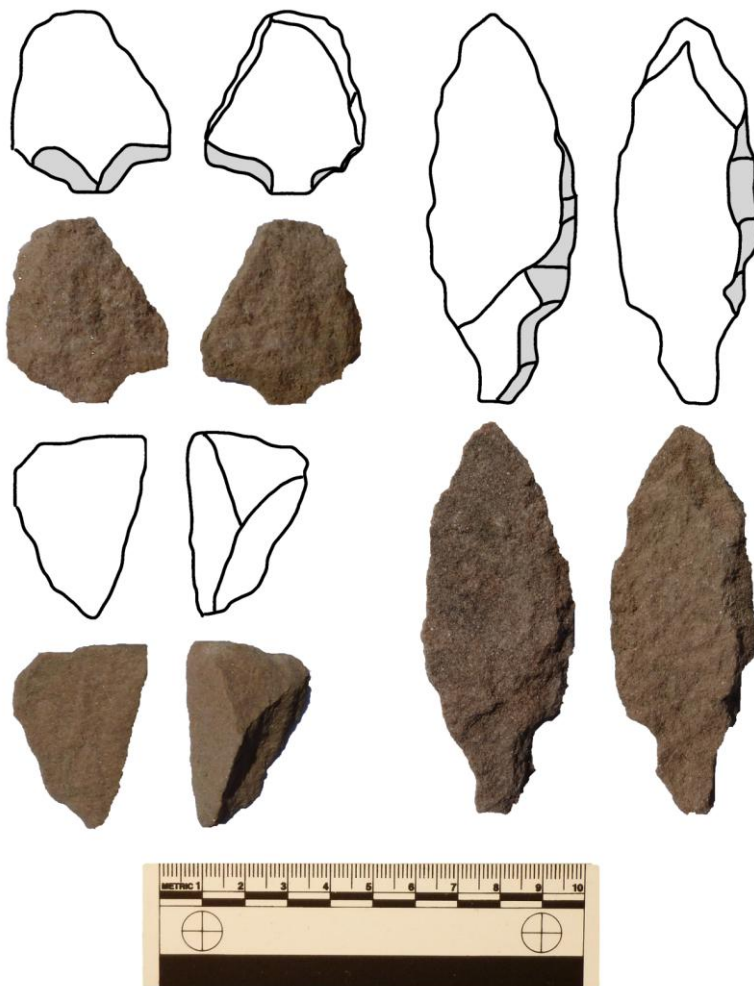


Figure 6.14: Artefacts from Chamu. Top-left: Shouldered flake from CHA1; Bottom-left: Levallois point from CHA1; Right: Bifacial stemmed point.

Survey of Lacustrine Sites

Little archaeological attention has been paid to either Sambhar Lake or the Jaisalmer Raans, whereas they have both been subject to palaeoenvironmental studies, including chronometric dating of lake sedimentation. Lake cores offer a useful line of evidence for understanding patterns of palaeoenvironmental change, yet little attention has been paid to the lake shores although they are likely to preserve more diverse sedimentary features and evidence of human activity. Significantly, Sambhar Lake is located at the edge of the desert while the Jaisalmer Raans occur at the arid core, and so have been subject to different levels of environmental variability that are likely to impact upon how Palaeolithic hominins have exploited these locations in the past, which may be reflected in their lithic technologies.

Sambhar Lake

Research at Sambhar has mostly focused upon Holocene lacustrine deposits (e.g. Jakher et al. 1990; Singh et al. 1972; 1974), although a number of important observations regarding the Pleistocene sediments of the region have been made (Sinha et al. 2006). A number of researchers report heterogeneity amongst sand dunes surrounding the lake, indicating repeated episodes of aeolian activity are present at the site (Allchin et al. 1978; Sinha et al. 2006). Secondly, the cross-section of stratigraphy presented by Agrawal (1971) relates aeolian deposits found within the modern lake boundary, overlain by Holocene lacustrine horizons, to sand dunes at the edge of the lake and radiocarbon dates from these upper lacustrine deposits suggests that major aeolian encroachment upon the lake had halted by the start of the Holocene (Allchin et al. 1978; Singh et al. 1972; 1974). Finally, Allchin et al. (1978) identified a clay pan upon which the modern lake sits and indicated that the ecology of the lake environs may have changed significantly following the formation of this impermeable layer, which effectively drives the salinity of the lake by preventing mixture with fresh groundwater.

With regards to previous archaeological research at Sambhar Lake, Allchin et al. (1978) undertook surveys of both the north and south shores, but encountered few archaeological sites. Two Palaeolithic sites are reported on the southern shore, including a collection of 20 fresh artefacts from an alluvial fan formed by a *nalla* (small gully) from nearby hills near the lake edge, and a second site occurring on the crest of an obstacle dune (Allchin et al. 1978). Renewed survey was undertaken at Sambhar Lake due to the ecological significance of the site, and its geographic location, occurring in a major pass through the Arravallis.

Archaeological survey around Sambhar Lake was predominately focused on the eastern side of low hill of banded gneiss, located to the east of the village of Korsana, on the southern shore (Figure 6.15). A rich diversity of lithic assemblages were encountered, and although these extended on to the west side of the hill, including stratified lithic assemblages in rilled and pedogenised dune deposits, quarrying activity effectively prevented survey work. The most prominent form of archaeological evidence from this location was the numerous boulder cores that littered the slopes of the hill. Large flakes have been removed from boulders ranging in size from 0.125m³ to 125m³ on the lower slopes of the hill, and are also seen on exposures of gneiss at the top of the hill (Figure 6.16). A range of Palaeolithic artefacts can be found scattered on and within the colluvial deposits that support the boulder cores, and 19 artefacts found in three groups within the vicinity of boulder cores have been recorded (SMB1), albeit with a more limited set of attributes than the rest of the assemblages presented in this chapter.

On the lower slopes of the hill a small quarry has revealed a small section through the colluvial deposits. The sediments included a large quantity of quartz artefacts, and a sample of 78 have been analysed (SAM1). Survey of the dunes abutting the eastern edge of the hill, and overlying the colluvial deposits, failed to identify many artefacts, with only a small sample of 9 artefacts having been identified and recorded (SMB2). In contrast, the ridge of the hill was littered with

evidence of lithic reduction activities, focusing on both gneiss and quartz. Three small samples of gneiss artefacts were selected for analysis, comprising 12 (SMB3), 14 (SMB4) and 16 (SMB5).

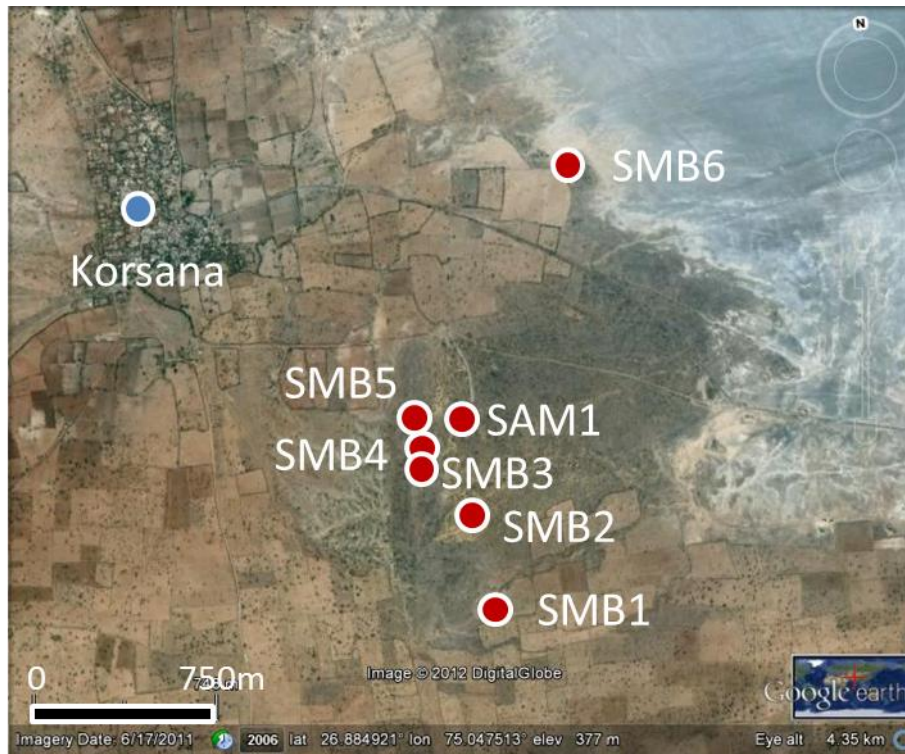


Figure 6.15: Map of locations of lithic assemblages recorded and sampled at Sambhar Lake.



Figure 6.16: Gneiss boulder core at SMB1.

Exploration of the lake shore identified a whitish clay horizon matching the description provided by Allchin et al. (1978), bracketed by two dark brown, pedogenised sandy clays and overlain by a spread of quartz gravels, all of which are overlain by modern lacustrine and aeolian deposits. A sample of 25 quartz artefacts were recorded from the gravels (SMB6) (Figure 6.17), while a number of quartz artefacts were seen stratified in the pedogenised sandy clays overlying the whitish clay and beneath the gravels, although none were recorded. This indicates the potential of further exploration of lake side environments for the recovery of archaeological assemblages in primary contexts, and to understand the stratigraphic and palaeoenvironmental development of lacustrine deposits at Sambhar Lake.



Figure 6.17: Lithic scatter from which SMB6 assemblage was sampled.

Jaisalmer Raans

The Jaisalmer Raans, a series of three linear lakes named Dandar, Kharia and Kanod (see Figure 6.18) offer a significantly different context to Sambhar Lake for investigating evidence of human occupation, occurring within the modern arid zone and presenting a significantly different suite of ecological and raw material resources. Unlike a number of the saline lakes that occur in central Rajasthan (e.g. Didwana), the modern topography and drainage pattern of the Jaisalmer Raans suggest that tectonic disruption of an ancient fluvial course, rather than sand dunes blocking a drainage basin, is responsible for their formation.

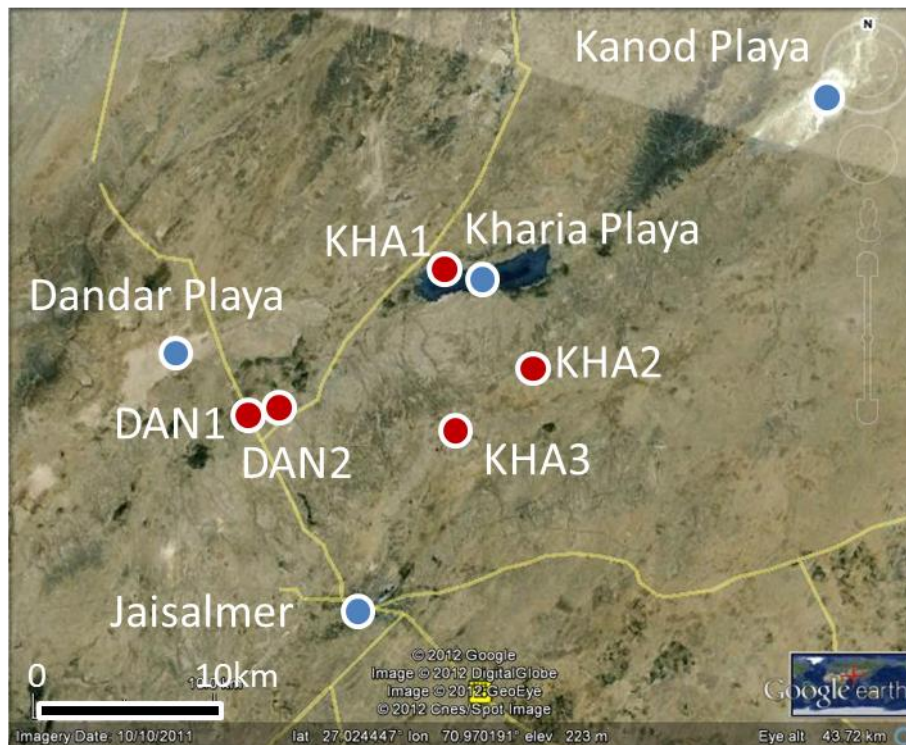


Figure 6.18: Map of locations of lithic assemblages recorded and sampled at the Jaisalmer Raans.

Recent work at Kanod playa presents the only dated evidence for lacustrine sedimentation amongst the three lakes, indicating that lake sediments have been deposited from the early Holocene onwards, and overlie terminal Pleistocene aeolian deposits and Mesozoic claystone

(Deotare et al. 2004). A range of both ceramic and aceramic Mesolithic sites are reported in the vicinity of Kanod playa, suggesting re-occupation of the central desert region is strongly associated with the availability of fresh water (Deotare et al 2004). In contrast, there has been little palaeoenvironmental research at either Kharia or Dandar playa, although three archaeological sites are reported from Dandar, including a Mesolithic (Late Palaeolithic) and two Middle Palaeolithic assemblages (Allchin et al. 1978).

Although there have been no targeted palaeoenvironmental studies undertaken at Kharia playa, a similar lacustrine sequence can be inferred, as the modern lake sediments are observed overlying poorly consolidated bedrock/marine sediment exposures of pre-Quaternary origin. The potential to preserve pre-Holocene lake sediments is limited by the inferred strength of aeolian erosion during the LGM. The surrounding landscape is covered in a blanket of recent sand dunes, although at a number of locations a more compact and pedogenised dune sand horizon, which is evidently more resistant to erosion, appears stratified beneath it. A discrete lithic scatter was identified overlying the pedogenised dune sand horizon at the break of slope between the lake shore dunes and the lake edge sediments (Figure 6.19) and a sample of 24 artefacts was recorded (KHA1).

Survey around a sandstone ridge overlooking the lake, and two fluvial channels that feed it, which display varied stratigraphic sequences that offer insights into palaeoenvironmental variability surrounding the lake. Exposures of cherty limestone and sandstone are abundant in the area, and a large volume of lithic debris is apparent on exposed bedrock surfaces (Figure 6.20), gravel spreads and thin, weathered dune deposits. A sample of 20 artefacts was recorded from gravel surface (KHA2) and bedrock (KHA3) contexts to the south of the playa.



Figure 6.19: Lithic scatter from which KHA1 assemblage was sampled.



Figure 6.20: Lithic scatter from which KHA2 assemblage was sampled.

A similar scenario was encountered at Dandar playa, with two phases of aeolian deposition overlying poorly consolidated bedrock/marine sediment exposures. However, exploration at the edge of the dune and lake sediments failed to identify any archaeological sites. As a result, a fluvial channel was targeted for survey, which revealed a more diverse sedimentary sequence including an alternating sequence of gravel and sand horizons. Further exploration of diverse sedimentary sequences surrounding the playa, rather than the playa sediments themselves, once again may offer the widest range of detail for investigating palaeoenvironmental variability at Dandar. A large volume of lithic material was exposed on the surface of both gravel and sand horizons on either side of the inspected fluvial channel, and two samples of 25 (DAN1) and 37 (DAN2) artefacts have been recorded.

Analysis of Lithic Assemblages

A basic typological breakdown of assemblages from Sambhar Lake and the Jaisalmer Raans is presented in Table 6.4. Sample sizes vary considerably within these assemblages, from 10 to 78 artefacts, which may have some impact upon the structure of variability described. Raw materials are widely available surrounding the sites under consideration here, except for at KHA1 where they are available within a short distance from the site (ca. 3km). A range of raw materials, with variable flaking properties and occurring in different clast sizes, are apparent amongst these sites (Table 6.5). A gross comparison of the size of all artefacts from these sites by raw material type indicates that artefacts on gneiss (seen only at Sambhar Lake) are substantially larger than those at the Jaisalmer Raans made on cherty limestone and sandstone, which are notably larger than quartz artefacts from Sambhar.

Artefact Type	DAN1	DAN2	KHA1	KHA2	KHA3	SAM1	SMB1	SMB2	SMB3	SMB4	SMB5	SMB6
Core	0	0	0	0	0	0	3	0	2	0	3	2
Single Platform	0	6	2	0	4	3	0	0	0	1	0	0
Multi Platform	0	4	11	3	0	3	5	0	0	1	0	0
Prepared	0	0	1	4	0	0	0	0	0	0	0	0
Flake	21	15	7	10	14	31	3	7	7	8	10	15
Broken Flake	3	5	0	3	2	8	1	0	0	0	0	0
Flake Piece	0	4	1	0	0	9	0	3	0	0	2	3
Single End	1	1	1	0	0	3	0	0	0	0	0	0
Single Side	0	1	0	0	0	8	0	0	0	3	0	1
Single End Single Side	0	0	0	0	0	8	0	0	2	0	0	1
Single End Double Side	0	1	1	0	0	2	0	0	0	0	0	0
Double End Single Side	0	0	0	0	0	1	0	0	0	0	0	0
Double End Double Side	0	0	0	0	0	2	0	0	1	1	0	0
Unspecified	0	0	0	0	0	0	1	0	0	0	0	0
Biface	0	0	0	0	0	0	3	0	0	0	0	0
Chopper	0	0	0	0	0	0	3	0	0	0	1	0
Total	25	37	24	20	20	78	19	10	12	14	16	25

Table 6.4: Typological breakdown of artefact assemblages from Sambhar Lake and Jaisalmer Raans.

It may be significant that the lower range of artefact size of quartz, sandstone and gneiss are very similar, suggesting that the capacity to produce small artefacts may not have influenced raw material choice, although the predictability of fracture mechanics may have been an important issue. The limited upper range of quartz artefacts is likely to reflect a real limit on the size of artefacts that can be produced from the narrow bands of quartz available around Sambhar Lake, which is not apparent for the other raw materials.

Site	Sandstone	Limestone	Cherty Limestone	Quartz	Gneiss
DAN1	21	4	-	-	-
DAN2	36	-	1	-	-
KHA1	-	-	24	-	-
KHA2	-	-	20	-	-
KHA3	-	-	20	-	-
SAM1	-	-	-	76	2
SMB1	-	-	-	5	14
SMB2	-	-	-	4	6
SMB3	-	-	-	-	12
SMB4	-	-	-	-	14
SMB5	-	-	-	-	16
SMB6	-	-	-	24	-

Table 6.5: Raw material use at Sambhar Lake and the Jaisalmer Raans.

Artefacts with cortical surfaces occur at most sites within this group (Table 6.6). The large numbers of cortical artefacts, mostly <50%, at SAM1 is likely to relate to the larger sample size and perhaps the size and shape of the bands of quartz available nearby. In contrast, at DAN1, DAN2 and KHA3 a greater proportion of artefacts with high levels of cortical coverage suggests that these assemblages preserve some evidence of early phases of lithic reduction.

Site	10%	20%	30%	40%	50%	60%	70%	80%	90%	100%
DAN1	-	-	-	1	-	-	1	-	2	6
DAN2	1	1	-	1	-	1	3	1	-	3
KHA1	2	-	-	-	2	-	-	-	1	1
KHA3	1	-	3	-	-	1	-	2	1	1
SAM1	6	-	1	3	1	1	3	1	-	-
SMB2	-	-	-	-	1	-	-	-	-	-
SMB3	-	-	-	1	-	-	-	-	1	-
SMB4	-	-	1	-	-	1	-	1	-	-
SMB5	-	1	1	1	-	-	2	-	-	-
SMB6	1	-	-	-	-	-	-	1	-	-

Table 6.6: Number of artefacts with different levels of cortical coverage at Sambhar Lake and the Jaisalmer Raans.

Cores

Typological Description

Cores at both the Jaisalmer Raans and Sambhar Lake are simple, with only five cores exhibiting evidence for the preparation of flaking surfaces. A single preferential Levallois core from KHA2 is present. In addition two microlithic cores are recorded at SAM1.

In addition to portable clasts that have been exploited as cores, a large number of gneiss boulders that litter the slopes of the surveyed hill near Korsana exhibit large negative flake scars. Measurements of 54 flakes from 23 boulders were recorded. The size range of these flakes is broad, with average dimensions of 204.6x249.1mm, although some are notably smaller (min=70x100mm). As a result, boulder cores can plausibly have been used to produce flake blanks for both heavy tools and smaller retouched pieces, as well as large flakes to be exploited as cores.

Technological Description

Core size attributes vary considerably with regards to raw material type. Quartz cores are smallest across all size variables, with an average length of 48.7mm, followed by limestone (mean=83.1mm), sandstone cores (mean=91.4mm); gneiss cores are largest (mean=99.5mm). The axial dimensions of last scars present a different pattern, with the axial length of sandstone cores (mean=23.5mm) smaller than that of quartz cores (mean=29.5mm), whereas limestone (mean=45mm) and gneiss (mean=52.9mm) are larger. The platform widths on gneiss cores (mean=68.4mm) are larger than those limestone (mean=41.3mm), sandstone (mean=40.3mm) and quartz (mean=31.9mm) cores. Blade proportioned scars are evident on quartz, limestone and gneiss cores, although elongate flakes are not typical (group mean=1.15).

Most cores on gneiss have not been classified, although examples of both single and multi-platform cores occur. Prepared cores only occur on limestone, whereas broadly equal proportions of single and multi-platform cores appear on quartz, limestone and sandstone. Dihedral platform types are only seen on limestone cores, whereas single and multiple conchoidal types are most common amongst all raw material types, and faceting is observed in low proportions on all raw materials. Feather terminations are most common across all raw material types, although a higher proportion of axial terminations are apparent on limestone cores. While prepared cores are only seen at KHA1 and KHA2, all other differences in core technology appear to relate more strongly to raw material type than to variation between sites.

Flakes

Typological description

Two unretouched pointed flakes present distinctive dorsal scar morphologies, both of which occur at KHA2. The first exhibits a number of small scars on both lateral margins, forming a medial ridge at the distal portion of the flake, and a single larger scar has been removed, originating from the proximal end. A small arise is also present at the distal end of the second piece, and a single, large, pointed removal originated from proximal is also evident on the flaking surface. The lateral margins exhibit trimming from both sides and from proximal. These both present examples of managed flaking surfaces organised for the production of pointed flakes.

Technological Description

Variability amongst flake attributes is predominately structured by raw material type. A small number of flakes produced on bioclastic limestone typically exhibit the largest sizes, with mean

length of 97.8mm. Gneiss flakes exhibit a mean length of 86mm, larger than that of limestone and sandstone (mean=70mm) and approaching twice the average size of quartz flakes (mean=46.1mm), with similar patterns extending to width and thickness measurements. Excluding bioclastic limestone pieces (min=61.4mm), limestone artefacts show the largest minimum length (43.5mm), over 10mm larger than average quartz, sandstone and gneiss flakes. The maximum range of quartz is limited (max=83.4mm) compared to other materials, all of which range between 115-200mm. Although axial lengths of limestone, sandstone and gneiss artefacts are similar (means range from 47-54mm), the axial widths of gneiss flakes (mean=78.9mm) and larger than sandstone and limestone (mean=56mm). Flake elongation is typically low (group mean=0.97), with quartz artefacts infrequently reaching blade proportions (max=2.12), although both limestone (max=1.89) and sandstone (max=1.98) artefacts come close to this level.

Proximal scar patterns are most common across raw material types (n=50), and weakly radial (n=23) and opposed/perpendicular (n=14) types are common. No side scar patterns occur on limestone flakes, whereas they appear on gneiss, sandstone and quartz flakes. Low numbers of bidirectional scar patterns are observed on all but bioclastic limestone flakes. Simple platform types, including cortical, plain and single conchoidal types, are most common. Low proportions of more reduced types are present on gneiss flakes, whereas higher proportions of dihedral and multiple conchoidal platforms are evident upon quartz and limestone flakes. Feathered terminations are most frequent across raw material types, whereas axial terminations are notably more frequent on quartz and limestone flakes.

Retouched Artefacts

Typological Description

A low number of retouched artefacts were recorded at the Jaisalmer Raan sites. At DAN2, two notches have been recorded, both on sandstone. A further notch is present on a limestone flake at KHA1. One of the most distinctive retouched pieces encountered throughout survey in Rajasthan occurred at KHA1, where a large limestone point has a clearly delineated tang (Figure 6.21). A large number of retouched quartz artefacts are present in the SAM1 assemblage (Figure 6.22). Three notches are present, and a single double notched pieces is recorded. Delineated types include four nosed pieces, two shouldered pieces and a single tanged piece. A single bifacial quartz point has also been recorded. SAM1 also includes two retouched gneiss pieces, one of which is nosed, whereas the other piece is tanged (Figure 6.23). In addition, single nosed artefacts are recorded in SMB4 and SMB6, and individual notched artefacts are recorded at both sites. SMB3 includes a unifacially retouched point, a shouldered piece and a tongued piece, and a single tanged piece is recorded at SMB6. Finally, one small and one large tanged gneiss point were also identified at the top of the hill overlooking Korsana, although neither was not analysed (Figure 6.23). Delineation repeatedly occurs at one of the maximum axis of the piece, typically opposite convergent margins.

Technological Description

Retouched artefacts vary substantially with regards to raw material type. The two limestone retouched artefacts are larger than quartz and sandstone pieces, and fall within the upper range of retouched gneiss artefacts. Sandstone and gneiss artefacts are, on average, similarly sized across most variables (e.g. mean length = 70.7mm and 73.8mm respectively) although the range of gneiss artefacts (38.11-155mm) is much larger than that for sandstone pieces

(64.4-77.2mm). Quartz artefacts are repeatedly smaller (mean=44.2mm; range=26.9-71.2mm). No clear preference for axially elongate flakes is evident. The extent of retouch varies considerably within and between raw material groups, with total retouch width ranging from 5.9-160mm. On average, the width of retouch on is lowest (mean=29.35) although the upper range (84mm) exceeds that of limestone (63.9mm) and sandstone (73mm) artefacts. Gneiss artefacts typically exhibit the largest retouch widths (mean=58mm).

Heavy Tools

A small group of gneiss heavy tools have been recorded at Sambhar Lake, predominately from SMB1, which include both bifacially worked pieces and choppers. The size ranges of these artefacts (length:81.98-141.68mm; width: 54.8-120.8mm) overlaps considerably with the flake and retouched populations from these sites. Imposition of form is somewhat limited, which may imply that these artefacts have been abandoned in early stages of reduction as heavy tools, or proved unsuitable for further reduction as cores.

Summary

The differences between raw materials appear to have had a significant impact upon lithic variability at these sites, which are most strikingly apparent at Sambhar Lake. Gneiss artefacts are substantially larger than the quartz artefacts found nearby although the occurrence of typologically similar artefacts suggests no clean distinction in overall reduction strategies for each raw material. The production of heavy tools on quartz is infeasible given the scale of available clasts, whereas examples of finely retouched gneiss artefacts at the same scale as quartz pieces indicates that raw materials may not have precluded common reduction strategies. The large size of gneiss artefacts may also relate to early stages in reduction sequences, some of which begin with removal of large flakes from boulder cores.

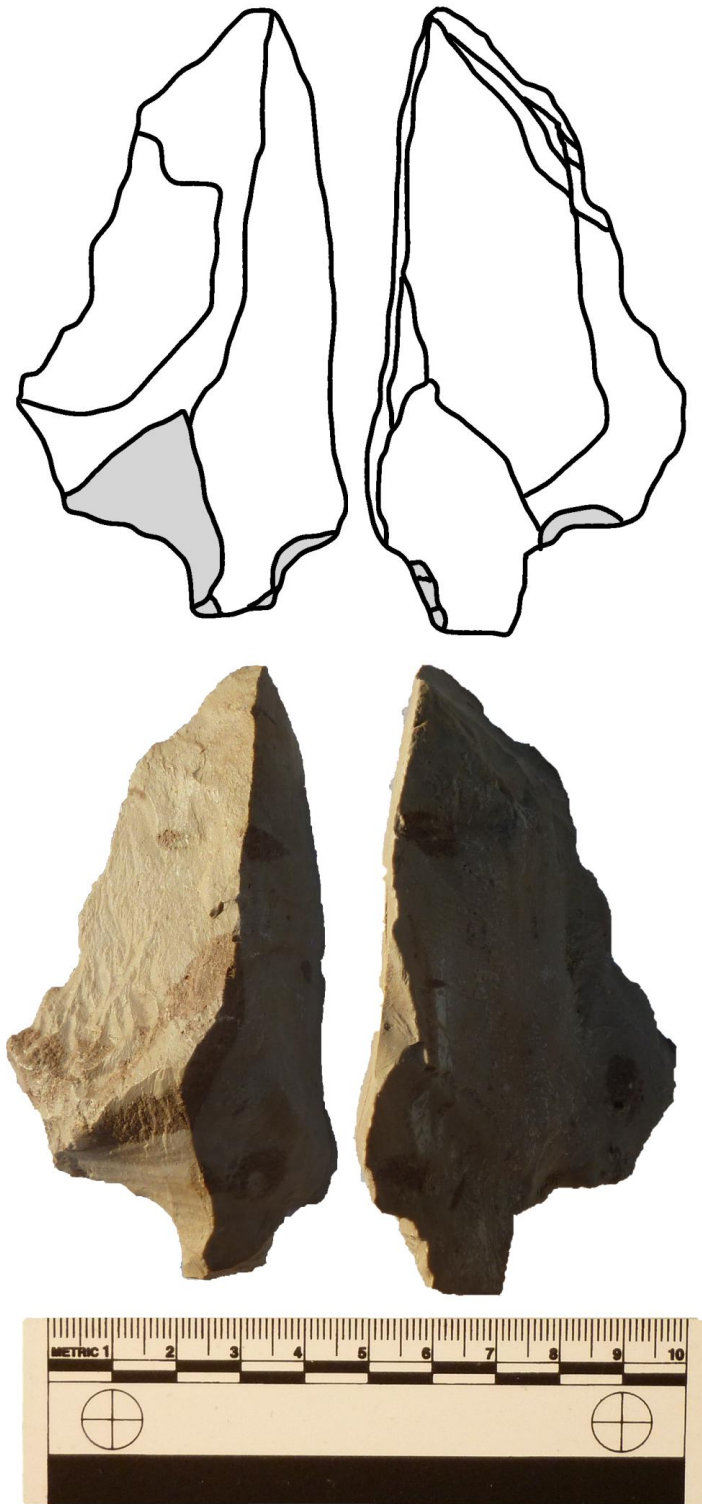


Figure 6.21: Tanged point from KHA1.

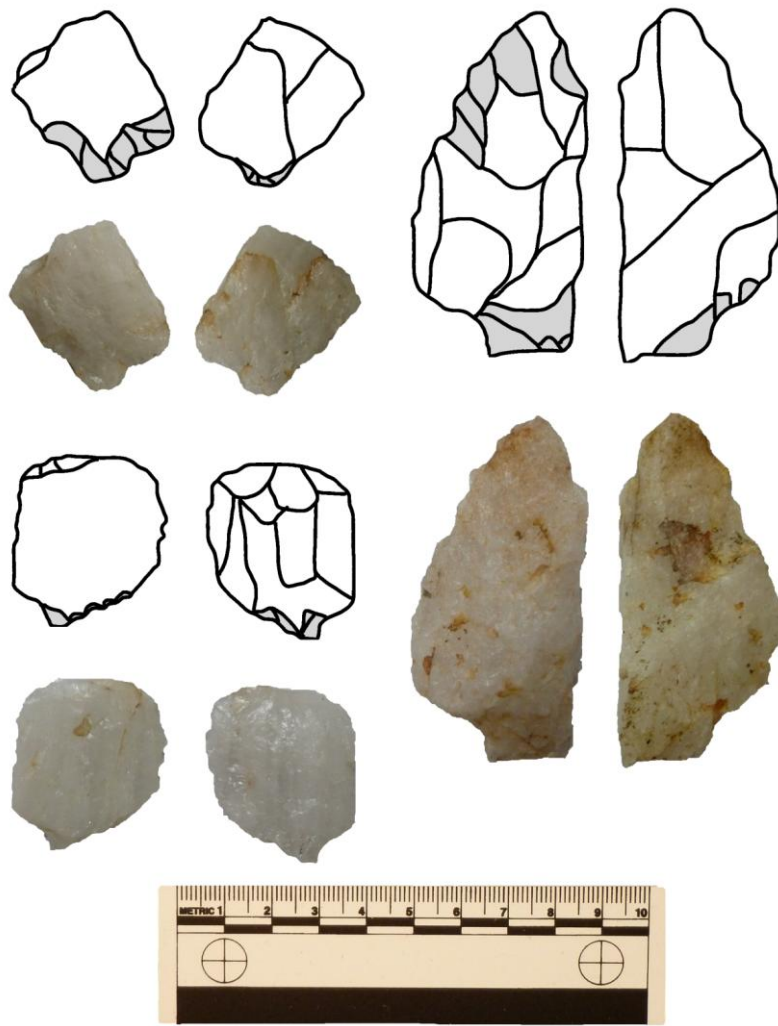


Figure 6.22: Delineated artefacts from SAM1. Top-left and Bottom-left: Nosed pieces; Right: Shouldered point.

The evidence from the Jaisalmer Raans illustrates a different pattern, with more fine grained raw materials than gneiss available in larger package sizes than quartz. The relative dearth of retouched tools accompanied by the occurrence of numerous, highly cortical artefacts and focus upon unidirectional reduction schemes, epitomised by the KHA3 assemblage, may indicate that these sites present evidence for early stages of reduction sequences, which is supported by the relatively easy to access raw materials available at most of these sites. KHA1 marks a significantly different trend, utilising more fine grained raw materials and occupying a

lake edge setting away from raw material resources. These artefacts appear to be more heavily reduced and may represent a secondary phase of lithic reduction, following preliminary work closer to a raw material source.

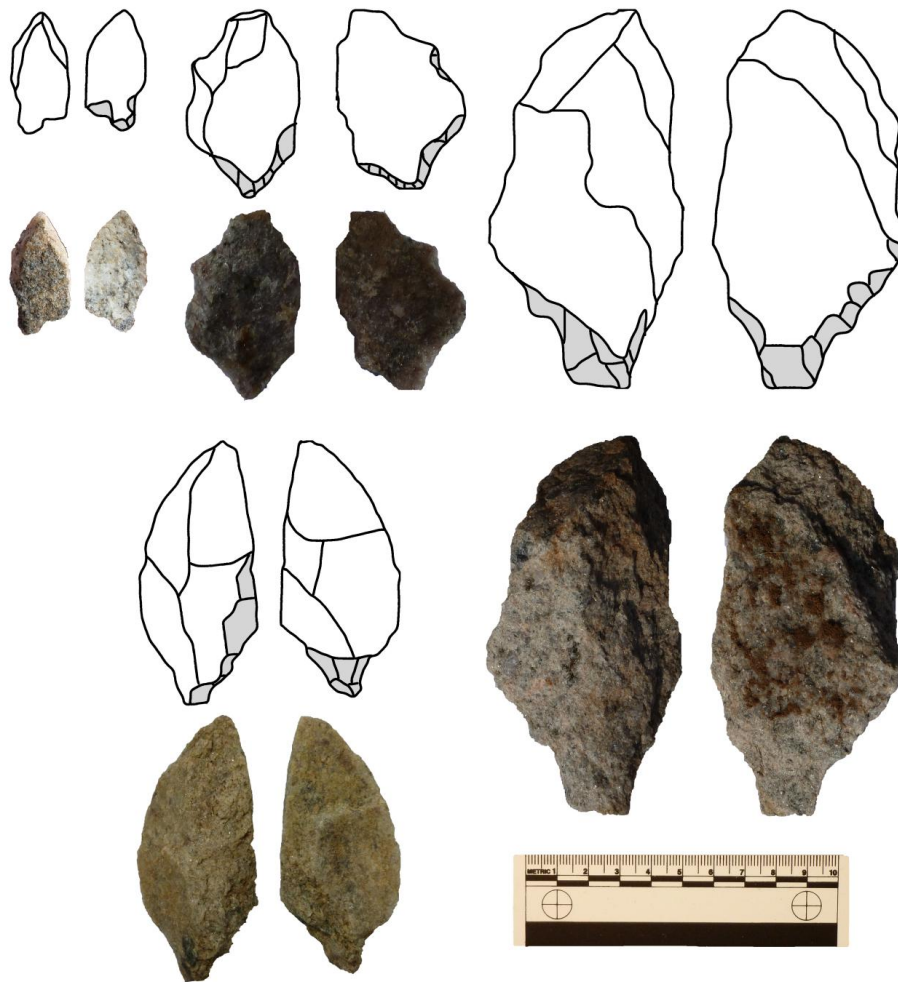


Figure 6.23: Delineated gneiss artefacts from Sambhar Lake. Top-left: Tanged point; Top-middle: Tongued piece from SMB3; Right: Tanged point ; Bottom-left: Tanged point from SAM1.

Although the different raw material resources have a profound effect upon lithic artefact variability, both Sambhar Lake and the Jaisalmer Raans present evidence for early stages of reduction following the exploitation of locally available resources. The co-occurrence of both geological and ecological resources in both areas is likely to have been a significant draw for

Palaeolithic populations. However, due to their location, the seasonal exploitation of these resources and their integration into mobility strategies may have differed significantly. The assemblages from Jaisalmer can tentatively be ascribed to the Middle Palaeolithic. At Sambhar, exploitation of boulder cores for production of heavy tools could feasibly stretch to the Lower Palaeolithic. However, lacking this or a clear blade/microlithic focus to reduction strategies, a range of both gneiss and quartz artefacts appear to fit best with descriptions of Middle Palaeolithic industries.

Survey of Pushkar Valley

The research undertaken by Allchin et al. (1978) in the Pushkar Valley documented the transition of Palaeolithic industries between the Middle and Upper Palaeolithic and Mesolithic (Late Palaeolithic). These researchers also situated the artefactual assemblages within an environmental framework that offered a relative chronology for the industries (Figure 6.24). To this day, few sites in South Asia appear to document these transitions and as a result the sites at Pushkar have remained significant for explaining the development of lithic technology in the Upper Pleistocene. As the transition between Middle and Late Palaeolithic industries has become a focal point in the debate surrounding the dispersal of modern humans into South Asia, developing a more detailed understanding of the similarities and differences amongst lithic assemblages in the Pushkar Valley offer a key means to investigate this issue. Exploration was concentrated at Budha Pushkar and Hokra (Figure 6.25), although survey of the valley margins also identified artefacts stratified in colluvial deposits and quartzite boulder cores.

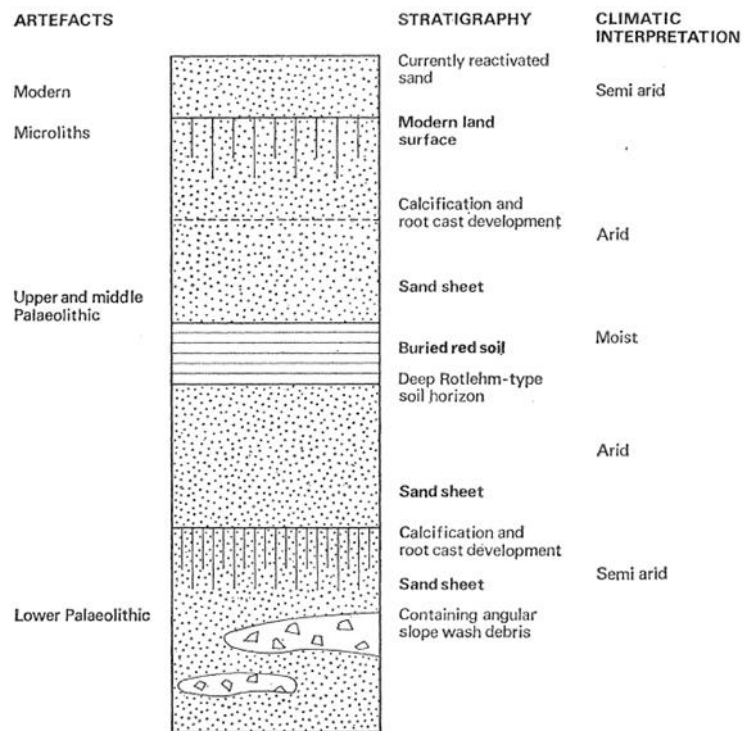


Figure 6.24: Composite stratigraphy from Pushkar (Allchin & Goudie 1974; Figure 22).

Budha Pushkar

A number of sites originally identified by Allchin and Goudie (1974; Allchin et al. 1978) were revisited, and many of the exposures of 'red soil' associated with archaeological finds remain present and easy to locate. Within the vicinity of Budha Pushkar G, on the top of a large stabilised dune overlooking the lake, two discrete lithic scatters were identified (Figure 6.26) and a sample of 20 artefacts recorded from each (BPG1 & BPG2). Further archaeological assemblages were identified at Budha Pushkar H, where friable aeolian sands have been stripped away revealing the compacted 'red soil'. An assemblage of 25 artefacts (BPH1) was recovered from the red soil where the overlying aeolian sands are eroding away, and do not appear to have been disturbed, as reported by Allchin et al. (1978). A second assemblage of 25 artefacts (BPH2) from the exposed red soil surface appears more obviously disturbed. The red

soils also appear to dominate the eastern edge of the Budha Pushkar basin, where a shallow but broad stream channel drains the steep valley slopes. Two isolated artefacts were identified in situ within the red soil horizon, presenting evidence for human occupation at the valley slopes, as well as close to the lake.



Figure 6.25: Map of Pushkar Valley sites.

Hokra

Significant expansion of agricultural activities within the Pushkar Valley appears to have engulfed the sites reported at Hokra by Allchin et al. (1978). Nevertheless, the recent construction of a train line through the Pushkar Valley has significantly disturbed the friable, yellowish dune sands. This appears to have led to the exposure of the red soil horizon, with numerous artefacts littering the surface that do not appear to have been significantly disturbed (Figure 6.27). Three assemblages of 25 artefacts each (HOKA, B & C) and one of 15 artefacts (HOKD) have been recorded from this context. Exploration within the vicinity of the



Figure 6.26: Lithic scatter from which the BPG1 assemblage was sampled.



Figure 6.27: Recently exposed red soil horizon at Hokra.

sites originally reported at Hokra led to the identification of an area of land that had not been disturbed by agricultural activity. This yielded another surface assemblage (HOKE) from the top of the red soil horizon. Finally, a rich scatter of lithics was identified at a roadside location near Hokra on top of the red soil that did not appear to have been significantly disturbed from its original location, and a sample of 104 artefacts were recorded (HOKF).

Analysis of Lithic Assemblages

A typological breakdown of assemblages from the Pushkar Valley is presented in Table 6.7.

Artefact Type	BPG1	BPG2	BPH1	BPH2	HOKA	HOKB	HOKC	HOKD	HOKE	HOKF
Core	0	0	2	0	0	0	0	0	0	7
Broken Core	1	0	0	0	0	0	0	1	0	0
Single Platform	3	7	4	4	5	0	3	3	3	33
Bidirectional	0	0	0	0	0	0	1	0	0	2
Multi Platform	1	3	1	2	11	6	6	4	1	21
Prepared	0	0	0	1	1	0	1	0	0	0
Flake	12	7	9	11	5	13	11	4	13	34
Broken Flake	2	1	3	3	1	2	1	1	0	3
Flake Piece	0	1	0	0	1	0	0	1	1	0
Retouched Flake	0	0	0	0	0	0	0	0	0	1
Retouched Flaked Piece	0	0	1	0	0	0	0	0	0	0
Single End	0	0	2	1	0	0	0	0	2	1
Single Side	0	0	2	1	0	1	2	1	2	0
Single End Single Side	1	1	1	1	0	0	0	0	1	1
Single End Double Side	0	0	0	0	1	2	0	0	2	1
Double Side	0	0	2	0	0	0	0	0	0	0
Double End Double Side	0	0	1	1	0	1	0	0	0	0
Total	20	20	28	25	25	25	25	15	25	104

Table 6.7: Typological breakdown of artefact assemblages from Pushkar Valley.

The majority of assemblages present similar sample sizes, although HOKF is substantially larger. In particular, HOKF includes a very large proportion of cores, and as a result these will be described separately. However, the flakes and retouched artefacts from HOKF will be described with the other assemblages. Overall, raw material use is evenly split between quartz and quartzite with minimal contribution from chert artefacts (see Table 6.8). Some gross differences in artefact size can be identified by raw material type. The low number of chert artefacts from BHP2 are particularly small, and overlap with the lower range of size variability of the other two raw material types. Substantial overlap occurs between quartz and quartzite artefacts, although across the different size variables roughly a quarter of quartzite artefacts are beyond the normal range of quartz artefacts.

	N	Quartz	Quartzite	Chert
BPG1	20	0	19	0
BPG2	20	0	20	0
BPH1	28	25	3	0
BPH2	25	10	9	6
HOKA	25	0	25	0
HOKB	25	3	22	0
HOKC	25	0	25	0
HOKD	15	0	15	0
HOKE	25	0	25	0
HOKF	104	104	0	0

Table 6.8: Raw material use in Pushkar Valley sites.

Some variation in presence of cortex occurs between the sites (Table 6.9). Cortical artefacts are most commonplace at BPG1, BPG2, with slightly lower frequencies occurring at BPH1, BPH2 and HOKE. There is a minimal presence of cortical artefacts at HOKA, HOKB, HOKC, HOKD and HOKF. Overall, the occurrence of coverage of cortex at these sites is low, suggesting preliminary reduction occurred elsewhere, although given the ready availability of raw materials in the Pushkar Valley, this may not have occurred at a great distance to these sites.

Site	10%	20%	30%	40%	50%	60%	70%	80%	90%	100%
BPG1	2	1	1		3	1	2			2
BPG2	1	2	1	3				1		1
BPH1	1		1	1			1		1	2
BPH2				2	1	1	1	1		
HOKA	1	1	2							
HOKB				1						1
HOKC								1		
HOKD	1			2		1				
HOKE	2				1	2	1		2	2
HOKF										

Table 6.9: Number of artefacts with different levels of cortical coverage at Pushkar Valley sites.

Cores

Typological Description

The majority of cores from the Pushkar Valley are informal Single and Multiple platform types. Two microlith cores are present, one in BPH1 and the other at BPH2. A single blade core is present at BPG2, whereas a small preferential Levallois cores is present at HOKC. Amongst the HOKF sample, 11 blade cores are present, all of which show multiple blade removals that have produced a number of longitudinal arises (Figure 6.28). Two of these exhibit bidirectional removals, whereas the remaining blade cores are unidirectional.

Technological Description

The average dimensions of cores from Buddha Pushkar and Hokra (A-E) are 70.1x48.6x29.2mm, with average last scar dimensions of 39.3x33.9mm. The size range evident is large, with core length varying between 24.7-145.6mm, although half of all cores fall between 53.2-84.9mm. Last scar elongation range between 0.56-3.54, but most scars not reach blade proportions, with 50% of scars between 1.13-1.52. Multi Platform (46.7%) and Single Platform (42.7%) comprise the majority of core flaking patterns, with 3 prepared cores and a single bidirectional cores present. Three quarters of flake scars exhibit feather

terminations, although a substantial proportion (20%) present axial terminations. Platform types are typically simple, dominated by cortical (33.3%), single conchoidal (24%) and plain (21.3%) types. Low numbers of dihedral (n=5), faceted (n=4), multiple conchoidal (n=3) and crushed (n=3) are present.

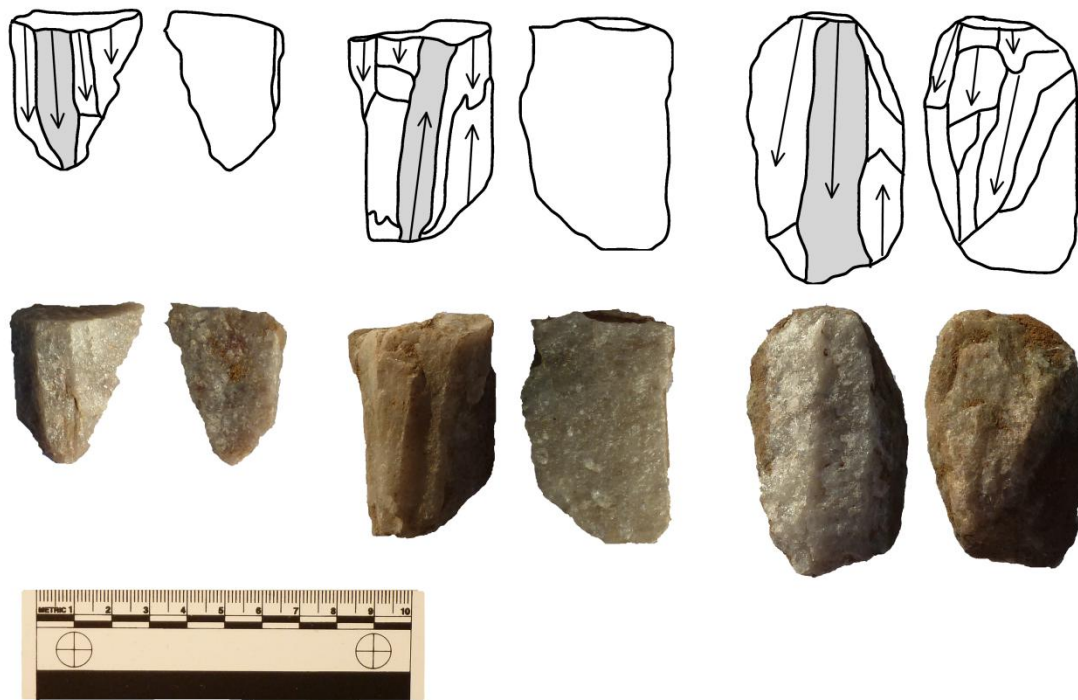


Figure 6.28: Blades cores from HOKF.

The single bidirectional core and four unspecified core types are smaller across all size dimensions, although do not exceed the lower range of other core types. The remaining 70 cores do not differ substantially across either the size variables or last scar elongation. Similarly, no clear differences occur in the proportions of platform types of last scar terminations between the core types.

Cores from three sites, BPG2, BPH2 and HOKB, are typically smaller (mean length=54-56mm) than the other sites (group mean=70.9mm), and similar patterns exist across other size variables. Blade proportioned scars occur in BPG1, BPG2, BPH1, HOKA and HOKB, although these are not typical (group mean=1.26). Single Platform cores are most common at the

Buddha Puskar sites, whereas multi-Platform cores are more prominent at Hokra, although there is little variability between platform or termination types.

Cores from HOKF are typically smaller than other sites, with average dimensions of 52.6x38.2x22.7mm. Half of these cores measure 45.9-60.1mm length and 32.5-43.3mm width. Last scars typically measure 37.1mm in length, although the range in length is wide, from 11.9-64.3mm. Average last scar elongation is 1.91, with 25% of last scars exhibiting elongation indices >2.4, whereas 25% are below 1. Over half of these cores (52.6%) are single platform cores, with a third of cores presenting multi-platform reduction patterns, and two bidirectional cores are present; the remaining 7 cores do not have a recorded scar pattern. Plain (23.8%), single conchoidal (23.8%) and cortical (22.2%) types comprise the majority of platforms. Multiple conchoidal cores make up 11.1% of cores, with other types occurring infrequently. Although no size differences occur between core types, blade proportioned last scars occur across all core types, but are more common with single platform (mean=2.19) types than multi platform (mean=1.53). Single platform cores types have a greater proportion of single conchoidal platforms, whereas multiple platform cores have larger proportion of multiple conchoidal platforms.

Flakes

Typological description

Few typologically distinct flake types are present. Two microblades have been recorded, one from BPG2 and the other from BPH2. Beyond this, no intentionally prepared flake types are evident.

Technological Description

The average flake dimensions from the Pushkar Valley are 52.4x35.3x14.8mm, with half of flakes within a 10mm bracket of this size, although some flakes range up to 136mm length and 102mm width. The average axial dimensions are smaller, at 38.6x39.5mm and half of flakes occur with a 10mm bracket of this. The average axial elongation is 1.09, and although some blade proportioned flakes are present, the majority of flakes are not. Proximal dorsal scar patterns are most common (42.7%), followed by side patterns (21.4%) and weakly radial (11.7%). Bidirectional (4.9%), distal (4.9%), opposed/perpendicular (6.8%) and radial (7.8%) occur at low frequency. Single conchoidal (25.9%) and plain (24.1%) platform types are most common, with dihedral (17.2%), multiple conchoidal (12.1%) and cortical (11.2%) platforms regular occurrences. Feather terminations occur on 79.5% of flakes, with 10.7% possessing axial terminations, and rare outrepasse (4.5%), step (4.5%) and hinge (n=1) types.

Flakes with bidirectional and opposed/perpendicular scar patterns are typically 10mm smaller in maximum dimension than average flakes, whereas radial and distal flakes are 10-20mm larger. A similar pattern is evident in the axial dimensions, with bidirectional flakes notable shorter (mean=23.7mm) than average (group mean=39.1mm). Although average axial elongation is low (mean=1.11), blade proportioned flakes occur on proximal and side scar flakes.

Proximal flakes are most frequent in sites at Buddha Pushkar, whereas side scar, weakly radial and radial flakes are relatively more common at Hokra. No clear differences in the proportion of either platform type or termination types occur with regards to the different sites. Typical size ranges at most sites are 30-80mm, although a number of substantial larger (>100mm) flakes are present at BPH1, BPH2 and HOKA. Flakes from HOKA repeatedly show mean

dimensions of >10mm above average. Blade proportioned flakes are present at BPG1, BPG2, HOKB and HOKF, although average elongation is low (mean=1.09).

Retouched Flakes

Typological Description

Retouched tools are found at all sites, and various types are present. Two burins have been recorded, one at BPH1 and the other at HOKC. Two simple notches occur at BPH1, and a further example is present at HOKE. Three unifacially retouched points have been recorded at HOKE, two of which exhibit medially breaks. A number of artefacts have undergone varying degrees of delineation, with a nosed piece in both HOKB and HOKF, while single shouldered pieces occur in BPG2, BPH1, HOKB and HOKE. More extensive delineation has produced tongues on artefacts at BPG1, BPH2 and HOKB, whereas tanged pieces occur at BPH2, HOKA and HOKF. Delineation typically includes retouching an end and a side, and frequently both sides are retouched. This frequently occurs at one end of the piece orientated by maximum axis, with convergent margins present at the opposite end.

Technological Description

Average measurements of retouched artefacts in the Pushkar Valley are 56.5x32.9x13mm, although average axial dimensions are smaller at 38.2x40.9mm. While the largest retouched artefact has a length of 95.9mm, half of all artefacts range in length between 44.3-66.5mm. Axial elongation of 17 artefacts indicated relatively squared flakes have been retouched (mean=1.13), with no blade proportion flakes selected. However, in many cases axial elongation may not be a good indicator of shape, as the retouched artefacts are typically more elongate around the axis of maximum length. Average retouched dimensions are 36.2x16.3mm. Maximum retouch width extends to 86mm, although half of all artefacts exhibit

retouch widths between 20-47mm. Limited variation between retouched artefacts occurs between sites, which appears to relate primarily to a small number of larger pieces at HOKA and HOKD.

Summary

Sufficient overlap in size ranges between quartz and quartzite artefacts in the Pushkar Valley occurs that raw material quality may not explain the variability observed, although different package sizes may have influenced the differences in size of artefacts. A clear focus upon unidirectional reduction strategies is broadly evident across the majority of sites, apparent in both flake and core populations. Blade production appears to be a recurrent reduction strategy, most evident amongst the core population from HOKF. Blades are notably lacking from the flake populations, suggesting they have been selectively removed from the site. The retouched flakes do not appear to have been produced upon blade blanks, and may represent a different reduction strategy. Although some size differences between single and multi-platform cores are evident, a number of single platform blade cores appear exhausted. As a result, differences in reduction strategy rather than reduction intensity may explain some of the observed variability. The assemblages from Buddha Pushkar appear to contain a mix of both Middle and Late Palaeolithic artefacts. The assemblages from HOKA-E fit well with definitions of Middle Palaeolithic industries, whereas the clear systematic production of blade blanks suggests HOKF may be defined as a Late Palaeolithic industry. However, these blades are frequently too large to be described as microblades.

Discussion

The results of the first Palaeolithic survey in the Rajasthan Thar Desert in a decade illustrate the wealth of Palaeolithic assemblages in the region, and the potential for further surface surveys to expand our understanding of the Palaeolithic occupation of the desert. Many of the sites reported here have not previously been identified with archaeological assemblages, whereas in some cases, and most clearly at Sambhar Lake, renewed survey has shown a more substantial and diverse body of evidence for Palaeolithic occupation than previously known. In spite of problems with sample size and sampling strategy, it is possible to make a number of preliminary observations regarding variability in lithic technology.

A wide range of raw material types has been exploited in the Thar Desert, which have had some impact upon artefact variability. Artefacts produced on coarse raw material types are repeatedly larger than finer materials between similar artefact types. However, the presence of distinct artefact types, such as tanged, tongued or shouldered points, occurring on a wide range of raw materials suggests some flexibility in the application of reduction strategies in the sampled assemblages.

Reduction intensity plays a clear role in structuring artefact variability at a number of sites. Cores analysed from sites in the Jaisalmer Raans and Chamu are typically large and have undergone fairly minimal reduction. Similarly, a number of large gneiss artefacts from Sambhar appear to have resulted from primary raw material extraction activities, widely evident from the large flake scars observed on boulder cores. In contrast, cores from the Pushkar Valley frequently appear exhausted, even when recorded presenting a single, simply prepared platform. In the case of Shergarh Tri-Junction, heavily reduced core types are present, despite the immediate access to raw material resources. While reduction intensity differs significantly

between sites, the application of particular reduction strategies also impacts artefact variability.

Two distinct core reduction strategies are evident amongst these sites. Levallois reduction schemes are best represented at Shergarh Tri-Junction, occurring in association with sedimentary contexts dated to <60ka. The presence of a single Nubian Type 2 point core at the nearby site of SHR1 is a particularly evocative of the application of prepared core techniques to produce formally shaped blanks. The prepared points from KHA2 may offer examples of such blanks. The second reduction strategy includes systematic blade production, most evident at HOKF. The range of sizes of blades produced is large, extending beyond regional definitions for microblade technologies (e.g. Clarkson et al. 2012). The appearance of a single bidirectional blade core at TRI1 similar to those at HOKF is notable, and in this context it is likely to have been produced <60ka. This co-occurrence of Levallois and systematic blade cores may indicate some overlap between core reduction strategies typically separated between Middle and Late Palaeolithic industries.

Occasional evidence for these two core reduction types are evident amongst the flake populations, with pointed flakes with tapered distal margins a more common occurrence than blades. However, a more coherent trend is the repeated appearance of retouched artefacts with a delineated margin, ranging from nosed and shouldered to tongued and tanged pieces. This retouching typically occurs at one end of the maximum axis of the artefact, with convergent margins at the opposite end, producing a pointed extremity. In a number of instances medial breaks are apparent along the axis perpendicular to the delineated portion. These occur in association with sediment contexts dated contexts from MIS5 at Chamu and Karna, although they may also be younger than this, yet they are absent from dated contexts at Shergarh Tri-Junction.

The trends identified through surface survey should be treated cautiously, although they help to build a clearer chronometric and environmental framework with which to understand the Palaeolithic occupation of the Thar Desert. Palaeolithic sites were repeatedly identified in sediment contexts formed through humid conditions, and particularly those dating to MIS5 and early MIS3. The sites reported here corroborate widely reported evidence for points as a prominent feature of Middle Palaeolithic sites in the region. Significantly this study has identified the widespread presence of retouched points, and in particular those with delineated margins, including tanged and shouldered types. Systematic blade production marks a notable departure from the mostly Middle Palaeolithic assemblages recorded, and may offer the clearest insight into the development of Late Palaeolithic technologies in the Thar Desert.

Chapter 7

Excavations at Katoati

Excavation undertaken at the site of Katoati (Fig 7.1) have been undertaken to permit the integration of typo-technological analyses of Palaeolithic assemblages within a chronological and environmental framework. The results of this excavation, reported in this chapter, and the resultant lithic analyses (Chapter 8) present a fresh means to evaluate the relationship between both existing and new archaeological evidence from the Thar Desert with palaeoenvironmental proxies. This will permit a more comprehensive characterisation of the Palaeolithic occupation of the Thar Desert, and ultimately new insight into southern Asian hominin demography.

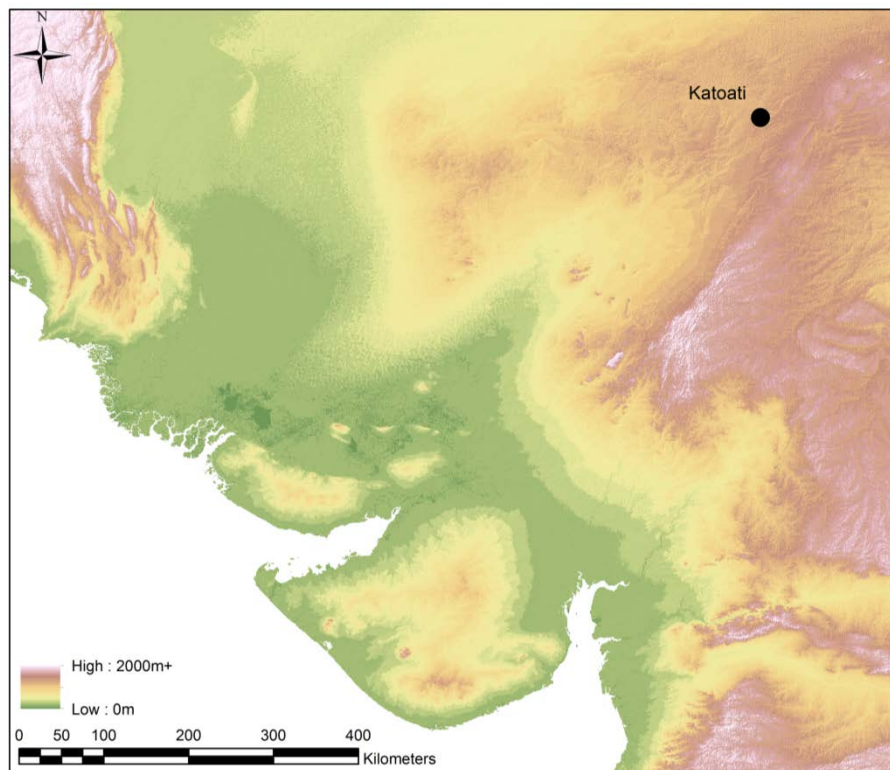


Figure 7.1: Location map of Katoati.

The objective of this chapter is to develop the landscape, environmental and depositional context for lithic assemblages recovered from excavations at Katoati. Following a brief review of existing studies from the area, the results of a preliminary survey season, undertaken in 2006 by Prof. Hema Achyuthan (Anna University, Chennai), Prof. M. Petraglia (University of Oxford), Dr. P. Ditchfield (University of Oxford) and Prof. R. Roberts (University of Wollongong), and an excavation, undertaken in 2011 by the author with Prof. H. Achyuthan, will be presented. Firstly, the geology and sedimentology at Katoati will be discussed, followed by more detailed consideration of three chronometrically dated sedimentary sections. The excavation and sedimentary sequence will then be examined and integrated with the results of palaeoenvironmental and geochronological studies, to present a scheme of natural formation processes relevant for the analysis of the lithic assemblages.

Previous Research

A number of field studies undertaken in the late 1970's and early 1980's (Agrawal et al. 1980; Misra et al. 1980; 1982) focused upon the Jayal gravel ridge (see Fig. 7.2) resulting in the inclusion of the Jayal Formation as the oldest member of a tripartite scheme of stratigraphic development for this region of Nagaur District (see Figure 7.3). The Jayal Formation is reported as an extensive and thick boulder-cobble gravel, comprised of orthoquartzites, quartzitic sandstone, quartz, gneiss and sandstone, lying unconformably upon Neogene bedrock (Misra 1995). The boulder beds are the product of a powerful fluvial regime thought to rise in the Himalaya, with some potential inputs from the Arravallis (Misra 1995). The gravel beds most prominently occur as a fericretised conglomerate ridge resting up to 20m higher than the surrounding landscape, resulting from tectonic uplift, and extend to a depth of 60m below surface (Agrawal et al. 1980; Misra 1995). Gravel deposits below the ridge are separated by a massive crystalline calcareous cement, suggested to have formed through groundwater

enrichment of carbonates, enhanced by the local availability of pre-Cambrian limestones in the area (Agrawal et al. 1980). This cemented formation is resistant to erosion, and occurs at a slightly raised level in comparison to the present fluvio-aeolian plain. Overlying deposits include calcretized gravels, low energy fluvial sediments and aeolian dune deposits, and the presence of carbonates throughout indicates continued exposure to moisture deficient environments (Agrawal et al. 1980).

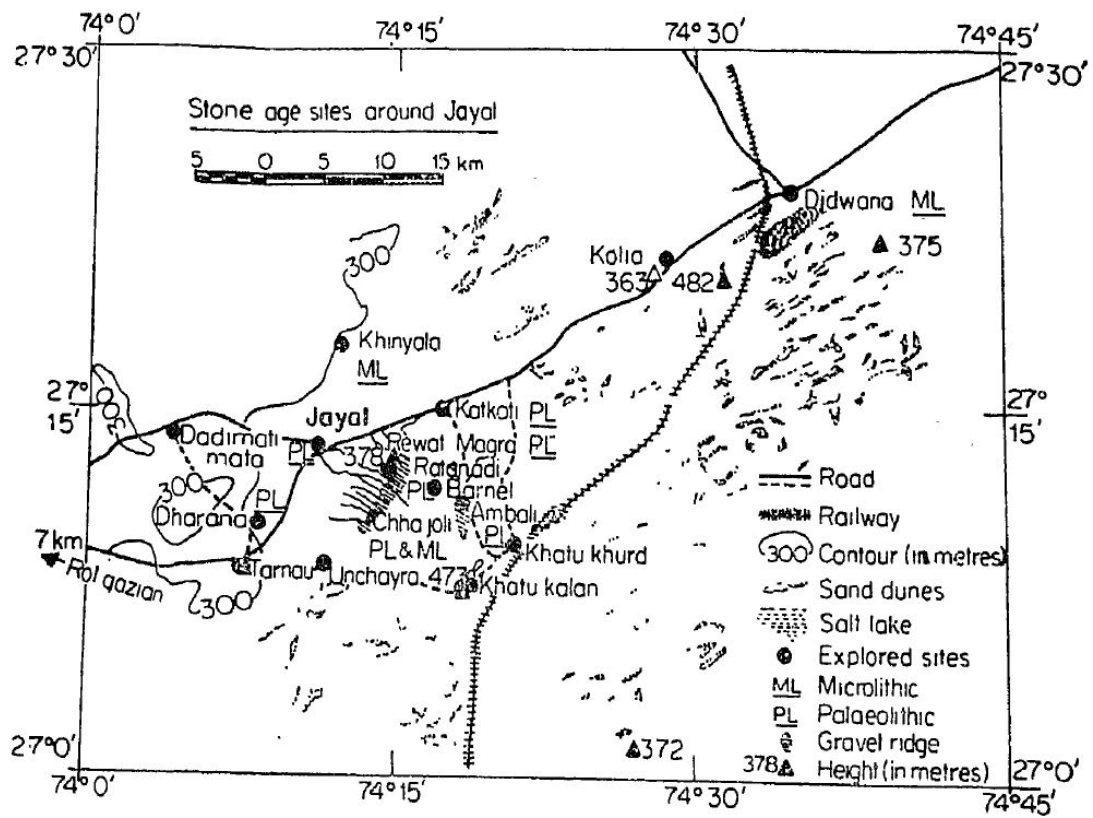


Figure 7.2: Location of Palaeolithic sites in Jayal area (Agrawal et al. 1980; Figure 3).

Lower, Middle and Late Palaeolithic artefacts have been reported in the area from surface surveys indicating repeated occupation of the area, with excavations at Jayal and Chhajoli indicating Lower Palaeolithic exploitation of the gravel beds (see Chapter 5)(Misra et al. 1980; Misra 1995). Excavations at Jayal indicate that only the uppermost boulder horizons have been

exploited by Lower Palaeolithic populations, and there is no basis to suggest a hominin occupation contemporary with the deposition of the boulder horizons (Misra et al. 1980).

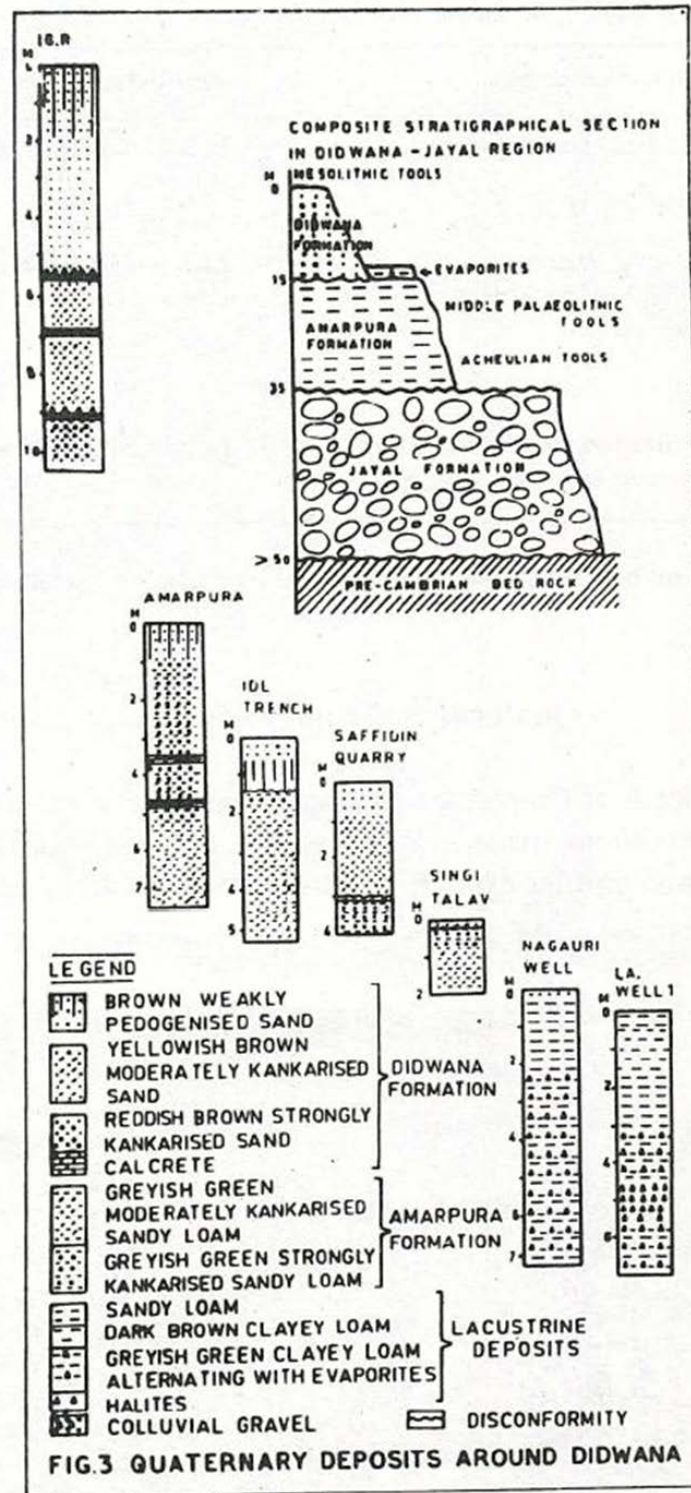


Figure 7.3: Scheme of quaternary deposition around Didwana (Misra 1995; Figure 3)

Preliminary Research at Katoati

Renewed fieldwork at Katoati in 2006 and 2011 has led to further insights into the evolution of this landscape and the evidence for Palaeolithic occupations that it preserves (locations discussed in text shown in Figure 7.4 & 7.5). A number of observations made by the author during the 2011 field season are useful to expand and refine the model of landscape development offered by Agrawal et al. (1980) and will be presented first. Following this, two sites visited at Katoati in 2006, reported as Jayal Formation Locality (JFL) 1 and 2, will be discussed, for which sedimentological logs have been produced (by Dr. P. Ditchfield), a number of OSL samples have been recovered and processed (by Prof. R. Roberts), a range of archaeological artefacts were recorded (by Prof. M. Petraglia) and a single piece of ostrich eggshell was recovered from a stratified context (by Dr. P. Ditchfield). Finally, the recovery of rich accumulations of ostrich eggshell from shallow stratified contexts by Prof. H. Achyuthan and the author will be reported.

The impact of tectonic uplift in the region is clearly evident in the appearance of the oldest sedimentary units occurring at the greatest elevation. This is exemplified by the quarry section at Ambali, a local topographic high point, where the thickest exposure of ferecretised boulder conglomerates can be observed (Figure 7.6 & 7.7). The erosion and transport of the uppermost gravel deposits appears to present the source material for younger gravel deposits observed elsewhere in the Katoati landscape, including the upper calcretised gravels overlying the cemented calcrete horizon reported by Agrawal et al. (1980). The recent erosion of highly ferrous sediments may also account for the rich reddish brown colour of aeolian sediments across the landscape.

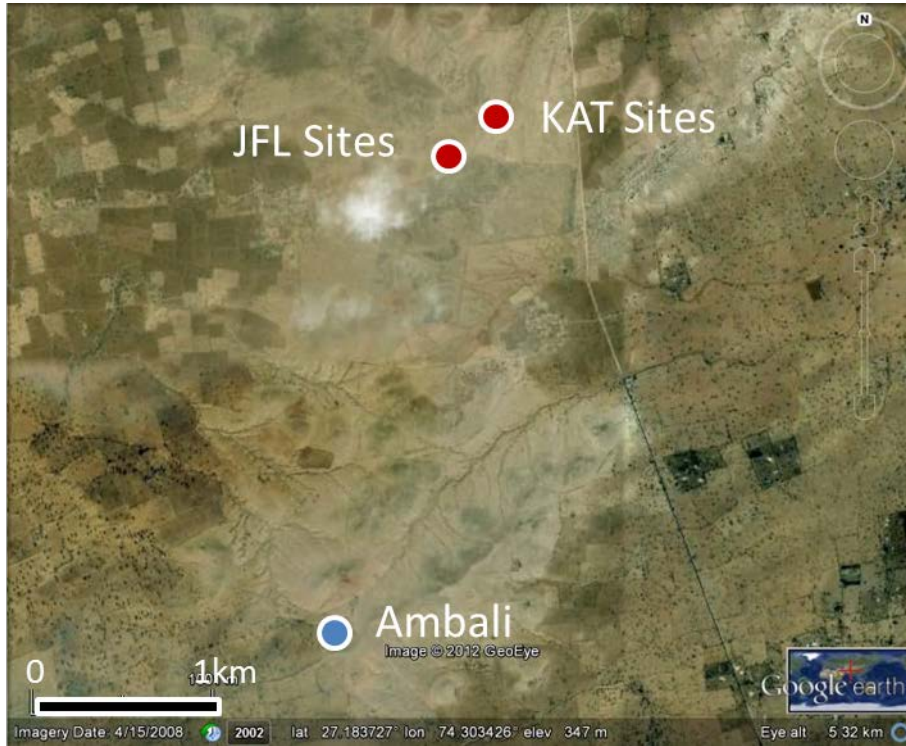


Figure 7.4: Site locations in Katoati landscape.

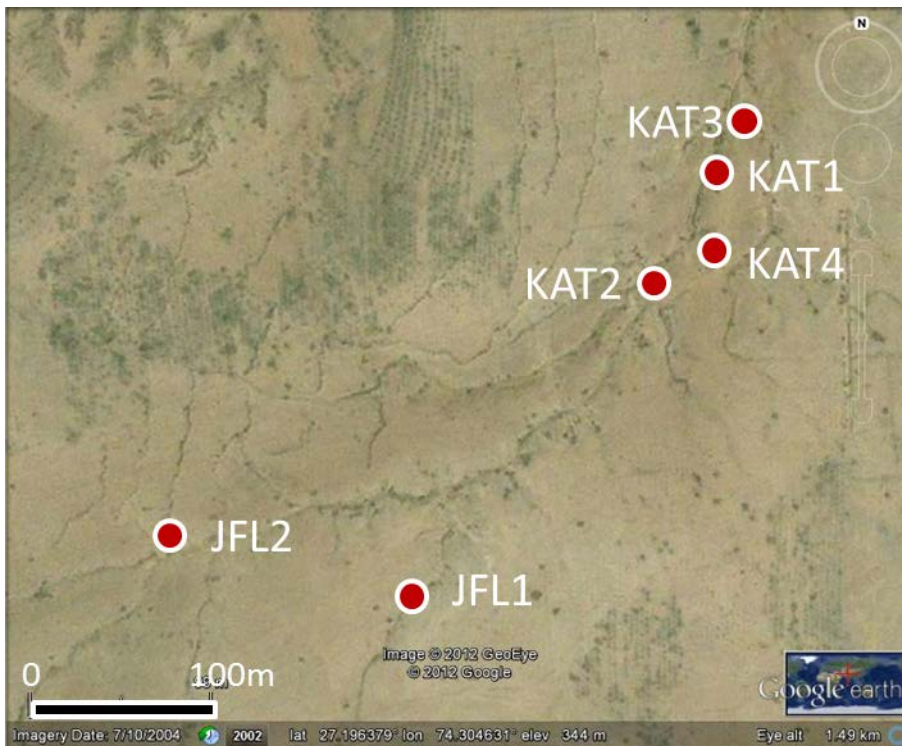


Figure 7.5: Detailed locations of JFL and KAT sites.



Figure 7.6: Ferricretised boulder conglomerate overlying sandstone basement at Ambali.



Figure 7.7: View over Katoati landscape from Ambali.



Figure 7.8: Uppermost horizon of calcretised horizon overlain by thin aeolian deposit.



Figure 7.9: Quarrying of calcrete horizon, with fluvio-aeolian deposits in background.

The presence of the cemented calcrete horizon is spatially heterogeneous, increasing in thickness and degree of carbonate development with decreasing elevation toward a palaeochannel (Figure 7.8 & 7.9). Given their location it is proposed that alluvial deposits, such as overbank or floodplain facies, are the substrate that have undergone significant calcretisation as a result of groundwater fluctuations over a considerable period of time. With increasing levels of cementation, it is likely that the calcrete horizon has had a changing role upon local drainage and channel morphology as fluvial margin deposits became more resistant to erosion. In some areas, thin aeolian deposits are preserved overlying the calcrete deposit, whereas elsewhere gravel deposits can be observed. Where gravels are present a number of fresh and abraded lithic artefacts can easily be located and the widespread presence of loose and discrete calcrete nodules, which are distinct from the cemented calcrete horizon, indicative of a deflated landscape.

Jayal Formation Locality 1

The sediments observed at JFL1 present a 3.5m sequence of alternating fluvial conglomerates and sands capped by an aeolian deposit (Figure 7.10). Preliminary results of OSL dating at the site, reported by Prof. R. Roberts, are presented in Table 7.1. The size of clasts in the conglomerate horizons is greatest at the base of the observed sequence and decreases towards the surface. This suggests a higher level of fluvial energy was responsible for deposition of the lowest facies, with an overall decrease in the capacity for coarse sediment mobilisation observed through time. Alternations between gravels and sands may indicate more immediate changes in fluvial discharge or channel morphology. The presence of carbonate nodules within the sand horizons indicates periods of fluctuating humidity following sedimentary deposition. Finally, the sequence is capped by an early Holocene aeolian deposit. Flake tools are reported from the lowermost fluvial sand horizon, indicating a hominin

presence in the area in MIS 6-5. A small sample (n=16) of single platform, multiplatform, radial and Levallois cores has been collected and analysed from the three conglomerate horizons stratified between JFL1-1 and JFL1-4 OSL samples, suggesting further occupation during MIS 5-3.

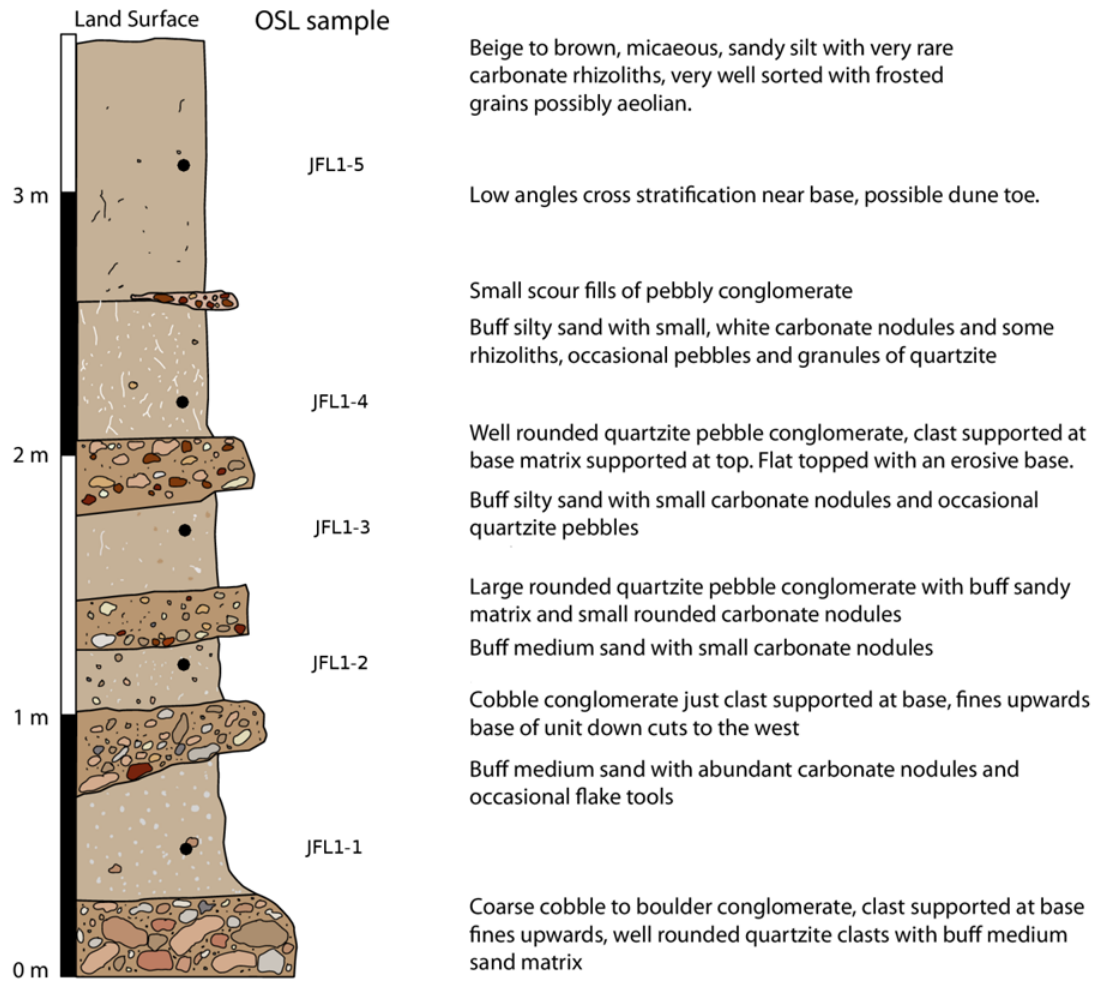


Figure 7.10: Schematic section drawing of sediment section at JFL1, showing location of OSL samples (modified from illustration by Dr. P. Ditchfield).

Sample	Final Age (ka)	Minimum Age (ka)	Median Age (ka)
JFL1-5	8	-	-
JFL1-4	-	15	36
JFL1-3	-	37	57
JFL1-2	-	38	87
JFL1-1	-	67	134

Table 7.1: Preliminary OSL dates from JFL1 (pers. Comm. Prof. R. Roberts, 12/2011).

Jayal Formation Locality 2

The 4m sequence observed at JFL2 presents a simpler sequence of sediment deposits revealed down to bed rock (Figure 7.11), however the preliminary results of OSL dating at this site are more problematic (Table 7.2). While the uppermost sample (JFL2-3) offers a reliable minimum and median age estimate, the results from the lower two samples (JFL2-2 & JFL2-1) present dispersed results. AMS radiocarbon dating of a piece of ostrich eggshell sampled from a similar level to JFL2-2 offers an independent means to assess the chronology of sedimentation at the site. Duplicate age estimates from a single sample have been processed by Dr. P. Ditchfield, providing uncalibrated ages of $45,350 \pm 650$ ka (OxA 19407) and $44,000 \pm 600$ ka (OxA 19408), which are in good agreement with one another. As a result, the upper part of the sedimentary sequence shares features with JFL1, with an early Holocene aeolian deposit, overlying alternating horizons of fluvial conglomerates and pedogenised sandy silts deposited in mid-MIS 3 and perhaps earlier too. However, the base of the sequence is notably different, as the basal sandy silt deposit presents evidence for pedogenic alteration, with abundant large pedogenic carbonate nodules directly overlying ferricrete coated boulders and sandstone basement. Although no archaeological collections were made at JFL2, bifacial flaked tools are reported to occur in the lower cobble conglomerate, which appears to date between 101-193ka.

Sample	Minimum Age (ka)	Median Age (ka)	Low Dispersed Age (ka)	High Dispersed Age (ka)
JFL2-3	9	14	-	-
JFL2-2	-	-	7	101
JFL2-1	34	101	-	193

Table 7.2: Preliminary OSL dates from JFL2 (pers. Comm. Dr. R. Roberts, 12/2011).

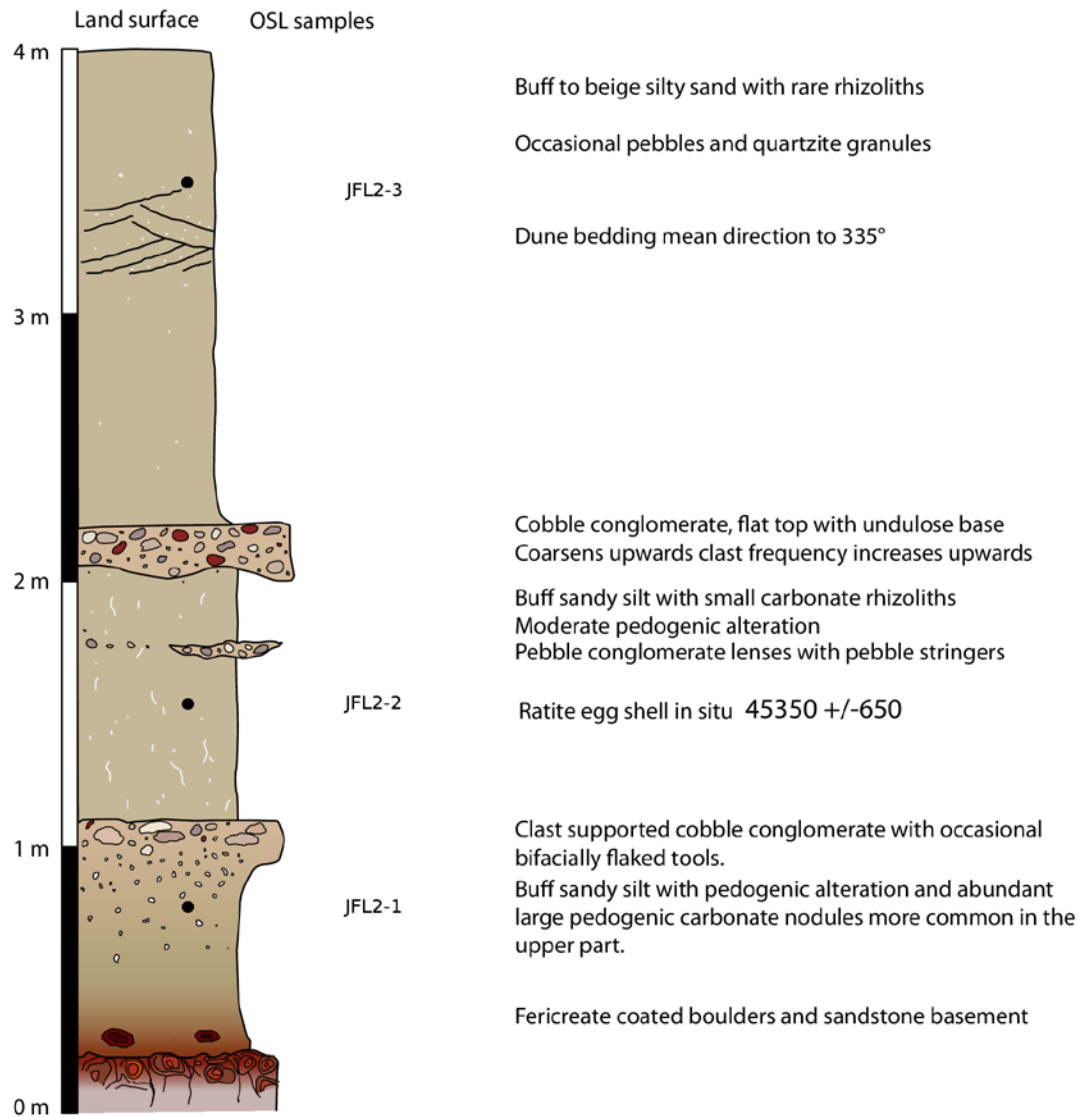


Figure 7.11: Schematic section drawing of sediment section at JFL2, showing location of OSL samples (modified from illustration by Dr. P. Ditchfield).

Katoati Ostrich Eggshell Sites

Prospection of the fluvio-aeolian sediment sequences (Figure 7.12) during the 2011 season led to the identification of a number of sites and near surface sites yielding fragments of ostrich eggshell. Shallow excavation at one site, KAT2, uncovered a rich assemblage of eggshell fragments that preserve distinctive spatial arrangements interpreted as discrete ‘egg’ clusters (Figure 7.13). Large samples of ostrich eggshell fragments from three of these clusters and have been subject to radiocarbon dating (Table 7.3) and stable isotope analyses (discussed with results from KAT1 below). This OES assemblage occurs at the interface of two sediment horizons, although the sediments adhering to the OES fragments were clearly related to the lower deposit. OSL samples were recovered in sediments 5cm above and below the stratigraphic horizon of the ostrich eggshell assemblage, and a small number of chert microliths were observed in the disturbed sediments from the recovery of the upper tube. The OSL samples have been submitted by Prof H. Achyuthan to the Wadia Institute for Himalayan Studies (Dheradun, India), and the results are presented in Table 7.4. Surface finds of OES pieces occurring in a similar stratigraphic context were also recovered at two further sites, KAT3 and KAT4, and samples have also been subject to AMS dating.

Site	Sample	AMS ¹⁴ C Date (BP)
KAT2	OxA-25899	>59,900
KAT2	OxA-25900	35,210±220
KAT2	OxA-25901	49,500±800
KAT3	OxA-25902	52,100±1,100
KAT4	OxA-25903	45,100±500

Table 7.3: Results of AMS radiocarbon dating of OES fragments from KAT2, KAT3 and KAT4; the dates are presented in uncalibrated radiocarbon years (Half-life=5,568 years).

Sample	Minimum Age (ka)	Mean Age (ka)
5cm Above OES assemblage	19±1	21±3
5cm Below OES assemblage	32±4	40±8

Table 7.4: Results of OSL dating of samples bracketing the OES assemblage at KAT2.



Figure 7.12: Prospection of fluvio-aeolian sediments in 2011, with Prof. H. Achyuthan.



Figure 7.13: Exposed clusters of ostrich eggshell at KAT2.

As the radiocarbon results occur at either background or near-background levels, some caution is required in accepting these results. Nevertheless, the radiocarbon dates on OES at KAT2 fit well with the OSL dates for sediments directly below the OES assemblage, corroborating the suggestion the OES derives from the lower strata. Similar age ranges at KAT3 and KAT4 indicate that this stratigraphic division is laterally extensive, and that OES is a relatively common occurrence in this horizon. These results match the AMS ¹⁴C chronology based on ostrich eggshell from JFL2, whereas the lower OSL date is also comparable with sample JFL1-4. This presents support for the mid-Upper Pleistocene age of the upper fluvio-aeolian sequence at Katoati.

Excavations at Katoati

In May 2011, a site in the fluvio-aeolian sediments with a similar stratigraphic sequence to JFL1, designated KAT1 (Figure 7.14), was selected for excavation. A 3m wide step trench was excavated (Figure 7.15) in 32 spits to a total depth of 4.48m (see Table 7.5), respecting context changes where they could be identified. Excavated sediments were dry sieved through 2mm mesh, although only a 50% sample was sieved in levels 16, 17 and 18, perceived to be sterile dune sands. Overall, the sediment sequence can be separated into eight distinct strata, labelled S1-S8 (Table 7.6; Figure 7.16). A total of 42 samples for sedimentological analyses were collected at ~10cm intervals, as well as seven samples for micro-morphological analyses and eleven OSL samples for dating, of which five samples have been processed so far (Table 7.7). A rich assemblage of lithic artefacts were recovered (n=1519) (Table 7.8). Two ceramic pieces were recovered from the uppermost stratum and two ostrich eggshell fragments were also identified and have been AMS dated (Table 7.9). A range of sedimentological analyses have been performed upon samples from the excavated sequence, which offer more detailed insights into depositional and post-depositional processes at the site.



Figure 7.14: KAT1 prior to excavation.



Figure 7.15: KAT1 excavated section.

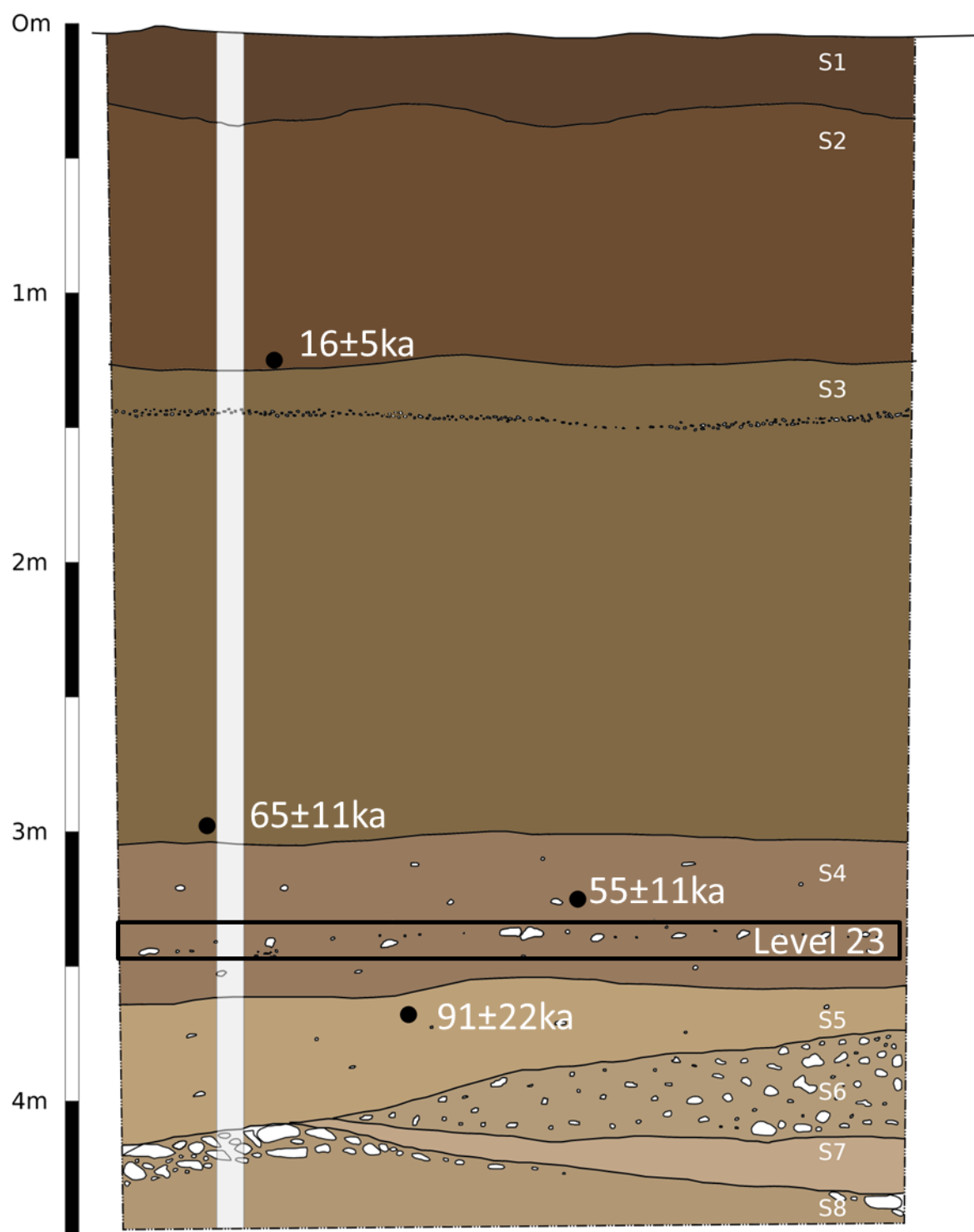


Figure 7.16: Schematic section diagram of excavation at KAT1 identifying individual strata (S1-S8) and showing the location of sedimentological (highlighted) and OSL sampling (black circles), and the excavation horizon yielding dated ostrich eggshell (Level 23).

Excavation Level	Depth (m)
1	0.1
2	0.15
3	0.2
4	0.25
5	0.34
6	0.44
7	0.61
8	0.7
9	0.78
10	0.98
11	1.07
12	1.2
13	1.38
14	1.49
15	1.67
16	2
17	2.4
18	2.68
19	2.83
20	3.04
21	3.22
22	3.33
23	3.43
24	3.61
25	3.73
26	3.88
27	4.04
28	4.14
29	4.24
30	4.36
31	4.44
32	4.48

Table 7.5: Basal depths of excavated horizons.

Stratum	Depth from surface (m)	Description
1	0-0.38	Mid reddish-brown silty sand with some rooting evident and rare powdery calcretes.
2	0.38-1.3	Mid brown silty sand with rare powdery and small, nodular calcretes.
3	1.3-3.04	Mid yellowish-grey sand with occasional small nodular calcretes, with a thin granule to pebble conglomerate horizon occurring in the top of the deposits (depths).
4	3.04-3.64	Mid yellowish/brownish-grey sand with common small calcrete nodules and occasional pebbles and small cobbles.
5	3.64-4.16	Mid yellowish grey sand with common nodular calcretes and rare granule and pebble inclusions.
6	3.74-4.14	Mid yellowish grey sand matrix supporting frequent pebbles and cobbles.
7	4.1-4.35	Mid yellowish grey sand with common nodular calcretes and rare granule and pebble inclusions.
8	4.16-4.48	Mid reddish-orangish brown sand matrix supporting frequent pebble and cobble inclusions with common nodular calcretes with some fusing of nodules evident.

Table 7.6: Description of sediment strata in excavated sequence at KAT1.

Sample	Depth	Least Age (ka)	Mean Age (ka)
KAT1-1	1.25m	9±1	16±5
KAT1-10	2.97m	55±5	65±11
KAT1-3	3.22m	45±7	55±11
KAT1-11	3.67m	66±8	91±22

Table 7.7: OSL age estimates of samples from KAT1.

Assemblage	Level	Artefact Total
S3a	13	5
	14	41
	15	12
S3b	18	2
	19	6
S4	20	49
	21	119
	22	144
	23	88
	24	36
S5	25	62
S6	26	219
	27	316
	28	92
S8	29	34
	30	141
	31	120
	32	32

Table 7.8: Details of excavated lithic assemblages from KAT1, grouped by excavation horizon and assemblage, relating to sedimentary strata.

Excavation Level	Sample	AMS ¹⁴ C Date (BP)
23	OxA-25897	>57,900
23	OxA-25898	>62,000

Table 7.9: Results of AMS radiocarbon dating of OES fragments from KAT1; the dates are presented in uncalibrated radiocarbon years (Half-life=5,568 years).

Sedimentological Studies

Grain size analysis, X-Ray Fluorescence (XRF) analysis, CaCO₃ composition analysis and stable isotope analyses have been applied to sediment samples from the excavated sequence at KAT1. Grain size and XRF analyses were undertaken in the Quaternary Palaeoenvironment and Geochemistry Lab, Anna University, Chennai with assistance from Mr. Nagasundaram Mohan and Dr. Vijay Raj. CaCO₃ composition analysis was undertaken in the Tephrochronology Lab at the Research Laboratory for Archaeology and History of Art (RLAHA), University of Oxford (support and materials provided by Mr. Cassian Bramham-Law and Dr. Christine Lane). Preparation of carbonate samples for stable isotope analysis was undertaken in the Diet Lab at

RLAHA, and submitted to Dr N. Charnley for analysis by Dr. P. Ditchfield. In addition to these sedimentological studies, macro-scale observations of pebbles and cobbles recovered during excavation and quantified measures of lithic artefact size and intensity of both weathering and rounding were conducted. These will offer further insight into depositional processes at KAT1.

Grain size analysis

A ~100g sub-sample of fine sediment (<2mm) from all 42 samples was weighed (with 0.01g resolution) and sieved for 15 minutes in a mechanical shaker with 9 sieves between 0 ϕ and 4 ϕ to differentiate between different sizes of sands and separate out the silt and clay fraction. The sediments retained in each sieve and the basal container was then weighed individually and the results were entered into GRADISTAT v.4 (Blott 2000) to produce summary statistics and descriptions.

The presence of coarse sediments (clasts >2mm) offers an informal index for the presence of fluvial activity within this sequence, and similarly larger sized, more frequent and poorly sorted pebbles and cobbles presents some measure of the increased strength of fluvial activity.

Quantitative measure of clast size was not undertaken, although a subjective appraisal is permitted through a photographic record of clast inclusions.

X-Ray Fluorescence

A ~10-15g sub-sample of sediment from all 42 samples were homogenised in an agate pestle and mortar and placed in plastic sample bags, to ensure the requisite stability of the device during analysis. Analysis was undertaken using Thermo Scientific Niton XL2 X-Ray Fluorescence Analyzer and recorded using Niton Data Transfer v.7.1 software complying with the device's Standard Operating procedure. Each sample was subject to 90 seconds analysis using the 'Main Range' filter following calibration to on-board standards, and downloaded

directly into the Niton Data Transfer program, detailing the percentage composition of each element.

CaCO₃

As the preparation of samples for XRF did not chemically alter the sediments, these samples were subject to further analysis to establish the proportion of CaCO₃ within the sediments. A ~1-1.5g sub sample from all 42 sediments was weighed (with 0.0001g resolution) and placed in a 50ml plastic test tube. Each sample was then reacted with 10ml 10% HCl for 72 hours until fully evolved. The samples were subsequently rinsed with 25ml distilled water and separated from suspension using a centrifuge, spinning at 4,500rpm for 5 minutes, and the process repeated three further times. The consolidated and drained sediment was subsequently dried in an oven at 70°C for 24 hours until completely desiccated and then the remaining sediment was reweighed. The percentage of CaCO₃ is calculated as 227.4 x weight loss/initial sample weight, following Allison & Moodie (1965). In addition, percentage of CaCO₃ will be calculated from XRF data for Ca using a conversion factor of 2.4973.

Stable Isotope Analyses

Stable Isotope analysis was conducted on both pedogenic carbonates and twelve ostrich eggshell samples, including those from KAT2-5. Of the 42 sediment samples, individual pedogenic carbonate samples, comprised of small nodules or rhizoliths, were analysed from samples 4, 5, 9 and 11, whereas two pedogenic carbonate samples were analysed from sediment samples 12 to 42. The nodules selected were analogous to both those observed in deflated contexts overlying the cemented calcrete horizon and within the *nalla* bed in the immediate vicinity of the excavation site. This indicates a rapid cementation of nodules prior to deep burial, supporting the suggestion that the samples are pedogenic, rather than groundwater carbonates.

Each pedogenic carbonate sample was prepared individually by the author, including rinsing in ethanol to remove any adhering sediments prior to crushing in an agate pestle and mortar, drying at 40°C before placing the sample in a test tube. A similar methodology was employed for processing the ostrich eggshell samples. Subsequent methodology is reported by Dr. P. Ditchfield and analysis undertaken by Dr. N. Charnley. Oxygen and carbon stable isotopic results were obtained using a VG Isogas Prism II mass spectrometer with an on-line VG Isocarb common acid bath preparation system. Each sample was reacted with purified phosphoric acid (H₃PO₄) at 90°C with the liberated carbon dioxide cryogenically distilled prior to admission to the mass spectrometer. Both oxygen and carbon isotopic ratios are reported relative to the VPDB international standard. Calibration was against the in-house NOCZ Carrara Marble standard with a reproducibility of better than 0.2%. Stable isotope ratios are expressed using the notation as difference in parts per thousand (permil, ‰) relative to the standard, calculated as $\delta\text{‰} = ([R_{\text{sample}}/R_{\text{standard}}] - 1) \times 1000$, where $R = {}^{13}\text{C}/{}^{12}\text{C}$ or ${}^{18}\text{O}/{}^{16}\text{O}$.

In addition a further seven $\delta^{13}\text{C}$ results have been provided as part of the radiocarbon analyses, which have undergone physical and chemical abrasion, reported and analysed by Prof. T. Higham (Oxford Radiocarbon Accelerator Unit). These samples were sandblasted in aluminium oxide powder, etched in ~0.2M HCl for 2 minutes, rinsed in distilled water and dried prior to acid hydrolysis for producing CO₂ for graphitisation for AMS dating and mass spectrometer analysis (see *Radiocarbon* 46 (1) 17-24, 155-163, and *Archaeometry* 44 (3) S1 1-149 for further details of methodology). The quoted $\delta^{13}\text{C}$ values are measured independently on a stable isotope mass spectrometer to ~0.3‰ relative to the VPDB international standard.

Size Sorting, Weathering and Rounding of Lithic Artefacts

As the only quantified measures of coarse sediment mobility that has been recorded, the size of lithic artefacts and degree of both rounding and weathering are significant indices for understanding both stratigraphic development of the sedimentary sequence and site formation processes. It has only been possible to address the impact of fluvial reworking by evaluating size sorting within the excavated assemblages, as there was insufficient time to record the spatial configuration, dip and orientation of lithic artefacts. Size sorting will be assessed upon maximum dimension and maximum surface area (MaxL x MaxW). Description of rounding is based upon observations of the character of the edges and arrises of lithic artefacts, whereas descriptions of weathering account for the appearance of all artefact surfaces, and are recorded as 'none', 'low', 'medium' and 'high'. While microscopic techniques can offer a robust means to quantify artefact rounding and weathering (e.g. Shackley 1974), it has not been practical to employ such methods due to timing and availability of suitable equipment at Anna University, Chennai.

Results

In the following section, the results of the various sediments analyses undertaken at KAT1 will be reported. A combined discussion of the various results will be presented in the subsequent section.

Grain Size Analysis

The results of the grain size analysis are presented in Figures 7.17-7.18, with descriptive statistics presented in Table 7.10.

Depth (m)	Mean		Sorting		Skewness		Kurtosis	
0.08	3.612	Very Fine Sand	1.554	Poorly Sorted	0.42	Very Fine Skewed	2.14	Very Leptokurtic
0.18	2.995	Fine Sand	1.378	Poorly Sorted	0.079	Symmetrical	2.572	Very Leptokurtic
0.28	2.764	Fine Sand	1.519	Poorly Sorted	-0.028	Symmetrical	2.105	Very Leptokurtic
0.38	2.859	Fine Sand	1.645	Poorly Sorted	0.051	Symmetrical	2.235	Very Leptokurtic
0.48	2.757	Fine Sand	1.445	Poorly Sorted	-0.005	Symmetrical	2.091	Very Leptokurtic
0.58	2.807	Fine Sand	1.457	Poorly Sorted	0.04	Symmetrical	2.276	Very Leptokurtic
0.68	2.744	Fine Sand	1.471	Poorly Sorted	-0.014	Symmetrical	2.309	Very Leptokurtic
0.78	2.943	Fine Sand	1.475	Poorly Sorted	0.043	Symmetrical	2.808	Very Leptokurtic
0.92	2.811	Fine Sand	1.615	Poorly Sorted	-0.043	Symmetrical	2.598	Very Leptokurtic
1.04	3	Very Fine Sand	1.369	Poorly Sorted	0.081	Symmetrical	2.728	Very Leptokurtic
1.15	2.874	Fine Sand	1.393	Poorly Sorted	-0.034	Symmetrical	2.681	Very Leptokurtic
1.26	2.826	Fine Sand	1.639	Poorly Sorted	-0.054	Symmetrical	2.56	Very Leptokurtic
1.38	2.539	Fine Sand	2.056	Very Poorly Sorted	-0.084	Symmetrical	1.388	Leptokurtic
1.5	1.849	Medium Sand	2.093	Very Poorly Sorted	0.12	Fine Skewed	0.85	Platykurtic
1.6	2.525	Fine Sand	2.316	Very Poorly Sorted	-0.004	Symmetrical	1.076	Mesokurtic
1.7	2.347	Fine Sand	2.232	Very Poorly Sorted	-0.021	Symmetrical	1.06	Mesokurtic
1.8	2.324	Fine Sand	2.23	Very Poorly Sorted	-0.016	Symmetrical	0.974	Mesokurtic
1.9	2.479	Fine Sand	2.392	Very Poorly Sorted	0.065	Symmetrical	0.926	Mesokurtic
2	2.643	Fine Sand	2.549	Very Poorly Sorted	0.112	Fine Skewed	0.822	Platykurtic
2.1	2.596	Fine Sand	2.492	Very Poorly Sorted	0.123	Fine Skewed	0.993	Mesokurtic
2.2	2.517	Fine Sand	2.474	Very Poorly Sorted	0.132	Fine Skewed	0.915	Mesokurtic
2.3	2.691	Fine Sand	2.528	Very Poorly Sorted	0.099	Symmetrical	0.901	Mesokurtic
2.4	2.421	Fine Sand	2.332	Very Poorly Sorted	0.07	Symmetrical	0.987	Mesokurtic
2.5	1.748	Medium Sand	1.995	Poorly Sorted	0.201	Fine Skewed	0.811	Platykurtic
2.6	1.982	Medium Sand	2.176	Very Poorly Sorted	0.168	Fine Skewed	0.849	Platykurtic
2.75	1.849	Medium Sand	2.215	Very Poorly Sorted	0.341	Very Fine Skewed	0.864	Platykurtic
2.85	1.875	Medium Sand	2.183	Very Poorly Sorted	0.287	Fine Skewed	0.866	Platykurtic
2.95	1.559	Medium Sand	2.052	Very Poorly Sorted	0.408	Very Fine Skewed	0.857	Platykurtic
3.05	1.496	Medium Sand	1.996	Poorly Sorted	0.414	Very Fine Skewed	0.868	Platykurtic
3.15	1.541	Medium Sand	2.032	Very Poorly Sorted	0.409	Very Fine Skewed	0.859	Platykurtic
3.25	1.518	Medium Sand	2.034	Very Poorly Sorted	0.426	Very Fine Skewed	0.866	Platykurtic
3.4	1.557	Medium Sand	2.03	Very Poorly Sorted	0.399	Very Fine Skewed	0.843	Platykurtic
3.5	2.231	Fine Sand	1.939	Poorly Sorted	-0.298	Coarse Skewed	0.756	Platykurtic
3.6	1.289	Medium Sand	1.931	Poorly Sorted	0.542	Very Fine Skewed	0.902	Mesokurtic
3.7	1.353	Medium Sand	1.962	Poorly Sorted	0.503	Very Fine Skewed	0.911	Mesokurtic
3.8	1.495	Medium Sand	1.986	Poorly Sorted	0.416	Very Fine Skewed	0.868	Platykurtic
3.9	1.432	Medium Sand	1.968	Poorly Sorted	0.44	Very Fine Skewed	0.883	Platykurtic
4	1.33	Medium Sand	1.951	Poorly Sorted	0.518	Very Fine Skewed	0.894	Platykurtic
4.1	0.893	Coarse Sand	1.805	Poorly Sorted	0.85	Very Fine Skewed	1.329	Leptokurtic
4.2	1.388	Medium Sand	1.968	Poorly Sorted	0.474	Very Fine Skewed	0.889	Platykurtic
4.3	1.316	Medium Sand	1.955	Poorly Sorted	0.531	Very Fine Skewed	0.887	Platykurtic
4.4	0.861	Coarse Sand	1.73	Poorly Sorted	0.835	Very Fine Skewed	1.205	Leptokurtic

Table 7.10: Description of sediment samples characteristics following Folk and Ward (1957) method.

The results of the grain size analysis broadly corroborate the identification of the separate sedimentary units recorded in the field, with clearly identifiable changes in grain size characteristics occurring at the interface between these units. However, a further significant change is observed within Stratum 3 that was not recognised in the field.

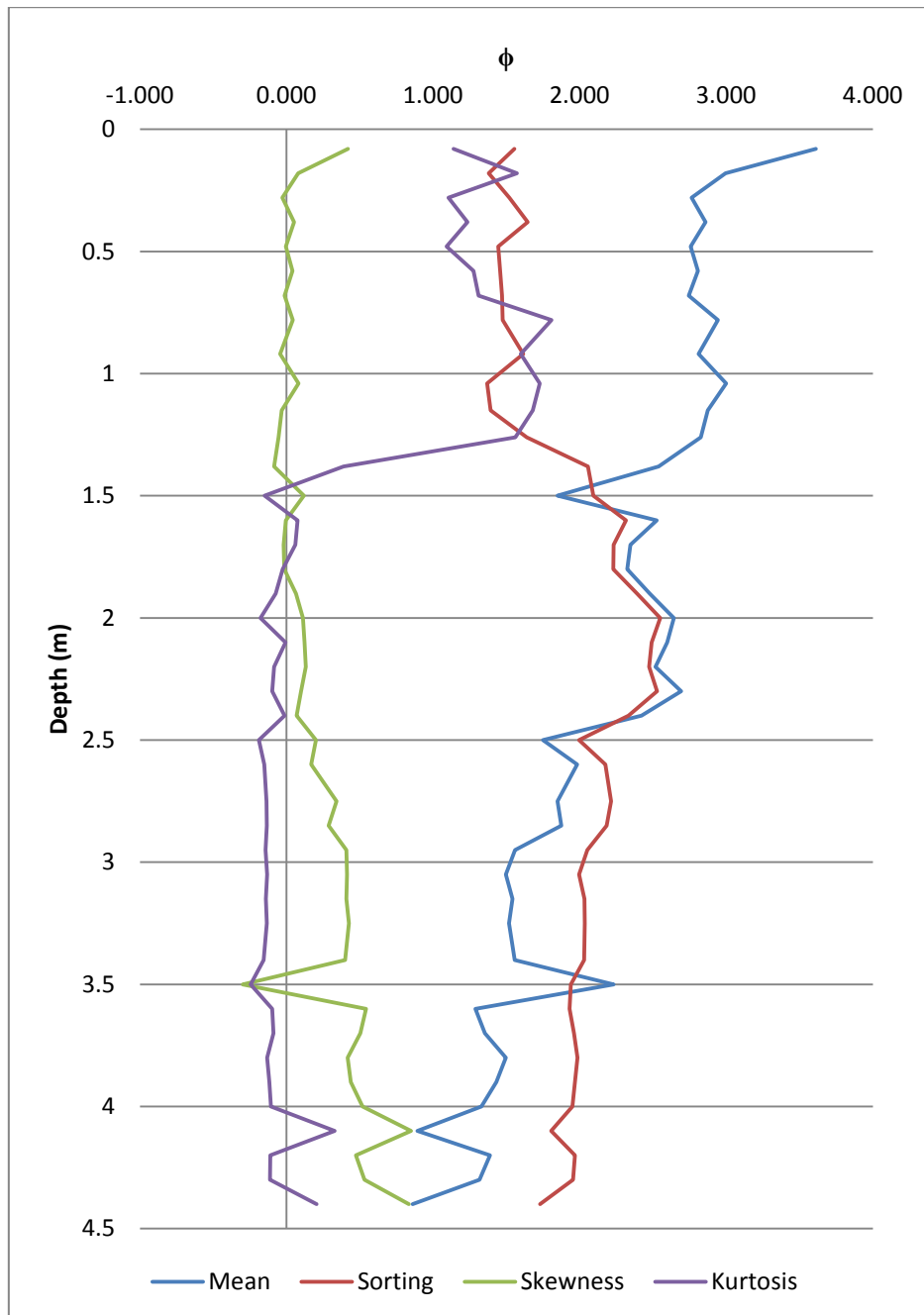
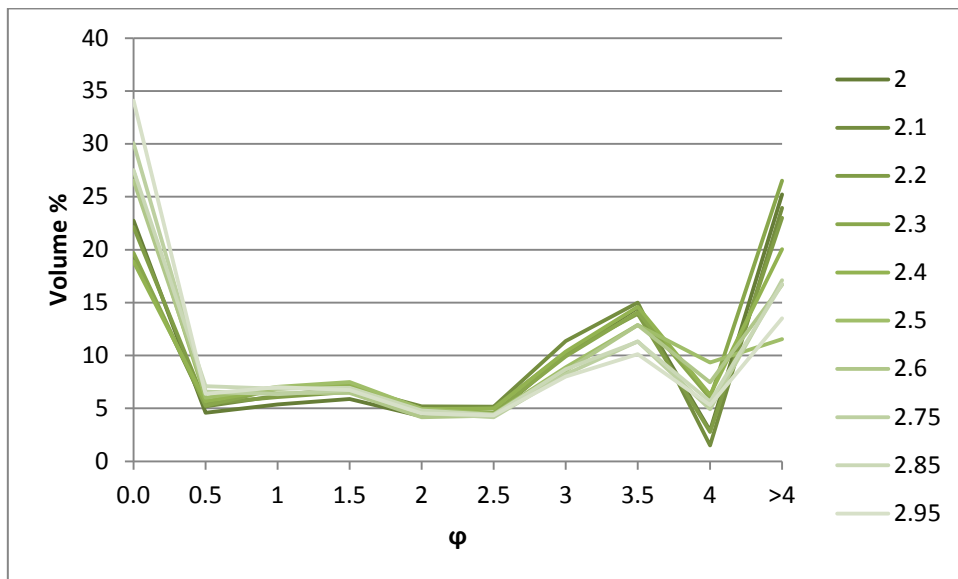
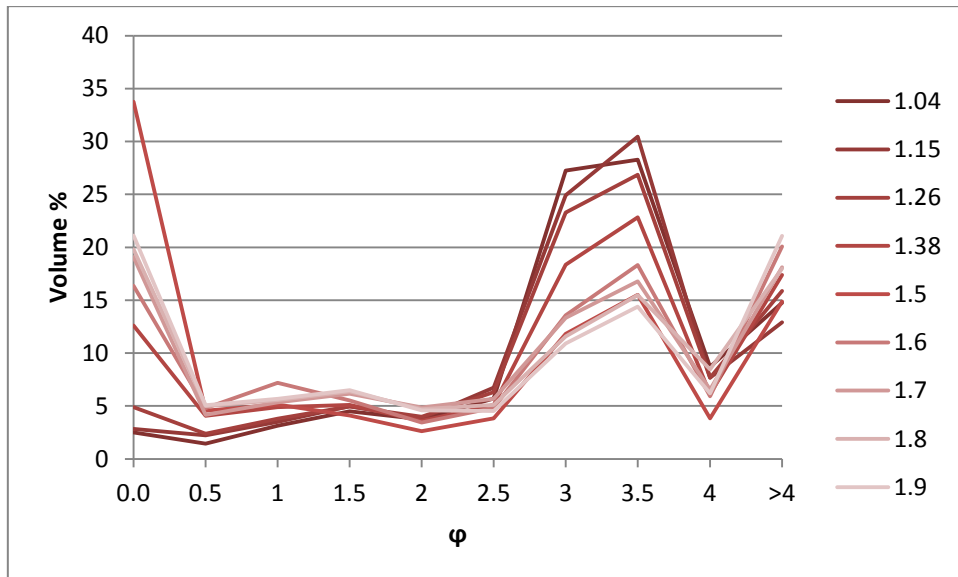
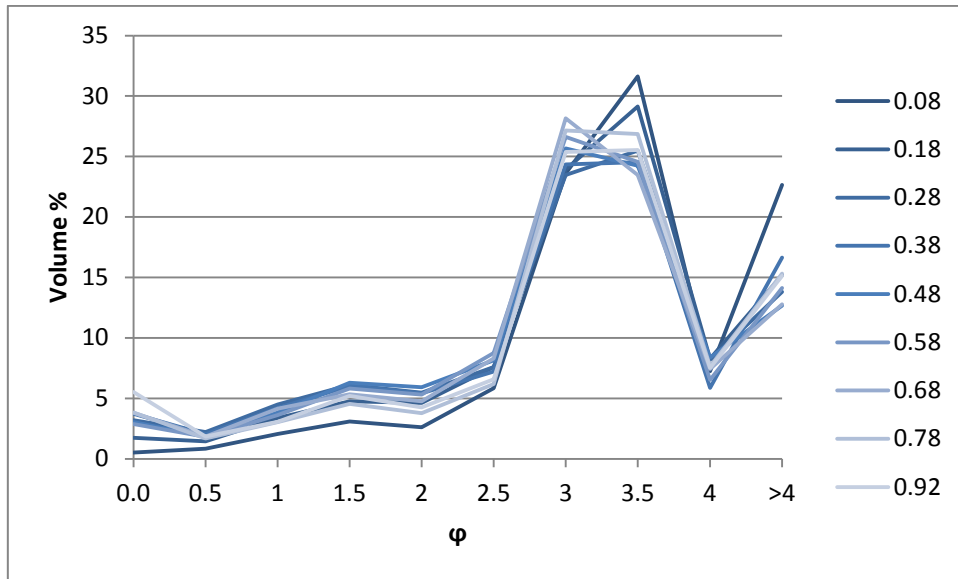


Figure 7.17: Mean grain size, sorting, skewness and kurtosis (ϕ) by depth in excavated profile. A value of 1ϕ was subtracted from kurtosis values so positive values correspond to leptokurtic distributions and negative values correspond to platykurtic distributions.



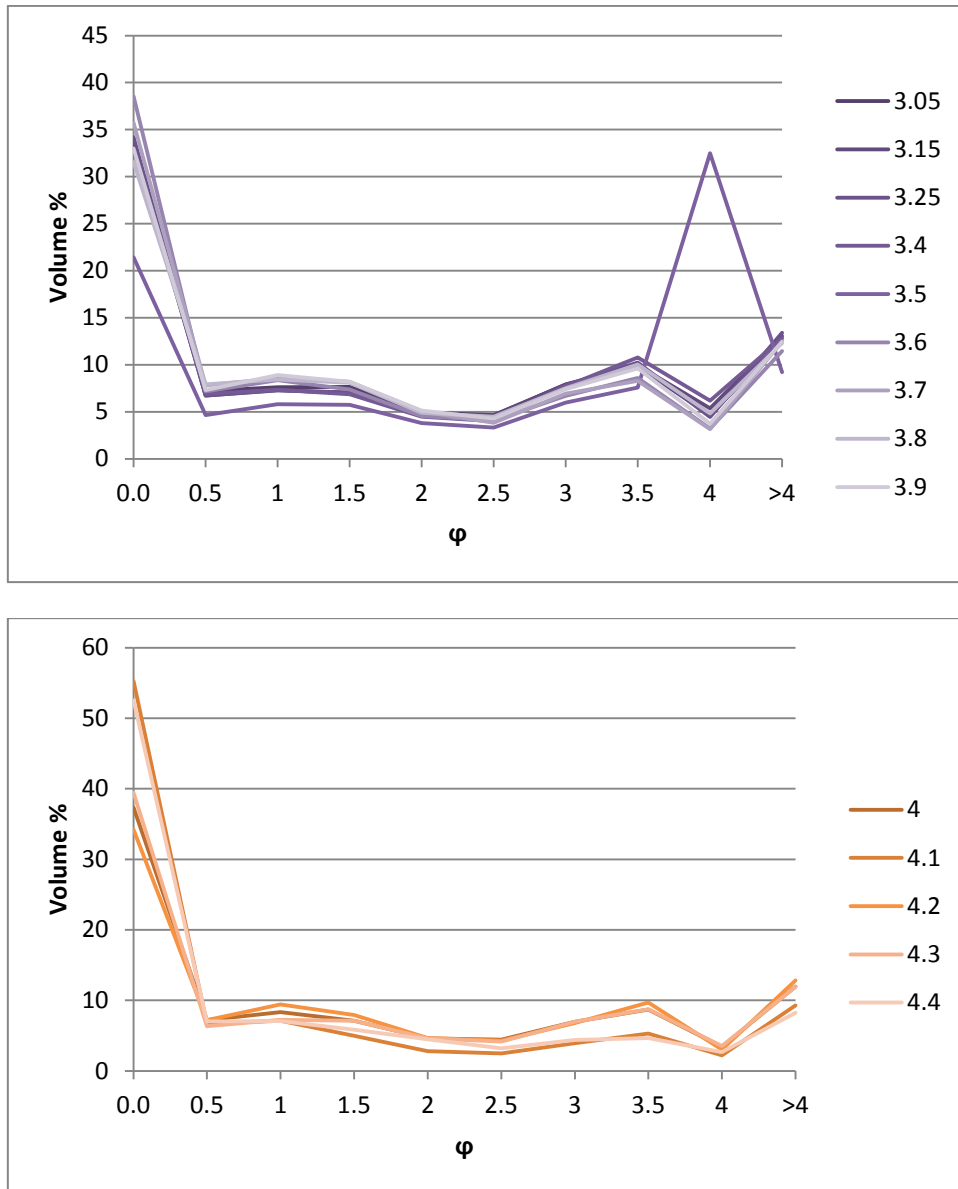


Figure 7.18: Grain size (ϕ) distributions of sediment samples (listed by arbitrary depth in profile) from KAT1, separated into 1m groups: a) (top) 0-1m; b) 1-2m; c) 2-3m; d) 3-4m; e) (bottom) 4-4.5m.

Grain size characteristics of Stratum 1 and Stratum 2 and distinctive from the other layers, typified as poorly sorted fine sands, all with mean grain size of $>2.8\phi$. A sharp break is observed in with the uppermost layers of Stratum 3, with a decrease in the level of sorting, overall drop in mean grain size, which is particularly clear at 1.5m, matching the thin pebble line observe in the section. Within this exception, the upper part of Stratum 3 comprises very poorly sorted fine sands to a depth of 2.4m. The lower part of Stratum 3, identified between

2.5-2.85m depth, shows larger mean grain sizes, which appears to relate to an increased contribution of coarse sands between 25-30%. The transition between Stratum 3 and 4 is similarly marked by a decrease in mean grain size relating to an increase in the proportion of coarse sands, whereas a poorly sorted fine sand is present at the basal boundary of Stratum 4 (3.5m depth). Stratum 5 is also comprised of medium sands, albeit with an increased level of sorting, although the mean size is again notably larger than the overlying level, ranging between 1.289-1.495 ϕ . Grain size analysis from Stratum 8 indicate the presence of both coarse and medium sands, with more than half of the samples from 4.1m and 4.4m depth comprised of sands <0 ϕ . Although the individual samples can be described as poorly sorted, the variation of grain size characteristics may indicate a lower degree of sorting may better describe the fine sediments from Stratum 8.

Coarse sediments

The upper deposits of the excavation (Stratum 1 & 2) yielded very rare if any clasts >2mm. A thin line of granules and pebbles was observed at a depth of 1.4m (see Figure 7.19) and a similar horizon can be observed throughout much of the fluvio-aeolian deposits at Katoati, with KAT2, KAT3, KAT4 and KAT5 all associated with this horizon. Very rare granule to gravel size clasts were encountered without any clear concentration during excavation of Stratum 3.

Excavations beneath 3m yielded a much greater quantity of coarse sediments than in the overlying deposits and clasts typically have a carbonate coating. Stratum 4 presents occasional bedded coarse sediments ranging from granules to large cobbles in an upward fining sequence, and this appears to be a laterally extensive deposit that can be observed extending throughout deposits surrounding the excavation site. Rare coarse sediments were encountered in Stratum 5, which did not occur in any clear concentrations. Both Stratum 6 and 8 contain denser concentrations of coarse sediments than Stratum 4. Overall, Stratum 6

contained a greater quantity of pebble sized clasts, whereas Stratum 8 included a larger number of cobbles. The thin horizon separating these two gravel layers, Stratum 7, contained extremely rare coarse sediments.

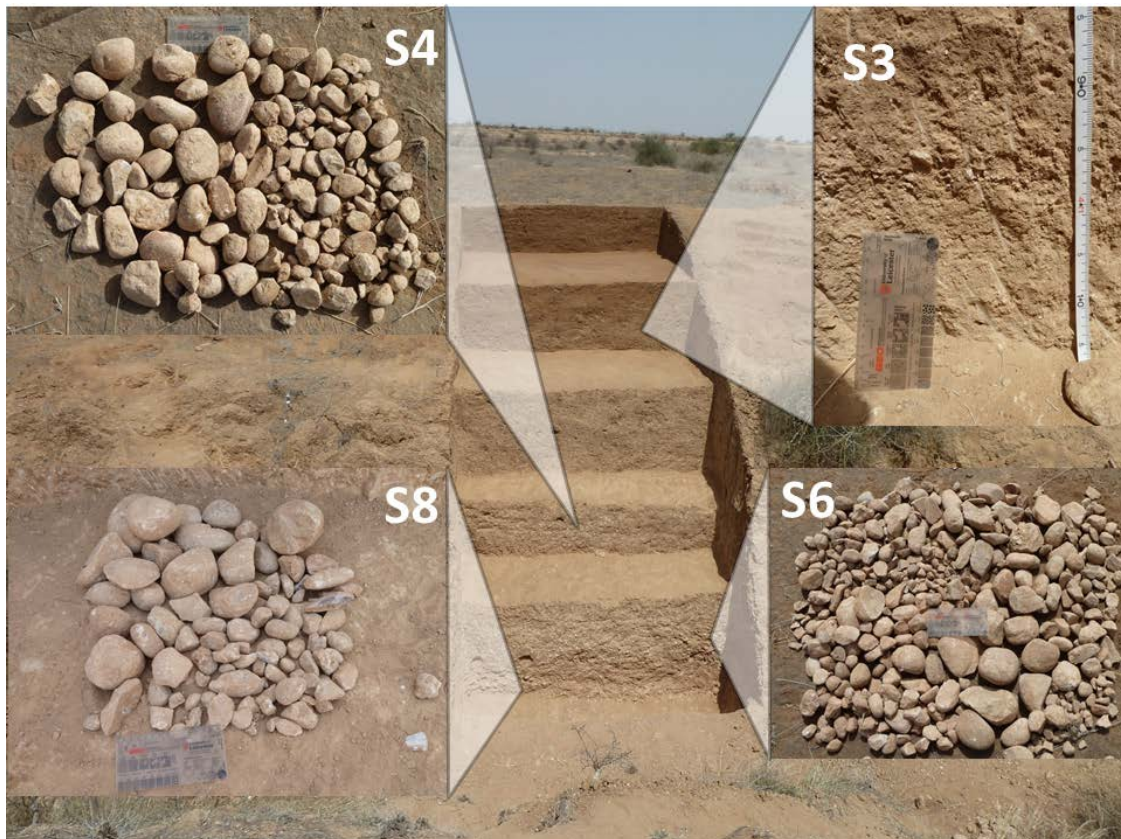


Figure 7.19: Coarse sediment inclusions from excavated strata 4, 6 and 8, and granule-pebble horizon *in situ* in Stratum 3.

X-Ray Fluorescence

Due to the limits of detection of the XRF device, it has not been possible to measure the contribution of sodium to the sediment samples and in a number of instances presence of aluminium fell below the limits of detection, preventing the calculation of standard indices of chemical weathering (e.g. WIP [Parker 1970]; CIA [Nesbitt & Young 1982]). As a result, the

individual contributions of mobile (Si, Ca, K) and immobile (Al) elements are presented in Figure 7.20.

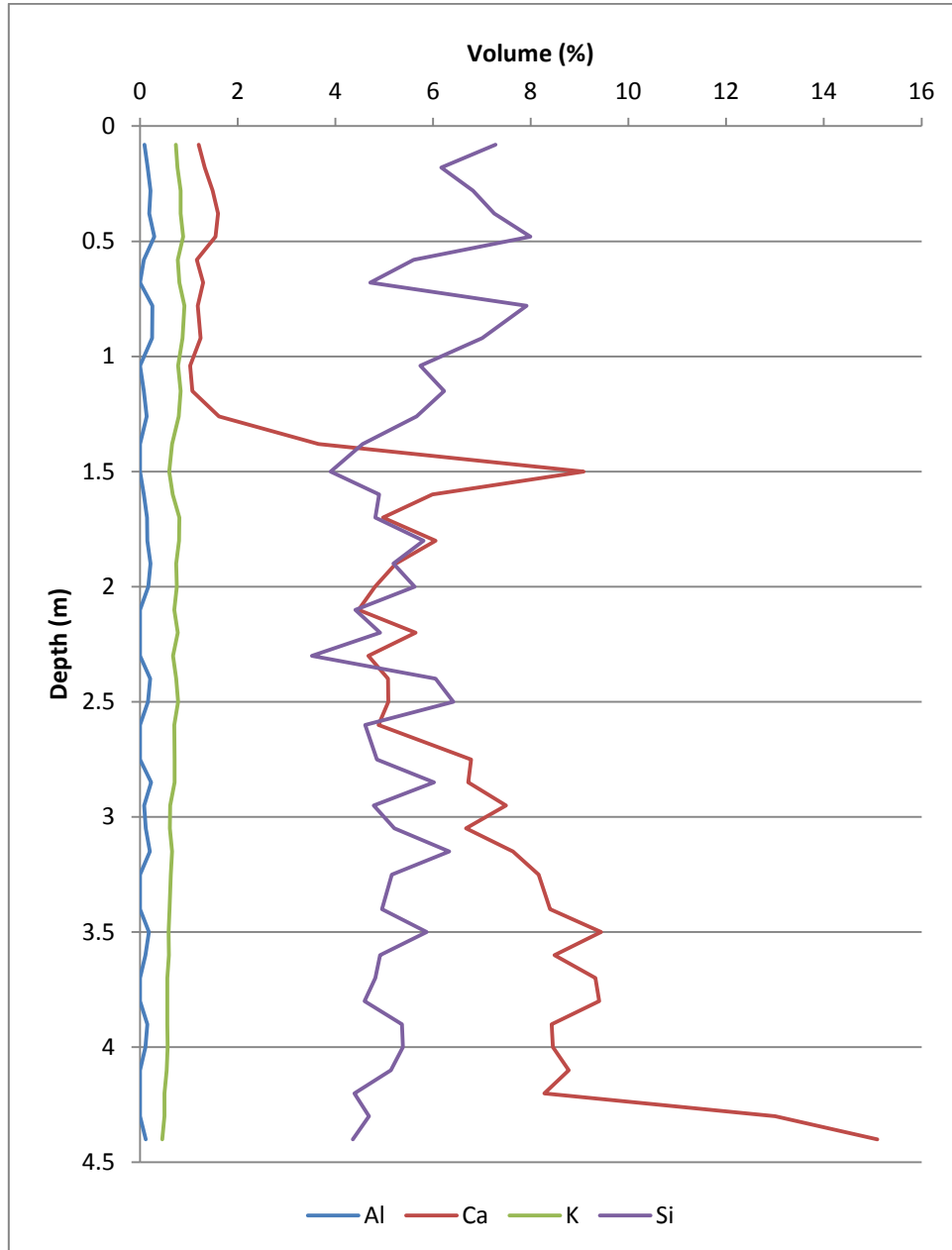


Figure 7.20: Proportional composition of aluminium, calcium, potassium and silicon within sedimentary samples from KAT1 based upon XRF analysis.

Very low levels of aluminium were observed throughout the excavated sequence with little variation with depth and frequently dropping below the XRF device's limits of detection, although this occurs more often with increasing depth. Potassium has been recorded in all

layers and the proportional composition remains remarkably stable, which is in contrast to both calcium and silicon. Silicon comprises between 4-8% of the composition of the sediment sample with much higher levels recorded in Stratum 1 and 2, a clear low point at 1.5m with broadly decreasing levels with depth below this, albeit with regular oscillations between 4.5-6%. The results for calcium composition are more variable, ranging from 1-15%, and bear general similarities to patterns observed for the grain size characteristics. Firstly, the results from Stratum 1 and 2 are considerably different from the lower levels, indicating a minimal presence of calcium ~1.5%. At 1.5m, a sharp spike is observed, peaking at ~9%, below which they remain stable at ca. 5-6% until 2.6m. Between 2.6-2.95m and 3.05-3.4m the proportion of calcium present increases fairly steadily with depth, reaching a plateau of ca. 9% between 3.4-4.2 before a further significant spike is observed at 4.3-4.4m.

CaCO₃

The percentage values of calcium carbonate within the sediment samples calculated from the results of titration and XRF analyses are presented in Figure 7.21.

The proportion of CaCO₃ present in sediments is likely to relate to the level of pedogenic carbonate formation and will increase with time since deposition, although contributions from groundwater carbonates cannot be discounted. As visible calcite nodules were removed prior to analyses, the results of both methods employed are liable to indicate a minimum estimate for the presence of calcium carbonate. Although the broad trends identified in % CaCO₃ in sediment samples are comparable between titration and XRF results, the latter are considerably smaller, whereas similarities between results from titration and grain size characteristics are more pronounced. The titration results indicate a low presence of CaCO₃ in Stratum 1 and 2, with a clear spike occurring at 1.5m after which CaCO₃ levels settle at >30-35% (see below). Notable increases in presence of CaCO₃ occur at 2.7m, 3.4m and 4.3m, which

broadly correlate with changes in grain size characteristics, and although similar changes are noted in the XRF results for calcium, they appear more muted when corresponding proportions of calcium carbonate are calculated. Although more precise experimental procedures for analysing % CaCO_3 content of soil are available (Loeppert & Suarez, 1996), the high concentrations of CaCO_3 indicated here suggest the differences with results obtained here would be negligible. The substantially lower estimates of the presence of CaCO_3 using results of the XRF analyses may be attributable to the limits of detection for the XRF device. This may indicate that the trends for other elements (Al, K & Si) are broadly representative of the composition of the analysed sediments, but the overall proportions may need to be significantly revised through using more controlled laboratory procedures.

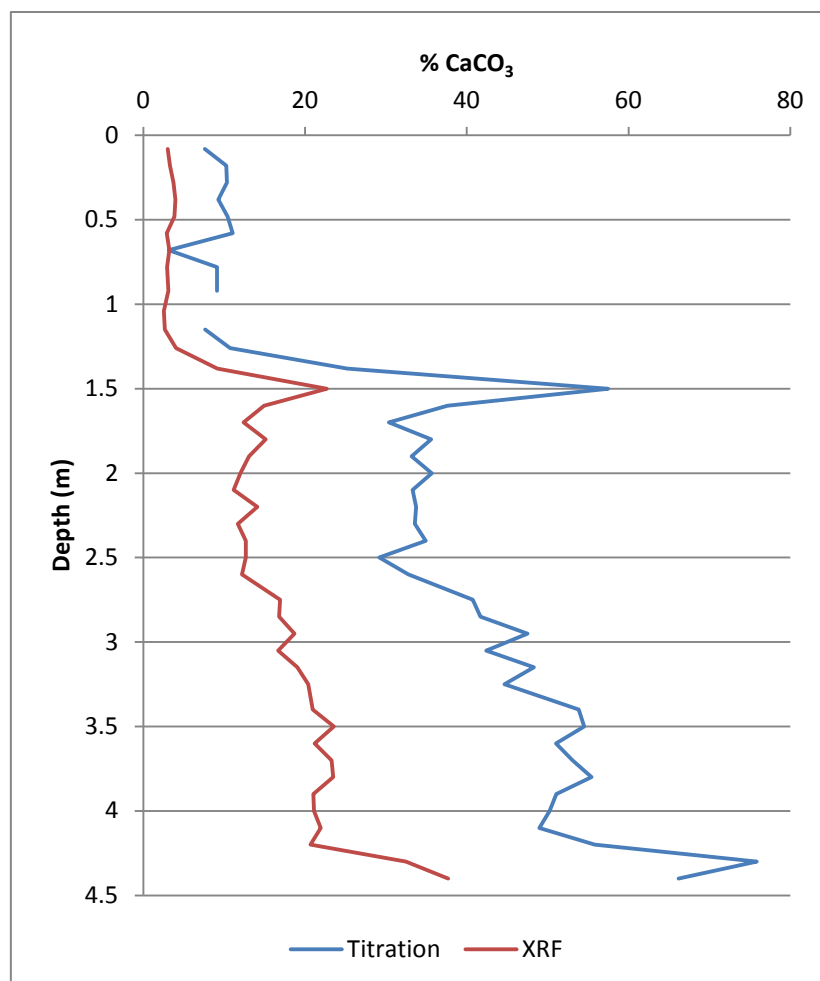


Figure 7.21: Percentage of calcite present in sediment samples plotted by depth.

Stable Isotopes

Results of stable isotope analyses of pedogenic carbonates from KAT 1 are presented in Table 7.11 and Figures 7.22 & 7.23.

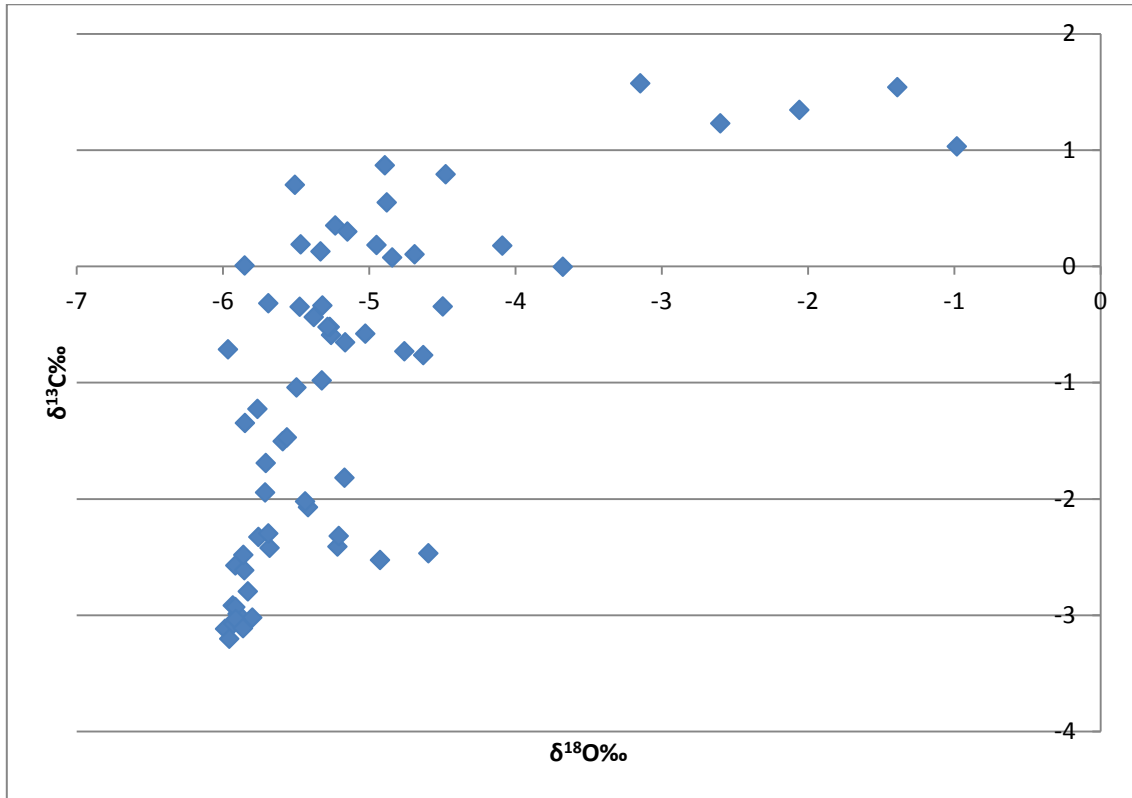


Figure 7.22: Stable oxygen and carbon isotope results from pedogenic carbonates from KAT1.

The majority of $\delta^{18}\text{O}$ results from pedogenic carbonates at KAT1 show fairly tight clustering between -4.5‰ to -6‰ , although slightly more enriched results are present beneath 3.4m depth. The relatively limited variability in $\delta^{18}\text{O}$ results suggests that either there has been little difference in meteoric water source over the period of carbonate formation exhibited in the excavated section, or the level of evaporitic fractionation of soil water has remained fairly constant. Given the extended time depth of the isotopic record at KAT1, spanning MIS 5-1, the latter appears a more plausible explanation. A major departure from this broad trend occurs in samples from 1.5-1.7m depth, which range between -4.1‰ to -0.98‰ .

Depth (m)	$\delta^{13}\text{C}$ (‰)		$\delta^{18}\text{O}$ (‰)		Depth (m)	$\delta^{13}\text{C}$ (‰)		$\delta^{18}\text{O}$ (‰)	
0.08					2.3	-2.41	-2.93	-5.71	-5.91
0.18					2.4	-2.07	-2.3	-5.22	-5.69
0.28					2.5	-2.32	-3.12	-5.42	-5.98
0.38	0.13		-5.33		2.6	-2.02	-3.2	-5.21	-5.96
0.48	-0.76		-4.63		2.75	-2.47	-2.48	-5.44	-5.86
0.58					2.85	-1.23	-3.02	-4.59	-5.8
0.68					2.95	-2.99	-3.07	-5.76	-5.93
0.78					3.05	0	-3.04	-5.9	-5.91
0.92	-1.38		-5.36		3.15	0.7	-3.11	-3.67	-5.86
1.04					3.25	-0.34	-1.47	-5.51	-5.56
1.15	-0.98		-5.35		3.4	-0.58	-0.73	-4.5	-4.76
1.26	1.03	-2.92	-5.32	-5.93	3.5	0.1	-0.35	-5.03	-5.47
1.38	1.54	1.35	-0.98	-2.06	3.6	0.08	-0.44	-4.69	-5.38
1.5	1.57	1.23	-1.39	-2.6	3.7	0.19	0.18	-4.84	-4.95
1.6	0.87	0.18	-3.15	-4.09	3.8	-0.59	-0.72	-5.47	-5.96
1.7	-0.65	-1.5	-4.89	-5.59	3.9	0.55	-0.52	-5.26	-5.27
1.8	-1.04	-2.57	-5.16	-5.91	4	0.35	-0.32	-4.88	-5.69
1.9	-1.94	-2.33	-5.5	-5.76	4.1	0.79	0.01	-5.23	-5.85
2	-2.42	-2.62	-5.71	-5.85	4.2	0.3	-0.52	-4.48	-5.29
2.1	-2.52	-2.8	-5.68	-5.83	4.3	-0.34	-1.35	-5.15	-5.85
2.2	-1.69	-1.82	-4.93	-5.17	4.4	0.95	0.68	-5.32	-5.57

Table 7.11: Results of stable isotope analysis of pedogenic carbonates.

The $\delta^{13}\text{C}$ ‰ results from pedogenic carbonates at KAT1 display greater variation than the oxygen isotope results, ranging from -3.2‰ to 1.57‰. Based upon an analogy with xerophytic plants in eastern Africa, pedogenic carbonates formed at a depth of >0.5m from surface in pure C_3 habitats are expected to range between -13.4‰ and -8.8‰ (mean=-11.1‰), whereas in pure C_4 habitats values between 0.2‰ and 3.8‰ (mean=2‰) are anticipated (Sikes et al. 1999; Cerling 1999; Cerling et al. 2010) (accounting for equilibrium fractionation between CaCO_3 and CO_2 of 9-11‰, kinetic diffusion effects of ~4.4‰, and errors introduced due to possible variation in soil respiration rates and temperature [Breecker et al. 2009]).

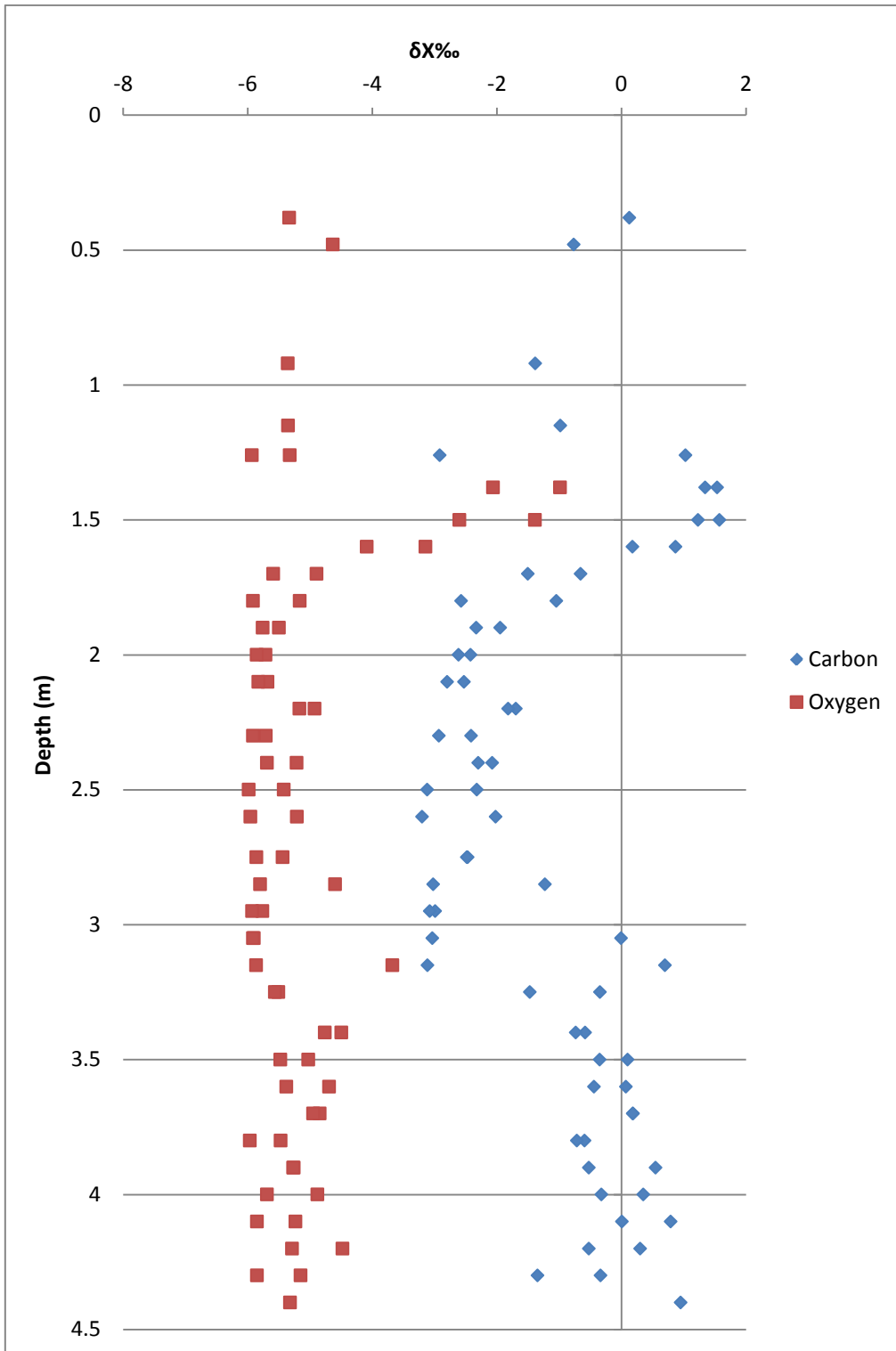


Figure 7.23: Stable oxygen and carbon isotope results of pedogenic carbonates from KAT1 plotted by depth.

The estimated proportion of C₄ plant coverage at KAT1 typically ranges between 60-90%, with a maximum of ~96% occurring at 1.5m depth, suggesting the dominance of C₄ grasses. Some notable variations in the proportion of C₄ plant coverage occur through the excavated sequence at KAT1. In the upper levels, where only single results are present, C₄ coverage is between 75-85%. Results from 1.26m depth are widely dispersed, suggesting between 62-92% C₄ plants. A peak in $\delta^{13}\text{C}\text{‰}$ values occurs at 1.38-1.5m depth, which rapidly decreases by 1.7-1.8m, which may either indicate a very strong signal of C₄ coverage or that the pedogenic carbonate nodules formed within 50cm from an ancient land surface. Between 1.9-2.95m the estimated cover of C₄ plants is typically between 60-70%, whereas dispersed results occur between 3.05-3.25, with estimated C₄ plant coverage ranging from 60-90%. Below this depth, estimated C₄ plant coverage is typically between 80-90%, although a notable drop in upper and lower estimates occurs at 4.3m.

The interpretation of stable isotope results from ostrich eggshell (Table 7.12 and Figure 7.24) is somewhat different from pedogenic carbonates. In particular, the isotopic composition of ostrich eggshell is characterised as a “snap-shot” of diet, averaged over 3-5 days, with breeding occurring after the rainy season when sufficient nutrient stores have been acquired (Johnson et al. 1998). Problematically, $\delta^{18}\text{O}$ in ostrich eggshell from modern populations exhibit wide variability with respect to localised surface water sources, exhibiting an inverse relationship with humidity (Johnson et al. 1998). As non-obligate drinkers, a range of fractionation processes within plant water sources as well as physiological responses of ostrich to humidity indicate that oxygen isotope data from ostrich eggshell may be best used as a qualitative measure of palaeoclimate (Johnson et al. 1998). The $\delta^{18}\text{O}$ results from the Katoati sites can be readily separated into three groups. The majority of samples range between -0.5‰ to 0.5‰, whereas the two samples from the KAT1 excavated sequence show a large step in enrichment of $\delta^{18}\text{O}$, returning results of ~6‰, and a similarly large step is observed

with KAT3a, returning results of ~12‰. As a result, it can be suggested that the majority of samples relate to eggs produced during more humid conditions, with those from KAT1 and KAT3a indicating an increasing impact of aridity.

Sample	$\delta^{13}\text{C}\text{‰}$	$\delta^{13}\text{C}\text{‰}^a$	$\delta^{18}\text{O}\text{‰}$	Age (ka)
KAT1-23a	-3.277	-5.1	6.057	>57,900
KAT1-23b	-3.413	-4.1	6.391	>62,000
KAT2a	-2.902	-3.9	0.173	>59,900
KAT2b	-2.948		-0.007	
KAT2c	-2.969	-2.8	0.139	35,210±220
KAT2d	-3.095		-0.062	
KAT2e	-2.655	-2.8	-0.538	49,500±800
KAT2f	-2.904		0.338	
KAT3a	-9.917	-9.9	11.937	52,100±1,100
KAT3b	-3.311		0.218	
KAT4	-3.015	-2.6	0.038	45,100±500
KAT5	-2.921		0.058	

Table 7.12: Results of stable isotope analysis of ostrich eggshell. ^a $\delta^{13}\text{C}$ results from radiocarbon analyses.

Carbon isotope results from ostrich eggshell appear to directly reflect the isotopic composition of the diet, with an enrichment of ~16‰ (Johnson et al. 1998; Segalen et al. 2006) such that a pure C₃ diet would produce an average $\delta^{13}\text{C}\text{‰}$ of -9.5‰ and a pure C₄ diet would return results of 4.2‰. Ostriches show a slight preference for C₃ shrubs and select against some vegetation (Johnson et al. 1998), which could relate to requirement for plant water intake where surface water supplies are not available. Overall, the results from most samples indicate that the estimated ostrich diets at Katoati show relatively equal proportions of C₃ and C₄ input, with a slight bias toward C₃ evident in the results of from 44.4 to 49.9% composition of C₄ plants. The results from KAT3a are different, indicating a pure C₃ diet.

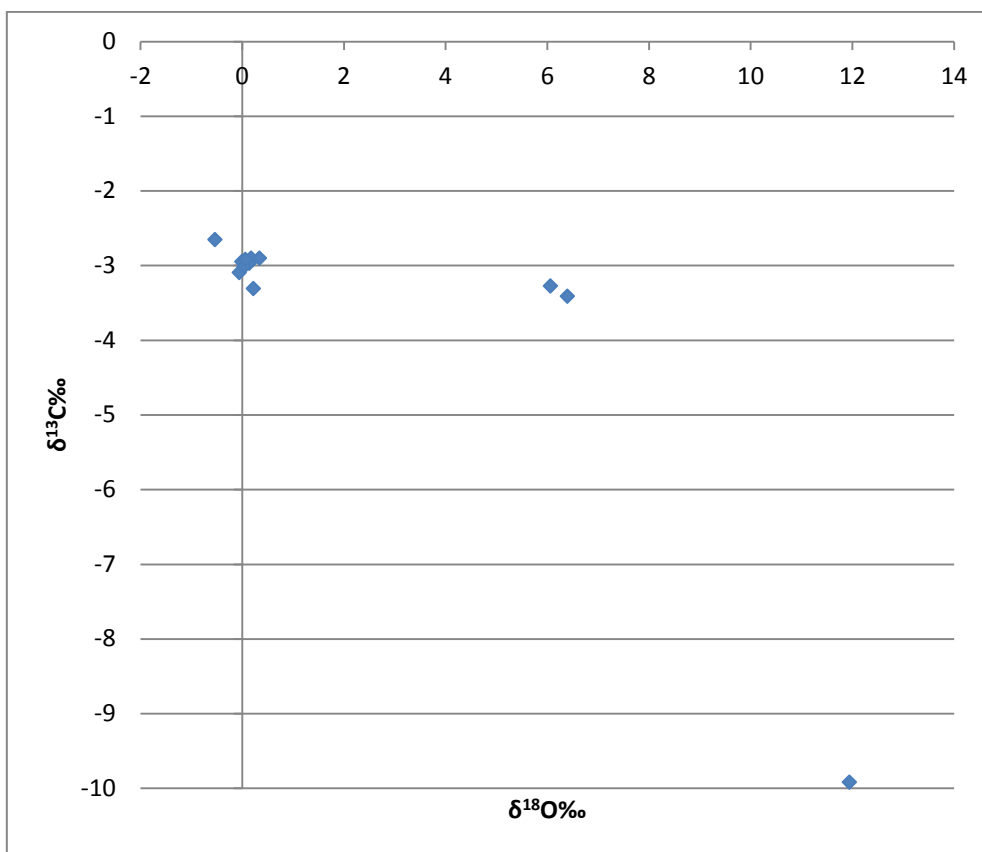


Figure 7.24: Stable oxygen and carbon isotope results of un-abraded ostrich eggshell samples from KAT1-KAT5.

The carbon isotope results of samples that were physically and chemically abraded match well with un-abraded samples in four of seven cases, suggesting limited impact of contamination from secondary carbonate sources. Analysis of the KAT1 samples and KAT2a returned more results showing they are more depleted in $\delta^{13}\text{C}\text{‰}$ than un-abraded samples. The un-abraded results appear to present an average between the abraded OES results and the pedogenic carbonate results from the source layer. For the samples from KAT1, the more depleted $\delta^{13}\text{C}\text{‰}$ results provide a better match with the enriched $\delta^{18}\text{O}\text{‰}$ results. The presence of secondary carbonates on the samples indicates the $\delta^{18}\text{O}\text{‰}$ results may also be averaged with pedogenic carbonates, and comparison with the relevant results would indicate that abraded samples may have returned more enriched results, further emphasising evidence for enhanced aridity.

Due to the rapid formation of ostrich eggshell, the isotopic signatures recorded are likely to present a very temporary snap-shot of ostrich diet and reproductive habits. Two different interpretations of these data can be made. Firstly, evidence for increased aridity and dependence upon C₃ resources between ca. 52ka to >62ka compared to ca. 50-35ka could indicate suppression of the summer monsoon in the earlier period, and that ostrich breeding coincided with the winter monsoon. However, as results from KAT2a dating to >60ka indicate decreased aridity and greater reliance upon C₄ resources, an alternative interpretation may be that two breeding seasons were possible during the earlier time bracket after both monsoons. As sedimentary deposition at Katoati changes from fluvial in the earlier time bracket to aeolian in the later time bracket, the latter explanation may be favoured although the analysis of a larger number of samples is required to corroborate this.

Size Sorting, Weathering and Rounding of Lithic Artefacts

Figure 7.25 presents a cumulative graph of the size classes present within archaeological assemblages between the different sedimentary strata. Assemblages S3a and S3b show a much higher proportion of small sized artefacts than the other assemblages, although they are also the smallest sample sizes. In contrast, S5 shows a greater proportion of larger artefacts than other assemblages while also including the greatest number within the smallest class (<10mm), although sample size may be a factor here too. However, S4, S6 and S8 present similar cumulative profiles with ca. 50% of artefacts smaller than 40mm. The cumulative proportion of <20mm artefacts is typically low (<10%), suggesting some winnowing of the smallest fraction of debitage in these assemblages, although no significant disturbance of artefacts above this level is suggested (Schick 1984).

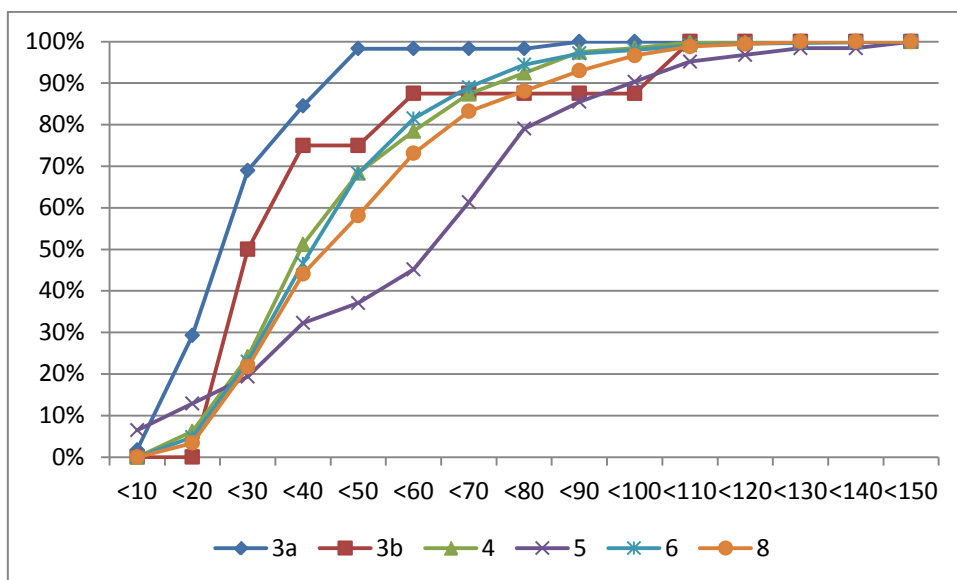


Figure 7.25: Cumulative composition of lithic artefacts within each assemblage grouped by 10mm size classes.

Table 7.13 presents the total number of artefacts displaying different levels of rounding and weathering. This indicates that two thirds of the artefacts show little or no rounding or weathering. Overall, a higher level of weathering in contrast to rounding is recorded, suggesting abrasive impacts upon artefacts have not been concentrated upon edges and arises, which may occur through aeolian and geochemical abrasion, as well as through fluvial factors.

		Weathering			
		None	Low	Medium	High
Rounding	None	179	292	1	0
	Low	4	458	146	2
	Medium	0	7	368	27
	High	0	0	3	28

Table 7.13: Total number of artefacts displaying different levels of rounding and weathering.

An evaluation of the cumulative size class distributions of artefacts showing different degrees of rounding offers further insight into potential post-depositional impacts on lithic assemblages (Table 7.14; Figure 7.26). S3a and S3b repeatedly show the smallest and most restricted distribution of artefact sizes across the different rounding categories.

Rounding										
Stratum	Level	None		Low		Medium		High		Total
3a	13	1	20.00%	3	60.00%	-	-	1	20.00%	5
	14	16	39.02%	18	43.90%	6	14.63%	1	2.44%	41
	15	5	41.67%	5	41.67%	2	16.67%	-	-	12
	Total	22	37.93%	26	44.83%	8	13.79%	2	3.45%	58
3b	18	1	50.00%	1	50.00%	-	-	-	-	2
	19		-	5	83.33%	1	16.67%	-	-	6
	Total	1	12.50%	6	75.00%	1	12.50%	0	0.00%	8
4	20	7	14.29%	29	59.18%	13	26.53%	-	-	49
	21	60	50.42%	46	38.66%	13	10.92%	-	-	119
	22	32	22.22%	87	60.42%	25	17.36%	-	-	144
	23	46	52.27%	25	28.41%	16	18.18%	1	1.14%	88
	24	12	33.33%	17	47.22%	7	19.44%	-	-	36
	Total	157	36.01%	204	46.79%	74	16.97%	1	0.23%	436
5	25	31	50.00%	14	22.58%	13	20.97%	4	6.45%	62
	Total	31	50.00%	14	22.58%	13	20.97%	4	6.45%	62
6	26	69	31.51%	98	44.75%	51	23.29%	1	0.46%	219
	27	95	30.06%	121	38.29%	96	30.38%	4	1.27%	316
	28	20	21.74%	33	35.87%	38	41.30%	1	1.09%	92
	Total	184	29.35%	252	40.19%	185	29.51%	6	0.96%	627
8	29	9	26.47%	12	35.29%	13	38.24%	-	-	34
	30	40	28.37%	42	29.79%	53	37.59%	6	4.26%	141
	31	27	22.50%	37	30.83%	45	37.50%	11	9.17%	120
	32	5	15.63%	16	50.00%	10	31.25%	1	3.13%	32
	Total	81	24.77%	107	32.72%	121	37.00%	18	5.50%	327

Table 7.14: Number of artefacts showing different degrees of rounding separated by excavation level and assemblage.

This is indicative of some size sorting, suggesting S3a and S3b may represent the winnowed portion of lithic assemblages. Due to the typically low sample sizes, the distribution of highly rounded artefacts are not highly informative, although the size class distribution from S5 and S8 indicate these artefacts are typically larger than the result of the population. Across the 'none', 'low' and 'medium' rounding categories, artefacts from S4, S6 and S8 show similar patterns within size class distributions. This suggests that they have been subject to very similar post-depositional processes, with some winnowing of the smallest fraction of artefacts, but fairly minimal impact upon >20mm artefacts. While S5 shows similarities with S4, S6 and S8 within the low rounded group, it is notably different in both 'none' and 'medium' classes,

indicating the increased presence of larger artefacts, potentially indicating an upstream lag deposit.

Fluvial transport of artefacts may explain the presence of some surface weathering on artefacts, although a number of other causes can be suggested. Abrasion of artefacts by flowing water and suspended fine sediments without artefact displacement offer one explanation (Petraglia & Potts 1994). Similarly, if artefacts are not immediately buried after their production, it is possible that they were subject to abrasion by fine sediments transported by aeolian forces. However, in situ geochemical weathering of artefacts may

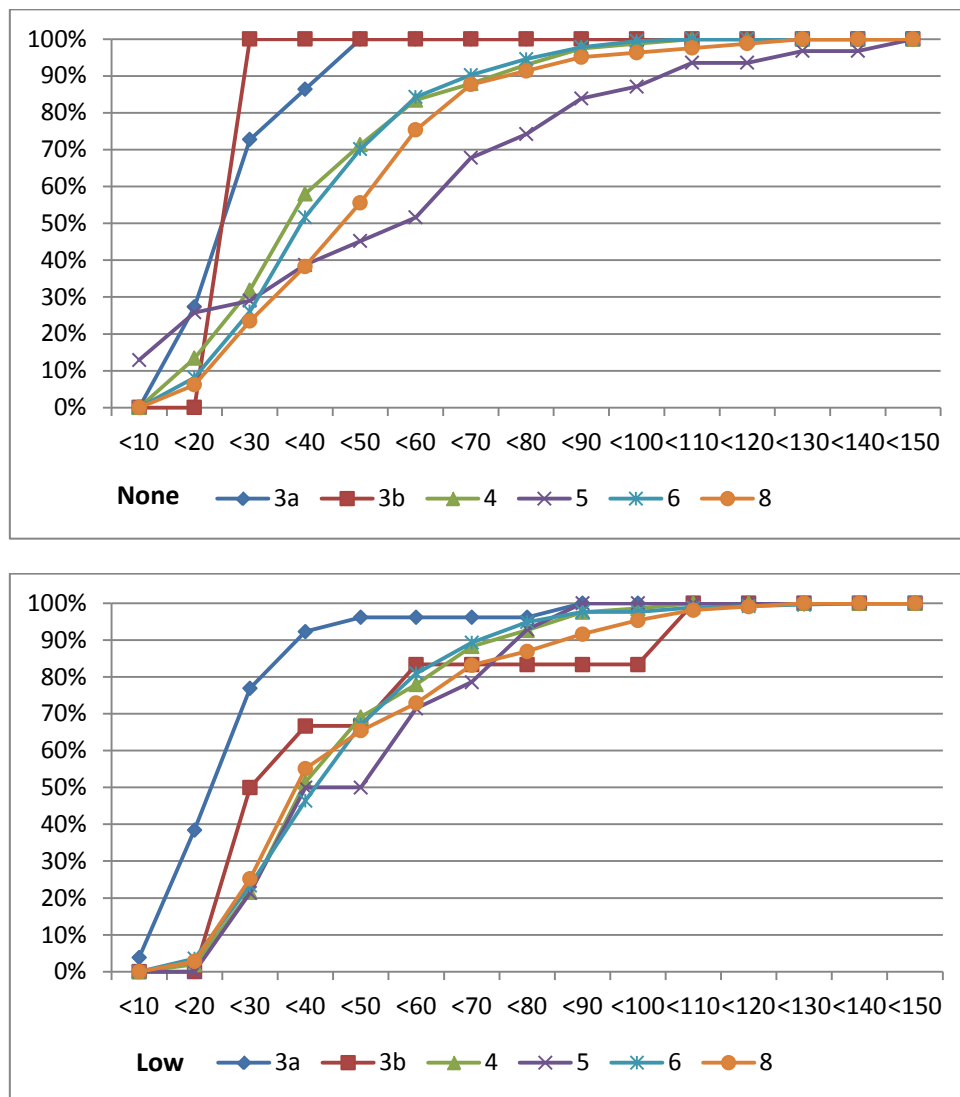


Figure 7.26: Cont.

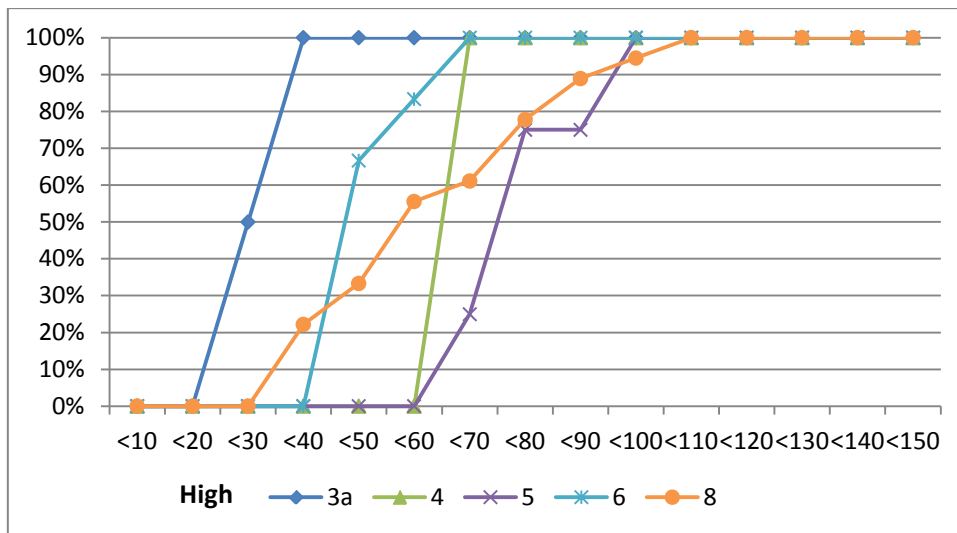
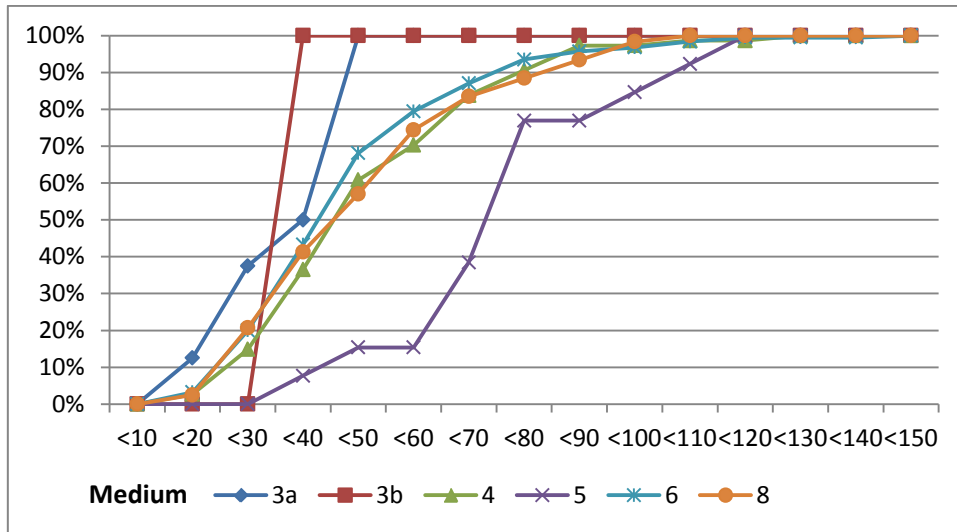


Figure 7.26: Cumulative composition of lithic artefacts within each assemblage grouped by 10mm size classes and degree of rounding.

tarnish artefacts that were rapidly buried after their production. The only limestone artefact recovered through excavations, from S6, has been de-calcified, attesting to the occurrence of acidic conditions and intense chemical weathering. The overwhelming majority of artefacts at KAT1 are quartzites, which are typically considered resistant to chemical weathering. However, dissolution of silica can occur at more advanced rates under conditions of high temperatures and in the presence of inorganic electrolytes in high pH solutions (Bennet 1991), both of which are feasible at Katoati. Equally, deposition of very fine silicate or carbonate crusts may also present the appearance of weathering.

The majority of artefacts are recorded with either low or medium weathering, while the proportion of medium and high weathered pieces, in contrast to low or no weathering, increases with depth (see Table 7.15). As all classes of weathering were recorded in all assemblages except S3b, it is unlikely that *in situ* geochemical weathering alone can explain the range of variability observed. As a result further analyses of the archaeological assemblages must take into account the possibility that more heavily weathered artefacts have spent a greater period of time exposed to physical weathering, due to their spatial configuration within an assemblage in relation to the rate of burial (e.g. Schick 1984) or deposition of artefacts of different ages in the same sedimentary context.

Highly weathered artefacts in S3a, S4, S5, S6 and S8 typically show the largest maximum surface areas sizes, in comparison to the other three weathering classes (see Figure 7.27). This may indicate that the more advanced state of weathering could be a product of greater *in situ* exposure. However, as size ranges overlap considerably it is also possible that they represent earlier activities at the site than the rest of the artefacts within the same stratum. The artefacts in S5 show the clearest pattern of increasing surface area with increasing levels of weathering, which may indicate an impact of greater size sorting occurring with extended periods of exposure. Artefacts with medium, low or no weathering exhibit a very similar range of surface areas in S4, S6 and S8, and as neither greater *in situ* exposure nor size sorting seem to explain this pattern, this could indicate the conflation of artefact assemblages of different ages.

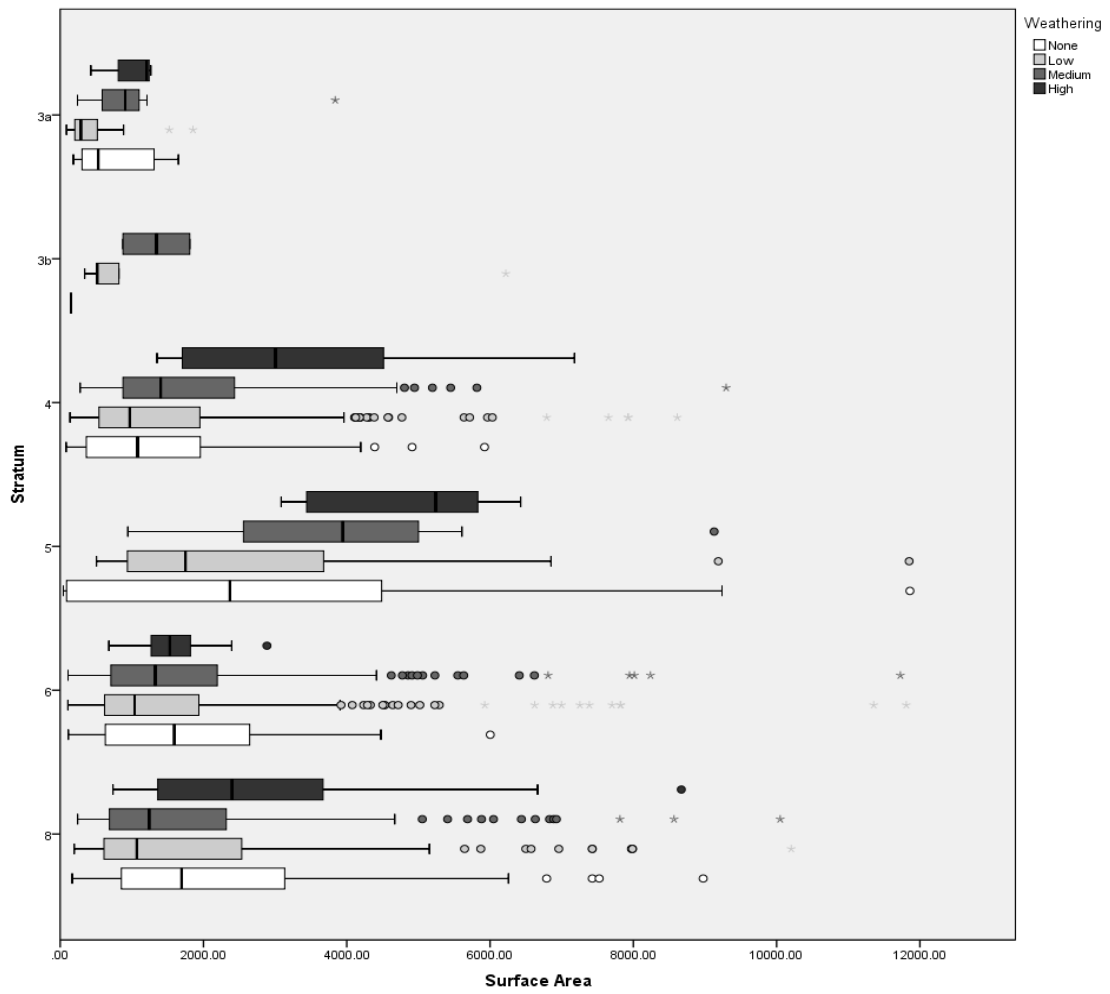


Figure 7.27: Boxplot of artefact surface area (mm²) separated by weathering classes and lithic assemblage.

Weathering										
Stratum	Level	None		Low		Medium		High		Total
3a	13	-		3	60.00%	1	20.00%	1	20.00%	5
	14	6	14.63%	26	63.41%	6	14.63%	3	7.32%	41
	15	4	33.33%	5	41.67%	3	25.00%	-		12
	Total	10	17.24%	34	58.62%	10	17.24%	4	6.90%	58
3b	18	1	50.00%	-		1	50.00%	-		2
	19	-		5	83.33%	1	16.67%	-		6
	Total	1	12.50%	5	62.50%	2	25.00%	-		8
4	20	2	4.08%	18	36.73%	26	53.06%	3	6.12%	49
	21	8	6.72%	87	73.11%	24	20.17%	-		119
	22	8	5.52%	80	55.17%	53	36.55%	4	2.76%	145
	23	22	25.00%	42	47.73%	23	26.14%	1	1.14%	88
	24	3	7.89%	23	60.53%	12	31.58%	-		38
	Total	43	9.79%	250	56.95%	138	31.44%	8	1.82%	439
5	25	21	33.87%	23	37.10%	13	20.97%	5	8.06%	62
	Total	21	33.87%	23	37.10%	13	20.97%	5	8.06%	62
6	26	28	12.79%	132	60.27%	57	26.03%	2	0.91%	219
	27	32	10.13%	162	51.27%	115	36.39%	7	2.22%	316
	28	2	2.20%	44	48.35%	42	46.15%	3	3.30%	91
	Total	62	9.90%	338	53.99%	214	34.19%	12	1.92%	626
8	29	4	11.76%	12	35.29%	18	52.94%	-		34
	30	25	17.73%	47	33.33%	59	41.84%	10	7.09%	141
	31	19	15.83%	37	30.83%	49	40.83%	15	12.50%	120
	32	2	6.25%	13	40.63%	14	43.75%	3	9.38%	32
	Total	50	15.29%	109	33.33%	140	42.81%	28	8.56%	327

Table 7.15: Number of artefacts showing different degrees of weathering separated by excavation level and assemblage.

Site formation processes at Katoati

The range of evidence presented above provides the means to develop a scheme of natural site formation processes at KAT1, which can be separated into depositional and post-depositional features.

The Depositional Environment at Katoati

The lowest three deposits observed at KAT1, Stratum 8, 7 and 6, can be characterised as gravel and sand bar deposits from a braided stream context, comprising of pebbles, cobbles and medium to coarse poorly sorted sands that have been deposited $>91\pm 22\text{ka}$. The occurrence of rare heavily rolled and weathered artefacts indicates that a small part of the archaeological assemblages in S8 and S6 have been transported to the site. The use of locally available quartzites suggests these gravels have been exploited as a raw material source. Some fluvial disturbance has occurred, and given the similar patterns of size sorting between no, low and medium weathering classes it is suggested that all three groups were subject to the same fluvial events. This may suggest the exploitation of a gravel bar that occurred in an infrequently active channel zone.

Overlying this, in Stratum 5, is a fluvial sand bar deposited $91\pm 22\text{ka}$, indicative of decreased fluvial energy in comparison to the underlying gravels or changes in channel morphology, although this may have been sufficient to winnow the lower archaeological assemblages. Size sorting within the archaeological assemblage from this stratum is pronounced and suggests that the more heavily rounded and weathered components have been undergone a greater level of transport, whereas the preservation of fresh and small debitage in this deposit indicate some activity on the site that was rapidly buried and not substantially reworked.

The return of gravel deposits in Stratum 4 suggests an increase in fluvial activity, including highly limited inward transport of lithic artefacts, although capacity for coarse sediment transport and deposition is more limited than in Stratum 6 and 8. Renewed exploitation of exposed gravel deposits occurred, and the appearance of fresh artefacts, including ostrich eggshell, indicates limited fluvial reworking of these deposits prior to burial. The presence of dated ostrich eggshell in this stratum offers a means to resolve the inverted chronology

presented by OSL samples KAT1-10 and KAT1-3. The background age estimates from the AMS dating programme fall within the upper confidence bracket of KAT1-3, suggesting the deposition of these sediments occurred between 58-66ka. Given the confidence bracket provided by KAT1-10, it can be suggested that fluvial activity at KAT1 was rapidly replaced by aeolian activity, as indicated in the overlying horizon.

A change in depositional environment is indicated by Stratum 3, which is comprised of medium and fine sands that either been deposited in a low energy fluvial environment or through aeolian activity, occurring from 66 ± 11 ka, although the lower end of the confidence bracket may be more probable given the dating of the underlying deposits. A sharp shift in grain size is apparent within Stratum 3 at 2.5m depth. The shift in sediment size within this stratum indicates a decrease in fluvial or aeolian activity, or potentially a change in sediment supply source. The presence of a thin line of coarse sediments between 1.4-1.5m indicates the top of this aeolian deposit has been scoured, which may suggest an episode of sheet-wash erosion including the introduction of small lithic artefacts that are likely to have been winnowed from a local source.

A sharp division between Stratum 3 and 2 is observed, with the latter comprised of finer sands with a higher level of sorting being deposited from 16 ± 5 ka. S2 and S1 are very similar in their sedimentary characteristics, and differences in colour may reflect organic contributions from contemporary vegetative and animal communities.

Post-Depositional Processes at Katoati

A clear spike in the presence of calcium carbonate is evident in Stratum 8, where it is considerably more abundant in contrast to the rest of the excavated sequence. Beyond the overall increase in the proportion of calcium carbonate with depth, which is likely to relate to more extended periods of calcite precipitation, this may be indicative of a greater flux of

humidity and evaporation that can be best explained by surface exposure. This is in agreement with the earlier suggestion that the gravel bar deposit may have been exposed for a long period of time, permitting different episodes of hominin activity. A similar significant spike in the presence of calcium carbonate occurs at 1.5m, marking the transition between the upper deposits in which CaCO_3 comprises ca. 10% of sediments and the lower deposits where CaCO_3 is >30%. This is concordant with the presence of a thin pebble horizon at this level, which may have supported a stable land surface that was more resistant to erosion than pure dune sands. As a result, increased presence of calcium carbonate may relate to greater levels of surface evaporation forcing precipitation.

Similar proportions of calcium carbonates within sediments suggest they have been subject to similar conditions and durations of carbonate precipitation, and step changes in % CaCO_3 may therefore indicate breaks in periods of calcite formation. Such a step increase occurs at 2.6-2.7m in Stratum 3, and potentially at 3.4m within Stratum 4. Both occur within sediment horizons, rather than at context boundaries, and may indicate a hiatus in sediment deposition where the depositional environment does not change. In the first instance, two phases of aeolian deposition may be inferred within S3, which is further supported by grain size analysis. The second case is less clear, due to more fluctuation in carbonate levels in Stratum 4 and 5 and the influence of fluvial activity upon their development.

The stable isotope record of pedogenic carbonates at KAT1 appear to record two environmental signatures, and two periods with either heavily enriched or dispersed results. Below 3.25m, the isotopic record preserves the signature of nearly purely C_4 vegetation at the site, with slightly more enriched $\delta^{18}\text{O}$ potentially indicating more evaporative conditions. The results from 2.75-3.25m are dispersed, and become increasingly split between more evaporative/higher % C_4 and less evaporative/lower % C_4 with depth. Between 1.85-2.75m more depleted $\delta^{13}\text{C}$ results indicate a greater presence of C_3 vegetation, with oxygen isotopes

slightly more depleted than the deeper levels suggesting less evaporative conditions. In contrast, between 1.38-1.85m strongly enriched oxygen and carbon results occur, indicative of C₄ dominated flora and enhanced evaporation.

Two different interpretations of these data can be made. The simpler explanation of these patterns would suggest a more evaporative and C₄ dominated environment existed during and immediately after the deposition of coarser fluvial sediments (i.e. >60ka), with decreased evaporation and increasing C₃ presence occurring through much of the fine fluvial/aeolian sequence (<60ka) and a spike in evaporation and C₄ dominance at the top of S3 relating to the scouring of the landscape (<16ka). However, this may not account for the impact of unrepresentative isotopic results due to increased atmospheric mixing at an exposed surface and directly relating the environmental conditions suggested by isotopic study with the sediments from which the samples are derived may be too simplistic.

A more complex interpretation of this data suggests that the hiatus in sediment accretion observed in Stratum 3 at ca. 2.5m depth presented a relatively stable land surface. The dispersion of isotopic results directly beneath this level may be indicative of the impact of increased atmospheric mixing, and the strong C₄/evaporative signal below preserving a more accurate picture of environmental conditions ca. 60ka. A similar scenario could be posited for the scoured, pebble lined upper surface of Stratum 3, with the heavily enriched results ca. 1.5m indicating some impact of surface proximity, indicating a less heavily C₄ dominated and evaporative environment occurring after this event. However, as the paired results are consistently enriched, an alternative explanation could be that these carbonates formed while a greater depth of aeolian sediment overlay the pebble horizon, thus presenting an accurate picture of environmental conditions for a period from most sedimentary evidence had been subsequently deflated. If such interpretations are correct, this would indicate that the isotopic record from KAT1 only relates to the aeolian environments at the site, and sampling and

analysis of larger carbonate nodules at a sub-nodule scale would be required to provide evidence for earlier environmental conditions.

Pleistocene Landscapes at Katoati

The foregoing discussion provides an immediate site formation context for the analysis and interpretation of the lithic assemblages from KAT1. Synthesising this with earlier observations from Katoati will permit a broader and more detailed picture of sedimentary and environmental history in this area, presenting the wider landscape in which hominin activities were embedded (see Figure 7.28).

There is no clear indication of a hominin occupation at Katoati prior to the uplift of the Jayal boulder beds, although poor chronological resolution of the period of existence of the powerful fluvial regime responsible for the boulder horizon, their subsequent tectonic uplift, and the production of the Lower Palaeolithic artefacts recovered from the excavations at Jayal and Chhajoli prevent a detailed discussion. The application of cosmogenic nuclide dating in the future would provide some means to resolve these issues, as this technique is well suited to both the materials available and the potential timescale under consideration.

The degree of cementation of calc-pan deposits suggest they have undergone a greater level of post-depositional change than the fluvio-aeolian deposits that have undergone more detailed study here, potentially indicating a Middle Pleistocene antiquity. Further stratigraphic, geochemical and chronological studies of this layer would facilitate comparisons with other, similar features reported from Rajasthan (e.g. Achyuthan et al. 2007). If this horizon is comprised of calcretised floodplain facies, this may present a potential context for the recovery of archaeological assemblages with relatively high integrity.

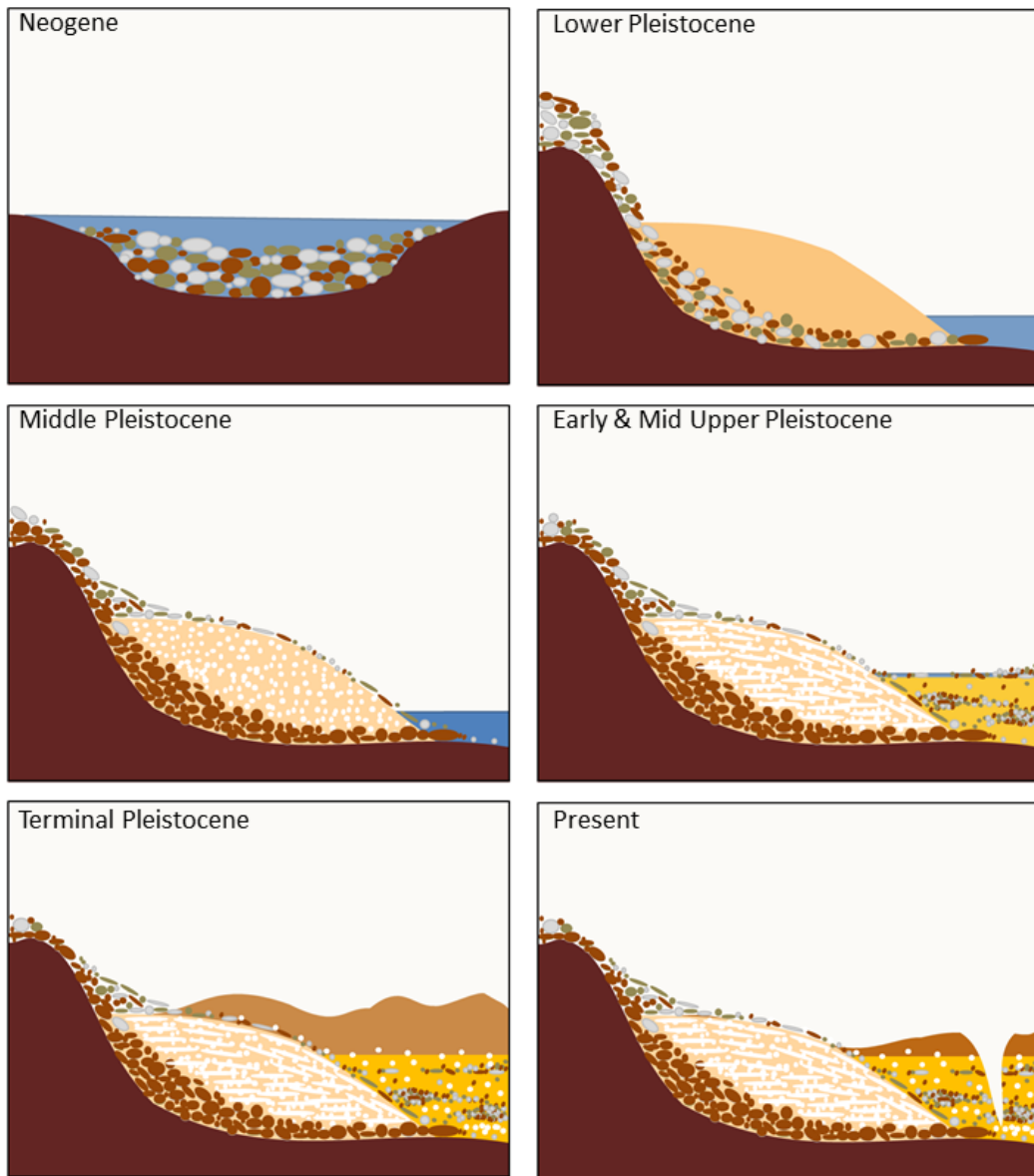


Figure 7.28: Schematic depiction of landscape development at Katoati: Top Left – existence of pre-Quaternary powerful fluvial system forming major boulder-cobble horizon overlying sandstone basement; Top Right – Tectonic uplift of sandstone basement alters depositional environment promoting deposition of overbank fine sediments; Middle Left – Weathering promotes ferricretisation of boulder horizon, while groundwater carbonate formation cements floodplain facies, making them resistant to erosion; Middle Right - Braided fluvial channels promote sedimentation, forming gravel and sand bars; Bottom Left – Aeolian deposition on top of fluvial horizons, with formation of pedogenic carbonates; Bottom Right – deflation of aeolian deposits and gullying of fluvio-aeolian horizons.

The exposure of bedrock at JFL2 suggest that any unconsolidated sediments relating to a Middle Pleistocene fluvial channel have since been eroded, and replaced by an Upper Pleistocene fluvial sequence, although upper age ranges of dates from JFL1 and JFL2 may indicate this phase of deposition began up to ca. 200ka. However, the majority of evidence from three dated sections indicates strong fluvial activity occurred during MIS 5, typified by the presence of braided channel deposits. The earliest clear evidence for the presence of hominins in the region is apparent in the occurrence of weather and rolled Lower Palaeolithic artefacts in the lowest fluvial sediments examined, suggesting they predate the development of fluvial facies. In comparison, a range of fresh, weathered and rolled artefacts were observed at all three sections with deposits dating to MIS 5, presenting clear evidence for hominin occupation during this period of enhanced humidity in the region.

Some evidence for fluvial activity during MIS 4 is presented at KAT1, whereas a mix of fluvial and dune deposits occur in MIS 3, suggesting intermittent humidity as well as aeolian activity. The presence of dated ostrich eggshells from >62ka provide the most oldest evidence for the appearance of ostrich in South Asia, and their presence is well attested throughout MIS 3. The arrival of large African fauna in the Thar Desert in MIS 4/MIS 3 may have significant implications for understanding broader patterns of biogeography and palaeoenvironmental change between Africa, South West and South Asia. Stable isotope analyses of ostrich eggshell appear to indicate a mixed C₃/C₄ diet, potentially indicative of both the dietary preference of ostrich for C₃ foliage due to higher water content as well as availability of C₄ foliage. Similar patterns of floral availability may have been critical to the eastward dispersal of ostrich.

The lack of sedimentary deposits dating from late MIS 3 and early MIS 2 suggest that either there was insufficient aeolian or fluvial activity to mobilise sediments, or that sediment deposits from this period have been eroded or deflated prior to the renewed onset of deposition ca. 20ka. The terminal Pleistocene and early Holocene present further evidence for

aeolian activity in the three dated sections, and microlithic artefacts have been observed within the lower parts of these deposits, suggesting the return of hominin groups to region following the LGM. Subsequent erosion of the fluvio-aeolian landscape within the Holocene is likely to explain the current configuration of the sedimentary deposits at Katoati.

Despite some winnowing of the smallest debitage, the majority of assemblages preserve sufficient numbers of fresh artefacts that can be correlated with the geochronology developed at KAT1. As a result, diachronic trends in lithic production can be assessed, and a range of explanation for variability can be examined. Given the presence of archaeological assemblages from KAT1 relating to fluvial activity in MIS 5 (S5, S6 and S8), less energetic fluvial activity in MIS 4(S4) and aeolian deposition in MIS 3 (S3a and S3b), some variability observed may be a response to different palaeoenvironmental conditions and available resource structures. As the site location within the landscape and availability of raw materials can be considered to have remained relatively similar, it is unlikely that these will explain much, if any variation between the archaeological assemblages. However, how the site and resources were integrated into broader seasonal rounds may have differed in response to palaeoenvironmental changes. Some variability between assemblages may be the product of demographic factors such as population size, and so relate to ability for hominins to exploit the range of floral and faunal resources available to them as well as technological adaptations to increase economic returns and environmental carrying capacities.

Chapter 8

Lithic Assemblages at Katoati

The sedimentary profile at Katoati, presented in the preceding chapter, provides a well dated context for the interpretation of the lithic assemblages. Three assemblages, S4, S6 and S8, do not appear to have undergone significant post-deposition modification. Due to the large sample size and their chronological assignment, these assemblages offer a unique opportunity to evaluate technological change through time in the Thar Desert. The objective of this chapter is to present the results of typological and technological analyses of the assemblages from Katoati (KAT1). Firstly, raw material use and overall assemblage composition divided by excavated strata will be discussed. Secondly, the analysis of typological and metric variability of cores, flakes, all retouched artefacts (flakes and flaked pieces) and heavy tools will be presented. Univariate description of the artefacts discussed in the text includes all strata; complete descriptive statistics are presented in Appendix C. Bivariate comparative analyses are focused upon the three largest assemblages, S4, S6 and S8, which appear to share similar site formation histories as outlined in Chapter 7. Significant results of statistical testing are discussed in the text, while test values are presented in Appendix C. Following this, the analysis of typological and metric variability of artefacts structured by excavated strata will be presented. Finally, an evaluation of the reduction activities present at the site will be undertaken, in order to characterise the lithic assemblages and relate them to interpretations of hominin behaviour, as set out in Chapter 3.

The Lithic Assemblages

A total of 1519 lithic artefacts were recovered from the excavations at KAT1. These artefacts are predominately produced from quartzites (96%) that are immediately available at the site, and are abundant in the Katoati landscape. A low number of quartz (n=50), chert (n=5) and sandstone (n=2) artefacts are present, and these materials are also locally available. A single limestone artefact, a pointed flake, presents the only clear evidence for the introduction of a raw material that is not immediately available at the site, suggesting that it has been imported to and discarded at the site. Preliminary statistical testing identified no significant differences in raw material use by gross artefact type (i.e. core, flake, flaked piece or heavy tool), artefact size or by excavated strata. As a result, raw material use has been excluded from further examination of lithic artefact variability within the KAT1 assemblages.

A typological categorisation of the artefacts from KAT1 is presented in Table 8.1, dividing the artefacts into gross types (i.e. core, flake, flaked piece or heavy tool) used for metric analysis, sub-types, as well as by strata and whether artefacts are complete or broken. The proportions of gross artefact types between strata are presented below. This is followed by more detailed discussion of sub-types of artefacts divided by cores, flakes, flaked pieces, retouched artefacts and heavy tools.

Statistically significant differences in gross assemblage composition are apparent between the strata (Table C.1; C.2). The appearance of a low number of heavy tools in S8 and a single heavy tool in S5 are particularly notable, marking the presence of a distinct gross category of artefact type. Significant differences remain when the ratio of cores, flakes and flaked pieces are compared by strata. Post-hoc testing identifies S4, S6 and S8 to include a significantly larger proportion of flakes and cores, with fewer flaked pieces, than S3a. A further significant

difference occurs in the proportion of retouched to un-retouched artefacts (flakes and flaked pieces), indicating a larger proportion of retouched pieces in S4 compared to S8.

Type	S3a	S3b	S4	S5	S6	S8	TOTAL
Core	1	0	3	0	4	0	8
Single Platform	6	0	41 (1)	8	57 (3)	42 (2)	154 (6)
Bidirectional	0	0	5	2 (1)	4	1 (1)	12 (2))
Multi Platform	1	0	21	3	31 (2)	17	73 (2)
Prepared			7	5	12 (2)	4	28 (2)
TOTAL CORES	8	0	77	18	108	64	275
Flake	24 (1)	3	230 (2)	23	340 (3)	165	785 (6)
Bipolar Flake	0	0	14	0	3	5	22
Redirecting Flake	0	0	1 (1)	1	1	0	3 (1)
Flaked Piece	25	5	73	16	125	73	317
TOTAL UN-RETOUCHED	49	8	318	40	469	243	1127
Single End	0	0	4	0	5	0	9
Single Side	1	0	13	2	13	4	33
Single Side (FP)	0	0	0	0	2	2	4
Single End Single Side	0	0	3	0	12	1	16
Single End Single Side (FP)	0	0	0	0	1	0	1
Single End Double Side	0	0	3	1	6	4	14
Double Side	0	0	9	0	5	1	15
Double End Double Side	0	0	0	0	2	0	2
Unspecified	0	0	1	0	3	1	5
Unspecified (FP)	0	0	9	0	1	0	10
TOTAL RETOUCHED	1	0	42	3	50	13	109
Heavy Tool	0	0	0	1	0	7	8
TOTAL	58	8	437	62	627	327	1519

Table 8.1: Basic typology of artefacts from each stratum at KAT1. Counts in brackets indicate the number of blades present.

Cores

A total of 275 cores have been recorded in the Katoati assemblages, including 256 complete specimens, appearing in all strata except for S3b. Firstly, the typology of cores from KAT1 will be discussed. A univariate description of all complete cores is then presented in four groups:

reduction strategy, core size and shape, platform characteristics and last scar characteristics. Subsequently, the results of bivariate analyses are set out, illustrating patterns of variability in core attributes structured by type, platform type and preparation, and last scar termination type. Finally, variation in core attributes between S4, S6 and S8 will be evaluated.

Typology

The majority of cores are relatively informal, exploiting a range of pebbles/cobbles, large flakes and flaked pieces to produce large numbers of single and multi-platform. Far fewer bidirectional cores are present, and most of these also appear informal. A few blade removals are recorded from these informal cores. However, there is no evidence to suggest that these are the result of intentional preparation of the flaking surface, such as organisation of longitudinal arises.

A low number of cores present evidence of more formal preparation of core flaking surfaces. This group comprises two bidirectional cores and the twenty-seven prepared cores, which includes three discoidal and thirteen Levallois (*sensu lato*) cores. A single bidirectional core from S5 exhibits a number of bidirectional flake removals that have produced a number of longitudinal arises. As the last flake scar is blade-proportioned, the organisation of longitudinal arises may have resulted from repeated blade removals.

The prepared cores are differentiated from multi-directional cores due to the presence of previous flake removals that have shaped the flaking surface from which the last flake has been removed. However, the lack of either a clear 'plane of intersection' between bifacial worked core surfaces or percussion perpendicular to this axis, centripetal reduction or sufficient reduction to control flaking surface convexities prevent the categorisation of many of these artefacts as either discoidal or Levallois cores. These artefacts have been discarded before meeting criteria set by archaeologists for formal 'types', although whether this is the

result of aborted attempts to produce these 'types', or because no further reduction was necessary, practical or possible is unclear.

A range of Levallois reduction strategies are apparent amongst the KAT1 assemblages, including cores with unidirectional, bidirectional, perpendicular and radial/centripetal flaking patterns. Two examples of a unidirectional core are present. The first, from S6, has two convergent prior removals forming a medial ridge, however the last flake scar has a stepped termination. The second, from S4, also has two convergent prior removals. As the last flake scar extends to the end of the flaking face, no medial ridge is now evident. However, given the scale of the artefact, it can be anticipated that the intersection of the previous convergent removals may have also created a medial-distal ridge.

Bidirectional flaking patterns are most common amongst Levallois cores, accounting for six artefacts. The most simple of these exhibits numerous proximal removals, including the last flake scar, with a single distal removal present (Figure 8.1a). Two cores, one from S8 and the other from S6, present convergent proximal scars with distal scars directed to a single side of the core (Figure 8.1b & 8.1f). One of these cores exhibits a medial-distal ridge, with a stepped final termination. One bidirectional core, from S5, presents a single proximal flake scar opposite two convergent distal scars that form a medial-distal ridge (Figure 8.1d). The final flake scar has removed the majority of the left margin. Two further examples, from S4 and S5, present two/three proximal flake scars and three divergent distal scars, both of which present a steep medial-distal ridge (Figure 8.1c & 8.1e).

Four cores present opposed scar patterns, combining distal and side scars. The first of these cores, from S6, has two parallel distal scars with a single sideways removal from the right side; the left margin has been removed by the last scar (Figure 8.2a). The second, from S4, has three divergent distal scars and a single sideways scar originating from the left side (Figure 8.3a). The

third, from S8, exhibits two divergent distal flake removals with a single sideways removal

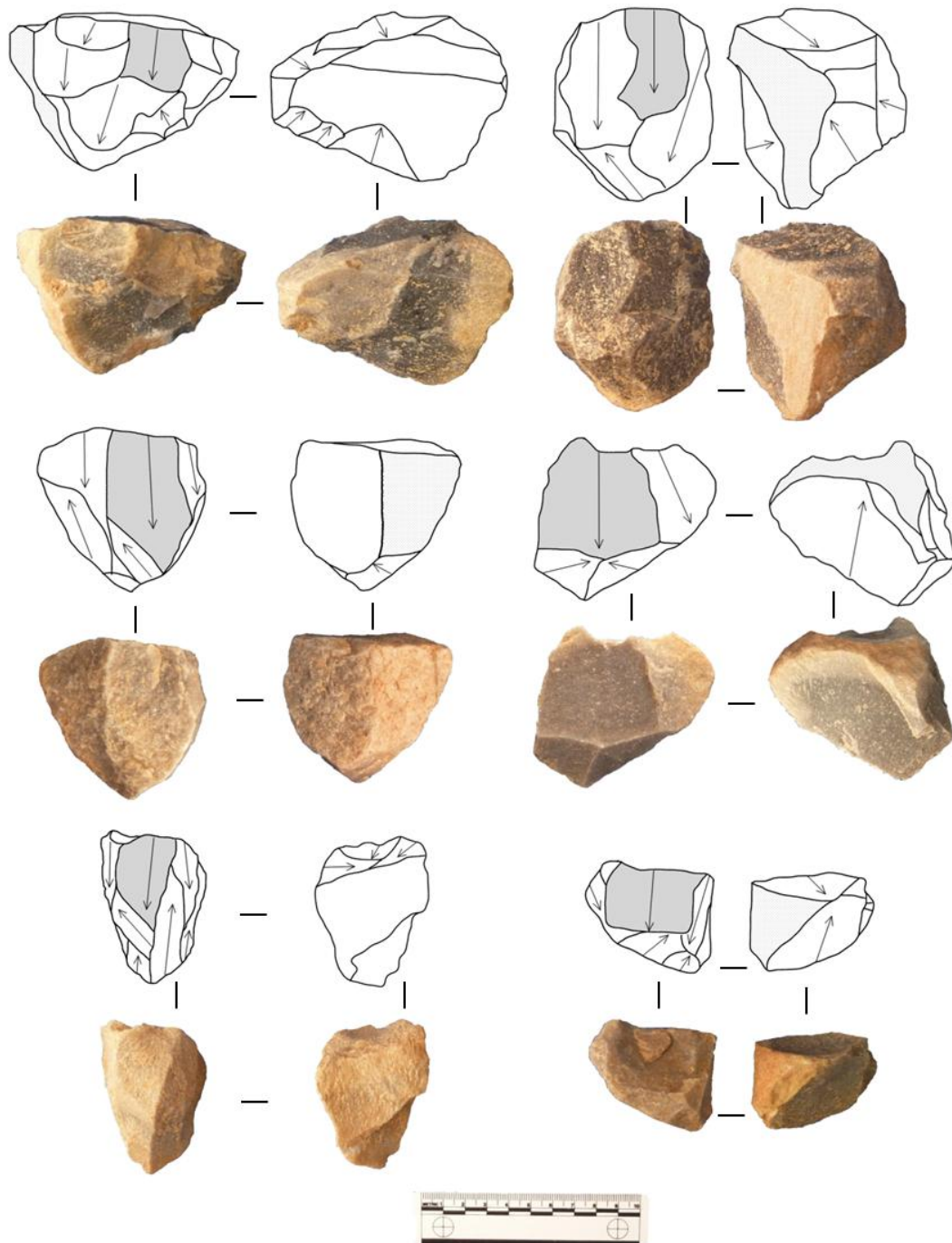


Figure 8.1: Levallois Cores: a) S8 - unidirectional (top left); b) S8 - convergent proximal and distal (top right); c) S5 proximal and divergent distal (middle left); d) S5 - proximal and convergent distal (middle right); e) S4 - proximal and divergent distal (Nubian Type 1-like) (bottom left); f) S6 -convergent proximal and distal (bottom right).

from orientated from medial to the left margin (Figure 8.3b). The fourth core, from S4, presents three convergent distal scars with a further sideways scar originating from the left side (Figure 8.2b). Whereas the last scar on the first of these cores is a large and broadly square, covering the majority of the flake surface, the latter three last scars are substantially smaller, covering roughly 1/3 of the flake surface with convergent margins.

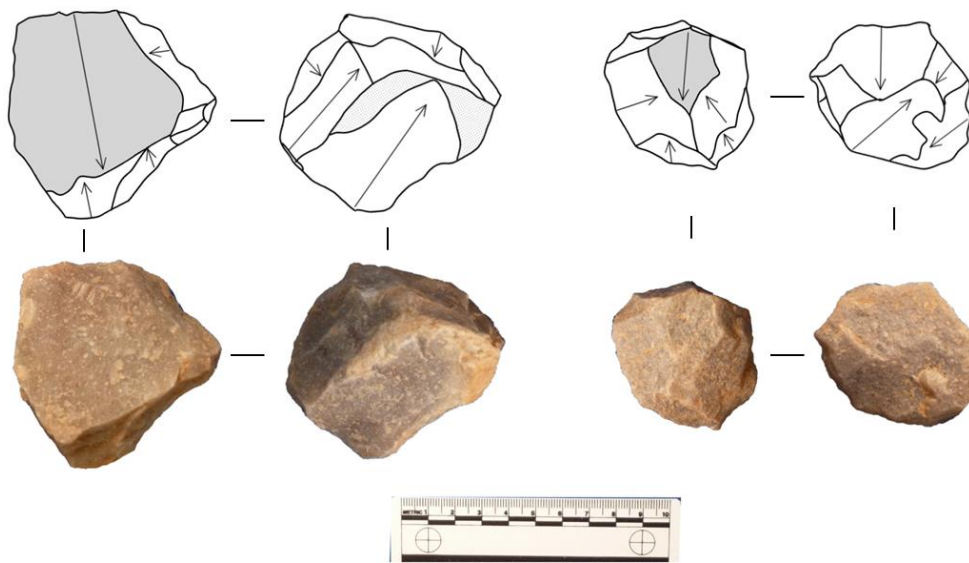


Figure 8.2: Levallois cores: a) S6 - distal and lateral (left); b) S4 - proximal and lateral convergent (Nubian Type 2-like) (right).

Four cores present radial scar patterns. The first two, from S6 (Figure 8.4) and S8 (Figure 8.5a) present proximal, distal and sideways flake scar, while the third exhibits removals from distal and both sides. These cores have produced squared or rectangular last scars covering at least half of the flaking surface. A single recurrent, centripetally flaked core is present in S6 (Figure 8.5b).

The last flake scars on these Levallois cores fall into three broad groups. Firstly, a number of last scars are broadly square in shape and cover much of the core's flaking surface. In these instances, the preparation of the flaking surface may have facilitated the production of large scars relative to the core. In two cases, the final flake scars have parallel edges and are

elongate to blade-like proportions, even though one exhibits a stepped termination. These may indicate intentional production of elongate flakes, but are not characteristic of systematic blade production, matching patterns observed in the flake population (see below). Finally, a recurrent trend amongst the unidirectional, bidirectional and perpendicular flaking patterns is the appearance of pointed flake removals and a medial-distal ridge. This combination suggests the preparation of the flaking surface to produce pointed flakes.

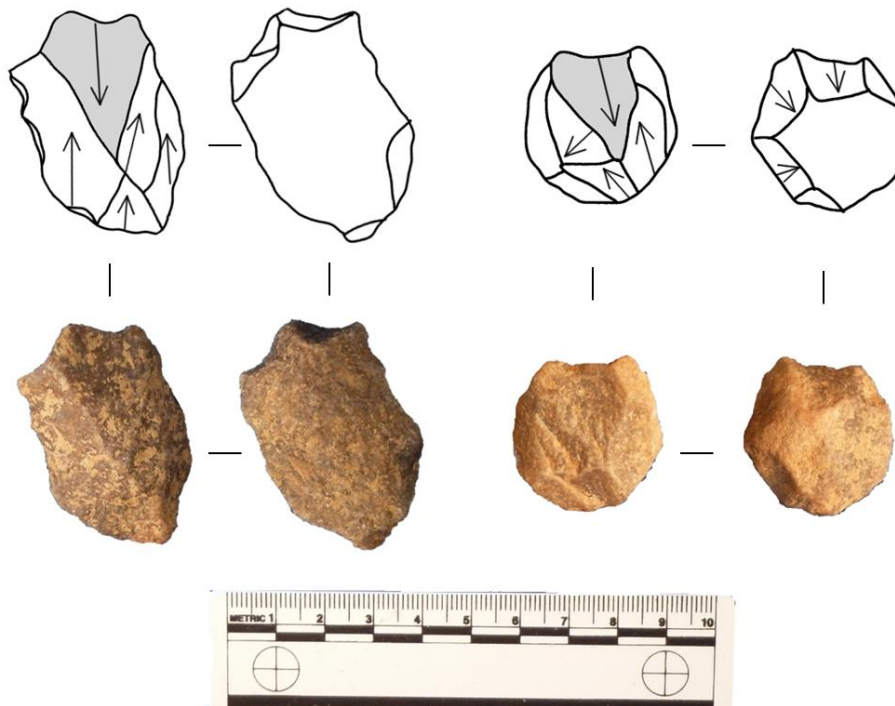


Figure 8.3: Levallois cores: a) S4 - distal divergent and lateral (Nubian Type 1/2-like) (left); b) S8 - distal divergent and lateral (right).

Univariate Description

Univariate descriptive statistics for core attributes are presented in Table C.3.

Reduction strategy

Over half of the cores are classified as single platform cores (56%), with multi-platform cores comprising roughly one quarter of the total (26%). Prepared cores, including Levallois and

discoidal cores, comprise 10% of the total, with a low proportion of bidirectional cores (4%) and uncategorised cores (3%) present. The majority of cores have not been rotated (64.4%),

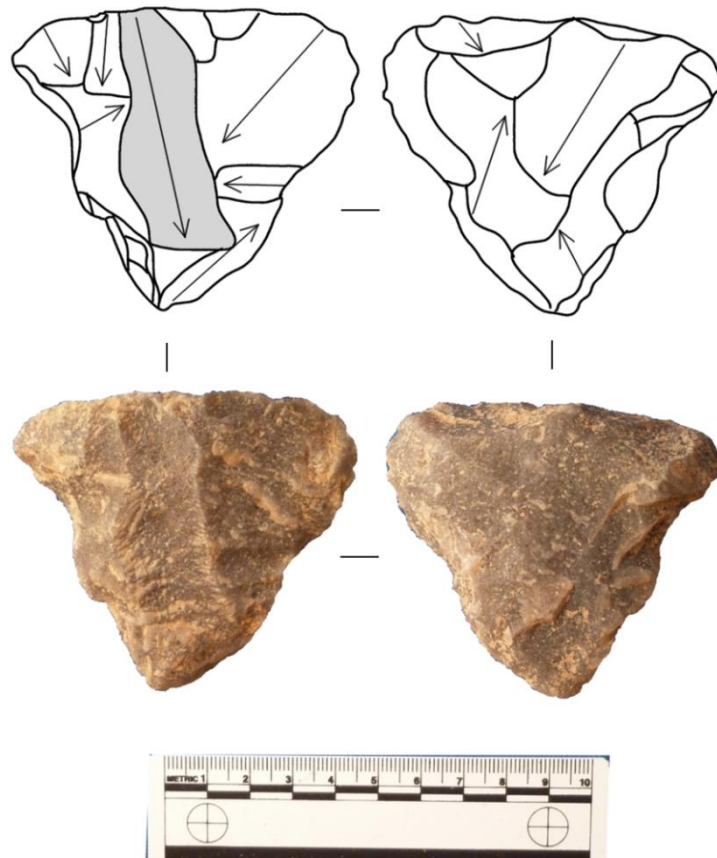


Figure 8.4: Radially flaked Levallois core from S6.

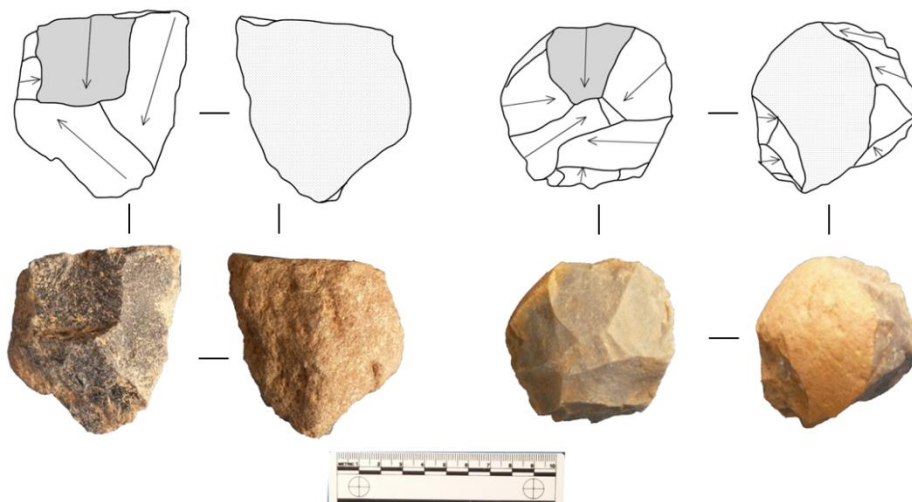


Figure 8.5: Levallois Cores: a) S8 - radial (left); b) S6 - recurrent centripetal (right).

with a substantial proportion (26.8%) exhibiting a single rotation of flaking axis. A low number of cores have undergone numerous rotations in flaking axis: 14 (5.6%) cores have been rotated twice, 6 (2.4%) cores have been rotated three times and 2 (0.8%) have been rotated four times. Most cores (40.3%) exhibit a single scar larger than 1/3 core length, with a substantial proportion of cores exhibiting two (24.5%), three (11.9%) and four (10.3%) scars. A low number of cores exhibit five (5.9%) and six (2.8%) scars, with the remaining 4.3% of cores exhibiting between seven and eleven scars. Cortical coverage on cores ranges from 0-90%, with a mean of 31% and interquartile range of 10-50%.

Core Size and Shape

A wide range in core sizes is present, illustrated by maximum dimension (23mm-147mm), with 50% of cores falling between 48-81mm. When orientated by flaking axis, mean core size (LxWxT) is 43x53x35mm, with 50% of cores ranging from 30-54mm (axial length), 37-64mm (axial medial width) and 24-43mm (medial thickness). However, the range of axial dimensions is large, from 6-15mm to 102-141mm across axial length, axial medial width and medial thickness. The distal thickness of cores is slightly smaller, ranging from 5-96mm, with an interquartile range (IQR) of 16-24mm. The proximal shape of cores is typically straight (mean=0.97; IQR=0.85-1.07) whereas distal shape is regularly tapered (mean=1.37; IQR=1.17-1.52). Wide variation in core elongation is observed, ranging between 0.28-2.56, although the majority of cores have a shorter flaking axis to width (IQR=0.59-1.07). Core flatness ranges from 0.51-4.97, with at least 50% of cores wider than they are thick (IQR=1.15-2.07).

Platform Characteristics

Both platform width (10.6-143.5mm) and platform depth (2.3-103.1mm) show an extreme range in size that parallel overall core size. However, the interquartile range of platform width

(36-62mm) and depth (19-41mm) suggests such proportions are uncommon. This is corroborated by the size corrected platform area, indicating that on average platform surface area is approximately half the core surface area (mean=0.5), and the interquartile range (0.35-0.67) suggests platform surface area regularly falls between 1/3-2/3 of core surface area. Platform shapes vary considerably ranging from narrow and thick (0.21) to very wide but thin (19.49). However, the interquartile range (IQR=1.23-2.25) suggests that platforms are typically twice as wide as they are thick. Single conchoidal platforms are most common, accounting for 40% of recorded types, followed by cortical (25%) and plain types (21%). Multiple conchoidal (10%) and dihedral (3%) are relatively uncommon. A single instance of a crushed platform (<1%) is present. Platform preparation is very limited, with only 12 instances of faceting (5%) and 3 occurrences of overhang removal (1%). The overwhelming majority of platforms (94%) exhibit no preparation. Although six examples (2.4%) of cores with 4 exploited platform quadrants are present, 68% of cores exhibit only a single exploited platform quadrant and 24.1% exhibit two exhibited platform quadrants; 5.5% of cores have three exploited platform quadrants.

Last Scar Characteristics

The last scar face length of cores closely matches the size of the axial core length, indicating flaking face typically comprises the entire axial surface. Last scar lengths range from 11-74mm, with an interquartile range of 22-40mm. Last scar widths closely match this, with a range between 11-78mm, and 50% of scar widths ranging between 24-39mm. On average, last flake elongation indicates relatively squared flakes were removed (mean=1.1; IQR=0.78-1.35). Only 13 last scars present blade-proportioned flake removals, with a maximum elongation of 3.3. A large proportion of last flake scars exhibit feather terminations (77.3%), with step terminations

accounting for 14.9%. A low frequency of axial (5.9%) and hinge (2%) terminations are observed.

Bivariate Analyses

The results of bivariate Kruskal-Wallis tests of core attributes are presented in Table C.4.

Core type

A number of trends are apparent from the attribute analysis of cores structured by core type (Figure 8.6a). Significant results of pairwise post-hoc Mann-Whitney tests of core type attributes and reported in Table C.5. With regards to the number of core rotations multi-platform cores (mean=1.2) have been rotated more than prepared cores (mean=0.89), and multi-platform, prepared and bidirectional cores (mean= 0.9) have all been rotated more than single platform cores (mean=0). Both multi-platform and prepared cores exhibit up to 4 core rotations. Single platform cores also exhibit fewer scars (mean=1.65) than multi-platform (mean=3.4), bidirectional (mean=3.8), and prepared cores (mean=4.21) (Figure 8.6b).

However, all core types include an example with either 9 or 10 scars present. Cortical coverage of prepared cores (mean=10.5%; range=0-30%) is significantly lower than either Multi-Platform (mean=28.7%; range=0-80%) or Single Platform cores (mean=35.1%; range=0-90%).

Prepared cores exhibit a greater maximum width (mean=58.7mm; range=50.8-65.7mm) than single platform cores (mean=45.9mm; range=19.6-84.6mm), resulting in a similar pattern for surface area. The axial length of prepared cores (mean=54.8; range=18.8-84.9mm) are larger than multi-platform cores (mean=44.6mm; range=17.7-80.4mm), which are both larger than single platform (mean=38.9mm; range=13.1-116mm) cores. Prepared cores are significantly flatter (mean=2.18; range=1.03-4.04) than both multi-platform (mean=1.49; range=0.55-3.06)

and single platform cores (mean=1.69; range=0.51-3.96). Beyond this, there are no significant differences in core size and shape between core types (e.g. Maximum length [Figure 8.6c]).

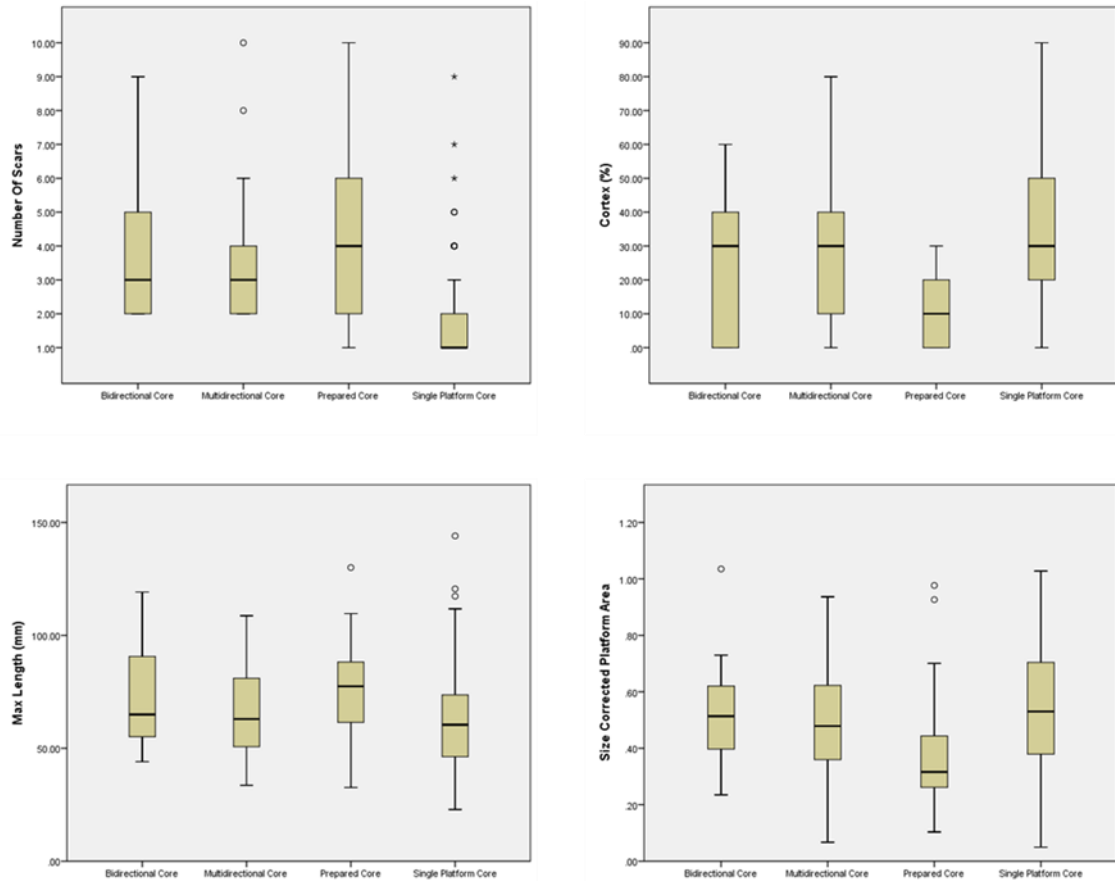


Figure 8.6: Boxplots of core attributes separated by core type; a) number of scars (top-left); b) cortex (%) (top-right); c) maximum length (bottom-left); d) size corrected platform size (bottom-right).

Two significant differences in platform size and shape occur. The shape of platforms on prepared cores are wider and thinner (mean=2.39; range=1.34-4.31) than those on either multi-platform (mean=1.92; range=0.58-14.3) or single platform (mean=1.85; range=0.21-6.57) cores. Single platform cores exhibit a larger ratio of platform surface area to core surface area (mean=0.54; range=0.05-1.03) than prepared cores (mean=0.4; range=0.1-0.98), although no overall difference in core size attributes occurs (Figure 8.6d).

Single platform cores present less elongate last scars (mean=1.04; range=0.27-3.3) than multiple platform cores (mean=1.21; range=0.52-2.27). In addition, single platform cores have a shorter last scar face length (mean=38.7mm; range=14.57-115.6mm) than either multi-platform (mean=44m; range=18.6-77.9mm) or prepared cores (mean=55.4; range=16.9-89.3mm). However, no difference in last scar length or width is evident.

Platform Type

Significant results of pairwise post-hoc Mann-Whitney tests of core platform type attributes and reported in Table C.6. Cores with cortical platforms exhibit a greater percentage of overall cortex coverage (mean=43.6%; range=0-90%) than cores with plain (mean=26.1%; range=0-80%), single conchoidal (mean=29.6%; range=0-80%), dihedral (mean=20%; range=0-40%), and multiple conchoidal (mean=15.9%; range=0-70%) platforms (Figure 8.7a). In addition, cores with single conchoidal platforms exhibit greater cortical coverage than cores with multiple conchoidal platforms. A greater number of core rotations is present on cores with multiple conchoidal (mean=0.9; range=0-3) and single conchoidal platforms (mean=0.6; range=0-4) than either plain (mean=0.19; range=0-2) or cortical platforms (mean=0.29; range=0-3). A similar pattern is evident for the number of scars present, with multiple conchoidal (mean=3.67; range=1-8) and single conchoidal platforms (mean=2.84; range=1-10) present on cores with a greater number of removals than either plain (mean=1.8; range=1-9) or cortical platform cores (mean=1.95; range=1-9).

A range of significant differences in core size and shape occur with respect to platform type. The maximum length and width of single conchoidal platform cores (length mean=68.5mm; range=32.6-130mm; width mean=51.5mm; range=26.9-90.8mm) are larger than plain platform cores (length mean=57.9mm; range=22.9-119.2; width mean=42.6mm; range=19.6-84mm) (Figure 8.7b). The surface area of plain platform cores (mean=2722mm²; range=503-

11809mm²) are smaller than both cortical platform (mean=3656mm²; range=755-11726mm²) and single conchoidal platform cores (mean=3773mm²; range=980-11809mm²) (Figure 8.7c).

The axial length of cores with plain platforms (mean=36.2mm; range=13.1-69.5mm) are smaller than those with cortical (mean=47.8mm; range=16.4-116.2mm) and multiple conchoidal platforms (mean=49.7mm; range=15.9-84.4mm), and the latter are also larger than cores with single conchoidal platforms (mean=40.6mm; range=15.9-84.9mm).

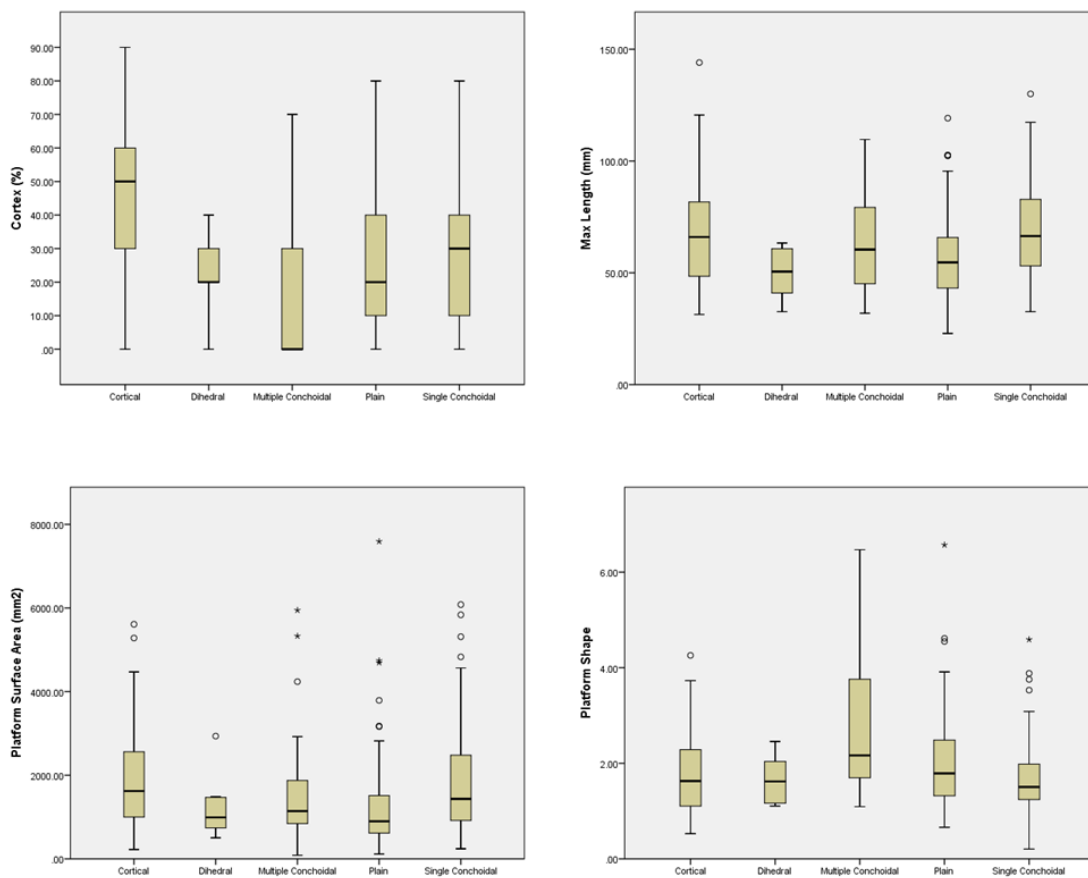


Figure 8.7: Boxplots of core attributes separated by platform type: a) cortex (%) (top-left); b) maximum length (top-right); c) platform surface area mm² (bottom left); d) platform shape (bottom right).

Multiple conchoidal platform cores are more elongate (mean=1.08; range=0.47-1.36) than either plain (mean=0.81; range=0.36-1.56) or single conchoidal platform cores (mean=0.78; range=0.32-0.7) (Figure 8.7d). With regards to proximal core shape, plain platform (mean=1.01;

range=0.63-1.39) and single platform (mean=0.99; range=0.6-1.66) cores are straighter than cortical platform cores (mean=0.91; range=0.47-1.38), which have more expanding margins.

The platform depths of cores with cortical (mean=34.8mm; range=7.75-103.1mm) and single conchoidal (mean=35.1mm; range=10.4-85.5mm) platforms are greater than both plain platform (mean=26.6mm; range=5.8-87.8mm) and multiple conchoidal platform (mean=25.3mm; range=3.65-63.5mm) cores. As a result, the surface area of cortical (mean=1975mm²; range=224-10082mm²) and single conchoidal (mean=1919mm²; range=241-6081mm²) cores is larger than that of plain platform (mean=1393mm²; range=115-7592mm²) cores. Multiple conchoidal platform shapes are wider and thinner (mean=3.38; range=1.09-14.13) than single conchoidal platforms (mean=1.66; range=0.21-4.59) and cortical platforms (mean=1.78; range=0.53-4.26). A greater number of platform quadrants are exploited on single conchoidal platforms (mean=1.58; range=1-4) compared to cortical platforms (mean=1.19; range=1-4).

The only significant difference between platform types relating to last flake scar characteristics is that both cortical (mean=45.6mm; range=16.2-115.6mm) and multiple conchoidal platform cores (mean=47.9mm; range=17.3-89.3mm) have larger last scar face lengths than plain platform cores (mean=35.9mm; range=16.6-68.8mm).

Platform Preparation

Bivariate attribute analysis structured by platform preparation is problematic due to the high frequency of unprepared platform types, although a number of significant relationships can be identified. Significant results of pairwise post-hoc Mann-Whitney tests of core platform preparation attributes and reported in Table C.7. Cores with faceted platforms have undergone more core rotations (mean=1; range=0-2) than unprepared platforms (mean=0.44; range=0-4). Faceted platform cores are thinner (mean=22.2mm; range=10-35.9mm) than

unprepared cores (mean=35.5mm; range=8.8-102.6mm), leading to a higher flatness index (faceted mean=2.73; range=1.8-4.97; unprepared mean=1.64; range=0.51-3.96). Faceted platform shapes are wider and thinner (mean=3.63; range=1.53-6.47) than unprepared platforms (mean=1.88; range= 1.8772). Unprepared platforms areas are larger relative to core surface area (mean=0.52; range=0.06-1.04) than faceted platforms (mean=0.32; range=0.05-0.8).

Last Scar Termination

Significant variation in the number of scars on cores occurs with regards to last scar termination type. Significant results of pairwise post-hoc Mann-Whitney tests of core termination type attributes and reported in Table C.8. Cores with axial terminations have fewer scars (mean=1.09; range=1-2) than cores with feather (mean=2.36; range=1-10), step (mean=3.45; range=1-10) and hinge (mean=4.4; range=1-10) terminations. In addition, cores with step terminations have more scars than those with feather terminations.

Across all core size variables, cores with step (e.g. surface area mean=5152mm²; range=1378-10203mm²) terminations are larger than those with feather terminations (e.g. mean=3175mm²; range=503-11809mm²). Cores with axial terminations have smaller axial distal widths (mean=36.7mm; range=18.2-61.9mm) than those with step terminations (mean=50.9mm; range=20-88.9mm).

Step terminations occur on cores with a larger number of exploited platform quadrants (mean=1.65; range=1-3) than those with axial terminations (mean=1.09; range=1-2). Cores with step terminations have larger platforms widths (mean=63.1mm; range=24.2-113.3mm) than those with feather terminations (mean=48.9mm; range=18.9-143.5mm).

Cores with axial terminations have larger last scar widths (mean=45.5mm; range=23.8-77.8mm) than those with feather terminations (mean=30.6mm; range=11.6-77.8mm), resulting in a similar pattern for last scar surface area. Equally, cores with step terminations also have smaller last scar surface areas (mean=960mm²; range=234-2190mm²) than cores with axial terminations (mean=1943mm²; range=437-4340mm²). Finally, step terminations occur on cores with a larger last scar face length (mean=54.3mm; range=16.3-115.6mm) than on cores with feather terminations (mean=39.5mm; range=14.6-94.3mm).

Diachronic Variability

Examination of core attribute variability structured by excavated strata amongst the three largest assemblages, S4, S6 and S8, has identified no significant differences across every analysed attribute (Table C.9). No differences in scalar and ordinal attributes are apparent, and as the majority of cores from KAT1 derive from these three horizons, no substantial differences occur with the all complete cores from the site as described above. The relative proportions of different core types are equal (Table 8.2), as are platform types (Table 8.3), presence of platform preparation (Table 8.4) and last scar termination types (Table 8.5). This indicates that core attribute variability is structured within and not between the strata.

	Single Platform	Bidirectional	Multi-Platform	Prepared	Total
S4	40	5	18	5	68
S6	57	4	29	11	101
S8	39	1	17	4	61
Total	136	10	64	20	230

Table 8.2: Core types by stratum.

	Cortical	Dihedral	Multiple Conchoidal	Plain	Single Conchoidal	Total
S4	17	3	5	16	27	68
S6	24	3	11	23	40	101
S8	16	1	6	12	26	61
Total	57	7	22	51	93	230

Table 8.3: Core platform types by stratum.

	Faceting	None	Overhang Removal	Total
S4	5	62	1	68
S6	4	96	2	102
S8	0	61	0	61
Total	9	219	3	231

Table 8.4: Core platform preparation by stratum.

	Axial	Feather	Hinge	Step	Total
S4	5	55	0	4	64
S6	4	79	4	12	99
S8	2	41	1	13	57
Total	11	175	5	29	220

Table 8.5: Core last scar termination type by stratum.

Summary

Core attribute variability offers a number of insights into reduction intensity and strategy at KAT1, although neither varies significantly between the three largest assemblages. The presence of a relatively high proportion of cores with cortical surfaces, including platform surfaces, supports the assertion that primary reduction was conducted at the site. This, combined with the high frequency of simple core types, appears to be based upon the exploitation of immediately available raw materials. This also explains the high upper range of sizes of cores present at the site. Although a range of significant size variability occurs amongst the cores, frequently the average difference is small (ca.10mm), indicating that statistical differences may have been identified due to the presence of the largest cores. The presence of Levallois core types suggests that some reduction sequences were conducted principally at the

site, although the export of some cores at earlier reduction stages is both possible and likely. The exploitation of cobbles at KAT1 for use as cores appears to be a common site use in all three main assemblages.

A number of patterns indicate the influence of reduction intensity upon core attribute variability. A common size range for core size, platform size and last scar sizes is 30-60mm, which may indicate a discard threshold. The ratio of platform size to core size is typically 1/3-2/3, which may be problematic to manage below this size threshold. Size differences indicate some impact of reduction intensity between cores with simpler morphologies (i.e. single platform; cortical/plain/single conchoidal platform). However, more reduced core types (multiple conchoidal/prepared; dihedral/multiple conchoidal platforms) are not smaller than the simpler cores, suggesting reduction intensity alone doesn't explain variability within this group. Aberrant terminations are rare, and typically occur on larger cores. The abandonment of these cores may not directly relate to a size-discard threshold, although management of the core to deal with the previous termination may have exceeded such a threshold.

The influence of flaking strategy is particularly apparent with regards to the prepared cores. Despite more intensive reduction, prepared cores are larger than other cores across a number of variables by up to 20mm. Prepared cores are typically flatter, with wider, thinner platforms that are relatively smaller in relation to core size. Including their typologically distinctiveness, these appear to mark particular reduction strategies that differ from more informal reduction evident across other core categories.

Other aspects of reduction strategy are also evident. Some simple cores appear to have undergone a greater degree of reduction than some more reduced core types, which may indicate differences in reduction strategy even amongst informal cores. Although rare, the use of faceting appears to have been employed to manage the relationship between the size of

platforms and flaking surface, and may indicate attempts to prolong reduction sequences. Cores with axial terminations are typically small but have yielded large flakes, which may reflect both increased reduction intensity and the use of increased force input to remove earlier flake scars from core surfaces.

Flakes

A total of 903 flakes have been recorded in the Katoati assemblages, including 608 complete flakes from all strata. A brief typological description of un-retouched flakes is presented (retouched flake typology is described separately below), and followed by a univariate description. Bivariate analyses examine variability in flake attributes with regards to dorsal scar pattern, termination type, platform type and platform preparation. In addition, a comparison of retouched and un-retouched complete flakes is presented to identify characteristics of blank selection. Finally, variation in flake attributes between S4, S6 and S8 will be evaluated.

Typology

Very limited typological diversity is evident amongst the flakes from KAT1, and variability amongst flakes is best described by the univariate description presented below. However, three types are worthy of further comment. Twenty-two bipolar flakes are present. These artefacts all preserve positive ventral features, although appear to be the result of splitting quartzite cobbles, and therefore mark the earliest reduction stages present at the site. Four redirecting flakes are present at KAT1, one of which has blade-like proportions and has been retouched. All four flakes preserve platform features on the dorsal surface, and offer an indication that some core-management strategies were employed at the site. Finally, three small (30-45mm length) Levallois points have been identified, one from S6 (Figure 8.8a) two

from S4 (Figure 8.8b & 8.8c). All three preserve steep, convergent margins formed by two or three flake scars, and a distal-medial ridge, although none exhibit clear evidence for platform preparation. Although a number of other pointed-flakes occur, showing contracting margins from the platform to distal tip, the organisation of flake scars on the dorsal surface offers equivocal evidence for the predetermination of flake shape.



Figure 8.8: Levallois points: a) S6 (left); b & c) S4 (middle; right).

Univariate Description

Univariate descriptive statistics for flake attributes are presented in Table C.10.

Reduction Strategy

The most common dorsal scar patterns present on complete flakes at KAT1 are proximal (24%) and cortical (17.9%). Sideways (15.6%), weakly radial (14.1%) and opposed/perpendicular

(13.4%) scar patterns occur in broadly equal proportions. Radial scar patterns are less common (8.6%), and distal (4.9%), and bidirectional (1.5%) scar patterns occur infrequently. Cortical coverage ranges from 0-100%, with 42.1% of flakes recorded with no cortex present, and 71.1% of flakes with less than 50% cortex present, resulting in a mean of 29.2%. Low frequencies of flakes with only cortical platforms (4%) and 100% cortical cover of dorsal and platform surface (3.8%) are observed. The majority of flakes present feather terminations (74%). Following this, axial terminations are most common (14.3%), with rarer occurrences of step (7.8%), outrepasse (2.8%) and hinge (1%) terminations.

Flake Size and Shape

Large size ranges are observed for both maximum length (9.7-127.6mm) and maximum width (8.5-91.5mm), although the interquartile range indicates 50% of flakes fall between 32-55.4mm maximum length and 22.3-38.7mm maximum width. Mean axial flake dimensions are 33.1x34.8x14.2mm, although both axial length and all three recorded axial widths range from <10mm to >90mm. The interquartile range indicates that 50% of flakes have an axial length of 22-40mm, a medial axial width of 23.2-43.6mm, and a medial thickness of 9.2-17.5mm. On average, flakes are as long as they are wide (mean elongation=1.02; IQR=0.73-1.26). A low number of blade proportioned flakes are present, with a maximum elongation of 2.54. Typical flakes are more than twice as wide as they are thick (mean flatness=2.6; IQR=1.98-3.15), with a maximum range of 0.76-6.84. Most flakes exhibit slightly expanding proximal margins (mean proximal shape=0.94; IQR=0.76-1.09), with a quarter of flakes exhibiting contracting proximal margins, leading to an upper proximal shape index of 1.73. In contrast, the distal shape index indicates that most flake exhibit contracting distal margins (mean=1.38; IQR=1.1-1.59). The highest distal shape index score is 2.89, indicating that the distal width is nearly 1/3 of the medial width.

Platform Characteristics

Single conchoidal platforms are the most common type (26.9%), followed by cortical (21.3%) and plain (19.2%) types. Multiple conchoidal (15.3%) and dihedral (14%) platforms occur in broadly equal proportion, with a low incidence of either punctiform (2.6%) and crushed (0.9%) platform types. Platform preparation is very rare, with 94.9% of platforms unprepared, 3.7% of platforms faceted, and 1.4% of platforms exhibit overhang removal. A wide range in platform size is evident, with platform width ranging from 5.4-99.4mm and platform depth ranging from 1.6-49.67mm. The mean platform size is 32.1x12.6mm, with interquartile ranges of 20.9-40mm x 7.7-16.1mm. The platform shape index indicates that platforms are typically elongate (mean=2.87), with over 75% of platforms twice as wide as they are thick. The size corrected platform area index indicates that most platforms sizes are equivalent to 20-40% of the flake surface area (mean=0.30; IQR=0.17-0.39), although a wide range is observed, from 0.01-1.02.

Bivariate Analysis

The results of bivariate Kruskal-Wallis tests of flake attributes are presented in Table C.11.

Dorsal Scar Pattern

Significant results of pairwise post-hoc Mann-Whitney tests of flake attributes by dorsal scar pattern and reported in Table C.12. The percentage of cortical coverage of flakes is significantly related to dorsal scar pattern. Cortical dorsal surfaces have the greatest amount of cortex (mean=85%; range=50-100%) of all types (Figure 8.9a). Proximal (mean=23.5%; range=0-90%), distal (mean=28.5%; range=0-90) and side (mean=31.3; range=0-90%) scar patterns preserve significantly more cortex than either opposed/perpendicular (mean=12.7%; range=0-80%) or weakly radial (mean=10.9%; range=0-70%) scar patterns, and all of these types, along with

bidirectional flakes (mean=20%; range=0-60%), preserve more cortex than radial flakes (mean=2.1%; range=0-10%).

Cortical flakes are larger than opposed/perpendicular, weakly radial flakes and proximal flakes across a number of size variables. Cortical flakes have larger maximum lengths (mean=52.2mm; range=16.54-127.57mm) than opposed/perpendicular (mean=42.3mm; range=16.3-97.4mm) and weakly radial flakes (mean=42.5mm; range=16.3-97.4mm) (Figure 8.9b). Cortical flakes also have larger maximum widths (mean=37.6mm; range=10.27-91.51mm) than proximal (mean=32.5mm; range=16.7-103.4mm), perpendicular/opposed (mean=29.6mm; range=9.28-70.1mm) and weakly radial (mean=30.2mm; range=11.2-68.5mm). As a result, cortical flakes exhibit larger surface areas than proximal, perpendicular/opposed and weakly radial flakes.

Cortical flakes exhibit larger proximal (mean=36.9; range=12.9-88.1), medial (mean=41.9; range=12.9-91.2mm) and distal (mean=31.6mm; range=6.8-67.8mm) widths and medial thicknesses (mean=17.3mm; range=2.9mm-52.4mm) compared to opposed/perpendicular (proximal mean=28.1mm; range=8.79-64.83mm; medial mean=30.8mm; range=9.7-86.8mm; distal mean=24.6mm; range=6.82-97.3mm; medial thickness mean=13.2mm; range=4.3-32.2mm) and weakly radial (proximal mean=28.3mm; 8.79-64.8mm; medial mean=32mm; range=10.8-85.7mm; distal mean=24.9mm, range=9.4-73.1mm; medial thickness mean=13.2mm; range=4.2-32.3mm) flakes. In addition, proximal flakes have smaller medial (mean=34.5mm; range=13.3-83.2mm) and distal (mean=26.9mm; 5.4-70.8mm) widths than cortical flakes. Radial flakes have a lower distal shape index (mean=1.2; range=0.72-2.36) than flakes with cortical (mean=1.39; range=0.69-2.27), proximal (mean=1.39; range=0.69-2.82), distal (mean=1.44; range=0.91-2.22) and side (mean=1.48; range=0.68-2.89) scar patterns (Figure 8.9c).

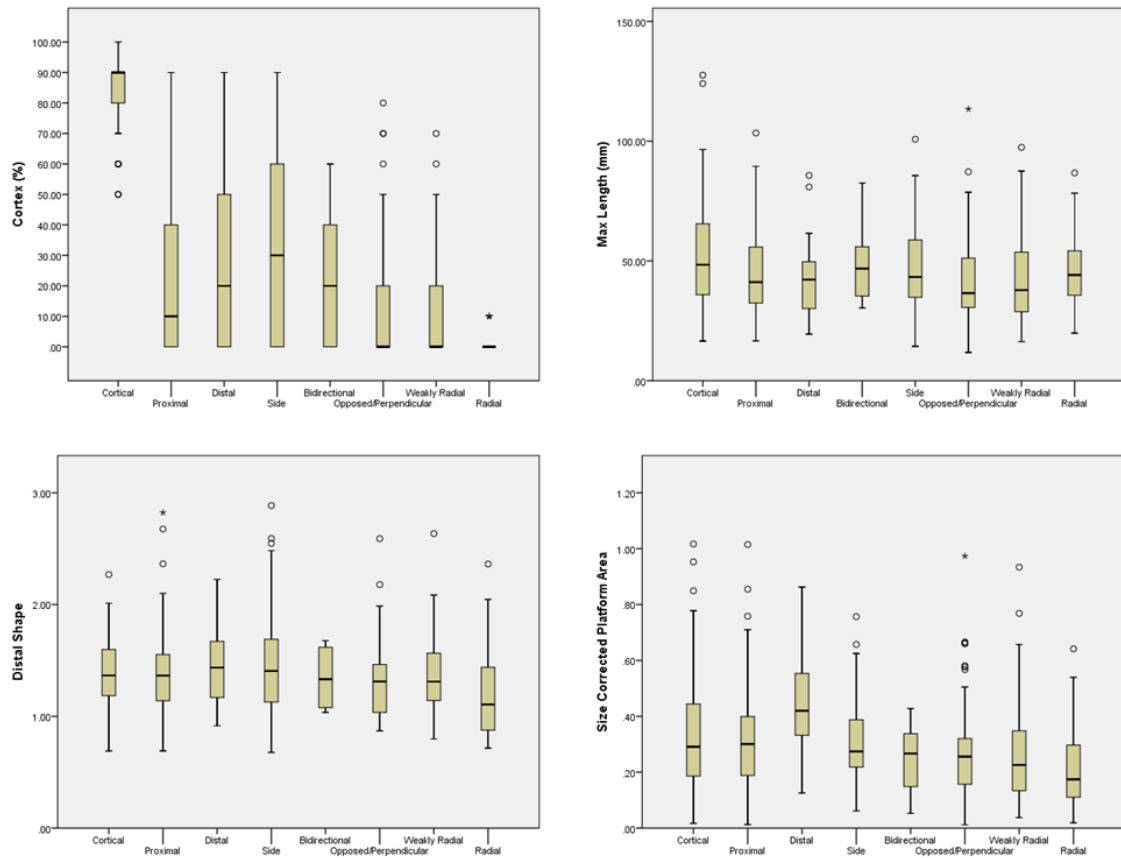


Figure 8.9: Boxplots of flake attributes separated by dorsal scar pattern: a) cortex (%) (top-left); b) maximum length (mm) (top-right); c) distal shape (bottom-left); d) size corrected platform area (bottom-right).

A number of differences in platform size are apparent between flakes with different scar patterns, and this variability is well characterised by differences in scar surface area. Flakes with cortical dorsal surfaces have larger platform surface areas (mean=673mm²; range=36-3255mm²) than flakes with proximal dorsal scar patterns (mean=485mm²; range=21-2876mm²), and both of these are larger than opposed/perpendicular (mean=365mm²; range=16-2222mm²) and weakly radial (mean=354mm²; range=42-2404mm²) flakes. Opposed perpendicular and weakly radial flakes also have smaller platforms than flakes with distal (mean=555mm²; range=87-1575mm²) and side (mean=527mm²; range=31-2033mm²) scar patterns. Cortical and side scar flakes have larger platforms than radial flakes (mean=343mm²; range=19-1132mm²). The size corrected platform area index indicates that platforms on flakes

with distal scar patterns are larger relative to flake size (mean= 0.45; range=0.13-0.86) than all other scar pattern types (group mean =0.31; range=0.01-1.02) (Figure 8.9d). Smaller platforms relative to flake size are apparent on weakly radial (mean=0.26; range=0.04-0.93) and radial (mean=0.21; range=0.02-0.64) flakes compared to those with cortical (mean=0.337; range=0.02-1.02); proximal (mean=0.31; range=0.01-1.01) and side (mean=0.31; range=0.06-0.76mm) scar patterns.

Termination type

The majority of significant differences in flake attributes between flakes with different termination types occur between those with axial terminations and the remaining three types. Significant results of pairwise post-hoc Mann-Whitney tests of flake attributes by termination type are reported in Table C.15. Axial flakes preserve more cortex (mean=52.2%; range=0-100%) compared to those with feather terminations (mean=25.3%; range=0-100%). Axial flakes are larger than feathered flakes across all flake and platform dimensions, as characterised by surface area (Axial mean=2209mm²; range=487-11355mm²; Feather mean=1528mm²; range=109-6789mm²) and platform surface area (Axial mean=709mm²; range=71-2803mm²; Feather mean=436mm²; range=19-3255mm²). However, flakes with feather terminations are flatter (mean=2.72; range=0.91-6.84) than axial flakes (mean=1.94; 0.76-3.23), and the proximal shape of feathered flakes more regularly exhibit straight of contracting proximal margins (mean=0.96; range=0.39-1.73) than axial flakes (mean=0.92; range=0.55-1.56).

Flakes with step terminations also have less cortex (mean=28.25; range=0-100) than axial flakes. The proximal width of stepped flakes is smaller (mean=28.5mm; range=8.96-73.3mm) than axial flakes (mean=35.5mm; range=13.7-76.6mm). Axial flakes present larger medial thicknesses (mean=21.5mm; range=9.5-53.2mm) than stepped flakes (mean=14.2mm;

range=5.9-45.4mm), resulting in flatter stepped flakes (mean=2.72; range=1.37-4.36) than axial flakes (mean=1.94; range=0.76-3.23). Axial flakes typically have straighter proximal margins (mean=0.92; range=0.55-1.56) and more contracting distal margins (mean=1.37; range=0.74-2.1) than stepped flakes (proximal mean=0.78; range=0.4-1.43; distal mean=1.16; range=0.69-2.07). The depth of platforms on axial flakes (mean=17.8mm; range=2.92-49.7mm) is larger than that of stepped flakes (mean=11.3mm; range=2.4-39.5mm). This results in a similar relationship in platform surface area, and a greater platform shape index for stepped flakes (mean=2.85; range=0.96-6.49) than axial flakes (mean=2.2; 0.84-8.28). Overall, axial flakes have larger platforms relative to flake size (mean=0.36; range=0.04-1.01) than stepped flakes (mean=0.21; range=0.01-0.48).

Feathered flakes have smaller distal widths (mean=25.7mm; range=5.37-100.35mm) than stepped flakes (mean=33.3mm; range=12.2-70.3mm). The proximal shape of hinged flakes exhibit more expanding margins (mean=0.69; 0.6-0.75) than axial flakes as do feathered flakes (mean=0.96; range=0.39-1.73). Feathered flakes have more contracting proximal and distal (mean=1.39; range=0.68-2.69) margins than stepped flakes. Outrepassé flakes also have more contracting distal margins (mean=1.56; range=0.87-2.68) than stepped flakes. Flakes are flatter with feather (mean=2.72; range=0.91-6.84) and step (mean=2.72; range=1.39-3.67) terminations than with outrepassé terminations (mean=2.16; range=1.39-3.67). Hinged flakes have smaller platform depths (mean=9.2mm; 5.67-13.27mm) than axial flakes, resulting in a smaller platform surface area and a lower ratio of platform to flake size (mean=0.16; range=0.06-0.35). Similarly stepped flakes have a small platform to flake surface area ration (mean=0.21; range=0.01-0.48) than feathered flakes (mean=0.31; range=0.01-1.02).

Platform Type

A number of significant differences occur in flake attributes when split by platform type, which predominately relate to platform size, with fewer significant relationships between platform type and flake size and reduction strategy. Significant results of pairwise post-hoc Mann-Whitney tests of flake attributes by platform type are reported in Table C.13.

Flakes with cortical platforms have a greater level of cortical coverage (mean=50.17%) than all other platform types (group mean=29.71%), although all types include some artefacts with cortical coverage ranging between 80-100%. In addition, flakes with dihedral platforms exhibit more cortex (mean=26.8%) than those with multiple conchoidal platforms (mean=15.65), which has the overall lowest mean value.

The axial length of flakes with cortical platforms (mean=36.7mm; range=8.58-123.7mm) is significantly larger than that of flakes with plain platforms (mean=29.9mm; range=8.83-79.7mm). With the exception of crushed platforms, flakes with all other platform types exhibit larger axial proximal widths (group mean=31.38; range=8.8-88.1mm) compared to flakes with punctiform platforms (mean=19.3mm; range=9.44-30.9mm). Flakes with punctiform platforms are typically more elongate (mean=1.33; range=0.53-1.97) than other platform types except for crushed types (group mean=1.01; range=0.28-2.54). With regards to proximal shape, plain platform flakes (mean=0.98; range=0.47-1.73) and single conchoidal platform flakes (mean=0.97; range=0.4-1.54) typically have straighter or more convergent margins than either cortical platform flakes (mean=0.92; range=0.52-1.72) or dihedral platform flakes (mean=0.88; range=0.39-1.59). However, plain, cortical, single conchoidal and multiple conchoidal (mean=0.94; range=0.49-1.58) platform flakes all typically have straighter or more contracting proximal margins in comparison to punctiform platform flakes (mean=0.71; range=0.51-1.15).

Punctiform platforms are significantly narrower (mean=10.26mm; range=5.9mm-24.2mm) than all other types except crushed platforms (group mean=32.01mm; range=5.86-99.41mm). Dihedral platforms are wider (mean=36.7mm; range=11.7-99.4mm) than crushed (mean=20.4; range=10.1-35.1mm), plain (mean=28.8mm; range=9.1-66.9mm), and single conchoidal (mean=31.2mm; range=7.69-91.59mm) platforms. Both multiple conchoidal (mean=34.95mm; range=11.57-85.95mm) and cortical (mean=33.67; range=10.39-74.16mm) platforms are also significantly wider than plain platforms. With the exception of crushed types, all other platform types are typically deeper (group mean =12.66mm; range=2.38-49.67mm) than punctiform platforms (mean=3.7mm; range=2.4-5.6mm). In addition, cortical platforms (mean=14.7mm; range=2.8-49.7mm) are significantly deeper than multiple conchoidal (mean=11.5mm; range=3.6-32.4mm). As a result, all platform types except crushed present larger surface areas (group mean=471mm²; range=16-3255mm²) than punctiform platforms (mean=38mm²; range=16-71mm²). Plain platforms have a smaller surface area (mean=413mm²; 48-2644mm²) than either cortical (mean=568mm²; range=44-2876mm²) or dihedral (mean=502mm²; range=31-2222mm²) platforms. The platform shape index indicates that multiple conchoidal (mean=3.36; range=1.2-9.9) and dihedral (mean=3.24; range=1.08-9.69) platforms are typically wider but thinner than cortical (mean=2.76; range=0.66-8.45), plain (mean=2.64; range=0.76-9.55) and single conchoidal (mean=2.57; range=0.96-5.64). Finally, all platform types are larger in proportion to flake surface area (group mean=0.3; range=0.01-1.02) than punctiform platforms (mean=0.04; range=0.01-0.08).

Platform preparation

Few significant differences occur between flakes with different types of platform preparation. Significant results of pairwise post-hoc Mann-Whitney tests of flake attributes by platform preparation are reported in Table C.14. The proximal axial width of flakes without platform

preparation (mean=31.4mm; range=8.8-88.1mm) and with faceted platforms (mean=34.3; range=16.7-57.9mm) are typically larger than those with overhang removal (mean=21.7mm; range=12.7-36.8mm). Faceted flakes are typically flatter (mean=3.01; range=2.27-4.32) than those without platform preparation (mean=2.58; range=0.76-6.84). Finally, faceted platform shapes are typically wider but thinner (mean=3.76; range=1.2-6.6) than unprepared platforms (mean=2.8; range=0.66-9.9).

Blank selection

Comparison of retouched and un-retouched complete flakes has identified a small number of significant differences. Significant results of pairwise Mann-Whitney tests of retouched and unretouched flakes are reported in Table C.16. A greater proportion of retouching occurs on complete flakes with punctiform platform types, compared to cortical, single, plain, dihedral and multiple conchoidal types. No significant differences in the proportion of retouched to un-retouched complete flakes occurs with respect to platform preparation type, termination type or dorsal scar pattern. Retouched flakes are significantly larger across a number of attributes, including maximum dimensions, axial length and axial widths. The mean maximum dimensions of retouched flakes are 53.7x36.7mm (range=19-127.6mm x 16.8x89.4mm), compared to 43.6x31.3mm (range=9.7-124mm x 8.5-91.5mm) on un-retouched flakes (Figure 8.10). Retouched flakes have significantly larger axial length (mean=39.2mm; range=15.2-108.1mm) and axial widths (e.g. medial width mean=41.3mm; range=15.9-85.7mm) compared to un-retouched axial length (mean=32.3mm; range=8.17x123.7mm) and axial widths (e.g. medial width mean=33.9mm; range=7.2-91.2mm). While no significant difference in medial thickness is apparent, the differences in axial widths results in relatively flatter retouched flakes (mean=2.85; range=1.16-6.84) compared to un-retouched flakes (mean=2.58; range=0.76-6.4). No significant difference occurs between un-retouched and retouched flakes with respect to

platform size, although the ratio of platform area to flake area indicates that un-retouched flakes typically have larger platforms (mean=0.31; range=0.1-1.02) than retouched flakes (mean=0.23; 0.1-0.57).

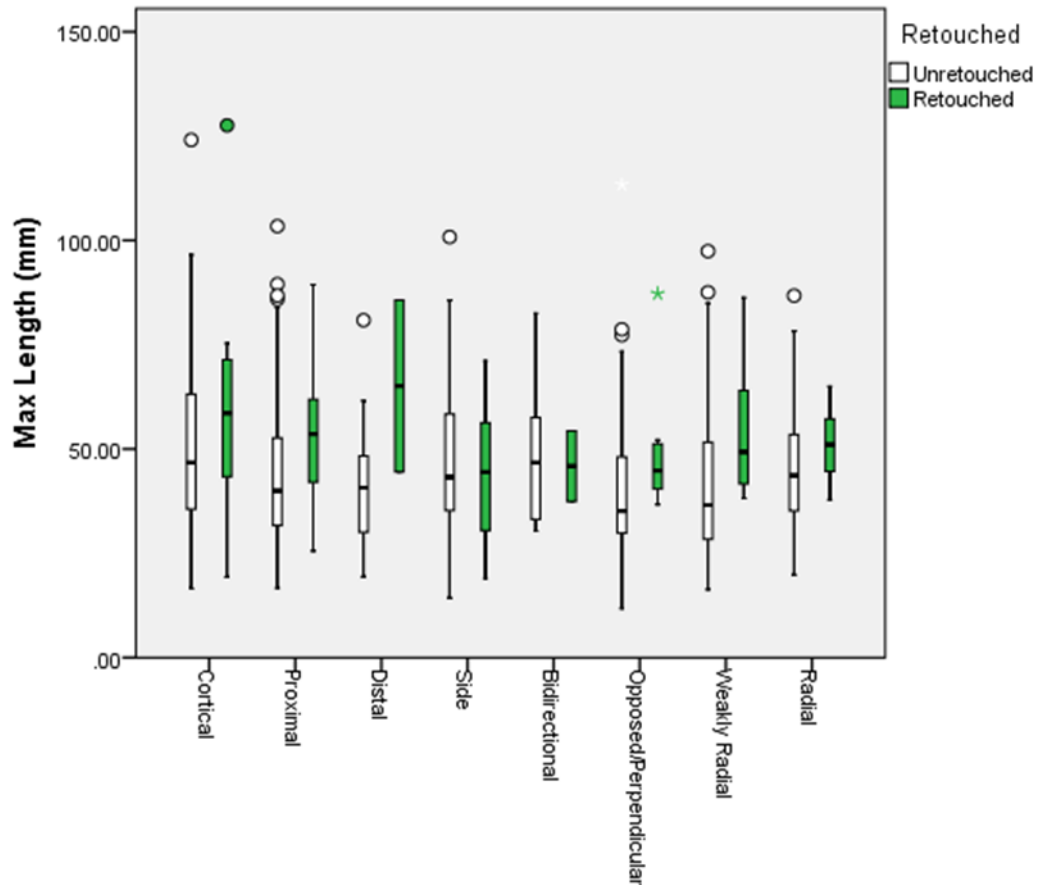


Figure 8.10: Box plot of complete flake maximum length separated by dorsal scar patterns and presence of retouch.

Diachronic Variability

A number of significant differences occur in flake attributes when structured by excavated strata amongst the three largest assemblages (Table C.17 & C.18). Significant variation in the proportion of flakes with different dorsal scar patterns occurs between the excavated strata (Table 8.6 & C.19). A relatively greater number of flakes with proximal, distal, side, bidirectional and weakly radial scar patterns occur in S4 than in S6 and S8. Proportionally

fewer opposed/perpendicular and radial flakes occur in S4 than in S6 and S8. A relatively larger number of flakes with cortical dorsal surfaces occur in S8 than in S4, and in S4 compared to S6, although no significant difference occurs between S6 and S8. No significant difference in the proportion of retouched to un-retouched flakes occurs with respect to the excavated strata.

Dorsal Scar Pattern	S4	S6	S8	Total
Bidirectional	4	3	1	8
Cortical	29	38	23	90
Distal	13	10	4	27
Opposed/Perpendicular	7	44	19	70
Proximal	46	53	25	124
Radial	10	24	10	44
Side	26	37	17	80
Weakly Radial	26	31	17	74
Total	161	240	116	517

Table 8.6: Number of flakes with different scar patterns separated by stratum.

Differences in the proportion of flake terminations occur between the excavated strata (Table 8.7 & C.21). A greater proportion of flakes with feather, hinge and step terminations occur in S6 than S8, and in S8 than S4. A relatively larger number of flakes with an outrepassé termination are present in S4 than S6, and in S6 than in S8. Finally, a larger proportion of axial terminations occur in S4 than in S8, and more appear in S8 than S6.

Termination Type	S4	S6	S8	Total
Axial	28	25	26	79
Feather	125	191	90	406
Hinge	0	4	1	5
Outrepassé	10	4	0	14
Step	8	26	6	40
Total	171	250	123	544

Table 8.7: Number of flakes with different scar patterns separated by stratum.

No significant difference in the proportion of platform preparation occurs between the three largest excavated assemblages, whereas significant variation does occur in the proportion of platform types (Table 8.8 & C.20). The lowest proportion of cortical flakes occurs in S4, with a

significantly larger proportion in S6, and a higher frequency than both these strata in S8.

Crushed and dihedral platforms appear in the largest proportion in S6, with fewer in S4, with the lowest proportion occurring in S8. S6 also has the largest proportion of multiple conchoidal platforms, with fewer appearing in S8, and the lowest frequency occurs in S4. A significantly higher frequency of plain and punctiform platforms occurs in S4, followed by S6, with the lowest proportion present in S8. Finally, the largest proportion of single conchoidal platforms appears in S8, followed by S4, with the lowest frequency present in S6.

Platform Type	S4	S6	S8	Total
Cortical	35	40	41	116
Crushed	1	3	0	4
Dihedral	26	44	5	75
Multiple Conchoidal	13	59	13	85
Plain	43	46	18	107
Punctiform	6	5	2	13
Single Conchoidal	46	55	46	147
Total	170	252	125	547

Table 8.8: Number of flakes with different platform type separated by stratum.

Flakes in S8 have a greater level of cortical coverage (mean=35.8%; range=0-100%) than either S6 (mean=25.9%; range=0-100%) and S4 (mean=27.6%; range=0-100%). Significantly larger axial distal widths occur in S8 (mean=30.35mm; range= 6.96-97.32mm) than S6 (mean=26.5mm; range= 6.8-73.1mm), both of which are larger than flakes in S4 (mean=25.5mm; 5.37-100.35mm). As a result, the distal shape of flakes in S4 typically have more contracting margins (mean=1.46; range=0.68-2.82) than either S6 (mean=1.35; range= 0.69-2.89) or S8 (mean=1.29; range= 0.74-2.27). The proximal shape index indicates flakes from S4 are typically straighter or exhibit contracting margins (mean=0.98; range= 0.45-1.73) than those from S8 (mean=0.89; range=0.4-1.55). A significant difference in medial thickness occurs, with flakes from S6 (mean=13.5mm; 3.81-52.38mm) thinner than those in S8 (mean=15.9mm; 3.5-45.9mm). Flakes in S6 are flatter (mean=2.67; 0.91-6.84) than those in S4

(mean=2.45; range= 0.92-5.47). More elongate flakes occur in both S4 (mean=1.08; range=0.39-2.17) and S6 (mean=1.01; range=0.32-2.54) compared to S8 (mean=0.91; range=0.28-1.91). Finally, the platform shape of flakes in S6 are wider but thinner (mean=2.93; range= 0.85-8.45) than those in S4 (mean=2.65; range=0.76-9.69).

Summary

The wide range in the size of flakes supports the suggestion that preliminary reduction activities were performed at KAT1. Average flake dimensions typically fall between 20-50mm, and the largest and smallest flakes present at the site are likely to have been by-products of reduction activity, rather than the outcome of specific reduction strategies. Although most flakes present minimal cortical cover, a substantial proportion exhibit considerable amounts of cortex, providing further evidence for likely exploitation of raw material resources present at the site. The presence of a small number of Levallois points indicates that although much of the reduction activity at the site was preliminary, some specific debitage products were produced at the site, matching evidence from the cores.

The presence of cortex decreases as more dorsal surfaces and platform types become more complex, and typically this is accompanied by a reduction in size characteristics, which may be explained by increasing reduction intensity. Notably, flakes exhibiting radial scar patterns do not fit this trend, suggesting that they may be the product of a different reduction strategy. Platform types are typically simple, and platform preparation is rare. Platforms are typically 20-40% of the size of the flake. Weakly radial and radial flakes show the smallest ratios of platform to flake size, which may indicate that they are the product of more intensive reduction sequences. Flakes with axial terminations are typically large, and appear to represent early reduction stages.

Of all scar patterns, radial flakes possess the least convergent margins, and coupled with the typically larger flake size, this may indicate that radial flaking was employed as a means to create big flakes with large perimeters. Flakes with punctiform platforms are also less pointed, but are more elongate and smaller than other flakes, which may represent an alternate strategy for producing large flake circumferences from more heavily reduced cores. However, there is little evidence overall for the targeted production of elongate flakes.

Differences in both reduction intensity and strategy occur between the three largest assemblages, in contrast to the core population. Variability in size and shape characteristics between strata are minor, which may best be explained by differences in reduction intensity. More cortical flakes and platforms occur in S8, implying more preliminary reduction compared to the other horizons. Radial flakes are most common in S6 and S8, whereas a range of more varied scar patterns are present in S4. It is unclear whether this marks different reduction strategies or simply that more intervening stages in reduction sequences are present in S4. Outrepassé and axial terminations are most common in S4, which may indicate strategies to rejuvenate flaking surfaces. While the largest proportion of aberrant terminations occur in S6, this is accompanied by the largest proportion of feather terminations, and may therefore relate to reduction intensity rather than differences in technique. Rare occurrences of blades are present in S4 and S6, although they are absent in S8.

Flaked Pieces

A total of 334 artefacts that are categorised as flaked pieces are present, which bear no clear ventral morphologies or negative flake scars originating from the margins of the artefacts, but have clearly undergone some reduction. Of these artefacts, 293 are recorded as complete, including 17 retouched pieces, and are described below. Typological description of retouched pieces is presented separately.

Univariate Description

Univariate descriptive statistics for flaked piece attributes are presented in Table C.22. The average maximum dimensions of flaked pieces are 34.5x24.1x11.9mm. The interquartile range for maximum length is 22.9-39.8mm, whereas the maximum range is 7.86-109.4. The interquartile range for maximum width is 16.2-28.3mm, with a maximum range of 4.71-94mm. For medial thickness, the interquartile range is 7.1-15.2mm, with a maximum range of 1.4-55mm. Cortical cover is typically low, with a mean occurrence of 15.2% and interquartile range of 0-30%, although some artefacts preserve 100% cover (apart from a single face that lacks clear ventral or flake scar characteristics).

Bivariate Analysis

Blank selection

Significant differences occur between retouched and un-retouched flaked pieces with regards to maximum length and width, and to cortical coverage. Significant results of Mann-Whitney tests comparing retouched and unretouched flaked pieces are presented in Table C.23. Retouched flaked pieces are significantly larger, with an average maximum length of 55mm (range=24.7x83.2mm) and average maximum width of 36.3mm (range=18.1-72.9mm), compared to un-retouched (maximum length mean=33.3mm; range=7.9-109.4; maximum width mean=23.3mm; range=4.71-94mm). Retouched flaked pieces typically have a greater level of cortical coverage (mean=32.9%) than un-retouched (mean=14.2%) flaked pieces, and flaked pieces with up to 90% cortex have been selected for retouch.

Diachronic Variability

No significant differences in size or cortical cover on flaked pieces occurs with respect to the three main excavated strata (Table C.24). However, a significant difference occurs in the proportion of retouched to un-retouched flaked pieces with respect to stratigraphic context (Table C.25). A larger proportion of flaked pieces from S4 have been selected for retouching than either S6 or S8 (Table 8.9).

	S4	S6	S8	Total
Un-retouched	68	110	61	239
Retouched	12	4	1	17
Total	80	114	62	256

Table 8.9: Number of retouched and un-retouched flakes separated by stratum.

Summary

The flaked pieces present at KAT1 are typically smaller than both flakes and cores, and predominately comprise debris from reduction sequences. However, opportunistic use of this debris is apparent, with the size of artefact selected for retouch closely matching that of retouched complete flakes. A greater proportion of flaked pieces have been selected for retouching in S4.

Retouched Artefacts

A total of 111 retouched flakes and flaked pieces are recorded at KAT1. The typological description of these artefacts, following terminology set out in Inizian et al. (1993) is followed by a univariate attribute description, bivariate analysis with respect to retouch location and blank type, and finally by analysis of diachronic variability of retouched artefacts.

Typology

A third of retouched artefacts present retouch only on a single side, with a further 8.1% retouched only on a single end. Retouch on a single end and side occurs on 14.4% of retouched pieces, with a further 11.7% retouched on a single end and both sides. Double sided retouch occurs on 12.6% of retouched pieces, with only two artefacts (1.8%) retouched on all four margins. Retouch on 18% of artefacts is unclassified. The application of retouch is typically limited, in terms of both extent and invasiveness (see below), suggesting that in most instances the application of retouch has made only minor modification to the blank shape and size. However, in a number of instances, artefacts have been retouched to either emphasise reshape blank morphology.

A single bifacial point is present in S4 (Figure 8.11), retouched on both proximal and distal ends of a flake. The artefact is roughly symmetrical around the maximum length/axial medial width (44.29mm), and is perpendicular to the axial length (29.9mm). The flake has a single conchoidal platform and terminated in a step.

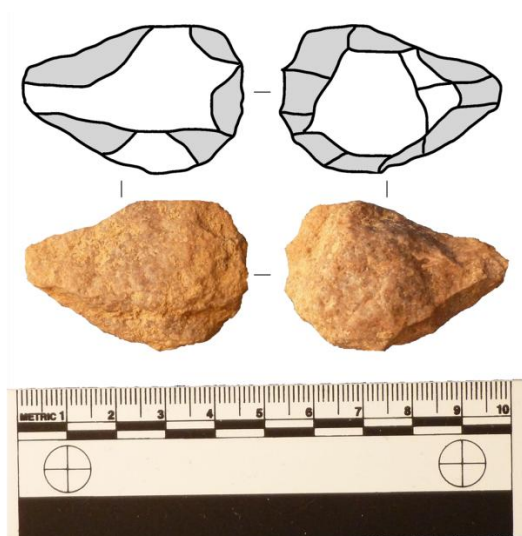


Figure 8.11: Bifacial point from S4; Ventral left, dorsal right; Platform at top.

Five artefacts present fairly simple notches, along with varying levels of further retouch. A simple notch occurs on the ventral face of a flake from S4, which has produced a protruding outline on one side of the artefact and a tapered edge on the other side (Figure 8.12a). The axial dimensions are 18.09x24.5mm, broadly perpendicular to the maximum dimensions. The flake has a cortical platform, a single sideways scar on the dorsal face and a feather termination. The delineation of a single side and end of a flake from S5 (Figure 8.12b) using a notch and a series of small retouch removals have produced a protruding artefact outline, which can be defined as a tang or tongue. The artefact, with axial length and width of 47x52mm, shows a lipped, single conchoidal platform and a bidirectional dorsal scar pattern. A flake from S6 (Figure 8.12c) has a single, simple notch adjacent to minor delineation on the side of the dorsal surface. Retouching has produced a simple shoulder/protrusion at one end of the maximum axis of the artefact, whereas the opposed flake side contracts to form a point where it meets the platform. The flake has a shallow, dihedral platform and opposed/perpendicular flaking dorsal scar pattern. The flaking axis is perpendicular to the maximum length of the artefact, which has dimensions of 52.1x26.1mm. A broken flake from S6 (Figure 8.12d), measuring 54.3x40.8mm, that presents a simple notch and delineated margin. This appears opposite to the axis of the break, which has created a protruding tongue or tang. Finally, a notch is present on the side of a broken flake from S8 (Figure 8.12e), with maximum dimensions of 49.7x34.04mm. This produces a distinct asymmetry to the piece, creating a shouldered protrusion, opposite sharply convergent flake margins formed by previous scars on the dorsal surface.

Six artefacts exhibited delineated margins, where retouch has typically been used to accentuate a protruding margin. Bifacial delineation along the side of a flake from S4 (Figure 8.13a) has resulted in a nosed artefact, with further retouch removal evident on the opposite

side of the ventral surface. This artefact has a single conchoidal platform and has been radially flaked. The maximum dimensions (37.8x29.9mm) are perpendicular to the flaking axis. The retouched side of a flake from S4 (Figure 8.13b) has delineated a protrusion that is perpendicular to both flaking and maximum axis of the artefact. Retouch is slightly more invasive toward the proximal end of the artefact, and the distal shape of the flake is convergent. The maximum dimensions are 37.5x31.1mm. Retouching of the proximal end and side of an artefact from S6 (Figure 8.13d) has removed the flaking platform, and a series of small removals have delineated a thin projection. The flake has a prominent longitudinal arise, created by two parallel scars on the dorsal surface, that splits in two in the distal portion. The retouched projection may be classified as a tongue. The artefact has maximum dimensions of 30.7x16.9mm. Two removals on the ventral surface of a flake from S6 (Figure 8.13e) have significantly thinned the longer side of a weathered flake. Delineation on the dorsal surface of the thinned side of the artefact has accentuated this thinned side, creating a shoulder. The axis of maximum dimensions (57.5x26x5mm) is perpendicular to the flake axis, the dorsal scar pattern is weakly radial, with a plain platform and feather termination present. Bifacial delineation of one end of a flaked piece from S6 (Figure 8.13c) has created a tongued artefact. Further retouching is present opposite this protrusion that has formed convergent margins. The maximum dimensions of the artefact are 61.6x27.1mm. Marginal trimming of a flake from S6 (Figure 8f) has delineated the side and distal portion of the artefact, creating a symmetrical outline from the extremity of the retouched portion to the opposing surface, where the platform surface meets the flake surface. The artefact measures 86.3x45.3mm around this axis, which is also the maximum axis.

These artefacts indicate that the application of retouch to flakes and occasional flaked pieces has been used to accentuate the shape of blanks and produce both symmetrical and asymmetrical protrusions. Following Inizian et al. (1993), a continuum of reduction is present

amongst delineated types, with shouldered and nosed pieces less invasively retouched compared to tongued or tanged artefacts. A number of further retouched pieces are present in the KAT1 assemblages that may present examples of the earliest aspects of these retouch strategies.

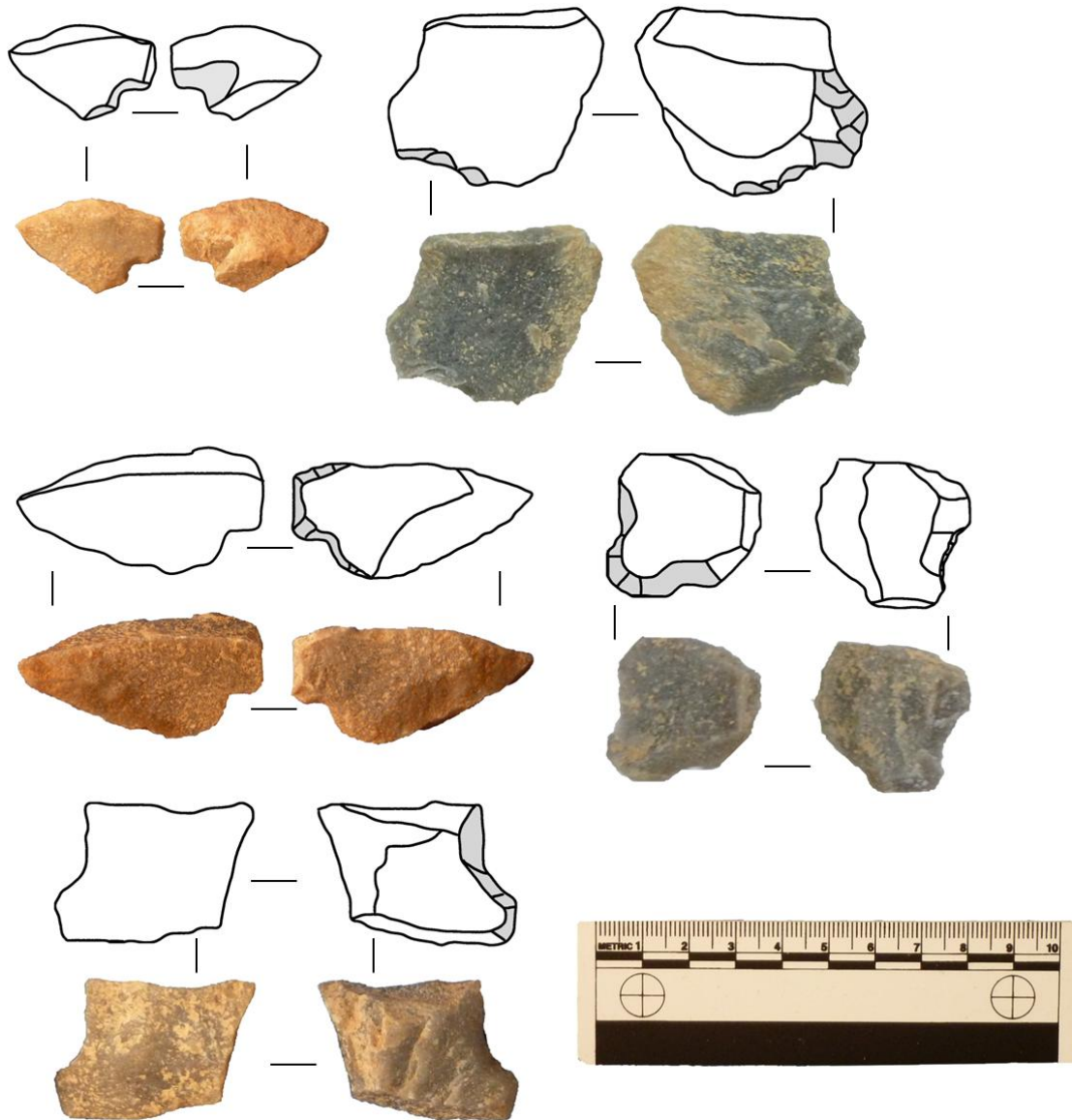


Figure 8.12: Notched artefacts: a) S4 – notch (top-left); b) S5 – tanged point (top-right); c) S6 – shouldered point (middle-left); d) S6 – broken tanged artefact (middle-right); e) S8 – notch/shoulder (bottom-left).

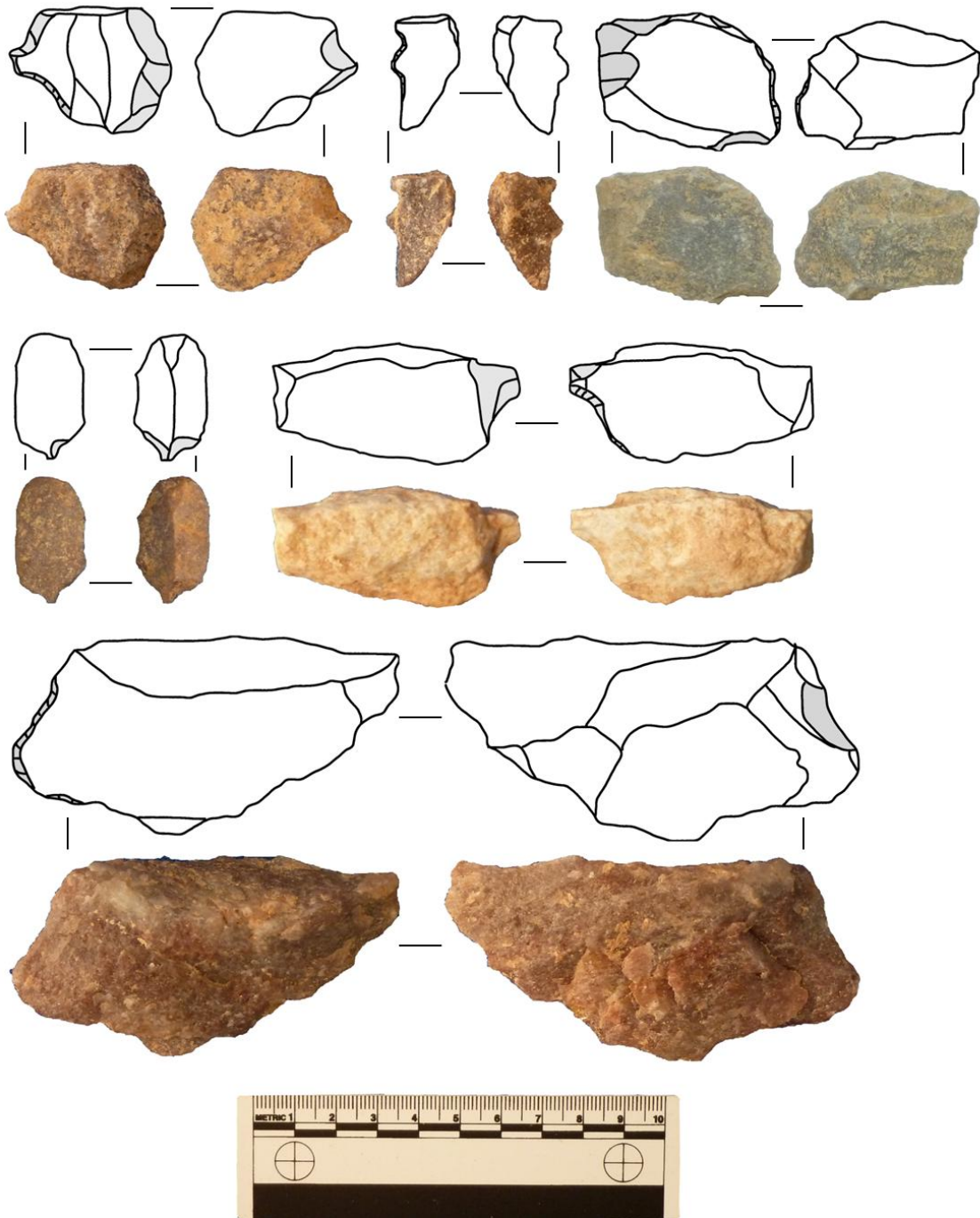


Figure 8.13: Delineated artefacts: a) S4 – nosed flake (top-left); b) S4 – delineated flake (top-centre); c) S6 - bifacially delineated tongued flake (top-right); d) S6 – tongued flaked (middle-left); e) S6 – shouldered flake (middle-right); f) S6 - delineated flake (bottom).

Univariate Description

Univariate descriptive statistics of retouched artefacts are presented in Table C.26. The average maximum dimensions of all retouched flakes and flaked pieces are 52.5x35.9x14.4mm. The maximum range of length is large, from 19mm-127.6mm, although 50% of artefacts range between 37.8-63.9mm. Similarly, the range of maximum width is 16.8-89.4mm, with an interquartile range of 26.6-42.2mm. Medial thickness ranges from 4.5-45.4mm, with 50% of artefacts ranging between 10.7-17.1mm. Average cortical coverage is 29.5%, with 45% of artefacts recorded with no cortex, 74.8% of artefacts with 50% or less cortex and 15.3% of artefacts have 90-100% cortical coverage.

With regards to retouch intensity, retouch width and depth on flakes and flaked pieces typically measure 36.4-10.9mm. Retouch width varies considerably, ranging from 12-115mm, with 50% of widths occurring between 23-45.5mm. Retouch depth variability is less extreme, ranging from 2-49mm, with an interquartile range of 4.7-14.5mm. The average index of invasiveness score is 0.1336, with a range of 0.03-0.44, and an interquartile range of 0.0781-0.1875.

Bivariate Analysis and Diachronic Variability

Blank size and cortex cover do not differ significantly with regards to retouch location in the three largest assemblages. Comparison of size, cortical coverage and retouch intensity by blank type (flake or flaked piece) indicates no significant differences. No significant difference occurs in the relative proportion of retouched flakes to flaked pieces between the three largest assemblages.

Similarly, no significant difference occurs between strata with regards to retouch location.

However, retouched artefacts from S4 exhibit significantly larger retouch widths (mean=44.4;

range=13-115m) than in S6 (mean=30.7mm; range=12-71mm) and S8 (mean=24.3; range=14-42mm) (Table C.27 & C.28).

Summary

The application of retouch is rarely extensive or highly invasive in the KAT1 assemblages. Blank selection appears to focus upon a size range of 40-60mm, including the shouldered, tongued and tanged pieces described above, regardless of blank type. A greater number of retouched pieces occur in S4 than in S8, and more extensive retouch, between 15-20mm difference in retouch width, is present in S4 compared to S6 and S8. The majority of retouched flakes are fairly simple. The typologically distinct artefacts described above share a focus upon delineating protrusions on one end of an artefact opposed to converging margins, typically creating some degree of symmetry around the axis of the maximum dimension. Without microwear and residue studies, it is problematic to outline the potential use of retouched artefacts, although shouldered, tongued and tanged artefacts are typically regarded as adaptations to facilitate hafting.

Heavy Tools

A total of 8 artefacts from KAT 1 are classified as heavy tools, one of which derives from S5 whereas the remaining seven come from S8. The metric characteristics of these artefacts are presented in Table 8.10. S8-1 is the most refined example of a bifacial tool (Figure 8.14a), with small flake removals evident around the perimeter of the piece, and can be classified as an ovate biface. S8-3 also shows a number of small margin trimming removals, coupled with a few large removals, and exhibits a broken tip. Marginal trimming of S8-5 occurs around roughly two thirds of the perimeter of the artefact, with the remaining third comprising a

cortical but to this bifacially worked artefact (Figure 8.14b). S8-6 is a ovate-shaped bifacial tool, but is predominately covered in cortex, with only a small number of flakes on either surface.

Categorisation of the remaining pieces is more problematic. S8-7 has been bifacially worked, yet it does not neatly fit into a 'classic' bifacial tool category. This is because one surface has been reduced primarily by three large removals in contrast to the finer and more intensive reduction evidence upon the opposite surface. A similar problem is present with S8-4, with marginal trimming evident upon the ventral surface of a large flake, and few, large flake removals evident the dorsal surface. S8-2 has been bifacially reduced with a small number of relatively large flakes compared to the overall artefact, resulting in a broadly triangular shape. These artefacts have been defined as heavy tools as opposed to cores based on qualitative comparisons with the rest of the core assemblage and the overall shape imposed upon the artefact by reduction. For both S8-7 and S8-4, bifacially tools may have been exploited as cores, whereas in the case of S8-2 the distinction of a bifacial tool compared to a prepared core is acknowledged as problematic.

The single heavy tool in S5 appears to have undergone considerable reduction. A distinct plane of intersection is evident for approximately half of the perimeter of the artefact, which has been bifacially worked. The remainder of the perimeter presents potential, thicker platform surfaces, although neither appear to have been heavily exploited. Given the availability of raw material at the site, and the contrasting degree of reduction evident upon this artefact and cores of a similar size, this piece is loosely classified as a 'chopping tool'.

Attribute	S5-1	S8-1	S8-2	S8-3	S8-4	S8-5	S8-6	S8-7
Max Length	110.8	77.11	84.37	109.12	103.67	80.78	75.65	120.95
Max Width	82.38	51.99	63.72	78.52	71.63	62.57	48.29	62.2
Cortex %	0	0	0	10	20	20	70	10
Axial Length	66.68	74.91	83.45	104.15	103.67	80.88	75.39	114.45
1/4 width	90.89	50.71	56.14	81.63	72.02	62.06	41.89	47.4
1/2 width	103.9 3	39.93	63.06	71.67	72.06	55.78	47.69	56.87
3/4 width	102.6 4	29.45	54.97	50.31	53	42.81	38.98	65.41
1/4 thickness	39.49	20.57	25.25	25.9	23.49	27.34	17.59	32.46
1/2 thickness	45.92	16.63	27.83	25.75	22.04	28.4	18.4	46.06
3/4 thickness	33.54	14.76	16.36	25.39	16.54	20.77	18.86	16.77
Max thickness	47.75	20.28	28.38	25.79	27.42	29.57	18.52	45.28

Table 8.10: Metric attributes of heavy tools from KAT1.

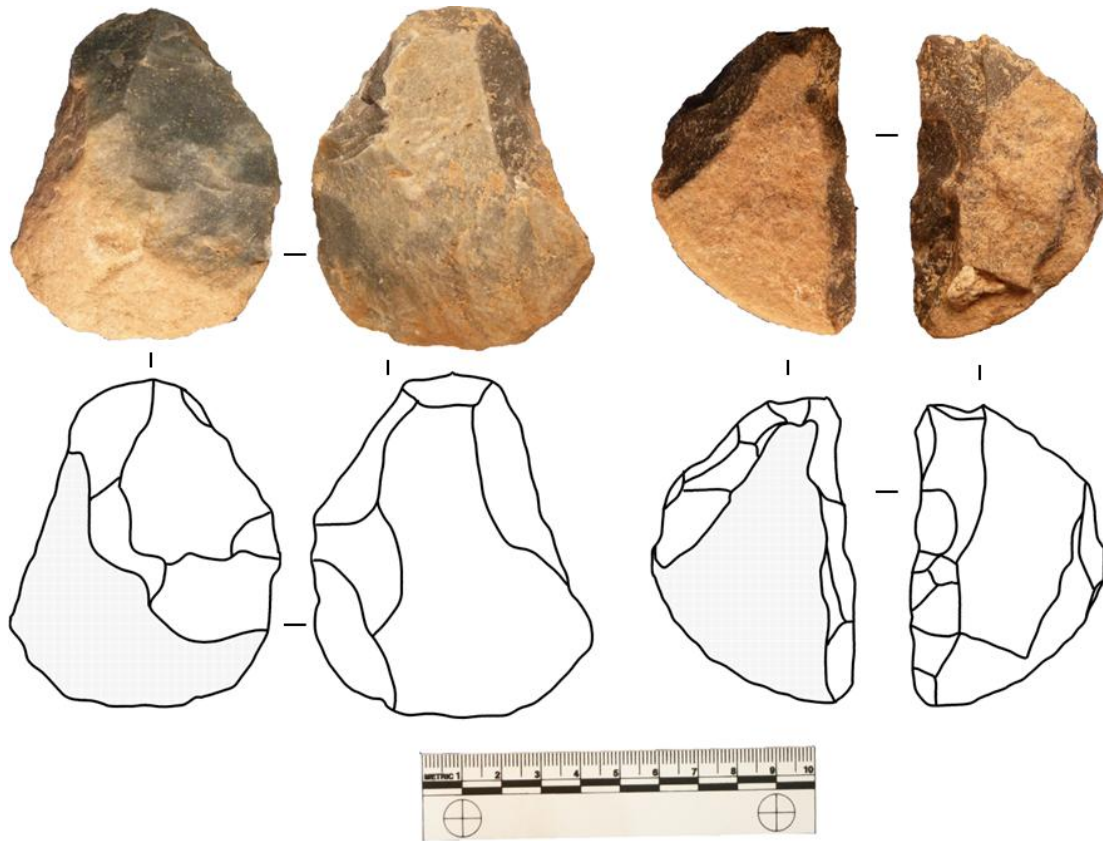


Figure 8.14: Heavy tools: a) Ovate biface (left); b) bifacial heavy tool (right).

Discussion

The analyses of the lithic assemblages from Katoati have identified a number of patterns, some of which are apparent across the basic artefact types used for analysis and transcend stratigraphic differences. All artefact types present some support for the assertion that primary exploitation of gravels and cobbles from Katoati were undertaken at the site, and the majority of artefacts across all basic types are dominated by relatively simple types with high proportions of cortex present. The upper range of artefact sizes present appears to repeatedly represent the earliest stages in reduction sequences, whereas the lower range of artefact sizes are most likely by production of reduction of activities. In many instances, different degrees of reduction intensity provide the grounds to explain attribute variability between artefacts.

Similarly, different patterns of statistical significance in the attribute analyses between the core and flake populations can best be explained by the different manner in which these complementary products of reduction sequences record the impact of reduction intensity.

In contrast, regular patterns in artefact size, typically between 30-60mm, may offer some indication of discard thresholds for more heavily exploited cores and both flakes and flaked pieces selected for retouching. Importantly, while some radial and prepared core reduction strategies appear to target the production of flakes at the larger end of this range, cores and their final flake removals are regularly reduced to smaller sizes. This may indicate the different outcomes of similar reduction strategies undertaken either to different levels of reduction intensity, or alternatively targeted to produce different sized flake products.

The presence of bifacially worked heavy tools are the result of significantly different reduction schemes, and some of the flakes may relate to these strategies, rather than the reduction of cores for flake products. Further analyses of the flakes are required to identify morphological

indicators for bifacial thinning flakes, such as differences in platform angles. However, as the bifaces appear to occur in relatively early stages of reduction or capitalise upon existing cobble shapes, it is not clear that distinctive characteristics will become apparent. Furthermore, potential continuity between bifacial reduction schemes and prepared core strategies may complicate the identification of such distinctions amongst the flake population.

A repeated trend amongst the Levallois cores is the presence of medial-distal ridges and point removals, particularly on cores with bidirectional flaking patterns, or where distally divergent flakes have been used to produce the medial-distal ridge. These cores fit the basic typological criteria of Nubian cores (Van Peer 1992; Rose et al. 2012), which are typically regarded as cores intended to produce pointed flakes. Two of the three Levallois points identified in the flake population match well with the size of point removals and anticipated dorsal scar patterns from these cores. This indicates that relatively complete un-retouched point production reduction sequences are present at the site. Notably, these points and flake scars occur at the lower end of the average spectrum of flake sizes.

At the larger end of the typical flake size spectrum occur a number of retouched artefacts than are classified as shouldered, tongued or tanged points. In a couple of instances, these artefacts present medial breaks along the maximum axis, which may have resulted from use. This could indicate that some of these pieces have been discarded following replacement with new points produced at Katoati. While the morphology of these artefacts may suggest they have been retouched to facilitate hafting, further analyses are required to confirm this. A number of pointed retouched and un-retouched flakes match similar sizes and shapes to both these retouched points and the Levallois points, presenting further support that a strategy of reduction at the site was point production, with differing levels of formality.

Significant diachronic differences between cores and flakes in the different strata may be best explained by different levels of reduction intensity, rather than major changes in reduction strategy. However, the presence of bifaces in S8 is a major categorical difference between the largest three assemblages. In addition, the most typologically distinct cores and retouched flakes are more common in S6 and S4, which may suggest differences between these specialised reduction strategies compared to the more generalised reduction sequences apparent in all assemblages.

Assemblages from S4 and S6 fit well with both regional and broader definitions of Middle Palaeolithic industries, focused primarily upon flake production making use of prepared core technologies. Characterising S8 is somewhat more problematic, primarily through the presence of bifacially worked heavy tools. The assemblage may meet regional definitions for both Middle Palaeolithic and Late Acheulean industries. A broader discussion of the distinction between these industries and its significance are discussed in the final chapter.

Chapter 9

Discussion

The new archaeological and environmental evidence presented in this thesis, including perspectives developed from a comprehensive literature review, offer a strong body of data from which to characterise the Palaeolithic occupation of the Thar Desert. The objective of this chapter is to put these new lines of evidence into their broader context. Firstly, the archaeological assemblages will be set within their chronological, environmental and landscape context. Following this, the relationship between results of new lithic analysis presented in this thesis and the existing Palaeolithic record will be discussed. The Palaeolithic archaeology of the Thar Desert will then be considered with respect to the environmental context, to identify the periods and conditions in which the region has been occupied by hominin populations. Finally, the archaeological, environmental and chronological records of the Thar Desert will be discussed in its broader geographic context and with respect to contemporary debates in human evolutionary studies.

The Katoati Assemblages in their Landscape Context

The results of archaeological, environmental and chronometric analyses presented from excavations at Katoati constitute a significant contribution to our understanding of the Palaeolithic occupation of the Thar Desert, and South Asia in general. Three main archaeological assemblages, S4, S6 and S8, present a number of similar reduction activities. These include an increase in prepared core technologies, including Levallois and point

production strategies, and occasional application of retouch to flakes and flaked pieces to form tangs and shoulders. The environmental record indicates that these three main assemblages are associated with periods of enhanced humidity, evident in the presence of fluvial sediments and an isotopic signature suggesting the dominance of C₄ plants, which typically thrive when the summer monsoon is strong. The smaller assemblage of S5 provides further support of occupation during these humid conditions. Archaeological evidence for occupation at Katoati becomes sparse as the sedimentological record indicates a shift from fluvial to aeolian sedimentation, accompanied by isotopic evidence of decreasing influence of C₄ vegetation. A sheet-wash event in S3, identified through the presence of a thin granule-small pebble horizon including lithic artefacts, marks a break in aeolian sedimentation. The sedimentological, isotopic and geochemical characteristics of the deposits above this pebble horizon indicate the continuation of an aeolian deposition regime that has been subject to less weathering and pedogenesis. Further evidence for Palaeolithic occupation at Katoati is based on distinctive lithic artefacts appearing across the landscape in sediments above the sheet-wash horizon.

The application of OSL and AMS ¹⁴C dating at Katoati provides the means to integrate this sequence of environmental variability and hominin occupation into a chronological framework. A major episode of fluvial activity occurs at KAT1 between ca. >91-55ka, and at JFL1 between ca. 134-36ka, apparent as alternating depositional cycles of gravels and coarse sand, occurring as braided stream deposits. Due to the relatively coarse chronological resolution, it is not clear whether these were continuous cycles or mark punctuated humid events, although a number of cycles of deposition appear to occur in both the upper and lower range of the chronological bracket. Aeolian deposition is evident in the landscape by 40ka and after 20ka, and these dates appear to bracket the widespread sheet-wash horizon.

Early Upper Pleistocene hominin occupation at Katoati is attested to by the presence of artefact assemblages dating to ca. 91ka. The appearance of bifaces in the lowest sediment

horizons, particularly at JFL2, may indicate a hominin occupation extending into the late Middle Pleistocene (MIS 6-7). The archaeological record indicates extensive occupation at Katoati coeval with the onset of fluvial sedimentation and humid environmental conditions, which appear to commence at in MIS 5 (ca.91-134ka). Further hominin occupation is evident in fluvial contexts between MIS 4 and early MIS 3, dating to 65-57ka at KAT1 and JFL1. Although evidence for more recent hominin occupation is present, the chronology for these is unclear. Excavated evidence for such occupations is problematic as the sample sizes are small and artefacts appear to have been size sorted through transportation, which could indicate mobilisation of cultural material. The presence of microlithic artefacts in sediments above the sheetwash horizon, as at KAT2, indicate the return of hominin populations in the terminal Pleistocene after 20ka.

Within this chronological and environmental framework (Table 9.1), a broader discussion of the lithic findings at Katoati is possible. Firstly, the presence of fluvial activity appears to have been a key reason for hominin occupation in the immediate vicinity of KAT1. The primary exploitation of river gravel and cobble deposits is a recurrent trend in the three largest assemblages at KAT1, which offers a rationale for site choice. The high proportion of cores, cortical artefacts, cores and simple reduction schemes on larger artefacts suggest reduction locally sourced raw materials. The availability of ecological resources, concentrated at sources of ground water, may also offer an explanation for occupation at this site. In the post-monsoon season, the Katoati landscape may have offered rich vegetative resources that would have been attractive to hominins and other fauna. Groundwater resources in and around drainage channels may have supported vegetation into the dry season, which may have made Katoati an attractive location as ecological resources became sparser elsewhere. Lithic raw materials are widely available in the Katoati landscape, not only within Upper Pleistocene fluvial contexts, including at locations such as Ambali, which offer panoramic views of the

surrounding area. KAT1 may have been chosen as a site for reduction activity specifically due to the co-occurrence of raw material and ecological resources. Some spatial variability may be observed in lithic technology as access to fluvial channels varies with distance and through time.

Age (ka)	Environment	Lithic Technology	Site/Assemblage
>200ka	Steady Middle Pleistocene fluvial activity resulting in landscape stability and intensive pedogenesis	Acheulean – Handaxes, cleavers, cores and flake tools	Jayal, Chhajoli
200 - >91ka	Onset of late Middle/Upper Pleistocene fluvial activity accompanied by C ₄ dominated vegetation	Late Acheulean – handaxes, cleavers, cores and flake tools	JFL2, <i>nalla</i> gravels at KAT1
		Late Acheulean/Middle Palaeolithic – bifacial tools, prepared & informal cores, flaked tools	KAT1-S8
>91-55ka	Cyclical fluvial activity involving alternating gravels and sands dominated by C ₄ vegetation	Middle Palaeolithic – informal, prepared and Levllois cores, including Nubian-style cores, delineated retouched tools including tanged and shouldered points	KAT1-S4, S5 and S6, JFL1
55-35ka	Onset of aeolian deposition; some landscape stability indicated by pedogenesis, increased presence of C ₃ vegetation	Hominin occupation evident but non-diagnostic	KAT1- S3b
35-21ka	Limited humid event apparent from sheet-wash event	Hominin occupation evident but non-diagnostic	KAT1-S3a
<21ka	Further aeolian deposition	Late Palaeolithic – occasional microlithic artefacts	KAT2

Table 9.1: Summary of hominin occupation at Katoati.

Much of the variability evident in the lithic assemblages at KAT1 can be explained by the primary exploitation of raw material resources. Larger artefacts typically present fewer attributes of intensive reduction compared to smaller artefacts, with the exception of prepared cores and radial flakes. A common discard threshold has been identified between 30-60mm present in all three main assemblages, with retouched artefacts typically occurring at

the upper end of this range. This threshold may therefore represent core exhaustion for the production of flakes selected for use.

A significant difference in reduction strategy is evident between the oldest assemblage at KAT1, S8, and the younger levels. The appearance of bifaces at Katoati is restricted to S8, with only a single, informal heavy tool evident in the overlying strata. Prepared core types, including Levallois cores, are less frequent in S8 than they are in the two other large assemblages, as well as S5. Retouched artefacts exhibiting delineated edges, such as tangs, tongues and shoulders, are most frequent in S6 and S4, with a single example in S8. Although the temporal gap between S8 and S6 is unclear, it would appear that a major change in reduction strategy occurs between the KAT1 assemblages in early MIS 5 (>91ka), with little significant difference apparent between the younger MIS 5 assemblages (S6 and S5) and the main assemblage from MIS 4-3 (S4).

Comparisons with 16R and Singi Talav

Examination of the lithic assemblages from 16R Dune and Singi Talav helps to contextualise the diachronic changes observed at Katoati. The larger Middle Palaeolithic assemblage from 16R Dune, 16R-Sup, is broadly contemporary (80-40ka) with S4 (55-65ka), whereas the majority of artefacts from 16R-Inf derive from an early MIS 5 context, corresponding with S5-S8 at Katoati. The chronology of the Singi Talav assemblages is problematic as no dated samples are directly associated with the lithic artefacts. While ESR dating at Amarpura has suggested lacustrine sedimentation is present in the area >797ka (Kailath et al. 2000) preliminary OSL age estimates from both the Singi Talav depression and Amarpura quarry suggest more recent sedimentation, returning results that fall within MIS 5-6 (Prof. R. Roberts, pers. comm.).

Artefact assemblages from 16R Dune and Singi Talav occur in low energy sedimentary contexts and as a result, the flake populations include a much greater proportion of artefacts measuring

<30mm compared to the Katoati assemblages. This may also reflect differences in reduction intensity and activities at these sites. Neither have raw material resources available in the immediate vicinity of the site and so larger flake sizes at Katoati may reflect more frequent primary reduction activities. The reporting of cores from 16R Dune and Singi Talav restricts direct comparisons with Katoati, as core reduction patterns are not described. However, no Levallois cores are noted in either 16R Dune or Singi Talav. In addition, cores and core tools from Singi Talav (mean=76.9x64.3x49.6mm) are typically larger than cores from Katoati (mean=43x53x35mm).

Retouched artefacts at these three sites exhibit comparable size ranges, typically between 44-53mm length, 33-38mm width and 14-30mm thickness. The reported typology of retouched artefacts from Singi Talav and 16R Dune presents a basic catalogue, indicating mostly marginal retouch with little imposition of form within the lower end of artefact size ranges. However, a larger artefact reported from 16R-Inf as a biface or core (Figure 5.28 – top right) exhibits a similar morphology to a delineated artefact from KAT1 (Figure 8.13f).

The most notable differences between these three sites relates to the production of heavy tools. Couché 4 at Singi Talav presents the clearest indication of reduction sequences that focus on biface production, including 20 handaxes and 3 cleavers. Low numbers of bifacial heavy tools occur in Couché 3 at Singi Talav (n=4), 16R-Sup (n=7), 16R-Inf (n=2) and S8 at Katoati (n=7). The average size of heavy tools from Singi Talav (113.3x70.6x37.8mm) is broadly equivalent with the larger bifaces from S8. The smaller bifaces from S8 (75-85x50-60x20-30mm) match the size range evident at 16R Dune. While an example of a finely reduced handaxe is present in the 16R-Sup sample, a number of artefacts recorded as heavy tools appear morphologically similar to Levallois cores (e.g. Figure 5.27: middle-right).

The Acheulean assemblages from Singi Talav appear distinct from those at Katoati and 16R-Dune due to the increased proportion of heavy tools present, which Gaillard (1993) indicates as the focus of reduction strategies. The oldest assemblages at Katoati, S8, may preserve aspects of similar reduction strategies, evident in the production of simple bifacial tools. These artefacts have also been identified at a number of sites in the Katoati landscape, including in the basal gravels observed in the *nalla* in which KAT1 was excavated (Figure 9.1), at JFL2, and in the excavations at Jayal (Misra et al. 1980). The finely crafted diminutive handaxe in 16R-Sup provides the clearest example for continuity in biface production within Middle Palaeolithic assemblages.



Figure 9.1: Biface observed in basal gravels in *nalla* at KAT1.

However, evidence for a bifacial point and bifacially retouched tanged and shouldered pieces at KAT1 may indicate how bifacial reduction has been employed to produce artefacts other than heavy tools. Similarly, definitions of Levallois core reduction schemes typically stress bifacial reduction. Overall, it appears that bifacial reduction practices have remained a feature of Lower and Middle Palaeolithic technologies in Nagaur District, although the objective of these strategies has changed through time, both in terms of reduction intensity and assemblage chronology. Future research focused upon the development of bifacial reduction strategies may be critical for the identification of technological distinctions between Lower and Middle Palaeolithic industries in the Thar Desert and in South Asia.

Palaeolithic Technology in the Thar Desert

The analyses of both excavated assemblages from KAT1 and surface assemblages from six areas surveyed in Rajasthan presents a significant investigation of lithic variability in the Thar Desert using an organisation of technology approach. This has offered a productive means to quantify the role reduction intensity and raw material differences have played in structuring lithic artefact variability. Significantly, this has permitted a number of trends in reduction strategy to be identified across survey sites in the Rajasthan Thar Desert that cross cut these contingent factors.

A number of Palaeolithic sites identified by surface survey present evidence for early reduction stages, partly due to the increased visibility of lithic assemblages close to raw material resources, such as at Sambhar Lake, Shergarh Tri-Junction and the Jaisalmer Raans. These three groups of sites present evidence of the exploitation of diverse raw material resources amongst Middle Palaeolithic assemblages in the Thar Desert, in terms of both the size of clasts

available and their differing fracture mechanics. Indeed, primary extraction of raw materials from boulder cores is evident at Sambhar Lake, Karna and the Pushkar Valley. Whereas many assemblages have been dominated by evidence for the early stages of reduction, those from TRI1 and TRI2 (as well as HOKF to a lesser extent), all occur close to raw material resources but exhibit a greater intensity of reduction, particularly evident in patterns of core exhaustion and discard. Primary reduction activities at some sites may have been undertaken to test and shape larger artefacts for export from raw material sources. It is clear that in some circumstances exhaustive reduction practices were undertaken despite the immediate availability of raw materials.

The use of prepared core technologies is evident in the Rajasthani Thar Desert sites. These are most apparent at Shergarh Tri-Junction, where a range of Levallois reduction strategies are evident, including a core exhibiting close similarity with a Nubian Type 2 point core. These typically exhibit a number of categorical indicators for more intensive reduction sequences, such as the use of more platforms and core rotations. However, unlike differences between single and multi-platform cores, these do not always result in decreased size attributes. Such contrasts help to differentiate the application of formal reduction strategies, which appear to target the production of certain flake products, and informal ones with a lesser degree of investment in preparation of flaking surfaces. This is in contrast to the evidence for systematic blade production strategies, which are most apparent at HOKF. Here, the size attributes of cores appear a more certain indicator of reduction intensity, as blade production has mostly resulted from unidirectional exploitation of a single, simple platform.

Points and tanged, shouldered and tongued artefacts are a key feature of Middle Palaeolithic assemblages across Rajasthan, regardless of raw material type. Indeed, one of the smallest of such artefacts occurs on one the coarsest raw material types and one of the larger specimens has been produced upon the most silicious material encountered (Figure 9.2). The recovery of

these artefacts in Middle Palaeolithic assemblages at the edge (Sambhar) and core (Jaisalmer) of the Desert, and in both sandy plains (Chamu) and river valleys (Karna) indicates that these forms are a significant feature throughout the region.



Figure 9.2: Large tanged point on silicious limestone from KHA1 (left) compared with small tanged point on gneiss from Sambhar Lake (right).

The technology and typology among the survey site assemblages correspond with those identified at Katoati. In particular, the production of delineated points and prepared core reduction strategies are apparent at Katoati and a number of other sites in the Rajasthan Thar Desert. Chronological similarities are also evident, with aspects of these distinctive reduction sequences typically apparent in contexts dating between MIS 5 and early MIS 3. The results of this study indicates that the hominin occupation of central and western Rajasthan, during the early and mid-Upper Pleistocene, is characterised by Middle Palaeolithic lithic assemblages including informal single and multi-platform cores with a repeated component of specialised prepared cores and tanged, tongued and shouldered points.

Blade core technologies do not feature at Katoati, but mark a distinct reduction strategy at Hokra. Whereas occasional blade proportioned flakes are encountered in Middle Palaeolithic assemblages, the core population from Hokra contains systematically produced parallel sided blades guided by longitudinal arises. The appearance of a single blade core, similar to those at Hokra, in the cores at Shergarh Tri-Junction is notable, suggesting both prepared and blade reduction strategies occur in similar landscape contexts. Furthermore, at TRI1 they appear to occur in a similar chronological context, relating to early MIS 3 colluvial and dune deposits. This may indicate contemporaneity between these reduction strategies at Hokra, previously suggested by Allchin et al. (1978) to relate to humid conditions at the start of MIS 3. It is significant to note that these blade reduction strategies do not meet regional definitions for micro-blade production that are typical of Late Palaeolithic industries. Changes in lithic technology in Rajasthan in MIS 3 do not appear to mark a wholesale change in reduction strategy from Middle to Late Palaeolithic industries, but instead exhibit some overlap of the two approaches.

Integrating technological and typological insights

The results of the fieldwork and lithic analyses presented herein offer new perspectives regarding Palaeolithic industries in the Thar Desert. Descriptions of core technology in the Palaeolithic literature for the Thar Desert have frequently been limited. The more detailed descriptions of core technology, particularly in Middle Palaeolithic assemblages, have indicated the use of prepared core strategies as a major feature of these industries. The emphasis on bifacial core types, including Levallois cores, is significant for investigating the nature of transitions between Lower and Middle Palaeolithic industries, which are otherwise focused on the elaboration of retouched tool typology and decreased size and frequency of heavy tool types.

A number of trends in the archaeological record of the Thar Desert have been identified in the new fieldwork. Typological analyses of Middle Palaeolithic assemblages highlighted the repeated occurrence of points within artefact catalogues, although little further description of these is available. The prevalence of delineated points in both the excavated and surface assemblages corroborates retouched points as a key feature of Middle Palaeolithic assemblages. The appearance of formal prepared point cores at both KAT1 and SHR1, as well as Levallois and prepared points at a number of sites, offer further support for the importance of points within Middle Palaeolithic assemblages, and may indicate some variability in techniques of production and use.

Middle Palaeolithic assemblages analysed here have indicated the use of a wide range of raw material types. In particular, these include the use of materials such as gneiss, sandstone and rhyolites that possesses very different flaking properties from the silicious materials typically evident in Late Palaeolithic assemblages. The deployment of similar reduction strategies across these raw material types is striking, suggesting that Middle Palaeolithic hominins could adapt reduction techniques to varying materials. Indeed, the use of formal prepared core technologies may have been significant to standardise techniques across raw material types. This would permit flexibility in resource exploitation patterns, both for raw material use and extraction in different geographic settings.

A number of factors may explain the prevalence of Middle Palaeolithic sites encountered, with few examples of Lower or Late Palaeolithic industries. Firstly, targeted survey of Upper Pleistocene sediment contexts may have precluded the identification of Lower Palaeolithic material in many, though not all, circumstances. Expansive exposures of sandstone and limestone around the Jaisalmer Raans are a clear exception to this, where dune coverage is minimal. Similarly, the existing archaeological record of the Thar suggests that Late Palaeolithic industries may not be apparent until after the LGM. As a result, such assemblages may relate

to the youngest episodes of dune formation, which were not targeted for survey. Furthermore, decreased visibility of Late Palaeolithic assemblages may be due to the smaller size of artefacts produced.

Distribution of raw material resources may have a significant impact influence on the distribution of Lower Palaeolithic sites. These industries are abundant at the fringes of the Thar, in the Rohri Hills, Saurashtra and the Aravallis, but not in the central Thar. This is true even where substantial geological outcrops occur, such as with the Malani volcanic group or Neogene sedimentary rocks of central and western Rajasthan. In many circumstances, the raised topography of these outcrops has prevented substantial aeolian accumulation, facilitating visibility. This suggests that a limited number of Lower Palaeolithic sites may represent the limited occupation of these regions. This distribution may also have related to differences in palaeoenvironmental conditions, suggesting that Lower Palaeolithic populations did not occupy the central regions of the desert due to increase aridity. However, given the longevity of Lower Palaeolithic occupations now evident in South Asia, it is surprising that Lower Palaeolithic populations rarely occupied the central Thar Desert during more humid phases.

Renewed, technologically orientated analyses of lithic assemblages from the Thar Desert are required to refine understanding of Late Palaeolithic assemblages and improve inter-regional comparisons, both within the Thar and beyond. In particular, a number of existing studies appear to highlight the dominance of microlithic reduction schemes, although this is rarely explicitly acknowledged. Metric analyses of Late Palaeolithic industries are vital to understand whether any discrete size difference occurs between artefacts such as blades, as such differences may differ between the Thar Desert and surrounding regions. This is particularly important given the potential co-occurrence of prepared cores and systematic blade cores. The blades produced here are often larger than metric definitions of microblades from other

regions (e.g. James 2011; Clarkson et al. 2012). Such insights may have a significant bearing for understanding regional trajectories of technological development as well as the origins of microlithic technologies in South Asia.

Palaeoenvironments and Palaeolithic Occupation in the Thar

Desert

Environmental conditions in the Thar Desert have had a significant bearing upon the distribution of Palaeolithic sites. This relates to both the palaeoenvironmental conditions that permitted hominin occupations and suitable contexts that preserve evidence for these occupations. Due to the extent of Upper and Middle Pleistocene sediment deposition, most suitable contexts for identifying the earliest hominin occupations of the Thar Desert are likely to be too deeply buried to be identified in the foreseeable future. However, if corroborated, the ESR date on carbonates from Nimbli Jordan of >1ma (Kailath et al. 2000) suggests some sediment contexts exist that may parallel the age of the oldest hominin occupation of South Asia. Similarly, the application of cosmogenic nuclide dating at Jayal may offer insight into the development of exogenous fluvial systems in the Thar Desert and their potential relationship to Lower Palaeolithic occupations. The application of parallel chronometric dating techniques in both Lower and Middle Pleistocene contexts is critical to understand environmental conditions in the Thar Desert, which otherwise remain in a relative, stratigraphic framework. As a result, the environmental context and chronology of hominin occupations of the Thar Desert >200ka remains obscure.

Repeated evidence for the Palaeolithic occupation of the Thar Desert is apparent from 200ka onwards. Hominin occupation in Saurashtra predates 190ka at Umrethi, which appears to be

oldest directly dated Palaeolithic artefacts in the region. Sporadic artefacts found throughout the dune sequence at 16R Dune attest to repeated, brief occupations at the site during MIS 6, and further dating of lacustrine sediments at Singi Talav may also indicate a similar pattern of occupation. Humid landforms dating to MIS 5 are repeatedly associated with Palaeolithic assemblages in both Gujarat and Rajasthan. Acheulean assemblages occur in alluvial contexts >100ka in Gujarat, and the oldest assemblages at Katoati (both KAT1-S8 and JFL2), may also share more in common with Lower Palaeolithic industries than the younger technologies at the site. The earliest Middle Palaeolithic assemblages at Katoati, S6 and S5, as well as from CHA2 and 16R Dune also offer evidence for hominin occupations of the Thar Desert during MIS 5. Fluvial sediments and pedogenesis dune sands suggest that these occupations occurred during more humid periods. Fresh artefacts cemented in gravels at Karna indicate further hominin occupation during the later stages of MIS 5 that overlaps with the upper age range for the main Middle Palaeolithic horizon at 16R Dune.

A number of Middle Palaeolithic assemblages relate to episodes of humidity in the latter half of MIS 4 and onset of MIS 3, apparent in Rajasthan and Gujarat. Humid landforms including fluvial sediments at Katoati, Jetpur, and the Orsang Valley dating between 65-49ka all contain Middle Palaeolithic assemblages. Further support for hominin occupation of the Thar Desert at this period is presented by the Middle Palaeolithic assemblages identified at Shergarh Tri-Junction, Karna and Chamu. This period also overlaps with the lower age range of the main Middle Palaeolithic assemblage at 16R Dune.

Evidence for the latter half of MIS 3 and the onset of MIS 2 are highly limited, for both environmental and archaeological records. This is likely to relate to the combination of the monsoonal minimum and glacial maximum. Increased aridity during the monsoonal minimum may have limited or prevented the occupation of the Thar Desert, and prevented the development of new humid sediment contexts. Increased monsoonal intensity linked with

cooler temperatures and sea surface temperatures over the glacial maximum is likely to have led to widespread aeolian mobilisation of surface sediments. Frequent remodelling of the landscape through dune mobility appears to have led to the disorganisation of drainage channels and other ecological resources. The clearest evidence for Late Palaeolithic occupation of the Thar Desert post-dates the LGM, with the appearance of microlithic industries between 21-16ka at 16R Dune and Katoati in the context of fluctuating humidity.

The lack of dated environmental records or archaeological sites from Sindh presents a significant problem for the integration of this sub-region into broader syntheses of hominin occupation in the Thar Desert. Critically, there is little evidence to indicate how the Lower Indus valley responded to palaeoclimatic variability during the Upper Pleistocene. Similarly, the role of the Ghaggar-Hakra throughout the Pleistocene is unknown. The delivery of fresh water from the mountain ranges to the north of the Thar Desert through some of the most arid parts of the region may have been significant for sustaining vegetative and faunal communities throughout monsoonal minima and glacial maxima. As a result these fluvial corridors may have preserved source populations for the colonisation of the Thar Desert with the amelioration of climates.

The Middle Palaeolithic archaeology of Sindh is limited, but distinct from the assemblages observed in Rajasthan due to the more extensive retouching of flakes. Further regional differences are also pronounced in Late Palaeolithic assemblages. While this may be the result of different cultural practices, the availability of highly silicious raw materials in large clast sizes may explain much of the variability between the regions. The different spatial distribution of raw material resources may also go some way to explain variability in artefact assemblages. The alluvial plains of the Indus and Ghaggar-Hakra valleys do not offer surface geological outcrops, which are more widely available in both Rajasthan and Gujarat. As a result, Palaeolithic hominins in Sindh may have had to produce more reliable lithic toolkits from more

limited but finer raw material resources to be used in landscapes in which it was not possible to replace broken or poorly functioning tools.

The Palaeolithic Occupation of the Thar Desert in Broader Context

This thesis has presented a comprehensive characterisation of the Palaeolithic occupation of the Thar Desert. The development of new technologically orientated evidence for lithic reduction strategies facilitates comparison with the Palaeolithic archaeology of other regions in South Asia and the Mid-Latitude Desert belt. Furthermore, by situating the archaeological record within a chronometric and palaeoenvironmental framework, a broader assessment of the role that the Thar Desert has played in hominin dispersals during the Upper Pleistocene is possible.

The identification of sizeable Middle Palaeolithic assemblages in early MIS 5 and at the boundary of MIS 4/3 at Katoati help to fill significant chronological lacunae identified in the South Asian Palaeolithic record (Figure 9.3). The best dated and most thoroughly analysed Middle Palaeolithic assemblages in South Asia are known from a series of excavations in the Jurerru Valley (Petraglia et al. 2007; 2009; 2012a; Haslam et al. 2012). Here, Middle Palaeolithic assemblages are found stratified in both palaeolsol and fluvial contexts that bracket a significant horizon of primary and reworked ash from the eruption of Toba at 74ka. The oldest assemblages, excavated at JWP22 and JWP3, are found directly below the Toba horizon and are dated by OSL to 71-77ka (Petraglia et al. 2012a), whereas assemblages dating to ca. 50ka and 38-34ka are identified overlying the Toba horizon, at JWP3, JWP23, JWP20 and JWP21 (Petraglia et al. 2009). Elsewhere in India, dated Middle Palaeolithic sites are rare and sample sizes are too small to effectively characterise lithic technology.

The results of the fieldwork in the Thar Desert complement that from the Jurreru Valley in a number of ways. Firstly, the chronology of Middle Palaeolithic assemblages at KAT1 interleave with those from the Jurreru Valley, supporting the suggestions that these industries are present in South Asia >80ka and continue to occur into MIS 3. Secondly, they support the suggestion for broad cultural continuity spanning the eruption of Toba, with few discernible differences between KAT1 assemblages S4 and S6. A number of similarities in artefact technology and typology are apparent. In both cases core technologies combine a mix of single and multiplatform methods with prepared core types, including Levallois cores (Clarkson et al. 2012). The presence of a tanged point, a bifacial point and Levallois points at JWP22 is paralleled at KAT1 by similar findings in both S4 and S6 (Figure 9.4). This is particularly significant as tanged points have not been documented in stratified contexts of South Asia prior to excavations at JWP22.

The earliest assemblage from KAT1, S8, presents a number of typological differences to both the younger assemblages at Katoati and those from the Jurreru Valley. In particular, the limited presence of Levallois cores and tanged and shouldered artefacts and the appearance of numerous bifacial heavy tools is notable. The presence of bifacial heavy tools in an artefact assemblage including both prepared cores and flake tools is comparable with the Late Acheulean assemblages reported from the sites of Bamburi and Patpara, in the Son Valley, dating between 140-120ka (Haslam et al. 2011). This also overlaps with the chronology of a number of the small artefact assemblages present in the 16R Dune sequence, and potentially with the younger horizons at Singi Talav. As a result, the excavated evidence from Katoati adds to a growing body of evidence indicative of the Late Acheulean occupation of South Asia during MIS 6 that also encompasses the onset of MIS 5 and interglacial climatic conditions.

The lack of clearly dated Late Palaeolithic industries in the Thar Desert preceding the LGM prevent comparisons with sites in Sri Lanka, the Jurreru Valley and at Patne that appear to

document the autochthonous origins of microlithic technologies. Nevertheless, the appearance of blade based industries at Hokra, and to a lesser extent at Shergarh Tri-Junction, as well as in Sindh, may indicate different regional trajectories in Late Palaeolithic lithic

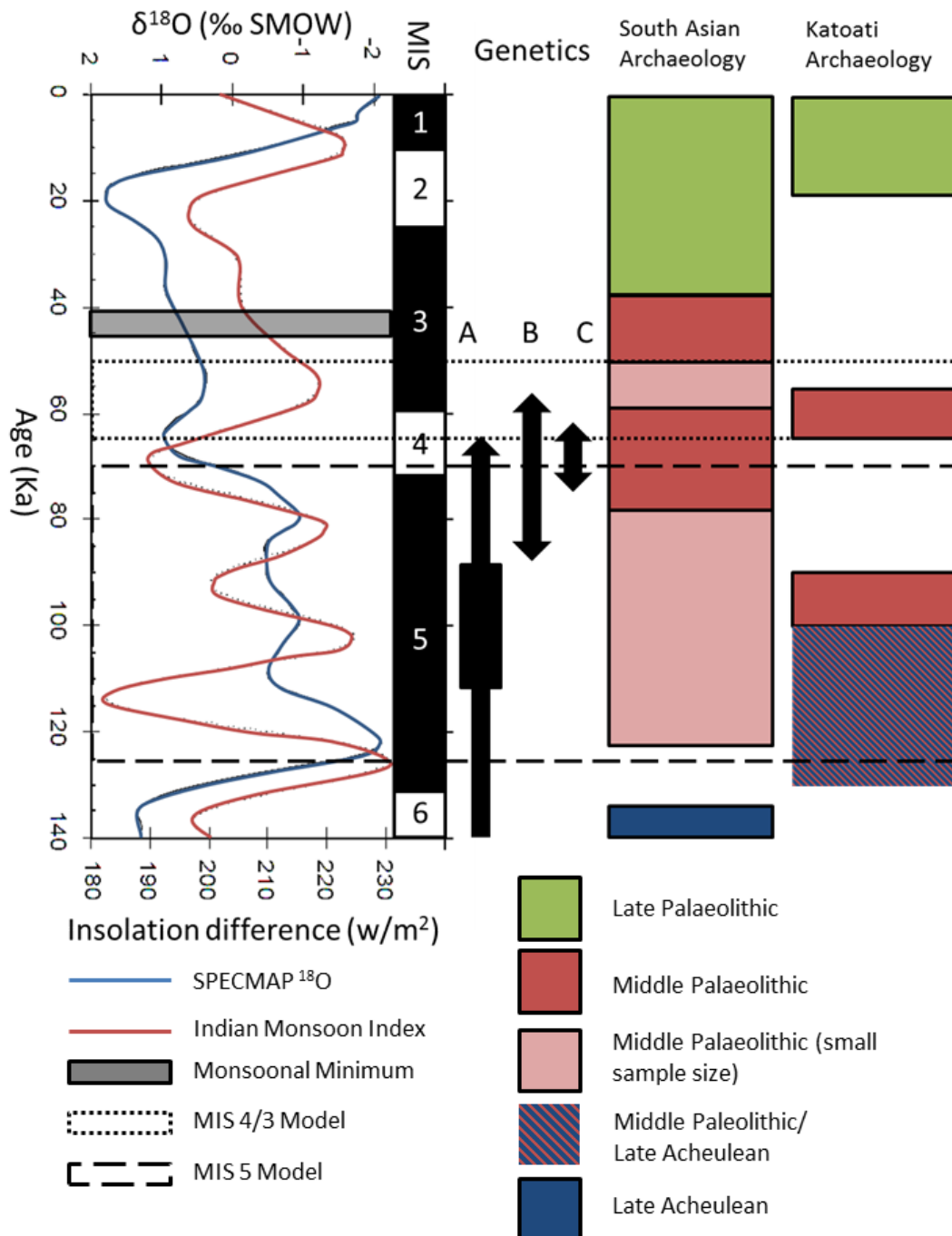


Figure 9.3: Synthesis of environmental and archaeological evidence from South Asia and Katoati, including genetic age estimates relating to human dispersals and suggested arrival of

modern humans in South Asia by two models. Environmental evidence includes SPECMAP Oxygen Isotope curve and associated Marine Isotope Stages (MIS) (following Imbrie et al. 1984), Indian Monsoon Index based upon variability in insolation at 30°N due to orbital tilt, precession and eccentricity (Leuschner & Sirocko 2003), and estimated monsoonal minimum based upon time averaged patterns of monsoonal intensity across 9 Lower and Middle glacial-interglacial cycles (Liu 2012). Archaeological evidence presented from South Asia is discussed in Chapter 2 and 5 (see also Petraglia 2012a; Haslam et al. 2011). Genetic results indicate age estimates for: A) Genomic estimate of split of Eurasian from African populations 112-88ka (C.I. 150-63ka) (Xing et al. 2009); B) mtDNA estimate of appearance of Hg L3 at 72ka. (C.I. 87-56ka) (Soares et al. 2009); and C) genomic estimate of split of East Eurasians from proto-Eurasian group (Rasmussen et al. 2011). MIS 4/3 model for the arrival of *Homo sapiens* in South Asia derived from Mellars (2006), MIS 5 model for the arrival of *Homo sapiens* in South Asia derived from Petraglia et al. (2010; 2012b).



Figure 9.4: Above – Tanged point from Jwalapuram 22 ca. 74ka (Haslam et al. 2012); Below – Tanged point from Katoati S5 ca. 91ka.

technologies that are not as reliant upon microlithisation as their southern counterparts at the end of MIS 3. The severity of aridity relating to the monsoonal minimum and glacial maximum are a likely cause for discontinuity in the hominin occupation of the Thar Desert in MIS 2. As a result, the microlithic technologies that accompanied renewed occupation of the Thar Desert

after 20Ka are likely to have their origins in surrounding regions that were able to support hominin occupation at the height of climatic instability.

The results of both the excavation at Katoati and survey in Rajasthan have identified a number of distinctive lithic artefacts that are also comparable to those found in sites in arid landscapes in both South West Asia and Saharan Africa. The appearance of Nubian-style cores at KAT1 dating to MIS 4/3 are a significant discovery, and may indicate a similar chronology for the Nubian core identified at SHR1. Nubian core technologies form an aspect of Middle Stone Age industries identified in the Nile Valley (Van Peer 2000; Van Peer et al. 2003, 2010; Chiotti et al. 2009; Olszewski et al. 2010) eastern Saharan oases (Wendorf et al. 1994; Smith et al. 2007), the Red Sea hills (Van Peer et al. 1996), and to a lesser extent in the Horn of Africa (Clark 1954; Kurashina 1978; Clark 1988). Recently, Nubian cores have also been reported from the Dhofar region, southern Oman (Rose et al. 2011; Usik et al. 2012), indicating that these reduction strategies are not solely restricted to Africa (Figure 9.5 and 9.6). Comparative studies with Nubian industries from Arabia and Africa will help to confirm the identification of these distinctive core types in the archaeological record of the Thar Desert. The discovery of several Nubian-style cores in the Thar Desert presents a significant expansion in their distribution, as well as diversification in the raw materials on which they are produced.

The occurrence of tanged, shouldered and nosed pieces in the Thar Desert, and the single tanged point from the Jurreru Valley, also draws parallels with Middle Stone Age assemblages from Saharan Africa. Aterian assemblages from the Sahara have been characterised by the presence of tanged points and pedunculates, although other aspects of reduction strategies at these sites appear spatially variable (Scerri 2012). Recent chronometric dating of Aterian sites indicates they typically occur from the end of MIS 6 to the onset of MIS 3 (Scerri 2012), which corresponds with the time span of Middle Palaeolithic sites in the Thar Desert that include tanged, shouldered and nosed pieces. The purpose of tanging and shouldering is typically

considered to relate to the hafting of lithic artefacts, yet both functional uses of hafted points and their broader cultural significance is debated (Shea 2006; Scerri 2012). The similarities between tanged and shouldered artefacts in the Sahara and Thar Deserts may indicate a shared cultural heritage or that they provided some adaptive significance for the occupation of arid landscapes.

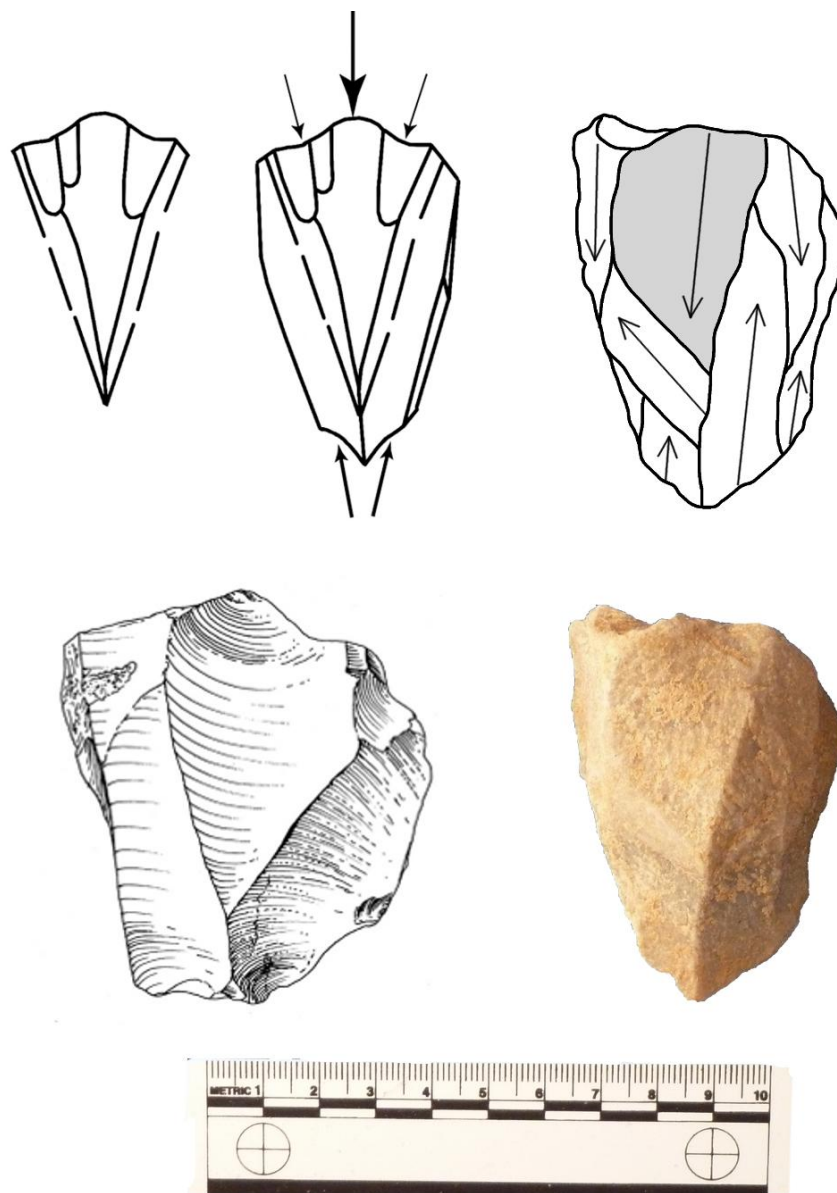


Figure 9.5: Nubian Type 1 reduction strategy. Top-left: Schematic depiction of Nubian Type 1 reduction strategy (from Figure 2 [Rose et al. 2011]); Bottom-left: Example of Arabian Nubian Type 1 core from Aybut Al Auwal (from Figure 9 [Rose et al. 2011]); Top-right: schematic depiction of Nubian Type 1-like core from KAT 1-S4; Bottom-right: photo of Nubian Type 1-like core from KAT 1-S4.

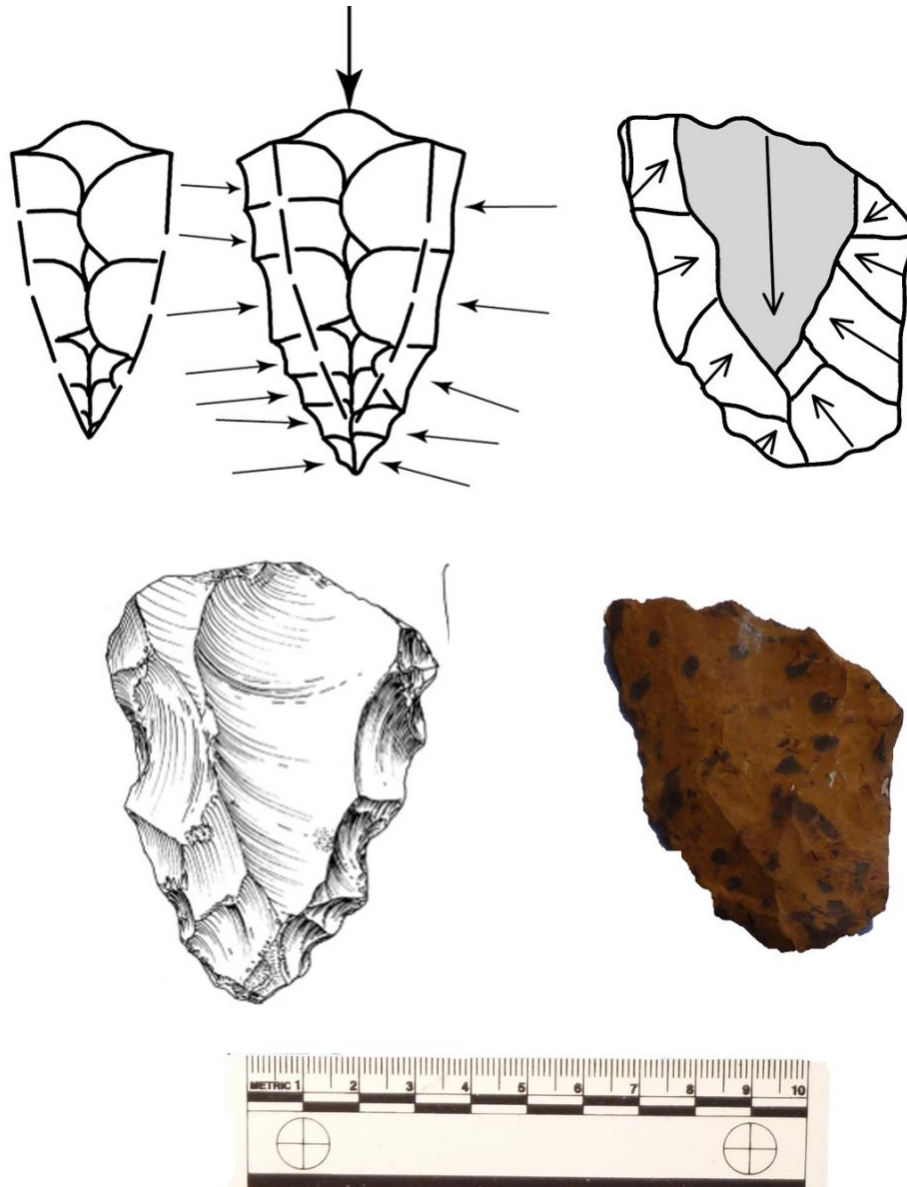


Figure 9.6: Nubian Type 2 reduction strategy. Top-left: Schematic depiction of Nubian Type 2 reduction strategy (from Figure 2 [Rose et al. 2011]); Bottom-left: Example of Arabian Nubian Type 2 core from Aybut Al Auwal (from Figure 9 [Rose et al. 2011]); Top-right: schematic depiction of Nubian Type 2-like core from SHR1; Bottom-right: photo of Nubian Type 2-like core from SHR1.

Relating archaeological assemblages to patterns of hominin demography is a difficult endeavour, complicated in a region such as South Asia owing to the lack of a hominin fossil record. The fossil hominin from Narmada is a likely candidate to represent the populations that produced Late Acheulean industries (Haslam et al. 2011). The relationship between the population represented by the Narmada specimen and either Pleistocene hominins in East Asia (see Norton & Jin 2009) or the genetically identified Denisovans (Reich et al. 2010) is unclear. However, the potential for some demographic continuity between South and East Asia cannot be discounted. Biagi and Starini (2011) raise the potential that Mousterian-like Middle Palaeolithic assemblages observed at sites such as Ongar in Sindh may mark the south-eastern extent of the range of Neanderthal populations. The biogeographic boundary that occurs in the Thar Desert, between the desert landscapes to the west and monsoon-dominated landscapes to the east, may have played a significant role in structuring this complex hominin milieu.

Recently, two different models for the dispersal of *Homo sapiens* into South Asia have been set out. The first suggests that a single dispersal of *Homo sapiens* from Africa resulted in the colonisation of South Asia 65-50ka, based upon mitochondrial DNA age estimates (Macaulay et al. 2005). Mellars (2006) suggests these populations are represented in the archaeological record by the appearance of a repertoire of material culture analogous to the Howieson's Poort cultures of southern and eastern Africa. Comparable material is identified at sites identified here as Late Palaeolithic, such as at Batadomba Lena and Patne (Mellars 2006). This model is presented as the MIS 4/3 model of Figure 9.3.

The second model proposes earlier and potentially numerous dispersals of populations of *Homo sapiens*, which are first identified in the fossil record of South West Asia during MIS 5 (Petraglia et al. 2010; 2012b). Analyses of Upper Pleistocene assemblages from Africa, southern Asia and Australia have indicated that Middle Palaeolithic technologies in South Asia

dated between 74-38ka show distinct similarities with African Middle Stone Age technologies, produced by modern humans (Petraglia et al. 2007; Clarkson et al. 2012). As Middle Palaeolithic technologies significantly overlap genetic estimates for the arrival of *Homo sapiens* in South Asia, unlike Late Palaeolithic industries, it is proposed that the former may have been produced by the earliest modern human populations in the subcontinent (Petraglia et al. 2010; 2012b). This is presented as the MIS 5 model on Figure 9.3.

The distinctive techno-typological features identified from Katoati and the survey sites in Rajasthan present further support for a relationship between Indian Middle Palaeolithic and African Middle Stone Age assemblages in MIS 5. The appearance of Middle Stone Age archaeological assemblages in Arabia during MIS 5 (Armitage et al. 2011; Rose et al. 2011) is broadly accepted to relate to a dispersal of African populations (Appenzeller 2012). The lack of MSA features in lithic assemblages east of Arabia has previously indicated to some that this was a limited and ultimately unsuccessful foray by African populations into new territories:

“There’s not a smell, not a whiff [of Nubian technologies] that has ever been detected in India,” says Mellars. “If Mike Petraglia could come to me with one of those Nubian cores and say, ‘Look, we found this in India,’ I would get down on my knees and say, ‘Sorry, Mike, I got it wrong’.” (Appenzeller 2012:26).

In the light of new discoveries made at Katoati and the Thar Desert, it is clear that parallels exist between lithic technologies in the MSA of the Sahara and Arabia and in the Middle Palaeolithic of the Thar Desert in MIS 5 and in MIS 4-3. The current level of understanding of the archaeological and environmental records of the Thar Desert permits a discussion only of the Palaeolithic *occupation* of the region. In order to investigate complex cultural and demographic scenarios, such as the dispersal of modern humans, a finer level of chronological resolution is required to address colonisation processes in the Thar Desert.

References Cited

- Achyuthan, H., 2003. Petrologic analysis and geochemistry of the Late Neogene-Early Quaternary hardpan calcretes of Western Rajasthan, India. *Quaternary International* 106-107, 3-10.
- Achyuthan, H., Quade, J., Roe, L., & Placzek, C., 2007. Stable isotopic composition of pedogenic carbonates from the eastern margin of the Thar Desert, Rajasthan, India. *Quaternary International* 162-3, 50–60.
- Agrawal, D.P., Datta, P.S., Husain, S., Krishnamurthy, R.V., Misra, V.N., Rajaguru, S.N., & Thomas, P.K., 1980. Palaeoclimate, stratigraphy and prehistory in North and West Rajasthan. *Proceedings of the Indian Academy of Sciences* 89, 51-66.
- Agrawal, D.P., & Ghosh, A. 1973. *Radiocarbon and Indian Archaeology*. Bombay: Tata Institute.
- Ajithprasad, P., 1988. *Pleistocene Stratigraphy and the Prehistoric Archaeology of the Orsang Valley*. Ph.D. Thesis. Vadodara: M.S. University of Baroda.
- Ajithprasad, P., 2005a. Early Middle Palaeolithic: a Transition Phase between the Upper Acheulian and Middle Palaeolithic cultures in the Orsang Valley, Gujarat. *Man and Environment* 30, 1-11.
- Ajithprasad, P., 2005b. Palaeolithic Cultural Sequence in the Sukhi valley, Gujarat. In: *River Valley Cultures of India*, K. K. Chakrabarty and G. L. Badam (Eds.). New Delhi: IGRMS Bhopal and Aryan Book International, pp 83-98.
- Allchin, B., 1959. The Indian Middle Stone Age. *Bulletin of the Institute of Archaeology, London* 2, 1-36.
- Allchin, B., 1995. Early Human Cultures and Environments in the northern Punjab, Pakistan: an Over view of the Potwar project of the British Archaeological Mission to Pakistan (1981-1991). In: *Quaternary Environments and Geoarchaeology of India*, Wadia, S., Korisettar, R., & Kale V.S. (Eds.). Bangalore: Geological Survey of India.
- Allchin, B., & Goudie, A., 1974. Pushkar: Prehistory and Climatic Change in Western India. *World Archaeology* 5, 358-68.
- Allchin, B., Goudie, A., & Hegde, K., 1978. *The Prehistory and Palaeogeography of the Great Indian Desert*. London: Academic Press.
- Allison, L.E., & Moodie, C.D., 1965. Carbonate. In: *Methods of Soil Analysis: Part 2 - Chemical and Microbiological Properties*, A.G. Norman (Eds.). Agronomy Monograph 9.2, American Society of Agronomy, Soil Science Society of America, pp. 1379-1396.

- An, Z., Clemens, S.C., Shen, J., Qiang, X., Jin, Z., Sun, Y., Prell, W. L., Luo, J., Wang, S., Xu, H., Cai, Y., Zhou, W., Liu, X., Liu, W., Shi, Z., Yan, L., Xiao, X., Chang, H., Wu, F., & Lu, F., 2012. Glacial-Interglacial Indian Summer Monsoon Dynamics. *Science* 333, 719-723.
- Andrefsky Jr., W., 2005. *Lithics: Macroscopic Approaches to Analysis*. Cambridge: Cambridge University Press (2nd Edition).
- Andrefsky Jr., W., 2009. The analysis of stone tool procurement, production and maintenance. *Journal of Archaeological Research* 17, 65–103.
- Andrews, J.E., Singhvi, A.K., Kailath, A.J., Kuhn, R., Dennis, P.F., Tandon, S.K., & Dhir, R.P., 1998. Do stable isotope data from calcrete record Late Pleistocene monsoonal climate variation in the Thar Desert of India? *Quaternary Research* 50, 240–251.
- Appenzeller, T., 2012. Human migrations: Eastern odyssey. *Nature* 485, 24-6.
- Armitage, S.J., Jasim, S.A., Marks, A.E., Parker, A.G., Usik, V.I., & Uerpmann, H.-P., 2011. The southern route “Out of Africa”: evidence for an early expansion of modern humans into Arabia. *Science* 331, 453-456.
- Athreya, S., 2007. Was Homo heidelbergensis in South Asia? A test using the Narmada fossil from central India. In: *The evolution and history of human populations in South Asia, Petraglia, M.D., & Allchin, B.* (Eds.). Dordrecht: Springer, pp 137–170.
- Badam, G. L., 1977. Inamgaon: human skeletal remains. *Man and Environment* 1, 56-58.
- Bailey, G., 2007. Time perspectives, palimpsests and the archaeology of time. *Journal of Anthropological Archaeology* 26, 198-223.
- Bajpei, V.N., Saha Roy, T.K., & Tandon, S.K., 2001. Subsurface sediment accumulation patterns and their relationships with tectonic lineaments in the semi-arid Luni river basin, Rajasthan, Western India. *Journal of Arid Environments* 48, 603-621.
- Banerjee, K.D., 1957. *Middle Palaeolithic Industries of the Deccan*. Ph.D thesis. Pune: Poona University.
- Baskaran, M., 1985. *Radiometric, mineralogical and trace elemental studies of Saurashtra Quaternary carbonate deposits: implications as to their age and origin*. Ph.D. Thesis. Ahmedabad: Gujarat University.
- Baskaran, M., Marathe, A.R., Rajaguru, S.N. & Somayajulu, B.L.K., 1986. Geochronology of Palaeolithic Cultures in the Hiran Valley, Saurashtra, India. *Journal of Archaeological Science* 13, 505-514.
- Baskaran, M., Rajagopalan, G., & Somayajulu, B.L.K., 1989. ²³⁰Th/²³⁴U and ¹⁴C dating of the Quaternary deposits of Saurashtra, India. *Chemical Geology (Isotope Geoscience Section)* 79, 65-82.

- Benjamini, Y., & Hochberg, Y., 1995. Controlling the false discovery rate: a practical and powerful approach to multiple testing. *Journal of the Royal Statistical Society, Series B (Methodological)* 57, 289–300.
- Bennet, P.C., 1991. Quartz dissolution in organic-rich aqueous systems. *Geochimica et Cosmochimica Acta* 55, 1781-1797.
- Berger, A., & Loutre, M.F., 1991. Insolation values for the climate of the last 10 million years. *Quaternary Science Reviews* 10, 297-317.
- Bhatt, N., 2003. The Late Quaternary bioclastic carbonate deposits of Saurashtra and Kachchh, Gujarat, Western India: A review. *Proceedings of the Indian National Science Academy* 69, 137-150.
- Bhatt, N., & Bhone, U., 2006. Geomorphic expressions of Late Quaternary sea level changes along the southern Saurashtra coast, Western India. *Journal of Earth System Science* 115, 395–402.
- Biagi, P. 1997. Flint assemblages from the Rohri Hills in British collections. *Ancient Sindh* 4, 19-30.
- Biagi, P., 2003-2004 - The Mesolithic Settlement of Sindh (Pakistan): A Preliminary Assessment. *Praehistoria* 4-5, 195-220.
- Biagi, P., 2007. Ongar revisited. *Sindhological Studies* 25, 1–21.
- Biagi, P., 2008. The Palaeolithic Settlement of Sindh: A Review. *Archäologische Mitteilungen aus Iranand Turan* 40, 1-26.
- Biagi, P., 2011. Late (Upper) Palaeolithic Sites at Jhimpir. In: *Studies in Honour of Isin Yalcinkaya*, Taskiran, H., Kartal, M., Ozcelik, K., Kosem, M.B., & Kartal, G. (Eds.). Bilgin Kulltur Sanat Yayolan, pp. 67-84.
- Biagi, P., & Cremaschi, M., 1988. The early Palaeolithic sites of the Rohri Hills (Sind, Pakistan) and their environmental significance. *World Archaeology* 19, 421-433.
- Biagi, P., & Shaikh, N., 1998–1999. Preliminary report of the surveys and excavations carried out by members of the “Joint Rohri Hills Project”. *Ancient Sindh* 5, 65–75.
- Biagi, P., & Starini, E., 2011. Neanderthals at the south-easternmost edge: the spread of Levalloisian Mousterian in the Indian subcontinent. In: *Papers in honour of Viola T. Dobosi*, Biro, K.T., & Marko, A., (Eds). Budapest: Hungarian National Museum 5-14.
- Biagi, P., Kazi, M.M., & Negrino, F., 1996. An Acheulian workshop at Ziarat Pir Shaban on the Rohri Hills, Sindh, Pakistan. *South Asian Studies* 12, 49–62.
- Biagi, P., Kazi, M.M., Madella, M., & Ottomano, C., 1998-2000. Excavations at the Late (Upper) Palaeolithic site of Ziarat Pir Shaban 2 (ZPS2) in the Rohri Hills, Sindh, Pakistan. *Estratto da Origini Preistoria e Protostoria delle Civiltà Antiche* 22, 111-113.

- Biswas, S.K., 1987. Regional tectonic framework, structure and evolution of the western marginal basins on India. *Tectonophysics* 135, 307-327.
- Blanford, W.T., 1877. Geological notes on the Great Indian Desert between Sind and Rajputana. *Records of the Geological Survey of India* 10, 10-21.
- Bleed, P., 2011. Loosening our Chains: Cognitive insights for the Archaeological Application of Sequence Models. *PalaeoAnthropology 2011 (Special Issue)*, 297-304.
- Blinkhorn, J., 2008. *In which context does symbolic behaviour first become manifest in the archaeological record: A case study from Kurnool District, India*. M.Phil. Thesis. Cambridge: University of Cambridge.
- Bordes, F. 1961. *Typologie du Paléolithique ancien et moyen*. Delmas: Publications de l'Institut de Préhistoire de l'Université de Bordeaux, Mémoire n° 1, réédition CNRS 1988
- Braconnot, P., Otto-Bliesner, B., Harrison, S., Jousaume, S., Peterchmitt, J.-Y., Abe-Ouchi, A., Crucifix, M., Driesschaert, E., Fichet, Th., Hewitt, C. D., Kageyama, M., Kitoh, A., Lâiné, A., Loutre, M.-F., Marti, O., Merkel, U., Ramstein, G., Valdes, P., Weber, S. L., Yu, Y., and Zhao, Y. 2003 Results of PMIP2 coupled simulations of the Mid-Holocene and Last Glacial Maximum – Part 1: experiments and large-scale features. *Climate Past* 3, 261-277.
- Breecker, D.O., Sharp, Z.D., & McFadden, L.D., 2009. Seasonal bias in the formation and stable isotopic composition of pedogenic carbonate in modern soils from central New Mexico, USA. *Geological Society of America Bulletin* 121, 630-640.
- Burnes, A., 1834. Papers descriptive of the North West Frontier of India: The Thurr or Desert; Jodhpur and Jaysalmer. *Journal of the Royal Geographic Society* 4, 88-129.
- Cammiade, L. A. & Burkitt, M. C., 1930. Fresh Light on the Stone Age in Southeast India. *Antiquity* 4 327-339.
- Carr, P.J., & Bradbury, A.P., 2011. Learning from Lithics: A perspective on the Foundation and Future of the Organisation of Technology. *PalaeoAnthropology 2011 (Special Issue)*, 305-319.
- Cerling, T.E., 1999. Palaeorecords of C4 plants and ecosystems. In: *C4 Plant Biology*, Sage, R.F., Monson, R.K. (Eds.). San Diego: Academic Press, pp. 445-469.
- Cerling, T.E., Levin, N.E., Quade, J., Wynn, J.G., Fox, D.L., Kingston, J.D., Klein, R.G., & Brown, F.H., 2010. Comment on the Paleoenvironment of *Ardipithecus ramidus*. *Science* 328, 1105.
- Chamyal, L.S., Maurya, D.M., & Raj, R., 2003. Fluvial systems of the drylands of western India: a synthesis of Late Quaternary environmental and tectonic changes. *Quaternary International* 104, 69-86.

Chauhan, P. R., 2009. The South Asian Paleolithic record and its potential for transitions studies. In: *Sourcebook of Paleolithic Transitions*, Camps, M., & Chauhan, P.R. (Eds.). Dordrecht: Springer, pp. 121-139.

Chauhan, P. R., 2010. Comment on 'Lower and Early Middle Pleistocene Acheulian in the Indian sub-continent' by Gaillard et al. (2009) (*Quaternary International*). *Quaternary International* 223-224, 248-259.

Chawla, S., Dhir, R.P., Singhvi, A.K., 1992. Thermoluminescence chronology of sand profiles in the Thar Desert and their implications. *Quaternary Science Reviews* 11, 25–32.

Chiotti, L., Dibble, H.L., McPherron, S.P., Olszewski, D.I., & Schurmans, U.A., 2009. Prospections sur le plateaux de désertiques du desert libyque égyptien (Abydos, Moyenne Egypte). Quelques exemples de technologies lithiques. *l'Anthropologie* 113, 341–355.

Chowesky, V., Maurya, D.M., Joshi, P., Khonde, N., Archana Das, & Chamyal, L.S., 2011. Lithostratigraphical development and neotectonic significance of the Quaternary sediments along the Kachchh Mainland Fault (KMF) zone, western India. *Journal of Earth System Sciences* 120, 979-999.

Clark, G., 1977. *World Prehistory in New Perspective*. Cambridge: Cambridge University Press (3rd Edition).

Clark, J.D., 1954. *The Prehistoric Cultures of the Horn of Africa*. Cambridge: Cambridge University Press.

Clark, J.D., 1988. Middle Stone Age of East Africa and the beginnings of regional identity. *Journal of World Prehistory* 2, 235–305.

Clarkson, C., 2007. *Lithics in the Land of the Lightning Brothers: The Archaeology of Wardaman Country, Northern Territory*. Canberra: Australia National University Press (Terra Australis 25).

Clarkson, C., Petraglia, M., Korisettar, R., Haslam, M., Boivin, N., Crowther, A., Ditchfield, P., Fuller, D., Miracle, P., Harris, C., Connell, K., James, H., & Koshy, J., 2009. The oldest and longest enduring microlithic sequence in India: 35 000 years of modern human occupation and change at the Jwalapuram Locality 9 rockshelter. *Antiquity* 83, 326-348.

Clarkson, C., Harris, C., Jones, S., 2012. Continuity and change in the lithic industries of the Jurreru Valley, India, before and after the Toba eruption. *Quaternary International* 258, 165-179.

Clemens, S., Prell, W., Murray, D., Shimmield, G.B., & Weedon, G., 1991. Forcing mechanisms of the Indian Ocean monsoon. *Nature* 353, 720-725.

Cronin, T.M. 2010. *Paleoclimates: understanding climate change past and present*. New York: Columbia University Press.

Cunningham, A. 1872-3. Archaeological Survey of India. *Report for the Year 1872-3*, 105-8.

- de Terra, H., & Paterson T. T., 1939. *Studies on the Ice Age in India and Associated Human Cultures*. Washington, D. C.: Carnegie Institute of Washington, Publication no. 393.
- Dennell, R., 2009. *The Palaeolithic Settlement of Asia*. Cambridge: Cambridge University Press.
- Dennell, R.W. & H. Rendell 1991. De Terra and Paterson, and the Soan flake industry: a perspective from the Soan Valley, Pakistan. *Man and Environment* 16, 2, 91-99.
- Dennell, R., Rendell, H., Halim, M., & Moth, E., 1992. A 45,000-Year-Old Open-air Paleolithic Site at Riwat, Northern Pakistan. *Journal of Field Archaeology* 19, 17-33.
- Dennell, R., & Roebroeks, W., 2005. An Asian perspective on early human dispersal from Africa. *Nature* 438, 1099-1104.
- Deotare, B.C., Kajale, M.D., Rajaguru, S.N., Kusumgar, S., Jull, A.J.T, & Donahue, J.D., 2004. Palaeoenvironmental history of Bap-Malar and Kanod playas of western Rajasthan, Thar desert. *Proceedings of the Indian Academy of Sciences (Earth and Planetary Sciences)* 113, 402-425.
- Deriyaganala, S. U., 1992. *The Prehistory of Sri Lanka: An Ecological Perspective*. Colombo: Department of Archaeology Survey, Government of Sri Lanka.
- Deutz, P., Montanez, I.P., & Monger, H.C., 2002. Morphology and stable and radiogenic isotope composition of pedogenic carbonates in Late Quaternary relict soils, New Mexico, USA: an integrated record of pedogenic overprinting. *Journal of Sedimentary Research* 72, 809–822.
- Dhir, R.P., Tandon, S.K., Sareen, B.K., Ramesh, R., Rao, T.K.G., Kailath, A.J., & Sharma, N., 2004. Calcretes in the Thar: genesis, chronology and palaeoenvironment. *Proceedings of the Indian Academy of Sciences (Earth and Planetary Sciences)* 113, 473–515.
- Dhir, R.P., Singhvi, A.K., Andrews, J.E., Kar, A., Sareen, B.K., Tandon, S.K., Kailath, A., & Thomas, J.V., 2010. Multiple episodes of aggradation and calcrete formation in late Quaternary aeolian sands, central Thar Desert, Rajasthan, India. *Journal of Asian Earth Sciences* 37, 10-16.
- Dookia, S., Rawat, M., Jakher, G.R., & Dookia, B.R., 2009. Status of the Indian Gazelle (*Gazella bennettii* Sykes, 1831) in the Thar Desert of Rajasthan, India. In: *Faunal Ecology and Conservation of the Great Indian Desert*, Sivaperuman, C. Baqri, Q.H., Ramaswamy, G., & Naseema, M. (Eds.). Leiden: Springer pp. 193-207.
- Enzel, Y., Ely, L.L., Mishra, S., Ramesh, R., Amit, R., Lazar, B., Rajaguru, S.N., Baker, V.R., & Sandler, A., 1999. High-resolution Holocene environmental changes in the Thar Desert, northwestern India. *Science* 284, 125-128.
- Fleitmann, D, Burns, S.J., Pekala, M., Mangini, A., Al-Subbary, A., Al-Aowah, M., Kramers, J., & Matter, A., 2011. Holocene and Pleistocene pluvial periods in Yemen, southern Arabia. *Quaternary Science Reviews* 30, 783-787.

Foley, R., & Lahr, M.M., 1997. Mode 3 Technologies and the Evolution of Modern Humans. *Cambridge Archaeological Journal* 7, 3-36.

Foote, R. B., 1866. On the occurrence of stone implements in laterite formations in various parts of the Madras and North Arcot Districts. *Madras Journal of Literature and Science* 3, 1-36.

Foote, R.B., 1898. *The Geology of Baroda State*. Madras: Madras Government Museum.

Foote, R.B., 1916. *The Foote Collection of Indian Prehistoric and Protohistoric Antiquities: Notes on Their Ages and Distribution*. Madras: Madras Government Museum.

Gaillard, C. 1993. *Contribution a la connaissance du Palaeolithique inferieur-moyen en Inde*. Ph.D. Thesis. Marseille: Universite de Provence.

Gaillard, C., 2006. Les premiers peuplements d' Asie du Sud: vestiges culturels. *C.R. Palevol* 5, 359–369.

Gaillard, C., Raju, D.R., Misra, V.N., & Rajaguru, S.N., 1983. Acheulian occupation at Singi Talav in the Thar Desert: a preliminary report on 1982 excavation. *Man and Environment* 7, 112–130.

Gaillard, C., Raju, D.R., Misra, V.N., & Rajaguru, S.N., 1986. Handaxe assemblages from Didwana region, Thar Desert, India: A metrical analysis. *Proceedings of the Prehistoric Society* 52, 189–214.

Gaillard, C., Mishra, S., Singh, M., Deo, S., & Abbas, R., 2010a. Lower and early Middle Pleistocene Acheulian in the Indian sub-continent. *Quaternary International* 223-224, 234-241.

Gaillard, C., Mishra, S., Singh, M., Deo, S., & Abbas, R., 2010b. Reply to: "Comment on 'Lower and early Middle Pleistocene Acheulian in the Indian sub-continent'" by P.Chauhan. *Quaternary International* 223-224, 260-264.

Geological Survey of India, 1999. *Geological and Mineral Map of Rajasthan*. Calcutta: Geological Society of India.

Goudie, A., Allchin, B., & Hegde, K. T. M., 1973. The former Extensions of the Great Indian Sand Desert. *Geographical Journal* 139, 243-57.

Gould, R. A., 1968. Living archaeology: the Ngatatjara of western Australia. *Southwestern Journal of Anthropology* 24, 101-122.

Green, R, Krause, J., Briggs, A., Maricic, T., Stenzel, U., Kircher, M., Patterson, N., Li, H., Zhai, W., Hsi-Yang Fritz, M. Hansen, N. F, Durand, E. Y. Malaspinas, A., Jensen, J. D., Marques-Bonet, T., Alkan, C., Prüfer, K., Meyer, M., Burbano, H., Good, J., Schultz, R., Aximu-Petri, A., Butthof, A., Höber, B., Höffner, B., Siegemund, M., Weihmann, A., Nusbaum, C., Lander, E., Russ, C., Novod, N., Affourtit, J., Egholm, M., Verna, C., Rudan, P., Brajkovic, D., Kucan, Ž., Gušić, I., Doronichev, V., Golovanova, L., Lalueza-Fox, C., de la Rasilla, M., Fortea, J., Rosas, A., Schmitz, R., Johnson, P., Eichler, E., Falush, D., Birney, E., Mullikin, J., Slatkin, M., Nielsen, R., Kelso, J.,

Lachmann, M., Reich, D., & Pääbo, S., 2010. A Draft Sequence of the Neandertal Genome. *Science* 328, 710-722.

Haslam, M., Roberts, R.G., Shipton, C., Pal, J.N., Fenwick, J., Ditchfield, P., Boivin, N., Dubey, A.K., Gupta, M.C., & Petraglia, M., 2011. Late Acheulean hominins at the Marine isotope stage 6/5e transition in north-central India. *Quaternary Research* 75, 670-682.

Haslam, M., Clarkson, C., Roberts, R.G., Bora, J., Korisettar, R., Ditchfield, P., Chivas, A., Harris, C., Smith, V., Oh, A., Eksambekar, S., Boivin, N., & Petraglia, M., 2012. A southern Indian Middle Palaeolithic occupation surface sealed by the 74 ka Toba eruption: further evidence from Jwalapuram Locality 22. *Quaternary International* 258, 148-164.

Idris, M, Singh, P. & Johari, 2007. Impact Assessment of the Indira Gandhi Canal on the Avifauna of the Thar Desert. In: *Faunal Ecology and Conservation of the Great Indian Desert*, Sivaperuman, C., Baqri, Q.H., Ramaswamy, G., & Naseema, M. (Eds). Leiden: Springer, pp 119-135.

Imbrie, J., Hays, J.D., Martinson, D.G., McIntyre, A., Mix, A.C., Morley, J.J., Pisias, N.G., Prell, W.L. & Shackleton, N.J., 1984. The orbital theory of Pleistocene climate: Support from a revised chronology of the marine N18O record. In: *Milankovitch and Climate, Part 1*, Berger, A.L., Imbrie, J., Hays, J.D., Kukla, G., Saltzman, B. (Eds.). Dordrecht: Reidel, pp. 269-305.

Immerzeel, W. W., van Beek, L.P.H. & Bierkens, M. F. P., 2010. Climate change will affect the Asian water towers. *Science* 328, 1382-1385.

Indian Archaeology - A Review (IAR). Delhi: Archaeological Survey of India.

Inizan, M-L., Roche, H., & Tixier, J., 1992. *Technology of Knapped Stone*. Meudon: CREP.

Isaac, N. 1960. *The Stone Age Cultures of Kurnool District*. Ph.D. Thesis. Pune: Poona University.

Jain, M., & Tandon, S.K., 2003. Fluvial response to Late Quaternary climate changes, western India. *Quaternary Science Reviews* 22, 2223–2235.

Jain, M., Tandon, S.K., Singhvi, A.K., Mishra, S., & Bhatt, S.C. 2005. Quaternary alluvial stratigraphical development in a desert setting: a case study from the Luni River basin, Thar Desert of western India. *Special Publications of the International Association of Sedimentologists* 35, 349-371.

Jakher, G.R., Bhargava, S.C., & Sinha, R.K., 1990. Comparative limnology of Sambhar and Didwana lakes (Rajasthan, NW India). *Hydrobiologia* 197, 245-256.

James, H.V.A., 2011. *Becoming Human: The emergence of modern human behaviour in South Asia*. Ph.D. Thesis. Cambridge: University of Cambridge.

James, H.V.A. & Petraglia, M.D., 2005. Modern Human Origins and the Evolution of Behavior in the Later Pleistocene Record of South Asia. *Current Anthropology* 46(Supplement), S3-S27.

James, H.V.A. & Petraglia, M.D., 2009. The Lower to Middle Palaeolithic Transition in South Asia and its Implications for Hominin Cognition and Dispersals. In: *Source book of Palaeolithic Transitions*, M. Camps, M., & Chauhan, P. (Eds.). Leiden: Psringer, 255-264.

Johnson, B.J., Fogel, M.L., & Miller, G.H., 1998. Stable isotopes in modern ostrich eggshell: A calibration for paleoenvironmental applications in semi-arid regions of southern Africa. *Geochimica et Cosmochimica Acta* 62, 2451-2461.

Juyal, N., Pant, R.K., Bhushan, R., & Somayajulu, B.L.K., 1995. Radiometric Dating of Late Quaternary Sea Levels of the Saurashtra Coast, Western India: an Experiment with Oyster and Clam Shells. In: *Quaternary Environments and Geoarchaeology of India*, Wadia, S., Korisettar, R., & Kale, V.S. (Eds.). Bangalore: Geological Society of India, pp. 372-379.

Juyal, N., Kar, A., Rajaguru, S.N. & Singhvi, A.K., 2003. Luminescence chronology of aeolian accretion during the Late Quaternary in the southern margin of Thar Desert. *Quaternary International* 104, 87-98.

Juyal, N., Chamyal, L.S., Bhandari, S., Bhushan, R. & Singhvi, A.K., 2005. Continental record of the south west monsoon during the last 130ka: evidences from the southern margin of the Thar Desert, India. *Quaternary Science Reviews* 25, 2632-2650.

Kailath, A. J., Rao, T. K. G., Dhir, R. P., Nambi, K. S. V., Gogte, V. D., & Singhvi, A. K., 2000. Electron spin resonance characterization of calcretes from Thar desert for dating applications. *Radiation Measurements*, 32, 371-383.

Kar, A., 1996. Morphology and evolution of sand dunes in the Thar desert as key to sand control measures. *Indian Journal of Geomorphology* 1, 177-206.

Kennedy, K. A. R., 2000. *God Apes and Fossil Men: Paleoanthropology in South Asia*. Ann Arbor: University of Michigan Press.

Khan, A. R., 1968. Ancient Settlements in the Karachi Region. *Dawn*, July 21 & 28 1968.

Khan A.R. 1979 Palaeolithic sites discovered in the Lower Sindh and their significance in the prehistory of the country. In: *Studies in the geomorphology and prehistory of Sind*, Khan, A.R. (Ed.). Jamshoro: Grassroots III Special Issue, vol. 2, pp. 81-86.

Kivisild, T., Bamshad, M., Kaldma, K., Metspalu, M., Metspalu, E., Reidla, M., Laos, S., Parik, J., Watkins, W., Dixon, M., Papiha, S., Mastana, S., Mir, M., Ferak, V., & Villems, R., 1999. Deep common ancestry of Indian and western-Eurasian mitochondrial DNA lineages. *Current Biology* 9, 1331-1334.

Kivisild, T., Rootsi, S., Metspalu, M., Mastana, S., Kaldma, K., Parik, J., Metspalu, E., Adojaan, M., Tolk, H., Stepanov, V., Gołge, M., Usanga, E., Papiha, S., Cinnioglu, C., King, R., Cavalli-Sforza, L., Underhill, P., & Villems, R., 2003. The Genetic Heritage of the Earliest Settlers Persists Both in Indian Tribal and Caste Populations. *American Journal of Human Genetics* 72, 313-332.

- Klein, R., 1995. Anatomy, Behavior and Modern Human Origins. *Journal of World Prehistory* 9, 167-198.
- Klein, R., 1999. *The Human Career: human biological and cultural origins*. Chicago: University of Chicago Press.
- Klein, R., 2000. Archeology and the Evolution of Human Behavior. *Evolutionary Anthropology* 9, 17-36.
- Korisettar, R., 2007. Towards developing a basin model for Paleolithic settlement of the Indian subcontinent: Geodynamics, Monsoon dynamics and habitat diversity and dispersal routes. In: *The evolution and history of human population in South Asia*, Petraglia, M.D. & Allchin, B. (Eds). Leiden: Springer. 69-96.
- Kumar, G., 1988. Ostrich Egg and Prehistoric Man: Some More Evidences from Chambal Valley. In: *Adaptation and Other Essays*, Ghosh, N.C. & Chakrabarti, S (Eds.). Santiniketan: Visva Bharati, pp. 69-74.
- Kumar, S., 2008. Conservation of Sambhar Lake - An important Waterfowl habitat and a Ramsar Site in India. In: *Proceedings of Taal2007: The 12th World Lake Conference*, Sengupta, M., & Dalwani, R. (Eds.). Delhi: Ministry of Environment and Forests, Government of India, pp.1509-1517.
- Kumar, S., & Pandey, S. K., 2010. Trace fossils from the Nagaur Sandstone, Marwar Supergroup, Dulmera area, Bikaner district, Rajasthan, India. *Journal of Asian Earth Sciences*, 38, 77-85.
- Kurashina, H., 1978. *An examination of prehistoric lithic technology in east central Ethiopia*. Ph.D Thesis. Berkeley: University of California, Berkeley.
- La Touche, T.H.D., 1910. Relics of the Great Ice Age in the Plains of Northern India. *Geological Magazine* 7, 193-201.
- Laghari, A. 2004. *Petrology of the Nagar Parkar granites and associated basic rocks, Thar District, Sindh, Pakistan*. Ph.D. Thesis. Peshawar: National Centre of Excellence in Geology, University of Peshawar.
- Lahr, M. M. & Foley, R., 1994. Multiple dispersals and modern human origins. *Evolutionary Anthropology* 3, 48-60.
- Lele, V.S., 1974. The Miliolite limestone at Saurashtra, Western India. *Sedimentary Geology* 10, 301-10.
- Leuschner, D.C., & Sirocko, F., 2003. Orbital insolation forcing of the Indian Monsoon - a motor for global climate changes? *Palaeogeography, Palaeoclimatology, Palaeoecology* 197, 83-95.
- Liu, Z., 2011. Glacial Cycles and Indian Monsoon - A Southern Push. *Science* 333, 706-707.

Loeppert, R. H., & Suarez, D. L., 1996. *Carbonate and gypsum*. Publications from USDA-ARS / UNL Faculty. Paper 504.

Logan, A. C., 1906. *Old Chipped Stones of India*. Calcutta: Thacker, Spink and Company.

Lycett, S. J., 2007. Is the Soanian technocomplex a Mode 1 or Mode 3 phenomenon? A morphometric assessment. *Journal of Archaeological Science* 34, 1434-1440.

Macaulay, V., Hill, C., Achilli, A., Rengo, C., Clarke, D., Meehan, W., Blackburn, J., Semino, O., Scozzari, R., Cruciani, F., Taha, A., Kassim Shaari, N., Maripa Raja, J., Ismail, P., Zainuddin, Z., Goodwin, W., Bulbeck, D., Bandelt, H., Oppenheimer, S., Torroni, A., & Richards, M., 2005. Single, Rapid Coastal Settlement of Asia Revealed by Analysis of Complete Mitochondrial Genomes. *Science* 308, 1034-1036.

Marathe, A., 1981. *Geoarchaeology of the Hiran Valley*. Poona: Deccan College.

Maurya, D.M., Chamyal, L.S., Merh, S.S., 1995. Tectonic evolution of the Central Gujarat plain, western India. *Current Science* 69, 610-613.

Maurya, D. M., Thakkar, M. G., Patidar, A. K., Bhandari, S., Goyal, B. & Chamyal, L. S., 2008. Late Quaternary geomorphic evolution of the coastal zone of Kachchh, western India. *Journal of Coastal Research* 24, 746-758.

Mellars, P., 2006. Going East: new genetic and archaeological perspectives on the modern human colonization of Eurasia. *Science* 313, 796-800.

Mellars, P., & Stringer, C., (Eds.) 1989. *The Human Revolution: Behavioural and biological perspectives on the origins of modern humans*. Princeton: Princeton University Press.

Michael, L., Gopala Rao, D., Krishna, K.S. & Vora, K.H. 2009. Late Quaternary seismic sequence stratigraphy of the Gulf of Kachchh, northwest of India. *Journal of Coastal Research* 25, 459-468.

Mishra, S., 1995. Chronology of the Indian Stone Age: the Impact of Recent Absolute and Relative Dating Attempts. *Man and Environment* 20, 11-16.

Mishra, S., & Rajaguru, S.N., 1993. Quaternary Deposits at Bhedaghat, near Jabalpur, Madhya Pradesh. *Man and Environment* 18, 7-13.

Mishra, S., Jain, M., Tandon, S.K., Sinhvi, A.K., Joglekar, P.P., Bhatt, S.C., Kshirsagar, A.A., Maik, S., & Deshpande-Muhkerje, A., 1999. Prehistoric Cultures and Late Quaternary Environments in the Luni Basin around Balotra. *Man and Environment* 24, 39-49.

Misra, V. N., 1961 Palaeolithic culture of western Rajputana; *Bulletin of the Deccan College Research Institute* 21, 85-156.

Misra, V.N., 1962. Problems of Terminology in Indian Prehistory. *The Eastern Anthropologist* 15, 113-124.

- Misra, V.N., 1967. *Pre-and Proto- History of the Berach Basin South Rajasthan*: Pune: University of Poona.
- Misra V.N., 1968. Middle Stone Age in Rajasthan. In: *La prehistoire: Problemes et tendances*, Bordes, F., & de Sonneville Bordes, D. (Eds.). Paris: Centre National de la Recherche Scientifique, pp. 295–305.
- Misra, V.N., 1978. The Acheulian industry of rock shelter III F-23 at Bhimbetka, central India — a preliminary study. *Australian Archaeology* 8, 63–106.
- Misra, V. N., 2001. Prehistoric human colonization of India. *Journal of Bioscience* 26, 491– 531.
- Misra, V.N., 1982. Evolution of the blade element in the Stone Industries of the Rock Shelter III F23, Bhimbetka . In: *Indian Archaeology, New Perspectives*, Sharma, K. (Ed.). Delhi: Agam Kala Prakashan: Delhi, pp. 7-13.
- Misra, V.N., 1985. The Acheulian succession at Bhimbetka, Central India. In: *Recent advances in Indo-Pacific Prehistory*, Misra, V.N., & Bellwood, P. (Ed.) New Delhi:IBH, pp. 35-47.
- Misra, V.N., 1989. Stone Age India: An Ecological Perspective. *Man and Environment* 14, 17-64.
- Misra, V.N., 1995. Geoarchaeology of the Thar Desert, North West India. In: *Quaternary Environments and Geoarchaeology of India*, Wadia, S., Korisettar, R. & Kale, V. (Eds.). Bangalore: Geological Society of India, pp.210-230.
- Misra V.N., & Rajaguru, S.N., 1986. Environment et culture de l’homme prehistorique dans le desert du Thar, Rajasthan, Inde; *L’ Anthropologie* 90, 407–437.
- Misra, V.N., Rajaguru, S.N., Agrawal, D.P., Thomas, P.K., Husain, Z., & Dutta, P.S., 1980. Prehistory and Palaeoenvironment of Jayal, Western Rajasthan. *Man and Environment* 4, 19-31.
- Misra, V. N., Rajaguru. S. N., Raju, D. R., Raghavan, H. & Gaillard, C., 1982. Acheulian occupation and evolving landscape around Didwana in the Thar Desert, India. *Man and Environment* 6, 72-86.
- Mohapatra, G. C., Bhatia, S. B. & Sahu, B. K., 1963. The Discovery of a Stone Age Site in the Indian Desert. *Research Bulletin (N.S.) Punjab University* 14, 205-23.
- Movius H.L., 1948. The Lower Palaeolithic cultures of Southern and Eastern Asia. *Transactions of the American Philosophical Society* 38, 329–420.
- Murty, M.L.K., 1974. A Late Pleistocene cave site in southern India. *Proceedings of the Philosophical Society* 118, 196-230.
- Murty, M.L.K., 1979. Recent research on the Upper Palaeolithic Phase in India. *Journal of Field Archaeology* 6, 301-320.

- Nambi, K.V.S., & Murthy, M.L.K., 1983. An Upper Palaeolithic Fireplace in the Kurnool Caves. *Bulletin of the Deccan College Post-Graduate and Research Institute* 42, 110-13.
- Negrino, F., & Kazi, M.M., 1996. The Palaeolithic industries of the Rohri Hills (Sindh - Pakistan). *Ancient Sindh* 3, 7-38.
- Nesbitt, H.W., & Young, G.M., 1982. Early Proterozoic climates and plate motions inferred from major element chemistry of lutites. *Nature* 299, 715-717.
- Norton, C.J., & Jin, J.J.H., 2009. The evolution of modern human behavior in East Asia: Current perspectives. *Evolutionary Anthropology* 18, 247-260.
- Olszewski, D.I., Dibble, H.L., McPherron, S.P., Schurmans, U.A., Chiotti, L., & Smith, J.R., 2010. Nubian Complex strategies in the Egyptian high desert. *Journal of Human Evolution* 59, 188-201.
- Otto-Bliesner, B. L., Marshall, S. J., Overpeck, J. T., Miller, G. H., & Hu, A., 2006. Simulating Arctic climate warmth and icefield retreat in the last interglaciation. *Science*, 311, 1751-1753.
- Paddayya, K., 1982. The Lower/ Middle Palaeolithic transition in the Hungsi valley, peninsula India. In: *The Transition from Lower to Middle Palaeolithic and the Origin of Modern Man*, Ronen, A. (Ed.). Oxford: BAR, pp. 257-264.
- Pandey, A. N., Parmar, T. D., & Tanna, S. R., 1999. Desertification: a case study from Saurashtra region of Gujarat state of India. *Tropical ecology*, 40, 213-220.
- Paddayya, K., Blackwell, B., Jhaldiyal, R., Petraglia, M. D., Fevrier, S., Chaderton, D., Blickstein, J., & Skinner, A., 2002. Recent findings on the Acheulian of the Hunsgi and Baichbal valleys, Karnataka, with special reference to the Isampur excavation and its dating. *Current Science* 85, 641-647.
- Pandey, D.K. & Bahadur, T., 2009. A review of the stratigraphy of Marwar Supergroup of West-central Rajasthan. *Journal of the Geological Society of India* 73, 747-758.
- Pant, R. K., & Juyal, N. (1993). Late Quaternary coastal instability and sea level changes: New evidences from Saurashtra coast, Western India. *Zeitschrift fur Geomorphologie*, 37, 29-29.
- Pappu, S., Gunnell, Y., Akhilesh, K., Braucher, R., Taieb, M., Demory, F., & Thouveny, N., 2011. Early Pleistocene presence of Acheulian hominins in south India. *Science* 331, 1596-1599.
- Parker, A., 1970. An index of weathering for silicate rocks. *Geological Magazine* 107, 501-504.
- Perera, N., Kourampas, N., Simpson, I.A., Deraniyagala, S.U., Bulbeck, D., Kamminga, J., Perera, J., Fuller, D.Q., Szabo, K., & Oliveira, N.V., 2011. People of the ancient rainforest: Late Pleistocene foragers at the Batadomba-lena rockshelter, Sri Lanka. *Journal of Human Evolution* 61, 254-269.

Petraglia, M.D., 1998. The Lower Palaeolithic of India and its bearing on the Asian record. In: *Early human behavior in global context: the rise and diversity of the Lower Palaeolithic record*, Petraglia M.D., & Korisettar, R. (Eds.). New York: Routledge. pp 343–90.

Petraglia, M.D., 2001. The Lower Palaeolithic of India and its behavioural significance. In: *Human roots: Africa and Asia in the Middle Pleistocene*, Robson-Brown, K., & Barham, L. (Eds.). Bristol: Western Academic & Specialist Press, pp 217–233.

Petraglia, M.D., & Potts, R., 1994. Water Flow and the Formation of Early Pleistocene Artifact Sites in Olduvai Gorge, Tanzania. *Journal of Anthropological Archaeology* 13, 228-254.

Petraglia, M.D. & Paddayya, K., 2005. New insights on the Acheulean: A case study from southern India. *Humankind* 1, 61-75.

Petraglia, M., Korisettar, R., Boivin, N., Clarkson, C., Ditchfield, P., Jones, S., Koshy, J., Lahr, M.M., Oppenheimer, C., Pyle, D., Roberts, R., Schwenninger, J.-L., Arnold, L., & White, K., 2007. Middle Palaeolithic assemblages from the Indian subcontinent before and after the Toba super-eruption. *Science* 317, 114-116.

Petraglia, M., Korisettar, R., Kasturi Bai, M., Boivin, N., Bora, J., Clarkson, C., Cunningham, K., Ditchfield, P., Fuller, D., Hampson, J., Haslam, M., Jones, S., Koshy, J., Miracle, P., Oppenheimer, C., Roberts, R., & White, K., 2009a. Human occupation, adaptation and behavioral change in the Pleistocene and Holocene of south India: recent investigations in the Kurnool District, Andhra Pradesh. *Eurasian Prehistory* 6, 119-166.

Petraglia, M., Clarkson, C., Boivin, N., Haslam, M., Korisettar, R., Chaubey, G., Ditchfield, P., Fuller, D., James, H., Jones, S., Kivisild, T., Koshy, J., Lahr, M.M., Metspalu, M., Roberts, R.G., & Arnold, L., 2009b. Population increase and environmental deterioration correspond with microlithic innovations in South Asia ca. 35,000 years ago. *Proceedings of the National Academy of Sciences* 106, 12261-12266.

Petraglia, M., Haslam, M., Fuller, D., Boivin, N., & Clarkson, C., 2010. Out of Africa: new hypotheses and evidence for the dispersal of *Homo sapiens* along the Indian Ocean rim. *Annals of Human Biology* 37, 288-311.

Petraglia, M.D., Ditchfield, P., Jones, S., Korisettar, R., & Pal, J.N., 2012a. The Toba volcanic super-eruption, environmental change, and hominin occupation history in India over the last 140,000 years. *Quaternary International* 258, 119-134.

Petraglia, M.D., Groucutt, H., & Blinkhorn, J., 2012b. Hominin evolutionary history in the Arabian Desert and the Thar Desert. In: *Changing Deserts: Integrating People and their Environment*, Mol, L., & Sternberg, T. (Eds.). Cambridge: White Horse Press, pp. 61-82.

Possehl, G. L., 2002. *The Indus civilization: a contemporary perspective*. Walnut Creek, CA: Alta Mira Press.

Powell, A., Shennan, S., & Thomas, M., 2009. Late Pleistocene demography and the appearance of modern human behavior. *Science* 324, 1298-1301.

Prins, M. A., Postma, G., Cleveringa, J., Cramp, A. & Kenyon, N.H., 2000. Controls on terrigenous sediment supply to the Arabian Sea during the late Quaternary: the Indus Fan. *Marine Geology* 169, 327-349.

Raghavan, H., Rajaguru, S. & Misra, V.N., 1989. Radiometric Dating of a Quaternary Dune Section. *Man and Environment* 13, 19-22.

Rajwat, A.S., Verma, P.K., & Nayak, S., 2003. Reconstruction of palaeodrainage network in northwest India: Restrospect and prospect of remote sensing studies. *Proceedings of Indian National Science Academy* 69, 217-230.

Rao, A. S. 2009. Climate and microclimate changes influencing the fauna of the hot Indian arid zone. In: *Faunal ecology and conservation of the Great Indian Desert*, Sivaperuman, C., Baqri, Q.H., Ramaswamy, G., & Naseema, M. (Eds). Leiden: Springer, pp. 13-23.

Rao, S. R., 1962-63. Excavations at Rangpur and other explorations in Gujarat. *Ancient India* 18-19, 5-207.

Rasmussen, M., Guo, X., Wang, Y., Lohmueller, K.E., Rasmussen, S., Albrechtsen, A., Skotte, L., Lindgreen, S., Metspalu, M., Jombart, T., Kivisild, T., Zhai, W., Eriksson, A., Manica, A., Orlando, L., De La Vega, F., Tridico, S., Metspalu, E., Nielsen, K., Ávila-Arcos, M.C., Moreno-Mayar, J.V., Muller, C., Dortch, J., Gilbert, M.T.P., Lund, O., Wesolowska, A., Karmin, M., Weinert, L.A., Wang, B., Li, J., Tai, S., Xiao, F., Hanihara, T., van Driem, G., Jha, A.R., Ricaut, F-X., de Knijff, P., Migliano, A.B., Gallego-Romero, I., Kristiansen, K., Lambert, D.M., Brunak, S., Forster, P., Brinkmann, B., Nehlich, O., Bunce, M., Richards, M., Gupta, R., Bustamante, C.D., Krogh, A., Foley, R.A., Lahr, M.M., Balloux, F., Sicheritz-Pontén, T., Villems, R., Nielsen, R., Jun, W., & Willerslev, E., 2011. An Aboriginal Australian Genome Reveals Separate Human Dispersals into Asia. *Science*. 334, 94-98.

Reich, D., Green, R.E., Kircher, M., Krause, J., Patterson, N., Durand, E.Y., Viola, B., Briggs, A.W., Stenzel, U., Johnson, P.L.F., Maricic, T., Good, J.M., Marques-Bonet, T., Alkan, C., Fu, Q., Mallick, S., Li, H., Meyer, M., Eichler, E.E., Stoneking, M., Richards, M., Talamo, S., Shunkov, M.V., Derevianko, A.P., Hublin, J.-J., Kelso, J., Slatkin, M., & Pääbo, S., 2010. Genetic history of an archaic hominin group from Denisova Cave in Siberia. *Nature* 468, 1053-1060.

Rendell, H. M., Dennell, R. W & Halim, M. A., 1989. *Pleistocene and Palaeolithic Investigations in the Soan Valley, Northern Pakistan. British Archaeological Mission to Pakistan*. Oxford: Bar International Series, no 544.

Rolland, N. & Dibble, H. L. 1990. A new synthesis of Middle Paleolithic variability. *American Antiquity* 55, 480–499.

Rose, J.I., Usik, V.I., Marks, A.E., Hilbert, Y.H., Galletti, C.S., Parton, A., Geiling, J-M., Ciktör, C., Morley, M.W., & Roberts, R.G., 2011. The Nubian Complex of Dhofar, Oman: An African Middle Stone Age Industry in Southern Arabia. *PLoS ONE* 6, e28239.
doi:10.1371/journal.pone.0028239

- Roy, A.B. 1999. Evolution of saline lakes in Rajasthan. *Current Science* 76, 290-296.
- Roy, A.B. & Jakhar, S. R., 2001. Late Quaternary drainage disorganisation, and migration and extinction of the Vedic Saraswati. *Current Science* 81, 1188-1195.
- Sali, S. A., 1989. *The Upper Palaeolithic and Mesolithic Cultures of Maharashtra*. Pune: Deccan College Post Graduate and Research Institute.
- Sankalia, H.D., 1946. *Investigations into Prehistoric Archaeology of Gujarat*. Baroda: Baroda State Press.
- Sankalia, H.D., 1955. Excavations at Langhnaj, Gujarat. *Man* 55, 26-26.
- Sankalia, H.D., 1956. Animal fossils and Palaeolithic industries from the Pravara basin at Nevassa, district Ahmadnagar. *Ancient India* 12, 35-52.
- Sankalia, H.D., 1964. Middle Stone Age Culture in India and Pakistan . *Science* 146, 365-75.
- Sankalia, H.D., 1974. *Prehistory and Protohistory of India and Pakistan*. Poona: Deccan College.
- Scerri, E.M.L, 2012. The Aterian and its place in the North African Middle Stone Age. *Quaternary International* <http://dx.doi.org/10.1016/j.quaint.2012.09.008>
- Schick, K.D., 1984. *Processes of Palaeolithic site formation: An experimental study*. Ph.D. Thesis. Berkeley: University of California.
- Schiffer, M.B. 1987. *Formation Processes of the Archaeological Record*. Albuquerque: University of New Mexico Press.
- Schiffer, M.B., 2010. *Behavioral Archaeology: Principles and Practice*. London:Equinox.
- Segalen, L., Renard, M., Lee-Thorp, J.A., Emmanuel, L., Le Callonnec, L., de Rafelis, M., Senut, B., Pickford, M., & Melice J-L., 2006. Neogene climate change and emergence of C4 grasses in the Namib, southwestern Africa, as reflected in ratite 13C and 18O. *Earth and Planetary Science Letters* 244, 725-734.
- Shackley, M. L., 1974. Stream abrasion of flint implements. *Nature* 248, 501-502.
- Shaikh, N., Veesar, G.M., & Mallah, Q.H., 2002-2003. Recent Discoveries of Sites/Industrial Complexes in Thar, Rohri Hills and Adjacent Plains: Regional Perspectives. *Ancient Sindh* 7, 27-66.
- Sharma, G.R., & Clark, J.D., 1983. *Palaeoenvironments and Prehistory in the Middle Son Valley*. Allahabad :Abinash Prakashan.
- Sharma, K.K. & Mehra, S.P. 2007. The Thar of Rajasthan (India): Ecology and Conservation of a Desert Ecosystem. In: *Faunal Ecology and Conservation of the Great Indian Desert*, Sivaperuman, C., Baqri, Q.H., Ramaswamy, G., & Naseema, M. (Eds). Leiden: Springer, pp 1-11.

- Shea, J.J., 2006. The origins of lithic projectile point technology: evidence from Africa, the Levant and Europe. *Journal of Archaeological Science* 33, 823-846.
- Shennan, S., 2001. Demography and Cultural Innovation: a Model and its Implications for the Emergence of Modern Human Culture. *Cambridge Archaeological Journal* 11, 5-16.
- Shetty, B.V. 1994. Flora of the Indian arid zone. In: *Sustainable development of the Indian arid zone*, Singh, R.P. & Singh, S. (Eds.): Jodhpur: Scientific, pp. 55–63.
- Sikes, N.E., Potts, R., & Behrensmeyer, A.K., 1999. Early Pleistocene habitat in Member 1 Olorgesailie based on paleosol stable isotopes. *Journal of Human Evolution* 37, 721-746.
- Singh, G., Joshri, R.D., & Singh, A.B., 1972. Stratigraphic and radiocarbon evidence for the age and development of three last-lake deposits in Rajasthan, India. *Quaternary Research* 2, 496-505.
- Singh, G., Joshri, R.D., Chopra, S.K., & Singh, A.B., 1974. Late Quaternary history of vegetation and climate of the Rajasthan Desert, India. *Philosophical Transactions of the Royal Society of London (Series B)* 267, 467-501.
- Singhvi, A.K., & Kar, A., 2004. The Aeolian sedimentation record of the Thar desert. *Proceedings Indian of the Academy of Sciences (Earth and Planetary Sciences)* 113, 371–402.
- Singhvi, A.K., Williams, M. A. J., Rajaguru, S.N., Misra, V.N., Chawla, S., Stokes, S., Chauhan, N., Francis, T., Ganjoo R.K. & Humphreys, G.S., 2010. A ~200 ka record of climatic change and dune activity in the Thar Desert, India. *Quaternary Science Reviews* 29, 3095-3105..
- Sinha, R., Smykatz-Kloss, W., Stüben, D., Harrison, S.P., Berner, Z., & Kramar, U, 2006. Late Quaternary palaeoclimatic reconstruction from the lacustrine sediments of the Sambhar playa core, Thar Desert margin, India. *Palaeogeography, Palaeoclimatology, Palaeoecology* 233, 252–270.
- Sivaperuman, C. & Baqri, Q.H., 2009. Avifaunal Diversity in the IGNP Canal Area, Rajasthan, India. In: *Faunal Ecology and Conservation of the Great Indian Desert*, Sivaperuman, C., Baqri, Q.H., Ramaswamy, G., & Naseema, M. (Eds). Leiden: Springer, pp. 113-118.
- Sivaperuman, C., Dookia, S., Kankane, P.L., & Baqri, Q.H., 2009. Structure of an Arid Tropical Bird Community, Rajasthan. In: *Faunal Ecology and Conservation of the Great Indian Desert*, Sivaperuman, C., Baqri, Q.H., Ramaswamy, G., & Naseema, M. (Eds). Leiden: Springer, pp 85-98.
- Smith J.R., Hawkins A.L., Asmerom, Y., Polyak, V., & Giegengack, R., 2007. New age constraints on the Middle Stone Age occupations of Kharga Oasis, Western Desert, Egypt. *Journal of Human Evolution* 52, 690–701.
- Soares, P., Ermini, L., Thomson, N., Mormina, M., Rito, T., Röhl, A., Salas, A., Oppenheimer, S., Macaulay, V., & Richards, M.B., 2009. Correcting for purifying selection: an improved human mitochondrial molecular clock. *American Journal of Human Genetics* 84, 740-759.

Sonakia, A., 1985. Skull cap of an early man from the Narmada valley alluvium (Pleistocene) of central India. *American Anthropologist* 87, 612–616.

Soressi, M., & Geneste, J-M., 2011. The History and Efficacy of the Chaîne Opératoire Approach to Lithic Analysis: Studying Techniques to Reveal Past Societies in an Evolutionary Perspective. *PalaeoAnthropology 2011 (Special Issue)*, 334-350.

Srivastava, P., Juyal, N., Singhvi, A.K., Wasson, R.J., & Bateman, M.D., 2001. Luminescence chronology of river adjustment and incision of Quaternary sediments in the alluvial plain of the Sabarmati River, north Gujarat, India. *Geomorphology* 36, 217-229.

Subbarao, B., & Deo, S. B., 1958. *The excavations at Maheshwar and Navdatoli, 1952-53*. Baroda: Maharaja Sayahirao University.

Subbarao, B., 1958. *The Personality of India*. Baroda: M.S.University, Baroda.

Szabo, B., McKinney Curtis, J., Dalbey, T., & Paddayya, K., 1990. On the age of the Acheulian Culture of the Hunsgi-Baichbal Valleys, Peninsular India. *Bulletin of the Deccan College Post-Graduate and Research Institute* 50, 317-321.

Taçon, P.S., 1991. The power of stone: symbolic aspects of stone use and tool development in western Arnhem Land, Australia. *Antiquity* 65, 197-207.

Tandon, S.K., Sareen, B.K., Rao, M.S., Singhvi, A.K., 1997. Aggradation history and luminescence chronology of Late Quaternary semi-arid sequences of the Sabarmati basin, Gujarat, western India. *Palaeogeography, Palaeoclimatology, Palaeoecology* 128, 339–357.

Tewari, R., Pant, P. C., Singh, L. B., Sharma, S., Sharma, M., Srivastava, P., Singhvi, A. K., Mishra, P. K., & Tobschall, H., 2002. Middle Palaeolithic Human Activity and Palaeoclimate at Kalpi in Yamuna Valley, Ganga Plain. *Man and Environment* 28, 1-13.

Thimma Reddy, K. & Sudarsen, V., 1978. Prehistoric Investigations in Sagileru Basin. *Man and Environment* 2, 32-40.

Todd, K.R.U., 1939. Palaeolithic Industries of Bombay. *The Journal of the Royal Anthropological Institute of Great Britain and Ireland* 69, 257-272.

Tripathi, J. K., Bock, B., Rajamani, V., & Eisenhauer, A., 2004. Is River Ghaggar, Saraswati? Geochemical constraints. *Current Science*, 87, 1141-1145.

Trumbore, S.E., 2000. Radiocarbon Geochronology. In: *Quaternary Geochronology: Methods and Applications*, Noller, J.S., Sowers, J.M., & Lettis, W.R. (Eds.). Washington D.C.: American Geophysical Union, pp 41-60.

Usik, V., Rose, J.I., Hilbert, Y.H., Van Peer, P., & Marks, A.E. Nubian Complex reduction strategies in Dhofar, Southern Oman. *Quaternary International*
<http://dx.doi.org/10.1016/j.quaint.2012.08.2111>.

- Van Peer, P., 1992. *The Levallois Reduction Strategy*. K.U.Leuven: Prehistory Press.
- Van Peer, P., 2000. Makhadma 6, a Nubian complex site. In: *Palaeolithic Living Sites in Upper and Middle Egypt*, Vermeersch, P.M. (Ed.). Leuven: Leuven University Press, pp 91–103.
- Van Peer, P., Vermeersch, P.M., Moeyersons, J., & Van Neer, W., 1996. Palaeolithic sequence of Sodmein Cave, Red Sea Mountains, Egypt. In: *Aspects of African Archaeology*, Pwiti, G., & Soper, R. (Eds.). Harare: University of Zimbabwe Publications. pp 149–156.
- Van Peer, P., Fullagar, R., Stokes, S., Bailey, R.M., Moeyersons, J., Steenhoudt, F., Geerts, A., Vanderbeken, T., De Dapper, M., Geus, F., 2003. The Early to Middle Stone Age transition and the emergence of modern human behaviour at site 8-B-11, Sai Island, Sudan. *Journal of Human Evolution* 45, 187-193.
- Van Peer, P., Vermeersch, P.M., Paulissen, & E., 2010. *Chert Quarrying, Lithic Technology and a Modern Human Burial at the Palaeolithic Site of Taramsa 1, Upper Egypt*. Leuven: Leuven University Press.
- Wakanker V.S., 1973. Bhim-betka excavations. *Journal of Indian History* L1, 23–33.
- Wasson, R.J., Smith, G.I., & Agrawal, D.P., 1984. Late Quaternary sediments, minerals and inferred geochemical history of Didwana Lake, Thar Desert, India. *Palaeogeography, Palaeoclimatology and Palaeoecology* 46, 345–372.
- Wendorf, F., Schild, R., Close, A.E., Schwarcz, H.P., Miller, G.H., Grün, R., Bluszcz, A., Stokes, S., Morawska, L., Huxtable, J., Lundberg, J., Hill, C.L., & McKinney, C., 1994. A chronology for the middle and late Pleistocene wet episodes in the eastern Sahara. In: *Late Quaternary Chronology and Paleoclimates of the Eastern Mediterranean*, Bar-Yosef, O., & Kra, R.S. (Eds.). Tucson: Radiocarbon. Department of Geosciences, University of Arizona, Tucson, pp. 147-168.
- Whittaker, J.C., 1994. *Flinkknapping: Making and understanding stone tools*. Austin: University of Texas Press.
- Wijeyapala, W.H., 1997. *New Light on the Prehistory of Sri Lanka in the Context of Recent Investigations of Cave Sites*. Ph.D. Thesis. Peradeniya: University of Peradeniya.
- Williams, M. & Clarke, M., 1995. Quaternary Geology and Prehistoric Environments in the Son and Belan Valleys, North Central India. In: *Quaternary Environments and Geoarchaeology of India*, Wadia, S., Korrisettar, R., & Kale, V. (Eds.). Bangalore: Geological Society of India Memoir 32, pp. 282-308.
- Xing, J., Watkins, W.S., Hu, W., Huff, C.D., Sabo, A., Muzny, D.M., Bamshad, M.J., Gibbs, R.A., Jorde, L.B., & Yu, F., 2010. Genetic diversity in India and the inference of Eurasian population expansion. *Genome Biology*, 11, R113.
- Zeuner, F. E. 1950. *Stone Age and Pleistocene Chronology in Gujarat*. Poona: Deccan College Monograph Series 6.

Appendix A: Gazetteer of Palaeolithic Archaeology in the Thar Desert

Table A.1: Palaeolithic site locations in the Thar Desert, Palaeolithic industry present (as defined in this thesis – 1= Lower Palaeolithic; 2=Middle Palaeolithic; 3=Late Palaeolithic; 4=Lower and Middle Palaeolithic; 5=Lower and Late Palaeolithic; 6=Middle and Late Palaeolithic; 7=Lower, Middle and Late Palaeolithic; 8=No Industry reported), presence of Raw Material, Artefact Type, Assemblage Composition and Artefact Size information, report on excavated or chronometrically dated assemblages, and references.

Site	Longitude	Latitude	Industry	Raw Material	Typology	Composition	Artefact Sizes	Excavation	Chronology	Source
16R	74.538346	27.371851	7	✓	✓	✓		✓	✓	IAR 1980-81; Gaillard 1993; Misra & Rajaguru 1986
25km NE Rajkot 1	71.024242	22.415927	6		✓		✓			Allchin et al. 1978
25km NE Rajkot 2	71.024242	22.415927	3	✓	✓					Allchin et al. 1978
47km S Nagaur	73.388062	26.917939	3	✓	✓					IAR 1979-80
60km South Jaisalmer	71.208487	26.486285	8	✓	✓					IAR 1979-80
6km E Pokaran	71.974461	26.895715	2	✓						IAR 1979-80
7.5 miles ENE Amreli	71.326193	21.636517	8	✓	✓					Foote 1916
797bis	68.85627	27.430786	7	✓	✓	✓		✓		Negrino & Kazi 1996
8km S Bikaner	73.28976	27.947455	3	✓						IAR 1983-84
Achali	73.616667	22.316667	5	✓	✓				✓	IAR 1988-89; Ajithprasad 2005a
Achhala	73.689784	22.726752	3							IAR 1972-73
Adadra	73.604074	22.635578	3							IAR 1972-73
Adam Khan-ka-Dera	71.878611	26.947222	4							IAR 1999-2000
Adhevada	72.156965	21.722713	3							IAR 1980-81
Ajivino Timbo	71.816667	23.616667	3							IAR 1990-91
Akhaj	72.516667	23.466667	8	✓	✓					Foote 1916
Akhaj N	72.516667	23.466667	3	✓	✓					Sankalia 1946
Akhaj SE	72.516667	23.466667	3	✓	✓					Sankalia 1946
Akkadia Mota	71.103932	21.645149	3	✓	✓					Foote 1916
Akora	74.523756	27.47178	3		✓					IAR 1965-66
Akvada	72.188248	21.736478	3							IAR 1980-81
Amarajina_muvada	72.864436	23.116467	3							IAR 1977-78
Amarpura	74.550891	27.408372	1	✓	✓					IAR 1979-80
Amba	71.316264	21.501601	6	✓	✓					IAR 1979-80
Ambakut	73.827879	22.435767	3	✓	✓			✓		IAR 1994-95
Ambali	74.297846	27.160421	8							Misra et al. 1980

Site	Longitude	Latitude	Industry	Raw Material	Typology	Composition	Artefact Sizes	Excavation	Chronology	Source
Ambaliara	73.043501	22.973808	3							IAR 1974-75
Ambasan	72.346434	23.480271	1							IAR 1980-81
Ambhakut	73.827879	22.435767	3		✓					IAR 1993-94
Anand	70.309356	22.667804	2							IAR 1979-80
Angadh	73.07861	22.384133	3							IAR 1977-78
Angia	69.348744	23.497344	1	✓	✓					IAR 1967-68
Anguria	72.438393	24.171181	3		✓					IAR 1964-65
Anguthala	72.835057	23.235261	3							IAR 1977-78
Anjar	70.021838	23.106667	2	✓	✓					IAR 1967-68
Anjar	70.021838	23.106667	3	✓	✓					IAR 1967-68
Ankodia	69.259893	23.35464	3							IAR 1967-68
Annas	74.253464	22.8323	3							IAR 1968-69
Arjunpura	74.501695	26.278617	3	✓	✓	✓				Allchin et al. 1978
Arzi Goth	68.287626	25.766448	6	✓	✓					Biagi 2008 (AMIT)
Atkot	71.147821	22.009852	1	✓	✓					IAR 1969-70
Atkot	71.147821	22.009852	1		✓					Marathe 1981
Aval-Javal	72.730125	23.008064	3							IAR 1971-72
Babapur	71.113658	21.52036	3	✓	✓	✓				Foote 1916
Babapur	71.112946	21.52141	7	✓	✓					IAR 1979-80
Babra	72.82	23.17	3							IAR 1977-78
Bacha	71.054423	20.906435	1		✓					IAR 1975-76
Badalpur	70.571649	21.387999	2	✓				✓		IAR 1971-72; Baskaran et al. 1986
Badela	74.43584	27.56864	2							IAR 1982-83
Badia to Sukhpar	71.331221	21.963419	2							IAR 1978-79
Bahadarpur	73.566322	22.187709	1	✓	✓			✓		IAR 1986-87; Ajithprasad 2005a
Bahadarpur	73.566322	22.187709	8	✓	✓					Sankalia 1946
Bahadarpur	73.616667	22.183333	3	✓	✓					Sankalia 1946
Bajawa	72.044149	25.789467	1	✓	✓					Mishra et al. 1999
Baklia	74.405688	27.603534	2							IAR 1982-83
Bakor	73.6167	23.133299	3							IAR 1975-76
Bakri Waro East	68.688833	27.132	3							Shaikh et al. 2002-03
Bakri Waro South	68.681001	27.127334	3							Shaikh et al. 2002-03
Bakrol	72.911173	22.5634	3							IAR 1972-73
Balani-Vav	71.36141	20.953015	1		✓					IAR 1975-76
Balasinor	73.336482	22.955907	3							IAR 1975-76
Bana	73.667944	25.958946	6	✓						IAR 1979-80
Bandharia Mota	71.101216	21.54585	8	✓	✓					Foote 1916
Bangur Canal	74.537865	27.372084	1		✓					Misra et al. 1982
Bar	73.847678	22.491195	1		✓					IAR 1993-94
Barala	71.126998	23.82541	3		✓					IAR 1964-65

Site	Longitude	Latitude	Industry	Raw Material	Typology	Composition	Artefact Sizes	Excavation	Chronology	Source
Baria	72.934842	23.047412	3	✓	✓	✓				Foote 1916
Baria	72.934842	23.047412	3							IAR 1977-78
Baridhani	72.285761	27.356887	2	✓	✓					Allchin et al. 1978
Bari-Khatu	74.473112	27.434554	3		✓					IAR 1965-66
Bariyari	71.204242	26.42791	2	✓	✓					IAR 1989-90
Barka	71.38	25.75	2	✓						IAR 1958-59
Barli	71.9	26.858333	8							IAR 1999-2000
Barnel	74.267853	27.191481	8							Misra et al. 1980
Baroragaon	71.878611	26.947222	4							IAR 1999-2000
Baska	73.445713	22.467061	3							IAR 1977-78
Baskario	73.666667	22.3	1	✓	✓					IAR 1986-87
Baskario	73.666667	22.3	4	✓	✓				✓	IAR 1988-89; Ajithprasad 2005a
Bavka	74.362102	22.726485	8	✓	✓					IAR 1958-59
Belaser	72.479431	26.39634	3	✓						IAR 1977-78
Beraja	69.608051	22.981739	3							IAR 1976-77
Bhadrajum	72.892741	25.597478	1		✓					IAR 1977-78
Bhadreshwar	69.903513	22.911096	2							IAR 1970-71
Bhagu-ka-Gaon	71.166667	25.916667	1							IAR 1999-2000
Bhagwanpura	73.583333	22.266667	3	✓	✓					IAR 1988-89
Bhahotalia	73.892799	23.189468	3							IAR 1972-73
Bhainsra	71.420833	26.611111	2							IAR 1999-2000
Bhajodi	69.859741	23.733733	1	✓	✓					IAR 1967-68
Bhamaria	73.471111	22.503333	3							IAR 1970-71
Bhandei	73.180783	25.904276	2	✓	✓					Misra 1963
Bhangsimala	73.892799	23.189468	3							IAR 1970-71
Bhanpur	73.748301	22.402427	1	✓	✓					IAR 1992-93
Bhanpur I	73.798689	22.424665	4	✓	✓					Ajithprasad 2005b
Bhanpur II	73.797013	22.42763	1	✓	✓					Ajithprasad 2005b
Bhanpur III	73.799828	22.43008	1	✓	✓					Ajithprasad 2005b
Bhanpur IV	73.802685	22.435252	4	✓	✓					Ajithprasad 2005b
Bhanpur IX	73.800032	22.433862	4	✓	✓					Ajithprasad 2005b
Bhanpur V	73.804935	22.433211	1	✓	✓					Ajithprasad 2005b
Bhanpur VI	73.80131	22.436255	1	✓	✓					Ajithprasad 2005b
Bhanpur VII	73.801091	22.439524	1	✓	✓					Ajithprasad 2005b
Bhanpur VIII	73.806544	22.436	1	✓	✓					Ajithprasad 2005b
Bhatpur	72.461636	22.894652	3							IAR 1971-72
Bhavada	72.483541	22.900805	3	✓	✓					IAR 1970-71
Bhavnagar	72.148904	21.763518	2	•	✓	✓				Marathe 1981
Bhavnagar/Triveni	72.148904	21.763518	3							IAR 1978-79
Bhawi	73.609828	26.196723	2	✓	✓					Misra 1963

Site	Longitude	Latitude	Industry	Raw Material	Typology	Composition	Artefact Sizes	Excavation	Chronology	Source
Bhetanda	73.293222	26.081059	2	✓	✓					Misra 1963
Bhitali	68.774	23.824	3		✓					IAR 1993-94
Bhojavadar	71.700882	21.869555	2							IAR 1971-72
Bhojka	71.161081	26.94427	1							IAR 1983-84
Bhojka	71.161081	26.94427	2	✓	✓					IAR 1984-85
Bhope-ki-dhani	71.266797	26.790311	1							IAR 1999-2000
Bhujodi to Mundra	69.738373	23.22457	2							IAR 1977-78
Bhukhi	73.59503	22.623875	3							IAR 1972-73
Bhulwan	73.633333	22.216667	3	✓	✓					Sankalia 1946
Bhungar	71.967571	21.251267	6	✓	✓					IAR 1979-80
Bhutia	73.231576	23.059372	6							IAR 1977-78
Bhuvad	69.873067	23.044233	3							IAR 1978-79
Bhuvel	72.766843	22.922485	3	✓	✓					IAR 1970-71
Bikaner	73.309342	27.959737	3	✓	✓	✓				Allchin et al. 1978
Bilara	73.66625	26.213769	3	✓						IAR 1958-59
Bilia	71.866622	26.916657	8		✓					IAR 1999-2000
Bisalpur	74.581966	26.519783	2		✓					Misra 1963
Bodeli	73.766667	22.283333	3	✓	✓					Sankalia 1946
Bolari	69.666932	23.242	3							IAR 1977-78
Boria Mound	72.803451	23.033859	3							IAR 1968-69
Bovadi	71.410294	21.369482	6	✓	✓					IAR 1979-80
Bridge Site	68.796664	27.313435	4	✓	✓					Biagi & Cremaschi 1988
Btw Umria and Bhard	74.05	22.75	8	✓	✓					Foote 1916
Budha Pushkar A	74.578788	26.520802	3	✓	✓	✓				Allchin et al. 1978
Budha Pushkar B	74.584818	26.51736	3	✓	✓	✓				Allchin et al. 1978
Budha Pushkar C	74.591484	26.516717	3	✓	✓	✓				Allchin et al. 1978
Budha Pushkar D	74.594975	26.516326	3	✓	✓	✓				Allchin et al. 1978
Budha Pushkar E	74.581638	26.519654	3	✓	✓	✓				Allchin et al. 1978
Budha Pushkar E-F	74.581966	26.519783	3	✓	✓					Allchin et al. 1978
Budha Pushkar F	74.582367	26.519929	3	✓	✓	✓				Allchin et al. 1978
Budha Pushkar G	74.584431	26.518243	3	✓	✓	✓				Allchin et al. 1978
Budha Pushkar H	74.587157	26.516722	2							Allchin et al. 1978
Bunglow Kot	68.742591	27.338516	4	✓	✓					Biagi & Cremaschi 1988
Central Processing Plant 3	69.237	27.123	3							Shaikh et al. 2002-03
Chachai	71.026944	21.325556	8	✓	✓					Foote 1916
Chakalia	73.681463	23.176981	3							IAR 1970-71
Chakrora nullah, S of Umria	74.05	22.75	8	✓	✓					Foote 1916
Chamol	71.668791	21.545765	3	✓	✓					IAR 1979-80
Chamu	72.582464	26.660875	3							IAR 1976-77

Site	Longitude	Latitude	Industry	Raw Material	Typology	Composition	Artefact Sizes	Excavation	Chronology	Source
Chancha Baluch	68.673374	27.325768	6	✓	✓	✓				Allchin et al. 1978
Chanda	71.714025	21.539616	3	✓	✓					IAR 1979-80
Char Baro North	68.673662	27.134005	3							Shaikh et al. 2002-03
Char Baro South 1	68.672333	27.127333	3							Shaikh et al. 2002-03
Char Baro South 2	68.675102	27.132408	3							Shaikh et al. 2002-03
Char Baro South 3	68.675999	27.124677	3							Shaikh et al. 2002-03
Charmadi Hill	71.910289	21.831998	3	✓	✓					Allchin et al. 1978
Chavodia	73.6167	23.133299	3							IAR 1972-73
Cekhala	72.853131	23.439433	1							IAR 1973-74
Chhajoli	74.223949	27.168292	1		✓	✓		✓		IAR 1978-79
Chotlia	71.195	22.423611	2							IAR 1974-75
Chuchhapura	73.605568	22.219465	1	✓	✓				✓	IAR 1986-87; Ajithprasad 2005a
Chundadi	73.618611	22.766667	3							IAR 1971-72
Chunkalia	74.152692	23.094412	3							IAR 1971-72
Dabla-ka-dhora	72.404652	25.457182	3	✓	✓					IAR 1967-68
Damrala	71.682909	21.483198	2	✓	✓					IAR 1979-80
Danasani	73.132352	25.929123	2	✓	✓					Misra 1963
Dandar	70.751105	27.024017	3	✓	✓	✓				Allchin et al. 1978
Dandar 2	70.834854	27.047229	2	✓	✓					Allchin et al. 1978
Dandar 3	70.837699	27.038275	2	✓	✓					Allchin et al. 1978
Dangarva	72.249222	23.386458	3							IAR 1977-78
Dangarwa Rabari-na-Gochara-no-Timbo	72.483333	23.383333	3	✓	✓					Sankalia 1946
Dangarwa Venu-no-Charo	72.483333	23.383333	3	✓	✓					Sankalia 1946
Dantali	72.821731	22.475296	3							IAR 1982-83
Daphro A	68.19139	25.159445	2	✓	✓					Biagi 2005
Daphro B	68.182222	25.163056	1	✓	✓					Biagi 2005
Datrana IV	71.133333	23.683333	3		✓			✓		IAR 1993-94
Datrana V	71.116665	23.766667	3	✓	✓			✓		IAR 1994-95
Deh Konkar	67.26916	25.063322	6							Biagi 2008
Delvada	72.974107	24.008256	3							IAR 1969-70
Desalpur	69.166574	23.460904	2	✓	✓					IAR 1967-68
Desalpur Guntali	69.166574	23.460904	1							IAR 1977-78
Deta	69.859741	23.733733	2	✓	✓					IAR 1967-68
Devalia	71.259491	21.523682	7	✓	✓					IAR 1979-80
Devisar	69.331707	23.405281	1	✓	✓					IAR 1967-68
Devnimori	73.357317	23.628333	3		✓					IAR 1960-61
Dhamod	73.411554	23.130339	3							IAR 1975-76
Dhaneri	73.70786	25.941748	6		✓					IAR 1960-61

Site	Longitude	Latitude	Industry	Raw Material	Typology	Composition	Artefact Sizes	Excavation	Chronology	Source
Dhaneri	73.70786	25.941748	2	✓	✓	✓				Misra 1963
Dhaneti	73.70786	25.941748	3							IAR 1970-71
Dharampur	72.853025	23.259015	3							IAR 1980-81
Dharana	74.134388	27.172606	8							Misra et al. 1980
Dharisana	72.853025	23.259015	3							IAR 1977-78
Dharwania	72.833333	23.933333	3	✓	✓					Sankalia 1946
Dhechu	72.327905	26.7669	3	✓						IAR 1977-78
Dhoraji	70.413068	21.747436	2	✓	✓					IAR 1967-68
Dhrangadhra	71.452847	22.98659	4	✓	✓					IAR 1967-68
Dhrangadhra	71.452847	22.98659	1							Lele 1972
Dhrud river	69.16089	23.40825	2	✓	✓					IAR 1967-68
Didwana	74.584222	27.390497	3	✓						IAR 1978-79
Diwada Colony	73.892799	23.189468	3							IAR 1972-73
Dohada	72.552374	22.402797	3							IAR 1971-72
Dokariya	73.766667	22.266667	3	✓	✓	✓				Sankalia 1946
Dolapura	73.396928	22.302569	3							IAR 1983-84
Don Dunker	73.699998	22.316666	1	✓	✓				✓	IAR 1988-89; Ajithprasad 2005a
Dubi 1	68.670333	27.137333	3							Shaikh et al. 2002-03
Dubi 2	68.670455	27.137333	3							Shaikh et al. 2002-03
Dubi 4	68.671434	27.137395	3							Shaikh et al. 2002-03
Dubi 5	68.672543	27.137406	3							Shaikh et al. 2002-03
Dubi 6	68.671667	27.136167	3							Shaikh et al. 2002-03
Duma	73.683334	22.300001	5	✓	✓					IAR 1986-87
Duma	73.683334	22.300001	4	✓	✓				✓	IAR 1988-89; Ajithprasad 2005a
Dundara	72.804781	25.879531	2	✓	✓					Misra 1963
Dungervant	73.853516	22.440847	1	✓	✓					Ajithprasad 2005b
Dunkri	73.65185	22.211893	3	✓	✓					IAR 1986-87
East of Lakes2	68.7295	27.150833	3							Shaikh et al. 2002-03
East of Lakes4	68.702505	27.130837	3							Shaikh et al. 2002-03
East of Lakes6	68.717997	27.114837	3							Shaikh et al. 2002-03
Eravada	71.876683	23.43993	3							IAR 1982-83
E-W (unnamed) Long Hill A	68.214167	25.159444	1	✓	✓					Biagi 2005
E-W (unnamed) Long Hill B	68.213333	25.160278	1	✓	✓					Biagi 2005
E-W (unnamed) Long Hill C	68.212778	25.160555	8	✓	✓					Biagi 2005
E-W (unnamed) Long Hill D	68.2125	25.161111	8	✓	✓					Biagi 2005
E-W (unnamed) Long Hill E	68.2075	25.160556	8	✓	✓					Biagi 2005
E-W (unnamed) Long Hill F	68.205556	25.161389	8	✓	✓					Biagi 2005

Site	Longitude	Latitude	Industry	Raw Material	Typology	Composition	Artefact Sizes	Excavation	Chronology	Source
Fala	70.316674	22.533333	2	✓	✓					IAR 1957-58
Fatehpur	71.21243	21.566957	3							IAR 1975-76
Gadhara (Hirpura)	72.783333	23.533333	3	✓	✓	✓				Sankalia 1946
Gadhara II (Hirpura)	72.783333	23.533333	3		✓	✓				Sankalia 1946
Gadhehundadi	73.618389	22.767042	3							IAR 1970-71
Galteswar	73.210179	22.797123	1							IAR 1975-76
Gamania-ni-Timbi	69.259893	23.35464	3							IAR 1967-68
Ganchhali	73.048056	24.031943	2							IAR 1973-74
Gebi	73.292652	23.459377	1							IAR 1973-74
Ghadhara Nala	72.85	23.6	8		✓					Sankalia 1946
Ghogamba	72.934842	23.047412	3							IAR 1970-71
Ghunada	70.828629	22.727867	3							IAR 1972-73
Ghuntia	73.847917	22.425879	1	✓	✓					IAR 1992-93
Ghuntia I	73.847917	22.425879	2	✓	✓					Ajithprasad 2005b
Ghuntia II	73.845901	22.423371	2	✓	✓					Ajithprasad 2005b
Ghuntia III	73.850801	22.423046	2	✓	✓					Ajithprasad 2005b
Girnar Hills	70.496368	21.49372	1							IAR 1975-76
GNR1	68.665791	27.104863	3	✓	✓					Biagi 2003-2004
GNR10	68.668016	27.097972	3	✓	✓					Biagi 2003-2004
GNR2	68.670167	27.105592	3	✓	✓					Biagi 2003-2004
GNR4	68.6756	27.099654	3	✓	✓					Biagi 2003-2004
GNR7	68.670135	27.096346	3	✓	✓					Biagi 2003-2004
GNR9	68.668993	27.094259	3	✓	✓					Biagi 2003-2004
Golio	73.307287	26.154353	2	✓	✓					Misra 1963
Goraj	73.483333	22.333333	1							IAR 1983-84
Gorwar II	69.2685	27.106833	3							Shaikh et al. 2002-03
Govindada	72.483541	22.900805	3							IAR 1971-72
Govindara	72.483541	22.900805	3	✓	✓					IAR 1970-71
Govindhgarh	74.380893	26.446985	4	✓						IAR 1958-59
Gudi	71.783333	26.816667	8		✓					IAR 1999-2000
Gunded	73.583334	22.15	3	✓	✓					IAR 1988-89
Gundiviri	73.65	22.333333	1	✓	✓				✓	IAR 1988-89; Ajithprasad 2005a
Gundiviri	73.65	22.333333	3	✓	✓					IAR 1988-89
Guntaligadh	69.259893	23.35464	1							IAR 1976-77
Gurha 1	72.991402	26.13929	2	✓	✓					Allchin et al. 1978
Gurha 2	72.991289	26.139976	2	✓	✓					Allchin et al. 1978
Guttiya	73.847917	22.425879	3	✓	✓					IAR 1992-93
Hadol	72.85	23.95	3	✓	✓					Sankalia 1946
Hadol Juna Nala gravel	72.85	23.95	8		✓					Sankalia 1946

Site	Longitude	Latitude	Industry	Raw Material	Typology	Composition	Artefact Sizes	Excavation	Chronology	Source
Hadol Juna Nala on bedrock	72.85	23.95	8		✓					Sankalia 1946
Halvad	71.222467	23.012563	4	✓	✓					IAR 1963-64
Handod	73.65185	22.211893	3	✓	✓					IAR 1986-87
Hanuman Kathi	71.833339	23.649989	3							IAR 1990-91
Haraniyava	72.760973	22.942272	3							IAR 1971-72
Harasoli	72.807544	23.078388	3							IAR 1977-78
Harihar no thumda	71.366667	23.883333	3							IAR 1992-93
Harsol	73.01531	23.361574	3							IAR 1978-79
Hathijan	72.665378	22.943069	3							IAR 1972-73
Hathipagla	73.816292	22.433804	1	✓	✓					IAR 1992-93
Hathipagla I	73.816292	22.433804	1	✓	✓					Ajithprasad 2005b
Hathipagla II	73.821198	22.433148	1	✓	✓					Ajithprasad 2005b
Hathipagla III	73.819838	22.434625	2	✓	✓					Ajithprasad 2005b
Hathipagla IV	73.822514	22.434753	1	✓	✓					Ajithprasad 2005b
Haveli	73.65	22.3	1	✓	✓				✓	IAR 1988-89; Ajithprasad 2005a
Hiran	70.432272	20.90382	1	✓	✓					IAR 1971-72
Hirpura	72.783333	23.533333	8	✓	✓					Sankalia 1946
Hokra 1A	74.605383	26.545323	2	✓	✓	✓				Allchin et al. 1978
Hokra 2A	74.605	26.546561	1	✓						Allchin et al. 1978
Hokra 2B	74.60547	26.547029	1	✓	✓		✓			Allchin et al. 1978
Hundgaon	73.421667	26.155426	2	✓	✓		✓			Misra 1963
Inder Singh-ki-Dhani	71.176389	26.870833	6							IAR 1999-2000
Inderwa no timbo II	71.466667	24.016667	3							IAR 1992-93
Indola-ki-Dhani	74.589904	27.396627	1	✓	✓	✓				IAR 1979-80
Indola-ki-Dhani	74.589904	27.396627	4		✓			✓		IAR 1980-81; Misra et al. 1982
Itari	73.140666	22.615673	3	✓	✓	✓				Allchin et al. 1978
Jadan and Kanaswas	73.491155	25.83311	3	✓						Allchin et al. 1978
Jaidak II	70.583369	22.683356	3		✓			✓		IAR 1991-92
Jakhel	71.740996	23.962165	3							IAR 1989-90
Jalampura	72.073956	22.992962	8	✓	✓					Foote 1916
Jalampura	73.083333	22.133333	3	✓	✓					Sankalia 1946
Jalat	74.310194	22.806409	3							IAR 1968-69
Jalor	72.619706	25.342245	3	✓						IAR 1977-78
Jamal Shah East 1	68.696618	27.115795	3							Shaikh et al. 2002-03
Jamal Shah East 2	68.692667	27.111	3							Shaikh et al. 2002-03
Jamal Shah North 1	68.69067	27.116833	3							Shaikh et al. 2002-03
Jamal Shah North 2	68.237838	27.120333	3							Shaikh et al. 2002-03
Jamal Shah North 3	68.685167	27.1245	3							Shaikh et al. 2002-03
Jamal Shah South 1	68.687	27.1065	3							Shaikh et al. 2002-03

Site	Longitude	Latitude	Industry	Raw Material	Typology	Composition	Artefact Sizes	Excavation	Chronology	Source
Jamal Shah South 2	68.691326	27.108497	3							Shaikh et al. 2002-03
Jamal Shah South 3	68.688857	27.109656	3							Shaikh et al. 2002-03
Jamla	72.994035	23.68566	3							IAR 1979-80
Jankpiura	74.546006	27.38716	1		✓					Misra et al. 1982
Jasdan	71.147821	22.009852	1							Lele 1972
Jawanpura	73.380826	22.586695	3	✓	✓					IAR 1959-60
Jayal	74.184015	27.221558	2	✓	✓					IAR 1977-78
Jayal	74.184015	27.221558	1	✓	✓	✓		✓		IAR 1978-79
Jenana	74.360705	27.4316	2		✓					Misra et al. 1982
Jesada	71.753558	23.779127	3							IAR 1982-83
Jetpur	70.625425	21.771685	8	✓	✓					Allchin et al. 1978
Jetpur	70.665777	21.744065	2	✓	✓				✓	IAR 1967-68; Baskaran et al. 1986
Jhab I	73.764818	22.431237	2	✓	✓					Ajithprasad 2005b
Jhab II	73.764869	22.436209	4	✓	✓					Ajithprasad 2005b
Jhab III	73.769724	22.438749	4	✓	✓					Ajithprasad 2005b
Jhab IV	73.775946	22.437322	1	✓	✓					Ajithprasad 2005b
Jhab V	73.770937	22.434701	4	✓	✓					Ajithprasad 2005b
Jhab VI	73.771591	22.431037	2	✓	✓					Ajithprasad 2005b
Jhak	72.82	23.17	3							IAR 1977-78
Jhaverpura	73.396928	22.302569	5							IAR 1982-83
JHP1	68.007283	25.001583	3	✓	✓	✓	✓			Biagi 2011
JHP10	68.006733	25.001633	3	✓	✓		✓			Biagi 2011
JHP11	68.007633	24.999417	3	✓	✓	✓	✓			Biagi 2011
JHP12	68.007506	24.999559	3	✓	✓	✓	✓			Biagi 2011
JHP13	68.00735	24.999683	3	✓	✓	✓	✓			Biagi 2011
JHP14	68.006317	25.0014	3	✓	✓		✓			Biagi 2011
JHP15	68.00515	24.999633	3	✓	✓		✓			Biagi 2011
JHP16	68.005017	24.996967	3	✓	✓					Biagi 2011
JHP19	68.001833	24.995183	3	✓	✓					Biagi 2011
JHP2	68.00605	24.996633	3	✓	✓		✓			Biagi 2011
JHP22	68.149067	25.086817	3	✓	✓		✓			Biagi 2011
JHP23	68.185731	25.118248	3	✓	✓					Biagi 2011
JHP26	68.089483	25.0946	3	✓	✓		✓			Biagi 2011
JHP27	67.992683	25.0278	3	✓	✓		✓			Biagi 2011
JHP4	68.00595	24.99835	3	✓	✓					Biagi 2011
JHP5	68.00635	24.999533	3	✓	✓					Biagi 2011
JHP6	68.006683	25.001217	3	✓	✓					Biagi 2011
JHP7	68.006667	25.001415	3	✓	✓	✓	✓			Biagi 2011
JHP8	68.006915	25.001433	3	✓	✓		✓			Biagi 2011
JHP9	68.006733	25.00125	3	✓	✓		✓			Biagi 2011

Site	Longitude	Latitude	Industry	Raw Material	Typology	Composition	Artefact Sizes	Excavation	Chronology	Source
Jinjar	72.763225	22.902403	3		✓					IAR 1971-72
Jira	71.303754	21.456462	8	✓	✓					Foote 1916
Jogpura	73.793161	22.467679	4		✓			✓		IAR 1993-94
Jogpura I	73.779765	22.461346	4	✓	✓					Ajithprasad 2005b
Jogpura II	73.780261	22.46237	1	✓	✓					Ajithprasad 2005b
Jogpura III	73.777341	22.462405	1	✓	✓					Ajithprasad 2005b
Jogpura IV	73.777961	22.460921	2	✓	✓					Ajithprasad 2005b
Jogpura V	73.779144	22.463185	1	✓	✓					Ajithprasad 2005b
Jogpura VI	73.784769	22.467836	2	✓	✓					Ajithprasad 2005b
Jogpura VII	73.786245	22.467292	2	✓	✓					Ajithprasad 2005b
Jojwaghode	73.6807	22.312998	3	✓	✓					IAR 1986-87
Jopa	73.65185	22.211893	3	✓	✓					IAR 1986-87
JS1	68.692253	27.112978	3	✓	✓					Biagi 2003-2004
JS2	68.692319	27.111542	3	✓	✓					Biagi 2003-2004
JS3	68.690132	27.114982	3	✓	✓					Biagi 2003-2004
JS4	68.692476	27.112369	3	✓	✓					Biagi 2003-2004
Juna	71.924988	25.565371	2	✓						IAR 1958-59
Juna Rampur	71.820713	21.855579	3							IAR 1980-81
Junagadh	70.457877	21.522184	1						✓	IAR 1975-76; Baskaran et al. 1986
Juni Shedhal-Bamaniyo Timbo	72.456016	23.400193	3	✓	✓					Sankalia 1946
K12	69.2265	27.190333	3							Shaikh et al. 2002-03
Kadadara	72.785623	23.086615	3							IAR 1977-78
Kakanpur	73.485105	22.83288	3							IAR 1971-72
Kalau	70.908344	26.915748	3							IAR 1983-84
Kalubhar	71.074199	22.502472	1	✓	✓					IAR 1976-77
Kalvad IV	70.380906	22.203448	2							IAR 1980-81
Kambolaj	73.090426	22.57744	3		✓		✓			Allchin et al. 1978
Kamboya Timbo	71.9	23.633333	3							IAR 1990-91
Kamod	72.542673	22.928227	3							IAR 1973-74
Kamol Nava	71.967407	21.366342	6	✓	✓					IAR 1979-80
Kamord	72.548161	22.927652	3	✓	✓	✓				Allchin et al. 1978
Kandava dam site	73.83823	23.289591	3							IAR 1972-73
Kandharki III	68.742	27.088333	3							Shaikh et al. 2002-03
Kaneria I (Rangpur)	72.8	23.916667	3	✓	✓					Sankalia 1946
Kaneria II (Rangpur)	72.8	23.916667	3	✓	✓					Sankalia 1946
Kanhathai	70.596005	23.606121	3		✓					IAR 1965-66
Kaniel	72.967284	22.950346	3	✓	✓					Foote 1916
Kanipur	72.876655	23.046282	3							IAR 1977-78
Kankawati	71.378292	23.10774	2							IAR 1963-64
Kankot	71.291717	21.512168	6	✓	✓					IAR 1979-80

Site	Longitude	Latitude	Industry	Raw Material	Typology	Composition	Artefact Sizes	Excavation	Chronology	Source
Kanod	71.182763	27.167999	3	✓	✓					Deotare et al 2004
Kantharapur-Juna	72.82	23.17	3							IAR 1977-78
Kapadvanj	73.056543	23.022297	2		✓					Allchin et al. 1978
Kapadvanj	73.071389	23.023056	8	✓	✓					Foote 1916
Karna I	71.941362	25.750937	8	✓	✓				✓	Mishra et al. 1999
Karna II	71.914843	25.753256	8	✓	✓				✓	Mishra et al. 1999
Kathore I	68.90517	27.069834	3							Shaikh et al. 2002-03
Kathoti	74.285078	27.24626	8							Misra et al. 1980
Kelamura	73.892799	23.189468	3							IAR 1972-73
Kelawa	71.816667	26.916667	8		✓					IAR 1999-2000
Kera	69.596271	23.078995	3							IAR 1976-77
Kesaria	70.941484	20.824582	1		✓					IAR 1975-76
Kevada	73.748541	22.433254	1	✓	✓					IAR 1992-93
Kevada	73.793347	22.466027	4		✓					IAR 1993-94
Kevada I	73.787451	22.455946	1	✓	✓					Ajithprasad 2005b
Kevada II	73.788281	22.455349	1	✓	✓					Ajithprasad 2005b
Kevada III	73.787275	22.454602	2	✓	✓					Ajithprasad 2005b
Khadeen	71.128285	25.727556	8	✓	✓					IAR 1979-80
Khairla Hill	73.191868	25.839948	3	✓	✓	✓				Allchin et al. 1978
Khairla Hill 2	73.191868	25.839948	2	✓	✓					Allchin et al. 1978
Khaksar	72.619408	22.313115	3							IAR 1971-72
Khari-no-Timbo	71.833333	23.6	3							IAR 1990-91
Khavda	69.731671	23.844291	2							IAR 1977-78
Khedoi	69.91667	23.066665	3							IAR 1970-71
Khidhadia Timbo	71.833333	23.6	3							IAR 1990-91
Khinsvar	73.406411	26.978315	3	✓	✓					IAR 1956-57
Khinyala	74.201579	27.293479	3	✓						IAR 1978-79
Khirwa	72.355574	27.210275	2							IAR 1976-77
Kikwada	73.876519	22.414078	1	✓	✓					Ajithprasad 2005b
Kiyal	72.483333	23.4	3	✓	✓					Sankalia 1946
Km 18	71.071852	26.919524	8	✓	✓					Allchin et al. 1978
Km 24	71.121135	26.927205	2	✓	✓					Allchin et al. 1978
Km 33	71.203117	26.940883	8	✓	✓					Allchin et al. 1978
Km 42	71.278336	26.992975	3	✓	✓	✓	✓			Allchin et al. 1978
Kodiar Mata	71.034919	21.343686	8	✓	✓					Foote 1916
Kodrali	72.827768	23.050932	3							IAR 1977-78
Kola	70.380906	22.203448	3							IAR 1980-81
Kolayat	72.956725	27.851045	2	✓	✓					IAR 1983-84
Koliya 1	74.483416	27.356709	1		✓					Misra et al. 1982
Koliya 2	74.483416	27.356709	1		✓					Misra et al. 1982

Site	Longitude	Latitude	Industry	Raw Material	Typology	Composition	Artefact Sizes	Excavation	Chronology	Source
Kolwa	73.65	22.266667	1	✓	✓				✓	IAR 1988-89; Ajithprasad 2005a
Kora	68.774	23.824	3		✓					IAR 1993-94
Kot	72.794677	23.725014	8	✓	✓					Foote 1916
Kot	72.800731	23.444921	8	✓	✓					Sankalia 1946
Kotada	69.199227	23.375952	2	✓	✓					IAR 1967-68
Kotada	69.199227	23.375952	3							IAR 1980-81
Krakach	71.44961	21.465313	7	✓	✓					IAR 1979-80
Krushnagadh	69.949418	21.972626	3							IAR 1978-79
Kubadthal	72.760696	23.031206	3							IAR 1971-72
Kujad	72.730125	23.008064	3							IAR 1971-72
Kukvav	72.042775	23.12632	3							IAR 1977-78
Kunda	71.905556	26.175	8		✓					IAR 1999-2000
Kuroli	74.516212	27.420875	3		✓					IAR 1965-66
Kuselpur	73.65185	22.211893	3	✓	✓					IAR 1986-87
Kutharivad	70.380906	22.203448	3							IAR 1980-81
Kutiyana	69.991502	21.620602	1	✓	✓					IAR 1976-77
Ladai	69.864376	23.452235	3	✓	✓					IAR 1955-56
Lakhavad	71.920655	21.484391	3	✓	✓					IAR 1979-80
Lakhiyar Viyaro	69.259893	23.35464	4							IAR 1970-71
Lakhond	69.833512	23.250182	1	✓	✓					IAR 1967-68
Lakhond	69.833512	23.250182	2	✓	✓					IAR 1967-68
Lakrora	?		8	✓	✓					Foote 1916
Landhi	67.203168	24.849544	2	✓	✓					Biagi 2008
Langer	73.680226	27.075132	3	✓	✓					IAR 1964-65
Laphni	73.683329	22.31666	1	✓	✓				✓	IAR 1986-87; Ajithprasad 2005a
Laphni	73.683329	22.31666	3	✓	✓					IAR 1988-89
Ler	69.666932	23.242	3	✓	✓					IAR 1967-68
Lever	73.633333	22.266667	3	✓	✓					IAR 1988-89
Limbuwani	73.771094	22.426211	1	✓	✓					Ajithprasad 2005b
Lonk	73.048056	24.031943	3							IAR 1970-71
Lordia	72.400391	27.065385	3							IAR 1976-77
Lordiya	72.404534	27.060424	7	✓	✓		✓			Deotare et al 2004
Lower Khaskheli Terrace	68.216391	25.156112	3	✓	✓					Biagi 2005
Luna	71.566676	26.699985	8		✓					IAR 1999-2000
Luni	70.078574	22.985725	3		✓					IAR 1955-56
Luni	73.004054	25.997038	4	✓	✓	✓	✓			Misra 1963
Madasar	71.495556	26.775	3							IAR 1999-2000
Madhapar	69.710953	23.229615	3							IAR 1970-71
Madhapar	69.710953	23.229615	2							IAR 1977-78
Madhavgad	?		8	✓	✓					Foote 1916

Site	Longitude	Latitude	Industry	Raw Material	Typology	Composition	Artefact Sizes	Excavation	Chronology	Source
Madhogarh	72.799256	23.426603	3	✓	✓					Allchin et al. 1978
Madhvas	73.621039	23.2003	3							IAR 1970-71
Madhvas	73.621039	23.2003	4							IAR 1975-76
Madhya Pushkar A	74.577707	26.508013	3	✓	✓	✓				Allchin et al. 1978
Madhya Pushkar B	74.576197	26.509607	3	✓	✓	✓				Allchin et al. 1978
Madhya Pushkar N	74.571233	26.50845	3	✓	✓	✓	✓			Allchin et al. 1978
Magra	74.284022	27.183237	8							Misra et al. 1980
Mahesha	71.68333	26.916664	8		✓					IAR 1999-2000
Maheshvari Hill I	73.472254	22.935422	3		✓					IAR 1974-75
Maheshvari Hill II	73.472254	22.935422	3		✓					IAR 1974-75
Malgad	72.132539	24.284535	3							IAR 1993-94
Malhar	72.382167	27.202134	6							IAR 1977-78
Malipara (Rangpur)	72.8	23.916667	3	✓	✓					Sankalia 1946
Malusar	71.420833	26.001389	6							IAR 1999-2000
Man	73.892799	23.189468	3							IAR 1972-73
Mandir wala thumda	71.616667	24.016667	3							IAR 1992-93
Mandor	73.034786	26.357385	3	✓	✓					IAR 1967-68
Mangadh	73.745387	23.141934	3							IAR 1971-72
Mangalpura	74.403814	27.626735	2		✓					Misra et al. 1982
Manpur	73.65185	22.211893	3	✓	✓					IAR 1986-87
Marwa	71.891666	26.749999	8		✓					IAR 1999-2000
Marwar Bagra	72.578648	25.212989	1	✓	✓		✓			Allchin et al. 1978
Marwar Bagra (a)	72.578648	25.212989	3		✓					Allchin et al. 1978
Marwar Bagra (b)	72.578648	25.212989	2	✓	✓	✓				Allchin et al. 1978
Mathal	69.177616	23.40705	2	✓	✓					IAR 1967-68
Mathawara	72.153864	21.392456	3	✓	✓					IAR 1979-80
Mehmudpura	73.336482	22.955907	3							IAR 1975-76
Mehreri	71.441111	26.544444	2							IAR 1999-2000
Mehreri Navi	71.451944	26.508611	1							IAR 1999-2000
Mekada	71.512351	21.416485	6	✓	✓					IAR 1979-80
Milestone 101 - general	68.182428	25.289621	7	✓	✓					Allchin et al. 1978
Milestone 101 1	68.182428	25.289621	3	✓	✓	✓	✓			Allchin et al. 1978
Milestone 101 2a	68.182428	25.289621	7	✓	✓					Allchin et al. 1978
Milestone 101 2b	68.182428	25.289621	3	✓	✓	✓				Allchin et al. 1978
Milestone 101 3	68.182428	25.289621	1	✓	✓		✓			Allchin et al. 1978
Milestone 101 4	68.182428	25.289621	1	✓	✓		✓			Allchin et al. 1978
Milestone 101 5	68.182428	25.289621	2	✓	✓					Allchin et al. 1978
Miroli	72.520513	22.884385	3							IAR 1974-75
Mitli	72.394534	22.419587	3	✓	✓	✓	✓			Allchin et al. 1978

Site	Longitude	Latitude	Industry	Raw Material	Typology	Composition	Artefact Sizes	Excavation	Chronology	Source
Mitli	72.395978	22.415907	3		✓					IAR 1963-64
Modasa	73.292652	23.459377	8	✓	✓					IAR 1958-59
Modha	71.994444	26.270833	8		✓					IAR 1999-2000
Mogra A1	72.979421	26.112264	1	✓	✓					Allchin et al. 1978
Mogra A2	72.978673	26.112545	2	✓	✓	✓				Allchin et al. 1978
Mogra A3	72.978759	26.112605	2	✓	✓					Allchin et al. 1978
Mogra B	72.986994	26.109921	3		✓	✓				Allchin et al. 1978
Mogra BN	72.986689	26.110389	8	✓	✓					Allchin et al. 1978
Mogra D	72.978478	26.112018	6	✓	✓	✓				Allchin et al. 1978
Mogra Hill	72.979421	26.112264	6							IAR 1977-78
Mokal	70.776046	27.092567	2	✓	✓					IAR 1984-85
Mokharia	72.310579	27.062904	6							IAR 1977-78
Moklat 1	71.041667	26.925	6							IAR 1999-2000
Monpur	73.65185	22.211893	3	✓	✓					IAR 1986-87
Moomal Ki Meri	70.908344	26.915748	3							IAR 1983-84
Morangana	74.013184	22.30868	3							IAR 1982-83
Morpur	69.815392	21.897435	3							IAR 1978-79
Mosabar	73.266667	22.216667	1	✓	✓					IAR 1986-87
Mosabar	73.266667	22.216667	1	✓	✓				✓	IAR 1988-89; Ajithprasad 2005a
Moti paneli	70.155831	21.871792	2							IAR 1958-59
Moti Pavthi	73.014591	23.135823	5							IAR 1974-75
Muai-Ashram	73.396928	22.302569	3							IAR 1983-84
Mudhiyari	73.746959	22.422501	2	✓	✓					Ajithprasad 2005b
Mulri Hills	67.113307	24.920803	6							Biagi 2008
Mulsan	72.533333	23.516667	3	✓	✓					Foote 1916
Mulsan	72.533333	23.516667	3	✓	✓					Sankalia 1946
Mum	69.259893	23.35464	3							IAR 1993-94
Muvada	73.815286	22.529513	8		✓					IAR 1985-86
N Kaneval Lake	72.515633	22.475783	3							IAR 1972-73
N of Bahadurpur	73.566322	22.187709	3	✓	✓	✓				Foote 1916
Nadisar	73.392655	22.885261	3							IAR 1971-72
Nagadia	69.5563	22.002855	3							IAR 1979-80
Nagri	73.376161	26.889732	6	✓	✓	✓				Allchin et al. 1978
Nagro Tikyo	73.65185	22.211893	3	✓	✓					IAR 1986-87
Naj	72.562214	22.880556	3							IAR 1973-74
Nakhoda	72.138942	25.792268	6							IAR 1977-78
Nakhtarana	69.259893	23.35464	1							IAR 1967-68
Nananiyai	71.754167	26.866667	8		✓					IAR 1999-2000
Nanawas	72.619706	25.342245	3							IAR 1977-78
Nand	74.466141	26.479251	3	✓						IAR 1977-78

Site	Longitude	Latitude	Industry	Raw Material	Typology	Composition	Artefact Sizes	Excavation	Chronology	Source
Nand Chandur	71.466667	23.6	3							IAR 1991-92
Nandol	72.815823	23.207875	3							IAR 1977-78
Nani	73.142701	23.157144	2							IAR 1974-75
Narvaniya	73.794349	22.436766	1	✓	✓					IAR 1992-93
Narvaniya I	73.794349	22.436766	1	✓	✓					Ajithprasad 2005b
Narvaniya II	73.792205	22.434334	1	✓	✓					Ajithprasad 2005b
Narvaniya III	73.791323	22.43835	8	✓						Ajithprasad 2005b
Narvaniya IV	73.785527	22.436175	1	✓	✓					Ajithprasad 2005b
Nasmed	72.409985	23.10889	3							IAR 1982-83
Navagam	71.792644	21.937846	3							IAR 1979-80
Navapura	71.833333	23.6	3							IAR 1990-91
Nawab Panjabi 1	68.680226	27.31537	6	✓	✓	✓				Allchin et al. 1978
Nawab Panjabi 2	68.680226	27.31537	6	✓	✓	✓				Allchin et al. 1978
nawab Panjabi 3	68.680226	27.31537	6	✓	✓	✓				Allchin et al. 1978
Nelya	74.379274	26.390525	3	✓						IAR 1977-78
Newa	74.747724	27.341961	3							IAR 1976-77
Nichadi	72.037934	21.244938	6	✓	✓					IAR 1979-80
Nigala Tappa	70.803457	21.961183	3	✓	✓					Foote 1916
Nijran Faliya	73.724126	22.420858	1	✓	✓					Ajithprasad 2005b
NNW Shivad	70.978069	21.307685	8	✓	✓					Foote 1916
nr Nakhtarana	69.356221	23.273892	2	✓						IAR 1967-68
nr Rojdi	70.917509	21.862114	2							IAR 1958-59
nr Rojdi	70.917509	21.862114	3							IAR 1958-59
Odd	72.565518	22.923163	3							IAR 1973-74
Ojat	70.51708	21.425151	1	✓	✓					Allchin et al. 1978
Okada Timbo	71.85	23.616667	3							IAR 1990-91
Olecha	71.455556	26.491667	1							IAR 1999-2000
Ongar 1	68.220833	25.176944	2	✓	✓					Biagi 2005
Ongar 10	68.22	25.16	3	✓	✓					Biagi 2005
Ongar 11	68.228611	25.161111	1	✓	✓					Biagi 2005
Ongar 2	68.229722	25.172222	8	✓	✓					Biagi 2005
Ongar 3	68.223333	25.172222	8	✓	✓					Biagi 2005
Ongar 4	68.226944	25.171667	2	✓	✓					Biagi 2005
Ongar 5	68.223621	25.171667	3	✓	✓					Biagi 2005
Ongar 6	68.229444	25.170278	3	✓	✓					Biagi 2005
Ongar 7	68.231389	25.164444	3	✓	✓					Biagi 2005
Ongar 8	68.228889	25.164167	3	✓	✓					Biagi 2005
Ongar 9	68.2225	25.164167	8	✓	✓					Biagi 2005
Opp Sadolia - R bank of Sabarmati	72.815057	23.442111	8	✓	✓					Foote 1916
Orana	72.824568	23.416395	3							IAR 1975-76

Site	Longitude	Latitude	Industry	Raw Material	Typology	Composition	Artefact Sizes	Excavation	Chronology	Source
Pachpadra Lake	72.22885	25.930427	3	✓						IAR 1977-78
Padardi	73.023727	24.042965	3							IAR 1970-71
Padra	73.085712	22.23988	3							IAR 1971-72
Pakhra Dungar	69.259893	23.35464	2		✓					IAR 1967-68
Paladi Karjan	72.54293	22.915164	3							IAR 1973-74
Palanpur	72.418722	24.177928	3	✓	✓	✓				Allchin et al. 1978
Palej	72.698609	23.221567	3							IAR 1974-75
Pali	73.323235	25.762817	4	✓	✓		✓			Misra 1963
Palsinda	73.900256	22.377355	3		✓					IAR 1993-94
Panchasar	71.753558	23.779127	3							IAR 1982-83
Panchwada	74.253464	22.8323	3							IAR 1970-71
Pandwa	73.400008	23.066554	3							IAR 1975-76
Pani	73.793347	22.466028	4		✓					IAR 1993-94
Panva	71.849408	23.366569	3							IAR 1982-83
Patharia	73.747786	22.820862	3		✓					IAR 1969-70
Pathodara	72.82	23.17	3							IAR 1974-75
Pavagadh	73.514774	22.462258	3		✓					IAR 1958-59
Pavagarh Dune 1	73.476758	22.284448	3	✓	✓	✓				Allchin et al. 1978
Pavagarh Dune 2	73.476758	22.284448	3	✓	✓		✓			Allchin et al. 1978
Pavagarh Dune 3	73.476758	22.284448	3	✓	✓	✓				Allchin et al. 1978
Pavagarh Hill	73.514774	22.462258	1	✓	✓					Allchin et al. 1978
Pedhamli	72.866623	23.666673	8	✓	✓					Foote 1916
Pedhamli	72.866623	23.666673	3	✓	✓					Sankalia 1946
Pedhamli in alluvium 30ft surface	72.866623	23.666673	8	✓	✓					Sankalia 1946
Pedhamli in alluvium 40-30ft	72.866623	23.666673	8	✓	✓					Sankalia 1946
Pedhamli in gravel	72.866623	23.666673	8	✓	✓					Sankalia 1946
Pedhamli on gravel	72.866623	23.666673	8	✓	✓					Sankalia 1946
Pedhamli-Karoli	72.866623	23.666673	3	✓	✓					Sankalia 1946
Peer Nango I	68.650833	27.0025	3							Shaikh et al. 2002-03
Peer Nango II	68.650833	27.002999	3							Shaikh et al. 2002-03
Peer Nango III	68.650833	27.003333	3							Shaikh et al. 2002-03
Pethapur	72.677113	23.26597	3							IAR 1974-75
Phalodi	72.361417	27.106821	3							IAR 1976-77
Pickak	73.688832	26.208683	2	✓	✓		✓			Misra 1963
Pindara	69.266832	22.254239	1		✓					IAR 1965-66
Pipad	73.54361	26.38552	2	✓	✓		✓			Misra 1963
Pipalsat	73.65185	22.211893	3	✓	✓					IAR 1986-87
Piperia	73.65185	22.211893	3	✓	✓					IAR 1986-87

Site	Longitude	Latitude	Industry	Raw Material	Typology	Composition	Artefact Sizes	Excavation	Chronology	Source
Pipiya	73.716661	22.316665	4	✓	✓				✓	IAR 1988-89; Ajithprasad 2005a
Pipli	71.879821	21.887371	3							IAR 1980-81
Pirana	72.510292	22.924577	3							IAR 1974-75
Pitavadi	71.506202	21.448279	6	✓	✓					IAR 1979-80
Pithad II	70.56714	22.684821	2							IAR 1979-80
Pitvajal	71.193791	21.518591	6	✓	✓					IAR 1979-80
Piyaj	72.45013	23.233043	1							IAR 1980-81
PN1	68.594659	27.045652	3	✓	✓					Biagi
PN2	68.594659	27.045652	3		✓					Biagi
PN3	68.594659	27.045652	3		✓					Biagi
Pokaran	71.930704	26.937226	2		✓					IAR 1977-78
Pokaran (x)	71.9	26.9	8		✓					IAR 1999-2000
Poylikothi	73.706471	22.457346	1	✓	✓					Ajithprasad 2005b
Pushkar L	74.547123	26.479956	1	✓	✓					Allchin et al. 1978
Rahib Sharik & Mutton Jugoth	68.862537	27.259299	1	✓	✓					Biagi & Cremaschi 1988
Raipur	73.825435	22.429058	1	✓	✓					IAR 1992-93
Raipur	73.825435	22.429058	3	✓	✓					IAR 1992-93
Rajasaro no Timbo	71.533333	23.583333	3							IAR 1991-92
Rajgarh	71.5	26.560556	6							IAR 1999-2000
Rajkot	70.80216	22.303894	8		✓					Marathe 1981
Rajpari	73.63331	22.31666	3	✓	✓					IAR 1988-89
Rajpipla	71.62576	21.885185	1		✓	✓				Marathe 1981
Rajpipla	71.62576	21.885185	1							IAR 1974-75
Rajpipla-2	71.62576	21.885185	2							IAR 1971-72
Rajthali	71.222271	21.508795	6	✓	✓					IAR 1979-80
Rajwada	70.380906	22.203448	3							IAR 1980-81
Rajwadio Timbo I	71.833333	23.6	3							IAR 1990-91
Rambhau	70.469224	23.481803	3		✓					IAR 1955-56
Ramji-ka-Gol	71.499263	25.117359	5	✓	✓					IAR 1979-80
Ramnod	70.92793	21.966442	3							IAR 1958-59
Rangpur	72.8	23.916667	1							IAR 1959-60
Rangpur	72.8	23.916667	3	✓	✓					Sankalia 1946
Ranodar	71.670842	24.960841	3	✓	✓					IAR 1979-80
Rasla	71.716667	26.75	8		✓					IAR 1999-2000
Ratadia	69.275092	23.00557	2	✓	✓					IAR 1963-64
Ratan Tekri	72.438393	24.171181	3		✓					IAR 1964-65
Rata-nadi	74.217107	27.17116	4	✓	✓	✓				IAR 1978-79; Misra et al. 1980; 1982
Ratanpur	73.616667	22.283333	4	✓	✓					IAR 1988-89
Ratanpur	73.616667	22.283333	3							IAR 1989-90

Site	Longitude	Latitude	Industry	Raw Material	Typology	Composition	Artefact Sizes	Excavation	Chronology	Source
Ratnakar	73.066168	23.022409	2							IAR 1974-75
Ratnal	69.89845	23.182613	3							IAR 1978-79
Ravaliya	73.09207	22.852137	3							IAR 1975-76
Rawad II	71.833339	23.649989	3							IAR 1990-91
Rawad III	71.833339	23.649989	3							IAR 1990-91
Raypur I	73.825435	22.429058	1	✓	✓					Ajithprasad 2005b
Raypur II	73.82567	22.426604	1	✓	✓					Ajithprasad 2005b
Raypur III	73.830532	22.427209	1	✓	✓					Ajithprasad 2005b
Raypur IV	73.834572	22.42996	1	✓	✓					Ajithprasad 2005b
Raypur IX	73.831262	22.434007	2	✓	✓					Ajithprasad 2005b
Raypur V	73.832745	22.428824	1	✓	✓					Ajithprasad 2005b
Raypur VI	73.82874	22.429348	1	✓	✓					Ajithprasad 2005b
Raypur VII	73.824971	22.435136	4	✓	✓					Ajithprasad 2005b
Raypur VIII	73.826662	22.432275	4	✓	✓					Ajithprasad 2005b
Red Hill	68.757321	27.355531	1	✓	✓					Biagi & Cremaschi 1988
Rehri	67.238452	24.815685	6							Biagi 2008
Reria	73.323235	25.762817	6							IAR 1977-78
RHBP 1	68.912167	27.656333	6							Shaikh et al. 2002-03
RHBP 10	68.913	27.661	4							Shaikh et al. 2002-03
RHBP 11	68.912339	27.661826	7							Shaikh et al. 2002-03
RHBP 12	68.912433	27.661933	4							Shaikh et al. 2002-03
RHBP 13	68.912533	27.661967	4							Shaikh et al. 2002-03
RHBP 14	68.912808	27.661881	7							Shaikh et al. 2002-03
RHBP 15	68.913167	27.662	7							Shaikh et al. 2002-03
RHBP 16	68.913383	27.66128	7							Shaikh et al. 2002-03
RHBP 17	68.913918	27.660583	6							Shaikh et al. 2002-03
RHBP 18	68.912377	27.66066	3							Shaikh et al. 2002-03
RHBP 20	68.912327	27.660353	2							Shaikh et al. 2002-03
RHBP 4	68.912459	27.660626	3							Shaikh et al. 2002-03
RHBP 5	68.912428	27.660667	3							Shaikh et al. 2002-03
RHBP 6	68.9125	27.660833	3							Shaikh et al. 2002-03
RHBP 7	68.912462	27.660871	3							Shaikh et al. 2002-03
RHBP 8	68.91243	27.660903	3							Shaikh et al. 2002-03
RHBP 9	68.913322	27.662155	3							Shaikh et al. 2002-03
Roda	73.292652	23.459377	8		✓					IAR 1958-59
Rohri	68.8993	27.679871	8	✓	✓					Foote 1916
Rohri (dT & P)	68.9181	27.665365	8	✓	✓					de Terra and Paterson 1939
Rohri Hills (generic)	68.913659	27.659751	7	✓						Allchin et al. 1978
Rohri Hills 5-6 (A)	68.913659	27.659751	6	✓	✓	✓				Allchin et al. 1978
Rohri Hills E	68.913659	27.659751	3	✓	✓	✓				Allchin et al. 1978

Site	Longitude	Latitude	Industry	Raw Material	Typology	Composition	Artefact Sizes	Excavation	Chronology	Source
Rojadi	70.848132	21.919912	2	✓	✓	✓				Allchin et al. 1978
Rojdi	70.917509	21.862114	2	✓	✓					IAR 1957-58
Rojdi	70.917509	21.862114	4							IAR 1961-62
Rugnathparu	71.239341	21.279148	6	✓	✓					IAR 1979-80
Runi	71.817585	23.937179	3							IAR 1989-90
Rupamore	70.058341	22.467219	3							IAR 1978-79
Rupavati	71.635992	21.501911	2	✓	✓					IAR 1979-80
Rupnagar	74.8597	26.785375	1	✓	✓					IAR 1984-85
Rustampura	73.321761	22.805084	1							IAR 1975-76
S of Chachai	71.026944	21.325556	3	✓	✓	✓				Foote 1916
S of Damnagar	71.517386	21.69496	3	✓	✓					Foote 1916
S of Khabarda	?		8	✓	✓					Foote 1916
Sabalpur	73.267714	23.476855	1							IAR 1973-74
Sabhrai	69.111391	23.012364	1		✓					IAR 1967-68
Sadolia	72.815057	23.442111	8		✓					Sankalia 1946
Sagdhra	73.616667	22.3	4	✓	✓				✓	IAR 1988-89; Ajithprasad 2005a
Salki	72.835244	23.221378	3							IAR 1977-78
Salt Dak Bungalow	74.564805	27.384076	3	✓						IAR 1979-80
Sam	70.546335	26.840463	8	✓	✓					IAR 1979-80
Samadhiala	71.074199	22.502472	4							IAR 1975-76
Samadhiala	71.074199	22.502472	1		✓			✓		IAR 1976-77
Samadhiala	71.074199	22.502472	1		✓	✓				Marathe 1981
Samadhiyala	71.074199	22.502472	1							IAR 1971-72
Sambhar Lake 1	75.067387	26.886396	2	✓	✓					Allchin et al. 1978
Sambhar Lake 2	75.062499	26.877128	2	✓	✓					Allchin et al. 1978
Samdari	72.576739	25.807007	2	✓	✓		✓			Misra 1963
Samdhi (A)	73.6	22.216667	4	✓	✓				✓	IAR 1988-89; Ajithprasad 2005a
Samdhi (B)	73.6	22.216667	3	✓	✓					IAR 1988-89
Sanawra	71.566667	26.85	8		✓					IAR 1999-2000
Sangana Nava	71.9861	21.351968	2	✓	✓					IAR 1979-80
Sangodara	70.576983	21.168926	1				✓			IAR 1977-78; Marathe 1981
Sankara	71.05	26.725	8		✓					IAR 1999-2000
Sanosara	69.666932	23.242	3							IAR 1980-81
Santhli	71.483333	23.9	3	✓	✓			✓		IAR 1993-94
Santhli III	71.483333	23.9	3							IAR 1993-94
Santhli V	71.483333	23.9	3							IAR 1993-94
Santhli VI	71.483333	23.9	3							IAR 1993-94
Santrampur	73.892799	23.189468	3							IAR 1972-73
Sanu	70.615072	27.279336	2	✓	✓					IAR 1984-85
Sar	72.939676	26.02544	6	✓	✓					Allchin et al. 1978

Site	Longitude	Latitude	Industry	Raw Material	Typology	Composition	Artefact Sizes	Excavation	Chronology	Source
Sarali	69.666932	23.242	3							IAR 1980-81
Sarangpur	71.674013	21.483354	6	✓	✓					IAR 1979-80
Sarkhej	72.884946	22.976328	1							IAR 1974-75
Sasan Gir	70.596393	21.170597	4	✓			✓			IAR 1974-75; Marathe 1981
Savitri Hill	74.544287	26.478885	1	✓	✓					Allchin et al. 1978
Sejakpur	71.457982	22.468321	2	✓	✓					IAR 1957-58
Sejakpur	71.457982	22.468321	3		✓					IAR 1957-58
Shaktari Timbo	71.533333	23.816667	3	✓	✓			✓		IAR 1992-93
Shamlaji	73.387	23.688	1							IAR 1979-80
Shedravadar	71.393601	21.463635	6	✓	✓					IAR 1979-80
Sherdi	70.138533	21.586385	1							IAR 1963-64
Shergarh Tri-Junction	72.282262	26.335354	6							IAR 1977-78
Shikapur	73.044742	26.035009	2		✓					Allchin et al. 1978
Shikarpura	73.04269	26.007774	2	✓	✓	✓	✓			Misra 1963
Shiyal/Magavana-no-Timbo	72.157366	22.687736	3							IAR 1976-77
Shyampura	74.416241	27.604779	2		✓					Misra et al. 1982
Sidsar	72.111123	21.719315	3							IAR 1980-81
Sigam Kanbi/Songir	73.683333	22.116667	3	✓	✓					Sankalia 1946
Silanwad	74.266657	27.349992	3		✓					IAR 1967-68
Singari	72.939524	25.90612	4	✓	✓		✓			Misra 1963
Singi Talav	74.554227	27.389404	4	✓	✓					IAR 1980-81
Singi Talav Quarry	74.554227	27.389404	1	✓	✓	✓		✓	✓	Misra et al. 1982
Sojat	73.655474	25.932118	8	✓	✓					IAR 1959-60
Sojet	73.655474	25.932118	2	✓	✓		✓			Misra 1963
Sokarna	72.697339	25.355365	3	✓						IAR 1977-78
Solankio-ki-Dhani-2	71.224975	26.895284	1							IAR 1999-2000
Solankio-ki-Dhani-I	71.206944	26.9	1							IAR 1999-2000
Sonada	73.066168	23.022409	3							IAR 1974-75
Suigam H	71.333337	24.116661	3							IAR 1993-94
Suigam I	71.333333	24.149981	3							IAR 1993-94
Sujan Singh-ki-Dhani	71.041667	26.886111	1							IAR 1999-2000
Sukhapur	69.288497	23.386559	1							IAR 1967-68
Sukkur	68.851421	27.688764	8	✓	✓					de Terra and Paterson 1939
Supadia	73.779024	22.432986	1	✓	✓					Ajithprasad 2005b
Suravali-jal	71.879821	21.887371	2							IAR 1979-80
Sureli	73.569053	22.65761	3							IAR 1975-76
Tadach	71.945321	21.407702	3	✓	✓					IAR 1979-80
Tajpur	72.920832	23.567031	1							IAR 1973-74

Site	Longitude	Latitude	Industry	Raw Material	Typology	Composition	Artefact Sizes	Excavation	Chronology	Source
Tajpura	72.920955	23.567202	3							IAR 1998-99
Talee	68.701498	27.155488	3							Shaikh et al. 2002-03
Talia	72.039125	21.355123	6	✓	✓					IAR 1979-80
Talioghoda	73.65185	22.211893	3	✓	✓					IAR 1986-87
Tanki	68.83471	27.256254	1	✓	✓					Biagi & Cremaschi 1988
Taranagar	71.583333	23.583333	3							IAR 1991-92
Tarpada	71.806478	21.844859	1							IAR 1974-75
Tarsang	73.473345	22.937254	3		✓					IAR 1974-75
Tarsang	73.472254	22.935422	3	✓	✓			✓		IAR 1977-78
Tarsang-Rena	73.473345	22.937254	3		✓					IAR 1974-75
That	71.85	26.833333	8		✓					IAR 1999-2000
Thesaria	72.438393	24.171181	3		✓					IAR 1964-65
Thob	72.39215	26.048142	8	✓	✓					Allchin et al. 1978
Thoriali	71.47503	22.230957	2	✓	✓					IAR 1958-59
Thoriali	71.47503	22.230957	2		✓					IAR 1961-62
Thumda II	71.566667	23.65	3							IAR 1991-92
Tikawada	73.847678	22.491195	1		✓					IAR 1993-94
Tikawada	73.847678	22.491195	3		✓					IAR 1993-94
Timana	71.992866	21.425948	3	✓	✓					IAR 1979-80
Timbi I	70.380906	22.203448	3							IAR 1980-81
Timbu	70.380906	22.203448	3							IAR 1980-81
Todiya	73.336482	22.955907	3							IAR 1975-76
Travada	71.10224	21.496864	4	✓	✓					IAR 1979-80
Uchhakalam	73.6807	22.312998	1	✓	✓				✓	IAR 1986-87; Ajithprasad 2005a
Uchhet	73.65	22.3	1	✓	✓					IAR 1986-87
Uchhet	73.65	22.3	4	✓	✓					IAR 1988-89
Uchhet	73.65	22.3	1	✓	✓				✓	IAR 1988-89; Ajithprasad 2005a
Udrel	72.779104	22.958063	3	✓	✓					IAR 1970-71
Udrel	72.779104	22.958063	3	✓	✓			✓		IAR 1971-72
Ukharda	69.259893	23.35464	3							IAR 1979-80
Umednagar	73.015417	26.56517	3	✓						IAR 1958-59
Umralla	71.806478	21.844859	1							IAR 1974-75
Umrasan	68.774	23.824	3	✓						IAR 1993-94
Umrethi	70.469222	21.020784	1	✓			✓		✓	IAR 1974-75; Marathe 1981; Baskaran et al. 1986
Umria	74.05	22.75	3	✓	✓	✓				Foote 1916
Una	70.966404	20.811949	3		✓					Allchin et al. 1978
Unchidhanal	72.967731	24.090181	3							IAR 1970-71
Undar	74.253464	22.8323	3							IAR 1968-69
Unnar	68.6833	27.318659	7	✓	✓					Biagi & Cremaschi 1988
Unnar Hill	68.679277	27.318065	4	✓	✓					Biagi & Cremaschi 1988

Site	Longitude	Latitude	Industry	Raw Material	Typology	Composition	Artefact Sizes	Excavation	Chronology	Source
Uparkot	70.566171	21.001761	1	✓	✓					IAR 1976-77
Upleta	70.28139	21.739722	2							Lele 1972
Uttam Singh-ki-Dhani	71.263348	26.812501	1		✓					IAR 1999-2000
Vadi	73.422844	22.9172	3							IAR 1971-72
Vakar Valley North East	68.706186	27.131841	3							Shaikh et al. 2002-03
Vakar Valley South	68.704	27.121	3							Shaikh et al. 2002-03
Valabhipur	71.879821	21.887371	6							IAR 1979-80
Vallavpur	73.395167	22.91895	3							IAR 1975-76
Valli (Vanthlino Tekro)	72.619408	22.313115	3							IAR 1972-73
Valothi I	73.745671	22.409336	2	✓	✓					Ajithprasad 2005b
Valothi II	73.749029	22.409333	1	✓	✓					Ajithprasad 2005b
Valothi III	73.750234	22.412356	4	✓	✓					Ajithprasad 2005b
Valothi IV	73.752134	22.405111	1	✓	✓					Ajithprasad 2005b
Vangadhra	71.74223	21.843071	8							Chakrabarti 1978
Vankia	71.135741	21.517829	7	✓	✓					IAR 1979-80
Vanzar	72.512018	22.955988	3							IAR 1973-74
Vasad	73.066667	22.45	3	✓	✓					Allchin et al. 1978
Vasad	73.066667	22.45	3	✓	✓					Sankalia 1946
Vasana	72.816221	23.305096	3							IAR 1974-75
Vasantgarh	73.847678	22.491195	1		✓					IAR 1993-94
Vasantgarh	73.847678	22.491195	3		✓					IAR 1993-94
Vastana	72.557597	22.58758	3							IAR 1972-73
Vatkiwalu kheter I	71.1	23.766667	3							IAR 1992-93
Vatkiwalu kheter II	71.1	23.766667	3							IAR 1992-93
Veesar Valley 10	68.74033	27.017832	3							Shaikh et al. 2002-03
Veesar Valley 11	68.740333	27.017833	3							Shaikh et al. 2002-03
Veesar Valley 12	68.740333	27.017873	3							Shaikh et al. 2002-03
Veesar Valley 13	68.740333	27.018	3							Shaikh et al. 2002-03
Veesar Valley 14	68.738333	27.018	6							Shaikh et al. 2002-03
Veesar Valley 15	68.738374	27.018	3							Shaikh et al. 2002-03
Veesar Valley 16	68.740667	27.018	6							Shaikh et al. 2002-03
Veesar Valley 17	68.741167	27.018	6							Shaikh et al. 2002-03
Veesar Valley 18	68.740167	27.018167	6							Shaikh et al. 2002-03
Veesar Valley 19	68.740667	27.018167	6							Shaikh et al. 2002-03
Veesar Valley 2	68.741333	27.009833	3							Shaikh et al. 2002-03
Veesar Valley 20	68.740994	27.018167	6							Shaikh et al. 2002-03
Veesar Valley 21	68.741167	27.018167	6							Shaikh et al. 2002-03
Veesar Valley 22	68.7405	27.018333	6							Shaikh et al. 2002-03
Veesar Valley 23	68.740667	27.018333	3							Shaikh et al. 2002-03

Site	Longitude	Latitude	Industry	Raw Material	Typology	Composition	Artefact Sizes	Excavation	Chronology	Source
Veesar Valley 3	68.741333	27.009833	3							Shaikh et al. 2002-03
Veesar Valley 4	68.739339	27.016646	3							Shaikh et al. 2002-03
Veesar Valley 5	68.740141	27.016828	3							Shaikh et al. 2002-03
Veesar Valley 50	68.74	27.019333	3							Shaikh et al. 2002-03
Veesar Valley 51	68.74	27.0195	6							Shaikh et al. 2002-03
Veesar Valley 52	68.74	27.0195	6							Shaikh et al. 2002-03
Veesar Valley 53	68.74	27.0195	6							Shaikh et al. 2002-03
Veesar Valley 54	68.7415	27.019667	6							Shaikh et al. 2002-03
Veesar Valley 55	68.741833	27.0195	3							Shaikh et al. 2002-03
Veesar Valley 56	68.739667	27.019667	6							Shaikh et al. 2002-03
Veesar Valley 57	68.741667	27.019667	6							Shaikh et al. 2002-03
Veesar Valley 58	68.7415	27.019667	6							Shaikh et al. 2002-03
Veesar Valley 59	68.75	27.0195	3							Shaikh et al. 2002-03
Veesar Valley 6	68.740167	27.016833	3							Shaikh et al. 2002-03
Veesar Valley 60	68.75	27.019649	3							Shaikh et al. 2002-03
Veesar Valley 61	68.741833	27.019667	3							Shaikh et al. 2002-03
Veesar Valley 62	68.743167	27.019833	6							Shaikh et al. 2002-03
Veesar Valley 63	68.741833	27.019833	6							Shaikh et al. 2002-03
Veesar Valley 64	68.741342	27.019833	3							Shaikh et al. 2002-03
Veesar Valley 65	68.741333	27.019833	3							Shaikh et al. 2002-03
Veesar Valley 66	68.739167	27.019833	3							Shaikh et al. 2002-03
Veesar Valley 67	68.739	27.019833	6							Shaikh et al. 2002-03
Veesar Valley 68	68.743167	27.019833	3							Shaikh et al. 2002-03
Veesar Valley 69	68.741333	27.02	3							Shaikh et al. 2002-03
Veesar Valley 7	68.740167	27.016992	6							Shaikh et al. 2002-03
Veesar Valley 70	68.741333	27.020167	6							Shaikh et al. 2002-03
Veesar Valley 71	68.739167	27.020167	6							Shaikh et al. 2002-03
Veesar Valley 72	68.743	27.020167	3							Shaikh et al. 2002-03
Veesar Valley 73	68.740513	27.020332	6							Shaikh et al. 2002-03
Veesar Valley 74	68.7405	27.020333	6							Shaikh et al. 2002-03
Veesar Valley 75	68.740609	27.020333	6							Shaikh et al. 2002-03
Veesar Valley 76	68.738833	27.020333	6							Shaikh et al. 2002-03
Veesar Valley 77	68.739	27.020333	6							Shaikh et al. 2002-03
Veesar Valley 78	68.7405	27.0205	6							Shaikh et al. 2002-03
Veesar Valley 79	68.741167	27.020667	6							Shaikh et al. 2002-03
Veesar Valley 8	68.740006	27.017161	3							Shaikh et al. 2002-03
Veesar Valley 80	68.739667	27.020833	6							Shaikh et al. 2002-03
Veesar Valley 81	68.739833	27.021	3							Shaikh et al. 2002-03
Veesar Valley 82	68.739833	27.021	6							Shaikh et al. 2002-03
Veesar Valley 83	68.739833	27.021	6							Shaikh et al. 2002-03

Site	Longitude	Latitude	Industry	Raw Material	Typology	Composition	Artefact Sizes	Excavation	Chronology	Source
Veesar Valley 84	68.740167	27.021167	3							Shaikh et al. 2002-03
Veesar Valley 85	68.741333	27.021167	6							Shaikh et al. 2002-03
Veesar Valley 86	68.740333	27.0215	6							Shaikh et al. 2002-03
Veesar Valley 87	68.74	27.021667	6							Shaikh et al. 2002-03
Veesar Valley 88	68.7405	27.021833	6							Shaikh et al. 2002-03
Veesar Valley 89	68.741	27.022	6							Shaikh et al. 2002-03
Veesar Valley 9	68.7397	27.017534	3							Shaikh et al. 2002-03
Veesar Valley 90	68.740167	27.022	3							Shaikh et al. 2002-03
Veesar Valley 91	68.740833	27.022	3							Shaikh et al. 2002-03
Veesar Valley 92	68.740667	27.022333	3							Shaikh et al. 2002-03
Veesar Valley 94	68.7415	27.022333	3							Shaikh et al. 2002-03
Veesar Valley 95	68.740333	27.0225	6							Shaikh et al. 2002-03
Veesar Valley 96	68.740833	27.022667	3							Shaikh et al. 2002-03
Veesar Valley 97	68.742667	27.022667	3							Shaikh et al. 2002-03
Veesar Valley 98	68.742667	27.023	3							Shaikh et al. 2002-03
Vejalpur	73.396928	22.302569	3							IAR 1982-83
Velavadar	72.034259	21.393677	6	✓	✓					IAR 1979-80
Venghdra	71.806478	21.844859	1							IAR 1970-71
Verai Mata-no-Timbo	72.483333	23.45	3	✓	✓					Sankalia 1946
Veraval	70.450306	20.997449	8		✓					Allchin et al. 1978
Vetalpur	72.736455	23.919136	3	✓	✓					Sankalia 1946
Vijayanagar	73.360553	24.005588	2							IAR 1973-74
Vijayapura/Pindara-Nazd	69.266832	22.254239	1							IAR 1978-79
Vinjhan	69.02575	23.104042	2	✓	✓					IAR 1967-68
Virani	69.270207	23.390444	1		✓					IAR 1967-68
Visadi	73.85393	22.4415	3	✓	✓	✓				Allchin et al. 1978
Visadi	73.85393	22.4415	3							IAR 1977-78
Visalpur	72.482245	22.93061	3							IAR 1973-74
Visangadh	73.838457	22.482599	1	✓	✓					Ajithprasad 2005b
Vyara	73.411762	22.251849	3							IAR 1977-78
W of Desar	73.291278	22.717741	8	✓	✓					Foote 1916
Wadeli	73.666667	22.3	1	✓	✓				✓	IAR 1986-87; Ajithprasad 2005a
Wadeli	73.609384	22.217131	3	✓	✓					Sankalia 1946
Wadi Sim North 1	68.689167	27.1395	3							Shaikh et al. 2002-03
Wadi Sim South	68.690495	27.13269	3							Shaikh et al. 2002-03
Wadu Kodivalo Timbo	72.55	23.366667	3	✓	✓					Sankalia 1946
Warsora	72.4	23.75	8		✓					Sankalia 1946
Yaksha	69.697657	23.23678	2	✓	✓					IAR 1967-68
Zanzaria no Timbo	71.733333	23.4	3							IAR 1991-92

Site	Longitude	Latitude	Industry	Raw Material	Typology	Composition	Artefact Sizes	Excavation	Chronology	Source
Zarmarmata (Navagam)	73.6167	23.133299	3							IAR 1975-76
ZPS 1	68.880278	27.457222	1			✓	✓	✓		Biagi 2008
ZPS 2	68.881111	27.457778	3			✓		✓		Biagi 2008
ZPS 4	68.876944	27.453611	3			✓		✓		Biagi 2008

Table A.2: Presence of artefact types at Palaeolithic sites in the Thar Desert (see Table A.1 for Industry description)

Site	Industry	Flake/Debitage	Blade	Blade parallel	Blade Flake	Blade backed	Blade crested	Retouched/Tool	Point	Borer	Burin	Awl	Denitulate	Notch	Scraper	Knife	Microlith	Geometric	Non-geometric	Lunate/Crescent	Triangle	Trapeze	Micro-Blade	Backed Blade	Core	Fluted Core	Blade Core	Levallois Core	Discooidal Core	Microlithic Core	Polyhedral Core	Heavy Tool	Handaxe	Chopper	Chopping Tool	Cleaver	Pick	Ovate				
16R	7	✓	✓					✓	✓	✓			✓	✓	✓									✓			✓															
25km NE Rajkot 1	6	✓	✓												✓										✓																	
25km NE Rajkot 2	3		✓																								✓															
47km S Nagaur	3	✓																							✓																	
60km South Jaisalmer	8	✓	✓																							✓																
7.5 miles ENE Amreli	8																✓																									
797bis	7	✓												✓	✓										✓																	
Achali	5	✓				✓		✓	✓	✓					✓				✓	✓	✓			✓																		
Akhaj	8	✓																																								
Akhaj N	3		✓					✓							✓																											
Akhaj SE	3		✓					✓							✓																											
Akkadia Mota	3	✓													✓										✓																	
Akora	3			✓																						✓																
Amarpura	1	✓																																								
Amba	6	✓			✓			✓	✓			✓			✓										✓				✓													
Ambakut	3					✓		✓	✓											✓	✓	✓			✓																	
Ambhakut	3					✓		✓											✓	✓	✓	✓			✓																	
Angia	1	✓																								✓														✓		
Anguria	3							✓		✓									✓				✓																			
Anjar	2							✓	✓						✓																											
Anjar	3		✓					✓							✓										✓	✓																
Arjunpura	3	✓	✓								✓				✓										✓	✓																
Arzi Goth	6	✓																																								
Atkot	1	✓													✓																											
Atkot	1	✓																																								
Babapur	3	✓							✓				✓		✓	✓									✓																✓	
Babapur	7	✓			✓			✓	✓			✓		✓	✓										✓				✓						✓	✓					✓	

Site	Industry	Flake/Debitage	Blade	Blade parallel	Blade Flake	Blade backed	Blade crested	Retouched/Tool	Point	Borer	Burin	Awl	Denitulate	Notch	Scraper	Knife	Microlith	Geometric	Non-geometric	Lunate/Crescent	Triangle	Trapeze	Micro-Blade	Backed Blade	Core	Fluted Core	Blade Core	Levallois Core	Discoidal Core	Microlithic Core	Polyhedral Core	Heavy Tool	Handaxe	Chopper	Chopping Tool	Cleaver	Pick	Ovate			
Bacha	1																																								
Bahadarpur	1	✓													✓	✓																									
Bahadarpur	3		✓						✓						✓																										
Bahadarpur	8	✓	✓																						✓			✓												✓	
Bajawa	1																																								
Balani-Vav	1								✓						✓																										
Bandharia Mota	8								✓																																
Bangur Canal	1	✓							✓				✓		✓														✓		✓										
Bar	1	✓													✓	✓																									
Barala	3								✓		✓								✓				✓																		
Baria	3	✓	✓						✓				✓		✓	✓									✓																
Baridhani	2	✓									✓				✓										✓		✓														
Bari-Khatu	3			✓																						✓															
Bariyari	2	✓						✓																					✓												
Baskario	1	✓													✓	✓																								✓	
Baskario	4	✓							✓						✓										✓																
Bavka	8		✓						✓						✓										✓																
Benara 'C'	2	✓																							✓																
Bhadrajum	1																																								✓
Bhagwanpura	3								✓	✓	✓				✓					✓	✓	✓			✓																
Bhajodi	1														✓																										✓
Bhandei	2		✓																																						
Bhanpur	1							✓							✓	✓																									
Bhanpur I	4	✓						✓	✓						✓	✓									✓																✓
Bhanpur II	1	✓						✓							✓										✓																✓
Bhanpur III	1	✓						✓							✓										✓																✓
Bhanpur IV	4	✓						✓	✓						✓	✓									✓																✓
Bhanpur IX	4	✓						✓	✓						✓	✓									✓																✓
Bhanpur V	1	✓						✓							✓										✓																✓
Bhanpur VI	1	✓						✓							✓										✓																✓

Site	Industry	Flake/Debitage	Blade	Blade parallel	Blade Flake	Blade backed	Blade crested	Retouched/Tool	Point	Borer	Burin	Awl	Denitulate	Notch	Scraper	Knife	Microlith	Geometric	Non-geometric	Lunate/Crescent	Triangle	Trapeze	Micro-Blade	Backed Blade	Core	Fluted Core	Blade Core	Levallois Core	Discoidal Core	Microlithic Core	Polyhedral Core	Heavy Tool	Handaxe	Chopper	Chopping Tool	Cleaver	Pick	Ovate			
Bhanpur VII	1	✓						✓							✓									✓																✓	
Bhanpur VIII	1	✓						✓							✓										✓																✓
Bhavada	3			✓					✓						✓					✓	✓																				
Bhavnagar	2	✓	✓						✓	✓	✓			✓	✓	✓									✓																
Bhawi	2	✓																																							
Bhetanda	2	✓																																							
Bhitali	3																								✓																
Bhojka	2	✓													✓										✓																
Bhulwan	3		✓						✓																✓																
Bhungar	6	✓			✓				✓	✓		✓			✓										✓				✓												
Bhuvel	3			✓					✓						✓					✓	✓																				
Bikaner	3		✓			✓														✓	✓																				
Bilia	8							✓																																	
Bisalpur	2	✓													✓																										
Bodeli	3		✓						✓						✓																										
Bovadi	6	✓			✓				✓	✓		✓			✓										✓				✓												
Bridge Site	4												✓		✓										✓																
Btw Umria and Bhard	8								✓																✓																
Budha Pushkar A	3	✓	✓								✓							✓							✓			✓													
Budha Pushkar B	3	✓							✓		✓				✓			✓							✓			✓													
Budha Pushkar C	3	✓	✓						✓		✓				✓			✓																							
Budha Pushkar D	3	✓	✓						✓		✓				✓										✓			✓											✓		
Budha Pushkar E	3	✓	✓						✓		✓	✓	✓		✓			✓							✓			✓													
Budha Pushkar E-F	3	✓							✓		✓				✓			✓							✓			✓													
Budha Pushkar F	3	✓	✓								✓				✓			✓							✓			✓													
Budha Pushkar G	3	✓	✓						✓		✓				✓			✓							✓			✓													
Bungalow Kot	4	✓																																							
Chachai	8	✓													✓										✓																
Chakrora nullah, S of Umria	8	✓																							✓																
Chamol	3	✓			✓										✓										✓																

Site	Industry	Flake/Debitage	Blade	Blade parallel	Blade Flake	Blade backed	Blade crested	Retouched/Tool	Point	Borer	Burin	Awl	Denitculate	Notch	Scraper	Knife	Microlith	Geometric	Non-geometric	Lunate/Crescent	Triangle	Trapeze	Micro-Blade	Backed Blade	Core	Fluted Core	Blade Core	Levallois Core	Discoidal Core	Microlithic Core	Polyhedral Core	Heavy Tool	Handaxe	Chopper	Chopping Tool	Cleaver	Pick	Ovate				
Chanda	3	✓		✓											✓									✓																		
Charmadi Hill	3	✓																							✓																	
Chhajoli	1						✓																																			
Chuchhapura	1	✓													✓	✓																		✓		✓						
Dabla-ka-dhora	3		✓												✓									✓																		
Damrala	2	✓							✓	✓		✓			✓														✓													
Danasani	2	✓							✓						✓																											
Dandar	3	✓	✓								✓				✓									✓			✓															
Dandar 2	2	✓													✓																					✓						
Dandar 3	2	✓													✓										✓																	
Dangarwa Rabari-na-Gochara-no-Timbo	3		✓						✓						✓									✓																		
Dangarwa Venu-no-Charo	3								✓						✓																											
Daphro A	2	✓																																								
Daphro B	1	✓																							✓														✓			
Datrana IV	3	✓																✓	✓																							
Datrana V	3								✓	✓					✓					✓	✓	✓																				
Desalpur	2								✓	✓					✓																											
Deta	2								✓	✓					✓																											
Devalia	7	✓		✓					✓	✓		✓			✓									✓				✓						✓	✓	✓	✓	✓		✓		
Devisar	1														✓																											
Devnimori	3				✓							✓							✓	✓	✓					✓																
Dhaneri	2	✓	✓	✓					✓	✓					✓	✓								✓				✓										✓				
Dhaneri	6																																									
Dharwania	3		✓												✓									✓																		
Dhoraji	2			✓					✓	✓					✓									✓																		
Dhrangadhra	4	✓													✓									✓																		
Dhrud river	2							✓	✓						✓									✓																		
Dokariya	3		✓						✓			✓			✓									✓																		
Don Dunker	1	✓																						✓																		
Duma	4	✓							✓						✓									✓																		

Site	Industry	Flake/Debitage	Blade	Blade parallel	Blade Flake	Blade backed	Blade crested	Retouched/Tool	Point	Borer	Burin	Awl	Denitculate	Notch	Scraper	Knife	Microlith	Geometric	Non-geometric	Lunate/Crescent	Triangle	Trapeze	Micro-Blade	Backed Blade	Core	Fluted Core	Blade Core	Levallois Core	Discoidal Core	Microlithic Core	Polyhedral Core	Heavy Tool	Handaxe	Chopper	Chopping Tool	Cleaver	Pick	Ovate			
Duma	5	✓													✓	✓	✓																								
Dundara	2	✓	✓						✓	✓					✓												✓														
Dungervant	1	✓						✓							✓											✓						✓				✓			✓		
Dunkri	3	✓	✓			✓			✓	✓	✓				✓					✓	✓	✓				✓														✓	
E-W (unnamed) Long Hill A	1	✓																							✓																
E-W (unnamed) Long Hill B	1																																								
E-W (unnamed) Long Hill C	8	✓													✓										✓																
E-W (unnamed) Long Hill D	8	✓																																							
E-W (unnamed) Long Hill E	8	✓																																							
E-W (unnamed) Long Hill F	8	✓																							✓																
Fala	2	✓							✓	✓					✓																										
Gadhara (Hirpura)	3		✓						✓						✓										✓																
Gadhara II (Hirpura)	3		✓						✓						✓										✓																
Ghadhara Nala	8	✓																																						✓	
Ghuntia	1							✓							✓	✓																									
Ghuntia I	2								✓						✓	✓																									
Ghuntia II	2								✓						✓	✓																									
Ghuntia III	2								✓						✓	✓																									
GNR1	3	✓							✓		✓															✓															
GNR10	3	✓							✓							✓						✓																			
GNR2	3	✓																																							
GNR4	3	✓					✓	✓																																	
GNR7	3	✓							✓																																
GNR9	3	✓					✓	✓	✓		✓				✓								✓			✓															
Golio	2	✓	✓						✓						✓	✓																									
Govindara	3			✓					✓											✓	✓																				
Gudi	8	✓																																							
Gunded	3								✓	✓	✓				✓					✓	✓	✓				✓															
Gundiviri	1	✓																																							
Gundiviri	3								✓	✓	✓				✓					✓	✓	✓				✓															

Site	Industry	Flake/Debitage	Blade	Blade parallel	Blade Flake	Blade backed	Blade crested	Retouched/Tool	Point	Borer	Burin	Awl	Denitculate	Notch	Scraper	Knife	Microlith	Geometric	Non-geometric	Lunate/Crescent	Triangle	Trapeze	Micro-Blade	Backed Blade	Core	Fluted Core	Blade Core	Levallois Core	Discoidal Core	Microlithic Core	Polyhedral Core	Heavy Tool	Handaxe	Chopper	Chopping Tool	Cleaver	Pick	Ovate			
Gurha 1	2	✓						✓																✓																	
Gurha 2	2	✓						✓							✓										✓												✓				
Guttiya	3					✓		✓												✓																					
Hadol	3		✓					✓																	✓																
Hadol Juna Nala gravel	8	✓																																						✓	
Hadol Juna Nala on bedrock	8	✓																											✓								✓		✓		
Halvad	4																																								
Handod	3	✓	✓			✓		✓		✓	✓				✓					✓	✓	✓			✓																
Hathipagla	1							✓							✓	✓									✓															✓	
Hathipagla I	1	✓						✓							✓										✓															✓	
Hathipagla II	1	✓						✓							✓										✓															✓	
Hathipagla III	2							✓							✓	✓									✓															✓	
Hathipagla IV	1	✓						✓							✓										✓															✓	
Haveli	1	✓																							✓																
Hiran	1														✓																										
Hirpura	8	✓																							✓																
Hokra 1A	2	✓						✓			✓				✓										✓															✓	
Hokra 2B	1	✓																																							✓
Hundgaon	2	✓			✓			✓		✓					✓	✓													✓												
Indola-ki-Dhani	1	✓																																							
Indola-ki-Dhani	4	✓						✓					✓		✓	✓																									
Itari	3	✓	✓												✓																										
Jaidak II	3	✓				✓		✓		✓															✓																
Jalampura	3		✓					✓							✓										✓																
Jalampura	8	✓													✓										✓																
Jankpiura	1	✓						✓						✓																											✓
Jawanpura	3		✓																																						
Jayal	1	✓												✓	✓	✓									✓																
Jayal	2	✓	✓												✓										✓																
Jenana	2	✓						✓							✓																										

Site	Industry	Flake/Debitage	Blade	Blade parallel	Blade Flake	Blade backed	Blade crested	Retouched/Tool	Point	Borer	Burin	Awl	Denitculate	Notch	Scraper	Knife	Microlith	Geometric	Non-geometric	Lunate/Crescent	Triangle	Trapeze	Micro-Blade	Backed Blade	Core	Fluted Core	Blade Core	Levallois Core	Discoidal Core	Microlithic Core	Polyhedral Core	Heavy Tool	Handaxe	Chopper	Chopping Tool	Cleaver	Pick	Ovate		
Jetpur	8	✓					✓								✓									✓																
Jhab I	2								✓						✓	✓															✓				✓	✓				
Jhab II	4	✓						✓	✓						✓	✓									✓						✓				✓	✓	✓		✓	
Jhab III	4	✓						✓	✓						✓	✓									✓						✓				✓	✓	✓		✓	
Jhab IV	1	✓						✓							✓										✓						✓				✓	✓	✓		✓	
Jhab V	4	✓						✓	✓						✓	✓									✓						✓				✓	✓	✓		✓	
Jhab VI	2								✓						✓	✓														✓			✓		✓	✓				
JHP1	3	✓					✓	✓	✓											✓				✓			✓			✓										
JHP10	3	✓					✓							✓													✓													
JHP11	3	✓					✓								✓									✓																
JHP12	3	✓															✓										✓													
JHP13	3	✓					✓										✓										✓													
JHP14	3	✓					✓										✓										✓													
JHP15	3	✓																									✓													
JHP16	3	✓																									✓													
JHP19	3	✓																												✓										
JHP2	3																													✓										
JHP22	3	✓																									✓			✓										
JHP23	3	✓																																						
JHP26	3	✓													✓															✓										
JHP27	3	✓																									✓													
JHP4	3	✓																										✓												
JHP5	3	✓																																						
JHP6	3						✓																																	
JHP7	3	✓					✓													✓							✓													
JHP8	3	✓																						✓	✓															
JHP9	3	✓					✓	✓												✓	✓			✓	✓		✓													
Jinjar	3					✓			✓						✓					✓	✓				✓				✓											
Jira	8																								✓															
Jogpura	4	✓													✓	✓																	✓		✓	✓				

Site	Industry	Flake/Debitage	Blade	Blade parallel	Blade Flake	Blade backed	Blade crested	Retouched/Tool	Point	Borer	Burin	Awl	Denitculate	Notch	Scraper	Knife	Microlith	Geometric	Non-geometric	Lunate/Crescent	Triangle	Trapeze	Micro-Blade	Backed Blade	Core	Fluted Core	Blade Core	Levallois Core	Discoidal Core	Microlithic Core	Polyhedral Core	Heavy Tool	Handaxe	Chopper	Chopping Tool	Cleaver	Pick	Ovate			
Jogpura I	4	✓						✓	✓						✓	✓								✓															✓		
Jogpura II	1	✓						✓							✓										✓															✓	
Jogpura III	1	✓						✓							✓										✓															✓	
Jogpura IV	2								✓						✓	✓									✓															✓	
Jogpura V	1	✓						✓							✓										✓															✓	
Jogpura VI	2		✓						✓						✓	✓									✓																
Jogpura VII	2		✓						✓						✓	✓																									
Jojwaghode	3	✓	✓			✓			✓	✓	✓				✓				✓	✓	✓			✓																	
Jopa	3	✓	✓			✓			✓	✓	✓				✓				✓	✓	✓			✓																	
JS1	3	✓					✓	✓	✓												✓	✓			✓																
JS2	3	✓				✓	✓	✓	✓		✓				✓							✓			✓																
JS3	3	✓						✓	✓		✓														✓																
JS4	3	✓						✓	✓		✓										✓	✓			✓																
Juni Shedhal-Bamaniyo Timbo	3		✓												✓																										
Kalubhar	1	✓													✓																										
Kambolaj	3	✓									✓				✓												✓														
Kamol Nava	6	✓			✓				✓	✓		✓			✓										✓				✓												
Kamord	3	✓	✓								✓						✓								✓			✓													
Kaneria I (Rangpur)	3	✓													✓										✓																
Kaneria II (Rangpur)	3		✓						✓						✓										✓																
Kanhathai	3	✓															✓								✓																
Kaniel	3	✓													✓										✓																
Kankot	6	✓			✓				✓	✓		✓			✓										✓					✓											
Kanod	3																✓																								
Kapadvanj	2	✓																							✓																
Kapadwanj	8	✓																							✓																
Karna I	8	✓																							✓																
Karna II	8	✓	✓																																						
Kelawa	8							✓																																	
Kesaria	1																																								

Site	Industry	Flake/Debitage	Blade	Blade parallel	Blade Flake	Blade backed	Blade crested	Retouched/Tool	Point	Borer	Burin	Awl	Denitulate	Notch	Scraper	Knife	Microlith	Geometric	Non-geometric	Lunate/Crescent	Triangle	Trapeze	Micro-Blade	Backed Blade	Core	Fluted Core	Blade Core	Levallois Core	Discoidal Core	Microlithic Core	Polyhedral Core	Heavy Tool	Handaxe	Chopper	Chopping Tool	Cleaver	Pick	Ovate			
Kevada	1							✓							✓	✓																									
Kevada	4	✓													✓	✓																									
Kevada I	1	✓						✓							✓										✓						✓									✓	
Kevada II	1	✓						✓							✓										✓						✓									✓	
Kevada III	2								✓						✓	✓															✓									✓	
Khadeen	8	✓																																							
Khairla Hill	3	✓	✓								✓				✓										✓		✓														
Khairla Hill 2	2	✓																																							
Khinsvar	3																																								
Kikwada	1	✓						✓							✓										✓							✓								✓	
Kiyal	3								✓						✓											✓															
Km 18	8	✓													✓										✓																
Km 24	2	✓													✓										✓																
Km 33	8	✓													✓										✓																
Km 42	3	✓	✓								✓	✓			✓					✓					✓		✓														
Kodiar Mata	8	✓																							✓																
Kolayat	2	✓													✓																										
Koliya 1	1	✓											✓		✓	✓														✓											
Koliya 2	1	✓													✓														✓												
Kolwa	1	✓																							✓																
Kora	3																								✓																
Kot	8	✓							✓																																
Kot	8	✓																																							
Kotada	2							✓	✓						✓										✓																
Krakach	7	✓			✓			✓	✓		✓				✓										✓					✓											✓
Kunda	8							✓																																	
Kuroli	3			✓																																					
Kuselpur	3	✓	✓			✓		✓	✓	✓					✓					✓	✓	✓			✓		✓														
Kutiyana	1																																								
Ladai	3			✓			✓																																		

Site	Industry	Flake/Debitage	Blade	Blade parallel	Blade Flake	Blade backed	Blade crested	Retouched/Tool	Point	Borer	Burin	Awl	Denitculate	Notch	Scraper	Knife	Microlith	Geometric	Non-geometric	Lunate/Crescent	Triangle	Trapeze	Micro-Blade	Backed Blade	Core	Fluted Core	Blade Core	Levallois Core	Discoidal Core	Microlithic Core	Polyhedral Core	Heavy Tool	Handaxe	Chopper	Chopping Tool	Cleaver	Pick	Ovate			
Lakhavad	3	✓			✓										✓										✓																
Lakhond	1														✓																				✓						
Lakhond	2								✓	✓					✓																										
Lakrora	8	✓													✓										✓																
Landhi	2								✓																																
Langer	3			✓																																					
Laphni	1	✓													✓	✓																			✓						
Laphni	3								✓	✓	✓				✓					✓	✓	✓			✓																
Ler	3		✓						✓						✓										✓	✓															
Lever	3								✓	✓	✓				✓					✓	✓	✓			✓	✓															
Limbuwani	1	✓						✓							✓										✓						✓						✓				
Lordiya	7	✓																																						✓	
Lower Khaskheli Terrace	3	✓																							✓																
Luna	8							✓																																	
Luni	3	✓	✓																																						
Luni	4	✓	✓		✓				✓	✓					✓	✓									✓		✓	✓	✓										✓		
Madhavgad	8																																								
Madhogarh	3	✓									✓															✓		✓													
Madhya Pushkar A	3	✓									✓				✓										✓		✓														
Madhya Pushkar B	3	✓	✓								✓				✓										✓		✓														
Madhya Pushkar N	3	✓	✓								✓				✓										✓		✓														
Mahesha	8							✓																																	
Maheshvari Hill I	3	✓	✓												✓										✓																
Maheshvari Hill II	3														✓																										
Malipara (Rangpur)	3		✓						✓						✓										✓																
Mandor	3		✓						✓			✓			✓												✓														
Mangalpura	2	✓							✓				✓	✓	✓																										
Manpur	3	✓	✓		✓				✓	✓	✓				✓										✓																
Marwa	8							✓																																	
Marwar Bagra	1	✓																																							

Site	Industry	Flake/Debitage	Blade	Blade parallel	Blade Flake	Blade backed	Blade crested	Retouched/Tool	Point	Borer	Burin	Awl	Denitculate	Notch	Scraper	Knife	Microlith	Geometric	Non-geometric	Lunate/Crescent	Triangle	Trapeze	Micro-Blade	Backed Blade	Core	Fluted Core	Blade Core	Levallois Core	Discoidal Core	Microlithic Core	Polyhedral Core	Heavy Tool	Handaxe	Chopper	Chopping Tool	Cleaver	Pick	Ovate			
Marwar Bagra (a)	3	✓	✓								✓				✓					✓						✓															
Marwar Bagra (b)	2	✓			✓						✓				✓										✓		✓														
Mathal	2								✓	✓					✓																										
Mathawara	3	✓			✓										✓										✓																
Mekada	6	✓			✓				✓	✓		✓			✓										✓																
Milestone 101 - general	7	✓	✓						✓		✓				✓										✓		✓	✓		✓		✓		✓		✓			✓		
Milestone 101 1	3	✓	✓								✓				✓												✓		✓											✓	
Milestone 101 2a	7	✓													✓										✓		✓														
Milestone 101 2b	3	✓	✓												✓												✓														
Milestone 101 3	1																																								
Milestone 101 4	1	✓													✓												✓														
Milestone 101 5	2	✓			✓				✓						✓																										
Mitli	3	✓	✓								✓				✓		✓										✓														
Mitli	3																✓																								
Modasa	8																																							✓	
Modha	8							✓																																	
Mogra A1	1	✓													✓																										
Mogra A2	2	✓									✓	✓			✓										✓		✓														
Mogra A3	2		✓								✓				✓		✓										✓		✓												
Mogra B	3	✓							✓		✓	✓			✓											✓		✓											✓		
Mogra BN	8	✓							✓						✓											✓		✓										✓		✓	
Mogra D	6	✓							✓		✓	✓			✓											✓		✓													
Mokal	2	✓							✓						✓											✓															
Monpur	3	✓	✓			✓			✓	✓	✓				✓					✓	✓	✓			✓		✓														
Mosabar	1	✓													✓	✓																							✓		
Mosabar	1	✓																								✓															
Mudhiyari	2								✓						✓	✓												✓		✓					✓	✓					
Mulsan	3	✓									✓				✓	✓	✓								✓																
Mulsan	3		✓						✓						✓																										
Muvada	8	✓																							✓																

Site	Industry	Flake/Debitage	Blade	Blade parallel	Blade Flake	Blade backed	Blade crested	Retouched/Tool	Point	Borer	Burin	Awl	Denitculate	Notch	Scraper	Knife	Microlith	Geometric	Non-geometric	Lunate/Crescent	Triangle	Trapeze	Micro-Blade	Backed Blade	Core	Fluted Core	Blade Core	Levallois Core	Discoidal Core	Microlithic Core	Polyhedral Core	Heavy Tool	Handaxe	Chopper	Chopping Tool	Cleaver	Pick	Ovate	
N of Bahadurpur	3	✓							✓				✓		✓	✓								✓															
Nagri	6	✓				✓					✓				✓						✓				✓								✓			✓	✓		
Nagro Tikyo	3	✓	✓			✓		✓	✓	✓					✓					✓	✓	✓			✓														
Nananiyai	8							✓																															
Narvaniya	1							✓							✓	✓																		✓		✓	✓		
Narvaniya I	1	✓						✓							✓										✓						✓		✓		✓	✓		✓	
Narvaniya II	1	✓						✓							✓										✓						✓		✓		✓	✓		✓	
Narvaniya IV	1	✓						✓							✓										✓						✓		✓		✓	✓		✓	
Nawab Panjabi 1	6	✓	✓												✓										✓		✓									✓			
Nawab Panjabi 2	6	✓	✓												✓										✓		✓												
nawab Panjabi 3	6	✓	✓												✓										✓		✓							✓					
Nichadi	6	✓			✓			✓	✓			✓			✓										✓				✓										
Nigala Tappa	3														✓	✓									✓														
Nijran Faliya	1	✓						✓							✓										✓						✓		✓		✓	✓		✓	
NNW Shivad	8																								✓														
Ojat	1	✓																																					
Ongar 1	2	✓																									✓												
Ongar 10	3	✓																												✓									
Ongar 11	1	✓																																					
Ongar 2	8	✓													✓																								
Ongar 3	8	✓																																					
Ongar 4	2	✓																																					
Ongar 5	3	✓			✓						✓																												
Ongar 6	3						✓																																
Ongar 7	3																	✓																					
Ongar 8	3				✓																																		
Ongar 9	8							✓							✓																								
Opp Sadolia - R bank of Sabarmati	8	✓																																					
Pakhra Dungar	2							✓																	✓														
Palanpur	3	✓									✓				✓										✓														

Site	Industry	Flake/Debitage	Blade	Blade parallel	Blade Flake	Blade backed	Blade crested	Retouched/Tool	Point	Borer	Burin	Awl	Denitculate	Notch	Scraper	Knife	Microlith	Geometric	Non-geometric	Lunate/Crescent	Triangle	Trapeze	Micro-Blade	Backed Blade	Core	Fluted Core	Blade Core	Levallois Core	Discoidal Core	Microlithic Core	Polyhedral Core	Heavy Tool	Handaxe	Chopper	Chopping Tool	Cleaver	Pick	Ovate			
Pali	4	✓		✓																								✓													
Palsinda	3				✓		✓											✓	✓	✓	✓																				
Pani	4	✓													✓	✓																		✓		✓	✓				
Patharia	3	✓							✓																✓																
Pavagadh	3				✓																				✓																
Pavagarh Dune 1	3	✓	✓								✓				✓		✓								✓																
Pavagarh Dune 2	3	✓									✓														✓		✓														
Pavagarh Dune 3	3	✓	✓								✓						✓									✓															
Pavagarh Hill	1	✓																						✓									✓								
Pedhamli	8																																						✓		
Pedhamli	3		✓						✓						✓										✓																
Pedhamli in alluvium 30ft surface	8	✓																						✓									✓	✓		✓		✓			
Pedhamli in alluvium 40-30ft	8	✓													✓									✓										✓	✓		✓		✓		
Pedhamli in gravel	8	✓													✓									✓				✓						✓	✓		✓		✓		
Pedhamli on gravel	8	✓													✓									✓										✓	✓		✓		✓		
Pedhamli-Karoli	3		✓						✓						✓									✓																	
Pickak	2	✓	✓	✓						✓					✓	✓								✓				✓													
Pindara	1	✓																																	✓		✓				
Pipad	2	✓	✓												✓										✓																
Pipalsat	3	✓	✓		✓			✓	✓	✓					✓				✓	✓	✓			✓																	
Piperia	3	✓	✓		✓			✓	✓	✓					✓				✓	✓	✓			✓																	
Pipiya	4	✓							✓						✓										✓									✓	✓						
Pitavadi	6	✓		✓				✓	✓		✓				✓									✓				✓													
Pitvajal	6	✓		✓				✓	✓		✓				✓									✓				✓													
PN1	3	✓	✓	✓				✓									✓			✓																					
PN2	3																																								
PN3	3																						✓						✓												
Pokaran	2	✓	✓						✓	✓					✓																								✓		
Pokaran (x)	8	✓																																							
Poylikothi	1	✓					✓								✓									✓					✓			✓	✓		✓	✓			✓		

Site	Industry	Flake/Debitage	Blade	Blade parallel	Blade Flake	Blade backed	Blade crested	Retouched/Tool	Point	Borer	Burin	Awl	Denitulate	Notch	Scraper	Knife	Microlith	Geometric	Non-geometric	Lunate/Crescent	Triangle	Trapeze	Micro-Blade	Backed Blade	Core	Fluted Core	Blade Core	Levallois Core	Discoidal Core	Microlithic Core	Polyhedral Core	Heavy Tool	Handaxe	Chopper	Chopping Tool	Cleaver	Pick	Ovate		
Pushkar L	1	✓									✓				✓									✓																
Rahib Sharik & Mutton Jugoth	1	✓									✓				✓																									
Raipur	1						✓		✓						✓	✓																								
Raipur	3					✓			✓						✓					✓																				
Rajkot	8	✓	✓							✓				✓	✓										✓															
Rajpari	3								✓	✓	✓				✓					✓	✓	✓			✓															
Rajpipla	1	✓													✓										✓															✓
Rajthali	6	✓			✓				✓	✓		✓			✓										✓				✓											
Rambhau	3																									✓														
Ramji-ka-Gol	5																	✓																						
Rangpur	3								✓						✓										✓															
Ranodar	3																	✓																						
Rasla	8							✓																																
Ratadia	2				✓				✓						✓										✓															
Ratan Tekri	3								✓		✓													✓		✓														
Rata-Nadi	4	✓											✓		✓	✓													✓											
Ratanpur	4	✓							✓						✓										✓															
Raypur I	1	✓						✓							✓										✓						✓									✓
Raypur II	1	✓						✓							✓										✓						✓									✓
Raypur III	1	✓						✓							✓										✓						✓									✓
Raypur IV	1	✓						✓							✓										✓						✓									✓
Raypur IX	2								✓						✓	✓															✓									✓
Raypur V	1	✓						✓							✓										✓						✓									✓
Raypur VI	1	✓						✓							✓										✓						✓									✓
Raypur VII	4	✓						✓	✓						✓	✓									✓						✓									✓
Raypur VIII	4	✓						✓	✓						✓	✓									✓						✓									✓
Red Hill	1													✓																										
Roda	8	✓																																						
Rohri	8	✓																							✓															
Rohri (dT & P)	8	✓	✓																						✓		✓	✓												

Site	Industry	Flake/Debitage	Blade	Blade parallel	Blade Flake	Blade backed	Blade crested	Retouched/Tool	Point	Borer	Burin	Awl	Denitculate	Notch	Scraper	Knife	Microlith	Geometric	Non-geometric	Lunate/Crescent	Triangle	Trapeze	Micro-Blade	Backed Blade	Core	Fluted Core	Blade Core	Levallois Core	Discoidal Core	Microlithic Core	Polyhedral Core	Heavy Tool	Handaxe	Chopper	Chopping Tool	Cleaver	Pick	Ovate		
Rohri Hills 5-6 (A)	6	✓	✓								✓				✓											✓	✓	✓												
Rohri Hills E	3	✓	✓																							✓														
Rojadi	2	✓													✓										✓											✓				
Rojdi	2	✓							✓	✓					✓																									
Rugnathparu	6	✓			✓				✓	✓		✓			✓											✓														
Rupavati	2								✓	✓					✓											✓														
Rupnagar	1	✓																							✓									✓						
S of Chachai	3	✓													✓										✓															
S of Damnagar	3																								✓															
S of Khabarda	8																								✓															
Sabhrai	1																								✓															
Sadolia	8	✓																																						
Sagdhra	4	✓							✓						✓										✓									✓	✓					
Sam	8	✓	✓																						✓															
Samadhiala	1	✓													✓										✓										✓	✓				
Samadhiala	1	✓						✓																	✓												✓			
Sambhar Lake 1	2	✓									✓				✓										✓											✓				
Sambhar Lake 2	2	✓									✓				✓										✓															
Samdari	2	✓							✓	✓															✓															
Samdhi (A)	4	✓							✓						✓										✓															
Samdhi (B)	3								✓	✓	✓				✓					✓	✓	✓			✓															
Sanawra	8	✓													✓										✓															
Sangana Nava	2	✓							✓	✓		✓			✓																									
Sankara	8							✓																																
Santhli	3				✓			✓										✓	✓	✓	✓	✓			✓		✓													
Sanu	2	✓																																						
Sar	6	✓									✓				✓										✓		✓											✓		
Sarangpur	6								✓	✓					✓										✓															
Savitri Hill	1	✓																											✓					✓			✓			
Sejakkpur	2	✓							✓	✓					✓																									

Site	Industry	Flake/Debitage	Blade	Blade parallel	Blade Flake	Blade backed	Blade crested	Retouched/Tool	Point	Borer	Burin	Awl	Denitculate	Notch	Scraper	Knife	Microlith	Geometric	Non-geometric	Lunate/Crescent	Triangle	Trapeze	Micro-Blade	Backed Blade	Core	Fluted Core	Blade Core	Levallois Core	Discoidal Core	Microlithic Core	Polyhedral Core	Heavy Tool	Handaxe	Chopper	Chopping Tool	Cleaver	Pick	Ovate			
Sejakpur	3			✓																					✓																
Shaktari Timbo	3					✓			✓											✓										✓											
Shedravadar	6	✓			✓				✓	✓		✓			✓										✓				✓												
Shikapur	2	✓							✓																✓																
Shikarpura	2	✓			✓				✓						✓									✓		✓			✓												
Shyampura	2	✓							✓						✓									✓										✓							
Sigam Kanbi/ Songir	3		✓						✓						✓									✓																	
Silanwad	3																						✓						✓												
Singari	4	✓	✓		✓				✓	✓					✓	✓									✓			✓	✓				✓								
Singi Talav	4	✓							✓	✓	✓		✓	✓	✓											✓			✓			✓		✓	✓	✓	✓	✓	✓	✓	
Singi Talav Quarry	1	✓											✓	✓															✓			✓		✓	✓	✓	✓				
Sojat	8		✓																								✓														
Sojet	2	✓	✓		✓				✓						✓	✓									✓			✓	✓												
Sukkur	8	✓	✓						✓						✓	✓									✓								✓								
Supadia	1	✓						✓							✓										✓					✓				✓						✓	
Tadach	3	✓			✓										✓										✓																
Talia	6	✓			✓				✓	✓		✓			✓										✓					✓											
Talioghoda	3	✓	✓		✓				✓	✓	✓				✓					✓	✓	✓			✓																
Tanki	1	✓																																							
Tarsang	3	✓			✓				✓	✓	✓						✓			✓	✓	✓			✓																
Tarsang	3																✓																								
Tarsang-Rena	3	✓															✓													✓											
That	8							✓																		✓															
Thesaria	3								✓		✓								✓				✓				✓														
Thob	8	✓													✓										✓																
Thoriali	2				✓				✓		✓				✓														✓												
Thoriali	2														✓																										
Tikawada	1	✓													✓	✓																			✓			✓	✓		
Tikawada	3				✓			✓										✓	✓	✓	✓																				
Timana	3	✓			✓										✓										✓																

Site	Industry	Flake/Debitage	Blade	Blade parallel	Blade Flake	Blade backed	Blade crested	Retouched/Tool	Point	Borer	Burin	Awl	Denitculate	Notch	Scraper	Knife	Microlith	Geometric	Non-geometric	Lunate/Crescent	Triangle	Trapeze	Micro-Blade	Backed Blade	Core	Fluted Core	Blade Core	Levallois Core	Discoidal Core	Microlithic Core	Polyhedral Core	Heavy Tool	Handaxe	Chopper	Chopping Tool	Cleaver	Pick	Ovate			
Travada	4	✓		✓											✓									✓															✓		
Uchhakalam	1	✓													✓	✓																							✓		
Uchhet	1	✓													✓	✓																							✓		
Uchhet	1	✓													✓										✓																
Uchhet	4	✓							✓						✓										✓																
Udrel	3								✓						✓					✓	✓		✓							✓											
Udrel	3			✓					✓						✓					✓	✓																				
Umrethi	1																																								
Umria	3	✓													✓	✓									✓																
Una	3	✓																		✓					✓		✓														
Unnar	7	✓											✓		✓																										
Unnar Hill	4	✓													✓																										
Uparkot	1																																								
Uttam Singh-ki-Dhani	1							✓																	✓																
Valothi I	2							✓							✓	✓																									
Valothi II	1	✓						✓							✓										✓																✓
Valothi III	4	✓						✓	✓						✓	✓									✓																✓
Valothi IV	1	✓						✓							✓										✓																✓
Vankia	7	✓			✓			✓	✓			✓			✓										✓					✓											✓
Vasad	3	✓													✓						✓				✓																
Vasad	3		✓						✓						✓										✓																
Vasantgarh	1	✓													✓	✓																									
Vasantgarh	3					✓		✓											✓	✓	✓	✓																			
Velavadar	6	✓			✓			✓	✓			✓			✓										✓					✓											
Verai Mata-no-Timbo	3		✓						✓						✓																										
Veraval	8																																								
Vetalpur	3		✓						✓						✓										✓																
Vinjhan	2							✓	✓						✓										✓																
Virani	1	✓						✓																																	✓
Visadi	3	✓	✓									✓			✓										✓		✓														

Table A.3: Presence of Raw Materials in Palaeolithic sites in the Thar Desert

Site	Silicious	Chalcedony	Agate	Jasper	Chert	Flint	Quartz	Quartzite	Sandstone	Shale	Granite	Dolerite	Basalt	Rhyolite	Tachylite	Trap	Volcanic	SHR	Ochre
16R Dune							✓	✓											
25km NE Rajkot 2							✓												
47km S Nagaur					✓														
60km South Jaisalmer									✓										
6km E Pokaran														✓					
7.5 miles ENE Amreli					✓														
797bis						✓													
8km S Bikaner					✓		✓												
Achali		✓	✓		✓		✓	✓											
Akhaj					✓														
Akhaj N		✓			✓		✓												
Akhaj SE	✓	✓			✓		✓	✓											
Akkadia Mota	✓	✓	✓		✓														
Amarpura							✓	✓											
Amba		✓			✓														
Ambakut							✓	✓											
Angia												✓	✓						
Anjar					✓		✓		✓										
Anjar		✓																	
Arjunpura							✓												
Arzi Goth						✓													
Atkot													✓						
Babapur					✓														✓
Babapur		✓		✓	✓														
Badalpur												✓	✓		✓				
Bahadarpur							✓	✓											
Bahadarpur	✓	✓	✓				✓												
Bahadarpur							✓	✓								✓			
Bajawa														✓					
Bana					✓														
Bandharia Mota					✓														
Baria	✓	✓	✓		✓		✓												✓
Baridhani							✓							✓					
Bariyari							✓												
Barka				✓															
Baskario							✓	✓											
Baskario		✓	✓		✓		✓	✓											
Bavka		✓			✓														
Belaser		✓			✓		✓	✓						✓					
Benara 'C'							✓												
Bhagwanpura		✓	✓		✓		✓												
Bhajodi							✓	✓											

Site	Silicious	Chalcedony	Agate	Jasper	Chert	Flint	Quartz	Quartzite	Sandstone	Shale	Granite	Dolerite	Basalt	Rhyolite	Tachylite	Trap	Volcanic	SHR	Ochre
Bhandei				<		<													
Bhanpur								<											
Bhanpur I							✓	✓											
Bhanpur II							✓	✓											
Bhanpur III							✓	✓											
Bhanpur IV							✓	✓											
Bhanpur IX							✓	✓											
Bhanpur V							✓	✓											
Bhanpur VI							✓	✓											
Bhanpur VII							✓	✓											
Bhanpur VIII							✓	✓											
Bhavada		✓			✓		✓												
Bhawi				✓		✓													
Bhetanda				✓		✓													
Bhojka								✓											
Bhulwan		✓	✓				✓												
Bhungar		✓			✓														
Bhuvel		✓			✓		✓												
Bikaner					✓		✓												
Bilara					✓		✓												
Bodeli		✓			✓		✓	✓											
Bovadi		✓			✓														
Bridge Site						✓													
Btw Umria and Bhard					✓														
Budha Pushkar A		✓					✓	✓											
Budha Pushkar B		✓					✓	✓											
Budha Pushkar C		✓					✓	✓											
Budha Pushkar D		✓					✓	✓											
Budha Pushkar E		✓					✓	✓											
Budha Pushkar E-F		✓					✓	✓											
Budha Pushkar F		✓					✓	✓											
Budha Pushkar G		✓					✓	✓											
Bungalow Kot						✓													
Chachai			✓		✓														
Chakrora nullah, S of Umria		✓			✓														
Chamol		✓			✓														
Chancha Baluch					✓														
Chanda		✓			✓														
Charmadi Hill														✓					
Chuchhapura							✓	✓											
Dabla-ka-dhora		✓	✓		✓														
Damrala					✓														
Danasani				✓		✓													
Dandar							✓												

Site	Silicious	Chalcedony	Agate	Jasper	Chert	Flint	Quartz	Quartzite	Sandstone	Shale	Granite	Dolerite	Basalt	Rhyolite	Tachylite	Trap	Volcanic	SHR	Ochre
Dandar 2							✓	✓						✓					
Dandar 3							✓	✓						✓					
Dangarwa Rabari-na-Gochara-no-Timbo					✓		✓												
Dangarwa Venu-no-Charo		✓			✓		✓												
Daphro A						✓													
Daphro B						✓													
Datrana V				✓	✓														
Desalpur					✓			✓		✓									
Deta					✓			✓		✓									
Devalia		✓		✓	✓														
Devisar								✓	✓										
Dhaneri	✓			✓		✓													
Dharwania							✓												
Dhechu		✓			✓		✓	✓						✓					
Dhoraji				✓	✓									✓	✓				
Dhrangadhra				✓	✓				✓										
Dhrud river		✓	✓	✓	✓														
Didwana		✓			✓														
Dokariya	✓	✓	✓	✓	✓		✓	✓											
Don Dunker							✓	✓											
Duma							✓	✓											
Duma		✓	✓		✓		✓	✓											
Dundara				✓		✓											✓		
Dungervant							✓	✓											
Dunkri		✓	✓		✓		✓												
E-W (unnamed) Long Hill A						✓													
E-W (unnamed) Long Hill B						✓													
E-W (unnamed) Long Hill C						✓													
E-W (unnamed) Long Hill D						✓													
E-W (unnamed) Long Hill E						✓													
E-W (unnamed) Long Hill F						✓													
Fala			✓		✓														
Gadhara (Hirpura)	✓	✓	✓	✓	✓		✓	✓											✓
Ghuntia								✓											
Ghuntia I							✓	✓											
Ghuntia II							✓	✓											
Ghuntia III							✓	✓											
GNR1						✓													
GNR10						✓													
GNR2						✓													
GNR4						✓													
GNR7						✓													
GNR9						✓													
Golio				✓		✓													

Site	Silicious	Chalcedony	Agate	Jasper	Chert	Flint	Quartz	Quartzite	Sandstone	Shale	Granite	Dolerite	Basalt	Rhyolite	Tachylite	Trap	Volcanic	SHR	Ochre
Govindara		✓			✓		✓												
Govindhgarh				✓		✓													
Gunded		✓	✓		✓		✓												
Gundiviri							✓	✓											
Gundiviri		✓	✓		✓		✓												
Gurha 1														✓					
Gurha 2														✓					
Guttiya							✓												
Hadol							✓												
Halvad				✓	✓			✓											
Handod		✓	✓		✓		✓												
Hathipagla								✓											
Hathipagla I							✓	✓											
Hathipagla II							✓	✓											
Hathipagla III							✓	✓											
Hathipagla IV							✓	✓											
Haveli							✓	✓											
Hiran												✓	✓		✓				
Hirpura					✓														
Hokra 1A								✓											
Hokra 2A								✓											
Hokra 2B								✓											
Hundgaon				✓		✓													
Indola-ki-Dhani							✓	✓											
Itari		✓			✓		✓												
Jadan and Kanaswas		✓																	
Jalampura	✓		✓				✓	✓											
Jalampura	✓		✓		✓														
Jalor		✓			✓		✓	✓						✓					
Jawanpura		✓	✓		✓														
Jayal								✓											
Jayal								✓											
Jetpur				✓	✓									✓	✓				
Jetpur																✓			
Jhab I							✓	✓											
Jhab II							✓	✓											
Jhab III							✓	✓											
Jhab IV							✓	✓											
Jhab V							✓	✓											
Jhab VI							✓	✓											
JHP1						✓													
JHP10						✓													
JHP11						✓													
JHP12						✓													

Site	Silicious	Chalcedony	Agate	Jasper	Chert	Flint	Quartz	Quartzite	Sandstone	Shale	Granite	Dolerite	Basalt	Rhyolite	Tachylite	Trap	Volcanic	SHR	Ochre
JHP13						✓													
JHP14						✓													
JHP15						✓													
JHP16						✓													
JHP19						✓													
JHP2						✓													
JHP22						✓													
JHP23						✓													
JHP26						✓													
JHP27						✓													
JHP4						✓													
JHP5						✓													
JHP6						✓													
JHP7						✓													
JHP8						✓													
JHP9						✓													
Jira			✓		✓														
Jogpura I							✓	✓											
Jogpura II							✓	✓											
Jogpura III							✓	✓											
Jogpura IV							✓	✓											
Jogpura V							✓	✓											
Jogpura VI							✓	✓											
Jogpura VII							✓	✓											
Jojwaghode		✓	✓		✓		✓												
Jopa		✓	✓		✓		✓												
JS1						✓													
JS2						✓													
JS3						✓													
JS4						✓													
Juna				✓															
Junagadh													✓						
Juni Shedhal-Bamaniyo Timbo					✓		✓												
Kalubhar														✓					
Kamol Nava		✓			✓														
Kamord							✓												
Kaneria I (Rangpur)	✓						✓												
Kaneria II (Rangpur)					✓		✓	✓											
Kaniel			✓		✓		✓	✓											
Kankot		✓			✓														
Kanod					✓		✓												
Kapadwanj	✓				✓														
Karna I														✓					
Karna II					✓		✓							✓					

Site	Silicious	Chalcedony	Agate	Jasper	Chert	Flint	Quartz	Quartzite	Sandstone	Shale	Granite	Dolerite	Basalt	Rhyolite	Tachylite	Trap	Volcanic	SHR	Ochre
Kevada								✓											
Kevada I							✓	✓											
Kevada II							✓	✓											
Kevada III							✓	✓											
Khadeen														✓					
Khairla Hill		✓					✓												
Khairla Hill 2														✓					
Khinsvar					✓														
Khinyala		✓			✓														
Kikwada							✓	✓											
Kiyal					✓		✓												
Km 18							✓	✓											
Km 24							✓	✓											
Km 33							✓	✓											
Km 42							✓												
Kodiar Mata	✓																		
Kolayat																		✓	
Kolwa							✓	✓											
Kot					✓			✓											
Kot					✓														
Kotada		✓	✓	✓	✓														
Krakach		✓		✓	✓														
Kuselpur		✓	✓		✓		✓												
Kutiyana														✓					
Ladai		✓																	
Lakhavad		✓			✓														
Lakhond								✓	✓										
Lakhond					✓			✓		✓									
Lakrora		✓			✓		✓												
Landhi						✓													
Langer		✓		✓	✓														
Laphni							✓	✓											
Laphni		✓	✓		✓		✓												
Ler		✓																	
Lever		✓	✓		✓		✓												
Limbuwani							✓	✓											
Lordiya					✓				✓										
Lower Khaskheli Terrace						✓													
Luni				✓	✓												✓		
Madhavgad							✓												
Madhogarh		✓					✓												
Madhya Pushkar A		✓					✓	✓											
Madhya Pushkar B							✓	✓											
Madhya Pushkar N		✓					✓	✓											

Site	Silicious	Chalcedony	Agate	Jasper	Chert	Flint	Quartz	Quartzite	Sandstone	Shale	Granite	Dolerite	Basalt	Rhyolite	Tachylite	Trap	Volcanic	SHR	Ochre
Malipara (Rangpur)		✓			✓		✓	✓											
Mandor		✓	✓	✓	✓														
Manpur		✓	✓		✓		✓												
Marwar Bagra														✓					
Marwar Bagra (b)														✓					
Mathal					✓			✓		✓									
Mathawara		✓			✓														
Mekada		✓			✓														
Milestone 101 - general					✓														
Milestone 101 1					✓														
Milestone 101 2a					✓														
Milestone 101 2b					✓														
Milestone 101 3					✓														
Milestone 101 4					✓														
Milestone 101 5					✓														
Mitli		✓					✓												
Modasa								✓											
Mogra A1														✓					
Mogra A2					✓									✓					
Mogra A3					✓														
Mogra BN					✓														
Mogra D					✓									✓					
Mokal								✓											
Monpur		✓	✓		✓		✓												
Mosabar							✓	✓											
Mosabar							✓	✓											
Mudhiyari							✓	✓											
Mulsan	✓	✓	✓		✓		✓												
Mulsan			✓		✓		✓	✓											
N of Bahadurpur		✓	✓	✓	✓														
Nagri					✓		✓							✓					
Nagro Tikyo		✓	✓		✓		✓												
Nand		✓			✓		✓	✓						✓					
Narvaniya								✓											
Narvaniya I							✓	✓											
Narvaniya II							✓	✓											
Narvaniya III							✓	✓											
Narvaniya IV							✓	✓											
Nawab Panjabi 1					✓														
Nawab Panjabi 2					✓														
nawab Panjabi 3					✓														
Nelya		✓			✓		✓	✓						✓					
Nichadi		✓			✓														
Nigala Tappa		✓			✓														

Site	Silicious	Chalcedony	Agate	Jasper	Chert	Flint	Quartz	Quartzite	Sandstone	Shale	Granite	Dolerite	Basalt	Rhyolite	Tachylite	Trap	Volcanic	SHR	Ochre
Nijran Faliya							<	<											
NNW Shivad					✓														
nr Nakhtarana					✓				✓										
Ojat														✓					
Ongar 1						✓													
Ongar 10						✓													
Ongar 11						✓													
Ongar 2						✓													
Ongar 3						✓													
Ongar 4						✓													
Ongar 5						✓													
Ongar 6						✓													
Ongar 7						✓													
Ongar 8						✓													
Ongar 9						✓													
Opp Sadolia - R bank of Sabarmati									✓										
Pachpadra Lake		✓			✓		✓	✓						✓					
Palanpur							✓												
Pali				✓		✓													
Pavagarh Dune 1			✓				✓			✓				✓					
Pavagarh Dune 2			✓				✓			✓				✓					
Pavagarh Dune 3			✓				✓			✓				✓					
Pavagarh Hill																		✓	
Pedhamli								✓											
Pedhamli	✓	✓			✓		✓	✓											
Pedhamli in alluvium 30ft surface								✓											
Pedhamli in alluvium 40-30ft								✓											
Pedhamli in gravel								✓											
Pedhamli on gravel								✓											
Pedhamli-Karoli	✓	✓		✓	✓		✓	✓											
Pickak				✓		✓													
Pipad				✓		✓													
Pipalsat		✓	✓		✓		✓												
Piperia		✓	✓		✓		✓												
Pipiya							✓	✓											
Pitavadi		✓			✓														
Pitvajal		✓			✓														
PN1						✓													
Poylikothi							✓	✓											
Pushkar L								✓											
Rahib Sharik & Mutton Jugoth						✓													
Raipur								✓											
Raipur							✓												
Rajpari		✓	✓		✓		✓												

Site	Silicious	Chalcedony	Agate	Jasper	Chert	Flint	Quartz	Quartzite	Sandstone	Shale	Granite	Dolerite	Basalt	Rhyolite	Tachylite	Trap	Volcanic	SHR	Ochre
Rajthali		✓			✓														
Ramji-ka-Gol														✓					
Rangpur					✓		✓												
Ranodar					✓														
Rata Nadi								✓											
Ratadia			✓	✓	✓			✓											
Ratanpur							✓	✓											
Raypur I							✓	✓											
Raypur II							✓	✓											
Raypur III							✓	✓											
Raypur IV							✓	✓											
Raypur IX							✓	✓											
Raypur V							✓	✓											
Raypur VI							✓	✓											
Raypur VII							✓	✓											
Raypur VIII							✓	✓											
Red Hill						✓													
Rohri						✓													
Rohri (dT & P)						✓													
Rohri Hills (generic)					✓														
Rohri Hills 5-6 (A)					✓														
Rohri Hills E					✓														
Rojadi					✓														
Rojdi			✓		✓														
Rugnathparu		✓			✓														
Rupavati																✓			
Rupnagar								✓											
S of Chachai		✓	✓		✓														✓
S of Damnagar			✓		✓														
S of Khabarda	✓																		
Sagdhra							✓	✓											
Salt Dak Bungalow							✓	✓											
Sam					✓		✓		✓										
Sambhar Lake 1							✓												
Sambhar Lake 2							✓												
Samdari				✓		✓												✓	
Samdhi (A)							✓	✓											
Samdhi (B)		✓	✓		✓		✓												
Sangana Nava		✓																	
Santhli		✓	✓	✓	✓		✓												
Sanu							✓												
Sar			✓		✓		✓		✓		✓			✓					
Sarangpur																	✓		
Sasan Gir		✓			✓							✓	✓			✓			

Site	Silicious	Chalcedony	Agate	Jasper	Chert	Flint	Quartz	Quartzite	Sandstone	Shale	Granite	Dolerite	Basalt	Rhyolite	Tachylite	Trap	Volcanic	SHR	Ochre
Savitri Hill								<											
Sejampur			✓		✓														
Shaktari Timbo		✓	✓	✓	✓														
Shedravadar		✓			✓														
Shikarpura				✓		✓													
Sigam Kanbi/ Songir		✓	✓				✓												
Singari				✓		✓											✓		
Singi Talav							✓	✓											
Singi Talav Quarry								<											
Sojat				✓	✓	✓													
Sojet				✓		✓													
Sokarna		✓			✓		✓	✓						✓					
Sukkur						✓													
Supadia							✓	<											
Tadach		✓			✓														
Talia		✓			✓														
Talioghoda		✓	✓		✓		✓												
Tanki						✓													
Tarsang		✓	✓	✓	✓		✓												
Thob														✓					
Thoriali		✓	✓																
Timana		✓			✓														
Travada				✓	✓														
Uchhakalam							✓	✓											
Uchhet							✓	✓											
Uchhet							✓	<											
Uchhet							✓	✓											
Udrel		✓			✓		✓												
Udrel		✓	✓	✓	✓		✓												
Umednagar				✓															
Umrasan	✓																		
Umrethi		✓			✓							✓	✓				✓		
Umria	✓	✓	✓		✓		✓												
Unnar						✓													
Unnar Hill						✓													
Uparkot													✓						
Valothi I							✓	✓											
Valothi II							✓	<											
Valothi III							✓	✓											
Valothi IV							✓	<											
Vankia		✓		✓	✓														
Vasad		✓			✓		✓												
Vasad		✓	✓		✓		✓	✓											
Velavadar		✓			✓														

Site	Silicious	Chalcedony	Agate	Jasper	Chert	Flint	Quartz	Quartzite	Sandstone	Shale	Granite	Dolerite	Basalt	Rhyolite	Tachylite	Trap	Volcanic	SHR	Ochre
	Verai Mata-no-Timbo		✓		✓	✓													
Vetalpur							✓												
Vinjhan		✓	✓	✓	✓														
Visadi							✓												
Visangadh							✓	✓											
W of Desar	✓		✓		✓														
Wadeli							✓	✓											
Wadeli		✓					✓	✓											
Wadu Kodivalo Timbo		✓			✓		✓	✓											
Yaksha					✓		✓			✓									

Table A.4: Artefact sizes from Palaeolithic sites in the Thar Desert

Site	Industry	Type	Jasper	Trap	Lava	Silicified Wood	Agate	Rhyolite	Chert	Flint	Quartz	Quartzite	Chalcedony	Length (mm)	Width (mm)	Thickness (mm)	# of Artefacts
Arjunpura	Late Palaeolithic	Scraper									✓			34	22	30	1
Arjunpura	Late Palaeolithic	Flake Core									✓			40	35	16.5	2
Arjunpura	Late Palaeolithic	Burin									✓			26.9	19.6	5.2	15
Bajawa	Lower Palaeolithic	Handaxe						✓						127.5	74.9	25.5	1
Budha Pushkar A	Late Palaeolithic	Flake Core									✓			21	19.7	16.5	3
Budha Pushkar A	Late Palaeolithic	Blade									✓			15.5	7.2		4
Budha Pushkar B	Late Palaeolithic	Flake Core										✓		39	29	25.3	3
Budha Pushkar C	Late Palaeolithic	Burin									✓			18.3	14.3	6.5	3
Budha Pushkar D	Late Palaeolithic	Flake Core										✓		55	47	14	1
Budha Pushkar E	Late Palaeolithic	Scraper										✓		43	26	25	1
Budha Pushkar E	Late Palaeolithic	Scraper									✓			32.5	34	13.5	2
Budha Pushkar E-F	Late Palaeolithic	Scraper									✓			24	37	13	1
Budha Pushkar E-F	Late Palaeolithic	Scraper										✓		39	26	24	1
Budha Pushkar E-F	Late Palaeolithic	Burin										✓		37	30	7	1
Budha Pushkar E-F	Late Palaeolithic	Flake Core										✓		86.3	91.3	53	3
Budha Pushkar E-F	Late Palaeolithic	Blade core										✓		38	20.5	18.5	3
Budha Pushkar F	Late Palaeolithic	Flake Core										✓		95	102	55	1
Budha Pushkar F	Late Palaeolithic	Blade									✓			17	9		2
Budha Pushkar F	Late Palaeolithic	Burin									✓			28	20	6.5	2
Budha Pushkar F	Late Palaeolithic	Blade Core										✓		39.5	35	29.5	3
Budha Pushkar F	Late Palaeolithic	Scraper										✓		35.3	31.7	17	3
Budha Pushkar G	Late Palaeolithic	Flake Core										✓		50.8	41.6	29	6
Chamardi	Late Palaeolithic	Blade core						✓						25	16	14	1
Danasani	Middle Palaeolithic	Scraper							✓					114	59	31	1
Dandar	Late Palaeolithic	Blade									✓			23	13	6	1
Dandar	Late Palaeolithic	Scraper									✓			21.7	13.7	10	3
Dandar	Late Palaeolithic	Flakes									✓			19.4	13.4	9.2	5
Dandar	Late Palaeolithic	Flake Cores									✓			21.6	18.6	10.1	8

Site	Industry	Type	Jasper	Trap	Lava	Silicified Wood	Agate	Rhyolite	Chert	Flint	Quartz	Quartzite	Chalcedony	Length (mm)	Width (mm)	Thickness (mm)	# of Artefacts
Dandar	Late Palaeolithic	Burin									✓			19.8	15.7	7.3	13
Dandar	Late Palaeolithic	Blade cores									✓			18.2	16.5	9.5	21
Dhaneri	Middle Palaeolithic	Scraper				✓								48	45	11	1
Dhaneri	Middle Palaeolithic	Scraper				✓								63	53	12	1
Dhaneri	Middle Palaeolithic	Handaxe							✓					107	56	28	1
Dhaneri	Middle Palaeolithic	Scraper							✓					93	60	46	1
Dhaneri	Middle Palaeolithic	Scraper							✓					34	31	7	1
Dhaneri	Middle Palaeolithic	Borer							✓					92	95	16	1
Dhaneri	Middle Palaeolithic	Point							✓					77	55	16	1
Dhaneri	Middle Palaeolithic	Point							✓					38	31	50	1
Dhaneri	Middle Palaeolithic	Blade							✓					40	18	6	1
Dhaneri	Middle Palaeolithic	Flake							✓					88	75	22	1
Dhaneri	Middle Palaeolithic	Flake							✓					43	32	9	1
Dundara	Middle Palaeolithic	Point			✓									91	47	20	1
Golio	Middle Palaeolithic	Point							✓					90	47	20	1
Golio	Middle Palaeolithic	Point							✓					77	55	35	1
Govindhgarh	Late Palaeolithic	Cleaver										✓		117	79	28	1
Govindhgarh	Late Palaeolithic	Cleaver										✓		85	54	21	1
Govindhgarh	Late Palaeolithic	Chopper										✓		125	97	60	1
Govindhgarh	Late Palaeolithic	Scraper										✓		110	78	30	1
Gurha	Middle Palaeolithic	Cleaver						✓						128.7	73.7	42	3
Gurha	Middle Palaeolithic	Handaxe						✓						121.2	79.3	49	3
Gurha	Middle Palaeolithic	Point						✓						88.9	59.2	20.2	5
Gurha	Middle Palaeolithic	Flake Core						✓						77.1	73.6	47.2	9
Gurha	Middle Palaeolithic	Flakes						✓						62	58.6	18.7	24
Hiran Valley	Lower Palaeolithic	Handaxe		✓										180	110	60	1
Hiran Valley	Lower Palaeolithic	Handaxe		✓										135	74	62	1
Hiran Valley	Lower Palaeolithic	Handaxe		✓										150	55	40	1
Hiran Valley	Lower Palaeolithic	Handaxe		✓										130	70	42	1

Site	Industry	Type	Jasper	Trap	Lava	Silicified Wood	Agate	Rhyolite	Chert	Flint	Quartz	Quartzite	Chalcedony	Length (mm)	Width (mm)	Thickness (mm)	# of Artefacts
Hiran Valley	Lower Palaeolithic	Handaxe		✓										140	80	33	1
Hiran Valley	Lower Palaeolithic	Handaxe		✓										147	90	60	1
Hiran Valley	Lower Palaeolithic	Handaxe		✓										200	135	80	1
Hiran Valley	Lower Palaeolithic	Handaxe		✓										132	110	70	1
Hiran Valley	Lower Palaeolithic	Handaxe		✓										130	90	53	1
Hiran Valley	Lower Palaeolithic	Handaxe		✓										140	90	82	1
Hiran Valley	Lower Palaeolithic	Cleaver		✓										137	90	40	1
Hiran Valley	Lower Palaeolithic	Cleaver		✓										130	90	35	1
Hiran Valley	Lower Palaeolithic	Cleaver		✓										125	70	50	1
Hiran Valley	Lower Palaeolithic	Cleaver		✓										145	90	55	1
Hiran Valley	Lower Palaeolithic	Chopper		✓										126	80	66	1
Hiran Valley	Middle Palaeolithic	Scraper	✓											72	72	28	1
Hiran Valley	Middle Palaeolithic	Point	✓											42	36	6	1
Hiran Valley	Middle Palaeolithic	Discoidal core	✓											82	73	46	1
Hiran Valley	Middle Palaeolithic	Scraper		✓										52	50	19	1
Hiran Valley	Middle Palaeolithic	Scraper		✓										46	36	14	1
Hiran Valley	Middle Palaeolithic	Scraper		✓										95	65	30	1
Hiran Valley	Middle Palaeolithic	Scraper		✓										85	50	25	1
Hiran Valley	Middle Palaeolithic	Scraper		✓										46	26	15	1
Hiran Valley	Middle Palaeolithic	Scraper		✓										35	32	8	1
Hiran Valley	Middle Palaeolithic	Scraper		✓										68	21	16	1
Hiran Valley	Middle Palaeolithic	Scraper		✓										58	46	17	1
Hiran Valley	Middle Palaeolithic	Scraper		✓										58	55	16	1
Hiran Valley	Middle Palaeolithic	Borer		✓										49	41	16	1
Hiran Valley	Middle Palaeolithic	Notch		✓										52	29	13	1
Hiran Valley	Middle Palaeolithic	Scraper							✓					48	47	14	1
Hiran Valley	Middle Palaeolithic	Scraper							✓					47	40	12	1
Hiran Valley	Middle Palaeolithic	Scraper							✓					57	53	15	1
Hiran Valley	Middle Palaeolithic	Scraper							✓					40	22	6	1
Hiran Valley	Middle Palaeolithic	Scraper							✓					73	52	12	1

Site	Industry	Type	Jasper	Trap	Lava	Silicified Wood	Agate	Rhyolite	Chert	Flint	Quartz	Quartzite	Chalcedony	Length (mm)	Width (mm)	Thickness (mm)	# of Artefacts
Hiran Valley	Middle Palaeolithic	Scraper							✓					51	36	14	1
Hiran Valley	Middle Palaeolithic	Scraper							✓					102	75	39	1
Hokra 1A	Middle Palaeolithic	Discoidal Core										✓		66	52.3	35.8	4
Hokra 1A	Middle Palaeolithic	Scrapers										✓		61.8	58	29.3	4
Hokra 1A	Middle Palaeolithic	Cleaver										✓		62.8	56	19.5	4
Hokra 1A	Middle Palaeolithic	Burin										✓		58.1	34.4	12.8	5
Hokra 1A	Middle Palaeolithic	Chopper/ing										✓		88.6	80.4	34.2	5
Hokra 1A	Middle Palaeolithic	Point										✓		63.7	56.7	16.3	6
Hokra 1A	Middle Palaeolithic	Scrapers										✓		52.7	37.8	21.8	6
Hokra 1A	Middle Palaeolithic	Flake Core										✓		72.1	91.9	53.7	9
Hokra 1A	Middle Palaeolithic	Scrapers										✓		47.6	49	14.5	13
Hokra 2B	Lower Palaeolithic	Handaxe										✓		186	94	65	1
Hokra 2B	Lower Palaeolithic	Cleaver										✓		104	77	46	1
Hokra 2B	Lower Palaeolithic	Flakes										✓		95	80	41	3
Hokra 2B	Middle Palaeolithic	Discoidal Core										✓		121.5	98.5	56.5	2
Hundgaon	Middle Palaeolithic	Scraper							✓					82	60	46	1
Hundgaon	Middle Palaeolithic	Scraper							✓					63	57	12	1
Hundgaon	Middle Palaeolithic	Borer							✓					57	35	15	1
Hundgaon	Middle Palaeolithic	Flake							✓					40	34	7	1
Hundgaon	Middle Palaeolithic	Prepared Core							✓					124	119	44	1
JHP 1	Late Palaeolithic	Microblade Core							✓					40	26	17	1
JHP 1	Late Palaeolithic	Microblade Core							✓					41	23	16	1
JHP 1	Late Palaeolithic	Microblade Core							✓					32	26	17	1
JHP 1	Late Palaeolithic	Microblade Core							✓					34	23	16	1
JHP 1	Late Palaeolithic	Microblade Core							✓					33	22	16	1
JHP 1	Late Palaeolithic	Microblade Core							✓					32	24	16	1
JHP 1	Late Palaeolithic	Microblade Core							✓					48	30	40	1
JHP 1	Late Palaeolithic	Microlith Core							✓					38	39	28	1
JHP 1	Late Palaeolithic	Backed Point							✓					30	13	7	1
JHP 1	Late Palaeolithic	Lunate							✓					22.5	7	2	1

Site	Industry	Type	Jasper	Trap	Lava	Silicified Wood	Agate	Rhyolite	Chert	Flint	Quartz	Quartzite	Chalcedony	Length (mm)	Width (mm)	Thickness (mm)	# of Artefacts
JHP 1	Late Palaeolithic	Backed Bladelet							✓					26	33	4	1
JHP 10	Late Palaeolithic	Microblade Core							✓					33	14	13	1
JHP 10	Late Palaeolithic	Notch							✓					32	17	6	1
JHP 11	Late Palaeolithic	Scraper							✓					18	24	90	1
JHP 11	Late Palaeolithic	Backed Microlith							✓					12	18	4.5	1
JHP 11	Late Palaeolithic	Backed Microlith							✓					16	10	4	1
JHP 11	Late Palaeolithic	Backed Microlith							✓					18	14	40	1
JHP 12	Late Palaeolithic	Microblade Core							✓					33	36	30	1
JHP 12	Late Palaeolithic	Microblade Core							✓					22	30	17	1
JHP 12	Late Palaeolithic	Microlith Core							✓					20	35	33	1
JHP 12	Late Palaeolithic	Backed Microlith							✓					16	12	4	1
JHP 12	Late Palaeolithic	Backed Microlith							✓					24	20	8	1
JHP 13	Late Palaeolithic	Microblade Core							✓					31	24	17	1
JHP 13	Late Palaeolithic	Microblade Core							✓					23	23	12	1
JHP 13	Late Palaeolithic	Microblade Core							✓					30	23	18	1
JHP 13	Late Palaeolithic	Backed Microlith							✓					24	15	8	1
JHP 14	Late Palaeolithic	Microlith Core							✓					46	51	28	1
JHP 15	Late Palaeolithic	Microblade Core							✓					67	53	27	1
JHP 2	Late Palaeolithic	Microlith Core							✓					26	37	22	1
JHP 22	Late Palaeolithic	Microblade Core							✓					27	22	21	1
JHP 22	Late Palaeolithic	Microlith Core							✓					36	50	28	1
JHP 22	Late Palaeolithic	Microlith Core							✓					26	39	37	1
JHP 26	Late Palaeolithic	Microlith Core							✓					22	47	24	1
JHP 26	Late Palaeolithic	Scraper							✓					31	29	9	1
JHP 27	Late Palaeolithic	Microblade Core							✓					25	14	8	1
JHP 7	Late Palaeolithic	Microlithic Core							✓					62	54	50	1
JHP 7	Late Palaeolithic	Microlithic Core							✓					43	55	35	1
JHP 7	Late Palaeolithic	Microblade Core							✓					37	32	23	1
JHP 7	Late Palaeolithic	Microlith Core							✓					38	31	25	1
JHP 7	Late Palaeolithic	Microlith Core							✓					24	26	19	1

Site	Industry	Type	Jasper	Trap	Lava	Silicified Wood	Agate	Rhyolite	Chert	Flint	Quartz	Quartzite	Chalcedony	Length (mm)	Width (mm)	Thickness (mm)	# of Artefacts
JHP 7	Late Palaeolithic	Lunate							✓					23	8	2.5	1
JHP 8	Late Palaeolithic	Microblade Core							✓					40	25	19	1
JHP 9	Late Palaeolithic	Microblade Core							✓					47	20	16	1
JHP 9	Late Palaeolithic	Microlith Core							✓					31	30	19	1
JHP 9	Late Palaeolithic	Microlith Core							✓					33	33	25	1
JHP 9	Late Palaeolithic	Lunate							✓					25	6	2	1
Kambolaj	Late Palaeolithic	Burin												23	21	9	1
Kambolaj	Late Palaeolithic	Blade core												22	15.3	9	3
Kamord	Late Palaeolithic	Burin									✓			22	19	7	14
Kamord	Late Palaeolithic	Blade core												20.5	19.5	17.5	15
Khairla Hill	Late Palaeolithic	Scraper											✓	25.3	17.8	8.2	26
KM 42	Late Palaeolithic	Lunate									✓			17	6	4	1
KM 42	Late Palaeolithic	Chopper/ing									✓			30.7	31.5	22.7	4
KM 42	Late Palaeolithic	Blade core									✓			35.6	19.4	13.5	11
KM 42	Late Palaeolithic	Flake Core									✓			33.9	20.8	10.9	16
KM 42	Late Palaeolithic	Scraper									✓			23.5	19.6	7.1	22
KM 42	Late Palaeolithic	Burin									✓			24.3	15.9	84	25
Lordiya	Lower Palaeolithic	Ovate												115	75	30	1
Luni	Middle Palaeolithic	Scraper			✓									77	54	13	1
Luni	Middle Palaeolithic	Scraper			✓									76	39	20	1
Luni	Middle Palaeolithic	Knife			✓									78	68	23	1
Luni	Middle Palaeolithic	Flake			✓									117	83	36	1
Luni	Middle Palaeolithic	Cleaver					✓							107	78	22	1
Luni	Middle Palaeolithic	Blade					✓							98	45	18	1
Luni	Middle Palaeolithic	Flake Core					✓							122	85	78	1
Luni	Middle Palaeolithic	Cleaver						✓						100	75	35	1
Luni	Middle Palaeolithic	Handaxe							✓					115	70	35	1
Luni	Middle Palaeolithic	Scraper							✓					81	41	38	1
Luni	Middle Palaeolithic	Scraper							✓					59	64	25	1
Luni	Middle Palaeolithic	Scraper							✓					59	44	12	1

Site	Industry	Type	Jasper	Trap	Lava	Silicified Wood	Agate	Rhyolite	Chert	Flint	Quartz	Quartzite	Chalcedony	Length (mm)	Width (mm)	Thickness (mm)	# of Artefacts
Luni	Middle Palaeolithic	Scraper							✓					45	38	10	1
Luni	Middle Palaeolithic	Scraper							✓					124	38	28	1
Luni	Middle Palaeolithic	Borer							✓					79	58	18	1
Luni	Middle Palaeolithic	Point							✓					62	44	19	1
Luni	Middle Palaeolithic	knife							✓					101	48	31	1
Luni	Middle Palaeolithic	knife							✓					73	44	22	1
Luni	Middle Palaeolithic	Blade							✓					54	29	14	1
Luni	Middle Palaeolithic	Flake							✓					89	66	18	1
Luni	Middle Palaeolithic	Flake							✓					68	42	11	1
Luni	Middle Palaeolithic	Flake							✓					44	42	13	1
Luni	Middle Palaeolithic	Handaxe								✓				82	65	26	1
Luni	Middle Palaeolithic	Blade core								✓				48	42	24	1
Luni	Middle Palaeolithic	Scraper										✓		81	52	32	1
Luni	Middle Palaeolithic	Point										✓		59	26	14	1
Madhya Pushkar A	Late Palaeolithic	Flake Core										✓		58	45	22	2
Madhya Pushkar A	Late Palaeolithic	Blade core										✓		36.2	32.6	24.8	5
Madhya Pushkar N	Late Palaeolithic	Scraper									✓			31	21	10	1
Madhya Pushkar N	Late Palaeolithic	Flake Core										✓		35	29	21	1
Madhya Pushkar N	Late Palaeolithic	Scraper									✓			28.3	19	16	3
Marwar Bagra	Lower Palaeolithic	Handaxe						✓						164	102	60	1
Marwar Bagra	Lower Palaeolithic	Cleaver						✓						139	80.5	49	2
Marwar Bagra	Lower Palaeolithic	Flakes						✓						135.5	95.2	42.6	8
Milestone 101 1	Late Palaeolithic	Scraper							✓					42	40	19	1
Milestone 101 1	Late Palaeolithic	Scraper							✓					45	37	29	1
Milestone 101 1	Late Palaeolithic	Burin							✓					48	32	10	1
Milestone 101 1	Late Palaeolithic	Chopper/ing							✓					85	44	27	1
Milestone 101 1	Late Palaeolithic	Cleaver							✓					116	66	19	1
Milestone 101 1	Late Palaeolithic	Handaxe							✓					78	55	21	1
Milestone 101 1	Late Palaeolithic	Scraper							✓					49	24	14	2
Milestone 101 1	Late Palaeolithic	Blade core							✓					57	42	25.5	4

Site	Industry	Type	Jasper	Trap	Lava	Silicified Wood	Agate	Rhyolite	Chert	Flint	Quartz	Quartzite	Chalcedony	Length (mm)	Width (mm)	Thickness (mm)	# of Artefacts
Milestone 101 1	Late Palaeolithic	Blade							✓					45	19.7		6
Milestone 101 1	Late Palaeolithic	Scraper							✓					58.9	43.9		19
Milestone 101 1	Late Palaeolithic	Flake							✓					58.4	39.3		32
Milestone 101 2b	Late Palaeolithic	Blade core							✓					74.5	51.5	40	2
Milestone 101 2b	Late Palaeolithic	Scraper							✓					69.7	75		3
Milestone 101 2b	Late Palaeolithic	Chopper/ing							✓					124.3	67	31.3	3
Milestone 101 2b	Late Palaeolithic	Blade							✓					66.5	21.5		4
Milestone 101 2b	Late Palaeolithic	Flake							✓					75.8	41.6		42
Milestone 101 3	Lower Palaeolithic	Handaxe							✓					120	55	35	1
Milestone 101 3	Lower Palaeolithic	Cleavers							✓					126	88.5	39.5	2
Milestone 101 4	Lower Palaeolithic	Blade core							✓					69	62	47	1
Milestone 101 4	Lower Palaeolithic	Flake							✓					105	90		2
Milestone 101 4	Lower Palaeolithic	Chopper/ing							✓					133	88.5	47	2
Milestone 101 4	Lower Palaeolithic	Scraper							✓					110.7	81.7	30.7	3
Milestone 101 4	Lower Palaeolithic	Handaxe							✓					123.8	70.2	38	5
Milestone 101 5	Middle Palaeolithic	Points							✓					80	62	14	2
Milestone 101 5	Middle Palaeolithic	Scrapers							✓					70.8	44.8		5
Milestone 101 5	Middle Palaeolithic	Blade-Flakes							✓					69	29		6
Milestone 101 5	Middle Palaeolithic	Flakes							✓					65.4	51.3		7
Mitli	Late Palaeolithic	Scraper											✓	19	22	5	1
Mitli	Late Palaeolithic	Burin											✓	20	9.5	5	2
Mitli	Late Palaeolithic	Blade core											✓	18.8	14.2	9.4	5
Mitli	Late Palaeolithic	Microlith											✓	14.9	6.6	2.2	18
Ojat	Lower Palaeolithic	Flake Core						✓						158	181.7		5
Ojat	Lower Palaeolithic	Flake						✓						134.8	96.5		6
Pali	Middle Palaeolithic	Discoidal Core									✓			84	74	25	1
Pavagarh Dune 2	Late Palaeolithic	Flake Core									✓			25	25	14	1
Pickak	Middle Palaeolithic	Blade							✓					47	20	7	1
Pipad	Middle Palaeolithic	Scraper							✓					76	60	33	1
Pipad	Middle Palaeolithic	Flake							✓					33	31	7	1

Site	Industry	Type	Jasper	Trap	Lava	Silicified Wood	Agate	Rhyolite	Chert	Flint	Quartz	Quartzite	Chalcedony	Length (mm)	Width (mm)	Thickness (mm)	# of Artefacts
Rodjadi	Middle Palaeolithic	Flake Core							✓					78	68.5	41.5	2
Rodjadi	Middle Palaeolithic	Scrapers							✓					49.5	36	20	2
Rodjadi	Middle Palaeolithic	Chopper/ing							✓					67.7	45	31	4
Rodjadi	Middle Palaeolithic	Scrapers							✓					62	45.8	18.3	6
Rodjadi	Middle Palaeolithic	Scrapers							✓					49.8	41.5	11.8	6
Rodjadi	Middle Palaeolithic	Scrapers							✓					54.3	39.6	20.7	14
Rohri Hills E	Late Palaeolithic	Blade core							✓					57.3	65	52	2
Rohri Hills E	Late Palaeolithic	Blades							✓					81.5	30		5
Samdari	Middle Palaeolithic	Point			✓									105	47	25	1
Savitri Hill	Lower Palaeolithic	Chopper/ing										✓		87	74.2	41.5	2
Savitri Hill	Lower Palaeolithic	Handaxe										✓		125.5	82.5	49	3
Savitri Hill	Lower Palaeolithic	Flakes										✓		93.3	75	17.3	5
Shirkapura	Middle Palaeolithic	Scraper					✓							49	31	15	1
Singari	Middle Palaeolithic	Borer			✓									84	43	16	1
Singari	Middle Palaeolithic	Knife			✓									87	53	20	1
Singari	Middle Palaeolithic	Borer							✓					42	43	7	1
Sojet	Middle Palaeolithic	Point							✓					60	42	12	1
Sojet	Middle Palaeolithic	Discoidal core							✓					98	91	73	1
Sojet	Middle Palaeolithic	Flake-Blade								✓				76	35	13	1
Visadi	Late Palaeolithic	Chopper/ing									✓			59	50.5	41.5	2
Visadi	Late Palaeolithic	Flake Core									✓			38.8	32	17.1	6
Visadi	Late Palaeolithic	Scraper									✓			36.6	25.4	16.5	8
Visadi	Late Palaeolithic	polyhedral core									✓			33.7	28.2	23.2	12
Visadi	Late Palaeolithic	Scraper									✓			31.9	28.3	24.2	16
Visadi	Late Palaeolithic	Blade core									✓			38.1	34.9	25	39
Visadi	Late Palaeolithic	Burin									✓			28.2	20.7	9.5	43
ZPS 1 E4	Lower Palaeolithic	Handaxe								✓				201	102	49	1
ZPS 1 E4	Lower Palaeolithic	Handaxe								✓				189	103	43	1
ZPS 1 E4	Lower Palaeolithic	Handaxe								✓				210	123	74	1
ZPS 1 E4	Lower Palaeolithic	Handaxe								✓				183	113	70	1

Site	Industry	Type	Jasper	Trap	Lava	Silicified Wood	Agate	Rhyolite	Chert	Flint	Quartz	Quartzite	Chalcedony	Length (mm)	Width (mm)	Thickness (mm)	# of Artefacts
ZPS 1 E4	Lower Palaeolithic	Handaxe								✓				176	83	40	1
ZPS 1 E4	Lower Palaeolithic	Handaxe								✓				169	107	56	1
ZPS 1 E4	Lower Palaeolithic	Handaxe								✓				213	111	60	1
ZPS 1 E4	Lower Palaeolithic	Handaxe								✓				175	117	52	1
ZPS 1 E4	Lower Palaeolithic	Handaxe								✓				129	76	40	1
ZPS 1 E4	Lower Palaeolithic	Handaxe								✓				156	85	80	1
ZPS 1 E4	Lower Palaeolithic	Handaxe								✓				105	75	53	1
ZPS 1 E4	Lower Palaeolithic	Handaxe								✓				223	106	95	1
ZPS 1 E4	Lower Palaeolithic	Handaxe								✓				214	109	80	1
ZPS 1 E4	Lower Palaeolithic	Handaxe								✓				125	70	38	1

Table A.5: Assemblage artefact type composition in Palaeolithic sites in the Thar Desert

Site	Flake/Debitage	Blade	Blade Flake	Blade backed	Blade crested	Retouched/tool	Point	Borer	Burin	Awl	Denitculate	Notch	Scraper	Knife	Microlith	Lunate/Crescent	Triangle	Backed micro-blade	Core	Blade Core	Levallois Core	Discoidal Core	Microlithic Core	Polyhedral Core	Heavy Tool	Handaxe	Chopper	Chopping Tool	Cleaver	Pick	Ovate	
16R Inf	32	5										2	5						2			1		1		2	4					
16R Sup	319	10					1	8	3		8	6	24						21			1		1		7	13	15				
797bis	315																															
Arjunpura	88	11							15				1						2													
Babapur	30							5			9		9	1					19												2	
Baridhani	20									6			11						13	1												
Barria	27	1					1				1		4	1					26								1					
Benara A & B	27	5							2						3				4	7												
Bhavnagar	128	15					4	18	1			13	208	1					8							4	10					
Bikaner		32		3												2	7															
Budha Pushkar A	55	4							3						7				3	8												
Budha Pushkar B	81						2		4				11		1				3	13												
Budha Pushkar C	149	11					2		3				2		4					19												
Budha Pushkar D	80	10					3		7				2						1	12							1					
Budha Pushkar E	74	5					10		7	2	2		3		2					5												
Budha Pushkar F	35	1							2				3		3				1	3												
Budha Pushkar G	156	9					2		7				8		3				6	21												
Chachai	5												2						44													
Chancha Baluch	103	33					3		1				14						40	16										2		
Chhajoli						41																										
Dandar	32	1							13				10						8	21												
Dhaneri	34	6	1				7	3					19	3					1			2				4			2			
Dokariya		16					1			1			29						7													
Gadhara (Hirpura)		67					4						81						16													
Gadhara II (Hirpura)		18					7						16						9													
Hokra 1A	57						6		5				19						9			4						5	4			
Indola ki Dhani	249							1				2		1									7					5				

Site	Flake/Debitage	Blade	Blade Flake	Blade backed	Blade crested	Retouched/tool	Point	Borer	Burin	Awl	Denitculate	Notch	Scraper	Knife	Microlith	Lunate/Crescent	Triangle	Backed micro-blade	Core	Blade Core	Levallois Core	Discoidal Core	Microlithic Core	Polyhedral Core	Heavy Tool	Handaxe	Chopper	Chopping Tool	Cleaver	Pick	Ovate		
Indola ki Dhani	411							7						7	2										3		2	6	3				
Itari	49	6							5				2		2					3		8											
Jayal	265										6	4	44	8					109						11		3	2					
Jetpur	62					1							2						3														
Jhir A & B	35	3							10				1		6				3	1													
JHP1	52				6	6	1									2		2		10			2										
JHP11	31				1								1					3															
JHP12	18														2					2			1										
JHP13	60				2										1					3													
JHP7	37				2											1				1			4										
Kamord	136	2							14						3					15													
Khairla Hill	146	13							44				32						12	58													
Km 42	48	1							25	1			22			1			16	11							4						
Luni	108	8	4				11	2					45	7					12	5	3	1			8				5				
Madhya Pushkar A	45								5				3		1				2	5													
Madhya Pushkar B	41	2							3				3						2	1							1						
Madhya Pushkar N	56	2							6				4						1	5													
Marwar Bagra (b)	32		2						1				1						8	1													
Milestone 101 - general	135	23					2		1				47						1	19	8	7		5		34		13	8		2		
Milestone 101 1	32	6							1				23							4					1	1		1					
Milestone 101 2a	28												12						1	7	2		4		6		5	3					
Milestone 101 2b	42	4											3							2							3						
Mitli	78	10											1		18					10													
Mogra A2	39								4	1			8						10	2													
Mogra B	44						2		7	1			14						8	5									1				
Mogra BN	33						8						11						2	1								2	1				
Mogra D	22						2		1	1			15						9	9					1			2					
N of Bahadurpur	81						1				3		5	3	1				30														
Nagri	55			1					6				14				1		11	5						3		2	1				

Site	Flake/Debitage	Blade	Blade Flake	Blade backed	Blade crested	Retouched/tool	Point	Borer	Burin	Awl	Denitculate	Notch	Scraper	Knife	Microlith	Lunate/Crescent	Triangle	Backed micro-blade	Core	Blade Core	Levallois Core	Discoidal Core	Microlithic Core	Polyhedral Core	Heavy Tool	Handaxe	Chopper	Chopping Tool	Cleaver	Pick	Ovate
Nawab Panjabi 1	291	3											3						2	4									1		
Nawab Panjabi 2	216	48											2						7	7											
nawab Panjabi 3	49	4											1						5	40					1			2			
Nimka Thana A & B	57	1				5		12					4		5				3	7											
Palanpur	34								3				5			1															
Pavagarh Dune 1	113	5							25				2		4				16												
Pavagarh Dune 3	70	5							8						3					7											
Pedhamli in alluvium 30ft surface	28																		4							8	4		3		6
Rajkot	70	3						4				1	102						5												
Rajpipla	80												73						16							52	21		32	16	
Rata-nadi	193										23		124	34								27				25	16	11	2		
Rohri Hills 5-6 (A)	59	1							1				2							1	2	2		2					1		
Rohri Hills E	14	5																		2											
Rojadi	19												28						2									4			
S of Chachai	6												2						58												
Samadhiala	68												49						15							33	17		24	16	
Shikarpura	44		1				6						6						2	1		3									
Singi Talav (Couche 3)	167						5	3				3	14						8			1		6		4	4	6			
Singi Talav (Couche 4)	357						5	7	5		3	9	32						3			3		5		20	5	6	3	1	
Singi Talav (Couche 5)	61						1		1			1	2																		
Umria	15												7	2					27												
Visadi	158	2							43				24						6	39			12				2				
ZPS 1 Sq E4	811												2						27							18					
ZPS 1 Sq E6-E7	398												2							26											
ZPS 2	1071	626	1143		3														35												
ZPS4					12														10	132											16

Appendix B: Surface Survey Sites

Site	Length						Width					
	N	Mean	S.D.	S.E.	Min	Max	N	Mean	S.D.	S.E.	Min	Max
BPG1	5	69.08	20.04	8.96	38.67	92.88	5	47.56	16.13	7.21	26.94	71.90
BPG2	10	55.85	20.39	6.45	35.18	98.84	10	36.65	14.02	4.43	18.57	64.59
BPH1	7	84.24	36.54	13.81	27.49	145.66	7	53.61	18.07	6.83	25.90	86.34
BPH2	7	54.22	18.65	7.05	24.66	76.40	7	42.35	15.25	5.76	20.89	60.47
CHA2	3	100.11	33.94	19.60	76.17	138.95	3	81.97	40.45	23.35	51.25	127.80
DAN2	10	92.41	14.38	4.55	60.37	109.35	10	64.53	17.76	5.62	29.70	87.41
HOKA	17	84.84	24.20	5.87	35.65	124.88	17	60.84	17.40	4.22	24.89	86.95
HOKB	6	55.47	20.65	8.43	26.05	81.16	6	37.38	13.61	5.56	19.26	59.57
HOKC	11	72.52	17.35	5.23	45.66	95.42	11	49.74	9.07	2.73	34.43	60.43
HOKD	8	70.55	17.20	6.08	50.33	96.92	8	49.72	13.59	4.81	33.37	69.63
HOKE	4	61.79	9.50	4.75	49.72	72.75	4	40.66	11.18	5.59	27.85	54.84
HOKF	63	52.64	10.85	1.37	15.99	74.71	63	38.21	9.00	1.13	17.31	68.61
KAR1	1	85.28			85.28	85.28	1	45.43			45.43	45.43
KAR2	6	95.66	13.44	5.49	72.79	109.22	6	71.98	13.02	5.32	60.55	95.80
KAR3	1	145.78			145.78	145.78	1	93.79			93.79	93.79
KHA1	14	85.70	13.10	3.50	62.15	111.17	14	57.76	13.11	3.50	43.07	93.80
KHA2	7	73.93	21.14	7.99	47.72	109.00	7	52.56	12.40	4.69	39.97	77.46
KHA3	4	61.38	47.22	23.61	10.53	117.67	4	69.71	30.43	15.21	30.52	104.78
SAM1	6	48.85	16.50	6.74	28.53	71.93	6	42.81	12.71	5.19	25.25	56.61
SHR1	6	77.29	29.69	12.12	41.30	114.09	6	59.77	24.02	9.80	36.36	97.24
SMB1	8	70.06	49.44	17.48	45.72	190.00	8	56.51	46.97	16.61	26.46	170.00
SMB3	2	108.47	21.71	15.35	93.12	123.82	2	72.94	36.36	25.71	47.23	98.65
SMB4	2	76.20	60.44	42.74	33.46	118.93	2	56.05	46.08	32.58	23.47	88.63
SMB5	3	102.04	14.88	8.59	91.05	118.97	3	64.68	7.34	4.24	56.38	70.33
SMB6	2	49.26	1.92	1.36	47.90	50.62	2	35.81	4.12	2.91	32.90	38.72
TRI1	23	58.63	13.34	2.78	37.18	96.80	23	43.78	10.33	2.15	27.53	65.59
TRI2	13	71.18	12.72	3.53	55.85	94.15	13	48.52	7.69	2.13	32.00	58.82

Table B.1: Descriptive statistics of core length and width from surface survey sites.

Site	Thickness						Axial Length					
	N	Mean	S.D.	S.E.	Min	Max	N	Mean	S.D.	S.E.	Min	Max
BPG1	5	33.14	12.90	5.77	14.82	45.76	4	44.68	6.35	3.17	36.48	51.84
BPG2	10	19.45	10.63	3.36	7.26	40.15	10	32.75	10.13	3.20	18.81	49.91
BPH1	7	33.66	12.71	4.80	17.04	55.45	7	43.96	18.65	7.05	22.21	70.17
BPH2	7	26.13	10.36	3.91	11.73	41.22	7	28.99	11.13	4.21	13.40	43.33
CHA2	3	21.82	6.49	3.75	17.19	29.24	3	59.67	17.79	10.27	47.00	80.00
DAN2	10	27.05	6.37	2.01	17.08	35.13	10	23.11	11.33	3.58	12.55	51.31
HOKA	17	38.70	13.92	3.38	14.90	71.30	17	51.23	16.45	3.99	21.86	72.95
HOKB	6	23.32	12.57	5.13	6.20	36.57	6	32.98	17.46	7.13	10.14	53.77
HOKC	11	24.27	6.20	1.87	15.96	35.74	11	37.51	9.13	2.75	22.20	52.51
HOKD	8	31.53	11.44	4.04	15.13	47.87	8	36.60	7.63	2.70	22.17	44.49
HOKE	4	23.48	2.23	1.12	21.41	26.65	4	28.32	10.03	5.01	21.41	43.16
HOKF	63	22.70	6.59	0.83	10.63	38.44	62	37.05	11.48	1.46	11.93	64.27
KAR1	1	29.07			29.07	29.07	1	40.10			40.10	40.10
KAR2	6	31.92	13.33	5.44	17.77	48.48	6	51.63	21.43	8.75	24.82	79.18
KAR3	1	41.67			41.67	41.67	1	49.06			49.06	49.06
KHA1	14	34.24	9.60	2.57	20.33	58.97	14	42.19	15.16	4.05	19.79	66.93
KHA2	7	28.43	15.72	5.94	15.78	60.43	7	47.15	15.34	5.80	31.02	72.84
KHA3	4	28.11	10.50	5.25	18.01	37.48	4	57.50	22.04	11.02	34.61	78.35
SAM1	6	29.61	10.98	4.48	19.16	49.38	6	29.32	10.61	4.33	13.47	44.29
SHR1	6	24.88	11.70	4.78	12.10	40.21	6	44.27	19.18	7.83	25.25	80.89
SMB1	8	24.57	14.61	5.17	10.65	50.00	5	36.53	13.70	6.13	24.36	60.00
SMB3	2	40.72	14.08	9.96	30.76	50.67	2	57.87	23.99	16.97	40.90	74.83
SMB4	2	27.76	14.06	9.94	17.82	37.70	2	53.96	43.90	31.05	22.91	85.00
SMB5	3	45.94	13.68	7.90	30.45	56.40	2	52.16	19.03	13.46	38.70	65.61
SMB6	2	22.23	4.62	3.27	18.96	25.49	2	30.20	2.26	1.60	28.60	31.79
TRI1	23	22.51	6.56	1.37	9.89	34.72	23	38.28	17.61	3.67	19.30	96.80
TRI2	13	27.88	6.94	1.93	15.46	38.10	13	42.02	13.26	3.68	29.25	72.57

Table B.2: Descriptive statistics of core thickness and axial length from surface survey sites.

Axial Width							Platform Width					
	N	Mean	S.D.	S.E.	Min	Max	N	Mean	S.D.	S.E.	Min	Max
BPG1	4	36.23	14.68	7.34	20.46	54.23	4	34.46	13.57	6.78	22.17	50.18
BPG2	10	33.00	12.11	3.83	13.00	51.50	10	36.56	14.03	4.44	16.04	56.72
BPH1	7	35.60	17.89	6.76	6.95	57.60	7	45.92	26.57	10.04	11.20	91.74
BPH2	7	25.31	9.24	3.49	11.22	36.46	7	30.49	14.83	5.60	13.71	60.42
CHA2	3	41.33	11.02	6.36	34.00	54.00	3	62.74	33.14	19.13	43.21	101.00
DAN2	10	34.95	12.92	4.08	15.67	57.40	9	40.08	12.75	4.25	23.32	62.03
HOKA	17	40.47	12.71	3.08	18.85	64.44	17	38.79	10.92	2.65	16.37	52.30
HOKB	6	22.10	6.89	2.81	12.65	32.55	6	22.33	5.84	2.38	15.54	29.51
HOKC	11	38.64	13.82	4.17	19.48	68.90	11	41.95	14.05	4.24	26.06	66.63
HOKD	8	32.64	7.61	2.69	22.11	45.10	8	40.46	15.14	5.35	14.59	69.19
HOKE	4	26.56	13.52	6.76	13.56	44.99	4	37.50	17.72	8.86	19.83	59.90
HOKF	62	24.48	10.90	1.38	8.03	53.39	63	34.72	11.79	1.48	11.04	62.56
KAR1	1	37.22			37.22	37.22	1	27.77			27.77	27.77
KAR2	6	36.42	12.47	5.09	25.09	59.76	6	30.28	7.97	3.26	20.10	41.19
KAR3	1	28.48			28.48	28.48	1	32.07			32.07	32.07
KHA1	14	37.75	13.05	3.49	9.62	58.71	14	40.03	14.99	4.01	13.70	68.44
KHA2	7	44.01	10.29	3.89	29.03	56.84	7	41.60	11.41	4.31	28.08	57.88
KHA3	4	47.95	19.71	9.85	18.86	61.85	4	45.88	29.49	14.74	15.58	82.73
SAM1	6	18.72	8.48	3.46	9.93	32.68	0					
SHR1	6	29.48	12.46	5.09	16.93	52.11	6	56.53	34.50	14.09	19.52	108.17
SMB1	5	37.16	30.37	13.58	14.53	90.00	0					
SMB3	2	39.26	14.86	10.51	28.75	49.77	2	81.59	59.73	42.24	39.35	123.82
SMB4	2	46.48	19.12	13.52	32.96	60.00	2	54.14	33.74	23.86	30.28	78.00
SMB5	2	44.13	7.67	5.43	38.70	49.55	2	69.57	37.52	26.53	43.04	96.10
SMB6	2	38.06	8.44	5.97	32.09	44.03	2	31.97	12.03	8.51	23.46	40.47
TRI1	23	30.08	13.34	2.78	11.65	60.96	23	23.85	10.35	2.16	7.64	45.09
TRI2	13	32.62	12.33	3.42	15.24	60.14	12	31.76	9.96	2.88	17.54	46.71

Table B.3: Descriptive statistics of core axial width and platform width from surface survey sites.

	Maximum Surface Area						Axial Elongation					
	N	Mean	S.D.	S.E.	Min	Max	N	Mean	S.D.	S.E.	Min	Max
BPG1	5	3462.61	1732.79	774.93	1041.77	5546.37	4	1.43	0.66	0.33	0.67	2.16
BPG2	10	2221.93	1534.60	485.28	653.29	5157.51	10	1.17	0.86	0.27	0.63	3.54
BPH1	7	5061.53	3724.64	1407.78	711.99	12576.28	7	1.55	0.85	0.32	0.57	3.20
BPH2	7	2528.33	1457.80	550.99	515.15	4276.11	7	1.18	0.38	0.14	0.84	1.91
CHA2	3	9072.60	7530.39	4347.67	4366.50	17757.81	3	1.56	0.75	0.43	0.87	2.35
DAN2	10	6108.64	2159.36	682.85	1792.99	9200.71	10	0.72	0.38	0.12	0.35	1.66
HOKA	17	5454.53	2558.75	620.59	887.33	9646.95	17	1.31	0.37	0.09	0.66	2.07
HOKB	6	2247.30	1380.81	563.71	501.72	4422.48	6	1.50	0.70	0.29	0.61	2.42
HOKC	11	3708.58	1323.34	399.00	1572.07	5230.82	11	1.04	0.29	0.09	0.56	1.45
HOKD	8	3662.77	1671.42	590.94	1776.62	5710.36	8	1.14	0.21	0.07	0.83	1.39
HOKE	4	2467.98	603.98	301.99	2026.09	3337.56	4	1.15	0.30	0.15	0.93	1.58
HOKF	63	2056.81	781.75	98.49	304.93	4713.51	62	1.91	1.25	0.16	0.28	6.59
KAR1	1	3874.27			3874.27	3874.27	1	1.08			1.08	1.08
KAR2	6	6968.77	2040.33	832.96	4783.76	10463.28	6	1.42	0.44	0.18	0.87	2.09
KAR3	1	13672.71			13672.71	13672.71	1	1.72			1.72	1.72
KHA1	14	5028.19	1824.70	487.67	3251.07	10427.75	14	1.20	0.43	0.11	0.65	2.06
KHA2	7	4094.86	2170.34	820.31	1940.14	8443.14	7	1.10	0.35	0.13	0.80	1.70
KHA3	4	4971.29	5384.45	2692.22	768.37	12329.46	4	1.30	0.43	0.21	0.80	1.84
SAM1	6	2262.49	1313.04	536.05	720.38	4071.96	6	1.70	0.66	0.27	0.98	2.73
SHR1	6	5186.80	3918.96	1599.91	1501.67	10911.30	5	1.42	0.11	0.05	1.25	1.55
SMB1	8	5972.45	10686.99	3778.42	1374.86	32300.00	0					
SMB3	2	8306.45	5527.30	3908.39	4398.06	12214.84	2	1.71	1.26	0.89	0.82	2.60
SMB4	2	5663.04	6898.15	4877.73	785.31	10540.77	2	1.01	0.45	0.32	0.70	1.33
SMB5	3	6532.52	348.40	201.15	6131.31	6758.71	2	1.16	0.23	0.16	1.00	1.32
SMB6	2	1767.96	271.60	192.05	1575.91	1960.01	2	0.81	0.12	0.08	0.72	0.89
TRI1	23	2636.72	1033.38	215.48	1187.53	4695.85	23	1.42	0.71	0.15	0.69	3.89
TRI2	13	3498.71	985.79	273.41	1816.32	5272.40	13	1.48	0.90	0.25	0.76	4.25

Table B.4: Descriptive statistics of core maximum surface area and axial elongation from surface survey sites.

Site	Unspecified	Cortical	Crushed	Dihedral	Faceted	Hammer and Anvil	Multiple Conchoidal	Plain	Punctiform	Single Conchoidal	Total
BPG1	1	3	1	0	0	0	0	0	0	0	5
BPG2	0	4	1	1	3	0	0	0	0	1	10
BPH1	0	4	0	0	0	0	0	2	0	1	7
BPH2	0	1	0	0	1	0	0	1	0	4	7
CHA2	0	0	0	0	1	0	0	2	0	0	3
DAN2	0	1	0	0	2	0	0	3	0	4	10
HOKA	0	5	1	1	0	0	0	4	0	6	17
HOKB	0	3	0	0	0	0	0	2	0	1	6
HOKC	0	2	0	2	0	0	2	2	0	3	11
HOKD	0	2	0	1	0	0	1	3	0	1	8
HOKE	0	1	0	0	0	0	0	2	0	1	4
HOKF	0	14	1	5	4	1	7	15	1	15	63
KAR1	0	0	0	0	0	0	0	1	0	0	1
KAR2	0	1	1	2	1	0	0	0	0	1	6
KAR3	0	0	0	1	0	0	0	0	0	0	1
KHA1	0	1	0	1	4	0	2	2	0	4	14
KHA2	0	0	0	2	0	0	2	0	0	3	7
KHA3	0	1	0	0	0	1	2	0	0	0	4
SAM1	0	1	0	0	0	0	0	3	0	2	6
SHR1	0	0	0	1	3	0	1	0	0	1	6
SMB1	5	0	0	0	3	0	0	0	0	0	8
SMB3	0	1	0	0	0	0	0	0	0	1	2
SMB4	0	0	0	0	0	0	0	1	0	1	2
SMB5	0	0	0	0	1	0	0	0	0	2	3
SMB6	0	0	0	0	0	0	2	0	0	0	2
TRI1	0	1	0	5	5	0	3	6	0	3	23
TRI2	0	0	0	2	6	0	0	3	0	2	13

Table B.5: Count of platform types in surface survey sites

Site	None	Axial	Feather	Hinge	Step	Total
BPG1	1	0	4	0	0	5
BPG2	0	2	7	1	0	10
BPH1	0	1	5	0	1	7
BPH2	0	2	5	0	0	7
CHA2	0	0	2	1	0	3
DAN2	0	3	4	0	3	10
HOKA	0	5	12	0	0	17
HOKB	0	2	3	1	0	6
HOKC	0	3	8	0	0	11
HOKD	0	0	8	0	0	8
HOKE	0	0	4	0	0	4
HOKF	2	4	55	0	2	63
KAR1	0	1	0	0	0	1
KAR2	0	2	4	0	0	6
KAR3	0	0	1	0	0	1
KHA1	0	4	7	1	2	14
KHA2	0	2	5	0	0	7
KHA3	1	2	1	0	0	4
SAM1	0	0	5	0	1	6
SHR1	0	1	4	1	0	6
SMB1	8	0	0	0	0	8
SMB3	2	0	0	0	0	2
SMB4	0	0	1	0	1	2
SMB5	1	0	2	0	0	3
SMB6	0	0	2	0	0	2
TRI1	0	6	15	0	2	23
TRI2	0	3	9	0	1	13
Total	15	43	173	5	13	249

Table B.6: Count of last scar termination types in surface survey sites.

	Length						Width					
	N	Mean	S.D.	S.E.	Min	Max	N	Mean	S.D.	S.E.	Min	Max
BPG1	12	45.43	15.73	4.54	19.44	74.91	12	23.72	7.37	2.13	15.02	37.34
BPG2	7	47.53	13.10	4.95	28.41	63.94	7	27.72	11.38	4.30	8.71	43.66
BPH1	9	63.80	30.95	10.32	42.77	136.56	9	41.09	25.04	8.35	24.46	95.78
BPH2	11	43.69	30.44	9.18	19.27	118.94	11	32.32	27.24	8.21	8.57	102.23
CHA1	20	62.48	24.21	5.41	25.05	133.18	20	42.51	18.45	4.13	17.52	74.99
CHA2	30	77.33	20.29	3.70	38.56	110.09	30	53.33	20.44	3.73	21.63	102.73
DAN1	21	78.14	22.78	4.97	44.08	138.56	21	52.09	23.19	5.06	20.12	116.01
DAN2	15	67.45	41.02	10.59	31.18	162.20	15	45.26	28.30	7.31	13.91	108.06
HOKA	5	74.19	19.02	8.51	54.60	100.51	5	50.40	11.28	5.04	42.54	70.21
HOKB	13	49.50	12.90	3.58	30.97	71.60	13	36.26	13.09	3.63	15.53	57.88
HOKC	11	57.84	18.13	5.47	34.56	86.87	11	37.81	8.83	2.66	25.30	50.15
HOKD	4	57.16	15.05	7.52	35.07	67.71	4	36.38	9.88	4.94	26.10	49.75
HOKE	13	49.97	16.42	4.55	24.00	79.94	13	38.35	13.94	3.87	20.09	67.56
HOKF	34	52.05	9.50	1.63	33.01	68.81	34	35.74	7.56	1.30	24.42	54.89
KAR1	4	52.06	13.04	6.52	40.35	67.56	4	38.44	7.49	3.75	33.04	49.48
KAR2	8	104.66	46.41	16.41	46.44	199.00	8	70.06	30.69	10.85	28.24	114.02
KAR3	16	71.73	33.82	8.45	38.81	177.00	16	45.41	20.86	5.22	22.78	104.49
KHA1	7	66.81	18.01	6.81	44.30	86.41	7	44.68	10.19	3.85	32.53	61.25
KHA2	10	61.71	20.16	6.38	43.49	100.69	10	41.92	10.15	3.21	27.66	62.13
KHA3	14	79.66	19.43	5.19	51.24	116.45	14	56.16	16.28	4.35	35.43	80.99
SAM1	30	47.29	13.64	2.49	29.93	83.38	30	33.05	9.92	1.81	17.77	54.99
SHR1	27	64.47	25.26	4.86	32.62	137.14	27	46.03	17.49	3.37	24.26	87.30
SMB1	3	123.27	27.57	15.92	99.51	153.50	3	71.68	13.79	7.96	56.13	82.44
SMB2	7	63.01	26.66	10.08	26.18	109.90	7	42.98	18.08	6.83	18.08	77.90
SMB3	7	65.16	30.29	11.45	33.76	117.96	7	39.05	25.35	9.58	10.90	81.52
SMB4	8	62.47	19.34	6.84	45.32	92.64	8	38.37	10.38	3.67	27.57	54.51
SMB5	10	113.98	43.68	13.81	61.63	200.00	10	74.02	19.62	6.20	46.86	105.98
SMB6	15	44.88	9.20	2.37	32.35	62.51	15	30.04	6.35	1.64	15.77	41.11
TRI1	15	61.86	10.54	2.72	39.08	78.27	15	43.08	8.63	2.23	33.07	60.60
TRI2	5	59.83	21.19	9.48	44.22	96.18	5	37.73	8.20	3.67	27.34	47.84
Total	391	63.46	27.34	1.38	19.27	200.00	391	42.82	19.36	0.98	8.57	116.01

Table B.7: Descriptive statistics of flake length and width from surface survey sites.

	Thickness						Maximum Surface Area					
	N	Mean	S.D.	S.E.	Min	Max	N	Mean	S.D.	S.E.	Min	Max
BPG1	12	10.93	5.18	1.49	3.27	18.58	12	1154.35	695.32	200.72	309.10	2431.58
BPG2	7	15.16	6.55	2.47	4.90	24.66	7	1435.79	893.87	337.85	247.45	2791.62
BPH1	9	12.85	6.76	2.25	7.95	29.75	9	3282.40	4029.55	1343.18	1093.85	13079.72
BPH2	11	14.80	14.74	4.44	3.75	53.68	11	2158.21	3573.05	1077.32	165.14	12159.24
CHA1	20	17.19	7.19	1.61	7.68	39.28	20	3003.36	2352.32	525.99	438.88	9987.17
CHA2	30	17.97	6.99	1.28	8.31	34.58	30	4439.13	2536.73	463.14	1193.99	10952.05
DAN1	21	17.71	7.87	1.72	7.83	33.46	21	4496.63	3432.38	749.01	1020.49	16074.35
DAN2	15	19.40	11.73	3.03	5.51	43.94	15	4030.29	4835.15	1248.43	433.71	17527.33
HOKA	5	16.76	6.25	2.80	9.50	23.93	5	3887.55	1896.59	848.18	2322.68	7056.81
HOKB	13	15.93	4.97	1.38	7.63	22.45	13	1914.45	1112.19	308.46	598.84	3739.67
HOKC	11	15.36	5.16	1.55	8.03	24.01	11	2310.02	1168.59	352.34	886.46	4356.53
HOKD	4	15.40	6.86	3.43	5.59	21.62	4	2139.06	878.00	439.00	915.33	3002.41
HOKE	13	12.54	4.09	1.13	5.48	20.55	13	2110.00	1493.02	414.09	482.16	5400.75
HOKF	34	16.39	4.59	0.79	7.50	24.79	34	1885.16	598.89	102.71	1016.38	3330.78
KAR1	4	17.91	6.93	3.46	11.12	24.21	4	2023.92	716.40	358.20	1333.16	2873.80
KAR2	8	23.50	12.70	4.49	7.45	45.63	8	8371.15	6829.32	2414.53	1672.77	22689.98
KAR3	16	17.55	13.47	3.37	4.40	60.84	16	3837.32	4256.20	1064.05	1163.14	18494.73
KHA1	7	23.74	10.53	3.98	12.54	42.50	7	3027.76	1194.73	451.56	1604.06	5021.89
KHA2	10	13.65	4.42	1.40	7.20	20.65	10	2683.46	1300.67	411.31	1308.87	4754.81
KHA3	14	19.40	6.07	1.62	6.83	28.03	14	4735.86	2467.02	659.34	2177.70	9431.29
SAM1	30	14.23	4.72	0.86	7.59	29.48	30	1665.48	962.09	175.65	585.34	4125.90
SHR1	27	18.03	12.60	2.43	7.93	73.50	27	3367.67	2712.69	522.06	828.83	11972.32
SMB1	3	34.79	7.54	4.35	26.08	39.17	3	9057.50	3536.18	2041.61	5585.50	12654.54
SMB2	7	17.77	7.33	2.77	5.51	29.77	7	3078.60	2582.55	976.11	473.33	8561.21
SMB3	7	15.54	8.91	3.37	5.20	26.37	7	3166.98	3292.98	1244.63	367.98	9616.10
SMB4	8	17.90	8.68	3.07	9.70	34.78	8	2547.61	1441.13	509.52	1249.47	4996.08
SMB5	10	30.08	11.23	3.55	12.69	44.50	10	8921.33	5105.15	1614.39	2887.98	19486.00
SMB6	15	15.08	4.33	1.12	8.48	22.91	15	1376.42	489.35	126.35	591.22	2083.46
TRI1	15	17.07	6.23	1.61	9.31	32.03	15	2708.75	881.65	227.64	1330.28	4363.20
TRI2	5	15.62	2.08	0.93	13.11	17.50	5	2331.47	1290.37	577.07	1503.04	4601.25
Total	391	17.07	8.61	0.44	3.27	73.50	391	3171.95	3054.56	154.48	165.14	22689.98

Table B.7: Descriptive statistics of thickness and maximum surface area from surface survey sites.

	Axial Width						Axial Length					
	N	Mean	S.D.	S.E.	Min	Max	N	Mean	S.D.	S. E.	Min	Max
BPG1	12	32.89	16.62	4.80	12.10	74.91	12	30.02	14.33	4.14	15.05	59.63
BPG2	7	32.13	13.03	4.93	8.71	46.78	7	33.09	12.47	4.71	19.48	53.58
BPH1	9	49.96	22.29	7.43	23.21	94.94	9	42.32	26.22	8.74	21.76	96.99
BPH2	10	37.63	30.71	9.71	12.88	116.48	10	39.87	27.20	8.60	8.57	98.07
CHA1	16	56.39	25.99	6.50	31.95	131.86	16	39.08	14.92	3.73	20.56	70.08
CHA2	21	65.46	19.39	4.23	35.67	109.33	21	55.89	18.78	4.10	17.85	77.32
DAN1	21	61.28	21.34	4.66	13.10	113.06	21	51.18	21.88	4.77	19.82	109.29
DAN2	15	54.38	42.10	10.87	20.44	162.20	15	46.17	25.94	6.70	14.25	108.06
HOKA	5	55.54	13.68	6.12	42.00	70.05	5	55.16	22.78	10.19	32.78	92.80
HOKB	13	34.04	12.46	3.46	15.59	58.76	13	39.99	12.62	3.50	23.04	62.25
HOKC	11	45.88	17.90	5.40	25.65	83.75	11	40.03	9.63	2.90	26.50	62.77
HOKD	4	45.14	13.80	6.90	24.45	52.24	4	35.41	8.76	4.38	26.77	47.61
HOKE	13	40.58	15.66	4.34	20.09	69.74	13	39.50	15.53	4.31	24.00	73.81
HOKF	34	39.00	10.48	1.80	13.80	65.12	34	39.11	12.87	2.21	17.66	68.81
KAR1	4	36.42	6.95	3.48	27.73	44.34	4	36.74	4.66	2.33	31.70	42.97
KAR2	8	83.67	30.34	10.73	27.55	134.33	8	68.48	36.08	12.76	26.77	139.83
KAR3	16	52.39	19.78	4.94	26.41	100.49	16	46.92	24.16	6.04	19.11	116.77
KHA1	7	47.59	11.42	4.32	37.79	64.53	7	43.83	13.96	5.28	28.82	63.16
KHA2	10	48.23	13.92	4.40	38.14	83.08	10	51.28	17.63	5.58	32.55	81.38
KHA3	14	63.27	20.22	5.40	35.43	103.64	14	57.38	14.43	3.86	36.58	80.20
SAM1	30	35.97	13.88	2.53	19.53	69.98	30	34.74	12.56	2.29	11.11	73.38
SHR1	27	49.52	19.23	3.70	23.91	97.70	27	50.72	20.98	4.04	22.95	125.86
SMB1	0	0
SMB2	3	71.56	19.17	11.07	55.22	92.66	3	49.56	19.65	11.35	32.96	71.26
SMB3	4	58.44	25.99	12.99	32.91	93.37	4	38.70	24.32	12.16	18.28	70.72
SMB4	4	59.72	17.43	8.72	41.12	76.78	4	42.51	15.08	7.54	29.39	60.18
SMB5	7	109.23	58.92	22.27	44.93	200.00	7	68.28	17.63	6.66	50.25	97.43
SMB6	10	33.61	10.10	3.19	21.29	56.11	10	34.86	10.14	3.21	21.42	58.64
TRI1	15	44.39	13.38	3.45	23.36	69.66	15	49.77	14.38	3.71	25.96	78.27
TRI2	5	38.62	7.93	3.55	27.34	47.84	5	58.21	22.91	10.25	36.15	96.18
Total	355	49.30	24.83	1.32	8.71	200.00	355	45.00	19.78	1.05	8.57	139.83

Table B.9: Descriptive statistics of flake axial length and axial width from surface survey sites.

	Platform Thickness						Platform Width					
	N	Mean	S.D.	S.E.	Min	Max	N	Mean	S.D.	S.E.	Min	Max
BPG1	12	8.44	4.94	1.43	1.11	18.07	12	27.55	19.32	5.58	7.91	73.31
BPG2	7	11.04	8.06	3.05	1.87	23.40	7	28.76	16.29	6.16	6.34	49.12
BPH1	9	11.74	8.41	2.80	3.56	32.78	9	46.16	21.12	7.04	30.81	97.12
BPH2	11	12.23	12.06	3.64	2.67	44.12	11	26.86	26.35	7.94	6.67	93.44
CHA1	20	15.20	8.48	1.90	6.17	45.96	19	46.32	26.35	6.05	15.68	127.18
CHA2	30	16.36	6.19	1.13	4.57	33.50	30	50.16	17.14	3.13	13.88	90.65
DAN1	21	15.24	9.07	1.98	2.22	38.68	21	55.02	20.03	4.37	22.29	106.94
DAN2	15	13.86	10.34	2.67	2.09	32.15	15	45.50	30.26	7.81	11.55	126.61
HOKA	5	11.58	4.17	1.86	6.65	17.31	5	35.67	10.06	4.50	27.03	49.15
HOKB	13	12.27	5.42	1.50	5.11	21.69	13	32.63	14.69	4.07	12.96	62.95
HOKC	11	13.66	4.65	1.40	6.83	20.85	11	42.23	18.43	5.56	24.91	84.46
HOKD	4	14.44	8.28	4.14	2.88	22.43	4	45.33	24.97	12.48	12.99	65.53
HOKE	13	10.08	4.26	1.18	3.99	17.26	13	27.06	14.51	4.02	8.22	61.51
HOKF	34	11.75	4.64	0.80	3.04	20.62	34	34.35	11.29	1.94	13.10	67.71
KAR1	4	13.65	6.20	3.10	8.92	22.67	4	43.05	17.19	8.59	30.67	67.56
KAR2	6	20.60	9.23	3.77	9.69	33.67	7	64.11	35.10	13.27	13.06	120.20
KAR3	15	15.51	17.07	4.41	4.79	70.43	15	48.51	23.00	5.94	26.63	101.38
KHA1	7	22.40	12.51	4.73	5.60	38.94	7	40.52	14.53	5.49	21.30	65.51
KHA2	10	9.52	6.18	1.95	4.26	21.94	10	34.23	20.52	6.49	13.45	80.26
KHA3	14	14.77	5.44	1.45	8.01	25.01	14	55.80	18.58	4.97	34.62	95.92
SAM1	30	11.19	4.28	0.78	4.16	23.23	30	31.74	11.43	2.09	12.38	57.38
SHR1	27	11.77	7.26	1.40	2.07	29.72	27	40.47	18.30	3.52	13.79	85.23
SMB1	0						0					
SMB2	7	13.32	8.79	3.32	3.56	26.65	7	40.78	27.86	10.53	17.03	97.07
SMB3	6	9.80	7.80	3.18	1.73	24.32	6	33.46	27.39	11.18	4.96	79.93
SMB4	8	11.57	7.70	2.72	2.00	26.41	8	35.86	14.58	5.15	20.78	63.05
SMB5	10	24.35	18.72	5.92	3.46	54.00	10	73.15	33.73	10.67	20.78	140.73
SMB6	15	12.06	6.06	1.56	0.00	23.39	15	25.79	10.83	2.80	10.75	52.00
TRI1	14	10.66	4.87	1.30	3.74	19.08	15	37.27	15.07	3.89	12.15	63.72
TRI2	5	11.01	3.18	1.42	7.22	15.25	5	27.52	4.89	2.19	23.07	34.61
Total	383	13.30	8.46	0.43	0.00	70.43	384	40.68	21.70	1.11	4.96	140.73

Table B.10: Descriptive statistics of platform thickness and platform width from surface survey sites.

	Maximum Elongation						Axial Elongation					
	N	Mean	S.D.	S.E.	Min	Max	N	Mean	S.D.	S.E.	Min	Max
BPG1	12	1.95	0.50	0.14	1.22	2.86	12	1.13	0.70	0.20	0.34	2.47
BPG2	7	1.90	0.64	0.24	1.34	3.26	7	1.32	0.95	0.36	0.47	3.26
BPH1	9	1.66	0.36	0.12	1.28	2.19	9	0.89	0.42	0.14	0.41	1.62
BPH2	11	1.53	0.40	0.12	1.14	2.25	10	1.14	0.43	0.13	0.44	1.93
CHA1	20	1.55	0.40	0.09	1.06	2.65	16	0.75	0.25	0.06	0.31	1.25
CHA2	30	1.56	0.43	0.08	1.04	2.67	21	0.87	0.28	0.06	0.41	1.64
DAN1	21	1.63	0.43	0.09	1.06	2.52	21	0.90	0.39	0.09	0.4	1.94
DAN2	15	1.57	0.37	0.10	1.1	2.24	15	1.00	0.47	0.12	0.37	1.88
HOKA	5	1.47	0.21	0.09	1.28	1.81	5	1.00	0.30	0.13	0.63	1.33
HOKB	13	1.47	0.48	0.13	1.07	2.48	13	1.24	0.38	0.11	0.73	2.08
HOKC	11	1.52	0.24	0.07	1.09	1.9	11	0.95	0.30	0.09	0.55	1.45
HOKD	4	1.60	0.38	0.19	1.21	2.02	4	0.86	0.37	0.19	0.52	1.36
HOKE	13	1.33	0.20	0.05	1.05	1.65	13	1.02	0.27	0.07	0.59	1.48
HOKF	34	1.50	0.33	0.06	1.04	2.21	34	1.13	0.63	0.11	0.4	3.39
KAR1	4	1.37	0.38	0.19	1.16	1.94	4	1.04	0.22	0.11	0.81	1.31
KAR2	8	1.57	0.47	0.17	1.01	2.53	8	0.82	0.24	0.09	0.38	1.17
KAR3	16	1.63	0.45	0.11	1.17	2.84	16	0.95	0.42	0.11	0.31	1.86
KHA1	7	1.54	0.54	0.20	1.11	2.61	7	0.93	0.26	0.10	0.69	1.37
KHA2	10	1.49	0.40	0.13	1.05	2.29	10	1.11	0.41	0.13	0.51	1.89
KHA3	14	1.44	0.21	0.06	1.21	1.92	14	0.97	0.33	0.09	0.49	1.75
SAM1	30	1.47	0.28	0.05	1.01	2.01	30	1.07	0.49	0.09	0.3	2.12
SHR1	27	1.41	0.20	0.04	1.07	1.87	27	1.07	0.33	0.06	0.57	1.71
SMB1	3	1.72	0.17	0.10	1.53	1.86	0					
SMB2	7	1.48	0.34	0.13	1.12	2.18	3	0.69	0.17	0.10	0.49	0.8
SMB3	7	1.94	0.66	0.25	1.28	3.1	4	0.63	0.16	0.08	0.39	0.76
SMB4	8	1.63	0.25	0.09	1.38	2.13	4	0.71	0.09	0.05	0.63	0.83
SMB5	10	1.55	0.42	0.13	1.09	2.21	7	0.78	0.41	0.16	0.33	1.35
SMB6	15	1.54	0.36	0.09	1.07	2.38	10	1.10	0.43	0.14	0.68	1.88
TRI1	15	1.46	0.29	0.07	1.15	2.07	15	1.20	0.41	0.11	0.38	1.95
TRI2	5	1.61	0.48	0.21	1.1	2.21	5	1.53	0.56	0.25	0.94	2.21
Total	391	1.55	0.38	0.02	1.01	3.26	355	1.02	0.45	0.02	0.3	3.39

Table B.11: Descriptive statistics of flake maximum and axial elongation from surface survey sites.

	None	Cortical	Proximal	Distal	Side	Bidirectional	Opposed/ Perpendicular	Weakly Radial	Radial	Total
BPG1	3	0	6	0	1	0	1	1	0	12
BPG2	0	0	5	0	2	0	0	0	0	7
BPH1	1	0	5	2	1	0	0	0	0	9
BPH2	0	0	3	0	1	2	1	3	1	11
CHA1	5	1	6	0	2	0	3	2	1	20
CHA2	4	1	8	1	5	0	3	7	1	30
DAN1	9	0	4	2	2	0	2	2	0	21
DAN2	5	0	5	2	1	1	0	1	0	15
HOKA	1	0	1	0	0	0	1	0	2	5
HOKB	2	0	3	0	3	0	1	3	1	13
HOKC	0	0	3	1	3	0	1	1	2	11
HOKD	0	0	1	0	1	1	0	1	0	4
HOKE	5	0	3	1	2	0	2	0	0	13
HOKF	4	0	11	1	8	2	3	3	2	34
KAR1	1	0	1	1	1	0	0	0	0	4
KAR2	4	0	1	0	3	0	0	0	0	8
KAR3	5	0	7	0	1	0	1	2	0	16
KHA1	3	0	0	0	0	0	1	2	1	7
KHA2	1	0	1	0	0	0	1	3	4	10
KHA3	1	1	11	0	0	1	0	0	0	14
SAM1	0	0	13	0	5	0	5	6	1	30
SHR1	2	0	6	2	2	0	6	4	5	27
SMB1	3	0	0	0	0	0	0	0	0	3
SMB2	0	0	1	1	2	0	0	3	0	7
SMB3	1	0	3	0	2	0	0	1	0	7
SMB4	0	0	1	0	1	1	4	1	0	8
SMB5	0	0	5	0	3	0	2	0	0	10
SMB6	0	0	7	0	1	1	2	4	0	15
TRI1	1	0	3	0	2	0	2	3	4	15
TRI2	0	0	3	0	0	0	2	0	0	5
Total	61	3	127	14	55	9	44	53	25	391

Table B.12: Count of flake dorsal scar patterns from surface survey sites.

	None	Cortical	Crushed	Dihedral	Faceted	Hammer and Anvil	Multiple Conchoidal	Plain	Punctiform	Shattered	Single Conchoidal	Stepped	Total
BPG1	0	1	0	1	2	0	2	2	0	0	4	0	12
BPG2	0	1	0	1	1	0	1	2	1	0	0	0	7
BPH1	0	3	0	2	0	0	3	1	0	0	0	0	9
BPH2	0	1	0	3	2	0	0	2	0	0	3	0	11
CHA1	2	1	0	2	0	0	0	9	0	0	6	0	20
CHA2	0	2	0	3	0	0	0	15	0	0	10	0	30
DAN1	0	4	0	5	1	0	1	4	0	0	6	0	21
DAN2	0	0	1	2	1	0	1	7	0	0	3	0	15
HOKA	0	3	0	0	0	0	2	0	0	0	0	0	5
HOKB	0	0	0	4	0	0	2	4	0	0	3	0	13
HOKC	0	0	0	4	0	0	0	3	0	0	4	0	11
HOKD	0	1	0	1	1	0	0	1	0	0	0	0	4
HOKE	0	2	0	0	0	0	0	6	1	0	4	0	13
HOKF	0	1	0	4	3	3	4	7	0	0	12	0	34
KAR1	0	0	0	1	1	0	0	2	0	0	0	0	4
KAR2	0	2	0	1	0	0	0	2	0	0	3	0	8
KAR3	0	4	1	2	1	0	2	3	0	0	3	0	16
KHA1	0	0	0	3	2	0	0	2	0	0	0	0	7
KHA2	0	0	0	2	1	0	3	0	0	0	4	0	10
KHA3	0	7	1	3	0	0	0	1	0	0	2	0	14
SAM1	0	1	1	7	0	0	5	6	0	0	10	0	30
SHR1	0	2	2	2	2	0	6	8	0	0	5	0	27
SMB1	3	0	0	0	0	0	0	0	0	0	0	0	3
SMB2	0	1	0	1	1	0	0	2	0	0	2	0	7
SMB3	1	1	0	1	0	0	0	0	1	0	3	0	7
SMB4	0	1	0	1	2	0	0	1	0	0	3	0	8
SMB5	0	1	0	2	2	0	0	3	0	0	2	0	10
SMB6	0	0	0	5	1	0	0	0	0	0	8	1	15
TRI1	0	1	0	4	3	0	3	1	0	1	2	0	15
TRI2	0	0	0	2	0	0	1	1	0	0	1	0	5
Total	6	41	6	69	27	3	36	95	3	1	103	1	391

Table B.13: Count of flake platform types from surface survey sites.

	None	Axial	Feather	Hinge	Outrepasse	Step	Total
BPG1	2	1	8	0	0	1	12
BPG2	0	0	6	0	1	0	7
BPH1	0	0	6	0	1	2	9
BPH2	1	0	9	1	0	0	11
CHA1	1	1	17	0	0	1	20
CHA2	2	0	26	0	0	2	30
DAN1	1	1	18	0	0	1	21
DAN2	0	2	10	2	0	1	15
HOKA	0	0	5	0	0	0	5
HOKB	0	1	12	0	0	0	13
HOKC	0	1	9	0	1	0	11
HOKD	0	0	4	0	0	0	4
HOKE	0	0	10	0	1	2	13
HOKF	4	9	20	0	1	0	34
KAR1	0	1	3	0	0	0	4
KAR2	0	1	6	1	0	0	8
KAR3	0	0	16	0	0	0	16
KHA1	0	1	6	0	0	0	7
KHA2	0	1	8	0	0	1	10
KHA3	0	3	8	2	0	1	14
SAM1	0	6	23	0	0	1	30
SHR1	1	0	22	4	0	0	27
SMB1	3	0	0	0	0	0	3
SMB2	1	1	4	0	0	1	7
SMB3	7	0	0	0	0	0	7
SMB4	1	0	6	0	0	1	8
SMB5	0	0	7	1	0	2	10
SMB6	1	1	12	0	0	1	15
TRI1	0	4	11	0	0	0	15
TRI2	0	1	4	0	0	0	5
Total	25	36	296	11	5	18	391

Table B.14: Count of flake termination type from surface survey type.

Site	Length						Width					
	N	Mean	S.D.	S.E.	Min	Max	N	Mean	S.D.	S.E.	Min	Max
BPG1	2	45.20	20.07	14.20	31.00	59.39	2	35.57	11.74	8.30	27.27	43.87
BPG2	2	55.73	8.53	6.03	49.70	61.76	2	38.43	8.08	5.71	32.72	44.14
BPH1	3	44.29	2.78	1.61	42.59	47.50	3	41.25	13.78	7.95	28.04	55.53
BPH2	3	30.07	7.30	4.22	21.73	35.31	3	21.04	10.28	5.94	9.27	28.30
CHA1	27	48.93	22.60	4.35	15.65	138.22	27	32.21	13.47	2.59	12.92	71.60
CHA2	12	78.83	25.40	7.33	43.13	116.33	12	53.29	17.35	5.01	29.50	96.32
DAN1	3	71.50	37.68	21.76	36.74	111.55	3	60.35	38.27	22.10	30.19	103.41
DAN2	9	65.50	21.58	7.19	36.04	97.51	9	43.41	12.62	4.21	29.60	59.52
HOKA	2	85.36	23.29	16.47	68.89	101.83	2	43.99	3.12	2.21	41.78	46.19
HOKB	2	59.58	23.23	16.43	43.15	76.00	2	44.63	32.58	23.04	21.59	67.67
HOKC	1	45.90			45.90	45.90	1	26.03			26.03	26.03
HOKD	2	69.75	19.57	13.84	55.91	83.59	2	41.72	11.33	8.01	33.71	49.73
HOKE	1	34.63			34.63	34.63	1	20.78			20.78	20.78
HOKF	3	46.41	1.78	1.03	44.48	47.99	3	38.84	8.21	4.74	31.30	47.58
KAR1	2	47.69	6.91	4.89	42.80	52.57	2	32.59	14.87	10.52	22.07	43.10
KAR2	5	71.98	7.57	3.38	62.99	80.08	5	39.85	9.75	4.36	28.43	51.77
KAR3	2	70.57	23.60	16.69	53.88	87.25	2	48.83	28.57	20.20	28.63	69.03
KHA1	1	78.56			78.56	78.56	1	37.63			37.63	37.63
KHA2	3	62.98	12.83	7.41	48.43	72.66	3	30.56	10.10	5.83	19.01	37.77
KHA3	2	85.41	36.56	25.86	59.55	111.26	2	70.69	34.15	24.15	46.54	94.84
SAM1	18	48.78	20.85	4.91	22.10	94.30	18	34.50	11.55	2.72	16.07	59.00
SHR1	12	61.81	14.38	4.15	36.98	85.93	12	44.01	12.84	3.71	24.43	62.27
SMB1	1	74.58			74.58	74.58	1	41.17			41.17	41.17
SMB2	3	50.49	28.73	16.59	27.86	82.81	3	29.54	20.25	11.69	16.80	52.89
SMB5	2	88.37	23.65	16.73	71.64	105.09	2	58.90	4.83	3.42	55.48	62.31
SMB6	3	42.96	10.86	6.27	35.81	55.46	3	25.80	9.36	5.40	18.55	36.36
TRI1	6	69.95	27.26	11.13	39.24	105.23	6	45.20	19.68	8.04	26.22	80.38
TRI2	2	57.11	20.16	14.26	42.85	71.36	2	37.49	3.45	2.44	35.05	39.93
Total	134	58.70	23.16	2.00	15.65	138.22	134	39.50	16.46	1.42	9.27	103.41

Table B.15: Descriptive statistics of flaked piece and broken flake length and width.

Thickness						
	N	Mean	S.D.	S.E.	Min	Max
BPG1	2	15.80	9.00	6.37	9.43	22.16
BPG2	2	15.33	0.21	0.15	15.18	15.47
BPH1	3	12.29	3.63	2.10	8.3	15.41
BPH2	3	7.09	4.35	2.51	2.25	10.67
CHA1	27	13.60	5.25	1.01	3.32	25.9
CHA2	12	20.88	7.06	2.04	7.92	34.12
DAN1	3	14.33	6.49	3.75	7.7	20.68
DAN2	9	17.10	6.92	2.31	6.32	25.79
HOKA	2	18.39	1.40	0.99	17.4	19.38
HOKB	2	13.96	5.70	4.03	9.93	17.99
HOKC	1	9.28			9.28	9.28
HOKD	2	14.62	3.69	2.61	12.01	17.23
HOKE	1	11.93			11.93	11.93
HOKF	3	13.73	4.57	2.64	10.04	18.84
KAR1	2	13.76	6.98	4.94	8.82	18.69
KAR2	5	14.98	2.49	1.12	13.18	19.24
KAR3	2	16.56	7.53	5.33	11.23	21.88
KHA1	1	28.90			28.9	28.9
KHA2	3	13.45	2.23	1.29	12.02	16.02
KHA3	2	20.35	8.85	6.26	14.09	26.6
SAM1	18	14.07	7.56	1.78	4.42	35.09
SHR1	12	16.33	11.30	3.26	5.39	49.7
SMB1	1	30.83			30.83	30.83
SMB2	3	17.77	7.71	4.45	10.44	25.81
SMB5	2	23.36	0.63	0.45	22.91	23.8
SMB6	3	14.38	0.87	0.50	13.75	15.37
TRI1	6	17.01	9.59	3.91	8.31	34.17
TRI2	2	17.59	0.54	0.38	17.21	17.97
Total	134	15.65	7.06	0.61	2.25	49.7

Table B.16: Descriptive statistics of flaked piece and broken flake thickness.

Site	Length						Width					
	N	Mean	S.D.	S.E.	Min	Max	N	Mean	S.D.	S.E.	Min	Max
BPG1	1	41.72			41.72	41.72	1	20.02			20.02	20.02
BPG2	1	45.71			45.71	45.71	1	20.49			20.49	20.49
BPH1	9	60.15	20.99	7.00	29.4	95.93	9	34.60	9.93	3.31	21.09	48.51
BPH2	4	37.26	11.99	6.00	24.27	53.25	4	21.27	7.08	3.54	15.07	27.45
CHA1	3	80.58	30.80	17.78	45.1	100.46	3	42.91	10.05	5.80	35.31	54.31
CHA2	5	85.75	22.05	9.86	61.43	121.53	5	47.92	14.53	6.50	30.21	60.7
DAN1	1	77.21			77.21	77.21	1	35.06			35.06	35.06
DAN2	3	68.56	5.95	3.44	64.43	75.38	3	46.20	8.82	5.10	36.59	53.94
HOKA	1	94.98			94.98	94.98	1	53.25			53.25	53.25
HOKB	4	57.05	20.52	10.26	36.34	84.95	4	34.10	4.75	2.37	31.15	41.19
HOKC	2	59.38	22.82	16.14	43.24	75.51	2	41.88	22.04	15.59	26.29	57.46
HOKD	1	88.50	.	.	88.5	88.5	1	54.16			54.16	54.16
HOKE	7	57.20	9.23	3.49	44.65	68.33	7	31.46	6.60	2.49	22.51	40.69
HOKF	4	53.38	5.93	2.96	46.04	59.66	4	33.53	8.62	4.31	20.88	40.1
KAR1	3	68.80	11.89	6.87	58.32	81.73	3	42.26	5.04	2.91	36.45	45.45
KAR2	1	86.25			86.25	86.25	1	60.76			60.76	60.76
KAR3	1	53.60			53.6	53.6	1	24.31			24.31	24.31
KHA1	2	96.06	7.51	5.31	90.75	101.37	2	73.66	35.40	25.04	48.62	98.69
SAM1	24	47.48	16.09	3.28	26.95	90.18	24	27.60	6.18	1.26	14.46	40.42
SHR1	5	74.33	14.11	6.31	65.24	99.24	5	53.39	9.18	4.11	45.14	67.81
SMB1	1	74.88			74.88	74.88	1	42.21			42.21	42.21
SMB3	3	87.99	58.57	33.82	46.57	155	3	47.72	33.72	19.47	19.37	85
SMB4	4	57.26	14.38	7.19	38.11	71.69	4	34.20	11.36	5.68	18.99	45.95
SMB6	5	44.73	14.12	6.32	29.98	63.79	5	28.12	9.19	4.11	22.17	44.25
TRI1	6	58.95	9.43	3.85	43.56	71.15	6	43.24	7.48	3.05	33.49	56
Total	101	60.10	21.96	2.19	24.27	155	101	36.35	14.28	1.42	14.46	98.69

Table B.17: Descriptive statistics of retouched artefact length and width.

Site	Thickness						Max Elongation					
	N	Mean	S.D.	S.E.	Min	Max	N	Mean	S.D.	S.E.	Min	Max
BPG1	1	10.97			10.97	10.97	1	2.08			2.08	2.08
BPG2	1	8.10			8.1	8.1	1	2.23			2.23	2.23
BPH1	9	12.59	5.49	1.83	6.21	23.36	9	1.76	0.45	0.15	1.07	2.35
BPH2	4	9.80	3.40	1.70	6.42	13.07	4	1.81	0.50	0.25	1.26	2.42
CHA1	3	18.65	7.43	4.29	10.07	23.04	3	1.87	0.65	0.38	1.28	2.57
CHA2	5	16.29	5.13	2.29	8.73	21.84	5	1.92	0.65	0.29	1.04	2.71
DAN1	1	17.46			17.46	17.46	1	2.20			2.2	2.2
DAN2	3	14.09	1.60	0.92	12.92	15.91	3	1.54	0.46	0.26	1.19	2.06
HOKA	1	15.25			15.25	15.25	1	1.78			1.78	1.78
HOKB	4	16.44	5.20	2.60	10.6	23.1	4	1.65	0.40	0.20	1.15	2.06
HOKC	2	11.63	4.77	3.37	8.26	15	2	1.48	0.23	0.17	1.31	1.64
HOKD	1	30.42			30.42	30.42	1	1.63			1.63	1.63
HOKE	7	11.19	2.47	0.93	9.29	16.27	7	1.85	0.28	0.11	1.53	2.29
HOKF	4	14.35	5.93	2.97	6.55	19.5	4	1.69	0.54	0.27	1.23	2.47
KAR1	3	17.74	1.85	1.07	15.62	18.98	3	1.67	0.51	0.29	1.28	2.24
KAR2	1	23.55			23.55	23.55	1	1.42			1.42	1.42
KAR3	1	13.27			13.27	13.27	1	2.20			2.2	2.2
KHA1	2	31.18	9.09	6.43	24.75	37.61	2	1.45	0.59	0.42	1.03	1.87
SAM1	24	12.53	4.60	0.94	6.34	24.55	24	1.72	0.40	0.08	1.19	2.84
SHR1	5	15.33	3.87	1.73	8.69	17.96	5	1.43	0.38	0.17	1.05	2.05
SMB1	1	14.92			14.92	14.92	1	1.77			1.77	1.77
SMB3	3	13.62	10.01	5.78	6.17	25	3	1.95	0.41	0.24	1.61	2.4
SMB4	4	14.47	5.59	2.80	7.47	20.55	4	1.72	0.20	0.10	1.56	2.01
SMB6	5	13.91	5.60	2.50	8.42	22.89	5	1.63	0.47	0.21	1.31	2.47
TRI1	6	19.93	6.56	2.68	12.27	29.73	6	1.39	0.27	0.11	1.06	1.73
Total	101	14.57	5.98	0.59	6.17	37.61	101	1.71	0.41	0.04	1.03	2.84

Table B.18: Descriptive statistics of retouched artefact thickness and maximum elongation.

	Retouch Width						Retouch Depth					
	N	Mean	S.D.	S.E.	Min	Max	N	Mean	S.D.	S.E.	Min	Max
BPG1	1	19.08			19.08	19.08	1	26.69			26.69	26.69
BPG2	1	45.71			45.71	45.71	1	20.49			20.49	20.49
BPH1	8	26.42	11.42	4.04	8	40.57	8	6.42	3.42	1.21	2.83	13
BPH2	4	40.39	31.14	15.57	15.79	85	4	14.16	8.93	4.46	7.97	27
CHA1	3	76.82	36.24	20.92	35	99.09	3	22.12	16.90	9.76	6	39.7
CHA2	5	44.99	19.65	8.79	14.59	64.37	5	12.43	6.63	2.97	2.5	20
DAN1	1	25.00			25	25	1	4.00			4	4
DAN2	3	39.25	29.29	16.91	20.48	73	3	14.36	12.68	7.32	6.98	29
HOKA	1	86.00			86	86	1	47.00			47	47
HOKB	4	19.58	5.93	2.96	13.63	25.3	4	5.33	3.66	1.83	1.75	10
HOKC	2	44.22	39.90	28.22	16	72.43	2	13.98	15.52	10.98	3	24.95
HOKD	1	63.50			63.5	63.5	1	14.55			14.55	14.55
HOKE	7	32.03	21.34	8.07	0	68.33	7	25.89	18.63	7.04	5.36	56.3
HOKF	4	45.25	10.38	5.19	30.74	54	4	22.49	9.97	4.98	14.51	36
KAR1	3	41.67	5.77	3.33	36.7	48	3	18.66	21.78	12.58	6	43.81
KAR2	1	80.00			80	80	1	34.00			34	34
KAR3	1	17.00			17	17	1	11.00			11	11
KHA1	2	50.96	18.33	12.96	38	63.92	2	10.78	7.08	5.01	5.77	15.78
SAM1	23	28.94	22.64	4.72	5.9	84	23	12.52	13.04	2.72	1.73	44.47
SHR1	5	30.45	5.59	2.50	25	38	5	8.11	5.80	2.59	4	18.14
SMB1	0						0					
SMB3	3	69.20	9.36	5.40	63.6	80	3	14.81	8.99	5.19	4.43	20
SMB4	4	66.73	62.35	31.17	31.54	160	4	18.81	11.18	5.59	3.57	30
SMB6	5	29.07	18.47	8.26	12.74	60.54	5	9.54	6.80	3.04	2.5	16.62
TRI1	6	31.60	12.82	5.23	9.22	46.69	6	6.36	3.83	1.57	3.29	12.21
Total	98	37.84	25.53	2.58	0	160	98	13.97	12.28	1.24	1.73	56.3

Table B.19: Descriptive statistics of retouched artefact retouch width and depth.

Appendix C – Statistical Results from Katoati

	Core	Flake	Flaked Piece	Heavy Tool	Total
S3a	8	25	25	0	58
S3b	0	3	5	0	8
S4	76	276	85	0	437
S5	18	27	16	1	62
S6	108	389	130	0	627
S8	64	181	75	7	327
Total	274	901	336	8	1519

Table C.1: Count of gross artefact types by stratum.

Comparison	Fisher's	N	p
All assemblages	50.686	1519	0
S3a-S4	14.69	495	0.01
S3a-S6	13.445	685	0.02
S3a-S8	8.987	378	0.11

Table C.2: Results of significant Fisher's Exact Test comparing gross artefact types by stratum.

Attribute	N	Mean	S.D.	Min	Max	Percentiles		
						25th	50th (Median)	75th
Cortex	256	30.94	23.11	0.00	90.00	10.00	30.00	50.00
Number Of Platforms Quadrants	253	1.42	0.71	1.00	4.00	1.00	1.00	2.00
Number Of Core Rotations	250	0.48	0.78	0.00	4.00	0.00	0.00	1.00
Number Of Scars	253	2.50	1.93	1.00	11.00	1.00	2.00	3.00
Max Length	256	65.60	22.44	22.89	146.84	48.05	62.29	80.57
Max Width	256	49.01	15.98	15.90	91.59	37.18	47.54	57.49
Surface Area	256	3518.05	2264.94	365.38	11860.27	1752.13	3095.89	4470.45
Medial Thickness	256	35.35	16.31	6.65	102.64	23.56	32.63	43.11
Distal Thickness	253	27.26	15.46	5.21	95.67	15.96	24.59	33.90
Axial Length	256	42.76	17.26	13.09	116.02	29.61	39.67	54.20
Axial Proximal Width	256	50.64	20.95	11.16	141.36	35.63	47.46	59.47
Axial Medial Width	256	53.17	20.56	15.28	133.58	37.08	50.70	64.30
Axial Distal Width	256	40.47	17.56	10.76	94.18	27.01	37.86	50.93
Elongation	256	0.86	0.35	0.28	2.56	0.59	0.83	1.07
Flatness	256	1.70	0.75	0.51	4.97	1.15	1.57	2.07
Proximal Shape	256	0.96	0.19	0.47	1.80	0.85	0.96	1.07
Distal Shape	256	1.37	0.27	0.89	2.38	1.17	1.32	1.52
Platform Width	256	50.29	20.70	10.59	143.52	35.77	46.32	61.88
Platform Depth	255	31.97	17.36	2.32	103.10	19.30	29.65	40.88
Platform Surface Area	255	1778.02	1506.42	24.57	10082.28	773.53	1312.00	2343.23
Platform Shape	255	2.00	1.68	0.21	19.49	1.23	1.62	2.25
Size Corrected Platform Area	255	0.50	0.23	0.04	1.04	0.35	0.49	0.67
Last Scar Length	253	32.46	12.80	11.10	73.88	22.37	30.47	39.50
Last Scar Face Length	253	42.24	17.31	14.57	115.62	29.71	39.19	53.55
Last Scar Width	253	31.42	11.19	11.35	77.82	23.58	28.66	38.91
Last Scar Surface Area	253	1074.18	707.16	191.02	4340.17	560.26	897.66	1301.25
Last Scar Elongation	253	1.11	0.47	0.27	3.30	0.78	1.04	1.35

Table C.3: Univariate descriptive statistics for core attributes.

Type	Core Type			Platform Type			Platform prep			Termination		
	χ^2	df	p	χ^2	df	p	χ^2	df	p	χ^2	df	p
Cortex	22.579	3	0	30.837	4	0	4.874	2	0.087	4.644	3	0.2
Number Of Platforms Quadrants	9.587	3	0.022	14.407	4	0.006	2.178	2	0.337	10.08	3	0.018
Number Of Core Rotations	164.631	3	0	24.431	4	0	7.287	2	0.026	7.069	3	0.07
Number Of Scars	91.761	3	0	28.28	4	0	6.806	2	0.033	23.302	3	0
Max Length	8.733	3	0.033	14.388	4	0.006	2.031	2	0.362	15.919	3	0.001
Max Width	13.582	3	0.004	14.214	4	0.007	0.518	2	0.772	17.299	3	0.001
Surface Area	11.448	3	0.01	15.221	4	0.004	1.244	2	0.537	17.706	3	0.001
Medial Thickness	8.304	3	0.04	9.654	4	0.047	7.728	2	0.021	2.975	3	0.395
Distal Thickness	5.877	3	0.118	5.383	4	0.25	6.937	2	0.031	0.407	3	0.939
Axial Length	21.284	3	0	17.973	4	0.001	2.593	2	0.274	10.297	3	0.016
Axial Proximal Width	6.25	3	0.1	7.267	4	0.122	0.216	2	0.897	11.805	3	0.008
Axial Medial Width	8.414	3	0.038	9.192	4	0.056	1.716	2	0.424	12.069	3	0.007
Axial Distal Width	9.483	3	0.024	7.719	4	0.102	1.452	2	0.484	15.824	3	0.001
Elongation	5.761	3	0.124	13.779	4	0.008	0.391	2	0.822	1.318	3	0.725
Flatness	14.994	3	0.002	2.484	4	0.648	13.098	2	0.001	1.447	3	0.694
Proximal Shape	1.177	3	0.759	14.654	4	0.005	2.446	2	0.294	3.9	3	0.272
Distal Shape	1.587	3	0.662	1.429	4	0.839	1.076	2	0.584	4.833	3	0.184
Platform Width	7.552	3	0.056	7.469	4	0.113	1.902	2	0.386	10.764	3	0.013
Platform Depth	1.673	3	0.643	17.62	4	0.001	6.742	2	0.034	3.208	3	0.361
Platform Surface Area	1.669	3	0.644	14.02	4	0.007	4.052	2	0.132	7.879	3	0.049
Platform Shape	9.741	3	0.021	14.783	4	0.005	8.165	2	0.017	1.588	3	0.662
Size Corrected Platform Area	9.469	3	0.024	3.312	4	0.507	7.693	2	0.021	2.703	3	0.44
Last Scar Length	3.42	3	0.331	5.284	4	0.259	0.942	2	0.624	6.907	3	0.075
Last Scar Face Length	17.543	3	0.001	11.621	4	0.02	1.853	2	0.396	16.274	3	0.001
Last Scar Width	3.556	3	0.314	5.181	4	0.269	0.746	2	0.689	10.402	3	0.015
Last Scar Surface Area	1.576	3	0.665	7.169	4	0.127	0.947	2	0.623	8.54	3	0.036
Last Scar Elongation	10.648	3	0.014	0.16	4	0.997	1.132	2	0.568	7.214	3	0.065

Table C.4: Results of Kruskal-Wallis test of core attributes separated by core type, platform type, platform preparation and termination type.

Attribute	Pair	Mann-Whitney U	Wilcoxon W	Z	Asymp. Sig. (2-tailed)
Cortex	Multiple Platform - Prepared	304.5	514.5	-3.641	0
	Single Platform - Prepared	519	729	-4.5	0
Number Of Core Rotations	Single Platform - Bidirectional	71.5	8982.5	-10.635	0
	Single Platform - Multiple Platform	490.5	9401.5	-12.622	0
	Multiple Platform - Prepared	437.5	627.5	-2.196	0.028
	Single Platform - Prepared	540	9451	-8.624	0
Number Of Scars	Single Platform - Bidirectional	181.5	9497.5	-4.423	0
	Single Platform - Multiple Platform	1166	10482	-8.929	0
	Single Platform - Prepared	501.5	9817.5	-4.896	0
Max Width	Single Platform - Prepared	748.5	10064.5	-3.242	0.001
Surface Area	Single Platform - Prepared	795	10111	-2.995	0.003
Axial Length	Single Platform - Multiple Platform	3309	12625	-2.88	0.004
	Single Platform - Prepared	645	9961	-3.79	0
	Multiple Platform - Prepared	410.5	2555.5	-2.481	0.013
Flatness	Multiple Platform - Prepared	295	2440	-3.678	0
	Single Platform - Prepared	809	10125	-2.921	0.003
Platform Shape	Multiple Platform - Prepared	327	2472	-3.106	0.002
	Single Platform - Prepared	799	10115	-2.69	0.007
Size Corrected Platform Area	Single Platform - Prepared	778	968	-2.804	0.005
Last Scar Face Length	Single Platform - Multiple Platform	3492.5	12808.5	-2.404	0.016
	Single Platform - Prepared	638.5	9954.5	-3.566	0
Last Scar Elongation	Single Platform - Multiple Platform	3169	12485	-3.243	0.001

Table C.5: Significant results of Mann-Whitney test of core attributes by core type.

Attribute	Pair	Mann-Whitney U	Wilcoxon W	Z	Asymp. Sig. (2-tailed)
Cortex	Cortical - Dihedral	85.5	113.5	-2.509	0.012
	Cortical - Multiple Conchoidal	272	525	-3.998	0
	Cortical - Plain	871.5	2197.5	-3.721	0
	Cortical - Single Conchoidal	1733	6104	-3.73	0
	Multiple Conchoidal - Single Conchoidal	602	855	-3.045	0.002
Number Of Core Rotations	Cortical - Multiple Conchoidal	319.5	1915.5	-3.686	0
	Cortical - Single Conchoidal	1977.5	3573.5	-2.701	0.007
	Multiple Conchoidal - Plain	261.5	1587.5	-4.15	0
	Plain - Single Conchoidal	1687.5	3013.5	-3.221	0.001
Number Of Platforms	Cortical - Single Conchoidal	1879.5	3532.5	-3.604	0
Number Of Scars	Cortical - Multiple Conchoidal	266.5	1919.5	-3.945	0
	Cortical - Single Conchoidal	1831	3484	-3.313	0.001
	Multiple Conchoidal - Plain	216	1542	-4.156	0
	Plain - Single Conchoidal	1576.5	2902.5	-3.46	0.001
Axial Length	Cortical - Plain	954.5	2280.5	-3.185	0.001
	Multiple Conchoidal - Plain	283	1609	-3.342	0.001
	Multiple Conchoidal - Single Conchoidal	645	5016	-2.688	0.007
Elongation	Multiple Conchoidal - Plain	339	1665	-2.669	0.008
	Multiple Conchoidal - Single Conchoidal	570	4941	-3.221	0.001
Max Length	Plain - Single Conchoidal	1607.5	2933.5	-3.191	0.001
Max Width	Plain - Single Conchoidal	1563.5	2889.5	-3.375	0.001
Proximal Shape	Cortical - Plain	902	2613	-3.504	0
	Cortical - Single Conchoidal	2023	3734	-2.579	0.01
Surface Area	Cortical - Plain	1028	2354	-2.739	0.006
	Plain - Single Conchoidal	1563	2889	-3.377	0.001
Platform Depth	Cortical - Multiple Conchoidal	399.5	630.5	-2.325	0.02
	Cortical - Plain	1001	2327	-2.903	0.004
	Multiple Conchoidal - Single Conchoidal	624	855	-2.577	0.01
	Plain - Single Conchoidal	1552.5	2878.5	-3.421	0.001
Platform Shape	Cortical - Multiple Conchoidal	353	2064	-2.841	0.004
	Multiple Conchoidal - Single Conchoidal	515	4886	-3.373	0.001
Platform Surface Area	Cortical - Plain	971	2297	-3.085	0.002
	Plain - Single Conchoidal	1619	2945	-3.143	0.002
Last Scar Face Length	Cortical - Plain	1035	2361	-2.575	0.01
	Multiple Conchoidal - Plain	310	1636	-2.794	0.005

Table C.6: Significant results of Mann-Whitney test of core attributes by platform type.

Attribute	Pair	Mann-Whitney U	Wilcoxon W	Z	Asymp. Sig. (2-tailed)
Number Of Core Rotations	None - Faceted	484	23920	-2.525	0.012
Medial Thickness	None - Faceted	449	494	-2.777	0.005
Flatness	None - Faceted	286	24596	-3.614	0
Platform Shape	None - Faceted	363	24673	-2.821	0.005
Size Corrected Platform Area	None - Faceted	438	474	-2.412	0.016

Table C.7: Significant results of Mann-Whitney test of core attributes by platform preparation.

Attribute	Pair	Mann-Whitney U	Wilcoxon W	Z	Asymp. Sig. (2-tailed)
Number Of Scars	Axial - Feather	439.5	505.5	-3.171	0.002
	Axial - Hinge	12.5	78.5	-2.235	0.025
	Axial - Step	31.5	97.5	-4.021	0
	Feather - Step	1535	16760	-3.5	0
Number Of Platforms	Axial - Step	79.5	145.5	-2.762	0.006
Max Length	Feather - Step	1440	16840	-3.727	0
Max Width	Feather - Step	1361	16761	-3.996	0
Surface Area	Feather - Step	1359	16759	-4.002	0
Axial Length	Feather - Step	1665	17065	-2.963	0.003
Axial Proximal Width	Feather - Step	1742	17142	-2.702	0.007
Axial Distal Width	Axial - Step	81	159	-2.665	0.008
	Feather - Step	1391.5	16791.5	-3.892	0
Axial Medial Width	Feather - Step	1578	16978	-3.259	0.001
Platform Width	Feather - Step	1610	17010	-3.15	0.002
Last Scar Width	Axial - Feather	435	15660	-3.031	0.002
Last Scar Surface Area	Axial - Feather	471	15696	-2.822	0.005
	Axial - Step	74	509	-2.59	0.01
Last Scar Face Length	Feather - Step	1409	16634	-3.804	0

Table C.8: Significant results of Mann-Whitney test of core attributes by termination type.

Attribute	χ^2	df	Asymp. Sig.
Cortex	1.082	2	0.582
Number Of Platforms Quadrants	2.197	2	0.333
Number Of Core Rotations	0.137	2	0.934
Number Of Scars	3.702	2	0.157
Max Length	2.083	2	0.353
Max Width	1.902	2	0.386
Surface Area	2.22	2	0.33
Medial Thickness	1.899	2	0.387
Distal Thickness	1.171	2	0.557
Axial Length	0.498	2	0.78
Axial Proximal Width	2.733	2	0.255
Axial Medial Width	2.491	2	0.288
Axial Distal Width	2.686	2	0.261
Elongation	1.126	2	0.569
Flatness	1.155	2	0.561
Proximal Shape	0.086	2	0.958
Distal Shape	0.01	2	0.995
Platform Width	1.804	2	0.406
Platform Depth	1.133	2	0.568
Platform Surface Area	2.291	2	0.318
Platform Shape	0.157	2	0.924
Size Corrected Platform Area	0.162	2	0.922
Last Scar Length	0.466	2	0.792
Last Scar Face Length	2.3	2	0.317
Last Scar Width	0.78	2	0.677
Last Scar Surface Area	0.283	2	0.868
Last Scar Elongation	0.658	2	0.72

Table C.9: Results of Kruskal-Wallis test of core attributes separated by stratum.

Attribute	N	Mean	S.D.	Min	Max	Percentiles		
						25th	50th (Median)	75th
Cortex	606	29.17	34.05	0.00	100.00	0.00	10.00	60.00
Max Length	606	44.83	18.52	9.69	127.57	32.03	40.97	55.40
Max Width	606	31.94	13.58	8.54	91.51	22.30	29.53	38.74
Surface Area	606	1649.30	1405.50	87.21	11354.56	702.30	1182.88	2068.30
Medial Thickness	606	14.25	7.41	2.67	53.18	9.17	12.73	17.53
Axial Length	569	33.13	15.63	8.17	123.70	21.97	29.39	40.13
Axial Proximal Width	574	31.55	14.26	8.79	97.26	21.27	28.51	38.41
Axial Medial Width	581	34.79	15.69	7.19	91.22	23.17	31.67	43.64
Axial Distal Width	576	26.95	14.09	3.84	100.35	16.69	23.57	33.65
Elongation	566	1.02	0.39	0.25	2.54	0.73	0.95	1.26
Flatness	581	2.61	0.89	0.76	6.84	1.98	2.51	3.15
Proximal Shape	573	0.94	0.24	0.39	1.73	0.76	0.94	1.09
Distal Shape	573	1.38	0.37	0.68	2.89	1.10	1.34	1.59
Platform Width	573	32.09	15.48	5.39	99.41	20.86	29.03	40.04
Platform Depth	575	12.61	7.01	1.61	49.67	7.71	11.15	16.10
Platform Surface Area	572	476.02	473.20	8.68	3255.11	168.83	327.77	634.39
Platform Shape	572	2.87	1.40	0.66	16.11	2.01	2.61	3.30
Size Corrected Platform Area	572	0.30	0.18	0.01	1.02	0.17	0.27	0.39

Table C.10: Univariate descriptive statistics for flake attributes.

Attribute	Scar Pattern			Platform Type			Platform Preparation			Termination Type		
	χ^2	df	p	χ^2	df	p	χ^2	df	p	χ^2	df	p
Cortex	248.239	7	0	86.741	6	0	4.691	2	0.096	41.95	4	0
Max Length	21.816	7	0.003	6.942	6	0.326	2.819	2	0.244	19.226	4	0.001
Max Width	23.001	7	0.002	10.437	6	0.107	1.885	2	0.39	24.744	4	0
Surface Area	23.471	7	0.001	9.173	6	0.164	2.246	2	0.325	22.681	4	0
Medial Thickness	19.417	7	0.007	10.43	6	0.108	3.967	2	0.138	76.1	4	0
Axial Length	15.57	7	0.029	14.429	6	0.025	0.954	2	0.621	12.927	4	0.012
Axial Proximal Width	24.756	7	0.001	19.766	6	0.003	7.138	2	0.028	11.84	4	0.019
Axial Medial Width	28.189	7	0	9.389	6	0.153	2.16	2	0.34	14.654	4	0.005
Axial Distal Width	20.007	7	0.006	6.23	6	0.398	3.767	2	0.152	20.628	4	0
Elongation	14.707	7	0.04	15.942	6	0.014	0.645	2	0.724	2.856	4	0.582
Flatness	5.964	7	0.544	11.182	6	0.083	7.198	2	0.027	64.459	4	0
Proximal Shape	5.713	7	0.574	29.343	6	0	1.615	2	0.446	28.33	4	0
Distal Shape	17.853	7	0.013	6.03	6	0.42	2.13	2	0.345	17.876	4	0.001
Platform Width	38.3	7	0	55.672	6	0	4.533	2	0.104	10.418	4	0.034
Platform Depth	35.572	7	0	42.946	6	0	4.258	2	0.119	48.905	4	0
Platform Surface Area	40.923	7	0	47.77	6	0	3.019	2	0.221	31.929	4	0
Platform Shape	10.536	7	0.16	36.691	6	0	11.489	2	0.003	44.171	4	0
Size Corrected Platform Area	42.48	7	0	45.694	6	0	3.371	2	0.185	22.048	4	0

Table C.11: Results of Kruskal-Wallis test of flake attributes separated by scar pattern, platform type, platform preparation and termination type.

Attribute	Pair	Mann-Whitney U	Wilcoxon W	Z	Asymp. Sig. (2-tailed)
Cortex	Bidirectional - Radial	84	1074	-3.005	0.003
	Cortical - Bidirectional	6	42	-4.716	0
	Cortical - Distal	153	531	-6.995	0
	Cortical - Opposed/Perpendicular	63.5	2548.5	-10.758	0
	Cortical - Proximal	396	8146	-11.718	0
	Cortical - Radial	0	990	-9.565	0
	Cortical - Side	513	3753	-9.735	0
	Cortical - Weakly Radial	22.5	2797.5	-11.102	0
	Distal - Opposed/Perpendicular	666.5	3151.5	-2.397	0.017
	Distal - Radial	274	1264	-4.401	0
	Distal - Weakly Radial	666	3441	-2.782	0.005
	Proximal - Weakly Radial	3404	6179	-3.225	0.001
	Proximal - Opposed/Perpendicular	3412.5	5897.5	-2.604	0.009
	Proximal - Radial	1414.5	2404.5	-5.104	0
	Side - Opposed/Perpendicular	1855	4340	-3.724	0
	Side - Radial	747	1737	-5.668	0
	Side - Weakly Radial	1849	4624	-4.24	0
Max Length	Opposed/Perpendicular - Radial	1056.5	2046.5	-3.29	0.001
	Weakly Radial - Radial	1211	2201	-2.783	0.005
Max Width	Cortical - Opposed/Perpendicular	2030.5	4515.5	-3.851	0
	Cortical - Weakly Radial	2307	5082	-3.381	0.001
Medial Thickness	Cortical - Opposed/Perpendicular	1985.5	4470.5	-4.005	0
	Cortical - Proximal	4226.5	11976.5	-3.027	0.002
	Cortical - Weakly Radial	2314	5089	-3.357	0.001
Surface Area	Cortical - Opposed/Perpendicular	2041	4526	-3.815	0
	Cortical - Weakly Radial	2301.5	5076.5	-3.399	0.001
	Cortical - Opposed/Perpendicular	1977	4462	-4.035	0
Axial Distal Width	Cortical - Proximal	4298	12048	-2.867	0.004
	Cortical - Weakly Radial	2280	5055	-3.47	0.001
	Cortical - Opposed/Perpendicular	2195	4610	-3.069	0.002
Axial Medial Width	Cortical - Proximal	4139.5	11520.5	-2.861	0.004
	Cortical - Weakly Radial	2253.5	4881.5	-3.232	0.001
	Cortical - Opposed/Perpendicular	1874	4359	-4.306	0
Axial Medial Width	Cortical - Proximal	4021.5	11771.5	-3.373	0.001
	Cortical - Weakly Radial	2039.5	4740.5	-4.07	0

Attribute	Pair	Mann-Whitney U	Wilcoxon W	Z	Asymp. Sig. (2-tailed)
Axial Proximal Width	Cortical - Opposed/Perpendicular	2026	4511	-3.778	0
	Cortical - Weakly Radial	2065	4766	-3.984	0
Distal Shape	Cortical - Radial	1286	2276	-3.214	0.001
	Distal - Radial	348	1338	-2.723	0.006
	Proximal - Radial	1831	2821	-3.062	0.002
	Side - Radial	1098	2088	-3.377	0.001
Platform Width	Cortical - Opposed/Perpendicular	1905.5	4390.5	-4.197	0
	Cortical - Proximal	4184	11565	-2.759	0.006
	Cortical - Weakly Radial	1871.5	4572.5	-4.635	0
	Distal - Weakly Radial	619	3320	-2.624	0.009
	Proximal - Weakly Radial	3308	6009	-2.926	0.003
	Side - Weakly Radial	1812	4513	-3.952	0
	Side - Opposed/Perpendicular	1849.5	4334.5	-3.482	0
Platform Depth	Cortical - Opposed/Perpendicular	1930	4415	-4.112	0
	Cortical - Radial	1142.5	2088.5	-3.744	0
	Cortical - Weakly Radial	2073	4774	-3.957	0
	Distal - Opposed/Perpendicular	550	3035	-3.179	0.001
	Distal - Radial	336	1282	-2.95	0.003
	Distal - Weakly Radial	596.5	3297.5	-3.02	0.003
	Side - Opposed/Perpendicular	2046.5	4531.5	-2.839	0.005
	Side - Radial	1191	2137	-2.806	0.005
	Side - Weakly Radial	2187	4888	-2.678	0.007
	Proximal - Opposed/Perpendicular	3384	5869	-2.391	0.017
	Platform Surface Area	Cortical - Opposed/Perpendicular	1850	4335	-4.389
Cortical - Proximal		4162	11543	-2.809	0.005
Cortical - Radial		1183	2129	-3.547	0
Cortical - Weakly Radial		1897	4598	-4.549	0
Distal - Opposed/Perpendicular		553	3038	-2.943	0.003
Distal - Weakly Radial		564	3265	-3.061	0.002
Proximal - Weakly Radial		3364	6065	-2.778	0.005
Proximal - Opposed/Perpendicular		3254	5739	-2.665	0.008
Side - Opposed/Perpendicular		1890	4375	-3.328	0.001
Side - Radial		1255	2201	-2.377	0.017
Side - Weakly Radial		1942	4643	-3.472	0.001

Attribute	Pair	Mann-Whitney U	Wilcoxon W	Z	Asymp. Sig. (2-tailed)
Size Corrected Platform Area	Proximal - Distal	862	8243	-3.61	0
	Cortical - Distal	741	4746	-2.781	0.005
	Distal - Bidirectional	37	73	-2.72	0.007
	Distal - Opposed/Perpendicular	380	2865	-4.37	0
	Distal - Radial	150	1096	-5.065	0
	Distal - Side	556	3716	-3.497	0
	Distal - Weakly Radial	384	3085	-4.493	0
	Proximal - Weakly Radial	3530	6231	-2.34	0.019
	Cortical - Radial	1202	2148	-3.455	0.001
	Cortical - Weakly Radial	2526	5227	-2.432	0.015
	Proximal - Radial	1643	2589	-3.584	0
	Side - Radial	994	1940	-3.775	0
Side - Weakly Radial	2203	4904	-2.51	0.012	

Table C.12: Significant results of Mann-Whitney test of flake attributes by dorsal scar pattern.

Attribute	Pair	Mann-Whitney U	Wilcoxon W	Z	Asymp. Sig. (2-tailed)
Cortex	Cortical - Dihedral	2394.5	5244.5	-5.28	0
	Cortical - Multiple Conchoidal	1596.5	5251.5	-8.293	0
	Cortical - Plain	2958.5	8736.5	-6.824	0
	Cortical - Punctiform	409	500	-2.722	0.006
	Cortical - Single Conchoidal	4589.5	15467.5	-6.517	0
	Dihedral - Multiple Conchoidal	2492	6147	-2.582	0.01
Axial Length	Cortical - Plain	4496.5	10061.5	-3.086	0.002
Axial Proximal Width	Cortical - Punctiform	263	354	-3.822	0
	Dihedral - Punctiform	227	318	-3.063	0.002
	Multiple Conchoidal - Punctiform	228	319	-3.367	0.001
	Plain - Punctiform	330	421	-3.086	0.002
	Punctiform - Single Conchoidal	360	451	-3.669	0
Elongation	Cortical - Punctiform	419	6860	-2.53	0.011
	Dihedral - Punctiform	237	3012	-2.905	0.004
	Multiple Conchoidal - Punctiform	278	3681	-2.761	0.006
	Plain - Punctiform	347	5912	-2.884	0.004
	Punctiform - Single Conchoidal	411	10707	-3.325	0.001
Proximal Shape	Cortical - Punctiform	282.5	373.5	-3.668	0
	Multiple Conchoidal - Punctiform	267	358	-2.954	0.003
	Plain - Punctiform	236	327	-3.859	0
	Punctiform - Single Conchoidal	333	424	-3.841	0
	Cortical - Plain	4937	11607	-2.438	0.015
	Cortical - Single Conchoidal	6537	13207	-2.91	0.004
	Dihedral - Plain	3025	5875	-2.736	0.006
	Dihedral - Single Conchoidal	4095	6945	-2.933	0.003
Platform Width	Plain - Punctiform	76.5	167.5	-5.227	0
	Punctiform - Single Conchoidal	98	189	-5.332	0
	Dihedral - Punctiform	14	105	-5.568	0
	Cortical - Punctiform	40	131	-5.581	0
	Crushed - Dihedral	47	57	-2.303	0.021
	Dihedral - Plain	2609	8387	-4.012	0
	Dihedral - Single Conchoidal	4064.5	14360.5	-2.934	0.003
	Multiple Conchoidal - Plain	3337.5	9115.5	-3.05	0.002
	Cortical - Plain	4837.5	10615.5	-2.75	0.006
Platform Depth	Cortical - Multiple Conchoidal	3865.5	7520.5	-2.526	0.012
	Cortical - Punctiform	50	141	-5.502	0
	Crushed - Punctiform	1	92	-2.832	0.005
	Dihedral - Punctiform	19	110	-5.509	0
	Multiple Conchoidal - Punctiform	29	120	-5.483	0
	Plain - Punctiform	26	117	-5.653	0
	Punctiform - Single Conchoidal	46.5	137.5	-5.67	0

Attribute	Pair	Mann-Whitney U	Wilcoxon W	Z	Asymp. Sig. (2-tailed)
Platform Shape	Cortical - Dihedral	3181	9851	-3.054	0.002
	Dihedral - Plain	2739	8517	-3.64	0
	Dihedral - Single Conchoidal	3715	14011	-3.724	0
	Cortical - Multiple Conchoidal	3376	10046	-3.624	0
	Multiple Conchoidal - Plain	2880	8658	-4.256	0
	Multiple Conchoidal - Single Conchoidal	3860	14156	-4.492	0
Platform Surface Area	Dihedral - Punctiform	8	99	-5.639	0
	Multiple Conchoidal - Punctiform	4	95	-5.739	0
	Plain - Punctiform	10	101	-5.788	0
	Punctiform - Single Conchoidal	31	122	-5.761	0
	Cortical - Punctiform	14	105	-5.786	0
	Crushed - Punctiform	3	94	-2.604	0.009
	Cortical - Plain	4894	10672	-2.632	0.008
Size Corrected Platform Area	Dihedral - Plain	3013	8791	-2.857	0.004
	Cortical - Punctiform	24	115	-5.707	0
	Crushed - Dihedral	34	44	-2.594	0.009
	Crushed - Punctiform	2	93	-2.717	0.007
	Dihedral - Punctiform	0	91	-5.733	0
	Multiple Conchoidal - Punctiform	1	92	-5.771	0
	Plain - Punctiform	13	104	-5.763	0
Punctiform - Single Conchoidal	15	106	-5.864	0	

Table C.13: Significant results of Mann-Whitney test of flake attributes by platform type.

Attribute	Pair	Mann-Whitney U	Wilcoxon W	Z	Asymp. Sig. (2-tailed)
Axial Proximal Width	None - Overhang Removal	1112	1148	-2.225	0.026
Axial Proximal Width	Overhang Faceting	25	61	-2.708	0.007
Flatness	None - Faceting	3154	134995	-2.613	0.009
Platform Shape	None - Faceting	2632	133960	-3.399	0.001

Table C.14: Significant results of Mann-Whitney test of flake attributes by platform preparation.

Attribute	Pair	Mann-Whitney U	Wilcoxon W	Z	Asymp. Sig. (2-tailed)
Cortex	Axial - Feather	9144.5	91765.5	-6.281	0
	Axial - Step	980.5	1800.5	-3.418	0.001
Max Length	Axial - Feather	11376.5	93997.5	-4.089	0
Max Width	Axial - Feather	10879.5	93500.5	-4.525	0
Surface Area	Axial - Feather	11030	93651	-4.393	0
Medial Thickness	Axial - Feather	6351.5	88972.5	-8.498	0
	Axial - Step	692	1512	-4.995	0
Axial Distal Width	Axial - Feather	12290.5	93696.5	-3.205	0.001
	Feather - Step	5380.5	86786.5	-3.47	0.001
Axial Length	Axial - Feather	12175.5	91576.5	-3.013	0.003
Axial Medial Width	Axial - Feather	11764.5	91964.5	-3.589	0
Axial Proximal Width	Axial - Feather	12275	90485	-2.994	0.003
	Axial - Step	1111.5	1931.5	-2.636	0.008
Proximal Shape	Axial - Hinge	49	64	-2.807	0.005
	Axial - Step	964	1784	-3.465	0.001
	Feather - Hinge	307	322	-2.649	0.008
	Feather - Step	4545	5365	-4.428	0
Distal Shape	Axial - Step	937	1757	-3.617	0
	Feather - Step	4956	5776	-3.97	0
	Step - Outrepassé	136	956	-2.842	0.004
Flatness	Axial - Feather	7351	10511	-7.515	0
	Axial - Step	580	3740	-5.625	0
	Feather - Outrepassé	1665	1770	-2.579	0.01
	Step - Outrepassé	152	257	-2.527	0.012
Platform Depth	Axial - Feather	8244.5	86850.5	-6.641	0
	Axial - Hinge	51	66	-2.77	0.006
	Axial - Step	760	1580	-4.613	0
Platform Shape	Axial - Feather	8493	11653	-6.376	0
	Axial - Step	1083	4243	-2.796	0.005
Platform Surface Area	Axial - Feather	9842	87657	-5.16	0
	Axial - Hinge	62	77	-2.562	0.01
	Axial - Step	888	1708	-3.893	0
Size Corrected Platform Area	Axial - Hinge	68	83	-2.448	0.014
	Axial - Step	867	1687	-4.011	0
	Feather - Step	5262	6082	-3.464	0.001

Table C.15: Significant results of Mann-Whitney test of flake attributes by termination type.

Attribute	Mann-Whitney U	Wilcoxon W	Z	Asymp. Sig. (2-tailed)
Cortex	18157.5	160468.5	-0.962	0.336
Max Length	13041.5	155352.5	-4.571	0
Max Width	14158.5	156469.5	-3.775	0
Surface Area	13381	155692	-4.329	0
Medial Thickness	16995.5	159306.5	-1.753	0.08
Axial Length	12628.5	136381.5	-4.037	0
Axial Proximal Width	14023	140779	-2.93	0.003
Axial Medial Width	13352	143147	-3.729	0
Axial Distal Width	13950	141210	-3.175	0.001
Elongation	17293	139558	-0.379	0.705
Flatness	14905	144700	-2.565	0.01
Proximal Shape	15750	18306	-1.586	0.113
Distal Shape	17911	143662	-0.095	0.924
Platform Width	16369	142622	-1.112	0.266
Platform Depth	17712	20340	-0.3	0.764
Platform Surface Area	17357	143108	-0.329	0.742
Platform Shape	15741	141492	-1.569	0.117
Size Corrected Platform Area	13028	15584	-3.65	0

Table C.16: Significant results of Mann-Whitney test comparing retouched and un-retouched complete flakes.

Attribute	χ^2	df	p
Cortex	8.094	2	0.017
Max Length	3.139	2	0.208
Max Width	6.06	2	0.048
Surface Area	4.797	2	0.091
Medial Thickness	7.463	2	0.024
Axial Length	2.177	2	0.337
Axial Proximal Width	1.79	2	0.409
Axial Medial Width	6.129	2	0.047
Axial Distal Width	15.746	2	0
Elongation	10.655	2	0.005
Flatness	8.295	2	0.016
Proximal Shape	7.272	2	0.026
Distal Shape	12.431	2	0.002
Platform Width	1.194	2	0.551
Platform Depth	5.763	2	0.056
Platform Surface Area	2.482	2	0.289
Platform Shape	11.007	2	0.004
Size Corrected Platform Area	3.124	2	0.21

Table C.17: Results of Kruskal-Wallis test of flake attributes separated by stratum.

Attribute	Pairs	Mann-Whitney U	Wilcoxon W	Z	Asymp. Sig. (2-tailed)
Cortex	S6 - S8	14305.5	49021.5	-2.733	0.006
	S4 - S8	10088	26741	-2.298	0.022
Medial Thickness	S6 - S8	14408.5	49124.5	-2.536	0.011
Axial Distal Width	S4 - S8	7832	22197	-3.789	0
	S6 - S8	13083.5	44709.5	-2.623	0.009
	S4 - S6	18695	33060	-2.061	0.039
Proximal Shape	S4 - S8	8419	16045	-2.623	0.009
Distal Shape	S4 - S8	8045	15795	-3.396	0.001
	S4 - S6	18039	49164	-2.476	0.013
Elongation	S4 - S8	7822	15203	-3.199	0.001
	S6 - S8	12848	20229	-2.241	0.025
Flatness	S4 - S6	18061	32596	-2.794	0.005
Platform Shape	S4 - S6	16987	31015	-3.341	0.001

Table C.18: Significant results of Mann-Whitney test of complete flakes by stratum.

Pair	Fisher's Test	N	Monte Carlo Sig. (2-sided)
S4- S6	24.244	401	0.001
S4 - S8	15.461	277	0.03

Table C.19: Results of significant Fisher's Exact Test comparing scar pattern by stratum.

Pair	Fisher's Test	N	Monte Carlo Sig. (2-sided)
S4 - S6	22.458	422	0.001
S4 - S8	21.985	295	0
S6 - S8	40.291	377	0

Table C.20: Results of significant Fisher's Exact Test comparing platform type by stratum.

Pair	Fisher's Exact Test	N	Monte Carlo Sig. (2-sided)
S4 - S6	15.22	421	0.004
S4- S8	10.388	294	0.023
S6 - S8	11.886	373	0.011

Table C.21: Results of significant Fisher's Exact Test comparing termination type by stratum.

Attribute	N	Mean	S.D.	Min	Max	Percentiles		
						25th	50th (Median)	75th
Cortex	293	15.2389	22.61828	0	100	0	0	30
Max Length	293	34.542	18.32177	7.86	109.38	22.92	30.03	39.825
Max Width	293	24.0521	13.3863	4.71	94	16.21	21.49	28.27
Surface Area	293	1054.698	1385.244	44.46	10049.54	380.3998	640.0758	1076.878
Medial Thickness	284	11.9236	7.39412	1.38	55	7.1325	10.05	15.2075

Table C.22: Univariate descriptive statistics for flaked piece attributes.

Attribute	Mann-Whitney U	Wilcoxon W	Z	Asymp. Sig. (2-tailed)
Cortex	1579	39805	-2.553	0.011
Max Length	1037	39263	-3.861	0
Max Width	1084	39310	-3.722	0
Surface Area	1027	39253	-3.89	0
Medial Thickness	1619.5	37665.5	-1.644	0.1

Table C.23: Significant results of Mann-Whitney test comparing retouched and unretouched flaked pieces.

Attribute	χ^2	df	p
Cortex	0.256	2	0.88
Max Length	0.147	2	0.929
Max Width	1.005	2	0.605
Surface Area	0.195	2	0.907
Medial Thickness	1.217	2	0.544

Table C.24: Results of Kruskal-Wallis test of flaked piece attributes separated by stratum.

	Fisher's Test	N	Sig
All assemblages	11.485	256	0.003
S4-S6	Exact	194	0.007
S4-S6	Exact	142	0.007

Table C.25: Results of significant Fisher's Exact Test comparing retouched and unretouched flaked pieces by stratum.

Attribute	N	Mean	S.D.	Min	Max	Percentiles		
						25th	50th (Median)	75th
Cortex	111	29.5045	34.6276	0	100	0	10	60
Max Length	111	52.4614	19.0774	19	127.57	37.81	49.74	63.91
Max Width	111	35.9367	13.06199	16.85	89.37	26.55	34.04	42.19
Surface Area	111	2080.94	1511.638	325.54	9296.03	1059.819	1667.214	2535.351
Medial Thickness	109	14.4294	6.26629	4.47	45.37	10.65	13.14	17.125
Retouch Width	78	36.38	18.512	12	115	23.02	32.56	45.45
Retouch Depth	78	10.95	9.157	2	49	4.73	7.57	14.51
Index of Invasiveness	102	0.1323	0.08029	0	0.44	0.0625	0.125	0.1875

Table C.26: Univariate descriptive statistics for retouched flake and flaked piece attributes.

Attribute	Location			Blank Type			Strata		
	χ^2	df	p	χ^2	df	p	χ^2	df	p
Cortex	8.622	6	0.196	0.02	1	0.889	df	2	0.475
Max Length	4.751	6	0.576	0.027	1	0.869	Asymp. Sig.	2	0.327
Max Width	5.433	6	0.49	1.125	1	0.289	1.437	2	0.487
Surface Area	4.607	6	0.595	0.192	1	0.661	1.209	2	0.546
Medial Thickness	10.031	6	0.123	1.241	1	0.265	2.567	2	0.277
Retouch Width	11.339	5	0.045	0.435	1	0.509	13.624	2	0.001
Retouch Depth	7.948	5	0.159	1.63	1	0.202	6.88	2	0.032
Index of Invasiveness	29.641	6	0	2.181	1	0.14	4.034	2	0.133

Table C.27: Results of Kruskal-Wallis test of retouched flake and flaked piece attributes separated by stratum.

Pair	Mann-Whitney U	Wilcoxon W	Z	Asymp. Sig. (2-tailed)
S4-S6	330.5	925.5	-3.175	0.001
S4-S8	32	53	-2.693	0.007

Table C.28: Significant results of Mann-Whitney test comparing retouch width by stratum.